Modern Breast Cancer Imaging

Su Jin Kim Hsieh
Elizabeth Anne Morris
Editors

Springer

Modern Breast Cancer Imaging

Su Jin Kim Hsieh • Elizabeth Anne Morris
Editors

Modern Breast Cancer Imaging

Springer

Editors
Su Jin Kim Hsieh
Breast Imaging Department
Hospital Sírio-Libanês and Instituto de Radiologia (INRAD), Hospital das Clinicas HCFMUSP, Faculdade de Medicina, Universidade de Sao Paulo
São Paulo, SP
Brazil

Elizabeth Anne Morris
Department of Radiology
University of California Davis
Sacramento, CA
USA

ISBN 978-3-030-84545-2 ISBN 978-3-030-84546-9 (eBook)
https://doi.org/10.1007/978-3-030-84546-9

This Springer imprint is published by the registered company Springer Nature Switzerland AG
The registered company address is: Gewerbestrasse 11, 6330 Cham, Switzerland

“To Mariana, Lucas and Pedro”
—Dr Su Jin Kim Hsieh

“For my two beautiful children, who are a wonder” —Dr Elizabeth Anne Morris

Foreword

Breast cancer has haunted the female universe for millennia. And this agony has been portrayed in many ways, both in history and in art. Sometimes in an accidental way as in some well-known paintings and sculptures, while at other times directly, as in hieroglyphic scripts that described it as an incurable disorder. Today, in the third millennium of the Christian era, our knowledge about this disease has completely changed. We already have the sequencing of the main genes related to breast cancer and specific targeted therapies, which totally altered its evolution. We know that early detection is still the best way to increase the chances of cure and the possibility of less aggressive surgical and adjuvant treatments. Currently there are imaging techniques capable of detecting increasingly smaller and biologically significant tumors. And this was only achieved thanks to the tireless work of doctors and scientists from different specialties, who joined together for a single objective: to reduce mortality from breast cancer and provide a better quality of life for women affected by it.

In the book *Modern Breast Cancer Imaging*, the editors, Su Jin Kim Hsieh and Elizabeth Morris, both with extensive expertise in breast radiology and international projection, brought a multidisciplinary approach to breast cancer, in the areas of pathology, oncology, radiotherapy, and surgery, in addition to an extensive update on diagnostic imaging applied to clinic. Divided into three large parts, the book initially brings the main advances in science from a clinical and pathological point of view. It covers from the molecular basis of breast cancer, risk factors, and genetic testing to advances in surgical and pathological treatment. In Part II, the imaging methods used in breast radiology, their indications and limitations, as well as their future perspectives are discussed, mainly how to transpose the information obtained to improve clinical outcomes. Part III presents the main clinical problems and how imaging methods can help: from screening to diagnosis, including treatment and follow-up of women diagnosed with breast cancer.

At last, despite breast cancer being one of the oldest and most studied diseases in science, we do have a lot to evolve. Mainly because fear and prejudice against this disease still exist, in the twenty-first century. And also, because we still witness many lives lost, despite being a potentially curable disease. We currently live in the

era of personalized medicine, in which there is no single-treatment disease. There is indeed a unique woman, with a unique history and genetic profile, who must be accompanied individually. And this is the kind of treatment our women need and deserve. And for this, the collaboration among the various professionals who are part of a breast center is essential: radiologists, pathologists, breast surgeons, oncologists, and geneticists, among many other specialties. And it is this integration and updating of knowledge and technology that this book brings in a spectacular way.

Linei Augusta Brolini Dellê Urban
Department of Breast Radiology
Clínica DAPI
Paraná, Brazil

Universidade Federal do Parana, UFPR
Paraná, Brazil

Brazilian College of Radiology, CBR
São Paulo, Brazil

Sociedad Iberoamericana de Imagen Mamaria (SIBIM)
São Paulo, Brazil

Preface

The field of breast imaging has been evolving very fast lately, especially concerning breast cancer. Not only screening protocols have suffered some adjustments over the past years, but also new imaging methods, software and even new types of procedures have emerged. New concepts regarding molecular and genetic basis and therapeutic regimens have changed greatly.

The understanding of these new concepts become essential to give the patient the best possible care, since the confection of a relevant and useful breast imaging report from the radiologist, and also for the other professionals to understand what type of imaging exams to order in each scenario and how to interpret the results.

Keeping up to date demanded a great deal of effort, considering the vast amount of information in the literature, not only in the area of imaging, but also in other fields such as pathology, surgery and oncology.

The idea of this book was to compile up-to-date and established information about breast cancer in all these areas, in a multimodality approach. It is intended to be useful for daily practice not only for breast radiologists, but also for everyone who is in this field of medical practice.

This book has been written by very experienced and renowned professionals and would not be possible without their valuable contributions!

Special thanks to Dr Morris, who believed in this project from the beginning!

São Paulo, Brazil — Su Jin Kim Hsieh

Contents

Part I Updates in Clinical and Pathological Aspects for Breast Cancer

1 Molecular Basis of Breast Cancer 3
Raquel Civolani Marques Fernandes

2 Risk Factors for Breast Cancer 17
Sergio Masili-Oku, Angela Trinconi, Gabriela Boufelli, and Jose Roberto Filassi

3 Genomic Tests 31
Laura Testa and Renata Colombo Bonadio

4 Updates in Surgical Approaches for Breast and Axilla 39
Bruna Salani Mota, Rodrigo Goncalves, and Jose Roberto Filassi

5 Pathological Aspects for Diagnosis 47
Marcelo Abrantes Giannotti and Fernando Nalesso Aguiar

Part II Update in Imaging Method

6 Radiation Based Imaging: Digital Mammography, Tomosynthesis 71
Almir Galvão Vieira Bitencourt and Carolina Rossi Saccarelli

7 Sonographic Based Imaging: Ultrasound, Color Doppler, Elastography, and Automated Breast Imaging 97
Juliana Hiraoka Catani

8 Magnetic Resonance Imaging: Regular Protocols and Fast Protocols 131
Joao V. Horvat and Sunitha B. Thakur

9 Nuclear Medicine Based Methods: PET FDG and Other Tracers . . . 141
Marcelo Tatit Sapienza and Poliana Fonseca Zampieri

10 Image-Guided Percutaneous Biopsies 161
Vitor Chiarini Zanetta

11 Breast Imaging Preoperative Localization Procedure 211
Heni Debs Skaf, Juliana Hiraoka Catani, and Vivian Simone De Medeiros Ogata

Part III Different Clinical Scenario: Clinical Management and Role of Imaging Modalities

12 Screening 247
Mila Trementosa Garcia, Laura Aguiar Penteado, Flávia Abranches Corsetti Purcino, and Jose Roberto Filassi

13 Diagnostic 259
Karina Belickas Carreiro, Juliana Pierobon Gomes da Cunha, Jose Roberto Filassi, and Caio Dinelli

14 Preoperative (Breast) 281
Jonathan Yugo Maesaka, Yedda Nunes Reis, and Jose Roberto Filassi

15 Systemic Staging (Total Body – When, How) 297
Fabiano de Almeida Costa and Rudinei Diogo Marques Linck

16 Neoadjuvant Systemic Therapy 307
Ana Carolina de Ataíde Góes, Heni Debs Skaf, and Laura Testa

17 Postoperative Breast 331
Larissa Muramoto Yano and Monica Akahoshi Rudner

18 Radiation Therapy 415
Paula de Camargo Moraes

19 Adjuvant Therapy 435
Laura Testa and Renata Colombo Bonadio

20 Follow-Up After Treatment 439
Bruno Salvador Sobreira Lima, Fernanda Barbosa, Maria Carolina Formigoni, Sergio Masili-Oku, and Jose Roberto Filassi

21 Breast Cancer During Pregnancy and Lactation 447
Yoon Seung Chang and Monica Akahoshi Rudner

Index 463

Contributors

Fernando Nalesso Aguiar, MD Departamento de Patologia, Instituto do Cancer do Estado de Sao Paulo ICESP, São Paulo, SP, Brazil

Fabiano de Almeida Costa, MD Departamento de Oncologia, Instituto do Cancer do Estado de São Paulo ICESP, São Paulo, SP, Brazil

Ana Carolina de Ataíde Góes, MD Instituto de Radiologia INRAD, Hospital das Clinicas HCFMUSP, Faculdade de Medicina, Universidade de Sao Paulo, São Paulo, SP, Brazil

Fernanda Barbosa, MD Departamento de Mastologia, Instituto do Cancer do Estado de Sao Paulo ICESP, São Paulo, SP, Brazil

Almir Galvão Vieira Bitencourt, MD A.C.Camargo Cancer Center, São Paulo, SP, Brazil

Diagnósticos da América SA, São Paulo, SP, Brazil

Renata Colombo Bonadio, MD Departamento de Oncologia, Instituto do Cancer do Estado de Sao Paulo ICESP, São Paulo, SP, Brazil

Gabriela Boufelli, MD Departamento de Mastologia, Instituto do Cancer do Estado de Sao Paulo ICESP, São Paulo, SP, Brazil

Paula de Camargo Moraes, MD Instituto de Radiologia INRAD, Hospital das Clinicas HCFMUSP, Faculdade de Medicina, Universidade de Sao Paulo, São Paulo, SP, Brazil

CDB (Centro Diagnóstico Brasil) – Grupo Alliar, São Paulo, SP, Brazil

Alta Medicina Diagnóstica – Grupo DASA, São Paulo, SP, Brazil

Karina Belickas Carreiro, MD Departamento de Mastologia, Instituto do Cancer do Estado de Sao Paulo ICESP, São Paulo, SP, Brazil

Juliana Hiraoka Catani, MD Instituto de Radiologia INRAD, Hospital das Clinicas HCFMUSP, Faculdade de Medicina, Universidade de Sao Paulo, São Paulo, SP, Brazil

Yoon Seung Chang, MD Breast Imaging Section, Centro de Diagnósticos Brasil (CDB – Alliar), São Paulo, SP, Brazil

Instituto de Radiologia INRAD, Hospital das Clinicas HCFMUSP, Faculdade de Medicina, Universidade de Sao Paulo, São Paulo, SP, Brazil

Juliana Pierobon Gomes da Cunha, MD Departamento de Mastologia, Instituto do Cancer do Estado de Sao Paulo ICESP, São Paulo, SP, Brazil

Caio Dinelli, MD Instituto de Radiologia INRAD, Hospital das Clinicas HCFMUSP, Faculdade de Medicina, Universidade de Sao Paulo, São Paulo, SP, Brazil

Raquel Civolani Marques Fernandes, MD Hospital Beneficência Portuguesa de São Paulo/Laboratório Bacchi, São Paulo, SP, Brazil

Pathology Department Director, Hospital Pérola Byington, São Paulo, SP, Brazil

Jose Roberto Filassi, MD, PhD Departamento de Mastologia, Instituto do Cancer do Estado de Sao Paulo ICESP, São Paulo, SP, Brazil

Maria Carolina Formigoni, MD Departamento de Mastologia, Instituto do Cancer do Estado de Sao Paulo ICESP, São Paulo, SP, Brazil

Mila Trementosa Garcia, MD Departamento de Mastologia, Instituto do Cancer do Estado de Sao Paulo ICESP, São Paulo, SP, Brazil

Marcelo Abrantes Giannotti, MD Hospital Sírio Libanês and Departamento de Patologia, Hospital das Clinicas HCFMUSP, Faculdade de Medicina, Universidade de Sao Paulo, São Paulo, SP, Brazil

Rodrigo Goncalves, MD Departamento de Mastologia, Instituto do Cancer do Estado de Sao Paulo ICESP, São Paulo, SP, Brazil

Joao V. Horvat, MD Department of Radiology, Memorial Sloan Kettering Cancer Center, New York, NY, USA

Bruno Salvador Sobreira Lima, MD Departamento de Mastologia, Instituto do Cancer do Estado de Sao Paulo ICESP, São Paulo, SP, Brazil

Rudinei Diogo Marques Linck, MD Departamento de Oncologia, Instituto do Cancer do Estado de São Paulo ICESP, São Paulo, SP, Brazil

Jonathan Yugo Maesaka, MD Departamento de Mastologia, Instituto do Cancer do Estado de Sao Paulo ICESP, São Paulo, SP, Brazil

Sergio Masili-Oku, MD Departamento de Mastologia, Instituto do Cancer do Estado de Sao Paulo ICESP, São Paulo, SP, Brazil

Vivian Simone De Medeiros Ogata, MD Instituto de Radiologia INRAD, Hospital das Clinicas HCFMUSP, Faculdade de Medicina, Universidade de Sao Paulo, São Paulo, SP, Brazil

Bruna Salani Mota, MD Departamento de Mastologia, Instituto do Cancer do Estado de Sao Paulo ICESP, São Paulo, SP, Brazil

Laura Aguiar Penteado, MD Departamento de Mastologia, Instituto do Cancer do Estado de Sao Paulo ICESP, São Paulo, SP, Brazil

Flávia Abranches Corsetti Purcino, MD Departamento de Mastologia, Instituto do Cancer do Estado de Sao Paulo ICESP, São Paulo, SP, Brazil

Yedda Nunes Reis, MD Departamento de Mastologia, Instituto do Cancer do Estado de Sao Paulo ICESP, São Paulo, SP, Brazil

Monica Akahoshi Rudner, MD Hospital Albert Einstein, São Paulo, SP, Brazil

Instituto de Radiologia INRAD, Hospital das Clinicas HCFMUSP, Faculdade de Medicina, Universidade de Sao Paulo, São Paulo, SP, Brazil

Hospital Moriah and Prevent Senior, São Paulo, SP, Brazil

Carolina Rossi Saccarelli, MD Diagnósticos da América SA, São Paulo, SP, Brazil

Hospital Sírio-Libânes, São Paulo, SP, Brazil

Marcelo Tatit Sapienza, MD, PhD Departamento de Radiologia e Oncologia, Hospital das Clinicas HCFMUSP, Faculdade de Medicina, Universidade de Sao Paulo, São Paulo, SP, Brazil

Heni Debs Skaf, MD Instituto de Radiologia INRAD, Hospital das Clinicas HCFMUSP, Faculdade de Medicina, Universidade de Sao Paulo, São Paulo, SP, Brazil

Laura Testa, MD Departamento de Oncologia, Instituto do Cancer do Estado de Sao Paulo ICESP, São Paulo, SP, Brazil

Sunitha B. Thakur, MD Department of Radiology, Memorial Sloan Kettering Cancer Center, New York, NY, USA

Angela Trinconi, MD Departamento de Mastologia, Instituto do Cancer do Estado de Sao Paulo ICESP, São Paulo, SP, Brazil

Larissa Muramoto Yano, MD Hospital Albert Einstein, São Paulo, SP, Brazil

Instituto de Radiologia INRAD, Hospital das Clinicas HCFMUSP, Faculdade de Medicina, Universidade de Sao Paulo, São Paulo, SP, Brazil

Poliana Fonseca Zampieri, MD Departamento de Medicina Nuclear, Instituto do Cancer do Estado de Sao Paulo ICESP, São Paulo, SP, Brazil

Vitor Chiarini Zanetta, MD Department of Radiology, Instituto de Radiologia INRAD, Hospital das Clinicas HCFMUSP, Faculdade de Medicina, Universidade de Sao Paulo, São Paulo, SP, Brazil

Part I
Updates in Clinical and Pathological Aspects for Breast Cancer

Chapter 1
Molecular Basis of Breast Cancer

Raquel Civolani Marques Fernandes

1.1 Introduction

Breast cancer is the second most common cancer among women, after non-melanoma skin cancer, with a one in eight probability of developing invasive carcinoma in a US woman during her lifetime. In 2021, an estimated 281,550 new cases of invasive breast carcinoma are expected to be diagnosed in American women, along with 49,290 new cases of in situ breast cancer [1].

About 5–10% of breast cancer can be linked to a hereditary mutation of a known gene, such as BRCA1 and BRCA2. On average, women with a BRCA1 mutation have up to a 72% lifetime risk of developing breast cancer, while the risk is 69% with BRCA2 mutation [2].

After the year 2000, with the sequencing of multiple types of tumors, the understanding of the molecular biology of breast cancer brought extremely important knowledge, which changed the clinical practice of its treatment. It has been recognized as a heterogeneous neoplasia by several biomarkers, now used in diagnosis, prognosis, and treatment according to each subtype.

The heterogeneity of breast carcinomas is due to the involvement of different genes, related to the proliferative activity, differentiation, and suppression of tumors, several of them studied alone or in small groups, regarding the implication in carcinogenesis and/or as prognostic factors. However, the enormous heterogeneity and the number of factors involved make interpretation difficult. With the development of genome analysis technologies with the possibility of concomitant analysis of thousands of genes, it was possible to identify intrinsic gene profiles in breast

R. C. M. Fernandes (✉)
Hospital Beneficência Portuguesa de São Paulo/Laboratório Bacchi, São Paulo, SP, Brazil

Pathology Department Director, Hospital Pérola Byington, São Paulo, SP, Brazil
e-mail: raquel@labbacchi.com.br

S. J. Kim Hsieh, E. A. Morris (eds.), *Modern Breast Cancer Imaging*,
https://doi.org/10.1007/978-3-030-84546-9_1

tumors called basal; HER2-enriched; luminal A, B, and C; and normal breast type according to the classification of Perou et al. [3–7]. These presentation profiles showed consistency even in different study groups and using different array techniques [4, 5, 8].

Over the past few years, there has been considerable effort to characterize and classify breast cancer at the molecular level in order to effectively tailor treatment. However, due to time and cost constraints, in the great majority of health-care systems, a surrogate molecular breast cancer classification is still largely based on immunohistochemical (IHC) assessment of biomarkers: ER (estrogen receptor), PR (progesterone receptor), HER2, and Ki-67. Nevertheless, the examination of global patterns of gene expression (especially of genes involved in the regulation of cell growth and other important aspects of cell behavior, such as invasion) has resulted in the identification of intrinsic molecular subtypes of biological and clinical relevance and of gene signatures predictive of outcome or response to therapy [9].

It is extremely important to remember that to avoid false-negative result for any molecular or IHC study, the biopsy or surgical specimen must be properly fixed at 10% buffered formalin to ensure pH range 7.0 and 7.4 within 1 hour after resection averting prolonged cold ischemic time, which may result in antigenic degradation. Under- or over-fixation is not recommended. Fixation for at least 6 hours and a maximum of 72 hours are recommendations from the College of American Pathologists (CAP) [10].

1.2 BC (Basal Carcinomas) and TNC (Triple Negative Carcinomas)

BC is characterized by the high expression of several genes that characterize the basal cells of the epithelium, which have the capacity to originate epithelial and myoepithelial cells in the terminal lobular duct unit, including the basal cytokeratins 5/6 and 17. These basal cytokeratins indicate smooth muscle differentiation, present in myoepithelial cells and their precursors [11]. Other markers can be used in order to improve accuracy in determining the phenotype and the expected evolution for these tumors, including expression of Epidermal growth factor receptor (EGFR) or HER1, c-Kit, and vimentin. With the possibility of comparing the IHC profile and the profile defined by the analysis of several genes, Nielsen et al. [12] demonstrated that a panel composed of four markers—a negative estrogen receptor, positive HER1, negative HER2, and a positive basal cytokeratin—could accurately identify the genetically determined basal subgroup.

BC generally correspond to high-grade invasive carcinoma of no special type (with or without medullary features) or metaplastic carcinoma [9].

Livasy et al. and Nielsen et al. also highlighted some morphological characteristics frequently present in these tumor subtypes [12, 13], including high histological and nuclear grade, high mitotic count, the presence of polygonal cells with abundant

eosinophilic or clear cytoplasm, geographic tumor necrosis, central scar, expansive tumor borders, and increased immune cells.

TNC are defined by the lack of expression of hormone receptors and HER2 protein, and today, IHC examination is the most accessible and the best diagnostic molecular tool for diagnosis [9]. Genetically, there is a 70–80% overlap between BC and TNC. Although almost 70% of basal intrinsic molecular carcinomas have a triple negative IHC profile, 20% of them have IHC expression of hormone receptors, and 10% are HER2 enriched [14]. BC and TNC have more frequent metastases to the brain and visceral organs than to the bone and nodes compared to ER-positive carcinomas and high risk of early recurrence within 5 years and death [15].

As for the prognosis, it is important to remember that TNC are a heterogeneous group of tumors. Among those with a favorable prognosis are low-grade adenosquamous carcinoma, adenoid cystic carcinoma, and secretory carcinoma; among those with intermediate prognosis is invasive carcinoma of no special type with medullary features, and among the unfavorable ones are the high-grade invasive carcinoma of no special type and metaplastic carcinoma [9].

The knowledge of the molecular biology of these tumors has been increasing every year. While until the middle of the last decade no specific therapeutic target was known, nowadays, antiandrogens, DNA damage response targeting, and immune checkpoint inhibitors are some of the promising clinical approaches that evolved from the concept that some tumors show poor prognosis due to overexpression of genes promoting proliferation and migration.

Lehman et al. in 2016 [16] updated the molecular classification of TNC through the analysis of TNC gene expression profiles, previously proposed by the same group in 2011. In this classification, four TNC subgroups were recognized, with their own clinical and molecular characteristics: basal subtype 1 (BL1) and basal subtype 2 (BL2), which have high proliferative activity with activation of various pathways to stimulate the cell cycle and response to DNA damage; mesenchymal subtype (M), which has activated signaling pathways of growth factors such as the IGF pathway/mTOR, a part of them still with low expression of claudins; and the luminal androgenic subtype (LAR), which has activation of signaling pathways associated with the androgen receptor. In this work, the authors highlighted the differences between age, grade, local and distant disease progression, and histopathology among these subgroups, in addition to the different responses to neoadjuvancy, depending on the subtype. Pathologic complete response (pCR) was reached in 41% of BL1, 18% of BL2, and 29% of LAR.

It is important to note that the characteristics of each subgroup, especially BL1, BL2, and M, can be modulated by the tumor microenvironment, with tumor-infiltrating lymphocytes (TILs) playing a fundamental role in this modulation.

Programmed death ligand 1 (PD-L1) is an immunoregulatory molecule that limits its antitumor immune activity. Both TILs and PD-L1 status predicted pathologic complete response (pCR) to neoadjuvant chemotherapy in univariate and multivariate analysis. PD-L1 expression was associated with TNC and receptor-negative status and high level of TILs [17].

In this scenario, immunotherapy with checkpoint inhibitors has made great progress. Early in 2019, atezolizumab, an anti-PD-L1 monoclonal antibody, was approved in combination with nanoparticle albumin-bound (nab) paclitaxel, a form of paclitaxel that does not require steroid premedication, for the treatment of patients with locally advanced or metastatic TNC whose tumors are positive for PD-L1 expression (≥1%) on immune infiltrate, evaluated by the Ventana PD-L1 (SP142) antibody [18].

The tumor mutational burden (TMB) is substantially lower in breast cancer than in other solid malignancies such as lung cancer or melanoma, with low ability to develop a competent immune response related only to this variant [19].

Along with BRCA1/2-mutation breast cancer, about 50% of sporadic TNC have the BRCAness phenotype, which gives them, clinical and pathological characteristics to be highlighted: large tumors (>2.0 cm), circumscribed with pushing borders, sheets of pleomorphic tumor cells, syncytial-like growth pattern, brisk lymphocytic stromal reaction, with geographic pattern necrosis or fibrosis, usually occurring in young patients and high KI-67 levels.

They are frequently associated with TP53 gene mutation and EGFR expression, deficient in homologous recombination and with sensitivity to (adenosine diphosphate-ribose) polymerase inhibitors and platinum salts [20, 21].

1.3 Luminal Carcinomas (LC)

Luminal carcinomas represent a group of tumors that corresponds to approximately 75–80% of all breast carcinomas and show a differentiated epithelial cell profile, with expression of estrogen and/or progesterone receptors and a better prognosis, particularly the subtype A. These tumors express markers of the epithelial cells of the ductal lining, such as luminal cytokeratins (8 and 18) and reflect a more advanced stage in differentiation, constituting a more heterogeneous group depending on the degree of differentiation. Fernandes et al. [22] showed that among the poorly differentiated invasive breast carcinomas (Nottingham classification between 2 and 3 with a maximum of 10% of solid arrangement), the luminal subtype was the most frequent (73 cases or 54.5%), followed by the triple-negative subtype (39 cases or 29.1%) and, more rarely, the HER2 subtype (22 cases or 16.4%).

The technology of DNA microarrays allowed subgroups of tumors to be analyzed in order to determine genes related to morphological characteristics of recognized prognostic impact. Thus, RE-positive carcinomas were subdivided into high and low genomic grade, determined by the expression of genes related to cell differentiation and proliferation [23]. In this study, the genomic grade determines two distinct subtypes of tumors in terms of evolution, regardless of the use of tamoxifen and consistent with the luminal profiles A and B. Luminal A carcinomas are characterized by a higher expression of ER, GATA3, and X-box-binding protein trefoil factor 3, hepatocyte nuclear factor 3 alpha, and LIV-1, besides low genomic grade, similar to the normal breast tissue. Luminal B carcinomas are generally

characterized by a lower expression of luminal-specific genes, a higher expression of genes involved in mitosis and cell proliferation, and high genomic grade and can also express in approximately 10–15% of cases, amplification and/or overexpression of the HER2 gene (ER+; PR+ and HER2+ or triple positive).

As to the IHC profile, the CAP and ASCO in the most recent update [24] maintained the definition of positive hormone receptor, any expression of ER or RP greater than or equal to 1% (which would correspond to an Allred score of 2 or more for the proportion of positive cells with any intensity of immunostaining) (Fig. 1.1). They also recommend that the result of the hormone receptors status be reported considering the average intensity and extent of immunostaining and not simply as positive or negative. In the same issue, invasive carcinomas with 1 to 10% of cells staining for ER (not PR) are reported as "low positive," and the following report comment is recommended: "The cancer in this sample has a low level (1–10%) of ER expression by IHC."

There are limited data on the overall benefit of endocrine therapies for patients with low level of ER expression (1–10%), but they currently suggest possible benefit, so patients are considered eligible for endocrine treatment. There are data that suggest that invasive cancers with these results are heterogeneous in both behavior and biology and often have gene expression profiles more similar to ER-negative cancers. The "low positive" designation applies only to invasive carcinoma and is not used for PR or ductal carcinoma in situ (DCIS).

When we attempt to correlate the histological with the molecular subtypes, the main studies were almost completely limited to invasive breast carcinoma of no special type, which can be of any molecular subtype, and did not take uncommon histologies into account. Thus, molecular classification is more a description of the heterogeneity of invasive breast carcinoma of no special type rather than an exhaustive representation of the entire breast cancer landscape. In this scenario, Dieci et al. [25] studied the special molecular types and histological subtypes, which represent 25% of all breast carcinomas. Some of the special

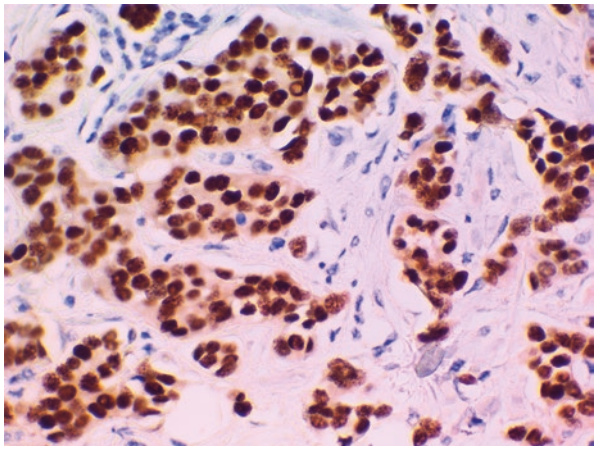

Fig. 1.1 Immunohistochemical reaction illustrating positive case for estrogen receptor. Nuclear staining in >1% of neoplastic cells

types with the best prognosis (pure mucinous and tubular carcinomas) presented the lowest levels of gene copy number changes and corresponded to the luminal subtype A.

In the 2013 St. Gallen consensus, the approximate cut-point in immunohistochemistry to separate the luminal subtypes A and B was KI67 ≤20% and/or PR <20% [26].

Currently, we also have genomic tests for HER-negative LCs, which can be used to define treatment in cases of discordant clinical and genomic risks, formerly used only to guide prognosis, such as the distance recurrence index determined by 21 genes [27] and the Amsterdam test of 70 genes [28]. These will be discussed in a specific chapter.

As for the metastatic scenario, Chen et al. [29] provided a large single center cohort to assess the frequency of receptor conversion in metastatic breast cancer. The overall discordant rates were 18.3%, 40.3%, and 13.7% for ER, PR, and HER2, respectively. The discordance was significantly higher for PR when compared with ER and HER2. The conversion occurred significantly as a switch from positive to negative receptor status when compared to the conversion from negative to positive for all three receptors. Semiquantitative analyses revealed a significantly decreased expression of both ER (25%) and PR (57%) in the metastases. There was a higher rate of PR discordance in bone metastases when compared to other common organs of relapse.

A positive ER status, in primary or metastatic breast cancer, was associated with a prolonged metastasis-free survival when compared with ER-negative primary tumors without conversion. Furthermore, a positive ER status in metastatic breast cancer regardless of the primary tumor was associated with a superior overall survival when compared with an ER-negative tumor without conversion. Thus, receptor conversion is a frequent event in the course of breast cancer progression and can also be seen between different metastatic sites. Moreover, some conversions are of prognostic significance. The findings may reflect tumor heterogeneity, sampling, or treatment effect but may also indicate alteration in tumor biology. Repeat biomarker testing is justified when making appropriate treatment plans in the pursuit of precision medicine.

Despite continuous expression of the ER, for unknown reasons, many ER+ breast cancers in the metastatic setting become refractory to the inhibition of estrogen action. Thirty-one biopsy samples collected after progression on hormonal therapy from patients with metastatic ER+ breast cancer were subjected to targeted DNA sequencing in a study [30]. ESR1 mutations (a total of 9/36 cases) were detected at much higher rates than in those reported by TCGA. The mutations in ESR1 clustered in the ligand-binding domain. Furthermore, analysis of the available paired primary samples showed that these mutations were an acquired event. The mutations clearly occurred in a population of patients with hormone refractory disease, and the biochemical and structural data demonstrated that these mutations promoted the agonist conformation of ER in the absence of ligand. Furthermore, the mutant ER isoforms were only partially inhibited by direct receptor antagonists such as tamoxifen or fulvestrant and needed higher doses than those used clinically

to achieve full inhibition. Thus, ESR1 mutations have emerged as predictors of acquired resistance to endocrine therapy and should help to select patients who are potential candidates for chemotherapy or other targeted agents [31].

Nowadays, there are important biomarkers still on the same scenario, such as genetic alterations of the phosphatidylinositol 3-kinase (PI3K)/AKT/mammalian target of rapamycin (mTOR) pathway, occurring in approximately 40% of patients with hormone receptor-positive, HER2-negative breast cancer. Thus, outcomes were not homogeneous, and it became evident that estrogen/ER signaling is more complex than initially believed. Apparently, feedback loops with growth factor signaling pathways play a vital role in resistance to antihormonal agents. Aberrant PI3K/AKT/mTOR signaling pathway is one mechanism of endocrine resistance acting via phosphorylation of the function domain 1 of the ER by S6 kinase 1, a substrate of mTOR complex 1. Targeting this pathway has been shown to have important clinical implications, demonstrated by the SOLAR-1 trial [32].

Dysregulation of the cell cycle is another important pathway targeted for drug development that led to the regulatory approval of a new drug. Several genetic alterations in key cell cycle regulatory proteins have been described in various cancers, including breast cancer. Here, the cyclin-dependent kinases (CDKs) were studied as targets of interest, especially CDK 4/6 molecule inhibitors [33].

1.4 HER2-Enriched Carcinomas

HER2 belongs to the family of four transmembrane receptors (HER1 or EGFR, HER2, HER3, and HER4), which use tyrosine kinase activity as a trigger in cell signaling. Other members of the tyrosine kinase growth factor receptor family are the c-Kit and the vascular endothelial growth factor receptor (VEGFR), factors that were initially studied in the assessment of breast cancer prognosis, and are now known to use the same activation pathways as HER2. Positivity for HER2 seems to be associated with relative but not absolute resistance to endocrine therapy in general [34]. Studies have suggested that this effect is specific with ER, since the non-genomic pathway of ER activity passes through the same pathways as HER, which would justify the failure to respond to hormonal block and resistance to endocrine therapy [35]. Retrospective results suggested that positivity for HER2 would be associated with the response with anthracyclines; however, this effect could be secondary to the co-amplification of the topoisomerase II alpha gene (TOP2A), a direct target of these agents and therefore another marker with therapeutic potential [36].

A subset of breast carcinomas (approximately 15%) overexpress human epidermal growth factor receptor 2 (HER2; Human Genome Organization (HUGO) nomenclature ERBB2). Protein overexpression is usually due to gene amplification. Assays for gene copy number, mRNA quantity, and protein generally give similar results; gene amplification correlates with protein overexpression in about 95% of cases. In a small subset of carcinomas (probably <5%), protein overexpression may occur by different mechanisms. Overexpression is both a prognostic and predictive

factor [10]. HER2 status is primarily evaluated to determine patient eligibility for anti-HER2 therapy. It may identify patients who have a greater benefit from anthracycline-based adjuvant therapy.

HER2 status can be determined in formalin-fixed paraffin-embedded tissue by assessing protein expression on the membrane of tumor cells using IHC or by assessing the number of HER2 gene copies using in situ hybridization (ISH). When both IHC and ISH are performed on the same tumor, the results should be correlated. The most likely reason for a discrepancy is that one of the assays is incorrect, but in a small number of cases, there may be protein overexpression without amplification, amplification without protein overexpression, or marked intratumoral heterogeneity. We must always keep in mind the intratumoral heterogeneity; when there is a negative result in a small biopsy sample, repeated testing on a subsequent specimen with a larger area of carcinoma sampled should be considered, particularly if the tumor has characteristics associated with HER2 positivity (i.e., tumor grade 2 or 3, weak or negative PR expression, increased proliferation index) [10]. When multiple invasive foci are present, the largest invasive focus should be tested. Testing smaller invasive carcinomas is also recommended if they are of different histologic type or higher grade.

The major challenge for the characterization of the HER2 group was the adequate laboratory standardization. The American Society of Clinical Oncology (ASCO) and CAP standardized criteria for positivity and laboratory control for adequate testing [10]. The immunohistochemical criteria are illustrated in Table 1.1 (Figs. 1.2 and 1.3), remembering that all HER2 2+ tumors (equivocal) must be subjected to ISH to confirm the real status of HER2. It is recommended that hormone receptor and HER2 testing be performed in all primary invasive breast carcinomas and in recurrent or metastatic tumors.

Fluorescence in situ hybridization (FISH), chromogenic in situ hybridization (CISH), and silver-enhanced in situ hybridization (SISH) studies for HER2 determine the presence or absence of gene amplification. Some assays use a single probe to determine the number of HER2 gene copies present, but most assays include a chromosome enumeration probe (CEP17) to determine the ratio of HER2 signals to copies of chromosome 17. Although 10% to 50% of breast carcinomas have more

Table 1.1 Reporting results of HER2 testing by immunohistochemistry

Result	Criteria
Negative (score 0)	No staining or incomplete or faint membrane staining within ≤10% of tumor cells
Negative (score 1+)	Incomplete or faint membrane staining within >10% of tumor cells
Equivocal (score 2+)	Weak to moderate complete membrane staining in >10% or intense complete membrane staining in ≤10% of tumor cells
Positive (score 3+)	Intense complete membrane staining in >10% of tumor cells

Adapted from 2018 CAP/ASCO Update recommendations

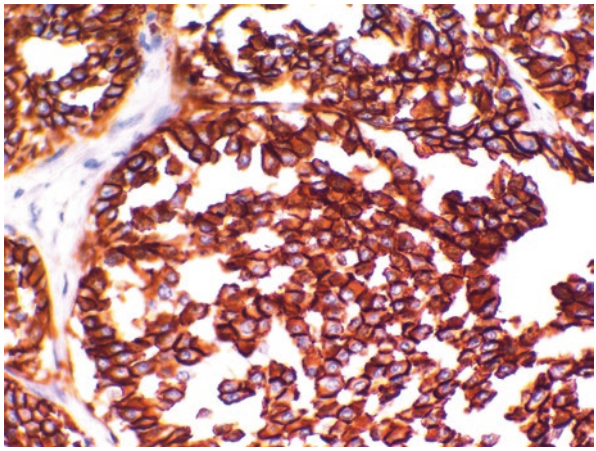

Fig. 1.2 Immunohistochemical reaction illustrating a positive case (score 3+) for HER2. Strong and complete membrane staining in >10% of neoplastic cells

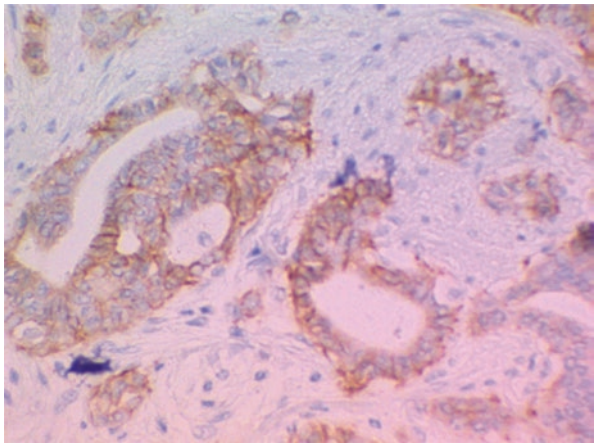

Fig. 1.3 Immunohistochemical reaction illustrating an equivocal case (score 2+) for HER2. Weak to moderate complete membrane staining in >10% of neoplastic cells

than two CEP17 copies, only 1% to 2% of carcinomas show true polysomy (i.e., duplication of the entire chromosome) (10).

Dual probe defines five groups by ISH: Group 1 = HER2/CEP17 ratio ≥2.0, ≥4.0 HER2 signals/cell; Group 2 = HER2/CEP17 ratio ≥2.0, <4.0 HER2 signals/cell; Group 3 = HER2/CEP17 ratio <2, ≥6.0 signals/cell; Group 4 = HER2/CEP17 ratio <2, ≥4.0 and <6.0 HER2 signals/cell; and Group 5 = HER2/CEP17 ratio <2.0, <4.0 HER2 signal/cell. Reporting results recommended by CAP/ASCO are shown in Table 1.2.

Group 1 is positive, group 5 is negative, and groups 2, 3, and 4 require a new count, together with immunohistochemistry and preferably by a second observer, to determine whether the result is positive or negative, without further misunderstanding after ISH. Regardless of the result, the group must be returned to the final report after the ISH.

Table 1.2 Reporting results of HER2 testing by in situ hybridization (dual-probe assay)

Result	Criteria (dual-probe assay)
Negative	Group 5
Negative – results based on concurrent review of IHC	Group 2 and concurrent IHC 0-1+ or 2+ Group 3 and concurrent IHC 0-1+ Group 4 and concurrent IHC 0-1+ or 2+
Positive – results based on concurrent review of IHC	Group 2 and concurrent IHC 3+ Group 3 and concurrent IHC 2+ or 3+ Group 4 and concurrent IHC 3+
Positive – results based on concurrent review of IHC	Group 1

Adapted from 2018 CAP/ASCO Update recommendations

The heterogeneity of HER2 breast cancer is a complex phenomenon. Before discussing true heterogeneity, it is important to discard pre-analytical problems that may have led to this result. Genomic heterogeneity refers to conditions where more than one population of tumor cells exists within the same tumor. This can occur in three separate manners: as discrete populations (clones) of amplified and non-amplified tumor cells, diffuse intermingling of amplified and non-amplified cells across the tumor, or as isolated 6 amplified cells in a predominantly non-amplified tumor [10]. This intrinsic heterogeneity reflects the lack of complete response to chemotherapy that these tumors present. lHC errors are more common in HER2 tumors, which had a low degree of amplification in the ISH [37].

As previously mentioned, there is biological resistance in positive hormonal tumors, HER2 positive. HER2 can induce ER phosphorylation (via MAPK and AKT) and cause hormonal resistance in these tumors. On the other hand, the ER pathway is an escape pathway that can drive tumor cell growth and survival in the presence of anti-HER2 therapy, via increased ER expression. In addition, non-genomic ER (associated with the membrane) can induce HER2 phosphorylation, causing resistance to anti-HER2 therapy [37–39].

Hou et al. [40], using the HER2 gene-protein assay (GPA) technique, simultaneously evaluated both HER2 gene signal and protein expression by means of a single-slide dual assay and observed that post-neoadjuvant pCR dropped from 76% (cases without heterogeneity for HER2) to 26% (cases with heterogeneity for HER2).

Another form of heterogeneity that occurs in these tumors is the conversion of status between the primary and the metastatic tumor and the conversion after neoadjuvant chemotherapy. Changes between the primary and metastatic profiles are expected in 10% of cases, most of them positive to negative. This is due to clonal selection and changes induced by treatment. It is more common for cases with low HER2 amplification, often HER2 2+ in immunohistochemistry [40–42]. Pusztai l during the 2020 ASCO meeting [42] divided the predictive factors of response to neoadjuvant treatment in HER2-positive breast carcinomas into two categories: sensitivity markers, with greater chance of pCR, and resistance markers, with less chance of pCR. Among the first are the ER-negative group, the intrinsic molecular

subtype HER2 enriched determined by PAM-50, tumors with intense immune infiltration (high TILs), and those with a high level of HER2 expression (immunohistochemistry, mRNA, copy number). Among the latter is the ER-positive group, with PIK3CA mutation, PTEN loss, HER2 copy number ratio <4.0, and focal HER2 positivity.

References

1. American Cancer Society. How common is breast cancer? Jan. 2021. Available at: https://www.cancer.org/cancer/breast-cancer/about/how-common-is-breast-cancer.html.
2. National Cancer Institute. BRCA mutations: cancer risk and genetic testing. Jan. 2018. Available at: https://www.cancer.gov/about-cancer/causes-prevention/genetics/brca-fact-sheet.
3. Perou CM, Sorlie T, Eisen MB, van de RM JSS, Rees CA, et al. Molecular portraits of human breast tumours. Nature. 2000;406(6797):747–52.
4. Sorlie T, Perou CM, Tibshirani R, Aas T, Geisler S, Johnsen H, et al. Gene expression patterns of breast carcinomas distinguish tumor subclasses with clinical implications. Proc Natl Acad Sci U S A. 2001;98(19):10869–74.
5. West M, Blanchette C, Dressman H, Huang E, Ishida S, Spang R, et al. Predicting the clinical status of human breast cancer by using gene expression profiles. Proc Natl Acad Sci U S A. 2001;98(20):11462–7.
6. Sotiriou C, Neo SY, McShane LM, Korn EL, Long PM, Jazaeri A, et al. Breast cancer classification and prognosis based on gene expression profiles from a population-based study. Proc Natl Acad Sci U S A. 2003;100(18):10393–8.
7. Sorlie T, Tibshirani R, Parker J, Hastie T, Marron JS, Nobel A, et al. Repeated observation of breast tumor subtypes in independent gene expression data sets. Proc Natl Acad Sci U S A. 2003;100(14):8418–23.
8. Van't Veer LJ, Dai H, van de Vijver MJ, He YD, Hart AA, Mao M, et al. Gene expression profiling predicts clinical outcome of breast cancer. Nature. 2002;415(6871):530–6.
9. WHO Classification of Tumours Editorial Board. Breast tumours, WHO classification of tumours series, vol. 2. 5th ed. Lyon: International Agency for Research on Cancer; 2019.
10. Cancer Protocols Templates of College of American Pathologists. Available at: https://www.cap.org/protocols-and-guidelines/cancer-reporting-tools/cancer-protocol-templates.
11. Birnbaum D, Bertucci F, Ginestier C, Tagett R, Jacquemier J, Charafe-Jauffret E. Basal and luminal breast cancers: basic or luminous? (review). Int J Oncol. 2004;25(2):249–58.
12. Nielsen TO, Hsu FD, Jensen K, Cheang M, Karaca G, Hu Z, et al. Immunohistochemical and clinical characterization of the basal-like subtype of invasive breast carcinoma. Clin Cancer Res. 2004;10(16):5367–74.
13. Livasy CA, Karaca G, Nanda R, Tretiakova MS, Olopade OI, Moore DT, et al. Phenotypic evaluation of the basal-like subtype of invasive breast carcinoma. Mod Pathol. 2006;19(2):264–71.
14. Stingl J, Caldas C. Molecular heterogeneity of breast carcinomas and the cancer stem cell hypothesis. Nat Rev Cancer. 2007;7(10):791–9.
15. Thike AA, Cheok PY, Jara-Lazro AR, Tan B, Tan P, et al. Triple-negative breast cancer: clinicopathological characteristics and relationship with basal-like breast cancer. Mod Pathol. 2010;23(1):123–33.
16. Lehmann BD, Jovanović B, Chen X, Estrada MV, Johnson KN, Shyr Y, et al. Refinement of triple-negative breast cancer molecular subtypes: implications for neoadjuvant chemotherapy selection. PLoS One. 2016;11(6):e0157368.

17. Wimberly H, Brown JR, Schlper K, Haack H, Silver MR, et al. PD-L1 expression correlates with tumor-infiltrating lymphocytes and response to neoadjuvant chemotherapy in breast cancer. Cancer Immunol Res. 2015;3(4):326–32.
18. Schmid P, Adams S, Rugo HS, Schneeweiss A, et al. Atezolizumab and Nab-Pacltaxel in advanced triple-negative breast cancer. N Engl J Med. 2018;379:2108–21.
19. Kandoth C, McLellan MD, Vandin F, Ye K, Niu B, Lu C, et al. Mutational landscape and significance across 12 major cancer types. Nature. 2013;502(7471):333–9.
20. Tian T, Shan L, Yang W, Zhou X, Shui R. Evaluation of the BRCAness phenotype and its correlation with clinicopathological features in triple-negative breast cancers. Hum Pathol. 2019;84:231–8.
21. Gross E, van Tinteren H, Li Z, Raab S, Meul C, Avril S, et al. Identification of BRCA1-like triple-negative breast cancers by quantitative multiplex-ligation-dependent probe amplification (MLPA) analysis of BRCA1-associated chromosomal regions: a validation study. BMC Cancer. 2016;16(1):811.
22. Fernandes RCM, Bevilacqua JLB, Soares IC, Siqueira SAC, Pires L, et al. Coordinated expression of ER, PR and HER2 define different prognostic subtypes among poorly differentiated breast carcinomas. Histopathology. 2009;55(3):346–52.
23. Loi S, Haibe-Kains B, Desmedt C, Lallemand F, Tutt AM, Gillet C, et al. Definition of clinically distinct molecular subtypes in estrogen receptor-positive breast carcinomas through genomic grade. J Clin Oncol. 2007;25(10):1239–46.
24. Allison KH, Hammond MEH, Dowsett M, McKernin SE, Carey AL, et al. Estrogen and progesterone receptor testing in breast cancer: ASCO/CAP guideline update. J Clin Oncol. 2020;38(12):1246–66.
25. Dieci MV, Orvieto E, Dominici M, Conte P, Guarneri V. Rare breast cancer subtypes: histological, molecular, and clinical peculiarities. Oncologist. 2014;19(8):805–13.
26. Goldhirsch A, Winer EP, Coates AS, Gelber RD, Piccart-Gebhart M, Thürlimann B, et al. Personalizing the treatment of women with early breast cancer: highlights of the St Gallen International Expert Consensus on the primary therapy of early breast cancer 2013. Ann Oncol. 2013;24:2206–23.
27. Sparano JA, Gray RJ, Makower DF, Pritchard KI, Albain KS, Hayes DF, et al. Adjuvant chemotherapy guided by a 21-gene expression assay in breast cancer. N Engl J Med. 2018;379(2):111–21.
28. Cardoso F, van't Veer LJ, Bogaerts J, Slaets L, Viale G, Delaloge S, et al. MINDACT Investigators. 70-gene signature as an aid to treatment decisions in early-stage breast cancer. N Engl J Med. 2016;375(8):717–29.
29. Chen R, Qarmali M, Siegal GP, Wei S. Receptor conversion in metastatic breast cancer: analysis of 390 cases from a single institution. Modern Pathol. 2020;33:2499–506.
30. Toy W, Shen Y, Won H, Green B, Sakr RA. ESR1 ligand-binding domain mutations in hormone-resistant breast cancer. Nat Genet. 2013;45:1439–45.
31. Aftimos P Jr, AAAJ, Sotiriou C. Tumours of the breast. In: Coleman WB, Tsongalis GJ, editors. Molecular pathology – the molecular basis of human disease. Academic Press; 2017. p. 583.
32. Andre F, Ciruelos E, Rubovszky G, Campone M, Loibl S, et al. Alpelisib for PIK3CA-mutated, hormone receptor–positive advanced breast cancer. N Engl J Med. 2019;380(20):1929–40.
33. Choi YJ, Anders L. Signaling through cyclin D-dependent kinases. Oncogene. 2014;33:1890–903.
34. Konecny G, Pauletti G, Pegram M, Untch M, Dandekar S, Aguilar Z, et al. Quantitative association between HER-2/neu and steroid hormone receptors in hormone receptor-positive primary breast cancer. J Natl Cancer Inst. 2003;95(2):142–53.
35. Ellis MJ. Neoadjuvant endocrine therapy for breast cancer: medical perspectives. Clin Cancer Res. 2001;7(12 Suppl):4388s–4391s.
36. Villman K, Sjostrom J, Heikkila R, Hultborn R, Malmstrom P, Bengtsson NO, et al. TOP2A and HER2 gene amplification as predictors of response to anthracycline treatment in breast cancer. Acta Oncol. 2006;45(5):590–6.

37. Godoy-Ortiz A, Sanchez-Munoz A, Parrado MRC, Alvarez M, Ribelles N, et al. Deciphering HER2 breast cancer disease: biological and clinical implications. Front Oncol. 2019;9:1124.
38. Turashvili G, Brogi E. Tumor heterogeneity in breast cancer. Front Med. 2017;4:article 227.
39. Griguolo G, Pascual T, Dierci MV, et al. Interaction of host immunity with HER2-targeted treatment and tumor heterogeneity in HER2-positive breast cancer. J Immunother Cancer. 2019;7:90.
40. Hou Y, Nitta H, Wei L, Banks PM, Portier B, et al. Her2 intratumoral heterogeneity is independently associated with incomplete response to anti-her2 neoadjuvant chemotherapy in HER2-positive breast carcinoma. Breast Cancer Res Treat. 2017;166:447–57.
41. Schettini F, Pascual T, Conte B, Chic N, Braso-Maristany F, et al. Her2-enriched subtype and pathological complete response in HER2-positive breast cancer: a systematic review and meta-analysis. Cancer Treat Rev. 2020;84:101965.
42. Pusztai L. Molecular predictors of response to neoadjuvant Her2 targeted therapies. ASCO Meeting, 2020.

Chapter 2
Risk Factors for Breast Cancer

Sergio Masili-Oku, Angela Trinconi, Gabriela Boufelli, and Jose Roberto Filassi

2.1 Introduction

Breast cancer is the second most common malignancy globally after lung cancer and the most frequent cancer among women.

About 2 million new cases of cancer occur each year. In 2020, there were 2,261,419 new cases and 684,996 deaths due to breast cancer worldwide [1, 2]. The incidence of breast cancer has been increasing in recent decades. In Brazil, the estimate for the year 2020 is 66,280 new cases, with 16,927 deaths [3]. Due to its significant incidence and prevalence, it is important to understand the risk factors for its development and what can be done to reduce the risk of acquiring it.

Studies in the literature show that about 10% of breast cancer cases are related to hereditary genetic mutations, while the other 90% occur randomly. Risk factors can be related to age, sex, and reproductive cycle. There are also behavioral factors. Other factors, such as precursor lesions and genetic mutations, must be evaluated.

2.2 Gender and Age

Breast cancer mainly affects women after 50 years old. Its incidence ranges from 14.5 to 55.6 (ASR-age standardized rate) per 100,000 women in Africa to 84.9 (ASR) per 100,000 in Brazil, 62.9 (ASR) per 100,000 in the United States, 93.6 (ASR) per 100,000 in the United Kingdom, and 99.1 (ASR) per 100,000 in France.

S. Masili-Oku (✉) · A. Trinconi · G. Boufelli · J. R. Filassi
Departamento de Mastologia, Instituto do Cancer do Estado de Sao Paulo ICESP, São Paulo, SP, Brazil
e-mail: sergio.masili@fm.usp.br; angela.trinconi@ambc.com.br; drfilassi@terra.com.br

S. J. Kim Hsieh, E. A. Morris (eds.), *Modern Breast Cancer Imaging*,
https://doi.org/10.1007/978-3-030-84546-9_2

The male sex corresponds to only 1% of cases, with one man per 100,000 standard population. When it affects men, they are generally older and may present some hormonal alteration, or it may be related to the BRCA2 gene mutation [4].

Regarding age, the incidence of breast cancer is higher among women after menopause. In the United States, about 77% of cases occur in women after 50 years of age, and the average age at diagnosis is 62 years old [5, 6]. In the United Kingdom, between 2015 and 2017, about 85% of cases were diagnosed in women over 50 years old [7]. Therefore, the population at the most significant risk for breast cancer are women over 50 years old, usually after menopause. They must undergo screening with annual or biannual mammograms according to each country's program [1, 8].

2.3 Reproductive Factors

Early menarche, nulliparity, and late pregnancy are risk factors for the development of breast cancer. In the literature, studies show a relationship between these factors and the appearance of positive hormone receptor breast cancer, which is not related to negative hormone receptor breast cancer. Probably the longer exposure time of the breast tissue to the hormonal action, such as estrogen and progesterone, the greater the likelihood of the appearance of breast neoplasms [9]. Thakur and collaborators [10] carried out a case-control study, which included 377 women with breast cancer and 346 controls. In this study, early menarche (<12 years) increased the risk for breast cancer by up to two times (odds ratio (OR) = 2.83, 95% confidence interval (CI) = 1.02–7.86); the same was found for late menopause (>50 years) (OR = 2.43, 95% CI = 1.2–4.9).

Huo and collaborators [11] also sought to assess menarche's influence on the onset of breast cancer. They carried out a case-control study, evaluating 819 patients with breast cancer and 569 controls, and found that for every 2 years of delay in menarche, there was a reduction in 7% risk of developing breast cancer.

2.4 Gestation and Lactation

Pregnancy and lactation are considered protective factors against developing breast cancer, and the age of the pregnancy and the duration of lactation are responsible for providing this protection. Ma and collaborators [12] evaluated that pregnancy decreases the risk of developing breast cancer by 11%. Still, it presents itself as a protective factor when it occurs before the age of 30 and can be a risk factor when it occurs at a late age. Women who became pregnant after the age of 30 were 27% more likely to have hormonal positive breast cancer than the patients who became pregnant before the age of 30. This difference is probably due to the breast's maturation stages, as it completes its embryological development with pregnancy. The

sooner this occurs, the less the chance of cellular changes that can be stimulated by the hormonal action of pregnancy, leading to the onset of neoplasms [13]. Thakur et al. [10], in a case-control study, found a risk of up to six times greater than having breast cancer when pregnancy occurs at an older age (>30 years) (OR = 6.34, 95% CI = 2.04–27).

A meta-analysis carried out by the collaborative group on hormonal factors of the breast [14] evaluated the impact of pregnancy on breast cancer; forty-seven studies were carried out, were conducted in 30 countries, and compared 12,214 nulligravid women with 16,900 women who had children but did not breastfeed. The result found that the earlier the pregnancy occurred, the lower the relative risk of developing breast cancer. The risk of developing breast cancer decreases by 7% with each delivery, demonstrating that pregnancy is a protective factor against the onset of breast cancer.

The practice of breastfeeding is a protective factor for breast cancer development, but there is still no consensus on the ideal breastfeeding time for its prevention [12, 15]. Huo and collaborators [11] found that every 12 months, lactation reduces the risk of developing breast cancer by 7%. A meta-analysis carried out by the collaborative group on hormonal factors of the breast [14] also identified breastfeeding as a protective factor. Every 12 months of breastfeeding, there is a decrease in the relative risk estimated at 4.5%.

2.5 Contraception and Hormone Replacement Therapy

Studies in the literature that have assessed the influence of hormonal contraceptives on breast cancer have shown variable findings ranging from no increased risk to a relative risk of 9.5, thus being a controversial subject [4, 16].

Marshbanks and collaborators [16] conducted a case-control study, evaluating 2282 women with breast cancer and 2424 women without breast cancer, and found no association between the use of hormonal contraceptives and an increased risk of developing breast cancer.

Mørch and collaborators [17], seeking a more recent analysis on the use of hormonal contraceptives and their relationship with breast cancer, conducted a cohort study evaluating approximately 1.8 million women between 15 and 49 years old, who were followed up by about 10.9 years. In this period, there were 11,517 cases of breast cancer. The relative risk found for women who used contraceptives compared to women who never used them was 1.20 (95% CI, 1.14–1.26). The risk increased from 1.09 (95% CI, 0.96–1.23) in women with less than 1 year of use to 1.38 (95% CI, 1.26–1.51) in women over 10 years of using hormonal contraceptives. The absolute risk for using hormonal contraceptives was 13 (95% CI, 10–16) per 100,000 women-years or approximately one extra breast cancer case for every 7690 women using hormonal contraceptives for 1 year. Therefore, the use of hormonal contraceptives should be discussed with the patient, individualizing personal risk factors and deciding with her the use thereof.

Regarding hormone replacement therapy, the Women's Health Initiative (WHI) randomized clinical trial evaluated 16,608 postmenopausal women aged 50–79.

With an intact uterus, one arm of 8506 women that received 0,625 mg of conjugated equine estrogen and 2.5 mg of medroxyprogesterone acetate daily was compared with the placebo group of 8102 women. A second arm of the study evaluated 10,739 hysterectomized women who received conjugated equine estrogen alone versus the group that received the placebo. The first arm of the study was designed for 8.5 years and was discontinued in 2002 (about 5.2 years) due to an increased risk of breast cancer (HR 1.26) [18]. The second arm was stopped in 2004 due to increased number of ischemic strokes (HR, 1.39; 1.10–1.77) [19]. In 2010, an analysis of the subgroups was carried out after discontinuation of hormone replacement therapy, and this analysis showed that in hysterectomized patients, the use of isolated estrogen (used for an average of 7.2 years) was a protective factor against the appearance of breast cancer with HR 0.79 (0.65–0.97) [20], raising the hypothesis that progesterone is more related to the risk of developing breast cancer.

Also, seeking to correlate the use of hormonal therapy (HT) with breast cancer, the Collaborative Group on Hormonal Factors of the Breast carried out a meta-analysis [21] comparing HT and breast cancer development. Fifty-three thousand eight hundred sixty-five women were evaluated, and 17,830 of them used hormone therapy (HT). The meta-analysis demonstrated a relative risk of 1.35 (1.21–1.49; $2p = 0.00001$) for women who used TH for more than 5 years. The risk increased with each year of using HT and returned to baseline 5 years after the end of treatment, associating HT as a risk factor for breast cancer development. Hormone therapy, then, is a risk factor for breast cancer development and should be used according to each patient's individual needs.

2.6 Obesity

Obesity has been described as a risk factor for the development of breast cancer. Adipose tissue is an androgen producer and allows more significant hormonal action in the breasts through their peripheral conversion [9].

Obesity is a risk factor for breast cancer in postmenopausal women. Kabat and collaborators [22] evaluated obesity and metabolic syndrome as a risk factor for breast cancer. An arm of the WHI study included 20,944 women with obesity and metabolic syndrome. Blood glucose, triglycerides, HDL-cholesterol, blood pressure, waist circumference, and body mass index (BMI) measurements were evaluated. Women were classified according to their BMI (18.5–<25.0, normal weight; 25.0–<30.0, overweight; and ≥30.0 kg/m2, obese) and the presence of metabolic syndrome (≥3 of the following: waist circumference ≥88 cm, triglycerides ≥150 mg/dL, HDL-C <50 mg/dL, glucose ≥100 mg/dL, and systolic/diastolic blood pressure ≥130/85 mmHg or treatment for hypertension), yielding six groups: metabolically healthy/normal weight (MHNW), metabolically unhealthy/normal weight (MUNW), metabolically healthy/overweight (MHOW), metabolically

unhealthy/overweight (MUOW), metabolically healthy/ obese (MHO), and metabolically unhealthy/ obese (MUO). These women were followed for 15 years, and during this period, 1176 cases of invasive breast cancer were diagnosed. Obesity, regardless of the metabolic part, has been associated with an increased risk of breast cancer. Being obese and metabolically unhealthy was associated with a higher risk: HR, 1.62 (95% CI, 1.33–1.96). These associations were strongest in women who had never used hormone therapy. This study demonstrates that both obesity and the metabolic part are related to the increase in breast cancer. These factors are modifiable with lifestyle changes, adequate diet, physical activity, and appropriate drug treatment, decreasing the patient's risk of breast cancer.

2.7 Alcohol and Smoking

Alcohol consumption and smoking are associated with the development of breast cancer. The greater the consumption before pregnancy, the greater the risk [4]. Park and collaborators [23] evaluated 85,089 women and alcohol consumption in a cohort with women from different ethnicities in Hawaii and California, with an average follow-up of 12.4 years. During this time, 3885 cases of breast cancer were identified. The hazard ratios (HRs) found demonstrated that alcohol consumption increases the risk of developing breast cancer compared to not consuming it. The HRs were 1.23 (95% CI, 1.06–1.42), 1.21 (95% CI, 1.00–1.45), 1.12 (95% CI, 0.95–1.31), and 1.53 (95% CI, 1.32–1.77) for 5–9.9, 10–14.9, 15–29.9, and ≥30 g/day of alcohol consumption, respectively.

A cohort between 1899 and 1975 with 302,865 Norwegian women evaluated the effect of smoking on cancer and concluded that women who smoked had a 15% increased risk of having breast cancer (HR = 1.15; 95% CI, 1.10–1.21) [24].

2.8 Thoracic Radiation Therapy

Chest radiotherapy performed to treat Hodgkin's disease increases the risk of developing breast cancer. Studies have shown that this risk is greater the younger the woman is when undergoing chest radiotherapy. The relative risk for developing breast cancer for women who received chest radiotherapy between the ages of 15 and 19 is 30.7; between 20 and 24 years, the RR is 14.0; between 25 and 29 years old, the RR is 5.5, and between 30 and 35 years old, the RR is 5.3. Thoracic radiotherapy after age 35 does not seem to increase this risk [25].

The risk of developing breast cancer is also related to the time that elapses after the end of chest radiotherapy. The RR is 2.9 after 5 years of the end of irradiation; the peak is after 15 to 19 years when this risk reaches an RR of 11.1, and after 20 to 25 years, there is a drop to an RR of 8.0 [25].

Wolden and collaborators [26] evaluated 71 cases of breast cancer in 65 women who had Hodgkin's lymphoma. The average age for diagnosis of lymphoma was 24.6 years, and the average age for breast cancer diagnosis was 42.6 years. The relative risk for developing invasive breast cancer was 4.7 (95% CI, 3.4–6.0).

Cutuli and collaborators [27] also identified a relationship between exposure to chest radiotherapy and breast cancer onset. When evaluating 117 women and two men who had been treated for Hodgkin's lymphoma, they found 133 diagnoses of breast cancer, with less than 5% of the cancer cases appearing before 5 years after the end of treatment and 27.8% of the patients between 11 and 15 years of therapy and 30% after 20 years of treatment.

2.9 Precursor Injuries

The proliferative intraductal lesions usually have their origin in the terminal duct lobular unit. They are composed of a heterogeneous group of lesions concerning cytology and architecture. Their presence confers an increased risk of developing an invasive lesion. The usual ductal hyperplasia, atypical hyperplasia, ductal carcinoma in situ, columnar cell lesion, columnar cell lesion with atypia, lobular carcinoma in situ, and flat epithelial atypia are part of this group. Since the increase in risk for breast cancer is 1.5 times in the presence of usual ductal hyperplasia, this rises to four to five times in ductal hyperplasia with atypia/columnar cell lesion with atypia and eight to ten times in ductal carcinoma in situ/lobular carcinoma in situ [28].

Atypical hyperplasia corresponds to a monotonous proliferation of epithelial cells inside the mammary duct. Without breaching through the myoepithelial layer, it does not compromise two consecutive mammary ducts and measures less than 2 mm. In terms of cytological characteristics, it is similar to low-grade ductal carcinoma in situ. It is classified when atypical cells affect two consecutive whole ducts and are present in an extension of 2 mm or more.

Columnar cell lesion with atypia is characterized by the proliferation of monotonous, noncohesive cells that fill the mammary duct and compromise less than 50% of the acini. In contrast, lobular carcinoma in situ is formed by these same cellular changes that occupy more than 50% of acini [28, 29].

The greater access to breast screening programs and the more significant number of mammograms performed have increased the diagnosis of atypia in percutaneous biopsies performed for detected masses and microcalcifications found in imaging exams. The presence of atypia in a breast biopsy, besides representing a greater risk for this patient to develop breast cancer, implies the need for surgical excision for the total removal of the lesion, since the percutaneous biopsy may underestimate the presence of an invasive lesion in 15% to 30% [29].

As for the flat epithelial atypia (FEA), few data establish its risk for breast cancer development as it is a rare finding. A study conducted by the Mayo Clinic [30] evaluating 11,591 women with benign breast biopsies found 282 biopsies with

FEA. Of these, 130 were associated with atypical hyperplasia (AH) (46%), and the others were associated with proliferative disease without atypia (PDWA). These patients were followed for an average of 16.8 years. The standardized incidence ratios (SIRs) were the following: SIR for breast cancer in women with AH + FEA was 4.74 (95% confidence interval [95% CI], 3.17–6.81) versus 4.23 (95% CI, 3.44–5.13) for AH without FEA ($P = 0.59$). SIR for PDWA + FEA was 2.04 (95% CI, 1.23–3.19) versus 1.90 (95% CI, 1.72–2.09) for patients with PDWA without FEA ($P = 0.76$), so the risk of developing breast cancer was mainly attributed to the presence of other hyperplasias with atypia rather than the presence of flat epithelial atypia itself.

In the literature, there is a conundrum about the evolution of a precursor lesion to an invasive breast cancer. It is known that breast cancer's natural course does not always follow this order: usual hyperplasia, atypical hyperplasia, ductal carcinoma in situ, and then to an invasive ductal carcinoma. Some studies demonstrate a more complex path, which does not follow these steps for the development of an invasive breast cancer. To et al. [31] followed 146 women for 25 years, 111 with ductal carcinoma in situ (DCIS) and 35 with lobular carcinoma in situ (LCIS). Among these, 26 (19 from the DCIS group and seven from LCIS) developed invasive breast cancer (17.8%), and 12 died of invasive cancer (8.2%). The average time for the diagnosis of invasive cancer was 6.3 years. The probability of progressing to invasive breast cancer was 10.0% in 5 years, 13.7% in 10 years, 17.6% in 15 years, and 19.7% in 20 years. Although 20% were related to the appearance of invasive cancer, in the other 80%, this relationship was not clear, allowing the discussion that not all in situ cancers evolve to invasive ones.

2.10 Hereditary Syndromes and Breast Cancer

Familial breast cancer is responsible for 5% to 10% of all breast cancers. Most of these cases may be associated with mutations in the BRCA1 or BRCA2 genes [32].

The lifetime risk of developing breast cancer for a woman is approximately 12.9%. That is, one in eight women will be diagnosed with breast cancer at some point in their lives, leading to the estimated prevalence of 3,577,264 women living with breast cancer in the United States in 2017 [33].

Several factors suggest a genetic contribution to breast cancer, such as [34]:

1. Increased incidence among individuals with a family history of these cancers
2. Several family members affected by these and other types of cancer
3. A cancer pattern compatible with autosomal dominant inheritance

Didactically, we can classify cancer cases [35]:

(a) Sporadic: when there are no cases of the same type of cancer in two generations, that is, brothers, children, parents, aunts, and uncles, and both pairs of unaffected grandparents.

(b) Familial: when there are two or more second-degree relatives with breast cancer, regardless of age, bilaterality, or other associated cancers. It corresponds to about 25% of the total diagnoses. Its etiology is multifactorial or random.
(c) Hereditary: its genealogy leads us to think of an autosomal dominant distribution characterized by early age onset, a more significant number of cases with bilaterality, and multiple primary cancers. It corresponds to about 10% of the total cases.

2.11 Genes and Associated Syndromes

Breast and ovarian cancers are present in several autosomal dominant cancer syndromes, although they are more strongly associated with highly penetrating pathogenic variants in BRCA1 and BRCA2. Other genes, such as PALB2, TP53 (associated with Li-Fraumeni syndrome), PTEN (associated with Cowden syndrome), CDH1 (associated with diffuse gastric and lobular cancer syndrome), and STK11 (associated with Peutz-Jeghers syndrome), confer risk for one or both cancers with relatively high penetrance [34].

2.11.1 Genes Associated with High Penetrance

(a) TP53

Mutations involving p53 are inherited in an autosomal dominant manner, which results in a familial predisposition to various cancers, with an estimated risk of breast cancer of around 49% at 60 years old and, according to several studies, a large percentage of diagnoses in young people (about 30 years old). It is associated with sarcomas, tumors of the central nervous system, leukemia, and adrenocortical carcinoma.

(b) STK11

Characterized by mutations in the serine-threonine kinase STK11, Peutz-Jeghers syndrome manifests itself by the appearance of hamartomas (perioral, hands, and genitals) and polyps in the gastrointestinal tract, in addition to malignant tumors, including uterus, ovary, and breast (relative risk, 15 times higher than the general population) [36].

(c) PTEN

Mutations in the tumor suppressor gene PTEN constitute an autosomal dominant inheritance known as Cowden syndrome, which is characterized by the development of multiple hamartomas on the skin and mucous membranes and an increased risk of developing thyroid, kidney, endometrial, and breast cancer (estimated risk of 85%) [37].

(d) BRCA

BRCA is a tumor suppressor gene responsible for maintaining the integrity of the genome since it makes possible the recombination of homologous bases of DNA, repairs the breakdown of the double helix, and controls DNA damage in the S phase [38].

A recent study [39] estimated that about 72% of women who inherit a harmful BRCA1 mutation and about 69% of women who inherit a harmful BRCA2 mutation would develop breast cancer at the age of 80 years old.

It is estimated that in 20 years after the first diagnosis of breast cancer, about 40% of women who inherit a BRCA1 mutation and about 26% of women who inherit a BRCA2 mutation will manifest cancer in their contralateral breast.

About 1.3% of women in the general population will develop ovarian cancer at some point in their lives. On the other hand, it is estimated that approximately 44% of women who inherit a deleterious BRCA1 mutation and about 17% of women who inherit a BRCA2 mutation will develop ovarian cancer at 80 years old [40].

The BRCA mutation increases the risk for several other types of cancer, including fallopian tube cancer and peritoneal cancer. Men with BRCA2 mutations are at increased risk of breast and prostate cancer. Men and women with BRCA mutations are at increased risk of pancreatic cancer [40].

Ashkenazi Jewish ancestry and Norwegian, Dutch, and Icelandic people have a higher prevalence of deleterious BRCA1 and BRCA2 mutations than people in the general population.

2.11.2 Genes Associated with Moderate Penetrance

(a) CHEK2

CHEK2 gene is a member of the Fanconi anemia (FA)-BRCA pathway and is involved in both the checkpoint function and repair mediated by BRCA1 and p53. CHEK * 1100delC mutations are associated with a three- to fivefold increase in breast cancer. The cumulative risk of breast cancer at the age of 70 years old among CHEK * 1100delC heterozygotes reaches 37% [41].

(b) PALB2

PALB2 is another gene on the FA-BRCA pathway. It encodes a protein that binds closely to BRCA2, stabilizing it and allowing it to perform its repairing functions. This interaction is essential for tumor suppression by BRCA2. Germline mutations in PALB2 increase the chance of early-onset breast cancer, with a five- to ninefold elevated risk. Unlike BRCA mutations, patients with a PALB2 mutation do not experience a statistically significant increase in ovarian cancer.

(c) ATM

Mutations in the ATM gene result in ataxia-telangiectasia, an autosomal recessive neurodegenerative disease that causes cerebellar dysfunction and a weakened immune response.

ATM protein is an essential kinase of the cell cycle within the FA-BRCA pathway and, among its functions, phosphoryl BRCA1. Studies have shown that patients with the ATM mutation have a breast cancer risk of approximately 2.37 [41].

2.12 Quantification of Mutation Risk

Risk assessment models have been developed to clarify the lifetime risk of developing breast cancer and the likelihood of having a pathogenic variant in BRCA1 or BRCA2 (3). When this risk is greater than or equal to 10%, conducting genetic testing should be suggested.

Among these risk calculators, we can mentio Claus and Gail's models, which estimate cancer-based risk only on personal and family characteristics.

To assess the probability of BRCA mutation, BRCAPRO, Penn II, Tyrer-Cuzick model, and BOADICEA can be utilized.

2.13 Genetic Testing for High-Risk Patients

The BRCA mutation analysis can range from direct, including only a specific mutation in BRCA1 or BRCA2 (single site analysis), to more complete tests that include sequencing of the entire gene [41].

Given the number of genes associated with an increased risk of breast cancer, several genes' massive sequencing may be available. Such an option may be of interest in patients whose family history is not very informative, that is, a restricted or unknown family structure (for instance, in case of adoption).

The strategy is to offer the broadest genetic test to the family member affected by the neoplasia and the guided analysis for the mutation then defined to the other family members.

Possible results for genetic tests are:

(a) True positive: the identified mutation is associated with an increased risk of cancer.
(b) True negative: no mutation is identified in an individual from a family known to have a mutation.
(c) Meaningless: no mutation is identified in an individual whose family also has no mutations.
(d) Uncertain meaning: a mutation has been identified; however, its clinical significance is unknown at the moment.

According to genetic diagnoses, the National Comprehensive Cancer Network (NCCN) guides the best practices for follow-up exams [42]. In general, the orientation is self-knowledge of the breasts from 18 years of age.

For women with BRCA mutation, the following are suggested:

- From 25 to 29 years old: screening with annual magnetic resonance imaging (MRI).
- From 30 to 75 years old: screening with mammography (MG) and annual MRI.
- Over 75 years old: assess individual life expectancy.
- If there is previously treated breast cancer: annual MG and MRI.
- Risk-reducing breast surgery is based on awareness and discussion of risk reduction.
- Bilateral salpingo-oophorectomy: for mutated BRCA1, it is most suitable between 35 and 40 years old or if she has constituted offspring. For BRCA2, surgery will be better indicated between 40 and 45 years old.

For men with BRCA mutation, the following are suggested:

- Annual self-examination and clinical breast examination from the age of 35 years old
- Annual MG if gynecomastia from 50 years old or 10 years before the youngest affected family member
- From the age of 40 years old, prostatic evaluation, particularly for those with the BRCA2 mutation

The other mutations mentioned above follow approximately the same scheme, varying the initial period for starting breast screening tests and other associated neoplasms.

Understanding genetic syndromes and their genes are essential to identify patients subject to more intense surveillance.

BRCA1 and BRCA2 gene mutations correspond to the majority of hereditary breast cancers. Identifying the high-risk patient is essential through a complete family history and adequate identification of the patients who must undergo genetic counseling for subsequent genetic testing.

References

1. Ferlay J, Colombet M, Soerjomataram I, Mathers C, Parkin DM, Piñeros M, et al. Estimating the global cancer incidence and mortality in 2018: GLOBOCAN sources and methods. Int J Cancer. 2019;144(8):1941–53.
2. Sung H, Ferlay J, Siegel RL, Laversanne M, et al. Global Cancer statistics 2020: GLOBOCAN estimates of incidence and mortality worldwide for 36 cancers in 185 countries. CA Cancer J Clin. 2021;0:1–41.
3. INCA INdC-. Câncer de mama 2020. Available at: https://www.inca.gov.br/tipos-de-cancer/cancer-de-mama.

4. Momenimovahed Z, Salehiniya H. Epidemiological characteristics of and risk factors for breast cancer in the world. Breast Cancer (Dove Med Press). 2019;11:151–64.
5. Tamimi RM, Spiegelman D, Smith-Warner SA, Wang M, Pazaris M, Willett WC, et al. Population attributable risk of modifiable and nonmodifiable breast cancer risk factors in postmenopausal breast cancer. Am J Epidemiol. 2016;184(12):884–93.
6. DeSantis C, Ma J, Bryan L, Jemal A. Breast cancer statistics, 2013. CA Cancer J Clin. 2014;64(1):52–62.
7. UK CR. Breast cancer risk Internet 2020. Available at: https://www.cancerresearchuk.org/health-professional/cancerstatistics/statistics-by-cancer-type/breast-cancer/incidence-invasive#heading-One.
8. Smart CR, Hendrick RE, Rutledge JH, Smith RA. Benefit of mammography screening in women ages 40 to 49 years. Current evidence from randomized controlled trials. Cancer. 1995;75(7):1619–26.
9. Althuis MD, Fergenbaum JH, Garcia-Closas M, Brinton LA, Madigan MP, Sherman ME. Etiology of hormone receptor-defined breast cancer: a systematic review of the literature. Cancer Epidemiol Biomark Prev. 2004;13(10):1558–68.
10. Thakur P, Seam RK, Gupta MK, Gupta M, Sharma M, Fotedar V. Breast cancer risk factor evaluation in a Western Himalayan state: a case-control study and comparison with the Western World. South Asian J Cancer. 2017;6(3):106–9.
11. Huo D, Adebamowo CA, Ogundiran TO, Akang EE, Campbell O, Adenipekun A, et al. Parity and breastfeeding are protective against breast cancer in Nigerian women. Br J Cancer. 2008;98(5):992–6.
12. Ma H, Bernstein L, Pike MC, Ursin G. Reproductive factors and breast cancer risk according to joint estrogen and progesterone receptor status: a meta-analysis of epidemiological studies. Breast Cancer Res. 2006;8(4):R43.
13. Aleitamento Materno MdO. 2006. Available at: https://www.febrasgo.org.br/images/arquivos/manuais/Manuais_Novos/aleitamento_.pdf.
14. Cancer CGoHFiB. Breast cancer and breastfeeding: collaborative reanalysis of individual data from 47 epidemiological studies in 30 countries, including 50302 women with breast cancer and 96973 women without the disease. Lancet. 2002;360(9328):187–95.
15. Wiseman M. The second World Cancer Research Fund/American Institute for Cancer Research expert report. Food, nutrition, physical activity, and the prevention of cancer: a global perspective. Proc Nutr Soc. 2008;67(3):253–6.
16. Marchbanks PA, Curtis KM, Mandel MG, Wilson HG, Jeng G, Folger SG, et al. Oral contraceptive formulation and risk of breast cancer. Contraception. 2012;85(4):342–50.
17. Mørch LS, Skovlund CW, Hannaford PC, Iversen L, Fielding S, Lidegaard Ø. Contemporary hormonal contraception and the risk of breast cancer. N Engl J Med. 2017;377(23):2228–39.
18. Rossouw JE, Anderson GL, Prentice RL, LaCroix AZ, Kooperberg C, Stefanick ML, et al. Risks and benefits of estrogen plus progestin in healthy postmenopausal women: principal results from the Women's Health Initiative randomized controlled trial. JAMA. 2002;288(3):321–33.
19. Anderson GL, Limacher M, Assaf AR, Bassford T, Beresford SA, Black H, et al. Effects of conjugated equine estrogen in postmenopausal women with hysterectomy: the Women's Health Initiative randomized controlled trial. JAMA. 2004;291(14):1701–12.
20. Manson JE, Chlebowski RT, Stefanick ML, Aragaki AK, Rossouw JE, Prentice RL, et al. Menopausal hormone therapy and health outcomes during the intervention and extended poststopping phases of the Women's Health Initiative randomized trials. JAMA. 2013;310(13):1353–68.
21. Collaborative Group on Hormonal Factors in Breast Cancer. Breast cancer and hormone replacement therapy: collaborative reanalysis of data from 51 epidemiological studies of 52,705 women with breast cancer and 108,411 women without breast cancer. Lancet. 1997;350(9084):1047–59.

22. Kabat GC, Kim MY, Lee JS, Ho GY, Going SB, Beebe-Dimmer J, et al. Metabolic obesity phenotypes and risk of breast cancer in postmenopausal women. Cancer Epidemiol Biomark Prev. 2017;26(12):1730–5.
23. Park SY, Kolonel LN, Lim U, White KK, Henderson BE, Wilkens LR. Alcohol consumption and breast cancer risk among women from five ethnic groups with light to moderate intakes: the Multiethnic Cohort Study. Int J Cancer. 2014;134(6):1504–10.
24. Bjerkaas E, Parajuli R, Weiderpass E, Engeland A, Maskarinec G, Selmer R, et al. Smoking duration before first childbirth: an emerging risk factor for breast cancer? Results from 302,865 Norwegian women. Cancer Causes Control. 2013;24(7):1347–56.
25. Bloom JR, Stewart SL, Hancock SL. Breast cancer screening in women surviving Hodgkin disease. Am J Clin Oncol. 2006;29(3):258–66.
26. Wolden SL, Hancock SL, Carlson RW, Goffinet DR, Jeffrey SS, Hoppe RT. Management of breast cancer after Hodgkin's disease. J Clin Oncol. 2000;18(4):765–72.
27. Cutuli B, Borel C, Dhermain F, Magrini SM, Wasserman TH, Bogart JA, et al. Breast cancer occurred after treatment for Hodgkin's disease: analysis of 133 cases. Radiother Oncol. 2001;59(3):247–55.
28. Board WCoTE. Breast Tumours. Lyon: International Agency for Research on Cancer; 2019.
29. Hartmann LC, Degnim AC, Santen RJ, Dupont WD, Ghosh K. Atypical hyperplasia of the breast--risk assessment and management options. N Engl J Med. 2015;372(1):78–89.
30. Said SM, Visscher DW, Nassar A, Frank RD, Vierkant RA, Frost MH, et al. Flat epithelial atypia and risk of breast cancer: a Mayo cohort study. Cancer. 2015;121(10):1548–55.
31. To T, Wall C, Baines CJ, Miller AB. Is carcinoma in situ a precursor lesion of invasive breast cancer? Int J Cancer. 2014;135(7):1646–52.
32. Ford D, Easton DF, Stratton M, et al. Genetic heterogeneity and penetrance analysis of the BRCA1 and BRCA2 genes in breast cancer families. Am J Hum Genet. 1998;62:676–89.
33. Female breast cancer — cancer stat facts. Available at: https://seer.cancer.gov/statfacts/html/breast.html. Accessed on 30/09/2020.
34. Genetics of Breast and Gynecologic Cancers (PDQ®)–Health professional version https://www.cancer.gov/types/breast/hp/breast-ovarian-genetics-pdq.
35. Lynch HT, Watson P, Lynch JF. Epidemiology and risk factors. Clin Obstet Gynecol. 1989;32(4):750–60.
36. Giardiello FM, Brensinger JD, Tersmette AC, Goodman SN, et al. Very high risk of cancer in familial Peutz–Jeghers syndrome. Gastroenterology. 2000;119(6):1447–53.
37. Tan MH, Mester JL, Ngeow J, Rybicki LA, et al. Lifetime cancer risks in individuals with Germline PTEN mutations. Clin Cancer Res. 2012;18(2):400–7.
38. De GrèveJ, Sermijn E, Brakeleer SD, et al. Hereditary breast cancer from bench to bedside. Curr Opin Oncol. 2008;20:605–13.
39. Kuchenbaecker KB, Hopper JL, Barnes DR, et al. Risks of breast, ovarian, and contralateral breast cancer for BRCA1 and BRCA2 mutation carriers. JAMA. 2017;317(23):2402–16.
40. BRCA mutations: cancer risk and genetic testing fact sheet. Available at: https://www.cancer.gov/about-cancer/causesprevention/genetics/brca-fact-sheet. Accessed on 30/09/2020.
41. Scalia-Wilbur J, Colins BL, Penson RT, Dizon DS. Breast cancer risk assessment: moving beyond BRCA 1 and 2. Semin Radiat Oncol. 2016;26(1):3–8.
42. NCCN Guidelines. Available at: https://www.nccn.org/professionals/physician_gls/pdf/genetics_bop.pdf. Accessed on 30/09/2020.

Chapter 3
Genomic Tests

Laura Testa and Renata Colombo Bonadio

3.1 Introduction

Localized hormonal receptor (HR)-positive breast cancer has a broad spectrum of disease behavior, influenced by numerous factors. Clinical and pathological features have a substantial impact on prognosis. For patients with a high risk of recurrence, intensification of treatment using neoadjuvant or adjuvant chemotherapy (CT) is usually recommended. Age, menopausal status, tumor size, lymph node status, tumor grade, angiolymphatic invasion, and expression of hormone receptor and HER2 are some of the factors influencing the risk of recurrence. However, these factors alone do not provide a precise estimation of prognosis. On the other hand, the indiscriminate use of chemotherapy is not appropriate since it is associated with potentially severe adverse events, and many patients would be cured without CT.

In this context, gene expression assays to assess patients' prognosis were developed. These tests evaluate genes related to tumor proliferation, invasion, angiogenesis, and oncogenic pathways. The most widely used tests provide information on recurrence risk based on the gene expression profile from tumor tissue, using microarray and reverse transcription polymerase chain reaction (RT-PCR) that assess mRNA expression. The assays available differ from one other in terms of number of genes evaluated, population in which the test was validated, number of risk categories provided, and validation as a predictor of chemotherapy benefit, as will be discussed ahead.

L. Testa (✉) · R. C. Bonadio
Departamento de Oncologia, Instituto do Cancer do Estado de Sao Paulo ICESP, São Paulo, SP, Brazil
e-mail: laura.testa@hc.fm.usp.br

S. J. Kim Hsieh, E. A. Morris (eds.), *Modern Breast Cancer Imaging*,
https://doi.org/10.1007/978-3-030-84546-9_3

3.2 Gene Expression Assays

3.2.1 Oncotype DX

The Oncotype DX assay evaluates 21 genes (16 tumor associated and five controls) and provides a recurrence score (RS) that ranges from 0 to 100. Depending on the RS, patients are classified as low risk, intermediate risk, or high risk. Oncotype DX was validated as a prognostication tool for estrogen receptor (ER)-positive early breast cancer in various trials [1–4].

Among patients with node-negative ER-positive breast cancer enrolled in the NSABP B-14 trial, recurrence scores (RS) of <18, 18–30, and ≥31 were associated with 10-year distant recurrence rates of 6.8%, 14.3%, and 30.5%, respectively [1]. A study with the population of another trial, the NSABP B-20, suggested that patients in the low-risk category (RS < 18) derived no benefit from the addition of adjuvant chemotherapy, while those with high risk (RS ≥ 31) had a significant reduction in distant recurrence with chemotherapy. Finally, for patients in the intermediate-risk category (RS 18–30), benefit from chemotherapy was uncertain [2].

The cutoff values for risk categories were refined in subsequent studies, and the ability of Oncotype DX to predict chemotherapy benefit was evaluated prospectively. The TAILORx trial enrolled patients with node-negative HR-positive breast cancer, tailoring adjuvant systemic therapy according to RS. Patients with an RS lower than 11 (low risk) were treated with endocrine therapy alone. Those with RS greater than 25 (high risk) received chemotherapy plus endocrine therapy. Finally, patients in the intermediate-risk category (RS 11–25) were randomized to receive endocrine therapy alone or chemotherapy plus endocrine therapy. Results showed similar outcomes from endocrine therapy and chemoendocrine therapy for patients in the intermediate group [5]. The study confirmed that Oncotype DX can be used to predict chemotherapy benefit.

Further analysis of the TAILORx trial suggested a different test behavior for women younger than 50 years. For those in the intermediate-risk group, patients with an RS of 16–25 seemed to benefit from chemoendocrine therapy. The absolute distant recurrence rate decreased 1.6% for RS 16–20 and 6.4% for RS 21–25 at 9 years with the addition of chemotherapy. A question that remains is if this difference observed in younger women is due to the effect of chemotherapy itself or the induction of menopause caused by it.

The RxPONDER trial evaluated the role of Oncotype DX for predicting chemotherapy benefit for patients with one to three positive lymph nodes. Patients with an RS ≤25 were assigned to receive either endocrine therapy or endocrine therapy plus standard chemotherapy. No benefit was seen for chemotherapy in postmenopausal women, but premenopausal women again had a different outcome. Five-year invasive disease-free survival rates were 91.9% for endocrine therapy plus chemotherapy vs 91.6% for endocrine therapy alone in the postmenopausal patient subset and 94.2% vs 89.0% in the premenopausal patient

subset [6]. The question remains as to whether this is a direct benefit of chemotherapy or an indirect effect of ovarian suppression.

3.2.2 MammaPrint

The MammaPrint assay classifies HR-positive early breast cancer patients into two categories, low risk and high risk, based on the evaluation of 70 genes. Retrospective and prospective studies have validated MammaPrint as a prognostic tool for breast cancer recurrence [7–9].

In the MINDACT trial, genomic risk based on MammaPrint was used together with clinical risk to define the use of adjuvant chemotherapy for patients with HR-positive breast cancer with negative lymph nodes or one to three positive lymph nodes. The clinical risk was defined using Adjuvant! Online, a web-based tool that provides recurrence risk according to clinical and pathological features [10]. Patients with low clinical and genomic risk received endocrine therapy alone, while patients with high clinical and genomic risk received chemoendocrine therapy. The cohort of patients with discordant results (low clinical risk and high genomic risk, or high clinical risk and low genomic risk) were randomized to receive adjuvant chemotherapy or not. The trial aimed to evaluate if patients with high clinical risk and low genomic risk could be spared chemotherapy. Results showed that 5-year distant metastasis-free survival (DMFS) rate was 94.7% (95% confidence interval 92.5–96.2%), which was considered satisfactory when compared with the noninferiority boundary of 92% established by the study. Additionally, in this group, the 5-year distant metastasis rate of survival (DMRS) was similar in patients with chemotherapy and without chemotherapy. The study suggested that MammaPrint can be used for patients with high clinical risk to select patients for whom chemotherapy can be avoided, although the trial was not powered for this comparison (yes versus no chemotherapy) [11].

Similar to what was observed with both randomized Oncotype DX trials, subgroup analysis of MINDACT suggested that for women younger than 50 years with high clinical risk and low genomic risk, a relevant absolute difference of 5% in 8-year DMFS was observed with the addition of chemotherapy [12]. Thus, for women younger than 50 years, additional studies are necessary to clarify the role of genomic assays for predicting chemotherapy benefit.

3.2.3 Other Assays

EndoPredict assay analyzes 12 genes (eight cancer-related genes and four reference genes), providing a risk score ranging from 0 to 15. The test also classifies patients into low- and high-risk groups. Moreover, an EndoPredict clinical score is

generated by incorporating clinical factors (tumor size and nodal status). EndoPredict's prognostic value was validated in prospective-retrospective cohorts of ER-positive patients with negative or positive lymph nodes [13–15].

Prosigna assay (or PAM50) uses 50 genes (plus eight reference genes) and distinguished breast cancer molecular subtypes (luminal A, luminal B, HER2 enriched, normal-like, and basal-like), which correlate with disease behavior. Moreover, a risk of recurrence (ROR) score is also provided by this test, ranging from 0 to 100. Validation of its prognostic impact occurred in prospective-retrospective trials of postmenopausal ER-positive patients, containing both lymph node-negative and positive cohorts [16–18]. Three risk group categories are provided for node-negative patients: low risk (ROR 0–40), intermediate risk (ROR 41–60), and high risk (ROR 61–100). For node-positive patients, only two categories are considered: low risk (ROR 0–40) or high risk (41–100). Prosigna's ability to predict late recurrences after adjuvant endocrine therapy has also been shown [19].

The Breast Cancer Index (BCI) assay evaluates seven cancer-related genes plus four reference genes, together with two other biomarkers (HOX-B13:IL17BR ratio and Molecular Grade Index). Similar to Prosigna, BCI has been shown to predict early and late recurrences in ER-positive lymph node-negative patients who received adjuvant endocrine therapy in prospective-retrospective trials [20–23]. These results generate the hypothesis that these tests (Prosigna and BCI) might help select patients for extended endocrine therapy.

3.3 Concordance of Expression Assays

Although genomic tests available have similar objectives, they differ in terms of genes evaluated and population in which the tests were validated. Importantly, discordances have been demonstrated among the tests. For instance, Barlett et al. showed that in a cohort of patients with early breast cancer, the proportion considered as low/intermediate risk was 82.1%, 65.6%, and 61.4% with Oncotype DX, Prosigna, and MammaPrint, respectively [24]. In another study, the concordance between Oncotype DX and MammaPrint was only 0.64 [25].

These results are similar to what was observed in a review that summarized head-to-head comparisons of Oncotype DX with other genomic tests. In this review, a high-risk score was observed: 11.5% with Oncotype DX, 16.2% with BCI, 30.7% with ROR (Prosigna), 63% with EndoPredict, and 45.8% with MammaPrint. Overall discordance between Oncotype DX and other tests ranged from 42% to 66% [26]. Thus, genomic tests for recurrence risk are not interchangeable, and careful selection of the appropriate test for a patient is necessary. A summary of these tests' characteristics is shown in Table 3.1.

Table 3.1 Summary of the characteristics of genomic tests for breast cancer recurrence risk

	Number of genes	Risk categories	Population evaluated	Current validation	Type of validation studies
Oncotype DX	21	Low Intermediate High	ER+/HER2- pT1-2 pN0-1	Prognostic Predictive of chemotherapy benefit	Prospective-retrospective [1–4] Prospective randomized [5, 6]
MammaPrint	70	Low High	pT1-2 pN0-1	Prognostic Predictive of chemotherapy benefit	Prospective-retrospective [7–9] Prospective randomized [11]
EndoPredict	12	Low High	ER+/HER2- pT1-2 pN0-1 Postmenopausal	Prognostic	Prospective-retrospective [13–15]
Prosigna (PAM50)	58	Low Intermediate High	ER+ pT1-2 pN0-1 Postmenopausal	Prognostic	Prospective-retrospective [16–18]
Breast Cancer Index	11	Low High	ER+/HER2- pT1-3 pN0	Prognostic	Prospective-retrospective [20–23]

3.4 Conclusion

Genomic tests are adding valuable information on recurrence risk for ER/PR-positive early breast cancer. Their use to estimate prognosis and predict the benefit of adjuvant therapy has been increasing in clinical practice [27]. Nevertheless, some challenges still need to be faced.

Despite the number of tests available, they were validated in different scenarios and are not totally concordant with one other. Carefulness is necessary for the appropriate test selection for a patient. More prospective validation is still required for some groups, such as premenopausal women and patients with positive lymph nodes. Moreover, tests' costs remain a barrier for wider access to these tests.

References

1. Paik S, Shak S, Tang G, Kim C, Baker J, Cronin M, et al. A multigene assay to predict recurrence of tamoxifen-treated, node-negative breast cancer. N Engl J Med. 2004;351(27):2817–26.
2. Paik S, Tang G, Shak S, Kim C, Baker J, Kim W, et al. Gene expression and benefit of chemotherapy in women with node-negative, estrogen receptor-positive breast cancer. J Clin Oncol. 2006;24(23):3726–34.

3. Dowsett M, Cuzick J, Wale C, Forbes J, Mallon EA, Salter J, et al. Prediction of risk of distant recurrence using the 21-gene recurrence score in node-negative and node-positive postmenopausal patients with breast cancer treated with anastrozole or tamoxifen: a TransATAC study. J Clin Oncol. 2010;28(11):1829–34.
4. Albain KS, Barlow WE, Shak S, Hortobagyi GN, Livingston RB, Yeh IT, et al. Prognostic and predictive value of the 21-gene recurrence score assay in postmenopausal women with node-positive, oestrogen-receptor-positive breast cancer on chemotherapy: a retrospective analysis of a randomised trial. Lancet Oncol. 2010;11(1):55–65.
5. Francis PA, Pagani O, Fleming GF, Walley BA, Colleoni M, Láng I, et al. Tailoring adjuvant endocrine therapy for premenopausal breast cancer. N Engl J Med. 2018;379(2):122–37.
6. Kalinsky K, Barlow W, Meric-Bernstam F, et al.. SWOG S1007: adjuvant trial randomized ER+ patients who had a recurrence score < 25 and 1–3 positive nodes to endocrine therapy (ET) versus ET + chemotherapy. Presented at: 2020 virtual San Antonio breast cancer symposium; December 8–11, 2020. Abstract GS3-00.
7. van de Vijver MJ, He YD, van't Veer LJ, Dai H, Hart AA, Voskuil DW, et al. A gene-expression signature as a predictor of survival in breast cancer. N Engl J Med. 2002;347(25):1999–2009.
8. Buyse M, Loi S, van't Veer L, Viale G, Delorenzi M, Glas AM, et al. Validation and clinical utility of a 70-gene prognostic signature for women with node-negative breast cancer. J Natl Cancer Inst. 2006;98(17):1183–92.
9. Bueno-de-Mesquita JM, van Harten WH, Retel VP, van't Veer LJ, van Dam FS, Karsenberg K, et al. Use of 70-gene signature to predict prognosis of patients with node-negative breast cancer: a prospective community-based feasibility study (RASTER). Lancet Oncol. 2007;8(12):1079–87.
10. Olivotto IA, Bajdik CD, Ravdin PM, Speers CH, Coldman AJ, Norris BD, et al. Population-based validation of the prognostic model ADJUVANT! for early breast cancer. J Clin Oncol. 2005;23(12):2716–25.
11. Cardoso F, van't Veer LJ, Bogaerts J, Slaets L, Viale G, Delaloge S, et al. 70-gene signature as an aid to treatment decisions in early-stage breast cancer. N Engl J Med. 2016;375(8):717–29.
12. Cardoso F, van't Veer L, Poncet C, et al. MINDACT: long-term results of the large prospective trial testing the 70-gene signature MammaPrint as guidance for adjuvant chemotherapy in breast cancer patients. J Clin Oncol. 2020;38(suppl; abstr):506.
13. Filipits M, Rudas M, Jakesz R, Dubsky P, Fitzal F, Singer CF, et al. A new molecular predictor of distant recurrence in ER-positive, HER2-negative breast cancer adds independent information to conventional clinical risk factors. Clin Cancer Res. 2011;17(18):6012–20.
14. Dubsky P, Filipits M, Jakesz R, Rudas M, Singer CF, Greil R, et al. EndoPredict improves the prognostic classification derived from common clinical guidelines in ER-positive, HER2-negative early breast cancer. Ann Oncol. 2013;24(3):640–7.
15. Martin M, Brase JC, Calvo L, Krappmann K, Ruiz-Borrego M, Fisch K, et al. Clinical validation of the EndoPredict test in node-positive, chemotherapy-treated ER+/HER2- breast cancer patients: results from the GEICAM 9906 trial. Breast Cancer Res. 2014;16(2):R38.
16. Dowsett M, Sestak I, Lopez-Knowles E, Sidhu K, Dunbier AK, Cowens JW, et al. Comparison of PAM50 risk of recurrence score with oncotype DX and IHC4 for predicting risk of distant recurrence after endocrine therapy. J Clin Oncol. 2013;31(22):2783–90.
17. Gnant M, Filipits M, Greil R, Stoeger H, Rudas M, Bago-Horvath Z, et al. Predicting distant recurrence in receptor-positive breast cancer patients with limited clinicopathological risk: using the PAM50 risk of recurrence score in 1478 postmenopausal patients of the ABCSG-8 trial treated with adjuvant endocrine therapy alone. Ann Oncol. 2014;25(2):339–45.
18. Liu S, Chapman JA, Burnell MJ, Levine MN, Pritchard KI, Whelan TJ, et al. Prognostic and predictive investigation of PAM50 intrinsic subtypes in the NCIC CTG MA.21 phase III chemotherapy trial. Breast Cancer Res Treat. 2015;149(2):439–48.
19. Sestak I, Cuzick J, Dowsett M, Lopez-Knowles E, Filipits M, Dubsky P, et al. Prediction of late distant recurrence after 5 years of endocrine treatment: a combined analysis of patients from the Austrian breast and colorectal cancer study group 8 and arimidex, tamoxifen alone

or in combination randomized trials using the PAM50 risk of recurrence score. J Clin Oncol. 2015;33(8):916–22.
20. Sgroi DC, Sestak I, Cuzick J, Zhang Y, Schnabel CA, Schroeder B, et al. Prediction of late distant recurrence in patients with oestrogen-receptor-positive breast cancer: a prospective comparison of the breast-cancer index (BCI) assay, 21-gene recurrence score, and IHC4 in the TransATAC study population. Lancet Oncol. 2013;14(11):1067–76.
21. Sgroi DC, Carney E, Zarrella E, Steffel L, Binns SN, Finkelstein DM, et al. Prediction of late disease recurrence and extended adjuvant letrozole benefit by the HOXB13/IL17BR biomarker. J Natl Cancer Inst. 2013;105(14):1036–42.
22. Zhang Y, Schnabel CA, Schroeder BE, Jerevall PL, Jankowitz RC, Fornander T, et al. Breast cancer index identifies early-stage estrogen receptor-positive breast cancer patients at risk for early- and late-distant recurrence. Clin Cancer Res. 2013;19(15):4196–205.
23. Sanft T, Aktas B, Schroeder B, Bossuyt V, DiGiovanna M, Abu-Khalaf M, et al. Prospective assessment of the decision-making impact of the breast cancer index in recommending extended adjuvant endocrine therapy for patients with early-stage ER-positive breast cancer. Breast Cancer Res Treat. 2015;154(3):533–41.
24. Bartlett JM, Bayani J, Marshall A, Dunn JA, Campbell A, Cunningham C, et al. Comparing breast cancer multiparameter tests in the OPTIMA prelim trial: no test is more equal than the others. J Natl Cancer Inst. 2016;108(9):djw050.
25. Denduluri N, Rugo H, Davis S, et al. Concordance between the 21-gene recurrence score (RS) and the 70-gene profile (MP) in breast cancer (BC) patients (pts). J Clin Oncol. 2011;27_suppl:13.
26. Varga Z, Sinn P, Seidman AD. Summary of head-to-head comparisons of patient risk classifications by the 21-gene Recurrence Score® (RS) assay and other genomic assays for early breast cancer. Int J Cancer. 2019;145(4):882–93.
27. Duffy MJ, Harbeck N, Nap M, Molina R, Nicolini A, Senkus E, et al. Clinical use of biomarkers in breast cancer: updated guidelines from the European Group on Tumor Markers (EGTM). Eur J Cancer. 2017;75:284–98.

Chapter 4
Updates in Surgical Approaches for Breast and Axilla

Bruna Salani Mota, Rodrigo Goncalves, and Jose Roberto Filassi

4.1 Introduction

Axillary surgery provides valuable staging information to guide the adjuvant treatment of breast cancer and is key to the local control of axillary disease, being a well-established procedure for the management of primary breast cancer.

However, the surgical management of the axilla has changed substantially in the last three decades, from the axillary lymph node dissection (ALND), which has a high morbidity and decreases the women's quality of life, to a sentinel lymph node biopsy for most patients.

This radical change in the surgical approach started in 1970; the Mayo Clinic published strong evidence for the axillary nodal metastases predictive values. All patients had undergone ALND, and the data showed 5-year survival rates of 86% in node-negative patients compared to 50% in node-positive patients. After that, the value of axillary clearance for all breast cancer surgery became questionable since it did not influence the survival rates and increased the chances of lymphedema [1].

In 1994, Giuliano et al. [2], after the successful use of sentinel lymph node biopsy (SLNB) for melanoma staging [3], published the first description of SLNB for breast cancer treatment, with the potential of axillary staging with less morbidity. Since then, its use has been widely accepted as the single axillary surgical procedure among all clinically node-negative (cN0) breast cancer patients and selected patients with low-volume axillary metastases. Those results significantly impacted breast cancer surgery management since it avoids as much as 70% of all complete axillary node dissections.

B. S. Mota · R. Goncalves (✉) · J. R. Filassi
Departamento de Mastologia, Instituto do Cancer do Estado de Sao Paulo ICESP, São Paulo, SP, Brazil
e-mail: rodrigo.g@hc.fm.usp.br; drfilassi@terra.com.br

S. J. Kim Hsieh, E. A. Morris (eds.), *Modern Breast Cancer Imaging*,
https://doi.org/10.1007/978-3-030-84546-9_4

We will discuss in this chapter the surgical management of the axilla according to the axillary stage: N (0), micrometastases (N1mic) or isolated tumor cells, clinically N0 with macrometastases in the pathological exam, and clinically positive axilla patients. This approach aims to facilitate the understanding of axillary treatment in different scenarios.

4.2 Axillary Management in Clinically Node-Negative Patients with Invasive Breast Cancer

The effectiveness of SLNB in clinically N0 breast cancer patients has been proven throughout the years with the publication of a comprehensive study assortment. These trials all have demonstrated low rates of axillary recurrences (0.2–0.5%) [4–7] when SLNB was compared to ALND (0–0.8%) in patients with a negative SLNB who had no further surgery.

The National Surgical Adjuvant Breast and Bowel Project (NSABP) B-32 trial is the most extensive study, with 5611 participants, to compare survival and regional control between SLNB alone and axillary lymph node dissection (ALND) in clinically node-negative patients. Patients were assigned to SLNB plus ALND or SLNB alone with ALND only if the sentinel node(s) was positive [5]. The latest report, in 2010, showed no difference in overall and disease-free survival between the two groups with a median follow-up of 8 years. Axillary recurrence as a first disease relapse event occurred in less than 1% of both the SLNB followed by ALND group (0.4%) and the SLNB-only group (0.6%), $p = 0.22$ [8].

In 2017, a meta-analysis from the Cochrane database, including seven clinical trials, compared ALND versus SLNB. There was no difference in overall survival in the comparison between SLNB and ALND (HR 1.05, 95% CI 0.89 to 1.25; 6352 participants; three studies; moderate-quality evidence) [9].

4.3 Axillary Management in Micrometastases (N1m1) or Isolated Tumor Cells N (+1) Patients with Invasive Breast Cancer

The pathology review of nodal specimens of SLNB negative patients in the NSABP B-32 trial presented the question about the role of ALND in the axillary treatment in micrometastases (N1m1) or isolated tumor cells N (+1) (ITC) patients. The absolute reduction in overall survival in those patients with ITC or micrometastases was only 1.2% in patients submitted to ALND in that trial [5].

The ACOSOG Z0010 trial confirmed that women with a low volume of nodal metastases who underwent an SLNB plus ALND did not have significant benefit in overall or disease-free survival over patients undergoing SLNB alone in this

multicentric prognostic study, which had 10.5% rates of occult sentinel node metastases [10].

The International Breast Cancer Study Group (IBCSG) 23-01 trial answered the question regarding the role of axillary surgery in breast cancer patients with N1mic definitively. In this trial, clinically node-negative patients with an SLNB containing micrometastases were randomized to ALND or no further axillary surgery. Thirteen percent of patients who had an ALND presented additional involved axillary nodes. However, 5-year disease-free survival did not significantly differ in the SLNB-alone (87.8%) vs. the ALND (84.4%) group. In patients who did not undergo ALND, the rate of disease recurrence was less than 1% [11].

4.4 Axillary Management in Clinically Node-Negative Patients and Macrometastases in the Pathology with Invasive Breast Cancer

In the past, the standard of care for patients who had positive sentinel lymph nodes with macrometastases (tumor deposits of more than 2.0 mm) was ALND to achieve local control. However, with the increasing use and efficacy of adjuvant chemotherapy, hormonal therapy, and radiation, the scientific community started questioning the real importance of ALND in providing regional control.

The American College of Surgeons Oncology Group Z0011 trial recruited patients with clinically T1 to T2, node-negative breast cancer selected to undergo breast-conserving surgery and SLNB. All patients who had a positive SLNB by routine H&E staining were randomized to ALND completion or no ALND and no further axillary specific radiotherapy. Any patient with three or more positive sentinel nodes was excluded. Accrual to the study and event rates were lower than expected, resulting in the trial's early closure. All patients received whole-breast irradiation, and almost all received adjuvant systemic therapy (58% chemotherapy, 46% hormonal therapy). Forty-one percent of the study patients had small volume metastases (micrometastases or ITCs). In the cohort who did undergo an ALND, additional positive axillary nodes were found in 27% of cases. At a median follow-up of 6 years, there were no differences between the SLNB followed by ALND and SLNB groups in the rates of overall locoregional recurrence (4.1% vs. 2.8%), breast recurrence (3.6% vs. 1.9%), and axillary recurrence (0.5% vs. 0.9). The 10-year follow-up publication confirmed the low rate of axillary recurrence of <2% in both groups, denying any concerns that a spate of late axillary recurrences may be seen with the SLNB-only group [12]. The trial's major weakness focused on the design of the radiotherapy fields; the tangential field whole-breast irradiation with high tangents used in both groups resulted in a portion of the axilla receiving radiation in patients on both arms of the study. However, trying to evaluate the radiotherapy as a confounder, further statistical analysis did not show a significant difference between treatment arms in the use of protocol-prohibited nodal fields [13].

The National Comprehensive Cancer Network (NCCN) guidelines adopted the surgical strategy evaluated in the ACOSOG Z011 to avoid the ALND in the setting of two or fewer metastatic lymph nodes on SLNB in patients with 5 cm or less tumors who have no clinically suspicious axillary lymph nodes and who are undergoing breast-conserving surgery and subsequent whole-breast irradiation and systemic therapy [14].

To investigate the same strategy of de-escalation of surgical treatment of the axilla, the European Organization for Research and Treatment of Cancer (EORTC) conducted and published the data from the AMAROS trial. This clinical trial enrolled 1400 patients with T1-T2 tumors and with positive SLN that were randomized to ALND versus axillary radiation [15]. Approximately 82% of the 1425 patients with a positive SLNB underwent breast-conserving surgery. In both arms, 60% of the sentinel node metastases were macrometastases. There was no difference in the 10-year axillary recurrence, overall survival (OS), and disease-free survival (DFS) rates. The axillary recurrence rates were 1.82% (11 of 681) in patients assigned to axillary radiotherapy versus 0.93% (seven of 744 patients) in those assigned to ALND. The OS rates were 81.4% and 84.6% and DFS rates were 78.2% and 81.7%, respectively [16].

There were a significant decrease in lymphedema with radiation and a nonsignificant trend toward decreased shoulder mobility.

4.5 Axillary Management in Clinically Node-Positive Patients and Neoadjuvant Chemotherapy (NAC) Treatment

According to the American Joint Committee on Cancer, clinical examination or imaging studies can identify positive axillary nodes. The core issue is detecting axillary disease in patients who are candidates directly to ALND without SLNB or planning to begin the treatment with neoadjuvant chemotherapy with a prospect of axillary downstaging [17].

The axillary downstaging (pathological complete response (pCR)) rate after neoadjuvant treatment is 37% in the NSABP B-18. The highest pCR rates (97%) are in patients with amplified HER2 disease, followed by estrogen receptor (ER)+/HER2+ with 70%, 47% in triple-negative and ER+ with 21% of pathological complete response rates [18].

Based on this, an accurate axillary evaluation is essential to make the best clinical decision. The NCCN recommends an axillary image with ultrasound (US) followed by fine needle aspiration (FNA) or core biopsy of any suspicious nodes in patients who would undergo neoadjuvant chemotherapy regardless of clinical axillary status [14]. The clinical examination has a sensitivity of 8.3%, a specificity of 94.8%, and a negative predictive value (NPV) of 46.6%. The ultrasound alone

revealed a sensitivity of 23.9%, a specificity of 91.7%, and an NPV of 50.3%. The association of both approaches (palpation and ultrasound) resulted in a sensitivity of 24.4%, a specificity of 91.4%, and an NPV of 50.3% [19].

Several clinical trials investigated the feasibility and accuracy of SLNB after NAC for axillary staging in initially clinically node-negative breast cancer patients. In 2016, a meta-analysis including 16 studies with 1456 patients showed an identification rate for SLNB of 96%, and the false-negative rate (FNR) was 6%. The negative predictive value (NPV) and accuracy were 94% and 98%, respectively [20]. Those values confirmed that SLNB is technically possible for axillary evaluation in clinically node-negative breast cancer patients after NAC.

The SLNB in clinically node-positive disease at presentation has identification rates ranging from 78% to 98% and false-negative rates as high as 40% in the initial studies [21–24]. Therefore, the enthusiasm for exploring SLNB surgery after NAC as a less aggressive alternative than ALND for those patients converted to clinically node-negative has lead to essential publications in this field. The accuracy of SLNB after neoadjuvant chemotherapy in clinically node-positive patients has been evaluated in three prospective trials [25]. The American College of Surgeons Oncology Group (ACOSOG) Z1071 trial reported a false-negative rate (FNR) of 12.6% for SLND in patients with cN1 disease who had at least two sentinel lymph nodes removed. A reduction in the false-negative rate was evident as the number of sentinel nodes removed increased: 31%, one node, and 21%, two nodes, dropping to a clinically acceptable 9% only when three or more nodes were removed [26].The mapping technique was the only factor found to impact SLN identification. The SLN identification rate was 78.6% with blue dye alone, 91.4% with radiolabeled colloid, and 93.8% with dual mapping agents. The patient features (age, body mass index), clinical tumor characteristics, pathologic nodal response, and site of tracer injection did not affect the SLN identification rate [25].

The European SENTinel NeoAdjuvant (SENTINA) trial and the Canadian Sentinel Node Biopsy Following Neoadjuvant Chemotherapy (SN FNAC) trial supported these findings with slight differences between them [27, 28]. The dual-tracer (blue dye and radioisotope) technique and removal of >2 SLNs were shown to lower the FNR in all three trials. In the SENTINA trial, the sentinel node detection rate was 80%, with a false-negative rate of 14%; it varied according to the number of sentinel nodes removed: 24%, one node; 18%, two nodes; and less than 8% when three or more nodes were removed [27]. The SN FNAC trial showed quite similar false-negative rates, 18% with one node and 5% with two or more nodes.

The applicability of SLNB in treating clinically node-positive patients who revert to clinically node-negative after neoadjuvant chemotherapy depends on the dual-modality mapping with both blue dye and radiocolloid followed by removal of three sentinel nodes to try to reduce the false-negative rates [26–28]. Added attention to avoid the false-negative rates is to use the clip to mark the metastatic axillary node(s) guided by ultrasound before neoadjuvant therapy. This procedure ensures that the positive node will be removed during the surgery, confirming the treatment

response. Caudle et al., in 2017, conducted a prospective study, including 208 participants, using iodine-125 seed localization. The marked node was not recovered as an SLN in 23% (31 of 134) of patients, including six with negative SLNs but metastasis in the clipped node. A total of 120 patients still had residual disease; from those, the clipped node showed metastases in 115 patients, resulting in a false-negative rate of 4.2% [29].

The routine use of SLNB using iodine-125 seed localization has not been established yet since there is an increase in treatment costs and questions regarding the technique due to the need of specialized breast radiologists, notably experienced in targeting techniques [29]. Otherwise, the trials published regarding this theme support the management of SLND with blue dye and radiocolloid with acceptable false-negative rates.

Although there are increasing efforts to avoid the ALND in patients identified as node-positive before systemic treatment that converted to negative after NAC, there are still almost 40% of patients who have residual axillary disease and need ALND following standard adjuvant treatment. The ALND is still the standard treatment in this setting; there is no scientific data to support radiotherapy as a unique treatment for this group of patients. The updated analysis of NSABP B-18 and B-27 neoadjuvant trials showed high rates of locoregional recurrence (LRR) observed in patients with pathologically positive nodes at surgery. The 10-year cumulative incidence of LRR was 12.3% for mastectomy patients and 10.3% for lumpectomy plus breast radiotherapy patients. The independent predictors of LRR in lumpectomy patients were age, clinical nodal status (before NAC), and pathologic nodal status/breast tumor response. In mastectomy patients, predictors of LRR were clinical tumor size (before NAC), clinical nodal status (before NAC), and pathologic nodal status/breast tumor response. The risk of LRR was increased by 2.71 times if residual axillary disease was present [30].

The Alliance A11202 study is a randomized clinical trial that evaluates the role of axillary radiotherapy (axilla, supraclavicular nodes, and internal mammary nodes) compared to ALND in patients who remain node-positive after NAC irrespective of the breast surgery type. The main outcome of this trial is recurrence-free survival rate in a non-inferiority design.

We will still observe extraordinary advances and practice changes in axilla management for the next decades due to preoperative image improvement and profile signatures. There are two exciting trials in the recruitment phase: the SOUND trial [31] and the SWOG RxPONDER trial [32]. In the first one, the research question is based on patients with a low burden of axillary disease, with a hypothesis that the results of SLNB are unlikely to alter adjuvant treatment decisions. Regarding this, the patients will be randomized to perform SLNB versus ultrasound only. The second protocol, SWOG RxPONDER trial, will assess gene expression profiling's ability in the setting of lymph node positivity to identify patients with excellent predicted long-term survival with adjuvant hormonal treatment alone in which chemotherapy would not confer any additional benefit.

References

1. Fisher B, Montague E, Redmond C, Barton B, Borland D, Fisher ER, et al. Comparison of radical mastectomy with alternative treatments for primary breast cancer. A first report of results from a prospective randomized clinical trial. Cancer. 1977;39(6 Suppl):2827–39.
2. Giuliano AE, Kirgan DM, Guenther JM, Morton DL. Lymphatic mapping and sentinel lymphadenectomy for breast cancer. Ann Surg. 1994;220(3):391–8. discussion 398–401.
3. Morton DL, Wen DR, Wong JH, Economou JS, Cagle LA, Storm FK, et al. Technical details of intraoperative lymphatic mapping for early stage melanoma. Arch Surg. 1992;127(4):392–9.
4. Mansel RE, Fallowfield L, Kissin M, Goyal A, Newcombe RG, Dixon JM, et al. Randomized multicenter trial of sentinel node biopsy versus standard axillary treatment in operable breast cancer: the ALMANAC trial. J Natl Cancer Inst. 2006;98(9):599–609.
5. Krag DN, Julian TB, Harlow SP, Weaver DL, Ashikaga T, Bryant J, et al. NSABP-32: phase III, randomized trial comparing axillary resection with sentinal lymph node dissection: a description of the trial. Ann Surg Oncol. 2004;11(3 Suppl):208S–10S.
6. Zavagno G, De Salvo GL, Scalco G, Bozza F, Barutta L, Del Bianco P, et al. A randomized clinical trial on sentinel lymph node biopsy versus axillary lymph node dissection in breast cancer: results of the Sentinella/GIVOM trial. Ann Surg. 2008;247(2):207–13.
7. Veronesi U, Paganelli G, Viale G, Luini A, Zurrida S, Galimberti V, et al. A randomized comparison of sentinel-node biopsy with routine axillary dissection in breast cancer. N Engl J Med. 2003;349(6):546–53.
8. Krag DN, Anderson SJ, Julian TB, Brown AM, Harlow SP, Costantino JP, et al. Sentinel-lymph-node resection compared with conventional axillary-lymph-node dissection in clinically node-negative patients with breast cancer: overall survival findings from the NSABP B-32 randomised phase 3 trial. Lancet Oncol. 2010;11(10):927–33.
9. Bromham N, Schmidt-Hansen M, Astin M, Hasler E, Reed MW. Axillary treatment for operable primary breast cancer. Cochrane Database Syst Rev. 2017;1:CD004561.
10. Giuliano AE, Ballman K, McCall L, Beitsch P, Whitworth PW, Blumencranz P, et al. Locoregional recurrence after sentinel lymph node dissection with or without axillary dissection in patients with sentinel lymph node metastases: long-term follow-up from the American College of Surgeons Oncology Group (Alliance) ACOSOG Z0011 randomized trial. Ann Surg. 2016;264(3):413–20.
11. Galimberti V, Cole BF, Viale G, Veronesi P, Vicini E, Intra M, et al. Abstract GS5-02: axillary dissection vs. no axillary dissection in patients with cT1-T2cN0M0 breast cancer and only micrometastases in the sentinel node(s): ten-year results of the IBCSG 23-01 trial. Cancer Res. 2018;78(4 Supplement):GS5-02-GS5-02.
12. Giuliano AE, Ballman KV, McCall L, Beitsch PD, Brennan MB, Kelemen PR, et al. Effect of axillary dissection vs no axillary dissection on 10-year overall survival among women with invasive breast cancer and sentinel node metastasis: the ACOSOG Z0011 (Alliance) randomized clinical trial. JAMA. 2017;318(10):918–26.
13. Haffty BG, McCall LM, Ballman KV, McLaughlin S, Jagsi R, Ollila DW, et al. Patterns of local-regional management following neoadjuvant chemotherapy in breast cancer: results from ACOSOG Z1071 (Alliance). Int J Radiat Oncol Biol Phys. 2016;94(3):493–502.
14. Gradishar WJ, Anderson BO, Abraham J, Aft R, Agnese D, Allison KH, et al. Breast cancer, version 3.2020, NCCN clinical practice guidelines in oncology. J Natl Compr Cancer Netw. 2020;18(4):452–78.
15. Straver ME, Meijnen P, van Tienhoven G, van de Velde CJH, Mansel RE, Bogaerts J, et al. Sentinel node identification rate and nodal involvement in the EORTC 10981-22023 AMAROS trial. Ann Surg Oncol. 2010;17(7):1854–61.
16. Rutgers EJ, Donker M, Poncet C, Straver ME, Meijnen P, van de Velde CJ, et al. Abstract GS4-01: radiotherapy or surgery of the axilla after a positive sentinel node in breast cancer patients: 10 year follow up results of the EORTC AMAROS trial (EORTC 10981/22023). Cancer Res. 2019;79(4 Supplement):GS4-01-GS4-01.

17. Singletary SE, Connolly JL. Breast cancer staging: working with the sixth edition of the AJCC Cancer staging manual. CA Cancer J Clin. 2006 Jan;56(1):37–47; quiz 50–1.
18. Mamtani A, Barrio AV, King TA, Van Zee KJ, Plitas G, Pilewskie M, et al. How often does neoadjuvant chemotherapy avoid axillary dissection in patients with histologically confirmed nodal metastases? Results of a prospective study. Ann Surg Oncol. 2016;23(11):3467–74.
19. Schwentner L, Helms G, Nekljudova V, Ataseven B, Bauerfeind I, Ditsch N, et al. Using ultrasound and palpation for predicting axillary lymph node status following neoadjuvant chemotherapy - results from the multi-center SENTINA trial. Breast. 2017;31:202–7.
20. Geng C, Chen X, Pan X, Li J. The feasibility and accuracy of sentinel lymph node biopsy in initially clinically node-negative breast cancer after neoadjuvant chemotherapy: a systematic review and meta-analysis. PLoS One. 2016;11(9):e0162605.
21. Lee S, Kim EY, Kang SH, Kim SW, Kim S-K, Kang KW, et al. Sentinel node identification rate, but not accuracy, is significantly decreased after pre-operative chemotherapy in axillary node-positive breast cancer patients. Breast Cancer Res Treat. 2007;102(3):283–8.
22. Shen J, Gilcrease MZ, Babiera GV, Ross MI, Meric-Bernstam F, Feig BW, et al. Feasibility and accuracy of sentinel lymph node biopsy after preoperative chemotherapy in breast cancer patients with documented axillary metastases. Cancer. 2007;109(7):1255–63.
23. Alvarado R, Yi M, Le-Petross H, Gilcrease M, Mittendorf EA, Bedrosian I, et al. The role for sentinel lymph node dissection after neoadjuvant chemotherapy in patients who present with node-positive breast cancer. Ann Surg Oncol. 2012;19(10):3177–84.
24. Newman EA, Sabel MS, Nees AV, Schott A, Diehl KM, Cimmino VM, et al. Sentinel lymph node biopsy performed after neoadjuvant chemotherapy is accurate in patients with documented node-positive breast cancer at presentation. Ann Surg Oncol. 2007;14(10):2946–52.
25. Boughey JC, Suman VJ, Mittendorf EA, Ahrendt GM, Wilke LG, Taback B, et al. Factors affecting sentinel lymph node identification rate after neoadjuvant chemotherapy for breast cancer patients enrolled in ACOSOG Z1071 (Alliance). Ann Surg. 2015;261(3):547–52.
26. Boughey JC, Suman VJ, Mittendorf EA, Ahrendt GM, Wilke LG, Taback B, et al. Sentinel lymph node surgery after neoadjuvant chemotherapy in patients with node-positive breast cancer: the ACOSOG Z1071 (Alliance) clinical trial. JAMA. 2013;310(14):1455–61.
27. Kuehn T, Bauerfeind I, Fehm T, Fleige B, Hausschild M, Helms G, et al. Sentinel-lymph-node biopsy in patients with breast cancer before and after neoadjuvant chemotherapy (SENTINA): a prospective, multicentre cohort study. Lancet Oncol. 2013;14(7):609–18.
28. Boileau J-F, Poirier B, Basik M, Holloway CMB, Gaboury L, Sideris L, et al. Sentinel node biopsy after neoadjuvant chemotherapy in biopsy-proven node-positive breast cancer: the SN FNAC study. J Clin Oncol. 2015;33(3):258–64.
29. Caudle AS, Yang WT, Krishnamurthy S, Mittendorf EA, Black DM, Gilcrease MZ, et al. Improved axillary evaluation following neoadjuvant therapy for patients with node-positive breast cancer using selective evaluation of clipped nodes: implementation of targeted axillary dissection. J Clin Oncol. 2016;34(10):1072–8.
30. Mamounas EP, Anderson SJ, Dignam JJ, Bear HD, Julian TB, Geyer CE Jr, et al. Predictors of locoregional recurrence after neoadjuvant chemotherapy: results from combined analysis of National Surgical Adjuvant Breast and Bowel Project B-18 and B-27. J Clin Oncol. 2012;30(32):3960–6.
31. Gentilini O, Veronesi U. Abandoning sentinel lymph node biopsy in early breast cancer? A new trial in progress at the European Institute of Oncology of Milan (SOUND: sentinel node vs observation after axillary UltraSouND). Breast. 2012;21(5):678–81.
32. Ramsey SD, Barlow WE, Gonzalez-Angulo AM, Tunis S, Baker L, Crowley J, et al. Integrating comparative effectiveness design elements and endpoints into a phase III, randomized clinical trial (SWOG S1007) evaluating oncotypeDX-guided management for women with breast cancer involving lymph nodes. Contemp Clin Trials. 2013;34(1):1–9.

Chapter 5
Pathological Aspects for Diagnosis

Marcelo Abrantes Giannotti and Fernando Nalesso Aguiar

5.1 Pre-analytical Procedures

Fixation of biopsies and surgical specimens in neutral buffered 10% formalin must be immediate, and an adequate volume of fixative (at least ten times the volume of the specimen – for biopsy fragments, about 10 ml) should be used for histological, immunohistochemical, in situ hybridization, and molecular studies (e.g., Oncotype DX). Large specimens should be sectioned in slices with a maximum thickness of 10 mm for adequate fixation.

Bar code identification and individual analysis in each step of histological processing are recommended to avoid errors.

5.2 Radiological-Pathological Correlation

The pathologist must have access to lesion imaging characteristics and clinical data. If the purpose of the biopsy is to study calcifications, the identification and segregation of biopsy fragments with calcifications may facilitate analysis and radiological-pathological correlation. Some rules are recommended to avoid mistakes:

M. A. Giannotti (✉)
Hospital Sírio Libanês and Departamento de Patologia, Hospital das Clinicas HCFMUSP, Faculdade de Medicina, Universidade de Sao Paulo, São Paulo, SP, Brazil
e-mail: mag1@uol.com.br

F. N. Aguiar
Departamento de Patologia, Instituto do Cancer do Estado de Sao Paulo ICESP, São Paulo, SP, Brazil
e-mail: fernando.aguiar@hc.fm.usp.br

S. J. Kim Hsieh, E. A. Morris (eds.), *Modern Breast Cancer Imaging*,
https://doi.org/10.1007/978-3-030-84546-9_5

1. To be considered adequate, the diagnosis of a benign lesion must explain the radiological findings. Eventually, some benign lesions may have suspicious aspects in image exams like microcalcifications or irregular masses, but before accepting a benign diagnosis, it is necessary to verify if the lesion was correctly sampled. Common suspect calcified benign lesions include fibroadenomatoid changes, columnar changes, cysts, and steatonecrosis. Suspect irregular lesions can be related to mastitis, diabetic changes, radial scars, desmoid fibromatosis, and granular cell tumors.
2. If there is a very high radiological probability of malignancy, a benign diagnosis should be dealt with caution, and surgical biopsy should be considered.
3. Invasion is detected when normal tissue (ducts, terminal ductal lobular unit (TDLU), adipose tissue) is infiltrated by carcinoma. Papillary (e.g., solid papillary carcinoma and encapsulated carcinoma) and sclerosing lesions may have findings similar to invasive carcinomas, and in order to avoid false-positive diagnosis, sampling the interface between the lesion and normal tissue is recommended.
4. "If it is malignant, is it primary?" Beware when diagnosing a "triple negative" carcinoma of the breast! Metastatic carcinomas and other epithelioid neoplasias (e.g., melanoma and high-grade lymphomas) are always a challenge, and immunohistochemistry should be employed if there is some doubt. The presence of in situ carcinoma and hormonal receptor positivity are suggestive of breast origin, but other tumors can also be estrogen positive (e.g., ovary carcinoma). Information of previous and coexisting diseases should always be informed to the pathologist.

5.3 Fibroepithelial Lesions

Fibroadenomas and phyllodes tumors are lesions that exhibit proliferation of epithelial and stromal cells. The architectural aspects of stromal growth can be divided into two patterns. In the peri-canalicular pattern, the stroma grows around rounded tubules, while in the intracanalicular pattern, the stroma compresses the ducts and forms arciform slit-like structures with epithelial revestment. In phyllodes tumors, this intracanalicular pattern is exaggerated and associated to stromal hypercellularity, with formation of leaf-like structures.

Fibroadenomas are benign lesions, may be multiple, and may increase with hormonal stimuli. If asymptomatic, excision of fibroadenomas is not required.

Phyllodes tumors are classified according to some histological findings: its cellularity, atypia, the presence of stromal overgrowth (i.e., areas greater than a lower magnification field with only stromal component), growth pattern (permeative x well defined), the presence of malignant heterologous elements, and, mainly, by their mitotic count. Although benign phyllodes tumors and fibroadenomas may have molecular differences [1], they share molecular alterations (e.g., MED12-mutant pathway) and recurrence rates, even when margins are positive [2]. In core needle

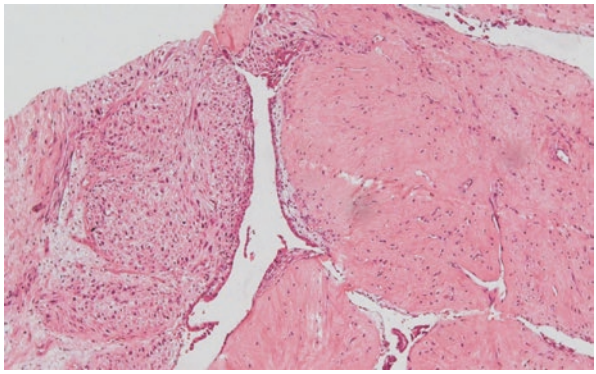

Fig. 5.1 Phyllodes tumor. Leaf-like structures and cellularity variation

Table 5.1 Differences between fibroadenomas and phyllodes tumors

Histological characteristics	Fibroadenoma	Phyllodes tumors		
		Benign	Borderline	Malignant
Mitotic count	Very low/absent	Less than 5/10 HPF	5–10/10HPF	More than 10/10 HPF
Stromal overgrowth	Absent	Absent	Absent/focal	Often present
Heterologous component	Absent	Absent	Absent (unless liposarcoma-like)	May be present
Atypia	Absent	Absent	Mild-moderate	Marked
Borders	Well defined	Well defined	May be focally permeative	Permeative
Cellularity	Scant to mild, uniform	Mild	Mild to moderate, heterogenous	Marked, heterogenous
Frequency	Common	Uncommon	Rare	Rare

* HPF = High-power field.

biopsies, the differences between them may be difficult to distinguish. Malignant and borderline tumors can be very heterogeneous, and final classification is sometimes possible only after complete excision (Fig. 5.1 and Table 5.1).

5.4 Papillary Neoplasms

Papillary lesions are characterized by fibrovascular cores covered by epithelial cells. When benign, myoepithelial cells are present. Malignant lesions can be classified as papillary ductal carcinoma in situ (DCIS), encapsulated, solid, and invasive. Ductal carcinoma in situ can also involve papillary lesions. Although encapsulated papillary carcinoma and solid papillary carcinoma usually do not have myoepithelial cells, they are considered in situ lesions and should be treated surgically.

Pure invasive papillary carcinoma is rare. The majority of invasive lesions related to encapsulated and in situ papillary carcinoma is carcinoma of no special type

Table 5.2 Differences between papillary lesions

	Histology	Clinical and radiological findings
Intraductal papilloma	Broad fronds, epithelial and myoepithelial cells around the fronds, epithelial hyperplasia with UDH features	Single nodule (central papilloma); incidental or calcifications (peripheral multiple papillomas)
Papilloma with DCIS	Broad fronds, myoepithelial cells present. Epithelial hyperplasia with features of DCIS	If high-grade DCIS is present, calcifications and nodules may be present
Papillary DCIS	Slender fronds. Myoepithelial cells absent in the fronds, present at the periphery	Similar to other types of DCIS
Encapsulated papillary carcinoma	Slender fronds; well-developed capsule. Myoepithelial cells absent	Single nodule
Solid papillary carcinoma	Solid pattern with delicate vascular septa. Myoepithelial cells absent	Nodule. May be multiple
Invasive papillary carcinoma	Infiltrative growth. Frond stroma with high cellularity. Myoepithelial cells absent. High-grade cytological findings may be present	Single nodule

DCIS ductal carcinoma in situ

(NST). Metastatic lesions should be excluded when invasive papillary carcinoma is diagnosed. Immunohistochemistry always shows diffuse estrogen receptor positivity in breast papillary carcinomas, and if this marker is negative, other primary lesions must be investigated.

The table below summarizes the differences between them (Table 5.2).

5.5 Benign High-Risk Lesions and Precursors, Including Classic Lobular Intraepithelial Neoplasia

With the improvement of biopsy devices, i.e., vacuum-assisted biopsies (VAB), the ratio of false-negative results in percutaneous biopsies has been reduced, and surgical approach to avoid underestimation is no longer recommended for some high-risk lesions [3], i.e., lesions with risk for subsequent development of breast cancer lower than 2.5-fold. When appropriate sampling is achieved on a percutaneous biopsy, patients diagnosed with papilloma, radial scar, mucocele-like lesion, flat epithelial atypia, lobular atypical hyperplasia, and classic in situ lobular carcinoma may be spared of surgical intervention. It is very important, however, before adopting a conservative approach, to verify if pathological and radiological aspects are compatible; for example, the diagnosis of in situ lobular carcinoma in a nodular lesion on mammogram should be considered inappropriate. The sampled proportion of the lesion should also be regarded. Large lesions, i.e., larger than 10 mm, will

probably benefit from surgical approach. It is recommended that the pathologist specify the amount of lesion represented in the biopsy so that the radiologist can estimate how much lesion was excised.

5.6 Atypical Ductal Hyperplasia and Low-Grade Carcinoma In Situ

Definition: Atypical ductal hyperplasia is characterized by epithelial proliferation similar to low-grade ductal carcinoma in situ (monomorphic cells with distinct borders, spaces with polarized cells, absence of streaming and overlapping) that does not meet the criteria of at least two TDLUs involved and 2 mm in size, necessary to the diagnosis of DCIS (Fig. 5.2). The difference between these diagnoses, therefore, is mostly quantitative.

Even with new biopsy devices, the underestimation rates of atypical ductal hyperplasia are not negligible, and surgery is recommended for the majority of cases. However, some very small lesions and atypical incidental findings (not related to the radiological findings) may be conservatively conducted [3]. Therapeutic decision in these cases will probably be influenced by the results of trials like COMET, LORD, and LORIS that study low-grade carcinoma in situ prognosis comparing conservative conduct to surgery.

Whenever high-grade atypia is found, even in very small lesions, the diagnosis of ADH is not adequate, and the diagnosis should alert for the possibility of high-grade ductal carcinoma in situ in the surroundings.

5.7 Intermediate and High-Grade Ductal Carcinoma In Situ

DCIS of intermediate grade is composed of cells without the polarization seen in low-grade DCIS nor the highly atypical cells seen in high-grade DCIS. The cells usually show mild to moderate variability in size and shape and also present

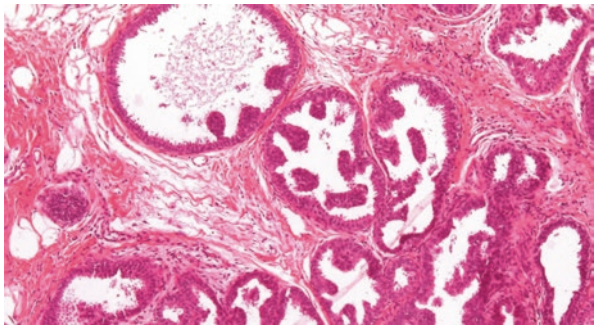

Fig. 5.2 Atypical ductal hyperplasia, micropapillary

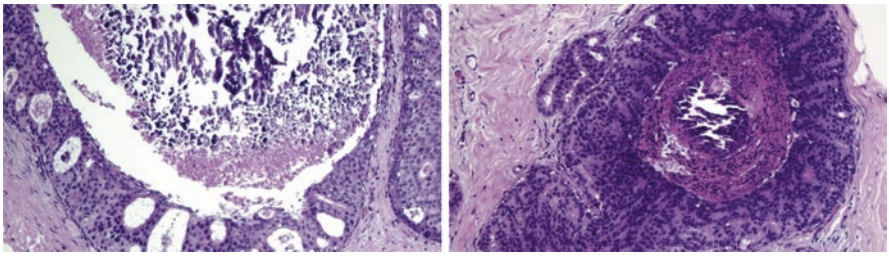

Fig. 5.3 Ductal carcinoma in situ (DCIS) of intermediate nuclear grade (grade 2)

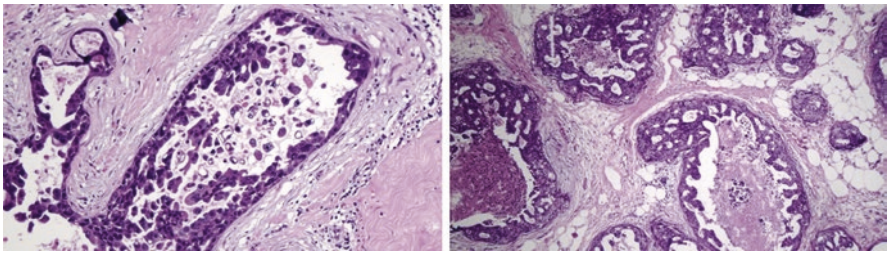

Fig. 5.4 Ductal carcinoma in situ (DCIS) of high nuclear grade (grade 3)

variably prominent nucleoli [4] (Fig. 5.3). Necrosis and microcalcifications in similar patterns seen in low- or high-grade DCIS may be present. By sharing some histological characteristics with low- and/or high-grade DCIS, it is no surprise that intermediate-grade DCIS has the least agreement between pathologists [5]. Studies show that the agreement is better when only two categories, low or high grade, are considered [6, 7]. Molecular studies support this as the intermediate-grade DCIS separates into these two and not into an individual category [8].

In summary, DCIS of intermediate grade can show any histological characteristics and immunohistochemical profile, overlapping with low- or high-grade DCIS.

High-grade DCIS presents highly atypical cells with pleomorphic nuclei, irregular contours, clumped chromatin, and prominent nucleoli [4]. Comedonecrosis is frequently seen, although not obligatory. Mitotic figures are common. High-grade DCIS may present as a mass or calcifications on mammography and as an enhancement on magnetic resonance imaging (MRI) [9] (Fig. 5.4).

5.8 Pleomorphic Lobular Carcinoma In Situ (PLCIS)

The pleomorphic LCIS variant has inactivation of e-cadherin which can be confirmed by immunohistochemistry, lacking membrane expression of e-cadherin and B-catenin and showing cytoplasmic expression of p120 [10]. Histologically, they are more similar to high-grade DCIS, showing higher nuclear grade and

comedonecrosis [11, 12] (Fig. 5.5). Compared with classic LCIS, PLCIS shows less expression of hormone receptors (estrogen and progesterone) and more chance of overexpression of HER2 [10, 11, 13].

PLCIS shares some genetic similarities with classic LCIS, including 16q loss and 1q gain, but might show a higher number of genetic alterations like gain of 16p, loss of 8p, and amplification of cyclin D1 gene [11, 14]. Biological behavior of PLCIS is more similar to high-grade DCIS [15].

5.9 Biomarkers in Ductal Carcinoma In Situ

Expression of hormonal receptors, at least estrogen receptor (ER), by immunohistochemistry is evaluated and recommended in all cases of DCIS, especially because they provide possibility of treatment with hormonal therapy [16]. Although not obligatory, HER2 evaluation in DCIS can help to understand its biological behavior and better plan its treatment as DCIS shows the same molecular classes seen in invasive carcinomas [17, 18] and more aggressive behavior in HER2 over-expressing DCIS [19] (Fig. 5.6).

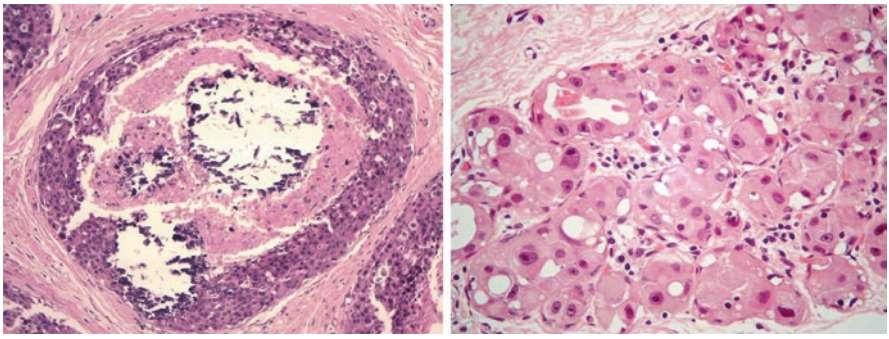

Fig. 5.5 Pleomorphic lobular carcinoma in situ (PLCIS)

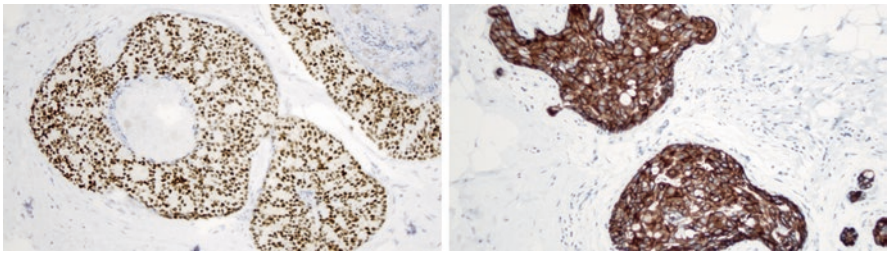

Fig. 5.6 Estrogen receptor expression and HER2 overexpression at immunohistochemistry in DCIS

The most studied characteristic of DCIS is the prediction of progression to invasive carcinoma. Several clinical studies and algorithms are known in this regard [20–23], although none can predict exactly the probability of invasion. With the improvement in the knowledge on breast carcinogenesis together with molecular technologies, other factors have been studied in DCIS, especially regarding the evolution or association with invasive carcinoma, including epithelial, myoepithelial, and microenvironment components and also combinations of those [24, 25].

The use of molecular or immunohistochemical methods to divide DCIS into classes [17, 26, 27] has provided some information as which is more (luminal-HER2) or less (triple-negative) prevalent when invasive carcinoma is present [28]; also high-grade DCIS, which includes HER2-expressing DCIS, is more associated with enhancement on MRI [29, 30]. The major genetic, molecular, and histological differences in the epithelial cells occur during progression from normal breast tissue to in situ carcinoma, and those are very similar to invasive carcinoma cells [31–33]. Although it is probably not the main driver in the progression to invasive carcinoma, there are some studies that show differences between cells in those components and possible markers helping in this prediction [34, 35].

With the improvement in the knowledge on breast carcinogenesis, the microenvironment became an integral part of the process of invasion, and it is reflected in numerous recent studies about microenvironment components. Stromal expression profile shows more differentially expressed genes between normal and DCIS-associated stroma than DCIS and invasive-associated stroma [36], although pure DCIS stroma is also different than stroma with DCIS and invasive carcinoma [37]. The vascular component of DCIS is also different compared to normal and also invasive carcinoma [38, 39]. The immune component of microenvironment also shows differences like more tumor-infiltrating lymphocytes (TILs) in DCIS with more DNA copy number aberration load [40] that histologically reflects in more TILs in high grade with HER2 overexpression and lack of ER and RP expression [41]. There are some promising studies regarding B lymphocytes in TILs, with some tumors having poor prognosis, but still they need large validation [16]. Another important component located between the DCIS neoplastic epithelial cells and the stroma is the basal membrane and myoepithelial cells; both need to be transposed for a diagnosis of invasive carcinoma [42]. Until recently, the general thought was that it was only a physical barrier, but now studies have shown that they are also an active part in the process of tumor suppressor function [43]. Also, DCIS-associated myoepithelial cells show different gene expression compared to normal breast tissue [44]. There is evidence that those gene expression differences may translate to immunohistochemical visible phenotypic alterations [45]. Based on that, it is likely that it can act as thermometers of what is happening on that interface, helping to evaluate risk of invasion in DCIS associated with other factors [24, 25].

Although there is no definite answer to which DCIS will or will not invade the adjacent stroma, the future looks promising in the discovery of more data that will help evaluate this risk even better.

5.10 Invasive Carcinoma of No Special Type

Previously known as invasive ductal carcinoma, invasive carcinoma of no special type (NST) is a diagnosis of exclusion. It is an invasive carcinoma that does not present enough histological features (more than 90% of the tumor) to be classified as any of the special types like lobular, metaplastic, tubular, and apocrine [46] (Fig. 5.7). It is the most common histological subtype of breast carcinoma, and all should be graded according to Nottingham criteria (see table below) (Table 5.3), which has direct correlation with prognosis, grade 3 carcinomas being the more aggressive ones [47].

Since the classic work of Perou [48] demonstrating the existence of different molecular classes of breast carcinomas, histologic grading is not the only important factor in its evaluation. Molecular classes also show differences in prognosis and

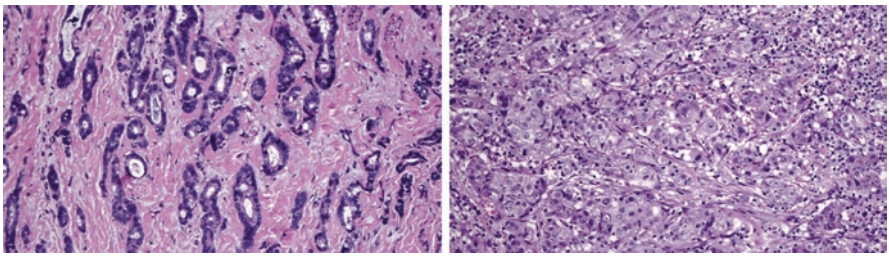

Fig. 5.7 Invasive carcinoma of no special type

Table 5.3 Nottingham criteria for invasive carcinomas of no special type (NST)

Feature	Score
Tubule and gland formation	
Majority of tumor (>75%)	1
Moderate degree (10–75%)	2
Little or none (<10%)	3
Nuclear pleomorphism	
Small, regular, uniform cells	1
Moderate increase in size and variability	2
Marked variation	3
Mitotic count (dependent on microscopic field area)	
Low	1
Moderate	2
High	3
Total score (add the scores)	*Final grading*
3–5	Grade 1
6 or 7	Grade 2
8 or 9	Grade 3

predictive factors [49]. Although the gold standard for identification of these classes is the molecular tests, in practice, immunohistochemical profile shows a good correlation with those [50, 51]. Based on that, the main molecular classes of invasive breast carcinoma can be correlated as this:

- Luminal A or B: carcinomas that express hormone receptors (ER and/or PR), without overexpression of HER2; the division between A and B has many options, but most incorporate Ki67 and the level of progesterone receptor expression – we follow this group criteria [52] (Table 5.4).
- Hybrid luminal/HER2: carcinomas that express hormone receptor (ER and/or PR) associated with overexpression of HER2 (Fig. 5.8).
- HER2: carcinomas that overexpress HER2 without expression of hormone receptors.
- Triple negative (TN): carcinomas that do not express hormone receptors nor HER2.

Invasive carcinomas of no special type are present in all of those groups, even though we can see some patterns of characteristics in some of them. Luminal A carcinomas are mostly Nottingham grade 1 with some grade 2. Hybrid, HER2, and

Table 5.4 Immunohistochemical profile and its correlation with molecular classes of invasive breast cancer

Luminal A	*All of:*
	ER positive
	HER2 negative
	And at least one of:
	Ki67 <14%
	Ki67 14–19% and PR ≥20%
Luminal B (HER2 negative)	*All of:*
	ER positive
	HER2 negative
	And at least one of:
	Ki67 14–19% and PR negative or <20%
	Ki67 ≥20%

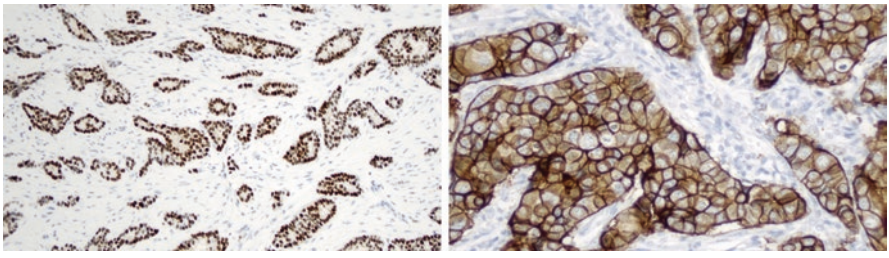

Fig. 5.8 Estrogen receptor expression and HER2 overexpression at immunohistochemistry in invasive carcinoma

TN are mostly grade 2 or 3 [53]. Special histological types show a more specific association with those classes: classic invasive lobular carcinoma is almost always luminal, predominantly A, and Nottingham grade 1 or 2. Pleomorphic lobular carcinoma can be luminal B (majority), but also hybrid, HER2, or even TN, being most Nottingham grade 2 or 3. Metaplastic and medullary carcinomas are TN and Nottingham grade 2 or 3. Some special types of carcinomas, such as adenoid cystic and secretory, can be TN and have a Nottingham low grade, but they are rare carcinomas.

With the improvement in the knowledge on breast carcinomas, its histological evaluation must have complementary immunohistochemistry to better understand its biology, predict the behavior, and offer adequate treatment.

5.11 Macroscopic Evaluation of the Breast Specimen, Including Those with Neoadjuvant Treatment

General rules for evaluation of breast specimens are well established and available in various publications like the College of American Pathologists [54] and other papers [55–57]. Here, we would like to reinforce some fundamental aspects in an attempt to better evaluate and obtain the best possible report for the other specialties that receive the anatomopathological summary.

The pathologist must have access to all data regarding the clinical, imaginological, and histological aspects about the specimen that he is evaluating. Most hospitals have integrated systems available to the pathologist, but in other scenarios, that may not be available. In this case, the pathologist must be proactive in looking for those data before evaluating and processing the specimen, as the optimal strategies in choosing which areas to evaluate happen in that first time – subsequent new cuts can be problematic as the tissue has already been cut before and its recomposition is difficult and also add to the delay in delivering the final pathological report.

Another extremely important factor in the evaluation of these specimens is the adequate fixation which does not mean just placing the specimens in formaldehyde, but it implies making sure that it can reach all areas of the specimen. Without an adequate fixation, morphological and biomarker evaluation will suffer [58, 59]. In larger specimens, it is necessary to make sections prior to fixation, so the maximum thickness should be of 10 mm or less. If the pathology laboratory is not integrated with the operating room or if the pathologist is not present at the surgery to make an evaluation and make the sections, the surgeon can do it himself.

With all specimen-related information and an adequate fixation, the pathologist can make optimal sections to provide the best anatomopathological report.

Low-grade DCIS specimens normally do not present any macroscopic lesions, so small specimens are entirely included for analysis and larger specimens can have only selected areas included, which should be chosen based on the lesion radiologic characteristics.

High-grade DCIS usually presents a macroscopic lesion, so the selection of the areas for microscopic analysis is clearer. Those which have a more extensive lesion on the radiologic exam than a visible macroscopically one - usually lesions with low cellularity and little desmoplasia - the area chosen for analysis should be bigger to not miss any lesion.

Most invasive carcinomas are macroscopically visible, the exception being some cases of low-grade carcinomas with little or no stromal reaction, as classic lobular carcinoma. At least one section per centimeter of the lesion is recommended for adequate analysis of the tumor, with the aid of radiologic data for those that do not appear macroscopically. Radiologic data can also help identify other lesions, such as in situ carcinoma, adjacent to or in other areas of the specimen, so the pathologist must have access and seek this data.

Invasive carcinomas might regress with neoadjuvant treatment, impacting survival rates [60]. Those with no response to treatment can be processed as stated above. The ones with clinical and/or radiologic response, complete or partial, provide a more complex challenge to the pathologist. Again, all the clinical, radiologic, and pathological information about the tumor is necessary for a better macroscopic evaluation and adequate selection of the areas for analysis. Triple-negative carcinomas and those that overexpress HER2 have a better chance to regress or even show complete pathological response [61–63]. At macroscopic evaluation, the pathologist can already see signs of regression and make adequate sections of the visible remaining areas of the tumor and also of the areas with regression (Fig. 5.9). Most carcinomas that have hormone receptor expression without overexpression of HER2 do not show great response to neoadjuvant treatment [61, 64, 65]. Knowing that, even with clinical and/or radiologic indication of partial regression, the pathologist must include sections that comprehend the initial area of the carcinoma so it can be adequately measured in microscopy. That is even more important in breasts with dense parenchyma or classic lobular invasive carcinomas.

If possible, all macroscopically free axillary lymph nodes should be processed as sentinel, i.e., maximum thickness of 2.0 mm, so any area with metastasis or regression will not be missed [55]. When the metastasis is macroscopically visible, only representative sections can be included.

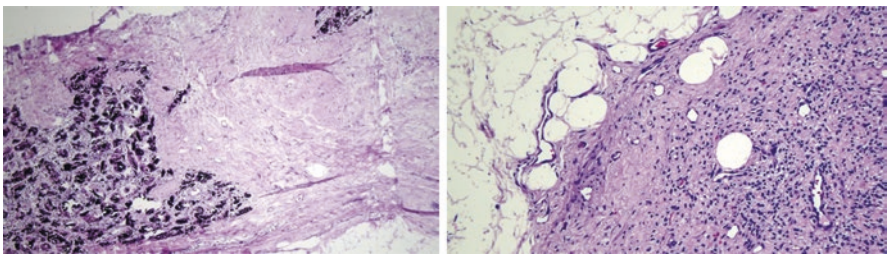

Fig. 5.9 Breast and lymph node with histological features of post-neoadjuvant chemotherapy regression

5.12 Special Subtypes

Before a diagnosis of invasive ductal carcinoma is rendered, the pathologist should verify if the clinical and morphological characteristics of the lesion do not correspond to one of the special subtypes.

The most common special subtype is invasive lobular carcinoma (approx. 15% of breast carcinomas) that is related to CDH1 gene mutation and loss of e-cadherin expression. Consequent to loss of cell-to-cell adhesion, invasive lobular carcinoma acquires different radiological findings and, not infrequently, are hard to find in screening tests (up to 19% false-negative rates) (Fig. 5.10). In spite of low nuclear grade and estrogen positivity, distant metastasis to bone, gastrointestinal tract (GIT) and ovary are more frequent than those of NST carcinoma. The incidence of contralateral tumors is also higher in this subtype. Cases with greater degree of atypia are classified as pleomorphic and exhibit association with pleomorphic LCIS.

Some of the special subtypes are related to better prognosis, e.g., mucinous (Fig. 5.11), cribriform, and tubular, and are usually estrogen positive, while others are worse, e.g., invasive micropapillary carcinomas that have higher lymph node metastasis rates. Radiological characteristics also differ among subtypes. Mucinous carcinomas may appear as benign masses on mammograms because of their regular margins, while most tubular carcinomas are spiculated. The table below summarizes these findings (Table 5.5).

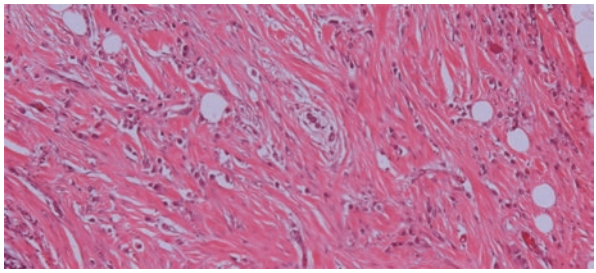

Fig. 5.10 Invasive lobular carcinoma. Isolated cells in desmoplastic stroma

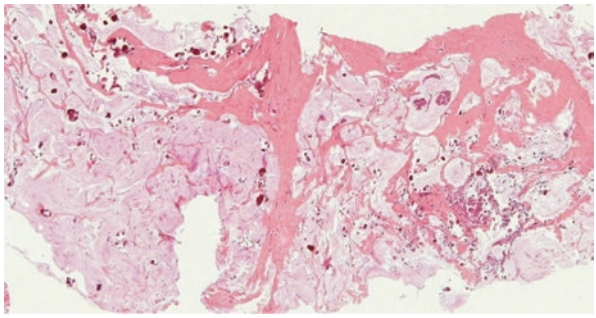

Fig. 5.11 Mucinous carcinoma. Small groups of neoplastic cells embedded in mucus

Table 5.5 Main characteristics of special subtypes of invasive carcinomas

Subtype	Clinical	Radiological	Immunohistochemical	Molecular	Prognosis
Lobular	Bilateral 5–19% Larger tumors Higher rate of node metastasis	False-neg mammo (up to 19%); irregular poor defined margins	Loss of e-cadherin ER+ HER2-	CDH1 PIK3CA	More long-term events (distant metastasis and recurrences) than IBC-NST
Tubular and cribriform	Age median 63 Small lesion	Small spiculated	ER+ HER2-	–	Favorable
Mucinous	Age median 71	Well circumscribed	ER+ HER2-	Low level of instability	Favorable (unless assoc. micropapillary pattern)
Micropapillary	Frequent axillary metastasis	Dense irregular tumors	Peripheral MUC1+	PIK3CA, TP53, GATA3, MAP2K4	Higher recurrence rate; overall similar to IBC-NST
Apocrine	Median age higher than IBC-NST	Poorly circumscribed tumors	ER- AR+ HER2+ (30–60%)	TP53, PIK3CA/ PTEN/AKT	–
Metaplastic (high grade)	Advanced stage Less node metastasis	–	ER- HER2- CK5/6+	Complex TP53, RB1, ARID1A, PI3K, MAPK, WNT	Worse than IBC-NST

A very aggressive breast carcinoma subtype is inflammatory carcinoma. Its incidence is higher in young women and among afro-descendants. The symptoms are similar to inflammatory diseases, with rapid enlargement and skin changes. Histologically, lymphovascular emboli are found, but their absence does not preclude this diagnosis. They are more frequently negative for hormonal receptors and are more HER2 positive than usual carcinomas.

5.13 Special Methods

5.13.1 Immunohistochemistry

Immunohistochemistry is the most used technique, and usual antibodies are well described in the carcinoma section. It is also used to help pathologists decide between typical and atypical hyperplasias, to define invasion (Fig. 5.12), and to subclassify carcinomas. Besides HER2 therapy, immune-checkpoint therapy is also based on immunohistochemical assays. The table below shows some of the most used antibodies (Table 5.6).

5.13.2 In Situ Hybridization

In situ hybridization allows the search of genetic alterations in slides from paraffin-embedded biopsies. In breast pathology, the main utility is to verify HER2 equivocal staining cases. The number of genes per cell and the ratio of genes and

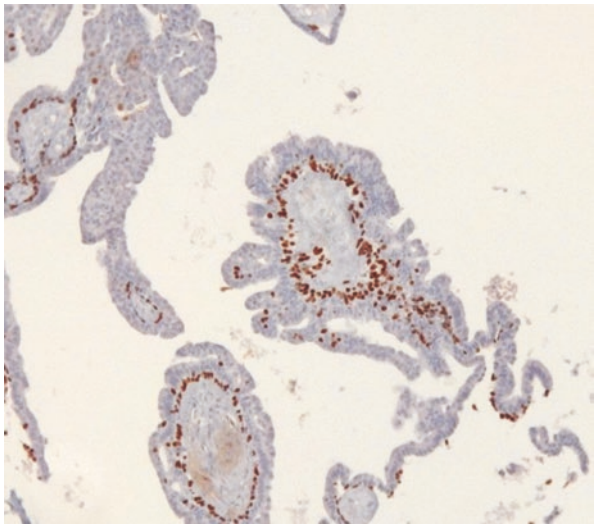

Fig. 5.12 P63 labeling myoepithelial cells in a papilloma

Table 5.6 Most common antibodies used for breast tumor evaluation

Antibody	Utility
P63, calponin, SMA, p40	Identify myoepithelial cells
CK5/6	ADH versus UDH
MUC1	Peripheral in micropapillary carcinoma
Cytokeratins	Diagnosis of spindle cell metaplastic carcinoma
E-cadherin, B-catenin, GP120	Loss of expression in ILC
GATA3, mammaglobin, Sox10	Breast primary tumors
Pax-8, Melan A, TTF1, Cdx2	Identification of metastasis to the breast
PD-L1	Identify cases that benefit from immuno-therapy (e.g., atezolizumab)

**ADH* = Atypical Ductal Hyperplasia, *UDH* = Usual Ductal Hyperplasia, *ILC* = Invasive Lobular Carcinoma

centromeres are calculated. Amplified cases are those with HER2/centromere ratio higher than 2.0 and more than 4.0 signals per cell [66].

5.14 Next-Generation Sequencing (NGS)

Next-generation sequencing is already feasible in many centers. The possibility of identification of mutations in up to 500 genes is a fantastic tool, and target specific drugs are already a reality. PIK3CA pathway inhibitors, for example, may be used in cases with diagnosed mutations. The same paraffin-embedded tissue used for routine histological analyses can be used to these molecular tests. Besides detecting specific gene mutations, investigation of tumor mutational burden and of genetic stability is also a promising tool [67].

References

1. Ng CCY, Md Nasir ND, Loke BN, Tay TKY, Thike AA, Rajasegaran V, et al. Genetic differences between benign phyllodes tumors and fibroadenomas revealed through targeted next generation sequencing. Mod Pathol. 2021;34:1320.
2. Lu Y, Chen Y, Zhu L, Cartwright P, Song E, Jacobs L, et al. Local recurrence of Benign, Borderline, and malignant Phyllodes tumors of the breast: a systematic review and meta-analysis. Ann Surg Oncol. 2019;26(5):1263.
3. Raza S. Management of high-risk breast lesions: counterpoint—time for personalized surveillance. Am J Roentgenol. 2020;216:1434.
4. Lakhani SR, Eliis IO, Schnitt SJ, Tan PH, van de Vijver MJ. WHO classification of tumors of the breast, vol. 4. Lyon: IARC Press; 2012. p. 240.

5. van Dooijeweert C, van Diest PJ, Willems SM, Kuijpers CCHJ, Overbeek LIH, Deckers IAG. Significant inter- and intra-laboratory variation in grading of ductal carcinoma in situ of the breast: a nationwide study of 4901 patients in the Netherlands. Breast Cancer Res Treat [Internet]. 2019 [cited 2020 Feb 1];174(2):479–88. Available at: http://www.ncbi.nlm.nih.gov/pubmed/30539380
6. Alghamdi SA, Krishnamurthy K, Garces Narvaez SA, Algashaamy KJ, Aoun J, Reis IM, et al. Low-grade ductal carcinoma in situ. Am J Clin Pathol [Internet]. 2020;153(3):360–7. Available at: https://academic.oup.com/ajcp/article/153/3/360/5643824
7. van Bockstal M, Baldewijns M, Colpaert C, Dano H, Floris G, Galant C, et al. Dichotomous histopathological assessment of ductal carcinoma in situ of the breast results in substantial interobserver concordance. Histopathology [Internet]. 2018;73(6):923–32. Available at: http://doi.wiley.com/10.1111/his.13741
8. Hannemann J, Velds A, Halfwerk JBG, Kreike B, Peterse JL, van de Vijver MJ. Classification of ductal carcinoma in situ by gene expression profiling. Breast Cancer Res. 2006;8(5):1–20.
9. Shehata M, Grimm L, Ballantyne N, Lourenco A, Demello LR, Kilgore MR, et al. Ductal carcinoma in situ: current concepts in biology, imaging, and treatment. J Breast Imag. 2019;1(3):166–76.
10. Dabbs DJ, Schnitt SJ, Geyer FC, Weigelt B, Baehner FL, Decker T, et al. Lobular neoplasia of the breast revisited with emphasis on the role of E-Cadherin immunohistochemistry. Am J Surg Pathol [Internet]. 2013;37(7):e1–11. Available at: http://journals.lww.com/00000478-201307000-00001
11. Wen HY, Brogi E. Lobular Carcinoma In Situ. Surg Pathol Clin [Internet]. 2018;11(1):123–45. Available at: https://linkinghub.elsevier.com/retrieve/pii/S1875918117301435
12. Ginter PS, D'Alfonso TM. Current concepts in diagnosis, molecular features, and management of lobular carcinoma in situ of the breast with a discussion of morphologic variants. Arch Pathol Lab Med [Internet]. 2017;141(12):1668–78. Available at: http://meridian.allenpress.com/aplm/article/141/12/1668/65743/Current-Concepts-in-Diagnosis-Molecular-Features
13. Shamir ER, Chen Y-Y, Chu T, Pekmezci M, Rabban JT, Krings G. Pleomorphic and florid lobular carcinoma in situ variants of the breast. Am J Surg Pathol [Internet]. 2019;43(3):399–408. Available at: http://journals.lww.com/00000478-201903000-00013
14. Chen Y-Y, Hwang E-SS, Roy R, DeVries S, Anderson J, Wa C, et al. Genetic and phenotypic characteristics of pleomorphic lobular carcinoma in situ of the breast. Am J Surg Pathol [Internet]. 2009;33(11):1683–94. Available at: http://journals.lww.com/00000478-200911000-00015
15. Foschini MP, Miglio R, Fiore R, Baldovini C, Castellano I, Callagy G, et al. Preoperative management of Pleomorphic and florid lobular carcinoma in situ of the breast: report of a large multi-institutional series and review of the literature. Eur J Surg Oncol [Internet]. 2019;45(12):2279–86. Available at: https://linkinghub.elsevier.com/retrieve/pii/S0748798319305487
16. Allison KH, Hammond MEH, Dowsett M, McKernin SE, Carey LA, Fitzgibbons PL, et al. Estrogen and progesterone receptor testing in breast cancer: American Society of Clinical Oncology/College of American Pathologists Guideline Update. Arch Pathol Lab Med [Internet]. 2020;144(5):545–63. Available at: http://meridian.allenpress.com/aplm/article/144/5/545/427509/Estrogen-and-Progesterone-Receptor-Testing-in
17. Tamimi RM, Baer HJ, Marotti J, Galan M, Galaburda L, Fu Y, et al. Comparison of molecular phenotypes of ductal carcinoma in situ and invasive breast cancer. Breast Cancer Res [Internet]. 2008;10(4):R67. Available at: http://breast-cancerresearch.biomedcentral.com/articles/10.1186/bcr2128
18. Mardekian SK, Bombonati A, Palazzo JP. Ductal carcinoma in situ of the breast: the importance of morphologic and molecular interactions. Human Pathol. 2016;49:114–23.
19. Miligy IM, Toss MS, Gorringe KL, Lee AHS, Ellis IO, Green AR, et al. The clinical and biological significance of HER2 overexpression in breast ductal carcinoma in situ: a large study from a single institution. Br J Cancer [Internet]. 2019;120(11):1075–82. Available at: http://www.nature.com/articles/s41416-019-0436-3

20. Sue GR, Lannin DR, Killelea B, Chagpar AB. Predictors of microinvasion and its prognostic role in ductal carcinoma in situ. Am J Surg [Internet]. 2013;206(4):478–81. Available at: https://linkinghub.elsevier.com/retrieve/pii/S0002961013002882
21. Badve S, A'hern RP, Ward AM, Millis RR, Pinder SE, Ellis IO, et al. Prediction of local recurrence of ductal carcinoma in situ of the breast using five histological classifications: a comparative study with long follow-up. Human Pathol [Internet]. 1998;29(9):915–23. Available at: https://linkinghub.elsevier.com/retrieve/pii/S0046817798901964
22. Silverstein MJ, Lagios MD. Choosing treatment for patients with ductal carcinoma in situ: fine tuning the University of Southern California/Van Nuys prognostic index. J Natl Cancer Inst - Monographs. 2010;41:193–6.
23. Silverstein MJ. The University of Southern California/Van Nuys prognostic index for ductal carcinoma in situ of the breast. Am J Surg [Internet]. 2003;186(4):337–43. Available at: https://linkinghub.elsevier.com/retrieve/pii/S0002961003002654
24. Hilson JB, Schnitt SJ, Collins LC. Phenotypic alterations in ductal carcinoma in situ-associated myoepithelial cells. Am J Surg Pathol [Internet]. 2009;33(2):227–32. Available at: http://journals.lww.com/00000478-200902000-00008
25. Aguiar FN, Cirqueira CS, Bacchi CE, Carvalho FM. Morphologic, molecular and microenvironment factors associated with stromal invasion in breast ductal carcinoma in situ: role of myoepithelial cells. Breast Dis. 2015;35(4):249–52.
26. Livasy CA, Perou CM, Karaca G, Cowan DW, Maia D, Jackson S, et al. Identification of a basal-like subtype of breast ductal carcinoma in situ. Human Pathol [Internet]. 2007;38(2):197–204. Available at: https://linkinghub.elsevier.com/retrieve/pii/S004681770600534X
27. Meijnen P, Peterse JL, Antonini N, Rutgers EJT, van de Vijver MJ. Immunohistochemical categorisation of ductal carcinoma in situ of the breast. Br J Cancer [Internet]. 2008;98(1):137–42. Available at: http://www.nature.com/articles/6604112
28. Doebar SC, van den Broek EC, Koppert LB, Jager A, Baaijens MHA, Obdeijn IMAM, et al. Extent of ductal carcinoma in situ according to breast cancer subtypes: a population-based cohort study. Breast Cancer Res Treat. 2016;158(1):179–87.
29. Chou S-HS, Gombos EC, Chikarmane SA, Giess CS, Jayender J. Computer-aided heterogeneity analysis in breast MR imaging assessment of ductal carcinoma in situ: correlating histologic grade and receptor status. J Magn Resonan Imag [Internet]. 2017;46(6):1748–59. Available at: http://doi.wiley.com/10.1002/jmri.25712
30. Esserman LJ, Kumar AS, Herrera AF, Leung J, Au A, Chen Y-Y, et al. Magnetic resonance imaging captures the biology of ductal carcinoma in situ. J Clin Oncol [Internet]. 2006;24(28):4603–10. Available at: http://ascopubs.org/doi/10.1200/JCO.2005.04.5518
31. Porter D, Lahti-Domenici J, Keshaviah A, Bae YK, Argani P, Marks J, et al. Molecular markers in ductal carcinoma in situ of the breast. Mol Cancer Res. 2003;1:362.
32. Hernandez L, Wilkerson PM, Lambros MB, Campion-Flora A, Rodrigues DN, Gauthier A, et al. Genomic and mutational profiling of ductal carcinomas in situ and matched adjacent invasive breast cancers reveals intra-tumour genetic heterogeneity and clonal selection. J Pathol [Internet]. 2012;227(1):42–52. Available at: http://doi.wiley.com/10.1002/path.3990
33. Aguiar FN, Mendes HN, Bacchi CE, Carvalho FM. Comparison of nuclear grade and immunohistochemical features in situ and invasive components of ductal carcinoma of breast. Revista Brasileira de Ginecologia e Obstetrícia [Internet]. 2013;35(3):97–102. Available at: http://www.scielo.br/scielo.php?script=sci_arttext&pid=S0100-72032013000300002&lng=en&nrm=iso&tlng=en
34. Pareja F, Brown DN, Lee JY, da Cruz PA, Selenica P, Bi R, et al. Whole-exome sequencing analysis of the progression from non–low-grade ductal carcinoma *in situ* to invasive ductal carcinoma. Clinical Cancer Res [Internet]. 2020;26(14):3682–93. Available at: http://clincancerres.aacrjournals.org/lookup/doi/10.1158/1078-0432.CCR-19-2563
35. Aguiar F, Mendes H, Cirqueira C, Bacchi C, Carvalho F. Basal cytokeratin as a potential marker of low risk of invasion in ductal carcinoma in situ. Clinics [Internet]. 2013;68(5):638–43. Available at: https://www.ncbi.nlm.nih.gov/pmc/articles/PMC3654300/?report=classic

36. Vargas AC, Reed AEM, Waddell N, Lane A, Reid LE, Smart CE, et al. Gene expression profiling of tumour epithelial and stromal compartments during breast cancer progression. Breast Cancer Res Treat [Internet]. 2012;135(1):153–65. Available at: http://link.springer.com/10.1007/s10549-012-2123-4
37. Sharma M, Beck AH, Webster JA, Espinosa I, Montgomery K, Varma S, et al. Analysis of stromal signatures in the tumor microenvironment of ductal carcinoma in situ. Breast Cancer Res Treat [Internet]. 2010;123(2):397–404. Available at: http://link.springer.com/10.1007/s10549-009-0654-0
38. Muggerud AA, Hallett M, Johnsen H, Kleivi K, Zhou W, Tahmasebpoor S, et al. Molecular diversity in ductal carcinoma *in situ* (DCIS) and early invasive breast cancer. Mol Oncol [Internet]. 2010;4(4):357–68. Available at: http://doi.wiley.com/10.1016/j.molonc.2010.06.007
39. Lee S, Stewart S, Nagtegaal I, Luo J, Wu Y, Colditz G, et al. Differentially expressed genes regulating the progression of ductal carcinoma in situ to invasive breast cancer. Cancer Res [Internet]. 2012;72(17):4574–86. Available at: http://cancerres.aacrjournals.org/cgi/doi/10.1158/0008-5472.CAN-12-0636
40. Hendry S, Pang J-MB, Byrne DJ, Lakhani SR, Cummings MC, Campbell IG, et al. Relationship of the breast ductal carcinoma *in situ* immune microenvironment with clinicopathological and genetic features. Clin Cancer Res [Internet]. 2017;23(17):5210–7. Available at: http://clincancerres.aacrjournals.org/lookup/doi/10.1158/1078-0432.CCR-17-0743
41. Pruneri G, Lazzeroni M, Bagnardi V, Tiburzio GB, Rotmensz N, DeCensi A, et al. The prevalence and clinical relevance of tumor-infiltrating lymphocytes (TILs) in ductal carcinoma in situ of the breast. Ann Oncol. 2017;28(2):321–8.
42. Man Y, Tai L, Barner R, Vang R, Saenger JS, Shekitka KM, et al. Cell clusters overlying focally disrupted mammary myoepithelial cell layers and adjacent cells within the same duct display different immunohistochemical and genetic features: implications for tumor progression and invasion. Breast Cancer Res [Internet]. 2003;5(6):R231. Available at: http://breast-cancer-research.biomedcentral.com/articles/10.1186/bcr653
43. Gudjonsson T, Adriance MC, Sternlicht MD, Petersen OW, Bissell MJ. Myoepithelial cells: their origin and function in breast morphogenesis and neoplasia. J Mammary Gland Biol Neoplas [Internet]. 2005;10(3):261–72. Available at: http://link.springer.com/10.1007/s10911-005-9586-4
44. Allinen M, Beroukhim R, Cai L, Brennan C, Lahti-Domenici J, Huang H, et al. Molecular characterization of the tumor microenvironment in breast cancer. Cancer Cell. 2004;6(1):17–32.
45. Hilson JB, Schnitt SJ, Collins LC. Phenotypic alterations in ductal carcinoma in situ-associated myoepithelial cells. Am J Surg Pathol. 2009;33(2):227–32.
46. Lokuhetty D, White VA, Watanabe R 1966-, Cree IA, WHO Classification of Tumours Editorial Board, International Agency for Research on Cancer. Breast tumours.
47. Elston CW, Ellis IO. pathological prognostic factors in breast cancer. I. The value of histological grade in breast cancer: experience from a large study with long-term follow-up. Histopathology [Internet]. 1991;19(5):403–10. Available at: http://doi.wiley.com/10.1111/j.1365-2559.1991.tb00229.x
48. Perou CM, Sørlie T, Eisen MB, van de Rijn M, Jeffrey SS, Rees CA, et al. Molecular portraits of human breast tumours. Nature [Internet]. 2000;406(6797):747–52. Available at: http://www.nature.com/articles/35021093
49. Sorlie T, Perou CM, Tibshirani R, Aas T, Geisler S, Johnsen H, et al. Gene expression patterns of breast carcinomas distinguish tumor subclasses with clinical implications. Proc Natl Acad Sci [Internet]. 2001;98(19):10869–74. Available at: http://www.pnas.org/cgi/doi/10.1073/pnas.191367098
50. Cheang MCU, Chia SK, Voduc D, Gao D, Leung S, Snider J, et al. Ki67 index, HER2 status, and prognosis of patients with luminal B breast cancer. J Natl Cancer Inst [Internet]. 2009;101(10):736–50. Available at: https://academic.oup.com/jnci/article-lookup/doi/10.1093/jnci/djp082

51. Nielsen TO. Immunohistochemical and clinical characterization of the basal-like subtype of invasive breast carcinoma. Clinical Cancer Res [Internet]. 2004;10(16):5367–74. Available at: http://clincancerres.aacrjournals.org/cgi/doi/10.1158/1078-0432.CCR-04-0220
52. Maisonneuve P, Disalvatore D, Rotmensz N, Curigliano G, Colleoni M, Dellapasqua S, et al. Proposed new clinicopathological surrogate definitions of luminal A and luminal B (HER2-negative) intrinsic breast cancer subtypes. Breast Cancer Res [Internet]. 2014;16(3):R65. Available at: http://breast-cancer-research.biomedcentral.com/articles/10.1186/bcr3679
53. Lopez-Garcia MA, Geyer FC, Lacroix-Triki M, Marchió C, Reis-Filho JS. Breast cancer precursors revisited: molecular features and progression pathways. Histopathology. 2010;57(2):171–92.
54. Protocol for the Examination of Resection Specimens From Patients With Invasive Carcinoma of the Breast [Internet]. 2020. Available at: www.cap.org/cancerprotocols.
55. Bossuyt V, Provenzano E, Symmans WF, Boughey JC, Coles C, Curigliano G, et al. Recommendations for standardized pathological characterization of residual disease for neoadjuvant clinical trials of breast cancer by the BIG-NABCG collaboration. Ann Oncol. 2015;26(7):1280–91.
56. Pinder SE, Rakha EA, Purdie CA, Bartlett JMS, Francis A, Stein RC, et al. Macroscopic handling and reporting of breast cancer specimens pre- and post-neoadjuvant chemotherapy treatment: review of pathological issues and suggested approaches. Histopathology. Blackwell Publishing Ltd. 2015;67:279–93.
57. Marchiò C, Maletta F, Annaratone L, Sapino A. The perfect pathology report after neoadjuvant therapy. J Natl Cancer Inst - Monographs. 2015;2015(51):47–50.
58. Khoury T. Delay to formalin fixation (cold ischemia time) effect on breast cancer molecules. Am J Clin Pathol. Oxford University Press. 2018;149:275–92.
59. Carson FL. Formaldehyde as a fixative for light and electron microscopy. Micros Today. 2000;8(5):30–1.
60. Cortazar P, Zhang L, Untch M, Mehta K, Costantino JP, Wolmark N, et al. Pathological complete response and long-term clinical benefit in breast cancer: the CTNeoBC pooled analysis. Lancet [Internet]. 2014;384(9938):164–72. Available at: https://linkinghub.elsevier.com/retrieve/pii/S0140673613624228
61. Battisti NML, True V, Chaabouni N, Chopra N, Lee K, Shepherd S, et al. Pathological complete response to neoadjuvant systemic therapy in 789 early and locally advanced breast cancer patients: the Royal Marsden experience. Breast Cancer Res Treat [Internet]. 2020;179(1):101–11. Available at: http://link.springer.com/10.1007/s10549-019-05444-0
62. Gianni L, Pienkowski T, Im Y-H, Roman L, Tseng L-M, Liu M-C, et al. Efficacy and safety of neoadjuvant pertuzumab and trastuzumab in women with locally advanced, inflammatory, or early HER2-positive breast cancer (NeoSphere): a randomised multicentre, open-label, phase 2 trial. Lancet Oncol [Internet]. 2012;13(1):25–32. Available at: https://linkinghub.elsevier.com/retrieve/pii/S1470204511703369
63. Santonja A, Sánchez-Muñoz A, Lluch A, Chica-Parrado MR, Albanell J, Chacón JI, et al. Triple negative breast cancer subtypes and pathologic complete response rate to neoadjuvant chemotherapy. Oncotarget [Internet]. 2018;9(41):26406–16. Available at: https://www.oncotarget.com/lookup/doi/10.18632/oncotarget.25413
64. Cottu P, D'Hondt V, Dureau S, Lerebours F, Desmoulins I, Heudel P-E, et al. Letrozole and palbociclib versus chemotherapy as neoadjuvant therapy of high-risk luminal breast cancer. Ann Oncol [Internet]. 2018;29(12):2334–40. Available at: https://linkinghub.elsevier.com/retrieve/pii/S0923753419342358
65. Haque W, Verma V, Hatch S, Suzanne Klimberg V, Brian Butler E, Teh BS. Response rates and pathologic complete response by breast cancer molecular subtype following neoadjuvant chemotherapy. Breast Cancer Res Treat [Internet]. 2018;170(3):559–67. Available at: http://link.springer.com/10.1007/s10549-018-4801-3

66. Wolff AC, Hammond MEH, Allison KH, Harvey BE, Mangu PB, Bartlett JMS, et al. Human epidermal growth factor receptor 2 testing in breast cancer: American Society of Clinical Oncology/College of American Pathologists Clinical Practice Guideline Focused Update. J Clin Oncol. 2018;36(20):2105.
67. Colomer R, Mondejar R, Romero-Laorden N, Alfranca A, Sanchez-Madrid F, Quintela-Fandino M. When should we order a next generation sequencing test in a patient with cancer? EClinicalMedicine. 2020;25:100487.

Part II
Update in Imaging Method

Chapter 6
Radiation Based Imaging: Digital Mammography, Tomosynthesis

Almir Galvão Vieira Bitencourt and Carolina Rossi Saccarelli

6.1 Introduction

Mammography is the most used imaging method for breast cancer screening in average-risk women. In fact, it is still the mainstay of breast cancer screening because it is broadly available, with established quality assurance, and has demonstrated within multiple historic randomized controlled trials to reduce breast cancer mortality in this population [1–4]. One of the main advantages of mammography over other modalities is the ability to identify calcifications, which are the only initial manifestation in about 30–50% of non-palpable breast cancers, especially in ductal carcinoma in situ (DCIS). However, mammography sensitivity for breast cancer detection varies with breast density and is lower for women with heterogeneously dense or extremely dense fibroglandular tissue [5].

Radiation-based breast imaging has undergone an impressive evolution in the past decades [6, 7]. The transition from conventional screen-film mammography to full-field digital mammography (DM) allowed higher accuracy for women younger than 50 years and women with heterogeneously dense or extremely dense breasts, in addition to improvement in mammography workflow, lower radiation dose, and faster localization procedures [8, 9]. More recently, digital breast tomosynthesis (DBT), which is an evolution of DM, has improved both screening and diagnostic

A. G. V. Bitencourt (✉)
A.C.Camargo Cancer Center, São Paulo, SP, Brazil

Diagnósticos da América SA, São Paulo, SP, Brazil
e-mail: almir.bitencourt@accamargo.org.br

C. Rossi Saccarelli
Diagnósticos da América SA, São Paulo, SP, Brazil

Hospital Sírio-Libânes, São Paulo, SP, Brazil
e-mail: carolina.srossi@hsl.org

S. J. Kim Hsieh, E. A. Morris (eds.), *Modern Breast Cancer Imaging*,
https://doi.org/10.1007/978-3-030-84546-9_6

imaging by decreasing the confounding effect of overlapping tissue, improving lesion detection, characterization, and localization [10, 11].

In this chapter, we will briefly discuss the technique of modern radiation-based breast imaging methods (DM and DBT), their indications, and basic interpretation.

6.2 Technique

Radiation-based breast imaging is formed by recording pattern of X-rays transmitted through the volume of the breast into an image receptor with high spatial resolution. While DM provides two-dimensional (2D) images based on stationary X-ray emission, DBT provides multiple projection images that are acquired, while the X-ray source makes an angular scanning motion and the acquired projections are reconstructed to provide sections parallel to the film. Although DBT images are acquired in low doses, the combination of DM and DBT approximately doubles the radiation exposure to the patient. Synthetic 2D mammography from DBT images has been developed to reduce the radiation dose with comparable diagnostic accuracy to DM; however, its use depends on the radiologists' learning curve [12].

Standard views in both DM and DBT include craniocaudal (CC) and mediolateral oblique (MLO) views (Fig. 6.1), which comprise routine screening exams. Diagnostic mammography sometimes requires obtaining additional views to further characterize inconclusive findings, which include:

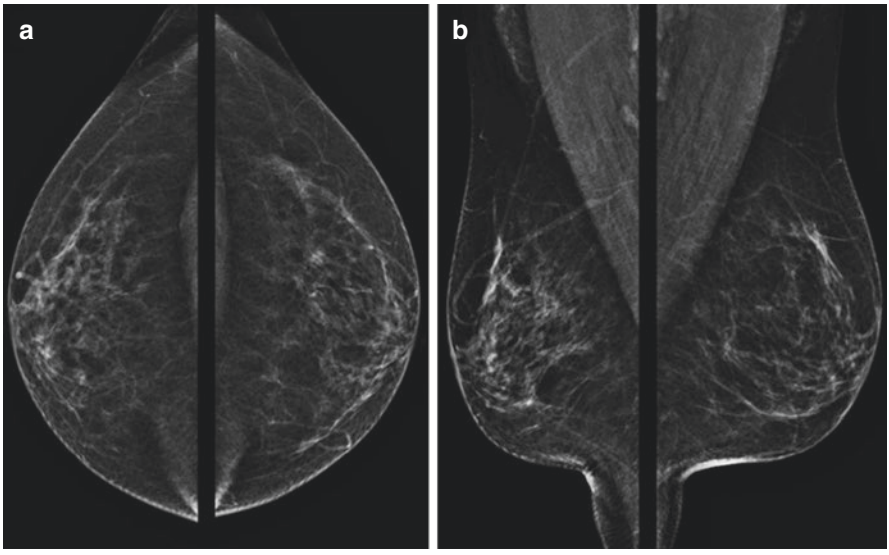

Fig. 6.1 Example of standard mammography views: (**a**) craniocaudal (CC); (**b**) mediolateral oblique (MLO)

- True lateral view: it is used to determine the exact location of a lesion, to guide stereotactic percutaneous procedures, and to evaluate calcifications of probable intracystic nature; it can be performed in mediolateral (ML) or lateromedial (LM) views; in both, the device will be positioned at 90° (it is usually positioned at 45° on MLO view) (Fig. 6.2).
- Magnification view: it is mandatory for the evaluation of the morphology and distribution of calcifications; the breast is positioned on a device which brings the breast closer to the X-ray source and allows the acquisition of magnified images (1.5–2x larger) of the region of interest (Fig. 6.3).
- Spot compression view: it is used on DM to perform a focal compression over asymmetries and masses, which is used to separate overlapping structures and improve lesion characterization (Fig. 6.4); this additional view is becoming less frequently used after the advent of DBT.

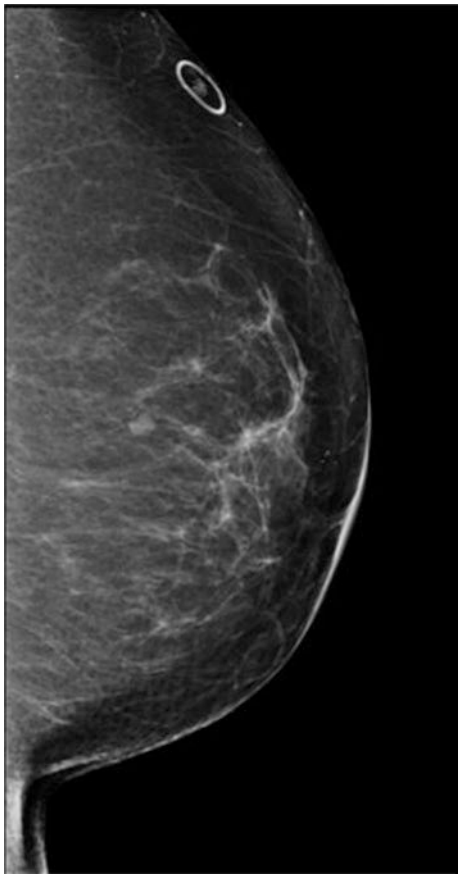

Fig. 6.2 Example of true lateral view on left mammography showing a circumscribed small mass in the posterior third of the upper quadrants

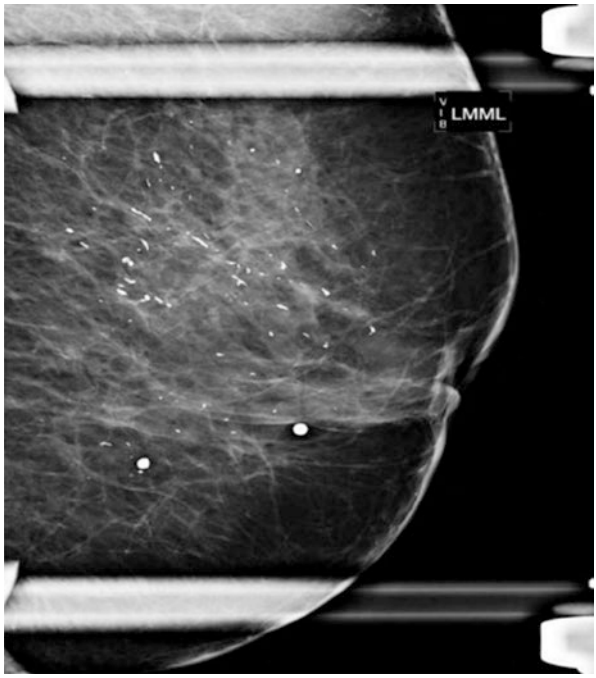

Fig. 6.3 Example of magnification view on left mammography showing large rod-like calcifications

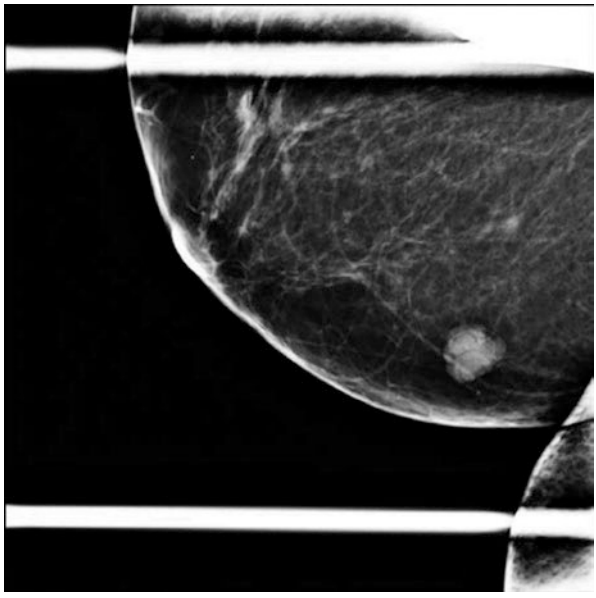

Fig. 6.4 Example of spot compression view on right mammography showing an irregular mass with microlobulated margins

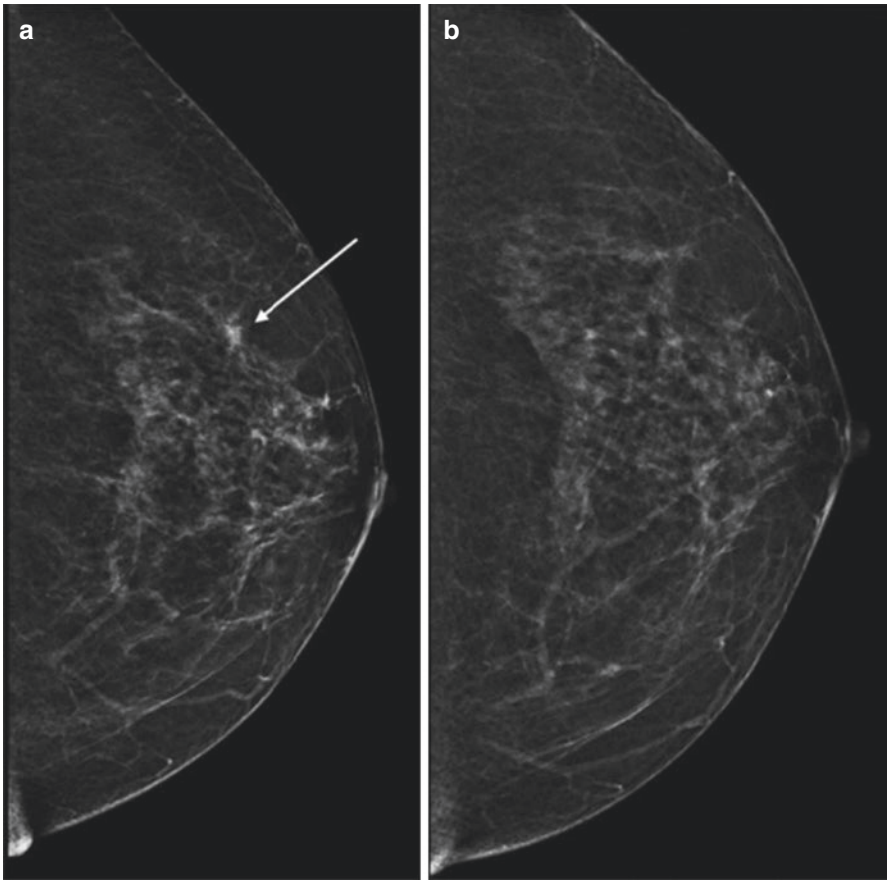

Fig. 6.5 Example of regular and rolled CC view on left mammography. Regular CC view (**a**) showed an asymmetry in the outer quadrants (arrow), which was not characterized on rolled CC view (**b**), corresponding to overlapped breast tissue

- Rolled CC view: it should be performed to confirm the presence and location of a lesion only visible in CC, which often turns to be not a true lesion, but a result of overlapped tissues in the standard view; as the spot compression, this additional view is also much less used after the advent of DBT (Fig. 6.5).
- Exaggerated CC views: also called the "Cleopatra view"; it should be performed to access deep and lateral tissue in the outer quadrants of the breast or axillary tail (Fig. 6.6).
- Cleavage view: also called the "valley view"; it should be used for the evaluation of lesions in the posterior and medial portion of both breasts (Fig. 6.7).
- Axillary view: it allows to characterize structures in the axillary tail, such as level I and II lymph nodes, palpable lesions, and metallic clips (Fig. 6.8).

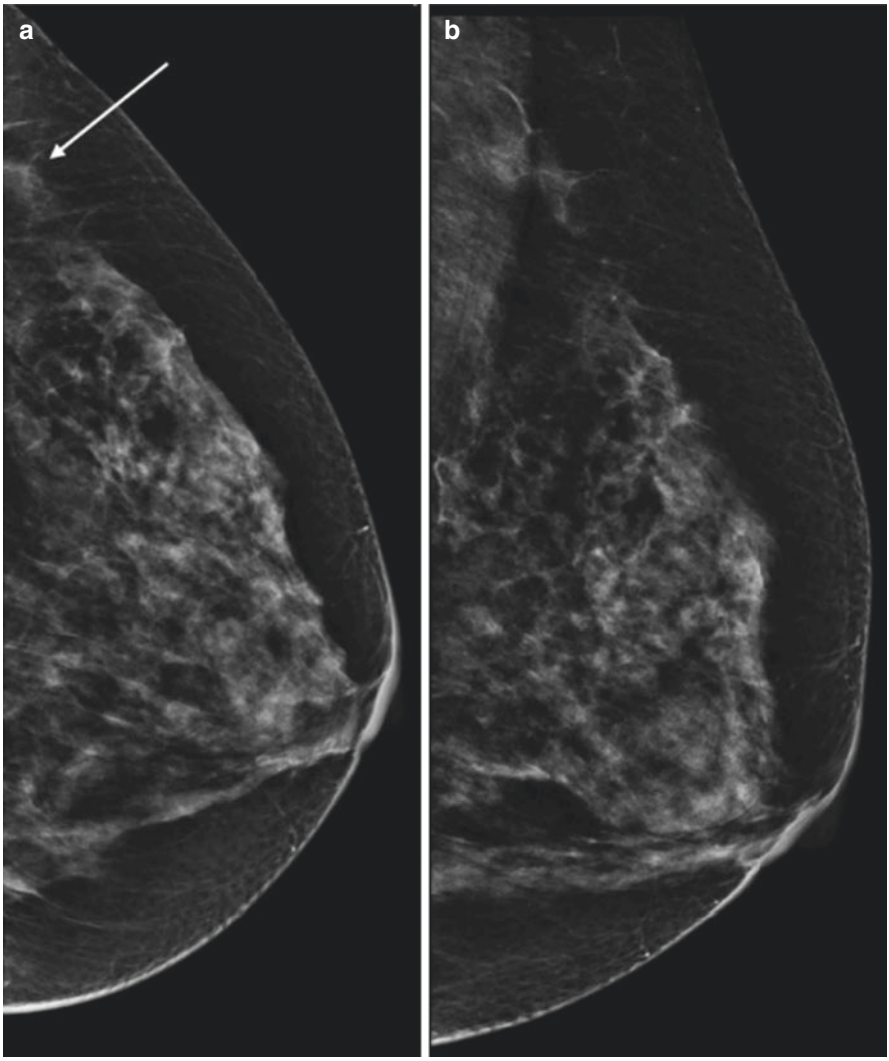

Fig. 6.6 Example of regular and exaggerated CC view on left mammography. Regular CC view (**a**) partially showed an asymmetry in the posterior third of the outer quadrants (arrow), which was better characterized on exaggerated CC view (**b**)

- Tangential view: it is useful to differentiate cutaneous from intraparenchymal calcifications and masses (Fig. 6.9); also less used after DBT, since the slices can demonstrate that the lesion is on the skin.
- Eklund technique: it is aimed at patients who have silicone implants and consists of posterosuperior displacement of the implants simultaneously to an anterior traction of the breast, allowing better visualization of the anterior breast tissue (Fig. 6.10).

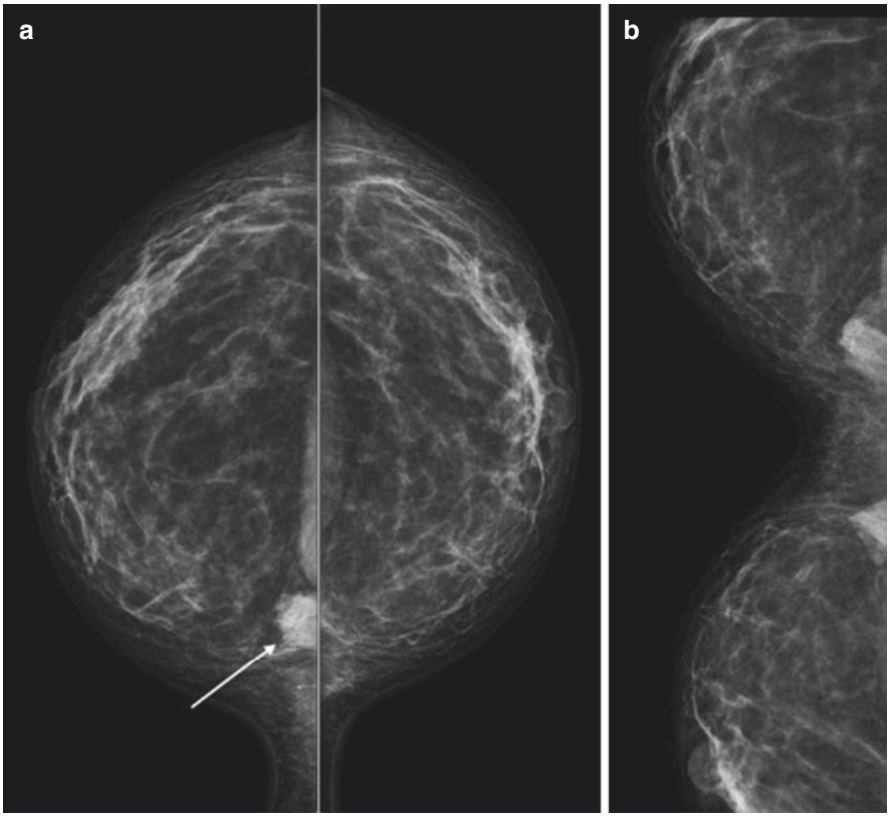

Fig. 6.7 Example of cleavage view on mammography. Regular CC view (**a**) showed an asymmetry in the inner quadrant of the right breast (arrow). Cleavage view (**b**) confirmed the finding and also showed a contralateral symmetric finding, compatible with sternalis muscle (anatomic variant)

6.3 Indications

Mammography is considered the best imaging modality for average-risk screening because it is the only method that has proven to be cost-effective and has shown a reduction in breast cancer mortality [2]. However, the sensitivity of screening mammography depends on factors such as the patient's age, density of breast tissue, and use of hormone replacement therapy. Thus, for young patients or those with dense breasts that are at higher risk of breast cancer, other imaging methods can be associated with mammography, with the aim of increasing the sensitivity of the screening.

The recommendations of different societies differ in relation to the periodicity (annual or biannual), age of beginning and stopping population screening [13–18]. Virtually all specialty societies recommend mammographic screening for women between 50 and 69 years old, with an interval never exceeding 2 years. In women

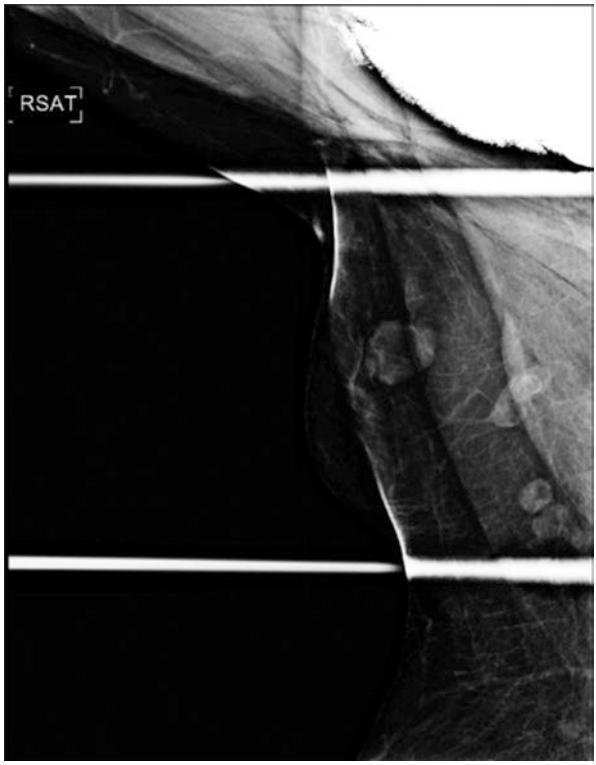

Fig. 6.8 Example of right axillary view with spot compression showing typical lymph nodes

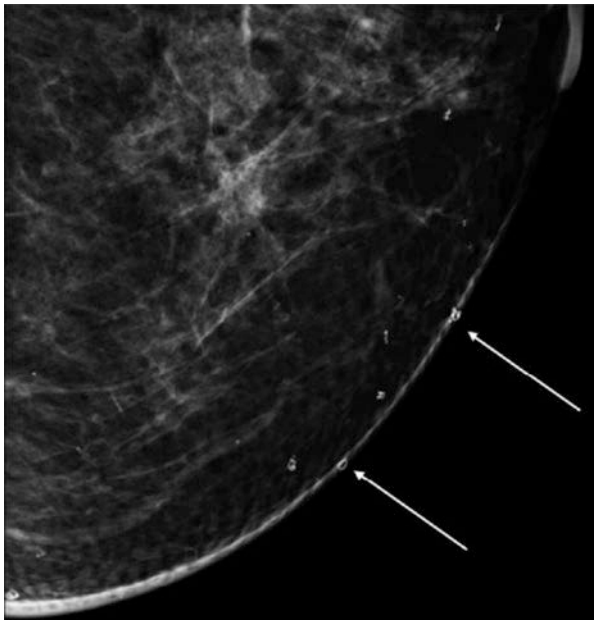

Fig. 6.9 Example of tangential view on left mammography, demonstrating cutaneous calcifications (arrows)

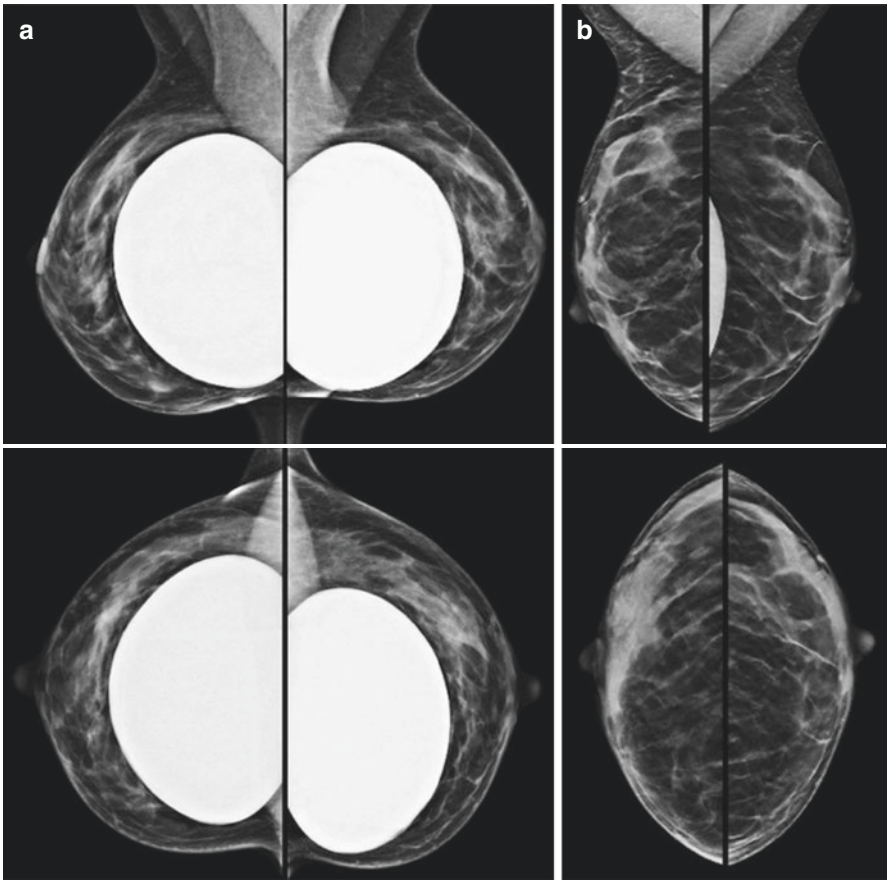

Fig. 6.10 Example of standard mammography views (**a**) and mammography views using Eklund technique (**b**) in a patient with breast implants

between age 40 and 49, the indication for screening is controversial, because in this population the incidence of cancer is lower and there is a higher frequency of dense breasts, reducing the effectiveness of screening. However, several studies have proven the benefit of mammographic screening also in this age group, especially with DM and DBT. For women under the age of 40 years, without a high risk of developing breast cancer, mammographic screening is not recommended due to the low frequency of the tumor, lower sensitivity of the mammogram, and greater radiosensitivity of the parenchyma. For women over age of 70, the decision to suspend screening should be individualized, considering global health, comorbidities, and life expectancy.

Several studies have demonstrated the benefit of DBT over DM for breast cancer screening, especially in women with dense breasts, with an increased rate of breast cancer detection, an increase in the positive predictive value of patients summoned for reassessment, and a reduction in the recall rates [19–24]. DBT also allows better

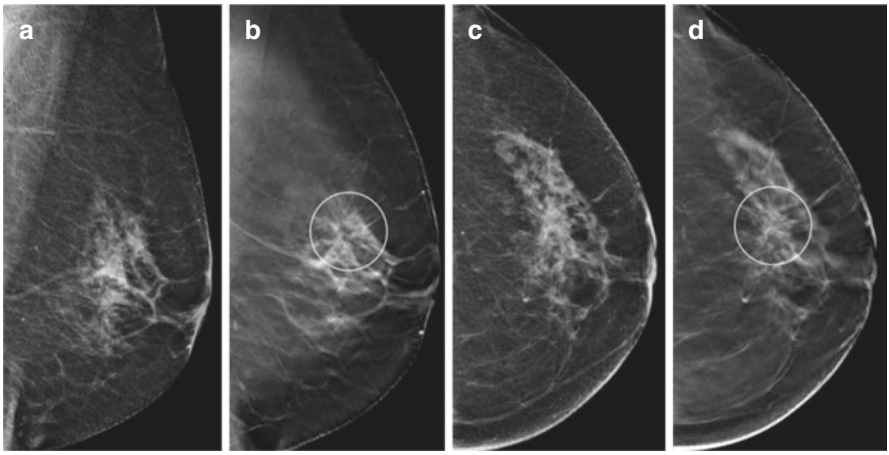

Fig. 6.11 Example of architectural distortion in the upper outer quadrant of the left breast (circle), better seen on tomosynthesis images ((**b**): MLO view; (**d**): CC view) than digital mammography images ((**a**): MLO view; (**c**): CC view), which was confirmed as an invasive lobular carcinoma

characterization of margins and location of breast lesions due to the elimination of tissue overlap, especially in spiculated lesions (Fig. 6.11).

In addition to breast cancer screening, DM or DBT is also indicated for evaluation of patients with clinical complaints (e.g., palpable lump, pain, or nipple discharge), complementary assessment of breast lesions identified in other imaging methods, staging and therapeutic planning for patients with diagnosed breast cancer, and to guide percutaneous biopsy and preoperative location of lesions identified on mammography, especially microcalcifications [25].

6.4 Interpretation

Both DM and DBT reports should follow the American College of Radiology – Breast Imaging Reporting and Data System (ACR-BI-RADS®) lexicon and must include indication of the exam, breast composition, and comparison with previous exams [26]. The report must also include an assessment category and management recommendation based on the relevant findings described on the exam and their probability of malignancy.

6.4.1 Breast Composition

Breasts can be presented to mammography in four composition subtypes: almost entirely fatty breasts; breasts with scattered areas of fibroglandular density; heterogeneously dense breasts, which may obscure small masses; and extremely dense

breasts, which lower the sensitivity of mammography (Fig. 6.12). Heterogeneously and extremely dense breasts may require supplemental imaging to avoid false-negative results, even on DBT.

6.4.2 Masses

They are three-dimensional findings and must be described according to the shape (oval, round or irregular), margins (circumscribed, obscured, indistinct, microlobulated and spiculated), and density in relation to the normal fibroglandular tissue (fat-containing, low, equal, or high density) (Figs. 6.13, 6.14, and 6.15).

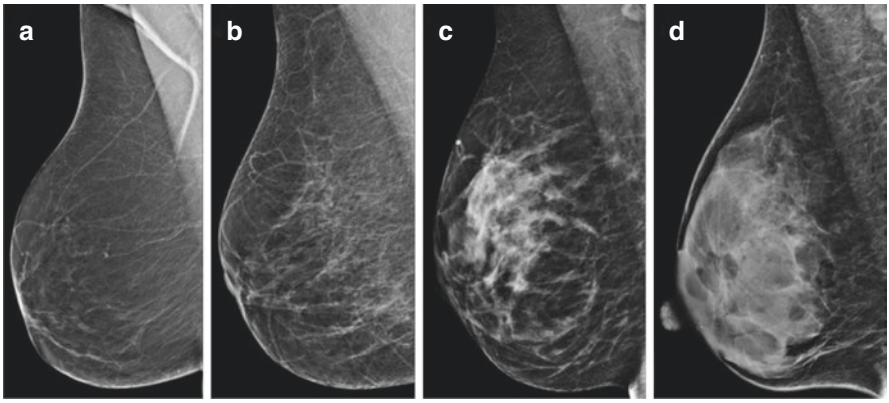

Fig. 6.12 Examples of different composition subtypes on mammography: (**a**) almost entirely fatty breast; (**b**) breast with scattered areas of fibroglandular density; (**c**) heterogeneously dense breast; (**d**) extremely dense breast

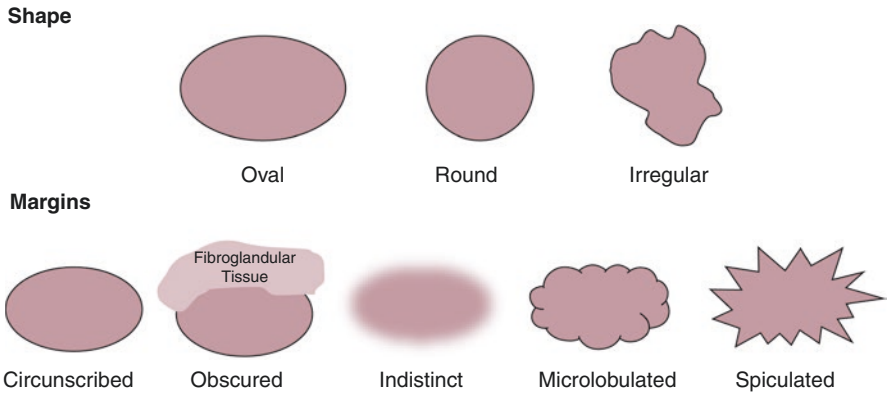

Fig. 6.13 Illustration of mass shape and margins according to the BI-RADS fifth edition

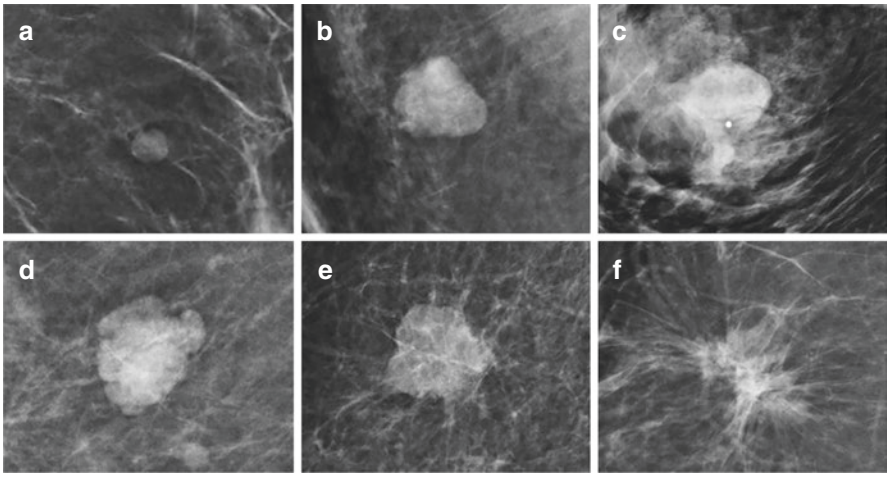

Fig. 6.14 Examples of masses with different shapes and margins on mammography: (**a**) round shape and circumscribed margins; (**b**) oval shape and circumscribed margins; (**c**) oval shape and obscured margins; (**d**) irregular shape and microlobulated margins; (**e**) irregular shape and indistinct margins;(**f**) irregular shape and spiculated margins

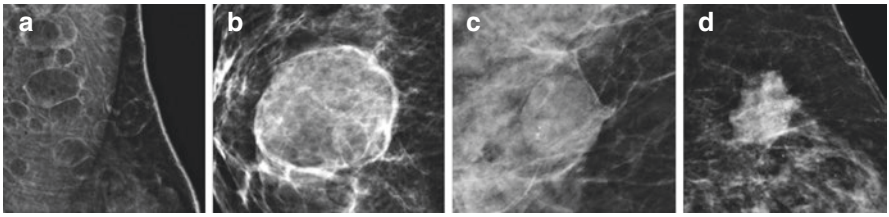

Fig. 6.15 Examples of masses with different densities on mammography: (**a**) fat-containing oval masses; (**b**) low-density oval mass; (**c**) equal-density (isodense) oval mass; (**d**) high-density irregular mass

6.4.3 Calcifications

Their morphology and distribution in the breast parenchyma must be taken into account. According to their distribution (Fig. 6.16), they should be classified as:

- Diffuse, when they are present in the entire breast.
- Grouped, when at least five calcifications are observed in a space of less than 1 cm^2, with the upper limit of 2 cm.
- Regional, when they occupy an area greater than 2 cm.
- Linear, suggesting ductal involvement.
- Segmental, inferring involvement of a ductal tree.

According to the morphology, calcifications should be classified as typically benign (skin, vascular, coarse or popcorn-like, large rod-like, rim, dystrophic, milk of calcium, and suture) or suspicious (amorphous, coarse heterogeneous, fine pleomorphic, fine linear, or fine linear branching) (Figs. 6.17 and 6.18). Round or

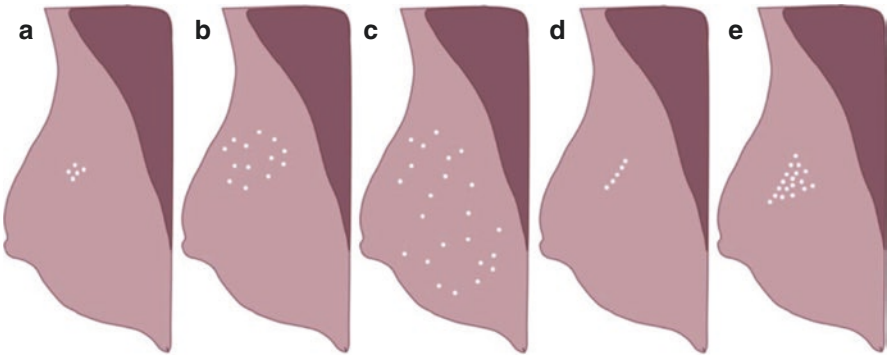

Fig. 6.16 Illustration of calcification distribution according to the BI-RADS fifth edition: (**a**) grouped; (**b**) regional; (**c**) diffuse; (**d**) linear; (**e**) segmental

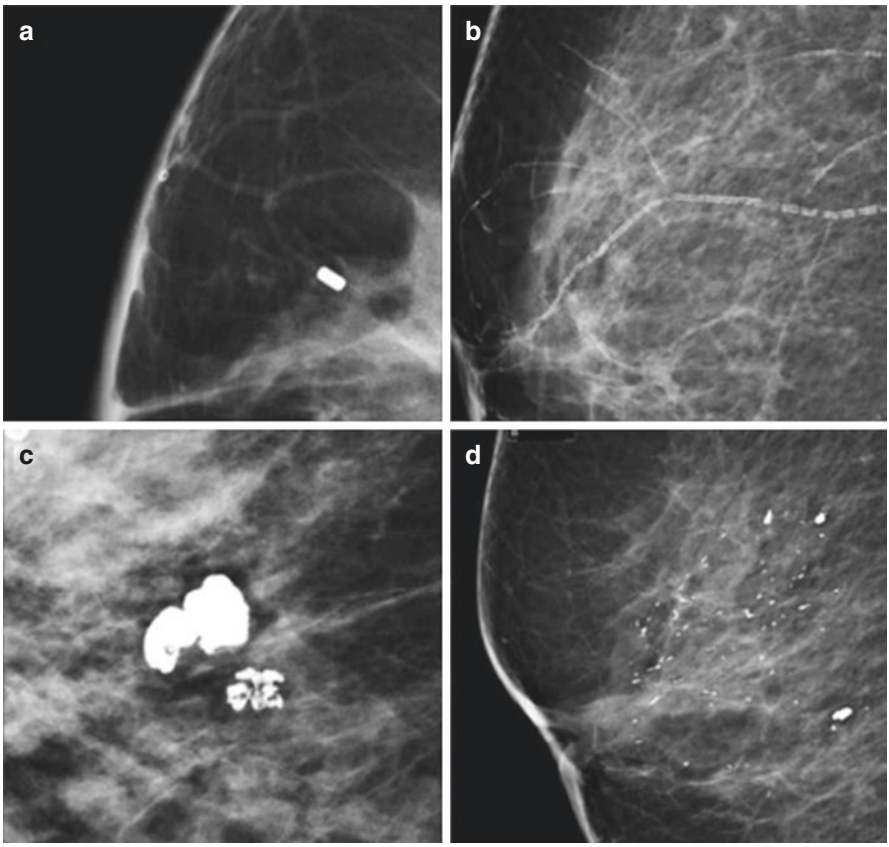

Fig. 6.17 Examples of typically benign breast calcifications on mammography: (**a**) skin lucent-centered calcifications; (**b**) vascular calcifications in blood vessels; (**c**) coarse or popcorn-like calcifications, typical of involuting fibroadenomas; (**d**) large rod-like intraductal calcifications; (**e**) rim "eggshell" calcification; (**f**) dystrophic calcifications; (**g**) suture calcifications; (**h**) milk of calcium sedimented calcifications in macro- or microcysts, usually more clearly defined on the true lateral view

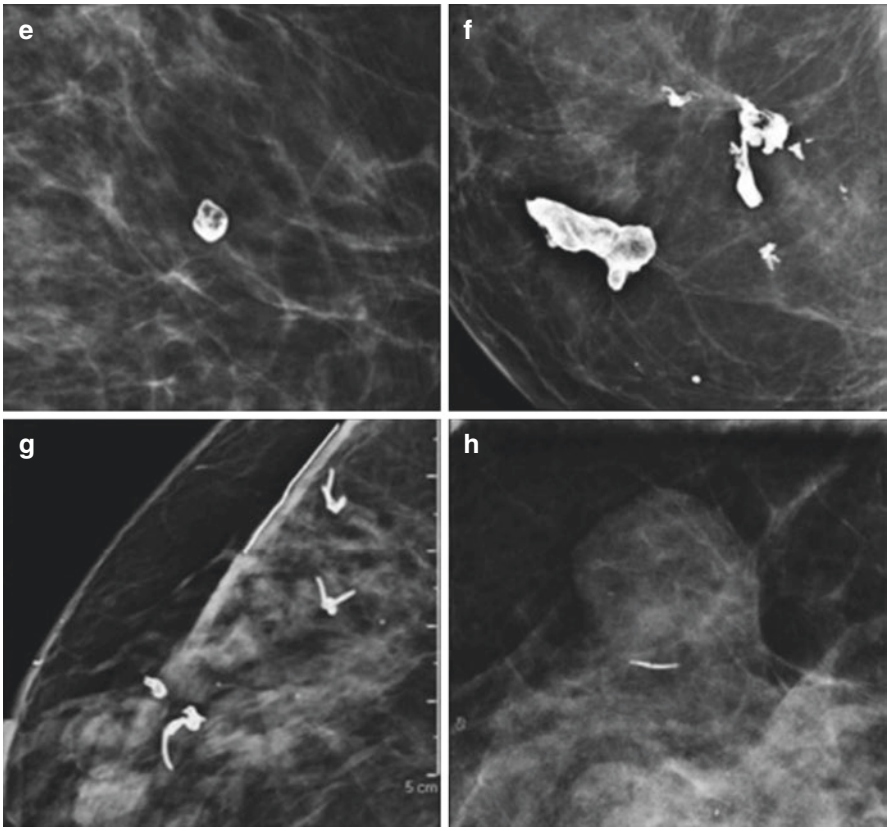

Fig. 6.17 (continued)

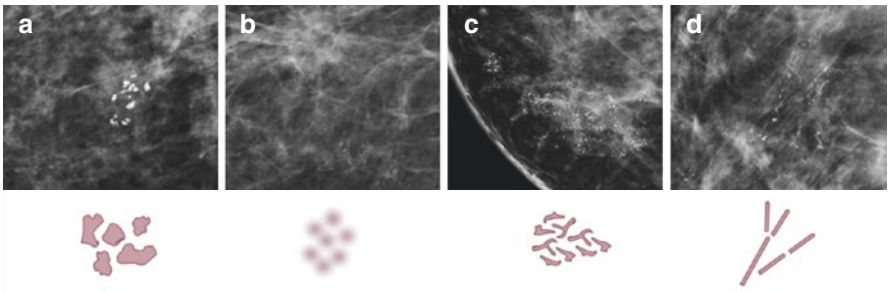

Fig. 6.18 Examples of calcifications with suspicious morphology on mammography: (**a**) coarse heterogeneous calcifications; (**b**) amorphous calcifications; (**c**) fine pleomorphic calcifications; (**d**) fine linear and fine linear branching calcifications

punctate calcifications are classified based on their distribution into benign (scattered or diffuse distribution), probably benign (grouped), or suspicious (linear or segmental distribution) (Fig. 6.19).

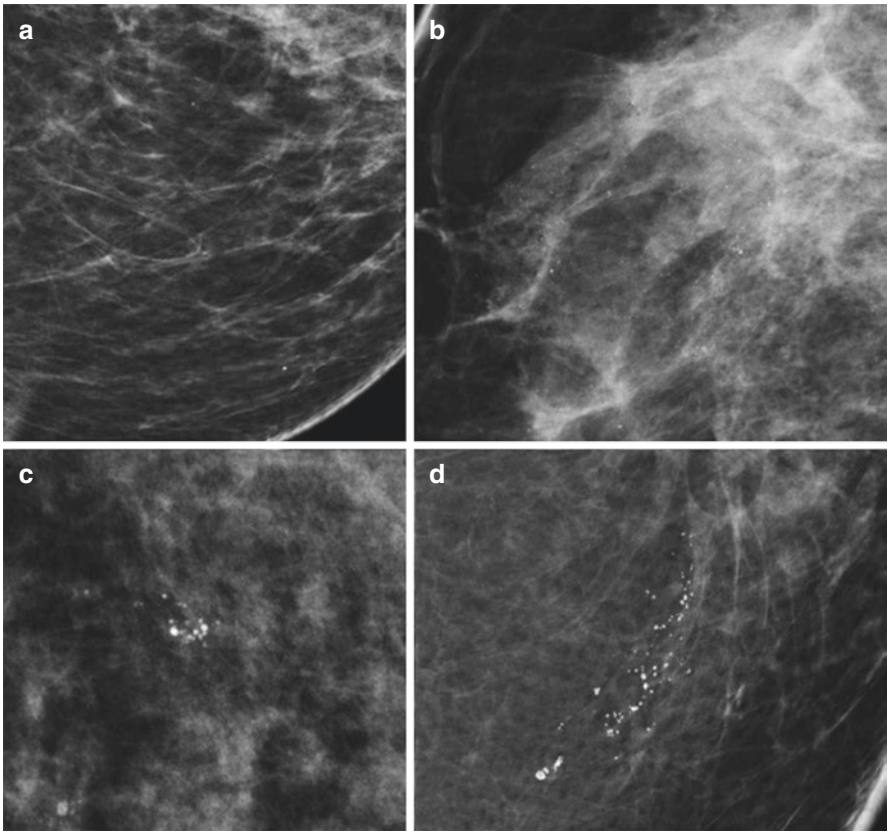

Fig. 6.19 Examples of round and punctate (<0.5 mm) calcifications with different distributions on mammography: (**a**) scattered isolated round calcifications (typically benign); (**b**) diffuse small punctate calcifications (typically benign); (**c**) grouped round calcifications (probably benign); (**d**) segmental round calcifications (suspicious)

6.4.4 Architectural Distortion

This finding may be related to previous surgeries and the presence or absence of other associated findings such as nodules or microcalcifications (Fig. 6.20). If there is no personal history of surgery, trauma, or radiation therapy, any architectural distortion should be considered suspicious for malignancy. These findings are particularly best characterized on DBT (Fig. 6.11) [27].

6.4.5 Asymmetries

According to the ACR-BI-RADS® classification, they should be named as:

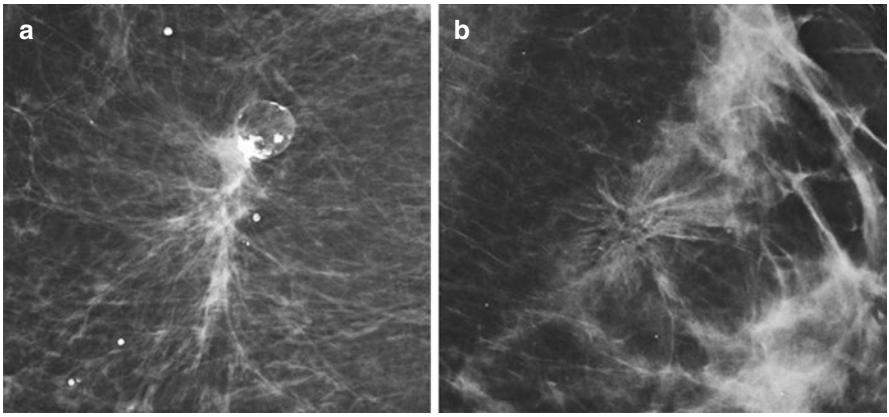

Fig. 6.20 Examples of architectural distortions on mammography: (**a**) postoperative changes; (**b**) invasive lobular carcinoma

- Asymmetry: Lesion seen in only one breast and in only one incidence of the mammographic exam. About 80% of the asymmetries are images formed by the overlapping of the breast tissue and complementary views such as magnification and compression or even the repetition of the exam can be sufficient to define whether the lesion is an image overlay or not (Fig. 6.21).
- Global asymmetry: They are seen in only one breast but in both views (caudal skull and oblique mediolateral) and occupy an area larger than one quadrant, being benign in most cases, except when there is an associated clinical symptom (Fig. 6.22).
- Focal asymmetry: Lesion seen in only one breast but in both views, occupying an area smaller than one quadrant. If there is no correspondent on ultrasound, they are considered ACR-BI-RADS® 3 because they have a malignancy index below 1%, when they are not associated with other suspicious findings (Fig. 6.23).
- Developing asymmetry: It has the same concept as a focal asymmetry, but it is more dense or larger when compared to the previous exam (Fig. 6.24). Therefore, for its characterization, it is mandatory to have a previous exam for comparison, and it has a malignancy index of 13 to 27% and should always be submitted to a histological study (ACR-BI-RADS 4) [28].

6.4.6 Intramammary Lymph Node

They are regular nodules with a fatty central hilum, often appear close to the vessels, and can present in any location of the breast, being more common in the upper outer quadrant (Fig. 6.25) [29].

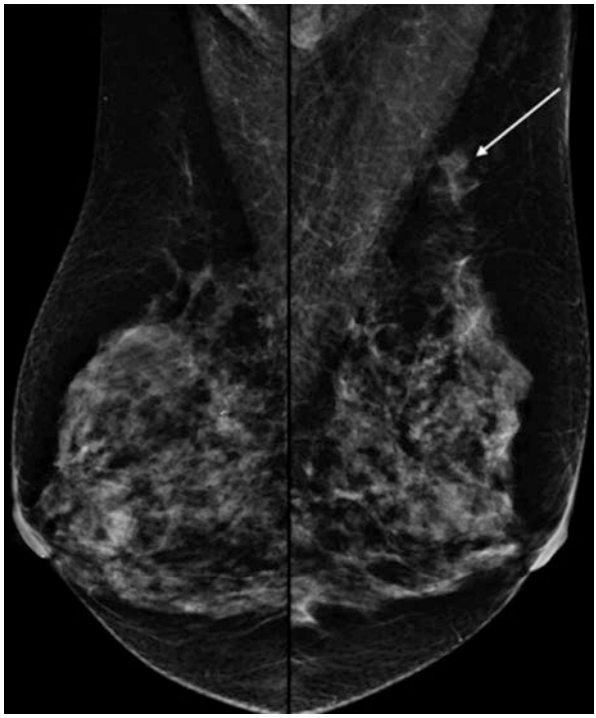

Fig. 6.21 Example of asymmetry in the upper quadrants of the left breast (arrow), not seen on CC view

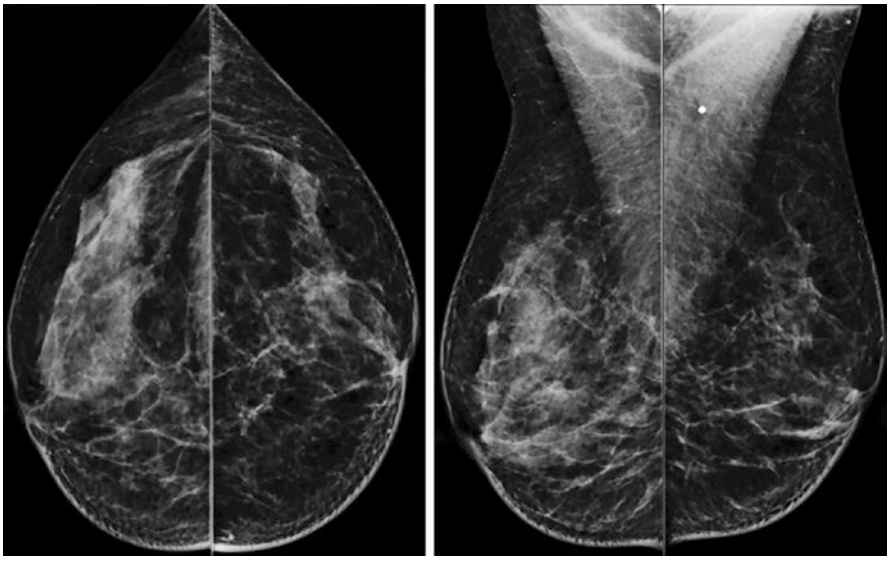

Fig. 6.22 Example of global asymmetry in the right breast

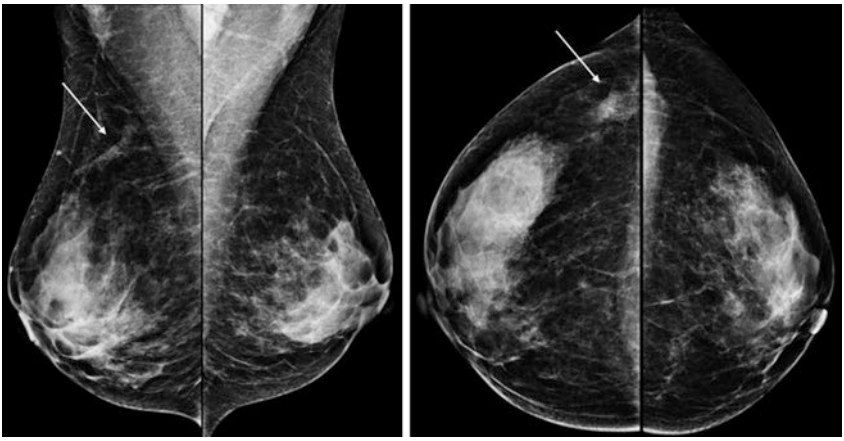

Fig. 6.23 Example of focal asymmetry in the upper outer quadrant of the right breast (arrows)

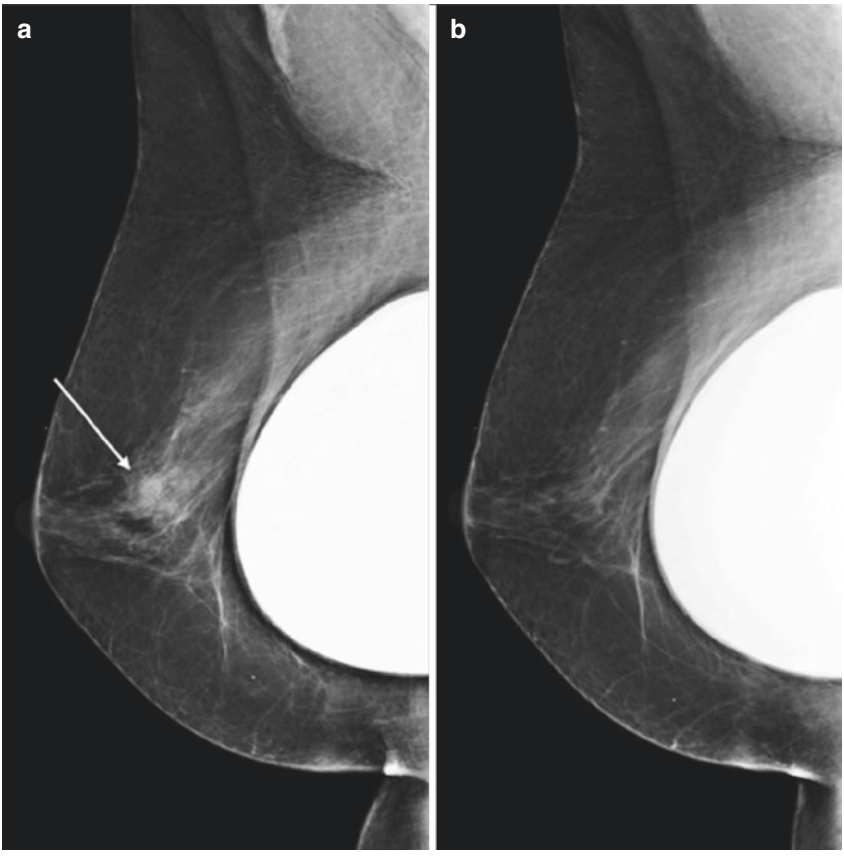

Fig. 6.24 Example of developing asymmetry in the central portion of the right breast (arrow in **a**), not seen on prior exam (**b**)

6.4.7 Skin Lesions

Skin breast lesions are usually associated to benign conditions; however, they may mimic breast lesions at mammography (Fig. 6.26). Placement of a metallic marker on skin lesions identified prior to mammography is essential to reduce additional

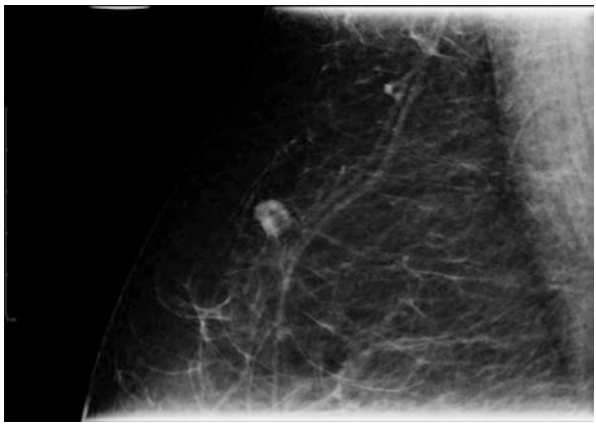

Fig. 6.25 Example of typical intramammary lymph node in the right breast

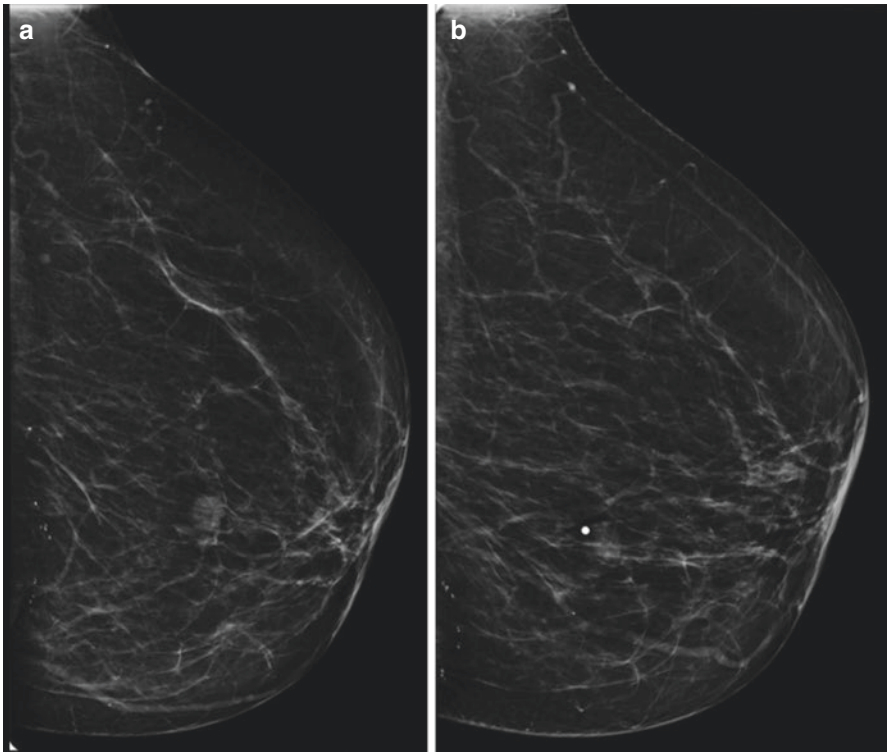

Fig. 6.26 Example of cutaneous cyst mimicking a mass in the left breast. (**a**) CC view with no marker. (**b**) CC view with metallic marker in the skin lesion

workup. On the other hand, breast cancer may present as a superficial lesion, and thus, any new, increasing, or suspicious superficial finding, not related to known skin lesions, should undergo additional imaging for further characterization [30].

6.4.8 Single Dilated Duct

It is a rare finding (Fig. 6.27), but it can be associated with DCIS. Recent studies have suggested that the positive predictive value of this findings is low and ultrasound should be performed to better assess ductal content [31].

6.4.9 Associated Findings

They are the result of the effect that a lesion can cause in the surrounding tissues, including skin thickening and retraction, nipple retraction, trabecular thickening (edema), axillary adenopathy, architectural distortion, and calcifications (Figs. 6.28 and 6.29).

6.4.10 Location of Lesions

Lesions identified on DM or DBT should be located in relation to its laterality, quadrant (or clock face), depth (anterior, middle, or posterior), and distance from the nipple. It is important to remember that the location of a lesion in the MLO view

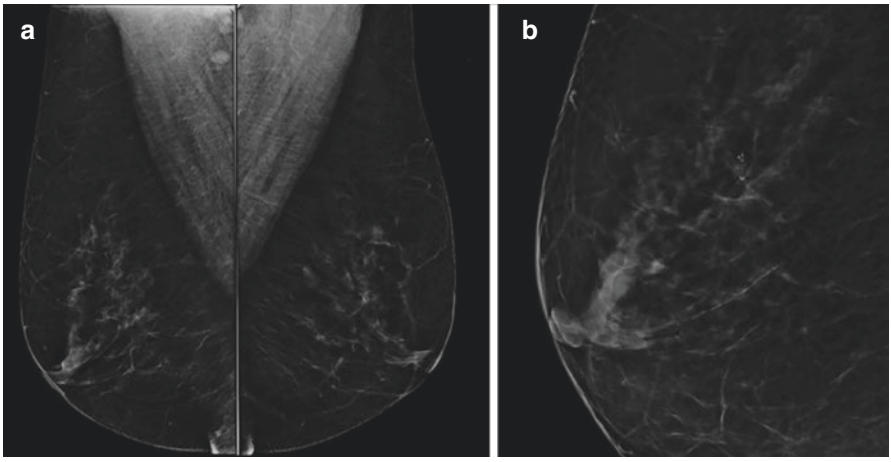

Fig. 6.27 Example of single dilated duct in the right breast. (**a**) MLO view of both breasts. (**b**) Spot compression view of the right breast

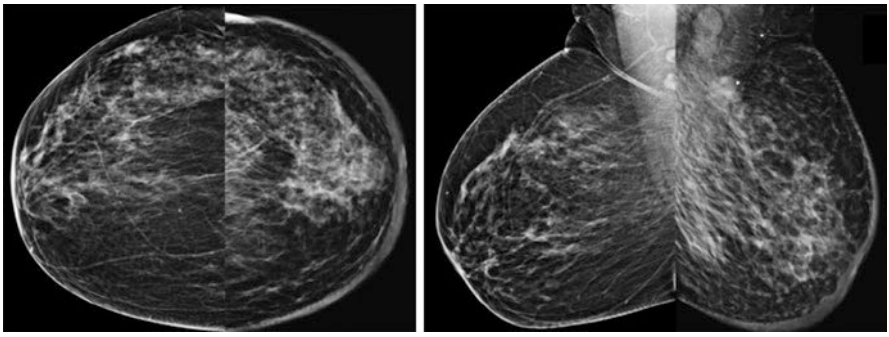

Fig. 6.28 Example of a malignant tumor with associated findings in the left breast, characterized by skin and trabecular thickening (edema) and axillary adenopathy

may be different in the true lateral view. Thus, it is important to know how to properly locate the lesions, both for correlation with other imaging methods and to indicate an additional incidence in the correct topography, when necessary. In general, lesions located in the inner quadrants tend to have an upper location in the true lateral view, when compared to the MLO view, while lesions located in the outer quadrants tend to have a lower location in the true lateral view.

6.4.11 ACR-BI-RADS® Final Assessment

Based on the positive predictive values of each finding, final assessment should be categorized in:

- BI-RADS 1 (negative; normal exam).
- BI-RADS 2 (benign findings): it includes typically benign calcifications, round or punctate calcifications with diffuse distribution, fat-containing masses or masses with typically benign calcifications (e.g., popcorn-like, rim or milk of calcium), architectural distortion related to prior surgery, asymmetry or global asymmetry with no other findings, and intramammary lymph node.
- BI-RADS 3 (probably benign; <2% likelihood of malignancy): it includes round or punctate calcifications with grouped or regional distribution, oval masses with circumscribed or obscured margins, and focal asymmetry with no other associated findings.
- BI-RADS 4 (suspicious; 2–95% likelihood of malignancy): calcifications with suspicious morphology, linear or segmental distribution, masses with irregular shape or non-circumscribed margins, architectural distortion not related to prior surgery, developing asymmetry, and other asymmetries with other suspicious findings. This category can be further subdivided into 4A,

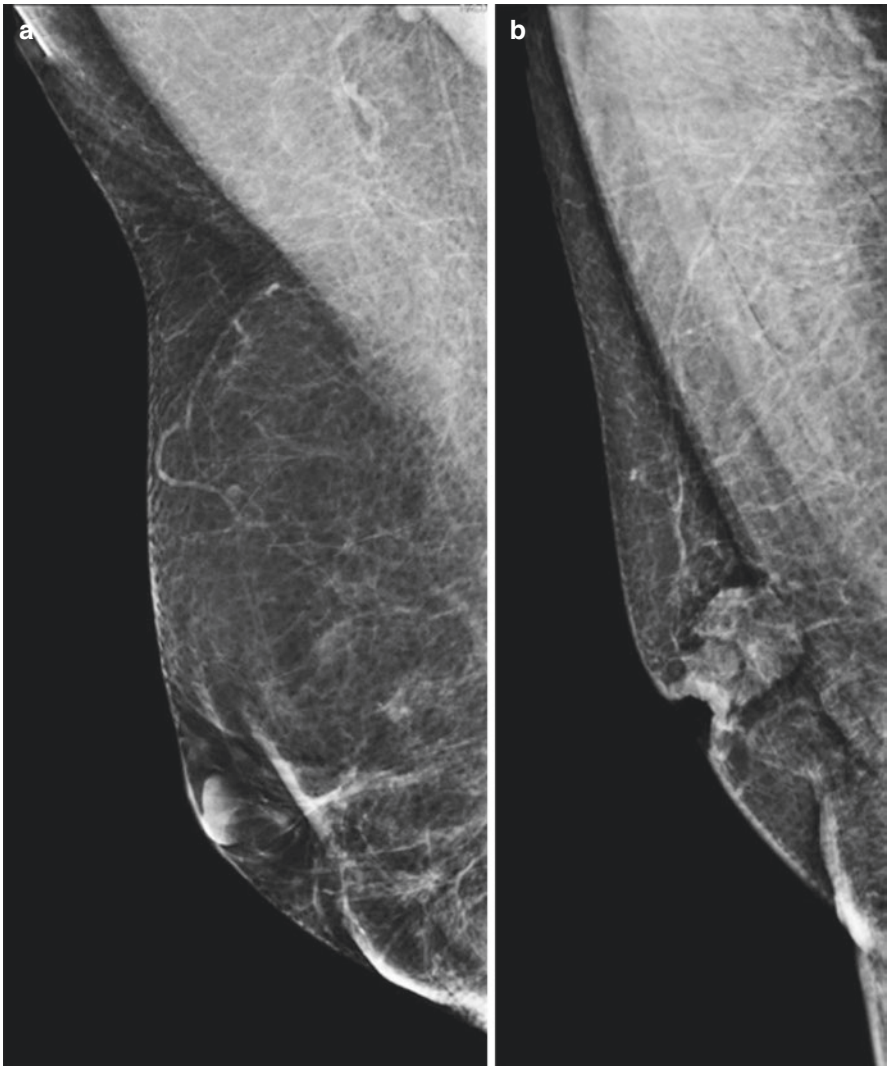

Fig. 6.29 Examples of nipple retraction on mammography: (**a**) postoperative changes; (**b**) invasive ductal carcinoma

4B, and 4C, with 2–10%, 10–50%, and 50–95% likelihood of malignancy, respectively.

- BI-RADS 5 (highly suggestive of malignancy; >95% likelihood of malignancy): more than one suspicious (BI-RADS 4) feature associated to additional findings.
- BI-RADS 6 (known biopsy-proven malignancy).
- BI-RADS 0 (incomplete; needs additional imaging evaluation or prior exams for comparison).

6.4.12 Recommendation

Usually, routine screening is recommended for BI-RADS categories 1 and 2 exams. Short interval (6 months) follow-up is recommended for BI-RADS category 3 exams, and tissue diagnosis (biopsy) is recommended for BI-RADS categories 4 and 5 exams. The fifth edition of the BI-RADS Atlas allows to disconnect the final assessment category from the recommendation in selected cases [32]. For example, in a patient with a palpable mass with normal mammography, it is possible to report the exam as negative (BI-RADS 1) and suggest complementation with other imaging tests if there is clinical suspicion. It is also possible to suggest appropriate treatment for benign lesions (BI-RADS 2) or with probably benign findings (BI-RADS 3), such as inflammatory cysts and abscesses, or to suggest follow-up for suspicious lesions (BI-RADS 4) in patients with known benign conditions, such as mastitis and steatonecrosis.

For follow-up of probably benign lesions (BI-RADS 3), the mammography should be repeated in 6 and 12 months of the initial examination, and in the case of stability, control can be performed 24 months after the initial examination (it is no longer necessary to perform follow-up exam 18 months after the initial examination if the findings are stable after the initial 12 months).

The presence of unilateral abnormal axillary lymph nodes, without known inflammatory or infectious etiologies, may be related to occult breast carcinoma and should be considered suspect (category BI-RADS 4). Ideally, ultrasound should be performed to confirm the finding as unilateral and suspicious. Bilateral lymph node enlargement with no known cause, especially if it is a new finding, could also be considered a suspicious finding.

6.5 Conclusions

Radiation-based breast imaging is still the most used method for screening and diagnostic workup in clinical practice. The advent of DM and DBT has improved mammography quality and results. Mammography findings should be reported according to the BI-RADS lexicon, which is widely available and universally accepted.

References

1. Myers ER, Moorman P, Gierisch JM, et al. Benefits and harms of breast cancer screening. JAMA. 2015;314:1615. https://doi.org/10.1001/jama.2015.13183.
2. Mainiero MB, Moy L, Baron P, et al. ACR appropriateness criteria ® breast cancer screeninG. J Am Coll Radiol. 2017;14:S383–90. https://doi.org/10.1016/j.jacr.2017.08.044.

3. Helvie MA, Bevers TB. Screening mammography for average-risk women: the controversy and NCCN's position. J Natl Compr Cancer Netw. 2018;16:1398–404. https://doi.org/10.6004/jnccn.2018.7081.
4. Saccarelli CR, Bitencourt AGV, Morris EA. Is It the era for personalized screening? Radiol Clin N Am. 2021;59:129–38. https://doi.org/10.1016/j.rcl.2020.09.003.
5. Vourtsis A, Berg WA. Breast density implications and supplemental screening. Eur Radiol. 2019;29:1762–77. https://doi.org/10.1007/s00330-018-5668-8.
6. Joe BN, Sickles EA. The evolution of breast imaging: past to present. Radiology. 2014;273:S23–44. https://doi.org/10.1148/radiol.14141233.
7. Garcia EM, Crowley J, Hagan C, Atkinson LL. Evolution of imaging in breast cancer. Clin Obstet Gynecol. 2016;59:322–35. https://doi.org/10.1097/GRF.0000000000000193.
8. Lewin JM, D'Orsi CJ, Hendrick RE. Digital mammography. Radiol Clin N Am. 2004;42:871–84. https://doi.org/10.1016/j.rcl.2004.06.004.
9. Bick U, Diekmann F. Digital mammography: what do we and what don't we know? Eur Radiol. 2007;17:1931–42. https://doi.org/10.1007/s00330-007-0586-1.
10. Kopans DB. Digital breast tomosynthesis from concept to clinical care. Am J Roentgenol. 2014;202:299–308. https://doi.org/10.2214/AJR.13.11520.
11. Nguyen T, Levy G, Poncelet E, et al. Overview of digital breast tomosynthesis: clinical cases, benefits and disadvantages. Diagn Interv Imaging. 2015;96:843–59. https://doi.org/10.1016/j.diii.2015.03.003.
12. Abdullah P, Alabousi M, Ramadan S, et al. Synthetic 2D mammography versus standard 2D digital mammography: a diagnostic test accuracy systematic review and meta-analysis. Am J Roentgenol AJR. 2020;20:24204. https://doi.org/10.2214/AJR.20.24204.
13. Oeffinger KC, Fontham ETH, Etzioni R, et al. Breast cancer screening for women at average risk. JAMA. 2015;314:1599. https://doi.org/10.1001/jama.2015.12783.
14. Siu AL. Screening for breast cancer: U.S. Preventive Services Task Force recommendation statement. Ann Intern Med. 2016;164:279. https://doi.org/10.7326/M15-2886.
15. Monticciolo DL, Newell MS, Hendrick RE, et al. Breast cancer screening for average-risk women: recommendations from the ACR commission on breast imaging. J Am Coll Radiol. 2017;14:1137–43. https://doi.org/10.1016/j.jacr.2017.06.001.
16. Sardanelli F, Aase HS, Álvarez M, et al. Position paper on screening for breast cancer by the European Society of Breast Imaging (EUSOBI) and 30 national breast radiology bodies from Austria, Belgium, Bosnia and Herzegovina, Bulgaria, Croatia, Czech Republic, Denmark, Estonia, Finland, France, G. Eur Radiol. 2017;27:2737–43. https://doi.org/10.1007/s00330-016-4612-z.
17. Qaseem A, Lin JS, Mustafa RA, et al. Screening for breast cancer in average-risk women: a guidance statement from the American College of Physicians. Ann Intern Med. 2019;170:547. https://doi.org/10.7326/M18-2147.
18. Cardoso F, Kyriakides S, Ohno S, et al. Early breast cancer: ESMO Clinical Practice Guidelines for diagnosis, treatment and follow-up. Ann Oncol. 201930(8):1194–220. https://doi.org/10.1093/annonc/mdz173.
19. Sharpe RE, Venkataraman S, Phillips J, et al. Increased cancer detection rate and variations in the recall rate resulting from implementation of 3D digital breast tomosynthesis into a population-based screening program. Radiology. 2016;278:698–706. https://doi.org/10.1148/radiol.2015142036.
20. Rose SL, Shisler JL. Tomosynthesis impact on breast cancer screening in patients younger than 50 years old. Am J Roentgenol. 2018;210:1401–4. https://doi.org/10.2214/AJR.17.18839.
21. Alsheik NH, Dabbous F, Pohlman SK, et al. Comparison of resource utilization and clinical outcomes following screening with digital breast tomosynthesis versus digital mammography: findings from a learning health system. Acad Radiol. 2019;26:597–605. https://doi.org/10.1016/j.acra.2018.05.026.

22. Conant EF, Barlow WE, Herschorn SD, et al. Association of digital breast tomosynthesis vs digital mammography with cancer detection and recall rates by age and breast density. JAMA Oncol. 2019;5:635.
23. Dang PA, Wang A, Senapati GM, et al. Comparing tumor characteristics and rates of breast cancers detected by screening digital breast tomosynthesis and full-field digital mammography. Am J Roentgenol. 2020;214:701–6. https://doi.org/10.2214/AJR.18.21060.
24. Bahl M, Mercaldo S, Dang PA, et al. Breast cancer screening with digital breast tomosynthesis: are initial benefits sustained? Radiology. 2020;295:529–539 https://doi.org/10.1148/radiol.2020191030.
25. Jackson VP. Diagnostic mammography. Radiol Clin N Am. 2004;42:853–70. https://doi.org/10.1016/j.rcl.2004.06.002.
26. Sickles EA, D'Orsi CJ, Mendelson EB, Morris E, et al. ACR BI-RADS® mammography. In: ACR BI-RADS® Atlas, breast imaging reporting and data system. 5th ed. Reston; 2013.
27. Durand MA, Wang S, Hooley RJ, et al. Tomosynthesis-detected architectural distortion: management algorithm with radiologic-pathologic correlation. Radiographics. 2016;36:311–21. https://doi.org/10.1148/rg.2016150093.
28. Chesebro AL, Winkler NS, Birdwell RL, Giess CS. Developing asymmetries at mammography: a multimodality approach to assessment and management. Radiographics. 2016;36:322–34. https://doi.org/10.1148/rg.2016150123.
29. Bitencourt AG, Ferreira EV, Bastos DC, et al. Intramammary lymph nodes: normal and abnormal multimodality imaging features. Br J Radiol. 2019;92:20190517. https://doi.org/10.1259/bjr.20190517.
30. Giess CS, Raza S, Birdwell RL. Distinguishing breast skin lesions from superficial breast parenchymal lesions: diagnostic criteria, imaging characteristics, and pitfalls. Radiographics. 2011;31:1959–72. https://doi.org/10.1148/rg.317115116.
31. Choudhery S, Simmons C, Woodard GA, et al. Outcomes of solitary dilated breast ducts in symptomatic and asymptomatic patients. Br J Radiol. 2020;93:20191039. https://doi.org/10.1259/bjr.20191039. https://doi.org/10.1001/jamaoncol.2018.7078
32. Rao AA, Feneis J, Lalonde C, Ojeda-Fournier H. A pictorial review of changes in the BI-RADS fifth edition. Radiographics. 2016;36:623–39. https://doi.org/10.1148/rg.2016150178.

Chapter 7
Sonographic Based Imaging: Ultrasound, Color Doppler, Elastography, and Automated Breast Imaging

Juliana Hiraoka Catani

Abbreviations

ABUS	Automated breast ultrasound
HHUS	Handheld ultrasound
MRI	Magnetic resonance imaging
ROI	Region of interest
SE	Strain elastography
SWE	Shear wave elastography
US	Ultrasound

7.1 Introduction

Ultrasound (US) is an interactive, dynamic, and real-time method that has become an indispensable resource for breast assessment, both together and complementary to mammography and magnetic resonance imaging (MRI). In the past, only mammography has been useful for population-based screening. However, high-resolution and quality-controlled ultrasound can further improve early cancer detection.

US has been used to classify benign, solid lesions with a negative predictive value of 99.5% [1].

US advantages include:

(a) No exposure to radiation and its related risks

J. H. Catani (✉)
Instituto de Radiologia INRAD, Hospital das Clinicas HCFMUSP, Faculdade de Medicina, Universidade de Sao Paulo, São Paulo, SP, Brazil
e-mail: juliana.catani@hc.fm.usp.br

S. J. Kim Hsieh, E. A. Morris (eds.), *Modern Breast Cancer Imaging*,
https://doi.org/10.1007/978-3-030-84546-9_7

(b) No tissue injury from US waves
(c) No contraindications

Ease of use and real-time imaging capability make breast ultrasound a method of choice for guiding breast biopsies and other interventions.

The limitations include:

(a) Inability to identify and characterize calcifications.
(b) Diagnostic performance is operator dependent.
(c) Large, mobile breasts will be difficult to scan thoroughly.

Currently accepted clinical indications include palpable lump; axillary adenopathy; first diagnostic approach for clinical abnormalities under 40 and in pregnant or lactating women; suspicious abnormalities at mammography or MRI; nipple discharge; recent nipple inversion; skin retraction; breast inflammation; surgical scar abnormalities; abnormalities in the presence of breast implants; screening high-risk women and locoregional staging of a known breast cancer when MRI is not performed; guidance for percutaneous interventions; and monitoring breast cancer neoadjuvant therapy. US can also be used as an adjunctive modality for breast cancer screening in women with dense breast tissue and negative mammography.

The ultrasound device emits and receives high-frequency electromechanical waves (ultrasound) that are generated by the piezoelectric crystals contained in the transducer. According to the impedance of each tissue, images in gray scale (B mode) are generated.

For the examination, proper positioning is essential, aiming at reducing breast thickness and mobility.

7.2 Scanning Technique

For positioning, the patient should lie down in the supine position with the chest undressed and with arms relaxed and flexed behind the head to flatten the breast. It might be necessary to roll the patient slightly to access the breast evenly.

The scan with the transducer should be done in at least two orthogonal planes, including the peripheral regions of the breasts and lymphatic drainage pathways. As the lactiferous ducts are arranged radially in the nipple, and the lesions tend to grow along the ducts, the radial scan is favored by being anatomically guided (Figs. 7.1 and 7.2).

Medial structures should generally be scanned in the supine position, and lateral structures including the armpit should generally be scanned with the patient in the contralateral oblique position. This allows for the elimination of possible artifacts secondary to inadequate compression of the breast tissue.

7.2.1 The Ideal Image

When examining the breast, a 12- to 18-MHz multifrequency linear transducer is commonly used (a minimum frequency of 10 MHz is required) [2, 3] and provides

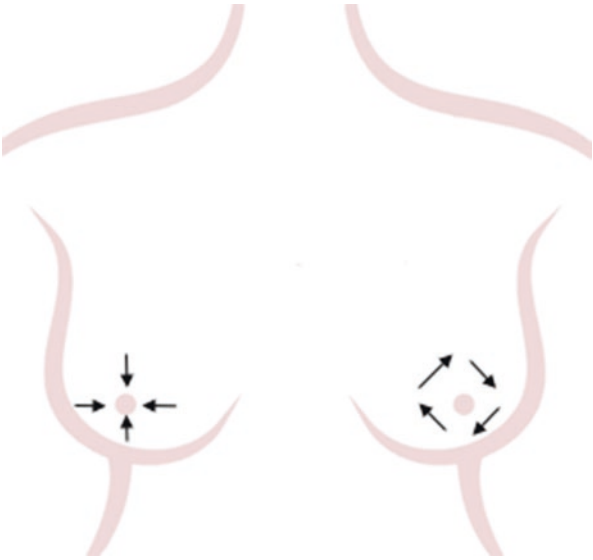

Fig. 7.1 Radial and anti-radial scanning

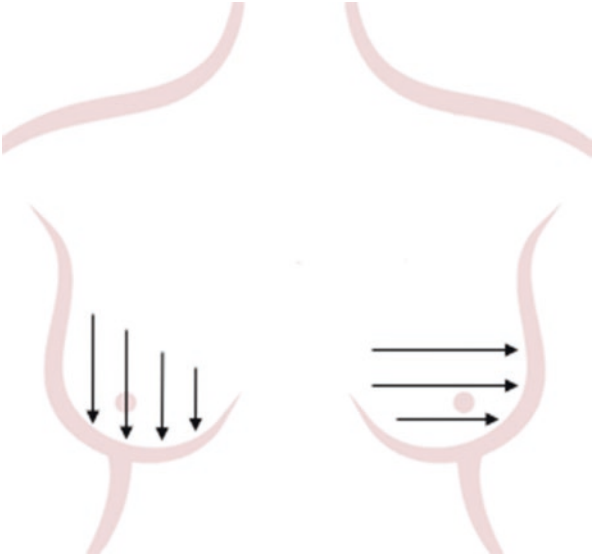

Fig. 7.2 Longitudinal and transverse scan

excellent spatial and soft tissue resolution, allowing for substantially improved differentiation of subtle shades of gray, margin resolution, and conspicuousness of the lesion at the bottom of normal breast tissue [2, 4–8].

The initial gain settings must be adjusted so that the fat at all levels is displayed as medium level gray (calibrated by the superficial fat to the breast area).

The echogenicity of the structures is determined by comparison with the echogenicity of the fat. In comparison with breast fat, most solid masses are hypoechoic and simple cysts anechoic, while skin, Cooper's ligaments, and fibrous tissue are echogenic.

Gentle pressure should be applied to the transducer during the examination. The smaller the thickness of the tissue, the higher the image resolution. The increase in pressure can have a beneficial effect on the acquired image, which can reduce artifactual shadows, as well as making it difficult to evaluate compressible structures (ducts and vessels).

7.2.2 Anatomy

The region of interest in the breast comprises the portion from the skin surface (a) and subcutaneous tissue (b) to the pleural surface/posterior chest wall (Fig. 7.3).

The areolopapillary complex is formed by the areola, papilla, and lactiferous ducts.

The mammary zone (c) is formed by glandular and adipose tissue and Cooper's ligaments, where most of the breast ducts and lobules are located, and therefore the main area of breast diseases.

The retromammary zone (d) is formed by retromammary fat, pectoral muscle, ribs, and pleural surface.

The axillary region is the pyramidal space inferior to the glenohumeral joint, at the junction between the arm and thorax, and contains many neurovascular structures, including the axillary artery, axillary vein, brachial plexus, and lymph nodes.

The anatomical repair used to classify lymph node levels in the axilla is the pectoralis minor muscle (highlighted in red in Fig. 7.4), being:

- Level I: lateral to the pectoralis minor muscle
- Level II: between the medial and lateral borders of the pectoralis minor muscle
- Level III: medial to the pectoralis minor muscle

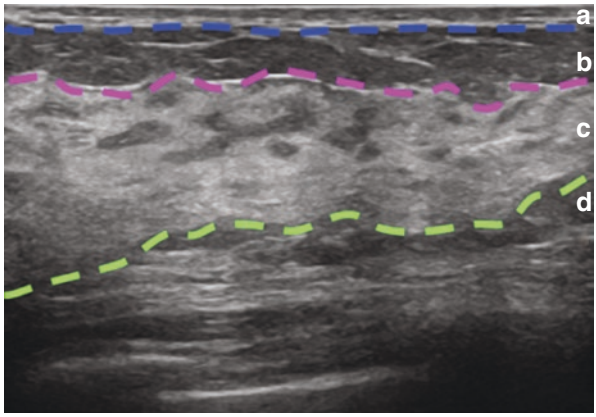

Fig. 7.3 (**a**) – Skin surface. (**b**) – Subcutaneous tissue. (**c**) – Mammary zone. (**d**) – Retromammary zone

7.2.3 *Harmonic*

The harmonic image can also be applied to better characterize a cyst or a subtle solid mass. The generation of harmonic images allows the higher harmonic waves to be selected and used to create the grayscale images with fewer artifacts [9].

Low-frequency surface reverberation echoes are thus reduced, allowing better characterization of simple cysts (particularly if small) by eliminating artificial internal echoes often seen in fluids (Fig. 7.5).

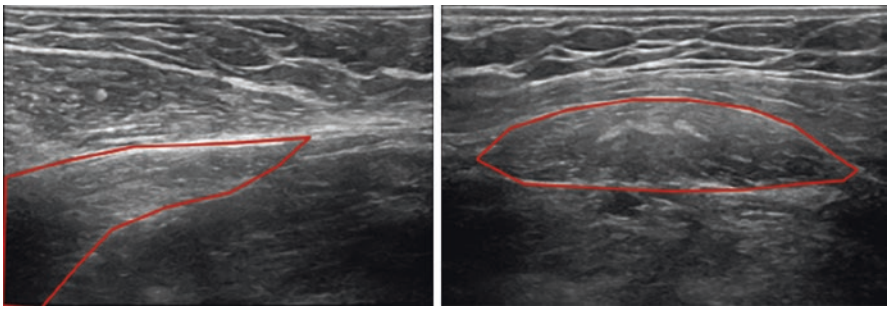

Fig. 7.4 Pectoralis minor muscle (highlighted in red, left axilla)

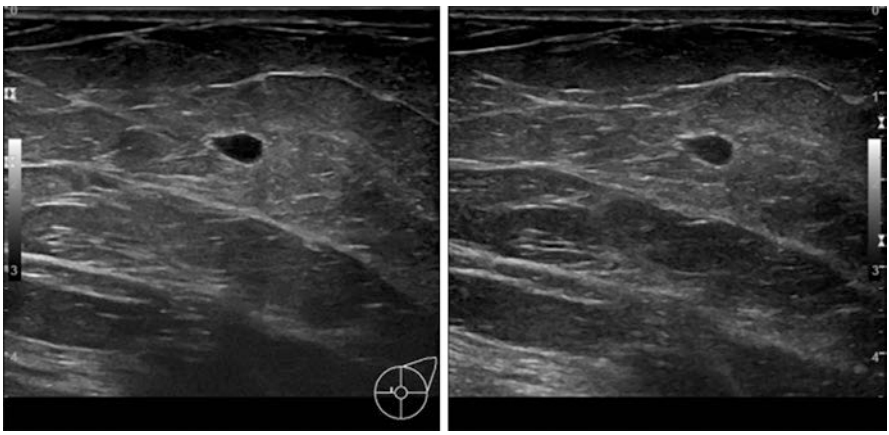

Fig. 7.5 Cyst with harmonic resource (left) and without harmonic resource (right), showing attenuation of internal echoes and confirming that it is a simple cyst

Harmonic imaging also improves lateral resolution and can improve the contrast between adipose tissue and subtle lesions, allowing for better definition of lesion margins and posterior shading.

7.2.4 Compound Imaging

Compound imaging shows improved image quality compared with conventional ultrasound, primarily because of reduction of speckle, clutter, and other acoustic artifacts.

The compound imaging feature acquires images at multiple angles from an insonation plane, reducing artifact echoes and increasing the image contrast, but there is a loss of image quality from the deepest planes (Fig. 7.6).

7.3 Doppler Evaluation

The evaluation through color mapping on the breast is based on the argument that malignant or inflammatory lesions can cause angiogenesis and these vessels are identified on the periphery or inside the lesions.

Currently, both power and color Doppler are complementary tools to the gray-scale image, although power Doppler mode is favored for being more sensitive when viewing small vessels, and factors such as flow direction and spectral evaluation are not relevant.

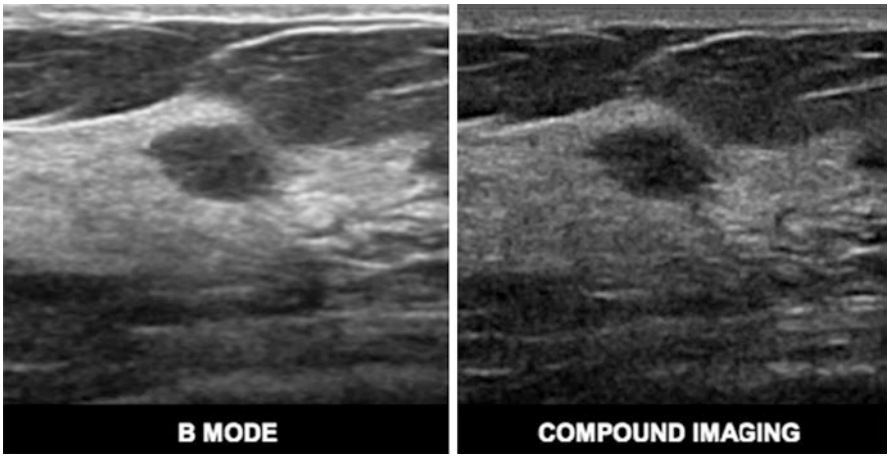

Fig. 7.6 Left – B mode. Right – compound imaging

Malignant breast lesions typically produce pro-angiogenic factors that stimulate neoangiogenesis and the growth of new irregular and branching vessels. Aggressive malignant lesions can exhibit little or no blood flow due to small lesions (bigger lesions tend to show more vascularization), the presence of posterior acoustic shadowing, and necrotic anechoic areas. Benign lesions usually do not show irregular branching, chaotic vessels, or formation of sinusoids and arteriovenous shunts [2, 3].

The evaluation of masses must be correlated with ultrasound findings, emphasizing that no vascular pattern is specific to a particular diagnosis.

The technique consists of visualizing the area of interest with the Doppler mode, performing small compression on the breast, as small vessels may not be identified with too much pressure from the transducer.

The demonstration of central or penetrating vascularization of irregular branching within a solid mass raises suspicion of malignant neovascularization [2, 3].

Color Doppler and power US are also useful for evaluating cysts and complex cystic masses that contain a solid component. The demonstration of flow within an apparently simple cyst, a complicated cyst, or a complex mass confirms the presence of a suspect solid component, which requires biopsy. The twinkle artifact seen with color Doppler is useful for identifying a biopsy marker or subtle echogenic calcifications.

By ACR BI-RADS, the findings on color Doppler mapping are classified as (Figs. 7.7, 7.8, and 7.9):

(a) Absent
(b) Internal vascularization
(c) Peripheral vascularization

It is important to note that these findings can overlap and sometimes benign lesions have internal and exuberant vascularization and malignant lesions can present absent or peripheral vascularization (Fig. 7.10).

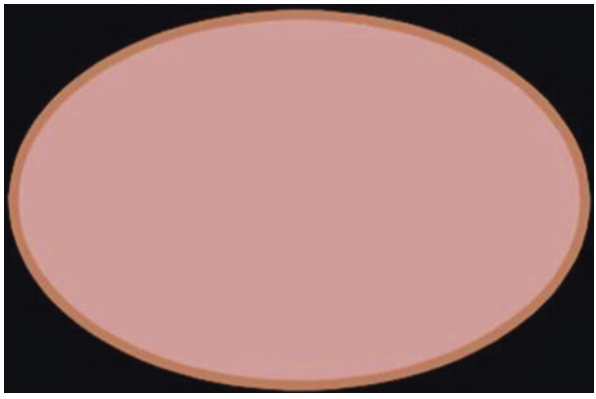

Fig. 7.7 Absent, when no vessel is identified in the region of interest, common in simple cysts and some benign masses

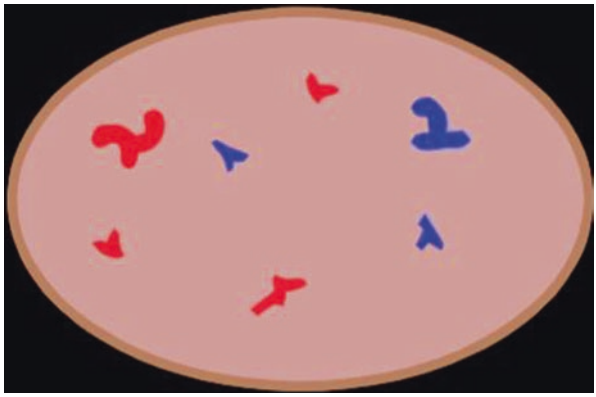

Fig. 7.8 Internal vascularization, when vessels (sometimes more than one) are identified inside the lesion, the most common finding in malignant neoplasms

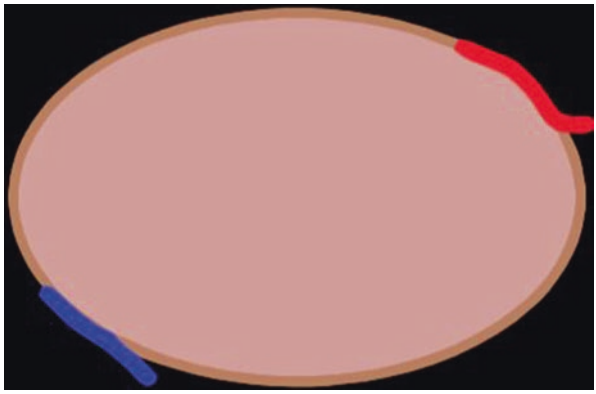

Fig. 7.9 Peripheral vascularization, when vessels are found surrounding the lesion, more common in inflammatory processes and benign solid masses

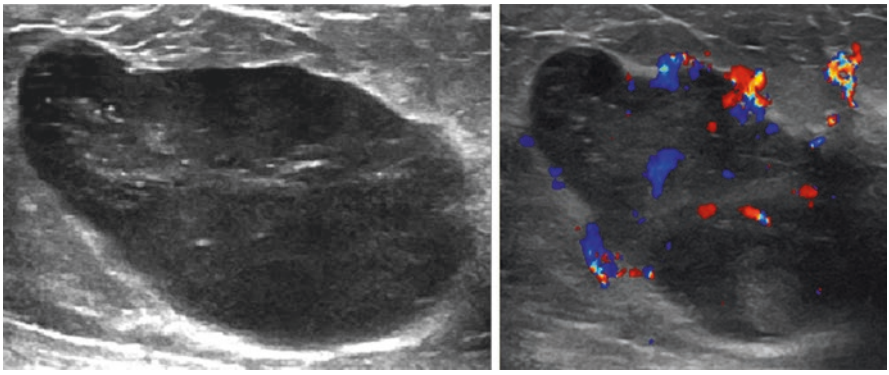

Fig. 7.10 New, solid, hypoechoic, oval, and circumscribed mass, with peripheral and central vascularization, and branched vessels on color Doppler. Patient underwent a percutaneous biopsy and was diagnosed with adrenal carcinoma metastasis

7.4 Elastography

Ultrasound elastography is an established method for characterization of focal lesions in the breast and can be used to measure tissue stiffness with the potential to improve specificity in the diagnosis of breast masses. There are two forms of elastography available: strain (SE) and shear wave (SWE).

This technique assesses tissue elasticity, which is the tendency of tissue to resist deformation with an applied force, or to return to its original shape after removal of the force [9–11].

Obtaining a good grayscale image is essential before changing to the elastography mode since SE and SWE images are often generated based on raw data from grayscale images.

Ultrasound elastography has 86.5% sensitivity, 89.8% specificity, and 88.3% diagnostic accuracy in the differentiation of benign from malignant solid breast masses [12].

Elastography is a useful complementary tool for undetermined breast lesions categorized as BI-RADS 4A or BI-RADS 3 or for cystic lesions but cannot avoid investigation if ultrasound features are clearly suspicious.

Some benign lesions can be poorly deformable, such as fibrous fibroadenomas or scars. The presence of implants can also change the strain of breast tissue around the implant, complicating elastography assessment.

The bull's eye cyst pattern can be seen with lesions that appear solid and suspicious on B-mode imaging. It occurs because of the fluid movement, and there is no correlation between images.

In ACR BI-RADS, the elastography findings are divided into:

(a) Stiff or hard.
(b) Intermediate.
(c) Soft, and this relationship is made with adjacent adipose tissue.

7.4.1 Strain Elastography

In this technique, a normal stress is applied to tissue (gentle compression or natural movement such as heartbeat, vascular pulse, or breathing), and the normal strain is measured. Under an equal amount of stress, a stiff region experiences less strain than the surrounding soft tissue.

For breast imaging, the region of interest (ROI) should extend anterior-posteriorly from the subcutaneous fat tissue to the pectoralis muscle, excluding the thoracic cage, and the width should be adjusted to keep the lesion of interest within 25% of the ROI width [13].

The information obtained with strain elastography provides qualitative information (hard, intermediate, soft).

Tsukuba Scoring System

A color-coded scoring system has been proposed by Itoh et al. [12], most commonly used for SE. The strain in lesion tissue is displayed in a color-coded image. The scoring system assigns a score from 1 to 5 (Fig. 7.11) with the risk of malignancy increasing from 1 to 5 (Fig. 7.12):

The risk of malignancy increases from 1 to 5.

7.4.2 Shear Wave Elastography

In contrast to strain imaging, SWE employs a higher intensity pulse to generate shear waves in the parallel or perpendicular dimensions.

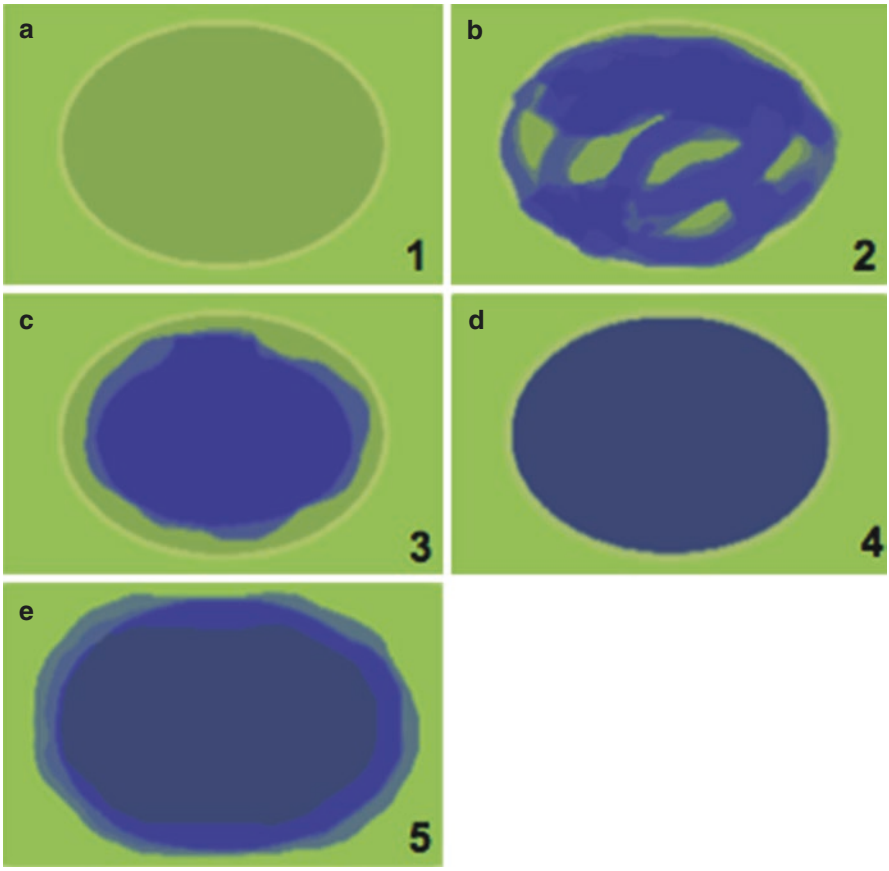

Fig. 7.11 (**a**) Score 1: complete deformability of lesion. (**b**) Score 2: most of the lesion is deformable although there are areas which are not deformable. (**c**) Score 3: presence of stiff area in center with peripheral deformability of lesion. (**d**) Score 4: no deformability throughout the entire lesion only. (**e**) Score 5: no deformation throughout the entire lesion or in adjacent tissue

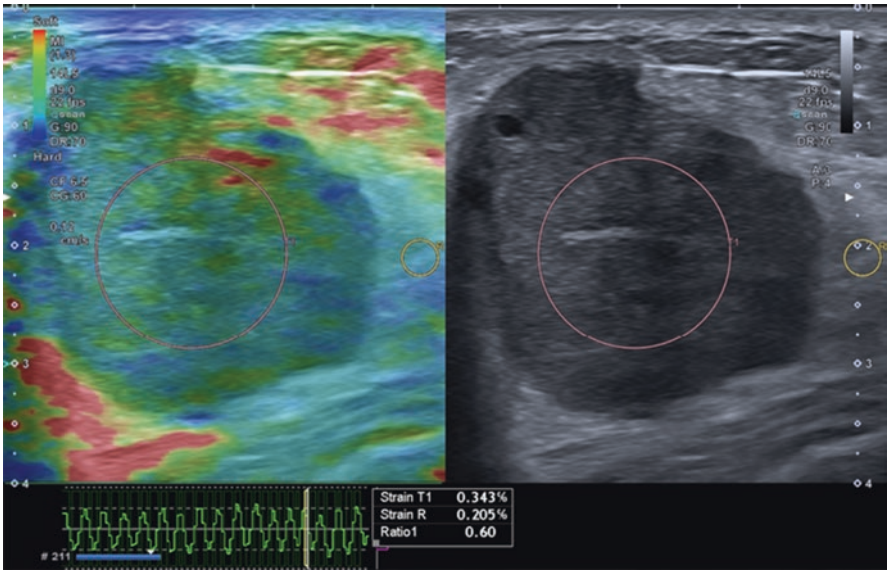

Fig. 7.12 Solid, hypoechoic, irregular, and microlobulated lesion on the grayscale B-mode image (right). Color mapping SE image (left) showing the same lesion shaded in blue color (hard lesion in the color scale used)

With the use of light transducer pressure, automatic transient pulses can be generated by the US probe, inducing shear waves transversely oriented in the tissue. The system captures the speed of these shear waves, which move faster in hard tissue compared to soft tissue.

To measure the elasticity quantitatively in SWE for breast lesions, the most common practice is to place a 2- to 3-mm circular ROI over the stiffest part of the lesion, including the immediately adjacent stiff tissue or halo [14].

Shear wave elastography provides quantitative information because tissue elasticity can be measured in meters per second or kilopascals, a unit of pressure. A value of over 80 kPa or velocity results of over 2 m/s are considered suspicious (Figs. 7.13 and 7.14).

7.5 Automated Breast Ultrasound

Automated breast ultrasound (ABUS) is used as a supplement to mammography for screening in asymptomatic women with dense breasts. It is an effective screening modality with diagnostic accuracy comparable to that of handheld ultrasound (HHUS) [10, 15].

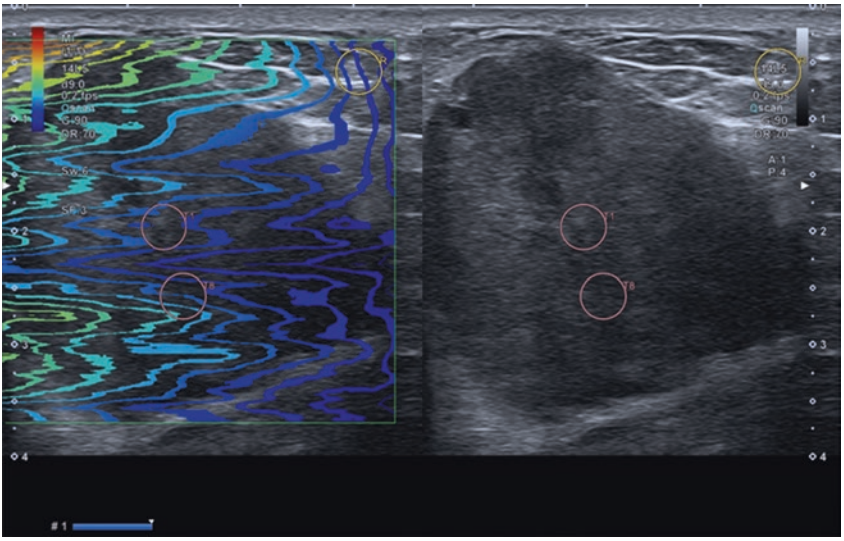

Fig. 7.13 Solid, hypoechoic, irregular, and microlobulated lesion on the grayscale B-mode image (right), poorly deformable in color-mode SWE (left)

	Speed[m/s]		Elasticity[kPa]		Dispersion[(m/s)/kHz]		
	Average	SD	Average	SD	Average	SD	Depth[cm]
1	6.14	1.45	104.8	45.4	***	***	1.4
2	7.51	0.74	139.8	46.0	***	***	1.2
3	3.70	1.06	45.0	21.7	***	***	1.7
4	5.61	1.17	95.1	37.6	***	***	2.3
5	8.18	0.58	111.0	68.2	***	***	1.2
6	3.50	0.76	38.8	16.3	***	***	2.2
7	4.49	1.45	64.3	32.1	***	***	2.6
8	7.94	0.56	139.1	60.9	***	***	0.9
9	4.48	0.56	61.5	15.3	***	***	1.6
10	5.54	0.94	95.3	32.8	***	***	2.4
11	5.10	0.80	80.2	23.9	***	***	2.0
12	5.16	0.64	81.4	18.8	***	***	2.1
R	1.78	0.09	9.3	0.9	***	***	0.7
Mean	5.32		82.0		***		
SD	1.77		36.8		***		
Median	5.16		81.4		***		
IQR	2.73		54.7		***		

Fig. 7.14 Velocities measured in the lesions are very high (>3 m/s), which suggests a malignant lesion

ABUS consists of a US scanner and special stationary device with a transducer, which moves automatically in a scan box. The slice thickness is adjustable from 0.5 mm to 8.0 mm, and up to 448 axial slices are acquired [10, 15].

The sequence of the technique consists of three steps: patient positioning, image acquisitions, and interpretation of data.

The patient lies down in the supine position with the ipsilateral hand raised above the head. A rolled towel is placed under each shoulder to help stabilize the breast with the nipple pointing to the ceiling. A hypoallergenic lotion is spread out evenly on the breast with an additional amount on the nipple area. A nipple marker is placed in every examination for accurate correlation of the reformatted views.

The exam is performed in anteroposterior, medial, and lateral views routinely and in the superior or inferior view additionally in cases of large breasts. Image acquisition in six views takes approximately 10–15 min.

The optimal image quality should be guaranteed for screening. However, the image quality and ultrasonic resolution diminish with poor contact, marked shadowing due to fibrotic breasts, and artifacts.

ABUS presents some limitations such as inability to assess vascularity and tissue elasticity and exclusion of axillary regions from the field of view. ABUS screening is also limited by its high recall rate and biopsy rate with low positive predictive value (PPV), similar to HHUS screening.

The most common artifacts in ABUS are:

(a) Corrugation, which is due to respiratory motion; this artifact can be avoided when women breathe calmly and do not speak or cough.
(b) Dropout shadowing deep to the skin, caused by insufficient lotion application and extreme compression.
(c) Nipple shadow and reverberation artifacts frequently occurred with ABUS.
(d) Skip artifacts present as a transverse anechoic line at the location of change in tissue stiffness due to a mass and can be used to detect isoechoic masses.
(e) In the study by Vourtsis and Kachulis [13], a "zigzag" sign was produced by disruption of the scanning process in 61.5% of women with palpable lesions.

Studies have shown that ABUS is a standardized and reproducible imaging modality that surmounts the limitations of HHUS, while offering valuable impact in the detection of breast lesions, and differentiates malignant from benign lesions, with a high inter-observer reliability [10, 13, 15, 16].

7.6 Correlation with Other Imaging Methods

When looking for a lesion initially identified on mammography or MRI, careful correlation must be made with the depth of the lesion and surrounding anatomical structures.

The location of the lesion can be affected by the patient's position, which differs during mammography, US, and MRI exams (Figs. 7.15 and 7.16).

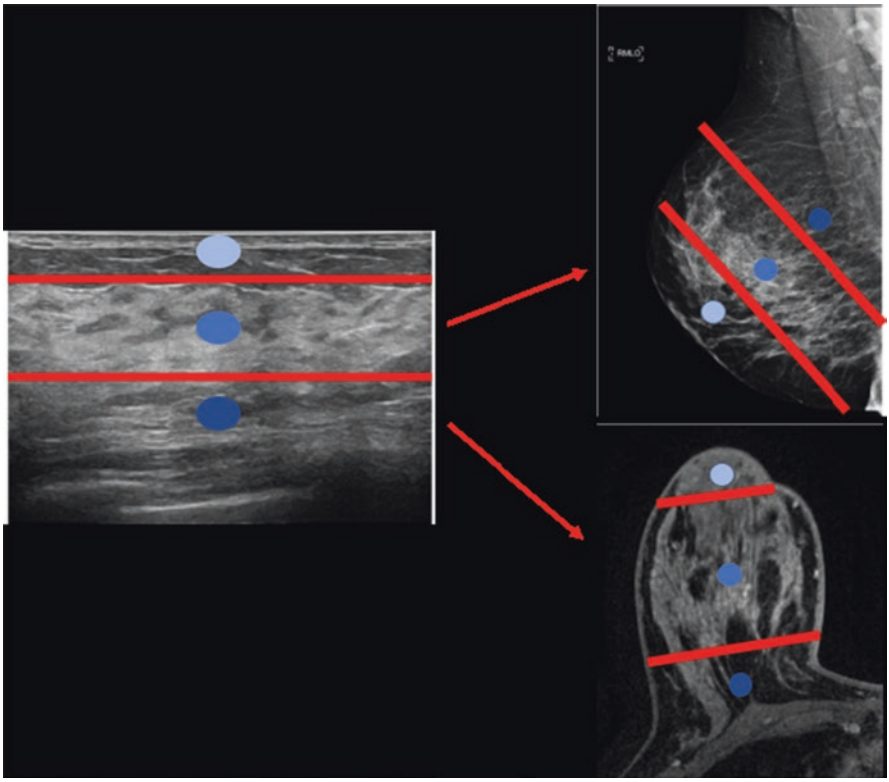

Fig. 7.15 When performing the correlation with mammography and MRI, take into account location (superficial, medium, and deep thirds), dimensions, shape, and margin

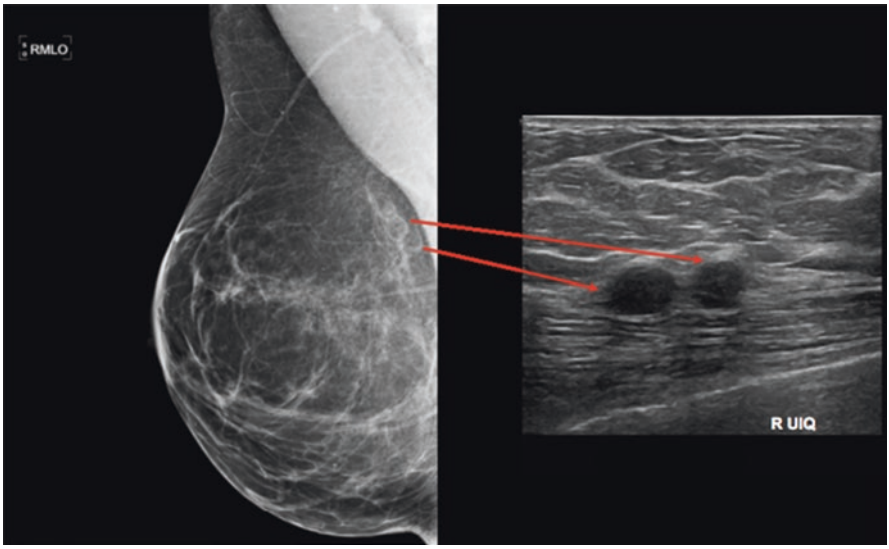

Fig. 7.16 Oily cysts in the posterior third of the right breast seen on mammography and their correspondence in the ultrasound study, next to the pectoral muscle

If a mass identified on mammography or magnetic resonance imaging is completely surrounded by adipose or fibroglandular tissue, on US, it must also be surrounded by hypoechoic tissue or echogenic fibroglandular tissue, respectively.

Lesions detected by MRI images are usually hidden in mammography, but many can be detected with the US. Along with the additional characterization of a lesion detected by MRI, US can be used to guide the intervention toward lesions initially detected in MRI (Fig. 7.17).

Likewise, careful attention is needed to the region of clinical interest when examining a palpable abnormality to ensure that the correct area is scanned. The examiner should place a finger on the palpable abnormality and then position the transducer directly over the region.

7.7 Exam Documentation

According to ACR BI-RADS®, the documentation must contain the breast that is being studied, the laterality, and the place of the "body mark," thus reducing any errors in laterality and quadrant (Fig. 7.18).

When documenting findings, the adjustment of focus and gain and frequency must be made and must contain images with and without measures to allow the evaluation of margins in still images. The location should be noted in laterality, quadrant, and/or clock face notation on the breast [9].

The size of the lesion should be measured in three dimensions, first reporting the longest diameter and the rest in the orthogonal plane (Figs. 7.19 and 7.20). The measurement can be made in millimeters or centimeters, rounding to just one decimal place [7].

In the presence of multiple cysts, documentation of the largest cyst in each breast and the measurement of its largest dimension can be made. In the presence of a normal lymph node, the same documentation can be performed.

Measure the longest axis (1) and perpendicular to the first (2). The third measure (3) should be taken from a plane orthogonal to the first image.

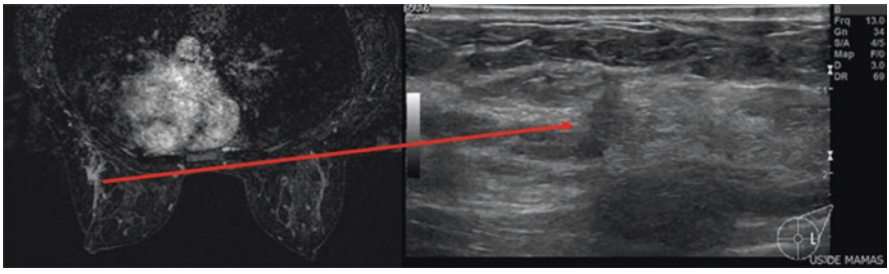

Fig. 7.17 Non-mass enhancement associated with architectural distortion in the posterior third of the outer quadrants of the left breast in the mammary zone (surrounded by fibroglandular tissue) and its ultrasound correspondence ("second-look" ultrasound)

Fig. 7.18 US documentation with laterality, quadrant, and body mark

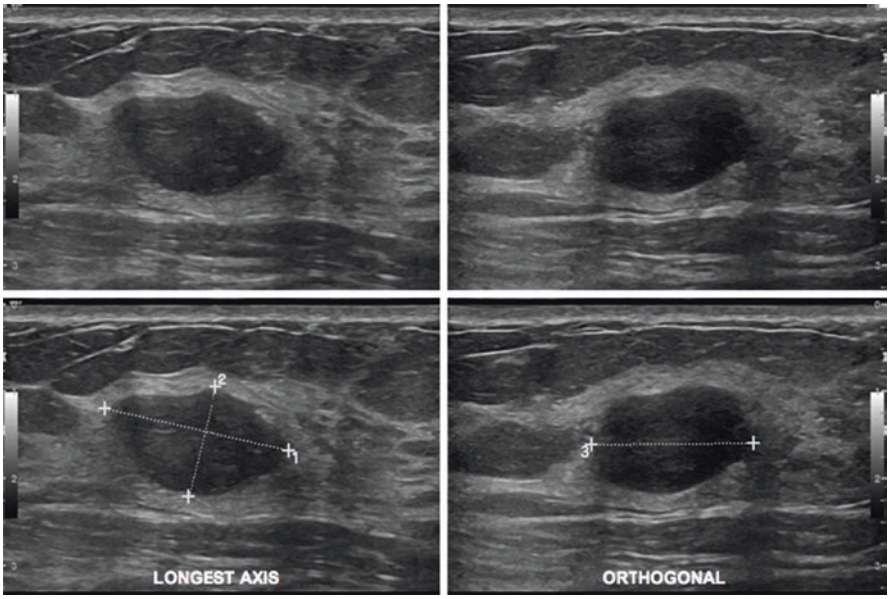

Fig. 7.19 Mass documentation in two plans without and with measures

The distance between the papilla and the lesion, and from this to the skin, is useful information and easy to identify by any operator, facilitating eventual localization during surgery and for evolutive control (Fig. 7.21).

A color Doppler/power Doppler image is recommended to assess the vascularization of the documented lesion (Fig. 7.22).

The documentation on breast screening without changes should contain the four quadrants and the retroareolar region.

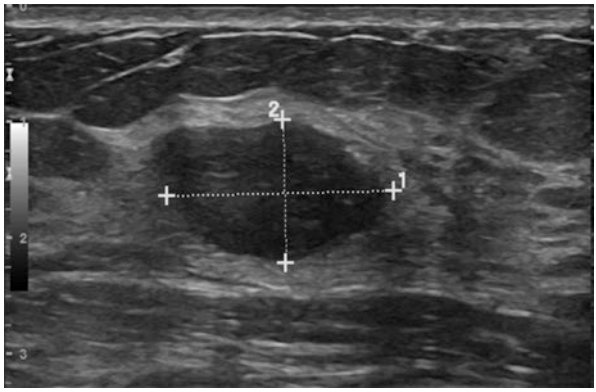

Fig. 7.20 Incorrect measurement, not respecting the largest axis of the lesion

Fig. 7.21 Distance between the mass and the papilla (1) and the skin (2)

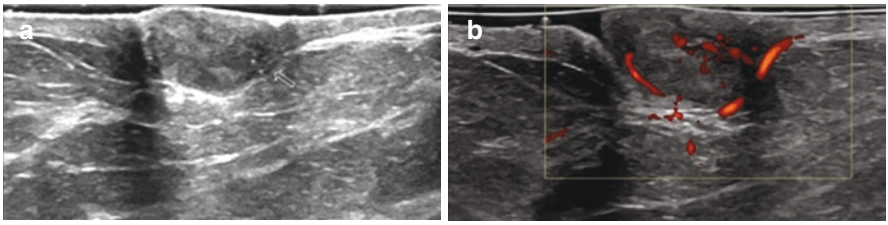

Fig. 7.22 Isoechoic mass that is difficult to characterize in B mode (**a**), but well delimited with the use of power Doppler (**b**)

Axilla documentation is not mandatory under the American College of Radiology (ACR) but can be performed as a courtesy when performing breast exams.

The ultrasound evaluation of breast implants must be performed in two separate steps, with adjustments of focus, gain, and depth for the evaluation of the parenchyma and later for the evaluation of the implant (Figs. 7.23 and 7.24).

7.8 BI-RADS® Lexicon

1. Breast composition
   Can be homogeneous background – fat or fibroglandular or heterogeneous background echotexture (Figs. 7.25, 7.26, and 7.27).

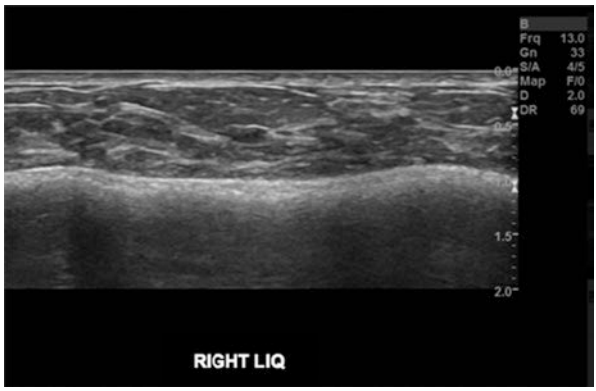

Fig. 7.23 Adjustment of focus and depth for evaluation of the breast parenchyma

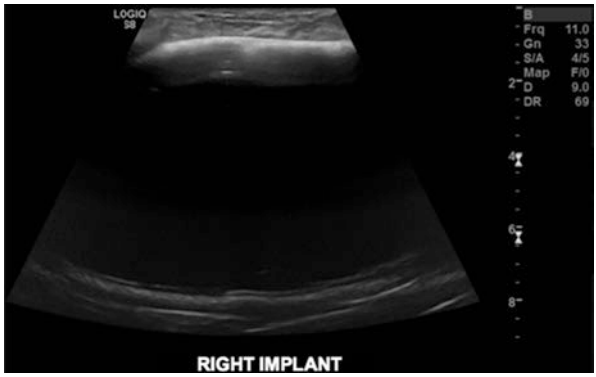

Fig. 7.24 Adjustment of focus and depth for evaluation of the implant

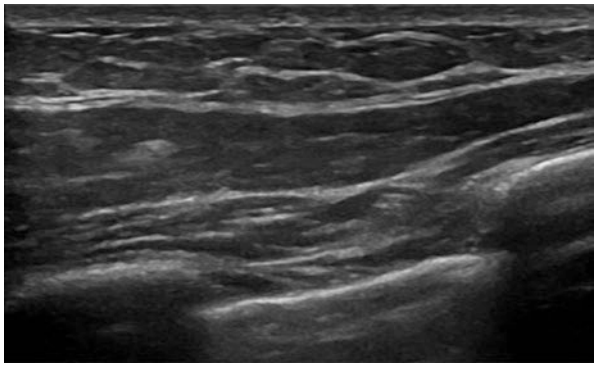

Fig. 7.25 Homogeneous background echotexture – fat

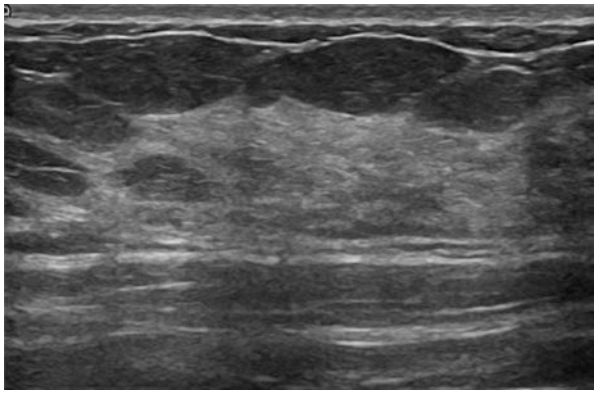

Fig. 7.26 Homogeneous background echotexture – fibroglandular

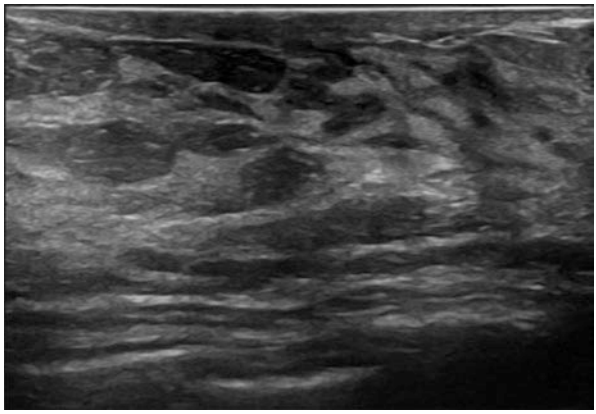

Fig. 7.27 Heterogeneous background echotexture

2. The characteristics of a mass that must be evaluated and included in the report include:

   (a) Shape
   Shape can be oval, round, or irregular (Figs. 7.28, 7.29, and 7.30).
   (b) Margin
   Can be circumscribed or non-circumscribed (indistinct, angular, microlobulated, or spiculated) (Figs. 7.31, 7.32, 7.33, 7.34, and 7.35).
   (c) Orientation (in relation to the skin surface)
   Parallel or non-parallel (Figs. 7.36 and 7.37).
   (d) Echogenicity
   Can be anechoic, hyperechoic, hypoechoic, isoechoic, complex cystic solid, or solid, heterogeneous (Figs. 7.38, 7.39, 7.40, 7.41, 7.42, and 7.43).
   (e) Posterior features

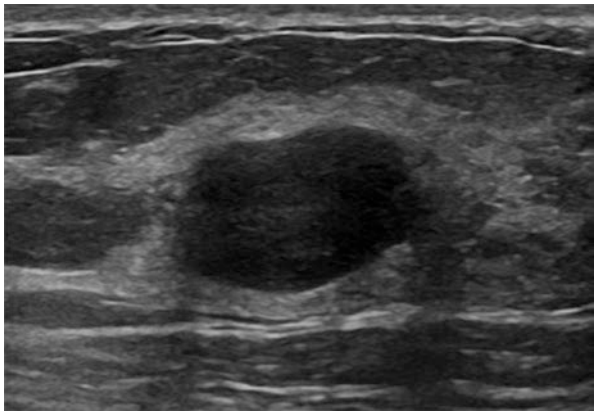

Fig. 7.28 Oval

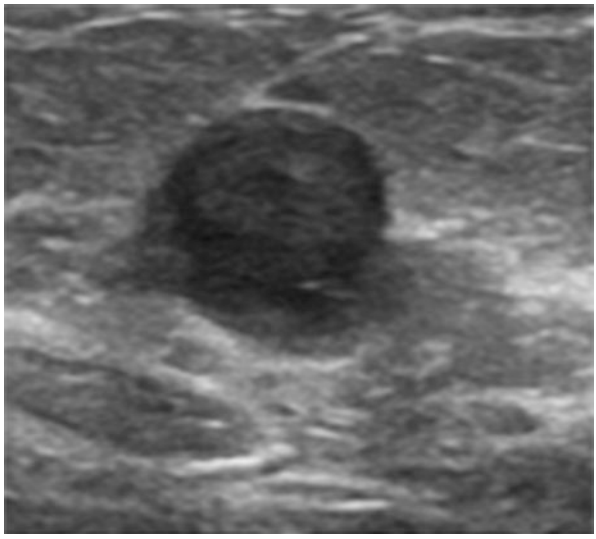

Fig. 7.29 Round

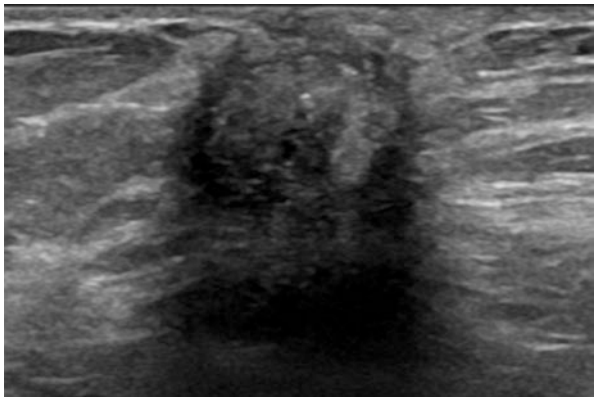

Fig. 7.30 Irregular

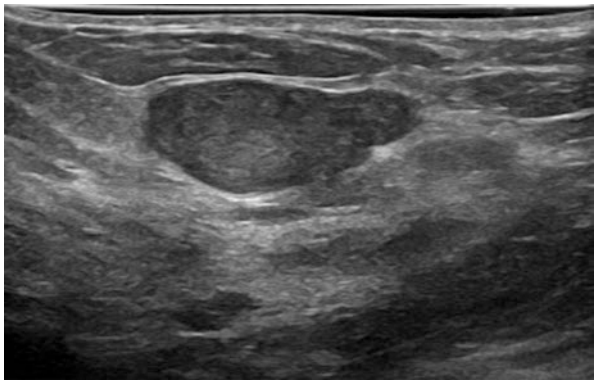

Fig. 7.31 Circumscribed

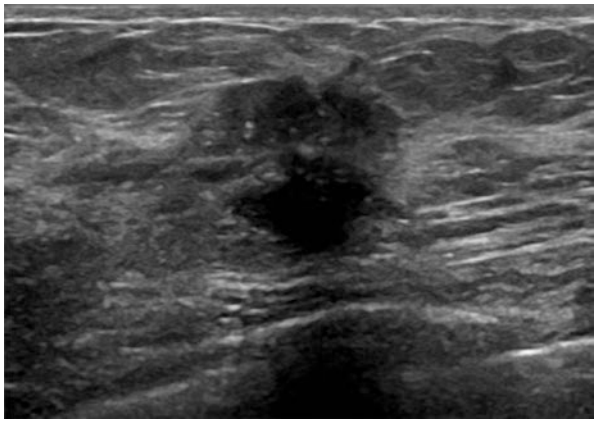

Fig. 7.32 Non-circumscribed – indistinct

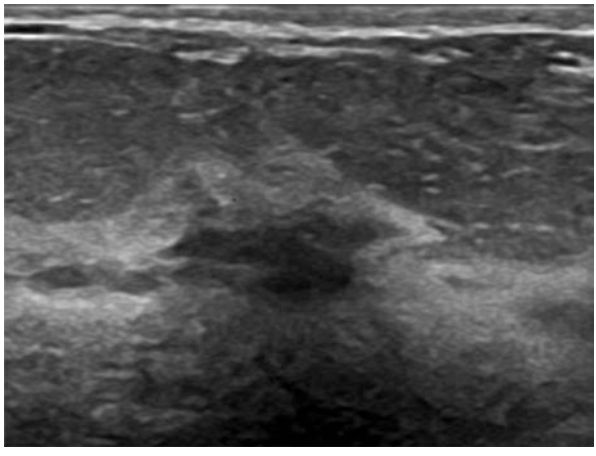

Fig. 7.33 Non-circumscribed – angular

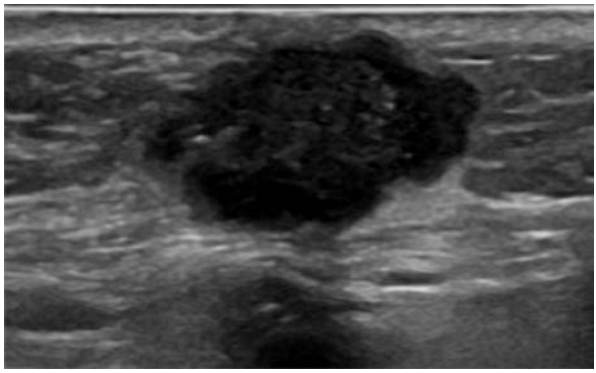

Fig. 7.34 Non-circumscribed – microlobulated

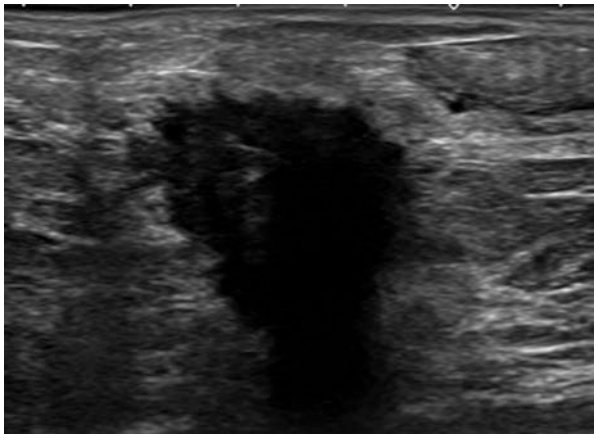

Fig. 7.35 Non-circumscribed – spiculated

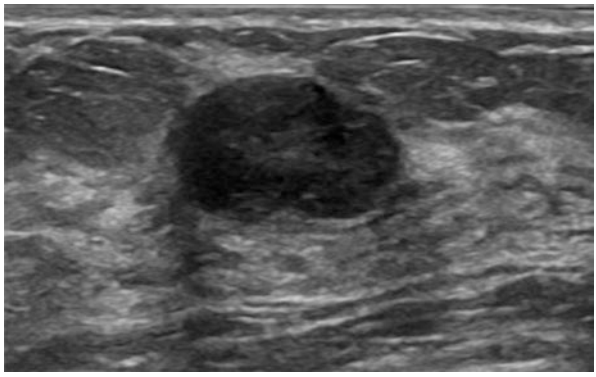

Fig. 7.36 Parallel

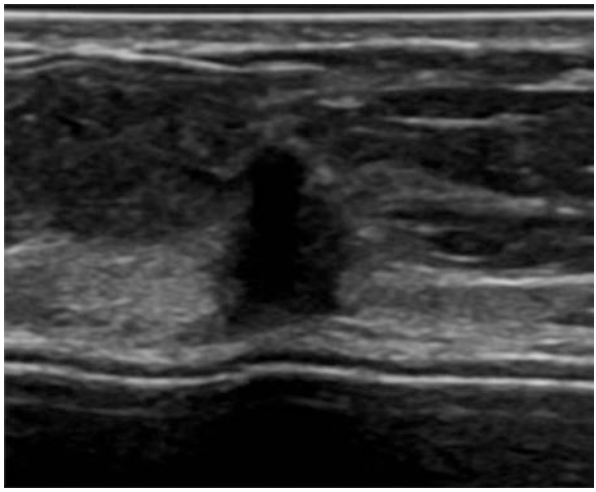

Fig. 7.37 Non parallel

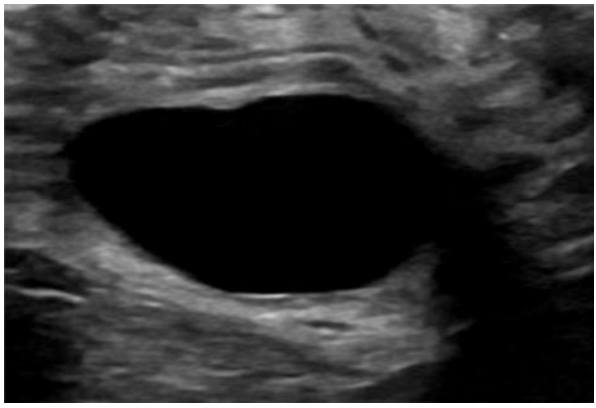

Fig. 7.38 Anechoic

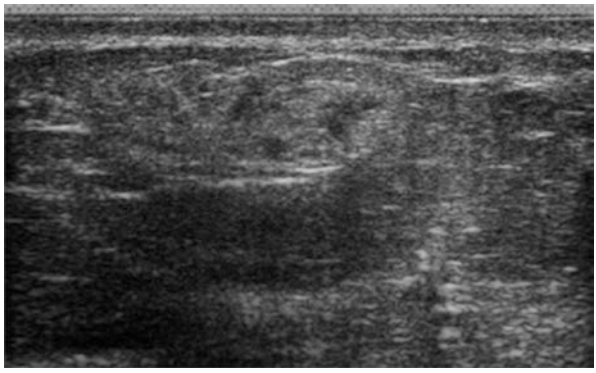

Fig. 7.39 Hyperechoic

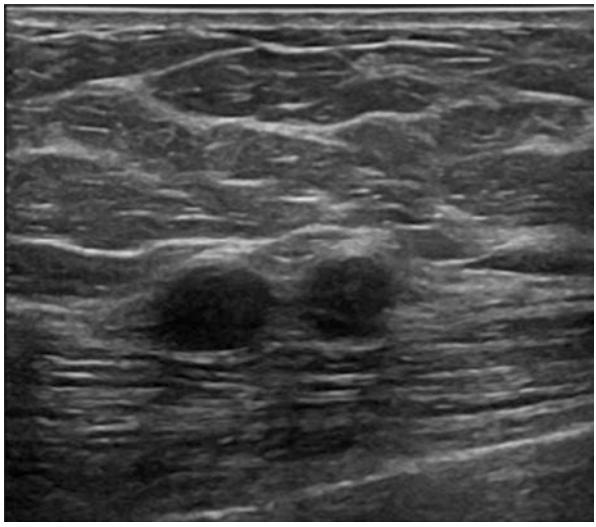

Fig. 7.40 Hypoechoic

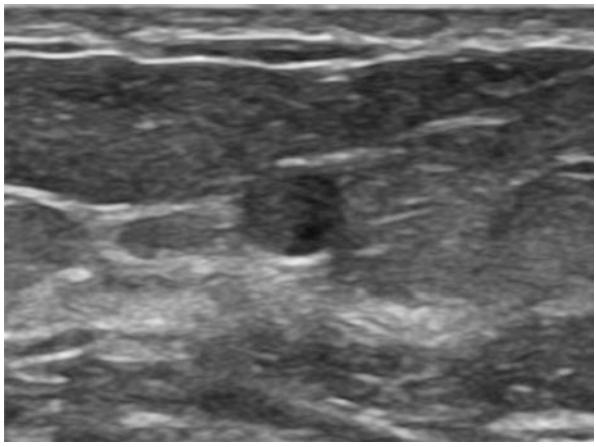

Fig. 7.41 Isoechoic

No posterior features, enhancement, shadowing, or combined pattern (Figs. 7.44, 7.45, and 7.46).

3. Calcifications
   Can be in a mass, outside a mass or intraductal (Figs. 7.47, 7.48, and 7.49).
4. Associated findings
   (a) Architectural distortion (Fig. 7.50).
   (b) Ductal changes (Fig. 7.51).
   (c) Skin changes
      (i) Skin thickening (Fig. 7.52).
      (ii) Skin retraction (Fig. 7.53).

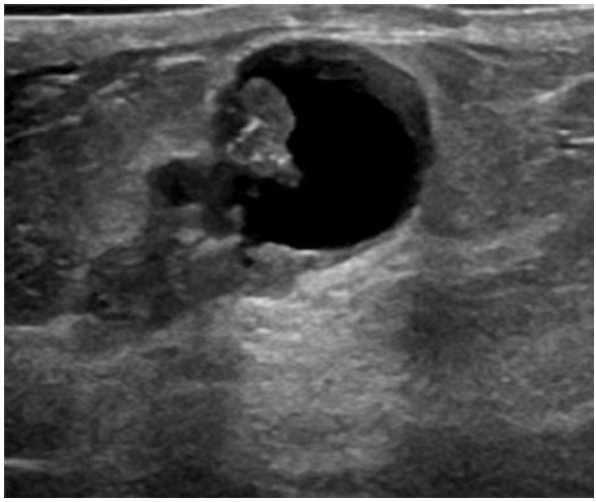

Fig. 7.42 Complex cystic solid

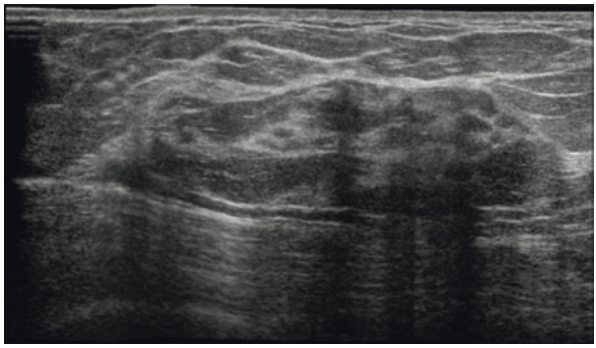

Fig. 7.43 Solid, heterogeneous

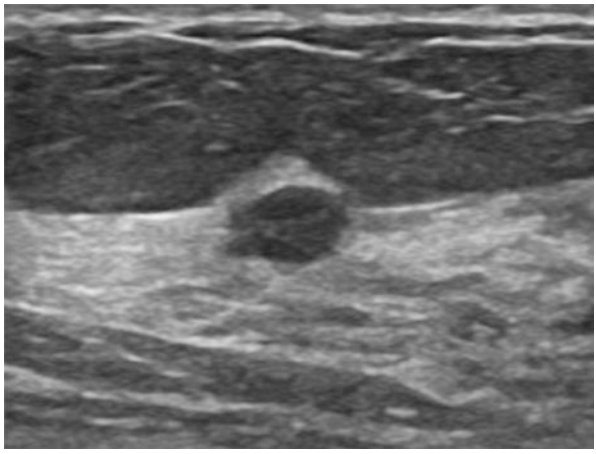

Fig. 7.44 No posterior features

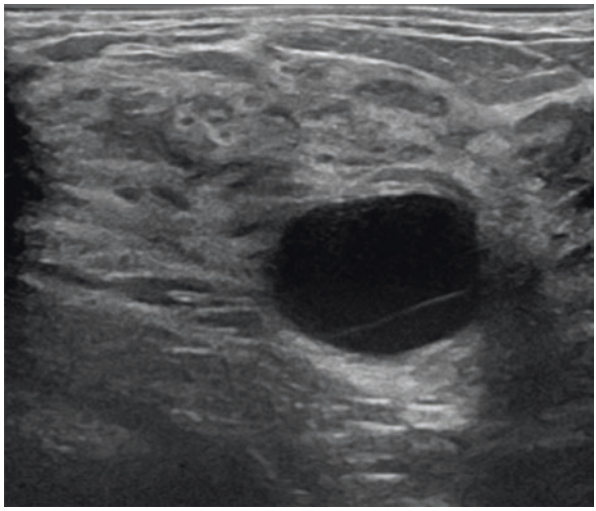

Fig. 7.45 Enhancement

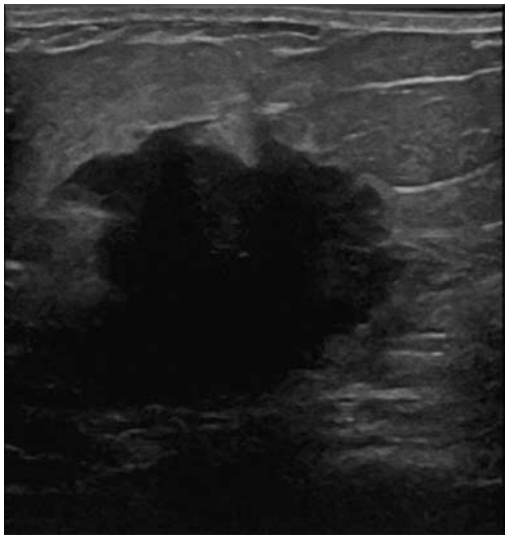

Fig. 7.46 Shadowing

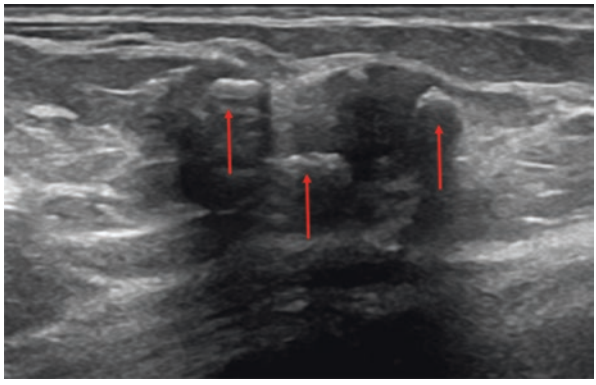

Fig. 7.47 Calcifications in a mass

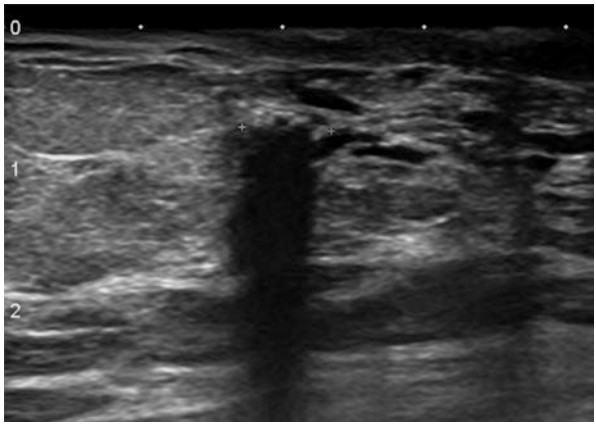

Fig. 7.48 Calcifications outside of a mass

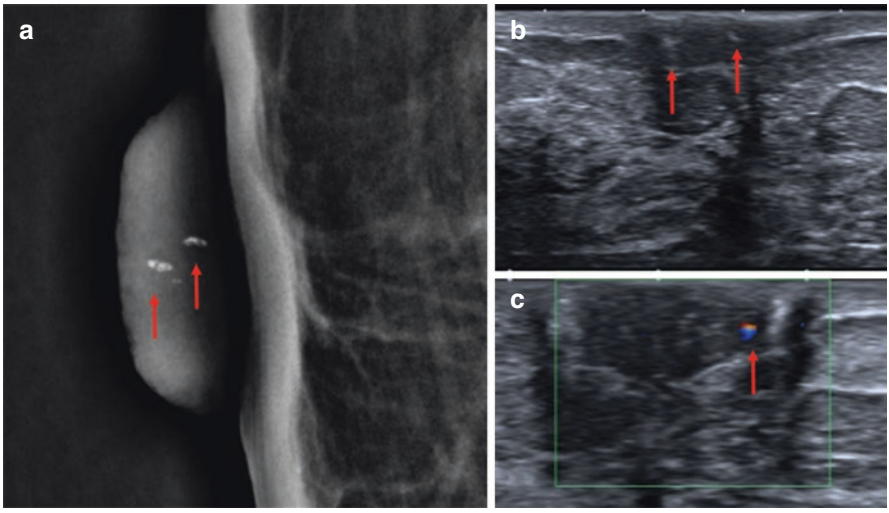

Fig. 7.49 A 75-year-old patient undergoing breast cancer screening. Linear calcifications on the right papilla on mammography (**a**). US shows hyperechoic foci within the papilla (**b**). In color Doppler (**c**), these foci have a "twinkle" artifact

(d) Edema (Fig. 7.54).
(e) Vascularity

(i) Absent
(ii) Internal vessels
(iii) Vessels in rim

(f) Elastography assessment

(i) Soft
(ii) Intermediate
(iii) Hard

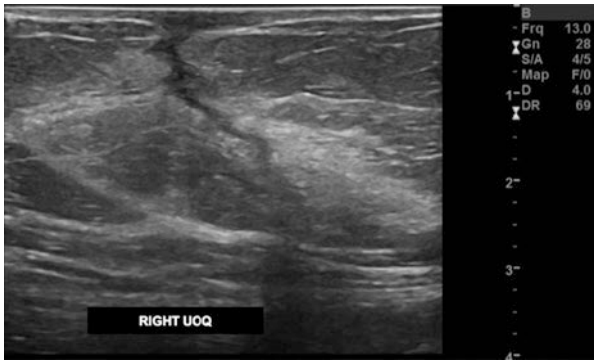

Fig. 7.50 Architectural distortion after breast conservation surgery

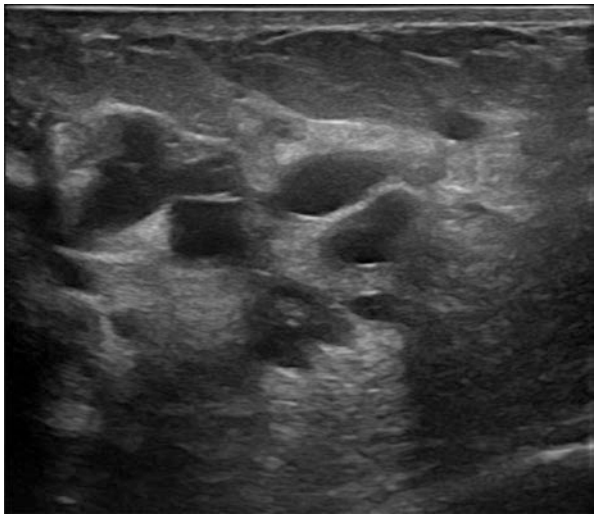

Fig. 7.51 Duct ectasia

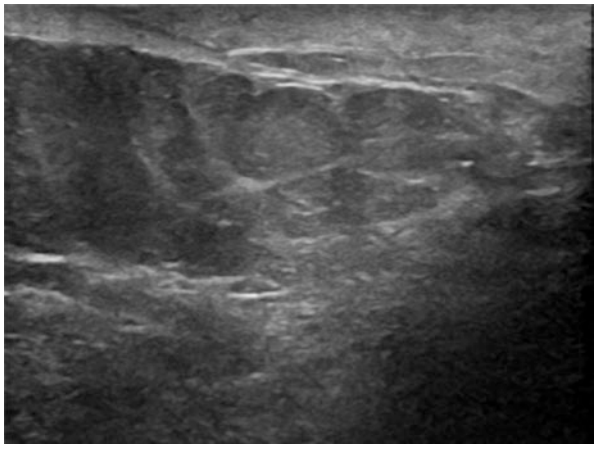

Fig. 7.52 Skin thickening

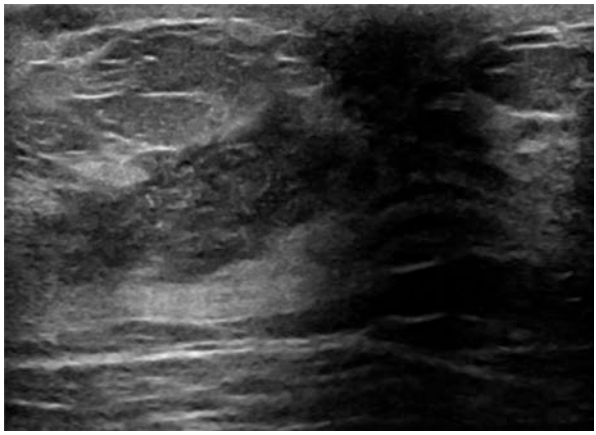

Fig. 7.53 Nipple retraction secondary to an irregular mass

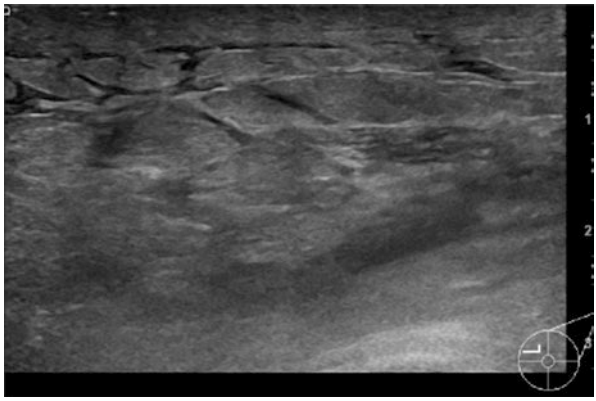

Fig. 7.54 Skin and parenchymal edema

5. Special cases

   (a) Simple cyst (Fig. 7.55).
   (b) Clustered microcysts (Fig. 7.56).
   (c) Complicated cyst (Fig. 7.57).
   (d) Mass in or on skin (Fig. 7.58).
   (e) Foreign body, including implants (Fig. 7.59).
   (f) Lymph nodes: intramammary, axillary (Fig. 7.60).
   (g) Vascular abnormalities (Fig. 7.61).
   (h) Postsurgical fluid collection (Fig. 7.62).
   (i) Fat necrosis (Fig. 7.63).

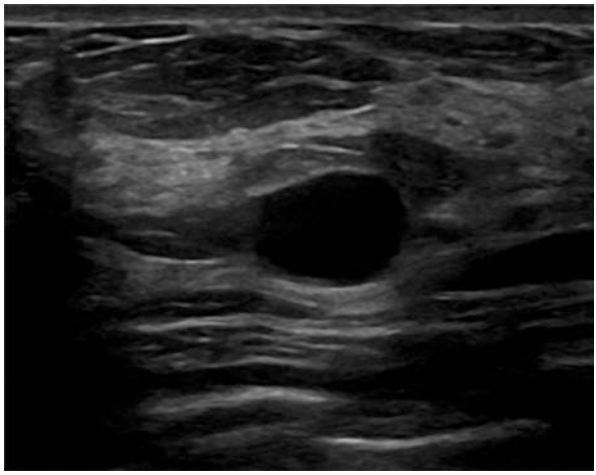

Fig. 7.55 Cyst

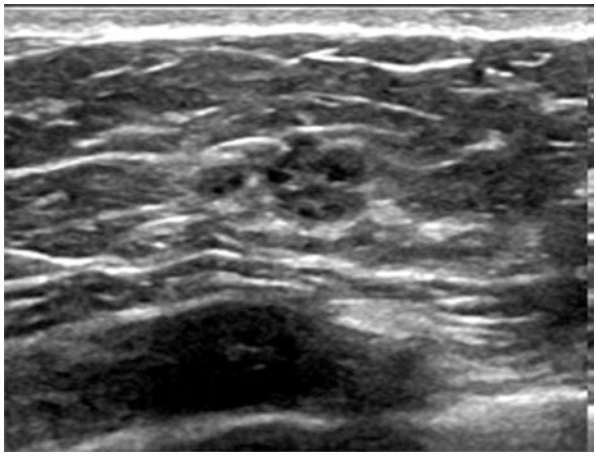

Fig. 7.56 Clustered microcysts

7.9 Report and Assessment

The preparation of the ultrasound report must contain the indication of the exam, the breast composition, a brief description of the lesion according to ACR BI-RADS, comparison with previous exams, final impression, and recommendation.

The report should conclude a summary of relevant US findings with a final assessment using BI-RADS® US categories 1–6 and the phrases associated with them.

If report of a US examination is integrated with a concurrently mammographic examination, the combined final assessment should reflect the highest likelihood of malignancy assessed by the two exams [7].

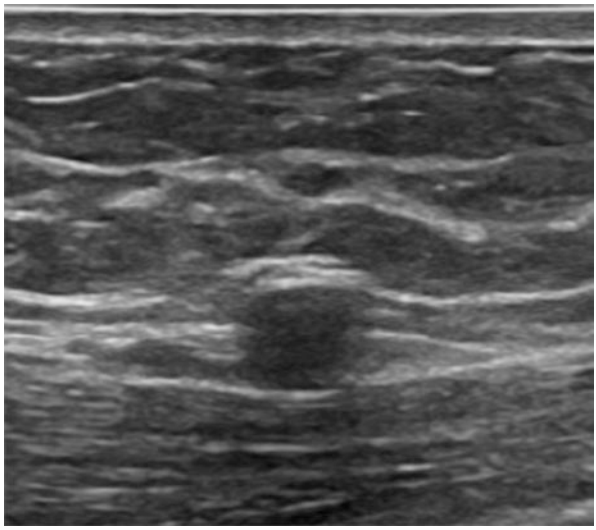

Fig. 7.57 Complicated cyst

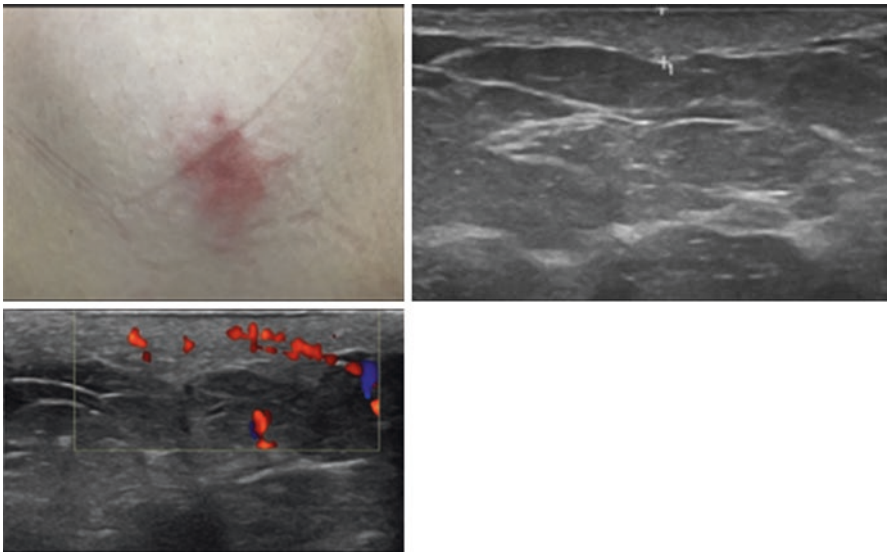

Fig. 7.58 Skin lesion. Ultrasound demonstrates skin thickening with increased vascularity

7.9.1 BI-RADS® Categories

1. Category 0: incomplete – need additional imaging evaluation.
2. Category 1: negative – 0% likelihood of malignancy – routine screening is recommended.

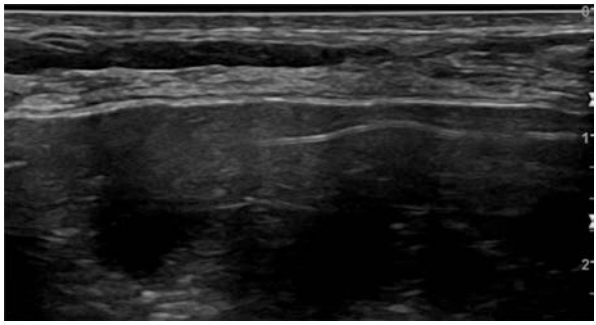

Fig. 7.59 Breast implant rupture

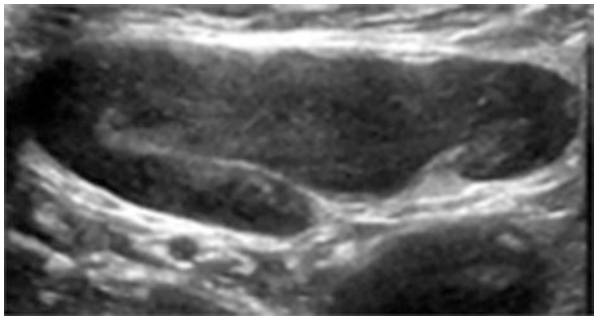

Fig. 7.60 Abnormal lymph node

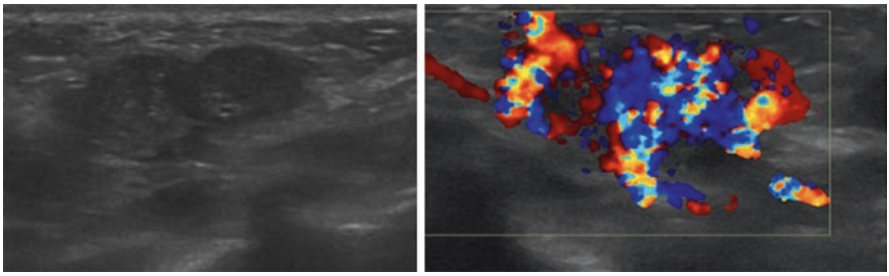

Fig. 7.61 An 8-month-old with circumscribed, hypoechoic, and heterogeneous mass in the upper outer quadrant of the left breast. Color Doppler shows high flow in the entire lesion with a vascular pedicle, consistent with arteriovenous malformation

3. Category 2: benign – 0% likelihood of malignancy – routine screening is recommended.
4. Category 3: probably benign – ≤2% likelihood of malignancy – follow-up is recommended (6 months, 12 months, 24 months, optional 36 months).
5. Category 4: suspicious – >2% but <95% likelihood of malignancy – tissue sampling is recommended.

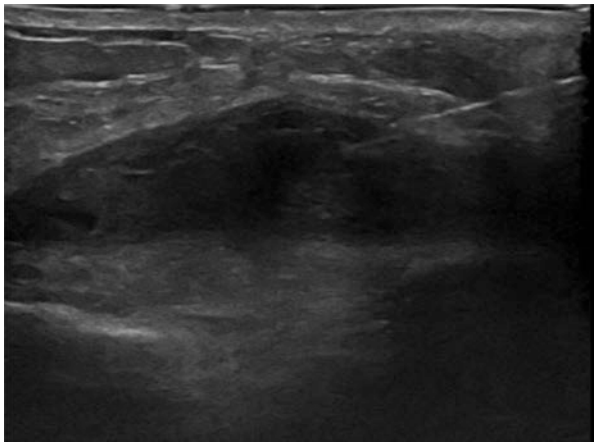

Fig. 7.62 Postsurgical fluid collection

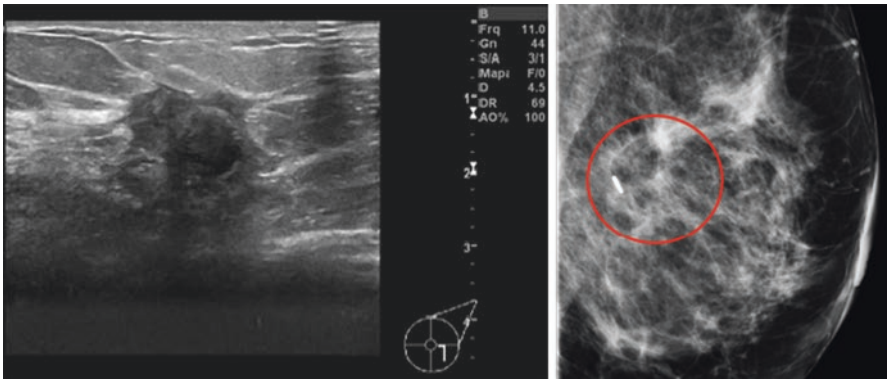

Fig. 7.63 Irregular mass in a patient with a history of surgical manipulation, requiring further evaluation with mammography. The correlation with mammography showed that it was steatonecrosis

BI-RADS subdivides category 4 assessments by likelihood of malignancy into categories 4A (>2% to ≤10%), 4B (>10% to ≤50%), and 4C (>50% to <95%).

6. Category 5: highly suggestive of malignancy – ≥95% likelihood of malignancy – tissue sampling is recommended.
7. Category 6: known biopsy-proven malignancy – surgical excision when clinically appropriate.

References

1. Stavros AT, Thickman D, Rapp CL, Dennis MA, Parker SH, Sisney GA. Solid breast nodules: use of sonography to distinguish between benign and malignant lesions. Radiology. 1995;196(1):123–34.
2. Watanabe T, Kaoku S, Yamaguchi T, Izumori A, Konno S, Okuno T, Tsunoda H, Ban K, Hirokaga K, Sawada T, Ito T, Nakatani S, Yasuda H, Tsuruoka M, Ueno E, Tohno E, Umemoto T, Shirakawa T. Multicenter prospective study of color Doppler ultrasound for breast masses: utility of our color Doppler method. Ultrasound Med Biol. 2019;45(6):1367–79. https://doi.org/10.1016/j.ultrasmedbio.2019.01.021. PMID: 30905536.
3. Cho N, Jang M, Lyou CY, Park JS, Choi HY, Moon WK. Distinguishing benign from malignant masses at breast US: combined US elastography and color doppler US–influence on radiologist accuracy. Radiology. 2012;262(1):80–90. https://doi.org/10.1148/radiol.11110886. PMID: 22084209.
4. Hooley RJ, Scoutt LM, Philpotts LE. Breast ultrasonography: state of the art. Radiology. 2013;268(3):642–59. https://doi.org/10.1148/radiol.13121606. PMID: 23970509.
5. https://www.acr.org/-/media/ACR/Files/Practice-Parameters/US-Breast.pdf. Assessed 15 Dec 2020.
6. Monticciolo DL, Newell MS, Moy L, Niell B, Monsees B, Sickles EA. Breast cancer screening in women at higher-than-average risk: recommendations from the ACR. J Am Coll Radiol. 2018;15(3 Pt A):408–14. https://doi.org/10.1016/j.jacr.2017.11.034. PubMed PMID: 29371086.
7. Mendelson EB, Bõhm-Vélez M, Berg WA, et al. ACR BI-RADS® ultrasound. In: ACR BI-RADS® atlas, breast imaging reporting and data system. Reston: American College of Radiology; 2013.
8. Leung JW, Sickles EA. Multiple bilateral masses detected on screening mammography: assessment of need for recall imaging. AJR Am J Roentgenol. 2000;175(1):23–9. https://doi.org/10.2214/ajr.175.1.1750023. PMID: 10882241.
9. Barr RG. Breast elastography: how to perform and integrate into a "best-practice" patient treatment algorithm. J Ultrasound Med. 2020;39(1):7–17. https://doi.org/10.1002/jum.15137. PMID: 31617225.
10. Vourtsis A. Three-dimensional automated breast ultrasound: technical aspects and first results. Diagn Interv Imaging. 2019;100(10):579–92. https://doi.org/10.1016/j.diii.2019.03.012. PMID: 30962169.
11. Hao SY, Jiang QC, Zhong WJ, Zhao XB, Yao JY, Li LJ, Luo BM, Ou B, Zhi H. Ultrasound elastography combined with BI-RADS-US classification system: is it helpful for the diagnostic performance of conventional ultrasonography? Clin Breast Cancer. 2016;16(3):e33–41. https://doi.org/10.1016/j.clbc.2015.10.003. PMID: 26639065.
12. Itoh A, Ueno E, Tohno E, Kamma H, Takahashi H, Shiina T, Yamakawa M, Matsumura T. Breast disease: clinical application of US elastography for diagnosis. Radiology. 2006;239(2):341–50. https://doi.org/10.1148/radiol.2391041676. PMID: 16484352.
13. Vourtsis A, Kachulis A. The performance of 3D ABUS versus HHUS in the visualisation and BI-RADS characterisation of breast lesions in a large cohort of 1,886 women. Eur Radiol. 2018;28(2):592–601. https://doi.org/10.1007/s00330-017-5011-9. PMID: 28828640.
14. Youk JH, Gweon HM, Son EJ. Shear-wave elastography in breast ultrasonography: the state of the art. Ultrasonography. 2017;36(4):300–9. https://doi.org/10.14366/usg.17024. PMID: 28513127; PMCID: PMC5621798.
15. Kim SH. Image quality and artifacts in automated breast ultrasonography. Ultrasonography. 2019;38(1):83–91. https://doi.org/10.14366/usg.18016. PMID: 30139244; PMCID: PMC6323315.
16. Kaplan SS. Automated whole breast ultrasound. Radiol Clin N Am. 2014;52(3):539–46. https://doi.org/10.1016/j.rcl.2014.01.002. PMID: 24792655.

Chapter 8
Magnetic Resonance Imaging: Regular Protocols and Fast Protocols

Joao V. Horvat and Sunitha B. Thakur

8.1 Introduction

Breast cancer diagnosis on magnetic resonance imaging (MRI) relies on the establishment of standard features for imaging acquisition. Patient positioning, temporal and spatial resolution, and pulse sequences should be standardized to provide high-quality images for adequate interpretation. The protocol should consist of sequences that can be obtained from different equipment within the same institution. The sequences obtained must provide images that are familiar to the radiology staff and that satisfy certain imaging interpretation objectives, such as differentiating cystic from solid lesions [1].

The imaging acquisition must not be extensively long. Long protocols can cause discomfort to the patient and may result in interruptions during the examination or patient motion that decreases the image quality. Long protocols reduce the number of patients that can be scanned within a certain amount of time, which may result in the elevation of costs. On the other hand, time should not be the most important factor in a protocol. If essential sequences are left out in a protocol, misdiagnosis may occur [2].

A reliable protocol must provide images that maintain a high sensitivity for the diagnosis of breast cancer and that are capable of differentiating between benign and malignant lesions [3]. Lesion morphology on gadolinium contrast-enhanced sequences is essential for this accomplishment. For malignant lesions, there are several morphological features that must be demonstrated, including shape, margin, internal enhancement pattern, and the presence of tumoral necrosis. Features that are typical of benign lesions such as the presence of fat should be clearly evident. A

J. V. Horvat (✉) · S. B. Thakur
Department of Radiology, Memorial Sloan Kettering Cancer Center, New York, NY, USA
e-mail: machadoj@mskcc.org; thakurs@mskcc.org

S. J. Kim Hsieh, E. A. Morris (eds.), *Modern Breast Cancer Imaging*,
https://doi.org/10.1007/978-3-030-84546-9_8

given protocol should be capable of preoperatively demonstrating local and regional staging for patients with breast cancer. The presence of chest wall invasion or axillary nodal disease may directly impact treatment management. These structures must be included in the field of view during the examination [4].

Standardization of MRI protocols is essential for patient care. Individuals with breast cancer may undergo a number of examinations in the same institution for a period of months to several years. Radiologists must be capable of comparatively evaluating these studies. This is of paramount importance, especially for the assessment of response to neoadjuvant treatment and to detect recurrence. Thus, protocols should remain unchanged as long as possible, unless modifications are proven to be highly necessary in order to improve diagnostic accuracy [1].

8.2 Standard Examination

The standard MRI examination consists of utilizing 1.5, 3, or 7 T equipment with a dedicated breast coil that frequently has between four and 16 channels. The patient lies in the prone position with the breasts hanging in the recesses of the coil. Care should be taken to make the breasts hang as free and straight as possible and to avoid much contact of the breasts with the surfaces of the coil as imaging artifacts may occur. Breasts are scanned from the clavicle to the inframammary fold. The axilla and the anterior chest wall should also be included in the examination. An intravenous access for the administration of gadolinium contrast media should be obtained. For contrast-enhanced sequences, a gadolinium-based agent should be administered at a dose of 0.1 mmol/kg of body weight with an injection rate of 2–3 mL/s followed by a 10–20 mL saline flush [5].

Although protocols may vary among institutions, there are universal goals that a given protocol must achieve. For an optimal diagnostic performance, a protocol must be able to detect enhancing lesions that measure 5 mm or more. A high signal-to-noise ratio and a high spatial resolution are necessary to demonstrate with fine detail lesion shape and margins. Acquisition slice thickness should be smaller than 3 mm, in-plane pixel resolution should be $\leq$1.0 mm, and interslice gap should be $\leq$0 mm [6]. A standard protocol usually includes T1-weighted and T2-weighted sequences and subtraction and 3D maximum intensity projection (3D MIP) post-processed images. Signal intensity of the most common structures in the breast on different MRI sequences is demonstrated in Table 8.1.

The sequences may be acquired in the axial, coronal, or sagittal planes or a combination of them. The advantage of the axial plane is a faster acquisition time and the possibility of comparing both breasts on the same image, facilitating lesion detection. Some breast imaging services may add other sequences to the protocol to improve accuracy, such as diffusion-weighted images with post-processed apparent diffusion coefficient (ADC) maps.

Table 8.1 Most common signal intensity of different structures in the breast on MRI sequences

Sequence	Fluid	Complicated cysts	Fat	Benign tumors	Malignant tumors	Lymph nodes (cortex)
T2 with fat sat	High	Low to high	Low	Low to high	Low	High
T1 without fat sat	Low	Low to high	High	Low	Low	Low
T1 with fat sat	Low	Low to high	Low	Low	Low	Low
T1 post contrast	Low	Low to high	Low	Low to high	High	High
Subtraction	Low	Low	Low	Low to high	High	High

8.3 T2-Weighted Images

T2-weighted images with fat suppression are the most important sequence for the detection of fluid [7]. Some facilities may opt to utilize a short tau inversion recovery (STIR) sequence instead with the same objective. Simple cysts present typical high signal intensity on T2 and have absence of internal enhancement on T1-weighted contrast-enhanced images. Complicated cysts may present high protein or hemorrhagic fluid content that may reduce T2 and increase T1 signal intensity. Subtraction images may be helpful in demonstrating the absence of internal enhancement within a complicated cyst.

T2-weighted images with fat suppression may aid in the identification of a solid portion on the wall of a cyst or a mass inside a fluid-filled duct. Cystic areas inside a mass are also visible on T2. The presence of tumoral necrosis is associated with poor prognosis and may also be identified as cystic areas with high signal intensity inside a tumor. Likewise, the presence of perilesional edema on T2-weighted images is also associated with malignancy and poor prognosis. Breast cancer on T2-weighted images usually presents low signal due to its high cellularity. Enhancing circumscribed masses that are T2 bright are most frequently benign [8]. Some tumors, on the other hand, may have a different biological profile and present high signal intensity on T2, like mucinous carcinomas [9].

Sequences without fat suppression, either T1 or T2, may be used to evaluate fat-containing lesions. Fat necrosis and mammary hamartoma, also known as fibroadenolipoma, can be easily detected as they present internal high signal similar to adjacent fatty tissue [10]. Due to its high resolution, radiologists may use this sequence to better visualize the margins of a mass, especially if it is surrounded by fat. Similarly, fat surrounding axillary lymph nodes may facilitate their identification and the diagnosis of nodal disease. Lastly, the distinction between a breast mass and an intramammary lymph node is not always easy. The identification of a fatty hilum in a sequence without fat suppression together with other morphological features may indicate that it corresponds to an intramammary lymph node. Some breast imaging services opt to include in their protocol only T2-weighted images with fat

suppression. As there is need for a sequence without fat suppression for the reasons mentioned, a T1-weighted sequence without fat suppression may be used instead.

8.4 T1-Weighted Images

Contrast-enhanced T1-weighted images are the core of breast cancer diagnosis on MRI. Most tumors present early and intense enhancement to gadolinium-based contrast media that is visually distinguishable from breast parenchyma and benign lesions. T1-weighted sequences are usually performed with fat suppression, but some breast imaging services may opt to utilize sequences without fat suppression. The advantage of fat suppression is to erase all of the high signal that comes from breast fatty tissue in order to better demonstrate enhancement to contrast media and to identify other lesions that might have high signal on unenhanced images [11].

Enhancing masses and non-mass enhancements are the main imaging findings on breast MRI. T1-weighted images must clearly demonstrate the morphology of enhancing lesions. For masses, shape and margins are the most important morphological features for imaging interpretation. For non-mass enhancements, distribution is a key factor. Some patterns like segmental distribution are frequently associated with malignancy. Given that lymph nodes enhance to gadolinium-based agents, contrast-enhanced sequences can be used to demonstrate nodal enlargement and cortical thickening, which are often associated with axillary metastatic disease. T1-weighted images can also be useful in the evaluation of pectoralis major muscle or skin malignant infiltration. The presence of abnormal enhancement in these structures is associated with neoplastic invasion.

Breast fibroglandular tissue may present background parenchymal enhancement to contrast media. The enhancement is symmetric, often seen in the periphery of the parenchyma, and shows persistent increase in signal intensity after gadolinium injection. In some patients, this enhancement may be markedly intense and jeopardize the identification of lesions, resulting in a decrease in sensitivity for the diagnosis of breast cancer. Occasionally, background enhancement may be highly heterogeneous and asymmetric, which can be confounded with a suspicious non-mass enhancement.

T1-weighted sequences consist of one acquisition before the administration of contrast agent and from one to seven or more contrast-enhanced dynamic phases that are repeatedly acquired in a certain time interval. There is no consensus on the number of phases that are adequate for a full multiparametric protocol. The first phase is acquired between 90 and 120 s after contrast injection followed by additional phases. Dynamic contrast-enhanced (DCE) acquisition is usually completed 4–7 min after contrast injection in most protocols. Nowadays, protocols often consist of one to three contrast-enhanced phases. Protocols that utilize more than one contrast-enhanced phase can demonstrate the enhancement kinetic curves of breast masses, while protocols that utilize a single post-contrast acquisition are more often seen in a screening scenario where abbreviated imaging studies are done.

8.5 Subtraction, Enhancement Curve, and 3D MIP

Post-processed images are extremely valuable in the analysis of breast MRI studies. Subtraction images correspond to the deletion of signal of the unenhanced T1-weighted sequence from a given contrast-enhanced phase. The result is the subtraction of all T1 signal except the signal from contrast enhancement. Subtraction images are capable of demonstrating only structures that truly present enhancement to gadolinium. There are, on the other hand, certain situations where the subtracted signal may not be optimal. Patient motion between pre- and post-contrast sequences may cause uneven subtraction. This may result in areas of false enhancement demonstrated in the subtraction images. When patient motion is suspected, visual comparison between pre- and post-contrast T1-weighted sequences is necessary to evaluate if it has occurred. Nowadays, there are several softwares that are capable of automatically correcting patient motion.

Variations in signal intensity between dynamic contrast-enhanced phases can be post-processed and graphically evaluated. Once a mass is visualized, it is possible to position a region of interest over it and create an enhancement kinetic curve. Three distinct enhancement curve patterns can be identified: persistent, plateau, and washout. Most malignant masses present a rapid increase in signal intensity followed by a contrast washout with a decay in signal intensity [12]. Most benign lesions, on the other hand, present a slow and persistent increase in signal intensity in the first 5 min after contrast injection [13].

3D MIP images have a significant contribution to the detection of breast cancer. They are obtained from subtracted images that are post-processed to create a three-dimensional volumetric display of both breasts. 3D MIP can better demonstrate abnormal enhancement with the comparison between both sides. Not only it is used to highlight malignancies, but it can also be useful in the comprehension of their position and distribution within the breast and the proximity to the papilla, skin, and chest wall.

8.6 Diffusion-Weighted Images

Diffusion-weighted images (DWI) are sometimes included in the standard protocol as it has been demonstrated to improve specificity in the evaluation of breast masses. This sequence can demonstrate features of breast tumors without the need of contrast injection. DWI demonstrates the diffusivity of water molecules in a tissue within a period of time [14, 15]. Two or more time points (b-values) are used to evaluate this diffusivity. A low b-value of 0 and a high b-value of 600–1500 s/mm^2 are typically used. Diffusion is reduced in the presence of high cellularity often found in malignant tumors that corresponds to high signal intensity on DWI. Previous studies have demonstrated that DWI may improve lesion diagnosis, especially in the differentiation between benign and malignant masses [16]. Traditional DWI sequences have

limited spatial resolution and are prone to artifacts that may jeopardize imaging interpretation [17]. Recent improvements in technique such as the use of readout-segmented echo planar imaging or multi-shot multiplexed sensitivity-encoding (MUSE) reduce these artifacts and improve lesion characterization [18, 19].

Post-processing images from the DWI sequence may be achieved with the creation of ADC maps that can be used to calculate the numerical amount of restriction in a mass. High-cellularity lesions present high diffusion restriction that is represented as low signal on ADC maps [20]. By drawing a region of interest on a lesion, ADC values can be calculated. Mean ADC values that are lower than 1.3×10^{-3} mm^2/s are associated with malignancy.

8.7 Breast Implants

Breast implants have become widely present in our society. MRI is the best modality for the evaluation of implant ruptures and other implant-related abnormalities. The vast number of different types of implants is specially challenging for radiologists. Implants may be filled with saline or silicone, which have different signal intensities on MRI. They may have one, two or, more lumens. They may present inner structures such as seals, valves, cannulas, markers, and chips that may cause confusion during imaging interpretation. Nevertheless, a standardized protocol to evaluate breast implants is necessary despite these variations [21].

Protocols to evaluate breast implants may be used alone or in addition to the standard protocol. Patients who are having an examination for the sole reason of evaluating implant rupture may opt not to receive intravenous contrast media. For these patients, a combination of unenhanced sequences of the standard protocol and sequences for implant evaluation should be used.

The sequences for implant evaluation consist of T2-weighted images with fat suppression and silicone or water suppression. These two sequences should be done in the same axis, as comparison between the two is of paramount importance. The suppression of silicone and water makes it possible for radiologists to evaluate abnormalities on the contours or within the implants that could be an indication of intracapsular rupture. The signal shift of silicone on the sequences with and without silicone suppression can demonstrate its presence within the breast parenchyma or inside internal mammary or axillary lymph nodes. Additionally, peri-implant fluid may be better depicted on the sequences with silicone suppression [22].

8.8 Abbreviated Protocol

Because of the high sensitivity of MRI for the detection of breast cancer, several studies have been conducted to evaluate its use in screening. There are a number of obstacles in MRI screening, including equipment lower availability, need of

intravenous contrast media, higher costs, and longer examination and reading times. To overcome some of these factors, abbreviated protocols with shorter examination times and with a reduced number of sequences have been proposed [23]. The main objective of these protocols is to maintain high sensitivity for breast cancer diagnosis [24]. Some protocols are proposed only to be used for patients with a previous full imaging protocol study, while others are used on the patient's first breast MRI examination [25].

The majority of abbreviated protocols consists of dynamic contrast-enhanced images with fat suppression. One pre-contrast and one post-contrast sequences are acquired followed by post-processed images, including subtraction and 3D MIP. Some authors have included other sequences such as more than one contrast-enhanced phase or T2-weighted images that may improve lesion characterization but increase examination and reading times. Since breast cancers usually present rapid contrast enhancement, images obtained 90–120 s after the injection of gadolinium depict the majority of malignancies on MRI.

8.9 Ultrafast Breast MRI

On MRI post-contrast sequences, breast malignant tumors enhance early, fast and avidly to gadolinium-based contrast agent. To evaluate the first stages of contrast inflow of breast lesions, ultrafast sequences were developed and have been investigated in several studies that were recently published. These sequences have high temporal resolution with an imaging acquisition of the whole breast that takes less than 7 s. Multiple repeated sequences can be obtained after contrast media injection or after it reaches the aorta. Kinetic curves of the first 1–2 min of contrast enhancement can demonstrate how early and intense a lesion enhances, and measurements of the enhancement curve slope can be obtained [26, 27]. These measurements have been used to improve specificity in the differentiation between benign and malignant lesions [28]. Some authors have proposed that ultrafast breast MRI can substitute the delayed standard dynamic contrast-enhanced sequences and reduce examination time [17].

8.10 Conclusion

Standardization of imaging protocols is necessary for consistent lesion detection and characterization. Protocols must be able to provide essential information to the radiologist in order to make the correct diagnosis. Protocols should not be extensively long but must include all the sequences needed to identify the most frequent breast lesions. Novel protocol proposals have been created to optimize lesion evaluation and to make breast MRI screening programs feasible and cost-effective. Abbreviated and ultrafast breast MRI have proven to be useful in clinical practice, maintaining high sensitivity for the diagnosis of breast cancer.

References

1. Newstead GM. MR imaging in the management of patients with breast cancer. Semin Ultrasound CT MR. 2006;27(4):320–32.
2. Clauser P, Mann R, Athanasiou A, Prosch H, Pinker K, Dietzel M, et al. A survey by the European Society of Breast Imaging on the utilisation of breast MRI in clinical practice. Eur Radiol. 2018;28(5):1909–18.
3. Huang W, Fisher PR, Dulaimy K, Tudorica LA, O'Hea B, Button TM. Detection of breast malignancy: diagnostic MR protocol for improved specificity. Radiology. 2004;232(2):585–91.
4. Thompson JL, Wright GP. The role of breast MRI in newly diagnosed breast cancer: an evidence-based review. Am J Surg. 2020;221(3):525–8.
5. Yitta S, Joe BN, Wisner DJ, Price ER, Hylton NM. Recognizing artifacts and optimizing breast MRI at 1.5 and 3 T. AJR Am J Roentgenol. 2013;200(6):W673–82.
6. Radiology ACo. Breast MRI clinical image review category D: spatial and temporal resolution 2019 [MRI and breast MRI accreditation]. Available at: https://accreditationsupport.acr.org/support/solutions/articles/11000070275-breast-mri-clinical-image-review-category-d-spatial-and-temporal-resolution
7. Santamaría G, Velasco M, Bargalló X, Caparrós X, Farrús B, Luis FP. Radiologic and pathologic findings in breast tumors with high signal intensity on T2-weighted MR images. Radiographics. 2010;30(2):533–48.
8. Lee JY, Jang M, Kim SM, Yun B, Jang JY, Ahn HS. Preoperative magnetic resonance imaging characteristics of oval circumscribed fast enhancing lesions in patients with newly diagnosed breast cancer. Medicine (Baltimore). 2018;97(19):e0704.
9. Pintican R, Duma M, Chiorean A, Fetica B, Badan M, Bura V, et al. Mucinous versus medullary breast carcinoma: mammography, ultrasound, and MRI findings. Clin Radiol. 2020;75(7):483–96.
10. Taboada JL, Stephens TW, Krishnamurthy S, Brandt KR, Whitman GJ. The many faces of fat necrosis in the breast. AJR Am J Roentgenol. 2009;192(3):815–25.
11. Carbonaro LA, Pediconi F, Verardi N, Trimboli RM, Calabrese M, Sardanelli F. Breast MRI using a high-relaxivity contrast agent: an overview. AJR Am J Roentgenol. 2011;196(4):942–55.
12. Partridge SC, Stone KM, Strigel RM, DeMartini WB, Peacock S, Lehman CD. Breast DCE-MRI: influence of postcontrast timing on automated lesion kinetics assessments and discrimination of benign and malignant lesions. Acad Radiol. 2014;21(9):1195–203.
13. Schnall MD, Blume J, Bluemke DA, DeAngelis GA, DeBruhl N, Harms S, et al. Diagnostic architectural and dynamic features at breast MR imaging: multicenter study. Radiology. 2006;238(1):42–53.
14. Iacconi C, Thakur SB, Dershaw DD, Brooks J, Fry CW, Morris EA. Impact of fibroglandular tissue and background parenchymal enhancement on diffusion weighted imaging of breast lesions. Eur J Radiol. 2014;83(12):2137–43.
15. Durando M, Gennaro L, Cho GY, Giri DD, Gnanasigamani MM, Patil S, et al. Quantitative apparent diffusion coefficient measurement obtained by 3.0Tesla MRI as a potential noninvasive marker of tumor aggressiveness in breast cancer. Eur J Radiol. 2016;85(9):1651–8.
16. Horvat JV, Durando M, Milans S, Patil S, Massler J, Gibbons G, et al. Apparent diffusion coefficient mapping using diffusion-weighted MRI: impact of background parenchymal enhancement, amount of fibroglandular tissue and menopausal status on breast cancer diagnosis. Eur Radiol. 2018;28(6):2516–24.
17. Mann RM, Cho N, Moy L. Breast MRI: state of the art. Radiology. 2019;292(3):520–36.
18. Naranjo I, Gullo R, Morris E, Larowin T, Fung M, Guidon A, et al. High-spatial-resolution multishot multiplexed sensitivity-encoding diffusion-weighted imaging for improved quality of breast images and differentiation of breast lesions: a feasibility study. Radiol Imaging Cancer. 2020;2(3):e190076.

19. Bogner W, Pinker K, Zaric O, Baltzer P, Minarikova L, Porter D, et al. Bilateral diffusion-weighted MR imaging of breast tumors with submillimeter resolution using readout-segmented echo-planar imaging at 7 T. Radiology. 2015;274(1):74–84.
20. Horvat JV, Bernard-Davila B, Helbich TH, Zhang M, Morris EA, Thakur SB, et al. Diffusion-weighted imaging (DWI) with apparent diffusion coefficient (ADC) mapping as a quantitative imaging biomarker for prediction of immunohistochemical receptor status, proliferation rate, and molecular subtypes of breast cancer. J Magn Reson Imaging. 2019;50(3):836–46.
21. Maijers MC, Niessen FB, Veldhuizen JF, Ritt MJ, Manoliu RA. MRI screening for silicone breast implant rupture: accuracy, inter- and intraobserver variability using explantation results as reference standard. Eur Radiol. 2014;24(6):1167–75.
22. Brenner RJ. Evaluation of breast silicone implants. Magn Reson Imaging Clin N Am. 2013;21(3):547–60.
23. Greenwood HI. Abbreviated protocol breast MRI: the past, present, and future. Clin Imaging. 2019;53:169–73.
24. Gao Y, Heller SL. Abbreviated and ultrafast breast MRI in clinical practice. Radiographics. 2020;40(6):1507–27.
25. Oldrini G, Derraz I, Salleron J, Marchal F, Henrot P. Impact of an abbreviated protocol for breast MRI in diagnostic accuracy. Diagn Interv Radiol. 2018;24(1):12–6.
26. Mori N, Abe H, Mugikura S, Takasawa C, Sato S, Miyashita M, et al. Ultrafast dynamic contrast-enhanced breast MRI: kinetic curve assessment using empirical mathematical model validated with histological microvessel density. Acad Radiol. 2019;26(7):e141–e9.
27. Shin SU, Cho N, Kim SY, Lee SH, Chang JM, Moon WK. Time-to-enhancement at ultra-fast breast DCE-MRI: potential imaging biomarker of tumour aggressiveness. Eur Radiol. 2020;30(7):4058–68.
28. Onishi N, Sadinski M, Gibbs P, Gallagher KM, Hughes MC, Ko ES, et al. Differentiation between subcentimeter carcinomas and benign lesions using kinetic parameters derived from ultrafast dynamic contrast-enhanced breast MRI. Eur Radiol. 2020;30(2):756–66.

Chapter 9
Nuclear Medicine Based Methods: PET FDG and Other Tracers

Marcelo Tatit Sapienza and Poliana Fonseca Zampieri

9.1 Introduction

9.1.1 Basic Aspects of ^{18}F-FDG-PET

Positron emission tomography (PET) allows the assessment of different metabolic parameters based on the detection of in vivo biodistribution of intravenously administered compounds, labeled with positron-emitting isotopes. Short-lived positron emitters are used to label several organic molecules, without interfering in their biological properties. During image acquisition, the positron emitted by the radiopharmaceutical interacts with an electron, and both undergo annihilation, emitting two gamma rays in opposite directions. In a typical PET equipment, these rays are detected simultaneously by scintillation crystals arranged like a ring around the patient in the detector system (Fig. 9.1). PET/CT cameras integrate PET imaging to a computed tomography (CT), adding the anatomical and morphological information of the CT to the functional information of PET. More recently, PET/MRI scan has also become available, allowing the integration of PET and magnetic resonance imaging (MRI) in a single study. This chapter will mainly review the application of PET/CT in breast cancer but will also discuss some aspects of PET/MR.

Fluorodeoxyglucose (FGD) is the most studied radiopharmaceutical in the evaluation of breast cancer. The FDG molecule is a glucose analog, in which a hydroxyl

M. T. Sapienza (✉)
Departamento de Radiologia e Oncologia, Hospital das Clinicas HCFMUSP, Faculdade de Medicina, Universidade de Sao Paulo, São Paulo, SP, Brazil
e-mail: marcelo.sapienza@hc.fm.usp.br

P. F. Zampieri
Departamento de Medicina Nuclear, Instituto do Cancer do Estado de Sao Paulo ICESP, São Paulo, SP, Brazil
e-mail: poliana.zampieri@hc.fm.usp.br

S. J. Kim Hsieh, E. A. Morris (eds.), *Modern Breast Cancer Imaging*,
https://doi.org/10.1007/978-3-030-84546-9_9

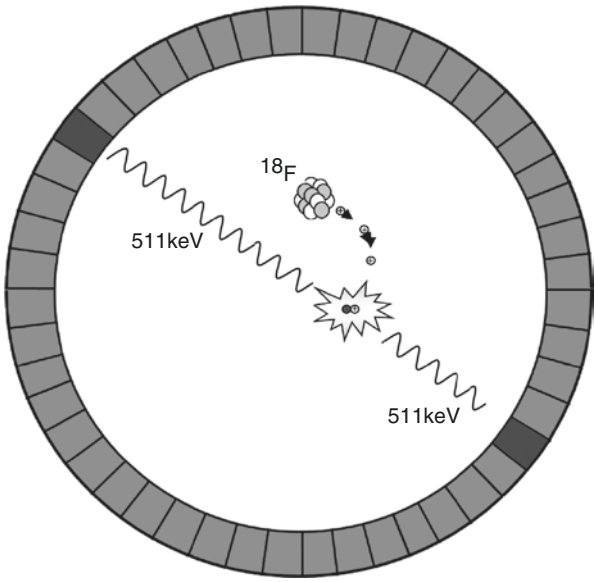

Fig. 9.1 Two gamma rays are emitted after a positron annihilation and detected simultaneously by the detectors in a PET equipment

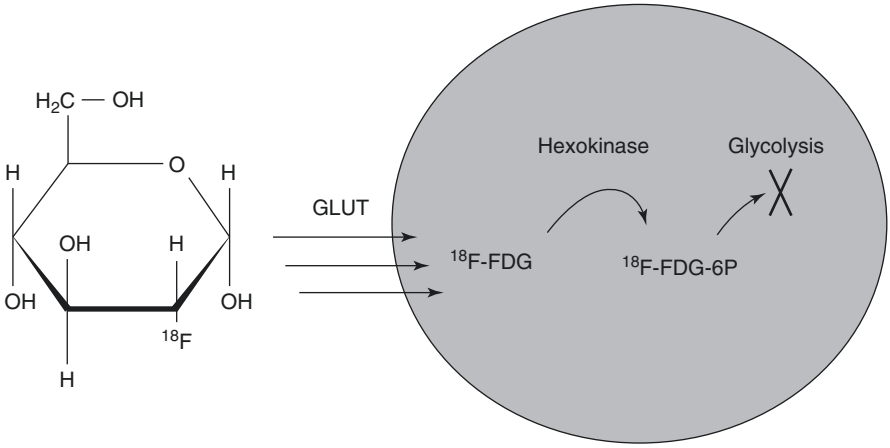

Fig. 9.2 FDG is transported by GLUTs and metabolized in FDG-6P by hexokinase but does not follow the subsequent glycolysis steps, being accumulated in the cell

group has been replaced by fluorine-18, obtained in a cyclotron. The uptake of ^{18}F-FDG by tumor cells occurs through non-insulin-dependent glucose transport systems (GLUTs 1 and 4) and, like glucose, undergoes phosphorylation due to hexokinase. Phosphorylated FDG does not progress in the metabolic pathway beyond this step and remains trapped in the tumor cell (Fig. 9.2). Most breast cancers present increased metabolic activity, although there are variations according to tumor characteristics and histology, to be discussed below.

PET/CT study is usually acquired 60 min after administration of ^{18}F-FDG to the fasting patient, who needs to remain at rest during the interval. Visual analysis is the basis for interpreting a PET/CT study. Semiquantitative measures can help to compare or monitor the degree of metabolic uptake, the most used being the SUV – standardized uptake value. SUV refers to the activity in a given volume of interest in relation to the total activity administered, corrected by the patient's weight.

$$\mathrm{SUV} = \frac{\text{Tissue activity concentration}\left(\dfrac{\mathrm{MBq}}{\mathrm{mL}}\right)}{\text{Injected dose}(\mathrm{MBq})} \times \text{body weight}(\mathrm{g})$$

Other tissues also show physiological uptake of FDG. Among the organs with intense physiological uptake of ^{18}F-FDG is the brain, impairing the ability to detect metastases at this site. Activity in the kidneys, ureters, and bladder resulting from the excretion of the radiopharmaceutical generally does not interfere with the interpretation of the study. It should also be remembered that inflammatory changes with infiltration by macrophages or granulation tissue (e.g., postoperative) have high metabolic activity and may lead to a false-positive study. Other causes of false-positive studies in the breast include benign conditions such as breast changes in pregnancy and lactation (Fig. 9.3), gynecomastia, mastitis, fat necrosis (Fig. 9.4), fibroadenoma, intraductal papilloma, and atypical ductal hyperplasia [1].

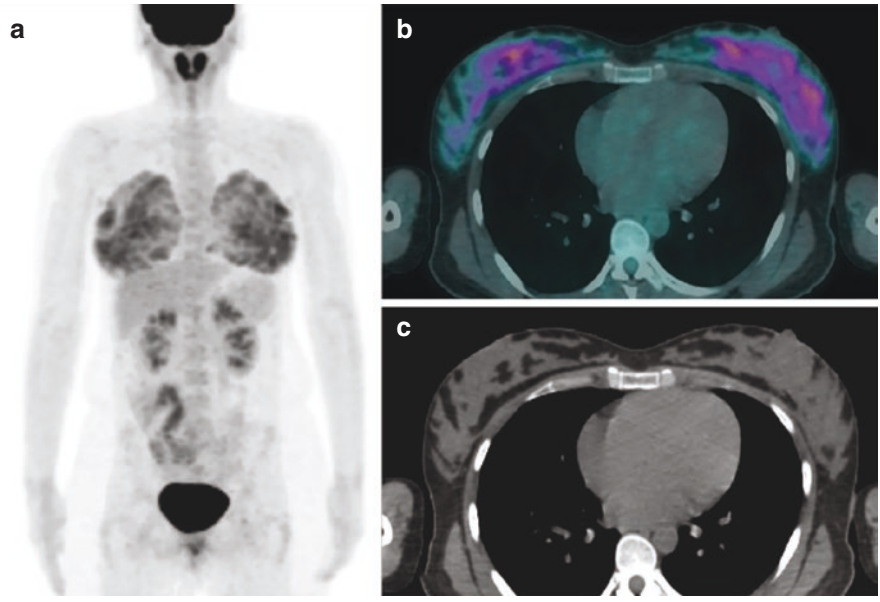

Fig. 9.3 FDG PET scan of a 39-year-old breastfeeding patient demonstrating diffuse intense activity in both breasts on MIP (**a**) and axial PET/CT (**b**), without tomographic lesions (**c**)

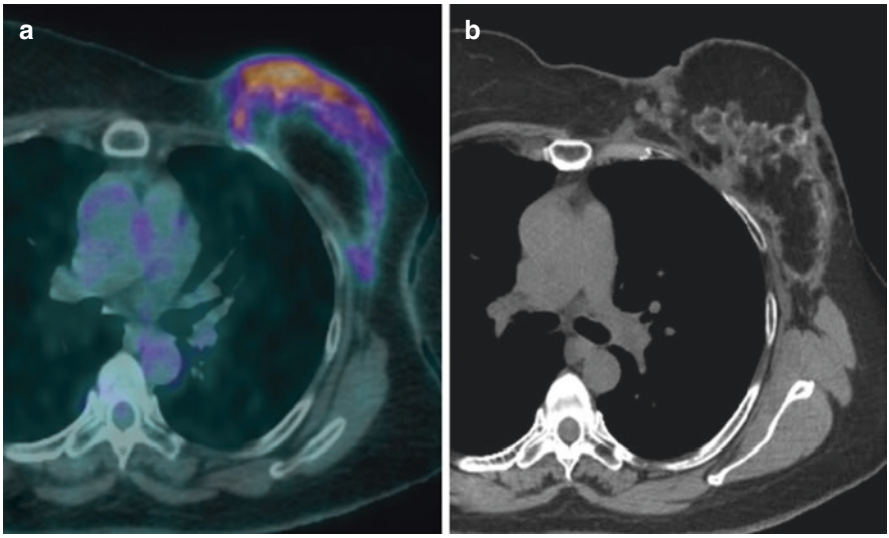

Fig. 9.4 Restaging FDG PET/CT scan in a patient suspected of having recurrent breast carcinoma. Axial fusion (**a**) and dedicated CT (**b**) images show areas of fat necrosis with increased FDG uptake

9.2 ^{18}F-FDG-PET/CT Indications in Breast Cancer

The National Comprehensive Cancer Network (NCCN) Guidelines do not indicate PET/CT in the staging of clinical stages I and II or operable stage III breast cancer. FDG PET/CT is suggested to be most helpful in situations where standard staging studies are equivocal or suspicious, especially in the setting of locally advanced or metastatic disease [2]. Regarding surveillance, the American Society of Clinical Oncology and NCCN guidelines recommend only regular history, physical examination, and mammography for breast cancer routine follow-up. Systematic ^{18}F-FDG PET/CT is not indicated [3].

Although not appropriate for all patients with breast cancer, the use of ^{18}F-FDG PET/CT can have an impact on patient care in multiple settings, including initial staging, treatment response assessment, and evaluation of suspected recurrence [4].

Influence of Histologic Subtypes and Receptor Status

Breast cancer is considered as a group of diseases with different molecular characteristics that originate in breast epithelial tissue but have different prognosis, patterns of recurrence, and dissemination after primary multidisciplinary treatments, leading to significant changes in diagnostic and therapeutic approaches [5].

^{18}F-FDG uptake depends on the histologic and biologic characteristics of the breast tumor and is influenced by its receptor status, grade, and histologic type [3, 4]. Invasive carcinoma of no special type (NST) exhibits higher uptake than invasive lobular carcinoma (ILC) [3, 6]. Lobular breast cancers may be occult at FDG PET even with large dimensions [4]. This is probably due to the lower density of tumor

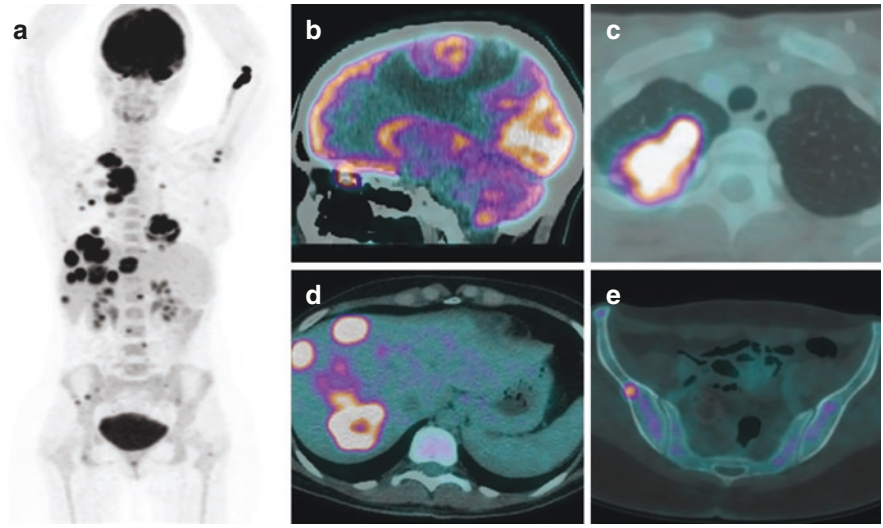

Fig. 9.5 Restaging with PET/CT in a patient with triple negative breast cancer presenting with reduction of strength in the left hemibody. MIP (**a**), sagittal PET/CT fusion (**b**), and axial PET/CT fusion (**c**–**e**) images show multiple metastasis with intense FDG uptake on the central nervous system, lungs, liver, and bones

cells in lobular carcinomas, lower expression of GLUT1, lower proliferation rates, and diffuse infiltrative tumor growth patterns into surrounding tissue, which may lead to false-negative scans [3]. Untreated osseous metastases from ILC are more likely sclerotic and missed by FDG PET than IDC metastases, showing a lower avidity and uptake similar to the background. In addition, ILC differs from NST in its patterns of metastatic spread, with a greater propensity to metastasize to the gastrointestinal tract and retroperitoneum, which are areas often difficult to assess with FDG PET as they are common sites of physiologic and variable FDG avidity [4].

Estrogen receptor (ER)-negative tumors and grade 3 cancers have significantly higher FDG avidity than ER-positive tumors and lower-grade malignancies [4]. Also, triple negative breast cancers demonstrate particularly elevated uptake of fluorodeoxyglucose (FDG) on PET. They are also known to result in early metastatic disease and have a propensity for extra skeletal metastases, increasing the importance of imaging for systemic staging [6] (Fig. 9.5).

Human epidermal growth factor receptor 2 (HER2)-positive breast cancers are characterized by a high expression of HER2 gene, which promotes tumor growth and progression and therefore tends to be more aggressive and FDG avid. Poorly differentiated tumors are more aggressive tumors and are more FDG avid [7]. There is also a positive correlation between the tumor proliferation index (Ki-67 expression) and the intensity of ^{18}F-FDG uptake [3].

Question Is the sensitivity of FDG PET similar for lobular and invasive carcinoma of no special type breast cancer? Why?

9.2.1 *Primary Breast Tumor Detection and Staging (T)*

FDG PET/CT is not indicated for screening in early-stage cancers [8]. Although it offers the opportunity to provide an overview of disease in a single procedure, the recommendation against the use of PET scanning is supported by many factors [3, 8]: it has low sensitivity for the primary breast tumor, and neither FDG PET nor CT is sensitive enough to detect breast cancers smaller than 1 cm [4]; the SUV in small lesions is susceptible to the partial volume averaging effect, which may lead to a lower value. This is further hampered by potential breathing motion artifact, as the PET acquisition is performed at tidal volume breathing [8]; ^{18}F-FDG imaging has lower sensitivity than the sentinel node technique in assessing axillary lymph node involvement, and the risk of distant metastases in early-stage cases is also low [3]. In addition to that, there is a high rate of false-positive scans in early-stage cancers, leading to unwarranted patient anxiety and delay of care in those patients [3].

However, in high-risk patients like those with inflammatory (T4d) or locally advanced breast cancer (LABC), the role of ^{18}F-FDG imaging in detecting local and distant metastasis has been highlighted [3]. FDG PET is helpful in local staging and particularly helpful in evaluation of internal mammary nodes and distant nodal metastasis [7]. It also helps to evaluate the equivocal findings on standard imaging and, in some cases, can detect unknown sites of distant metastasis even though the standard imaging is negative for lesions [7].

Any FDG-avid breast focus found during staging or surveillance of an extra-mammary malignancy should be thoroughly investigated in patients with reasonable life expectancy [8] (Fig. 9.6). These lesions have a 30–40% chance of being

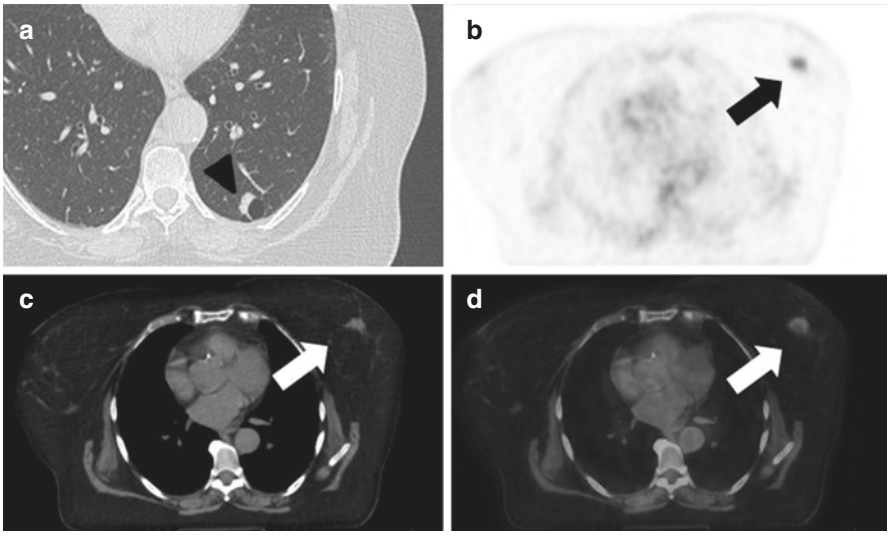

Fig. 9.6 FDG PET/CT used to stage lung cancer. Lung CT demonstrates partially cavitated pulmonary nodule (arrowhead in **a**), and PET/CT shows a solid nodule on the left breast (arrows in **b**, **c**, and **d**) with FDG uptake, which was later diagnosed as ductal invasive carcinoma by biopsy

malignant, including previously unsuspected primary breast malignancies, metastases to the breast, and breast lymphoma [4]. The likelihood that the lesion is a primary breast cancer is approximately 6%, and more than half of these will be early-stage disease, with potential for cure [8].

Question An intense area of FDG uptake was detected in the breast of a patient during the investigation of a solitary pulmonary nodule. Considering that FDG PET is not indicated for detecting a primary breast tumor, do you think this finding should be further evaluated?

9.2.2 Nodal Staging (N)

For the evaluation of locoregional nodal metastases, it is useful to make a distinction between axillary and regional extra axillary nodes [4]. Axillary lymph node status is one of the main prognostic factors in breast cancer. If there are no palpable lymph nodes on clinical examination, the currently accepted approach for axillary staging is sentinel lymph node biopsy. This technique has the advantage of detecting even micrometastases (<2 mm) or isolated tumor cells [9]. The sentinel lymph node biopsy predicts the state of axillary disease with an accuracy greater than 95%. FDG PET/CT has poor sensitivity for axillary nodal metastases compared with sentinel lymph node biopsy, because clinically relevant axillary nodal metastases are often subcentimeter in size. But the specificity of FDG PET/CT for axillary nodes has been shown to be far better than its sensitivity. Thus, the presence of an FDG-avid axillary node is likely to represent nodal malignancy [4].

Locoregional extra axillary nodes, including internal mammary, infraclavicular, and supraclavicular nodes, may be clinically occult and less commonly identified by sentinel node evaluation (Fig. 9.7). It is in this group of nodes where FDG PET/CT evaluation begins to show value in patient staging through the detection of unsuspected extra axillary nodal metastases [4]. Axillary node clearance by axillary dissection is usually limited to levels I and II. ^{18}F-FDG uptake suggesting involvement at level III (infraclavicular) or in extra axillary locoregional nodes (supraclavicular or internal mammary) may have important implications in surgical management and in the design of radiation therapy fields [3, 9].

Question A patient with a palpable axillary node had an FDG PET study acquired prior to the surgery. Intense FDG uptake was noted in multiple axillary nodes and also in the internal mammary node. What is the practical implication of this finding?

9.2.3 Metastatic Staging (M)

The most common sites of distant metastasis in breast cancer are bones, lungs, liver, and brain, and the conventional imaging studies for detecting distant metastasis include contrast-enhanced CT, bone scintigraphy, and MRI [10]. FDG PET/CT has

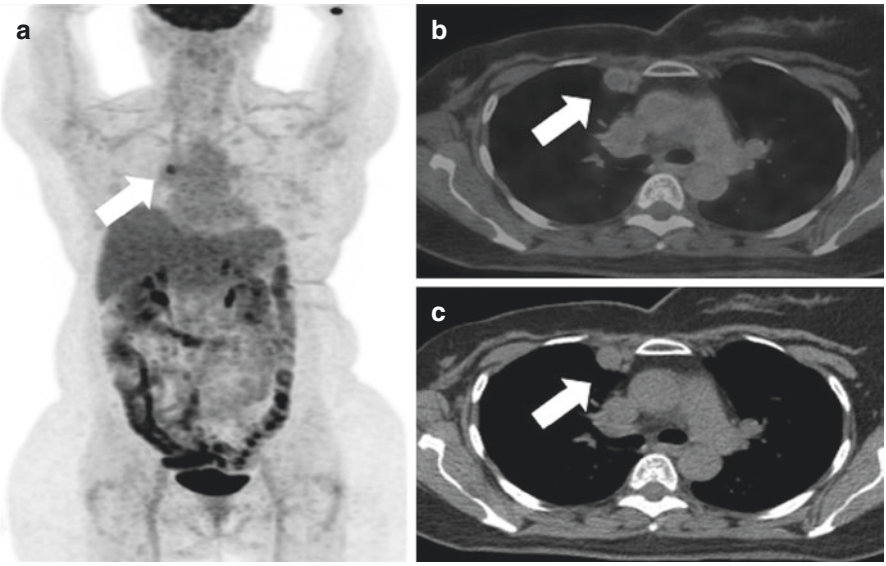

Fig. 9.7 Restaging with PET/CT in a patient with breast cancer presenting rising levels of CA 15-3. MIP (**a**), axial PET/CT fusion (**b**), and axial CT (**c**) images show intense FDG uptake in internal mammary lymph node (arrows in **a**, **b**, and **c**)

higher sensitivity than conventional modalities for detection of unsuspected distant metastasis in patients with locally advanced breast cancer, changing the patient's stage and converting patient's management from curative-intent therapy by surgery with or without neoadjuvant therapy to palliative systemic therapies [4].

Groheux et al. compared a conventional staging approach including bone scanning, chest radiography or dedicated CT, and liver ultrasound or contrast-enhanced CT for abdomen–pelvis with a single session of staging with ^{18}F-FDG PET/CT. ^{18}F-FDG PET/CT outperformed conventional imaging for bone, distant lymph nodes, and liver metastases, whereas CT was more sensitive for lung metastases [3]. PET lacks sensitivity for detection of infracentimetric pulmonary nodules because of the partial-volume effect and respiratory movements. Careful scrutiny of CT images from PET/CT can reveal small nodules without ^{18}F-FDG uptake. However, CT performed during free breathing is less efficient than standard diagnostic thoracic CT [3].

For evaluation of bone metastasis in breast cancer patients, both bone scintigraphy and FDG PET/CT are convenient whole-body imaging tools [11]. FDG PET acts as a tumor-specific tracer and reflects the glucose usage by tumor cells in viable metastatic lesions, while bone scintigraphy mainly reflects the response of surrounding bone to cancer. Bone scan may fail to show early response to effective therapy and may even show a "flare" related to bone healing. Similar findings may occur with other modalities including CT [11, 12]. Metabolic flare may be seen at FDG PET, with temporarily increasing FDG avidity after successful therapy; however, it occurs in the first 1–2 weeks and, thus, is not a confounding issue on scans

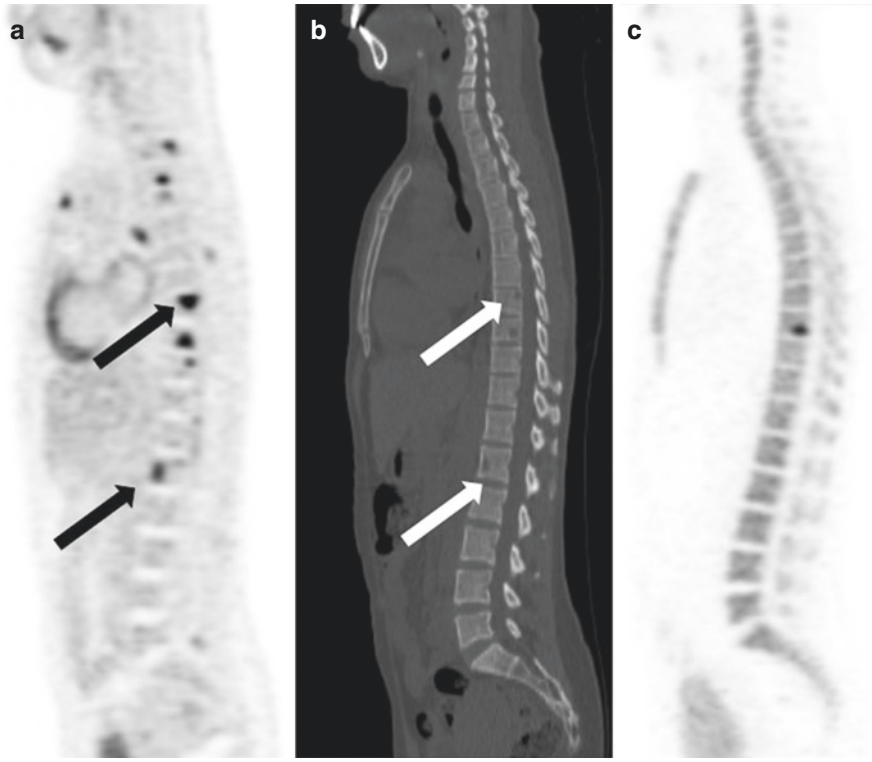

Fig. 9.8 Metastatic disease in a patient with biopsy-proven breast cancer. Arrows in sagittal PET (**a**) and sagittal CT (**b**) demonstrate FDG uptake in lytic bone lesions, with no uptake in ^{18}F-NaF (sodium fluoride) (**c**)

that are normally performed months after initiating therapy. Rather, FDG metabolic flare may be an indicator of future response to therapy [4].

PET is generally considered to be superior to CT and bone scintigraphy in detecting lytic or mixed bone metastases and bone marrow metastases (Fig. 9.8), but a multimodality approach is recommended for the investigation of bone metastases due to the low sensitivity of PET in detecting sclerotic bone metastases in some cases. In addition, sclerotic lesions without FDG accumulation can be detected on CT images of a PET/CT study [13].

FDG PET is not as sensitive as MRI in the evaluation of brain metastases. Cerebral cortex is highly FDG avid, and metastases often appear as focal areas of hypometabolism, which may also be seen in non-neoplastic entities. Some lesions do manifest as focal areas of hypermetabolism, although this can be difficult to detect in the setting of normal physiologic gray matter metabolism [14]. Furthermore, inflammatory tissue can also exhibit high FDG tracer uptake, diminishing diagnostic specificity [15].

Question Why, despite the high global sensitivity for breast cancer metastases, PET FDG is not indicated for the detection of brain lesions?

9.2.4 Recurrence

Breast cancer recurrence can be suggested by clinical symptoms, radiologic findings, or rising levels of tumor markers (carcinoma antigen 15-3, carcinoembryonic antigen or cancer antigen 125) [3]. ^{18}F-FDG PET/CT has a high diagnostic accuracy in detecting breast cancer recurrence in case of elevated levels of serum tumor markers, and it can be used in addition to conventional imaging techniques [16] (Figs. 9.9 and 9.10). The European Society for Medical Oncology (ESMO) guidelines and NCCN suggest that FDG PET/CT can be useful for identifying the site of relapse when traditional imaging methods are equivocal or conflicting, because it allows better discrimination between posttreatment scar or fibrosis and viable tumor tissue [17]. Moreover, this imaging modality can improve the identification of isolated locoregional relapse as well as isolated metastatic lesions, that is, a situation where patients may benefit from a more aggressive multidisciplinary approach [17]. PET/CT is also efficient in patients with suspected recurrence but with negative tumor marker results [3].

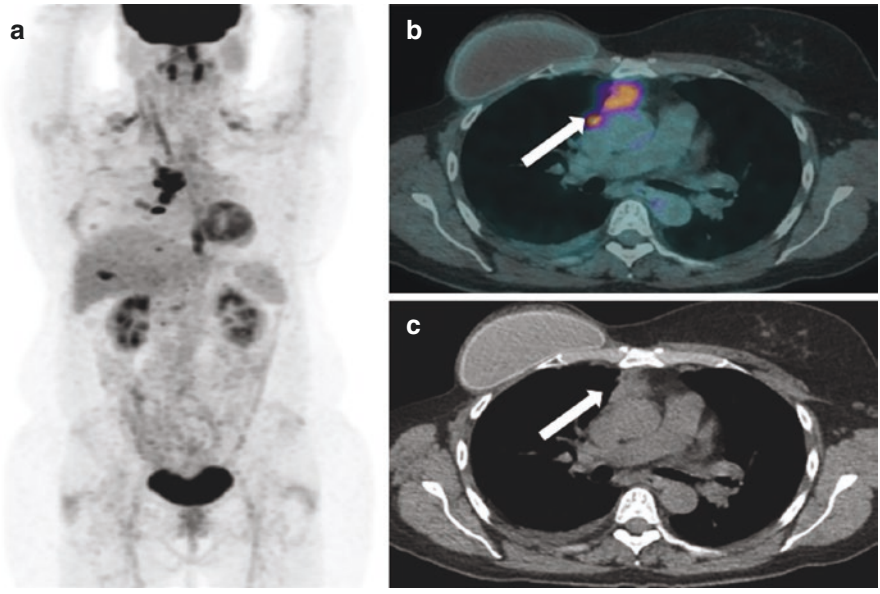

Fig. 9.9 PET/CT in a patient with breast cancer presenting rising levels of tumor markers. MIP (**a**), axial PET/CT fusion (**b**), and axial CT (**c**) images show FDG uptake on mediastinal soft tissue mass (arrows in **a**, **b**, and **c**)

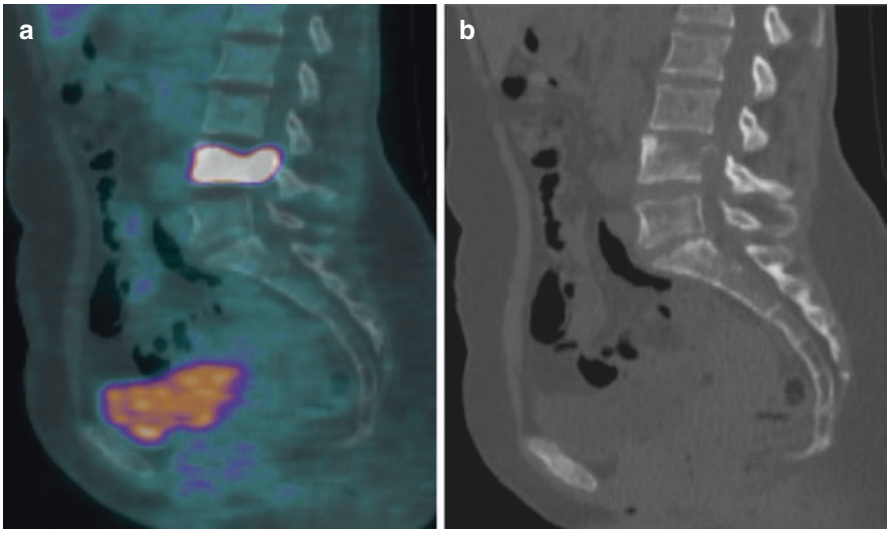

Fig. 9.10 PET/CT in a patient suspected of having recurrent breast carcinoma due to back pain. Sagittal PET/CT fusion (**a**) and sagittal CT (**b**) images show mixed bone lesion on the vertebral body of L4, consistent with metastatic disease

9.2.5 Response Assessment to Neoadjuvant Chemotherapy (NAC)

Breast cancer response to NAC has traditionally been assessed by conventional imaging modalities, which sometimes have difficulties in differentiating fibrosis from residual tumors. ^{18}F-FDG PET/CT and enhanced MRI are used in this clinical setting [18]. Studies using ^{18}F-FDG PET/CT to monitor early tumor responses to NAC showed a moderate accuracy to identify pathological responses in breast cancer patients, with better results than mammography, sonography, and MRI in predicting pathologic complete response (pCR) during NAC for locally advanced breast cancer [19].

^{18}F-FDG PET/CT can differentiate changes in tumor glucose metabolism before morphologic changes. The decrease in ^{18}F-FDG uptakes in tumors after chemotherapy is an indicator to assess the treatment response in triple-negative breast cancer (TNBC) and HER2-positive subtypes [18, 20]. Enhanced MRI can provide information on lesion microvasculature and depict changes in the physiologic characteristics of tumors [18]. PET/MRI holds the promise to improve therapy-response evaluation because it has the high sensitivity of PET and the high specificity of the MRI component [18].

9.2.6 *Response Assessment in Metastatic Disease*

Accurate assessment of treatment response is vital to provide the most effective therapy as well as to avoid unnecessary treatment escalation [21]. The current standard of measuring treatment response in metastatic breast cancer relies on size measurements of tumors, usually on CT [4]. Nonetheless, there are some inherent limitations in the size criteria. Distinguishing viable from nonviable residual tumor tissue is often difficult, and osseous metastases are in general nonmeasurable [22]. Metabolic changes measured by FDG PET may better predict treatment response than anatomic changes because PET/CT can differentiate active tumors from post-therapeutic changes and assess metabolic activity in osseous metastases [4, 22]. ^{18}F-FDG PET/CT seems to be accurate in directing treatment of metastatic bone disease as it reflects tumor activity, which is structurally difficult to be assessed by CT scan alone or by bone scintigraphy (Fig. 9.11). The latter reflects bone reaction against metastatic tumor that increases as the disease responds to treatment [21].

FDG PET was able to distinguish responders from nonresponders after distinct and varied courses of hormonal and chemotherapies of breast cancer metastases [4]. Riedl et al. showed that metabolic assessment by FDG PET/CT was a better predictor of both progression-free and disease-specific survival than Response Evaluation Criteria in Solid Tumors (RECIST) evaluation on CT, and this difference would alter overall patient management in 25% of the patients, reducing the morbidity and costs of ineffective therapies in clinical practice [22].

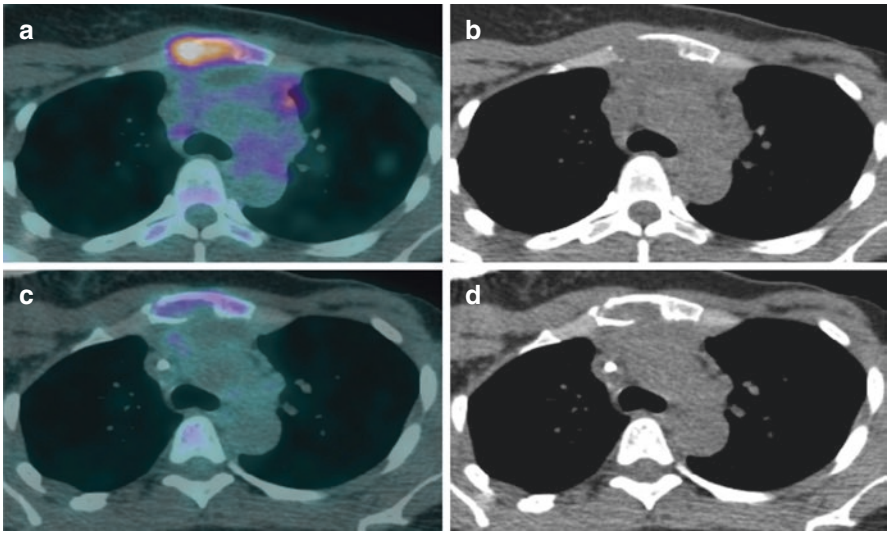

Fig. 9.11 Response assessment in a patient with metastatic breast cancer after chemotherapy. Pretreatment FDG PET/CT images (**a** and **b**) show intense bone lesion FDG uptake in the sternum. (**b**) Follow-up FDG PET/CT images after chemotherapy (**c** and **d**) show significant decrease in the intensity and extent of FDG uptake in the sternum

Question Is FDG PET a good method to assess whether a persistent residual mass after therapy corresponds to a viable tumor or fibrosis?

9.3 Prognostic Value

FDG PET has been found to have also a role in predicting the prognosis of breast cancer [23], indicating those patients more likely to progress, also with a correlation between SUV measurement and histologic grade, proliferation index, and triple-negative status [3]. High uptake reflects aggressive tumors and has poor prognosis [7]. Although SUVmax is one of the most widely used parameters in clinical settings, it does not show the uptake of the entire tumor mass and may not reflect the intratumor heterogeneity sufficiently [23]. Therefore, there has been an increasing interest in volumetric parameters such as metabolic tumor volume (MTV) and total lesion glycolysis (TLG), which are becoming easier to measure due to commercially available softwares [23]. The metabolic parameters SUVmax, MTV, and TLG of the lesion before treatment are related to the recurrence rate. The higher the metabolic parameters of the primary lesion, the greater the possibility of recurrence and distant metastasis [24].

9.4 Other PET Technologies and Tracers

9.4.1 PET/MR and Positron Emission Mammography (PEM)

After the rapid incorporation of PET/CT into clinical practice for staging and prognostic evaluation of breast cancer patients, hybrid PET/MRI equipment was developed. MRI provides not only high resolution but also high contrast images and the possibility of better tissue characterization with the combination of different pulse sequences. MRI sensitivity in the detection of breast lesions is well established, especially for patients with limitations in conventional mammographic/ultrasound evaluation, such as young women, dense breasts, and multifocal/multicentric lesions. Incorporation of metabolic information by FDG PET can increase the specificity of the method, but care must be taken with false-negative results in cases of small tumors (<1–2 cm) and histologic variations such as tubular carcinoma, well-differentiated, or in situ ductal carcinomas.

PET/MR for breast imaging includes specific position and pulse sequences. PET/MR mammography is acquired in the prone position with the breast hanging and allows better identification of lesions in the breast and regional lymph nodes [25]. MR imaging sequences usually include a T2 fat-suppressed sequence, a T1 non-fat-suppressed sequence, and post-contrast T1 sequences. Even though there is no increase in radiation dose, the additional time spent on a PET/MRI exam should

be considered in obtaining additional images. Among the additional MR sequences that may be indicated for FDG PET/MR mammography, diffusion-weighted imaging (DWI) is probably the most useful. Restricted diffusion and a low apparent diffusion coefficient (ADC) are observed in tissues with high cellularity, and this finding may provide prognostic information on breast cancer patients, although false-negative results may occur due to the association of necrotic tissues with aggressive tumors. Prognostic information obtained from DWI and FDG uptake may be incremental, as they reflect different biological properties of the tumor and are not directly correlated, even though when considered as isolated parameters, FDG uptake has a higher prognostic value than ADC values [26, 27].

Whole-body PET/MR is limited in the detection of breast lesions. A PET/MR mammography, with the acquisition of prone breast imaging using a breast coil, has better results in local assessment for determining the local extent of malignant lesions and for surgery planning [28, 29]. Another option is the fusion of breast PET and MR based on software. Post-acquisition fusion of PET/CT and MRI, guided by landmarks, has shown significant increases in specificity and positive predictive value (PPV) for breast lesions, as compared to MR alone [30].

MRI is generally considered to be of low effectiveness in preoperative lymph node evaluation. The same limitations of the PET component described in PET/CT apply to PET/MR. A PET/MR mammography allows better discrimination of lymph nodes than a whole-body study; however, the method is not able to detect minimal infiltrations and therefore does not replace a sentinel lymph node biopsy. Despite the limited sensitivity, there are situations in which a patient with locally advanced disease or during follow-up can benefit from the PET/MR study by detecting the metabolic alteration in lymph nodes that are not enlarged or by detecting previously unsuspected locoregional extra-axillary lymph node metastases [31]. Local staging may be well addressed by hybrid whole body PET/MR, combining the high sensitivity of MR for multifocal disease with the high sensitivity of PET for axillary nodal disease [32].

Regarding distant metastases detection, whole-body PET/MRI combination of structural and functional information in a single study may be valuable [33]. However, it is not yet clear whether there are advantages over performing sequential PET/CT and MRI studies. In the detection of distant metastasis, the MR component of a whole-body PET/MR will improve detection of lesions in the brain, liver, and bones and decrease the sensitivity for small lung lesions as compared to CT.

Low sensitivity of whole-body PET for breast cancer is due to the limited resolution of the method (5–6 mm). Resolution and lesion detectability can be improved using positron emission mammography (PEM). However, limitations arising from histological types with low metabolic activity are only partially resolved with these devices. PEM equipment consists of detectors arranged as plates, which compress the breast and allow the acquisition of images with greater spatial resolution and better sensitivity. There is also the configuration with the breast hanging through an opening in the examination table, with the PET detector ring positioned below. Both systems have limitations for lesions close to the thoracic wall.

PET mammography reports are preferentially described with a standardized interpretation lexicon similar to BI-RADS. Sensitivity and specificity of the method are higher than MR in a direct comparison and can contribute to a reduction in unnecessary biopsies [34]. Even without the CT exposure, administration of FDG implies in a whole-body radiation exposure more than ten times higher than that from a two-view screen film mammography [34]. Also, the technical complexity of the method, including those related to maintaining a nuclear medicine facility, makes it difficult to include PET mammography as a tool for screening or in primary patient evaluation.

Question Will PET/MR be a suitable equipment for breast cancer screening in the foreseeable future?

9.4.2 Non-FDG Tracers for Breast Cancer

While ^{18}F-FDG remains the most widely used radiopharmaceutical in PET studies, other tracers available or under development have a great prospect of clinical application in breast cancer imaging. New radiotracers allow a noninvasive method not only for staging but also for assessment of receptor status, metabolic activity, and proliferation [35]. The clinical introduction of these radiopharmaceuticals depends on factors such as local production and availability, clinical validation, and national regulatory agencies approval.

^{18}F-NaF (sodium fluoride) presents high affinity for areas of bone remodeling, determined by the fluoride ion exchange in hydroxyapatite crystals. Its higher and faster uptake, together with the improved resolution of PET in relation to scintigraphy, allows a higher sensitivity than a bone scan, especially for osteoblastic metastasis (Fig. 9.12). However, there is still a need for further cost-benefit analysis before the recommendation to replace the methods [36].

^{18}FMISO and *^{18}FAZA* are hypoxia markers that have prognostic value. Hypoxia, in addition to radioresistance, is associated with greater tumor aggressiveness and worse response to treatment, and a boost in hypoxemic tumors may allow optimization of radiotherapy results [37].

^{18}F-FLT (fluorothymidine) is a labeled nucleotide that traces DNA synthesis and correlates with Ki-67 expression, used as an imaging proliferation marker. FLT PET may be used in the assessment of early response to chemotherapy and endocrine therapy [38].

^{18}F-FES (fluoroestradiol) and other receptor tracers

^{18}F-FES is currently used to evaluate the estrogen receptor status in breast cancer patients, with the advantage of a simultaneous evaluation of multiple sites and of sites not accessible to a biopsy. Visual and semiquantitative measures (SUV) in a FES PET/CT can identify patients that will most likely benefit from endocrine

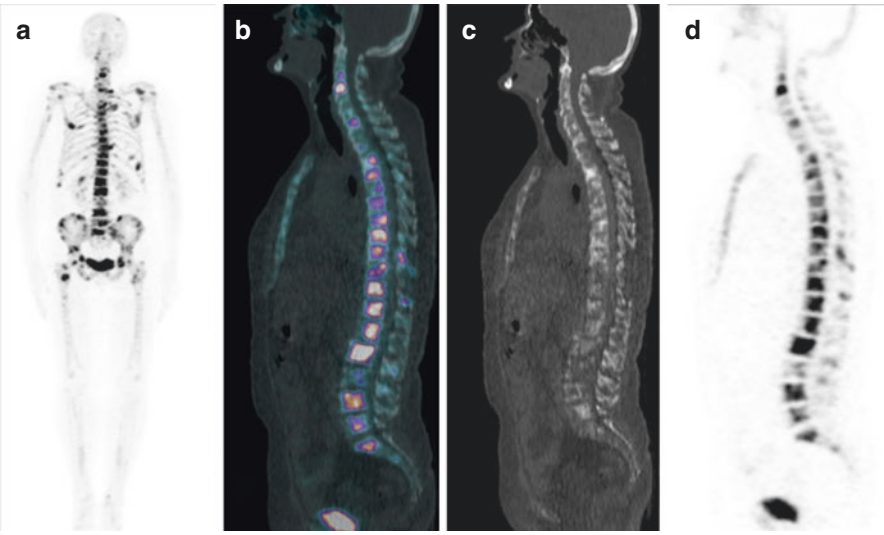

Fig. 9.12 ^{18}F-NaF PET shows multiple areas of increased radioactivity (**a**, **b**, and **d**), predominantly in the axial skeleton, consistent with osseous metastases. CT image (**c**) shows both lytic and sclerotic bone metastases, demonstrating fluoride uptake only on sclerotic lesions

therapy [39, 40]. Clinical trials are currently under way to assess the value of FES PET/CT as predictive marker of response to endocrine therapy.

^{18}F-Fluoro Furanyl Norprogesterone (^{18}F-FFNP) is a progesterone receptor tracer, also under evaluation to determine its value as a predictor of response to hormone therapy [41].

^{89}Zr-trastuzumab is one of many different tracers developed to study human epidermal growth factor type 2 (HER2) receptor status. HER2 PET is a possible method to predict response to trastuzumab-based therapy [41, 42].

Question FES PET can be used to evaluate hormone receptor status. Which lesions should be presumed to respond to hormonal therapy, those with high or with low radiopharmaceutical uptake?

9.5 Conclusion

^{18}F-FDG PET/CT is indicated for distant metastases detection in patients with advanced breast cancer, particularly when other methods are inconclusive. It is also indicated to detect suspected recurrence. New tracers and equipment may increase the future role of PET imaging in breast cancer patients.

References

1. Dong A, Wang Y, Lu J, Zuo C. Spectrum of the breast lesions with increased 18F-FDG uptake on PET/CT. Clin Nucl Med. 2016;41:543–57. https://doi.org/10.1097/rlu.0000000000001203.
2. Rashmi Kumar JB. NCCN Guidelines Version 6.2020 Breast Cancer. Version 6.2020 — September 8, 2020. NCCN Guidelines Version 6.2020 Breast Cancer. Version 6.2020 — September 8, 2020. [cited 2020 Sep 27]. Available at: https://www.nccn.org/professionals/physician_gls/pdf/breast.pdf
3. Groheux D, Cochet A, Humbert O, Alberini J-L, Hindie E, Mankoff D. 18F-FDG PET/CT for staging and restaging of breast cancer. J Nucl Med. 2016;57:17S–26S. https://doi.org/10.2967/jnumed.115.157859.
4. Ulaner GA. PET/CT for patients with breast cancer: where is the clinical impact? Am J Roentgenol. 2019;213:254–65. https://doi.org/10.2214/ajr.19.21177.
5. Hortobagyi GN, Connolly JL, D'Orsi CJ, Edge SB, Mittendorf EA, Rugo HS, et al. AJCC cancer staging manual. Breast. 2017;2017:589–636. https://doi.org/10.1007/978-3-319-40618-3_48.
6. Provenzano E, Ulaner GA, Chin S-F. Molecular classification of breast cancer. PET Clin. 2018;13(3):325–38.
7. Lebron L, Greenspan D, Pandit-Taskar N. PET imaging of breast cancer. PET Clin. 2015;10:159–95. https://doi.org/10.1016/j.cpet.2014.12.004.
8. Benveniste AP, Marom EM, Benveniste MF, Mawlawi O, Fox PS, Yang W. Incidental primary breast cancer detected on PET–CT. Breast Cancer Res Treat. 2015;151:261–8. https://doi.org/10.1007/s10549-015-3402-7.
9. Yararbas U, Avci NC, Yeniay L, Argon AM. The value of 18F-FDG PET/CT imaging in breast cancer staging. Bosn J Basic Med Sci. 2018;18(1):72–9.
10. Paydary K, Seraj SM, Zadeh MZ, Emamzadehfard S, Shamchi SP, Gholami S, et al. The evolving role of FDG-PET/CT in the diagnosis, staging, and treatment of breast cancer. Mol Imaging Biol. 2019;21:1–10. https://doi.org/10.1007/s11307-018-1181-3.
11. Park S, Yoon J-K, Lee SJ, Kang SY, Yim H, An Y-S. Prognostic utility of FDG PET/CT and bone scintigraphy in breast cancer patients with bone-only metastasis. Medicine. 2017;96:e8985. https://doi.org/10.1097/md.0000000000008985.
12. Peterson LM, O'Sullivan J, Wu Q, et al. Prospective study of serial 18F-FDG PET and 18F-fluoride PET to predict time to skeletal-related events, time to progression, and survival in patients with bone-dominant metastatic breast cancer. J Nucl Med. 2018;59:1823–30. https://doi.org/10.2967/jnumed.118.211102.
13. Aliyev A, Aksoy SY, Özhan M, Ekmekçioğlu Ö, Vatankulu B, Kocael PÇ, et al. The role of FDG PET/CT in detection of distant metastasis in theinitial staging of breast cancer. Turk J Med Sci. 2016;46:349–60. https://doi.org/10.3906/sag-1409-1.
14. Fink KR, Fink JR. Imaging of brain metastases. Surg Neurol Int. 2013;4(Suppl 4):S209–19.
15. Galldiks N, Langen K-J, Albert NL, Chamberlain M, Soffietti R, Kim MM, et al. PET imaging in patients with brain metastasis—report of the RANO/PET group. Neuro-Oncology. 2019;21:585–95. https://doi.org/10.1093/neuonc/noz003.
16. Göktaş İ, Cayvarlı H. The role of F-FDG PET/CT in evaluating elevated levels of tumor markers in breast cancer. Mol Imaging Radionucl Ther. 2018;27(1):3–9.
17. Piva R, Ticconi F, Ceriani V, Scalorbi F, Fiz F, Capitanio S, et al. Comparative diagnostic accuracy of ^{18}F-FDG PET/CT for breast cancer recurrence. Breast Cancer. 2017;9:461–71. https://doi.org/10.2147/bctt.s111098.
18. Liu Q, Wang C, Li P, Liu J, Huang G, Song S. The role of18F-FDG PET/CT and MRI in assessing pathological complete response to neoadjuvant chemotherapy in patients with breast cancer: a systematic review and Meta-analysis. Biomed Res Int. 2016;2016:1–10. https://doi.org/10.1155/2016/3746232.
19. Tian F, Shen G, Deng Y, Diao W, Jia Z. The accuracy of 18F-FDG PET/CT in predicting the pathological response to neoadjuvant chemotherapy in patients with breast cancer: a

meta-analysis and systematic review. Eur Radiol. 2017;27:4786–96. https://doi.org/10.1007/s00330-017-4831-y.
20. Grapin M, Coutant C, Riedinger J-M, Ladoire S, Brunotte F, Cochet A, et al. Combination of breast imaging parameters obtained from 18F-FDG PET and CT scan can improve the prediction of breast-conserving surgery after neoadjuvant chemotherapy in luminal/HER2-negative breast cancer. Eur J Radiol. 2019;113:81–8. https://doi.org/10.1016/j.ejrad.2019.02.005.
21. Al-Muqbel KM, Yaghan RJ. Effectiveness of 18F-FDG-PET/CT vs bone scintigraphy in treatment response assessment of bone metastases in breast cancer. Medicine. 2016;95:e3753. https://doi.org/10.1097/md.0000000000003753.
22. Riedl CC, Pinker K, Ulaner GA, Ong LT, Baltzer P, Jochelson MS, et al. Comparison of FDG-PET/CT and contrast-enhanced CT for monitoring therapy response in patients with metastatic breast cancer. Eur J Nucl Med Mol Imaging. 2017;44:1428–37. https://doi.org/10.1007/s00259-017-3703-7.
23. Pak K, Seok JW, Kim HY, Nguyen TL, Kim K, Kim SJ, et al. Prognostic value of metabolic tumor volume and total lesion glycolysis in breast cancer: a meta-analysis. Nucl Med Commun. 2020;41:824–9. https://doi.org/10.1097/mnm.0000000000001227.
24. Qu Y-H, Long N, Ran C, Sun J. The correlation of F-FDG PET/CT metabolic parameters, clinicopathological factors, and prognosis in breast cancer. Clin Transl Oncol. 2020;23(3):620–7. https://doi.org/10.1007/s12094-020-02457-w.
25. Heusner TA, Kuemmel S, Umutlu L, Koeninger A, Freudenberg LS, et al. Breast cancer staging in a single session: whole-body PET/CT mammography. J Nucl Med. 2008;49:1215–22. https://doi.org/10.2967/jnumed.108.052050.
26. Razek AAKA, Khalek AA, Gaballa G, Denewer A, Nada N. Invasive ductal carcinoma: correlation of apparent diffusion coefficient value with pathological prognostic factors. NMR Biomed. 2010;23:619–23. https://doi.org/10.1002/nbm.1503.
27. Kitajima K, Yamano T, Fukushima K, Miyoshi Y, Hirota S, Kawanaka Y, et al. Correlation of the SUVmax of FDG-PET and ADC values of diffusion-weighted MR imaging with pathologic prognostic factors in breast carcinoma. Eur J Radiol. 2016;85(5):943–9.
28. Grueneisen J, Nagarajah J, Buchbender C, Hoffmann O, Schaarschmidt BM, Poeppel T, et al. Positron emission tomography/magnetic resonance imaging for local tumor staging in patients with primary breast cancer. Investig Radiol. 2015;50:505–13. https://doi.org/10.1097/rli.0000000000000197.
29. Sasaki M, Tozaki M, Kubota K, Murakami W, Yotsumoto D, Sagara Y, et al. Simultaneous whole-body and breast 18F-FDG PET/MRI examinations in patients with breast cancer: a comparison of apparent diffusion coefficients and maximum standardized uptake values. Jpn J Radiol. 2018;36:122–33. https://doi.org/10.1007/s11604-017-0707-y.
30. Moy L, Noz ME, Maguire GQ Jr, Melsaether A, Deans AE, Murphy-Walcott AD, et al. Role of fusion of prone FDG-PET and magnetic resonance imaging of the breasts in the evaluation of breast cancer. Breast J. 2010;16(4):369–76. https://doi.org/10.1111/j.1524-4741.2010.00927.x.
31. Moon E-H, Lim ST, Han Y-H, Jeong YJ, Kang Y-H, Jeong H-J, et al. The usefulness of F-18 FDG PET/CT-mammography for preoperative staging of breast cancer: comparison with conventional PET/CT and MR-mammography. Radiol Oncol. 2013;47(4):390–7.
32. Melsaether A, Moy L. Breast PET/MR imaging. Radiol Clin N Am. 2017;55:579–89. https://doi.org/10.1016/j.rcl.2016.12.011.
33. Cho I-H, Kong E-J. Potential clinical applications of ^{18}F-Fluorodeoxyglucose positron emission tomography/magnetic resonance mammography in breast cancer. Nucl Med Mol Imaging. 2017;51:217–26. https://doi.org/10.1007/s13139-016-0446-5.
34. Narayanan D, Berg WA. Use of breast-specific PET scanners and comparison with MR imaging. Magn Reson Imaging Clin N Am. 2018;26(2):265–72.
35. Ulaner GA, Riedl CC, Dickler MN, Jhaveri K, Pandit-Taskar N, Weber W. Molecular imaging of biomarkers in breast cancer. J Nucl Med. 2016;57:53S–9S. https://doi.org/10.2967/jnumed.115.157909.

36. Arvola S, Jambor I, Kuisma A, Kemppainen J, Kajander S, Seppänen M, et al. Comparison of standardized uptake values between 99mTc-HDP SPECT/CT and 18F-NaF PET/CT in bone metastases of breast and prostate cancer. EJNMMI Res. 2019;9(1):6. https://doi.org/10.1186/s13550-019-0475-z.
37. Daimiel I. Insights into hypoxia: non-invasive assessment through imaging modalities and its application in breast cancer. J Breast Cancer. 2019;22:155. https://doi.org/10.4048/jbc.2019.22.e26.
38. Kostakoglu L, Duan F, Idowu MO, Jolles PR, Bear HD, Muzi M, et al. A phase II study of 3'-Deoxy-3'-^{18}F-Fluorothymidine PET in the assessment of early response of breast cancer to neoadjuvant chemotherapy: results from ACRIN 6688. J Nucl Med. 2015;56:1681–9. https://doi.org/10.2967/jnumed.115.160663.
39. Linden HM, Stekhova SA, Link JM, Gralow JR, Livingston RB, Ellis GK, et al. Quantitative fluoroestradiol positron emission tomography imaging predicts response to endocrine treatment in breast cancer. J Clin Oncol. 2006;24:2793–9. https://doi.org/10.1200/jco.2005.04.3810.
40. van Kruchten M, de Vries EG, Brown M, de Vries EF, Andor WJ, Rudi AJ, et al. PET imaging of oestrogen receptors in patients with breast cancer. Lancet Oncol. 2013;14:e465–75. https://doi.org/10.1016/s1470-2045(13)70292-4.
41. Website. [cited 2020 Aug 15]. Available from: (NCT02398773 and NCT 02455453, available at https://clinicaltrials.gov)
42. Gebhart G, Lamberts LE, Wimana Z, Garcia C, Emonts P, Ameye L, et al. Molecular imaging as a tool to investigate heterogeneity of advanced HER2-positive breast cancer and to predict patient outcome under trastuzumab emtansine (T-DM1): the ZEPHIR trial. Ann Oncol. 2016;27:619–24. https://doi.org/10.1093/annonc/mdv577.

Chapter 10
Image-Guided Percutaneous Biopsies

Vitor Chiarini Zanetta

10.1 Historical Perspective

The history of percutaneous breast biopsies is intrinsically associated with the development of mammography in the twentieth century as a diagnostic tool and the identification of non-palpable breast abnormalities, some of which are malignant tumors being detected prior to becoming palpable lesions. The cognizance that early detection improves survival rates urged the adoption of mammography as a screening tool for asymptomatic women in the 1970s. However, a drawback was quickly noted. Owing to the overlap between benign and malignant features in imaging, most of these clinical occult lesions are in fact benign lesions, and surgery was often needed to provide a definitive diagnosis. This meant a significant burden for the majority of women undergoing additional investigation as surgical biopsies are morbid and expensive procedures.

This problem was first addressed in the late 1980s with the development of stereotactic biopsy, using x-rays and triangulation to accurately sample lesions with needle biopsy, seeking to obviate unnecessary surgeries. In the early 1990s, core needles began to be used in stereotactic biopsy, showing encouraging results [1, 2].

In 1993, the first study evaluating the efficiency of ultrasound (US)-guided large core percutaneous breast biopsy in 181 cases was published, with 100% agreement between 49 malignant biopsy results and surgery, and no cancers were found during follow-up of the remaining 132 cases [3]. In the following years, stereotactic and ultrasound-guided procedures were endorsed by research, and percutaneous biopsy began to present as a reliable and safe alternative to open surgery [4]. In the last 20 years, technology has made tomosynthesis and magnetic resonance imaging

V. C. Zanetta (✉)
Department of Radiology, Instituto de Radiologia INRAD, Hospital das Clinicas HCFMUSP, Faculdade de Medicina, Universidade de Sao Paulo, São Paulo, SP, Brazil
e-mail: vitor.chiarini@einstein.br

S. J. Kim Hsieh, E. A. Morris (eds.), *Modern Breast Cancer Imaging*,
https://doi.org/10.1007/978-3-030-84546-9_10

(MRI)-guided biopsies possible, increasing the range of lesions that are amenable to percutaneous biopsy, while the development of more efficient sampling needles, including larger core needles and vacuum-assisted devices, has improved diagnostic accuracy.

Currently, the goal of the breast team is to obtain a definitive, nonoperative diagnosis of all potential breast abnormalities in a timely and cost-effective way [5]. The standard approach to potential breast abnormalities is the "Triple Assessment" derived from clinical evaluation, radiological information, and pathological assessment. When there is agreement between these three assessments, the level of diagnostic accuracy exceeds 99%. For cases without clinical information, such as nonpalpable breast lesions, similar levels of accuracy have been achieved by combining only imaging tests and pathological evaluation [5].

10.2 Understanding Imaging-Guidance and Needle Selection: Practical Considerations

Preferences for guidance methods and needle types for specific breast lesions vary across institutions. A major factor in choosing the adequate imaging modality to guide a biopsy procedure is lesion visibility. Breast lesions may be better depicted at one modality over another, to the point that some highly suspicious lesions in one modality may be completely invisible in another method.

For lesions that are well seen in all different modalities, the order of choice among imaging methods will usually be ultrasound, mammography, and MRI. It is easy to understand this order when comparing modalities. Ultrasound-guided biopsies have several advantages, including real-time sampling, lower cost, and the absence of radiation or gadolinium injection, and are more comfortable for patients when compared to MRI and mammographic guided procedures. These last two methods require breast compression and immobile position in order to target the lesion and complete the sampling, occasionally lasting more than 30 minutes. Whenever a suspicious lesion is first seen at mammography or MRI, a targeted ultrasound can be performed to look for a possible correlate, and if found, ultrasound is used to guide the procedure. Likewise, stereotactic and tomosynthesis-guided biopsies must be preferred instead of MRI-guided procedures, given the technical difficulties associated with MRI biopsy, higher costs, and limitations related to contrast injection.

Usually masses, cysts, and every other lesion detected on ultrasound will be submitted to ultrasound-guided biopsy. Calcifications, breast asymmetries, and architectural distortions without a sonographic correlate will undergo mammography-guided biopsy, and non-mass enhancements, foci, and masses without correlation in other modalities will undergo MRI-guided biopsy. It is thus critical to perform an adequate imaging workup before any procedure to ensure accurate targeting, safety of the procedure, and cost-effectiveness.

There are currently three different options of biopsy needles that are used for sampling breast lesions: fine needle aspiration (FNA), conventional core needle biopsy (CNB), and vacuum-assisted core needle biopsy (VAB). Although all imaging modalities can guide procedures using any kind of needles, VAB is preferably guided by mammography and MRI, while ultrasound is used for all types of biopsies and needles. This matter will be further discussed.

10.3 Pre-biopsy Assessment

Prior to any percutaneous breast biopsy, there are several common steps that should be undertaken regardless of the procedure. It is critical to ensure that complete imaging workup has been performed, to obtain confirmation that the lesion is real and requires tissue sampling, as well as to select the proper imaging guiding method. For instance, the radiologist should review all available images and assure that the lesion is not actually a benign finding with incomplete workup, such as skin calcifications without proper tangential mammographic views demonstrating them or fat necrosis presenting as a suspicious complex mass on ultrasound without proper mammographic correlation, that would reveal benign lucent-center calcification. If there is any concern about the biopsy need due to incomplete workup or doubts about what imaging guidance method is appropriate, additional studies may be performed, such as additional mammographic views or a second-look ultrasound looking for a sonographic correlate.

10.4 Patient Preparation, Biopsy Risks, and General Post-biopsy Information

The patient should be oriented to keep normal activities and medications until the day of the procedure; no fasting is required. Discontinuing blood thinning medications is a controversial topic. Blood thinning medications may increase the risk of bleeding and hematoma formation due to biopsy; however, there are potential life-threatening risks in stopping them, such as myocardial infarction and stroke. Current literature supports that it is safe to perform percutaneous breast biopsy under medications known to impact bleeding, such as aspirin and anticoagulants [6]. Decisions regarding discontinuing blood thinning medications should be made on a case-by-case basis and shared with referring physician. If the radiologist opts for cessation, it is necessary to ensure adequate timing for normalization of coagulation and, if needed, check laboratory tests such as international normalized ratio (IRN) before performing the procedure.

On the day of the procedure, the patient should be instructed to avoid applying deodorant, lotion, or powder in the chest and axilla, since these may cause

calcification-like artifacts in the image. The patient should be questioned about allergies related to medications used during the procedure and metal allergies for clip placement. The chance of pregnancy should also be assessed given the potential risks of ionizing radiation, MR field strength, and gadolinium injection.

All percutaneous breast biopsies require oral and written informed consent clearly informing about the (1) purpose of the procedure, (2) benefits, (3) risks, and (4) alternatives to diagnosis:

1. The purpose of the procedure is to obtain a satisfactory sample of tissue to evaluate a breast abnormality. A comprehensible explanation of how the procedure is performed should be given. The patient should be aware that the target may not be sampled, neither completely removed, and occasionally, the biopsy will not be performed due to non-visualization.
2. Percutaneous breast biopsy is a minimally invasive way of obtaining diagnosis of a breast abnormality and to provide the referring physician adequate information for patient care. It should be noted that depending on the result, additional surgery may be needed, and in case of inadequate sampling, a re-biopsy or surgical biopsy may be needed.
3. Complications in percutaneous breast biopsy are rare. The risks associated with the procedure are vasovagal reactions, hematoma formation, unstoppable bleeding requiring surgical intervention (extremely rare), infection, pneumothorax, pseudoaneurysm formation, implant rupture, and milk fistula in lactating patients. The post-biopsy marker (clip) placement should be addressed, informing that a tiny marker may be placed in the biopsy site, facilitating correlation between different imaging modalities and preoperative lesion localization. Occasionally, the clip may migrate to a different location. Potential complications related to post-biopsy markers, such as allergy, are restricted to few case reports, and the metallic marker will not trigger security metal detectors.
4. Surgical biopsy is usually the only alternative in obtaining tissue diagnosis.

Once the procedure is finished, the patient should be discharged with information on how to obtain the final diagnosis, contact information for problems and concerns, and general postprocedural orientations: avoid extreme physical activity in the following 4 or 5 days, appropriate care instructions for the sterile dressing, possible occurrence of minor bleeding or bruising, as well as the appearance of a small lump at the biopsy site and how to be vigilant for infection signs or abnormal bleeding.

Pre-biopsy assessment:

– Lesion is real.
– Lesion is suspicious.
– Modality and needle selection are adequate.
– Patient preparation and informed consent.

Post-biopsy orientations:

– How to obtain the final diagnosis.
– Patient education for surveillence of normal and abnormal post-biopsy healing.
– Contact information for problems or concerns.

10.5 Considerations Regarding Clip Placement

The radiologist may choose to deploy a post-biopsy marker (clip) at the biopsy site to facilitate the subsequent location. These markers are designed to be seen at different imaging modalities, allowing accurate localization of the biopsy site. Post-biopsy markers are useful for several reasons:

1. Correlation of imaging findings between MRI, US, and mammography. This is especially useful to check for accurate targeting when the lesion was first identified in one modality and biopsied using another one, for instance, a suspicious MRI finding, submitted to a second-look ultrasound-guided biopsy. A post-biopsy non-enhanced MRI T1-weighted sequence can be used to check for the marker location and whether it matches the original diagnostic MRI location.
2. Tissue markers allow for reliable re-identification of a biopsy site. Tissue markers are considered vital when the target is no longer visible after biopsy, for instance, after complete removal during percutaneous biopsy and the histologic results warrant surgical excision. In addition, re-identification of the biopsy assists in evaluation for sampling error and imaging-pathology concordance.
3. Malignant lesions submitted to neoadjuvant chemotherapy may reduce to the point of complete radiological response, becoming invisible in control examinations. The post-biopsy marker is usually a reliable landmark to guide additional surgical excision. For large lesions, more than one marker may be used for lesion extent bracketing.
4. Dealing with breasts containing multiple sampled lesions is facilitated when biopsy markers are used, clearly demonstrating which lesions have already been sampled. Multiple biopsy sites may require different management, and biopsy markers streamline this assessment. Post-biopsy markers are available in several different shapes, and specific clips can be used to mark different targets (Fig. 10.1).

Clips are frequently made of titanium or stainless steel. Other materials include metal alloys and non-metallic alternatives, such as carbon-coated ceramic. Metallic clips produce a susceptibility artifact on MRI, being easily identified, whereas non-metallic clips may be less evident. On the other hand, metallic clips cause an artifact on tomosynthesis that may obscure subtle findings.

Clips are available either alone, as bare clips, or associated with other materials, such as bio-absorbable materials or non-absorbable polymers. Examples of associated materials include beta glucan, polyethylene glycol (PEG)-based hydrogel, bovine collagen, polyvinyl alcohol (PVA) polymer, polyglycolic acid (PGA) microfiber pad, PGA microfiber–PVA polymer combinations, starch pellets, polylactic acid–PGA pellets, and suture-like netting [7]. These associated materials are designed by vendors to improve or confer the clips certain features, such as improved hemostasis, ultrasound visualization, or reduced clip migration.

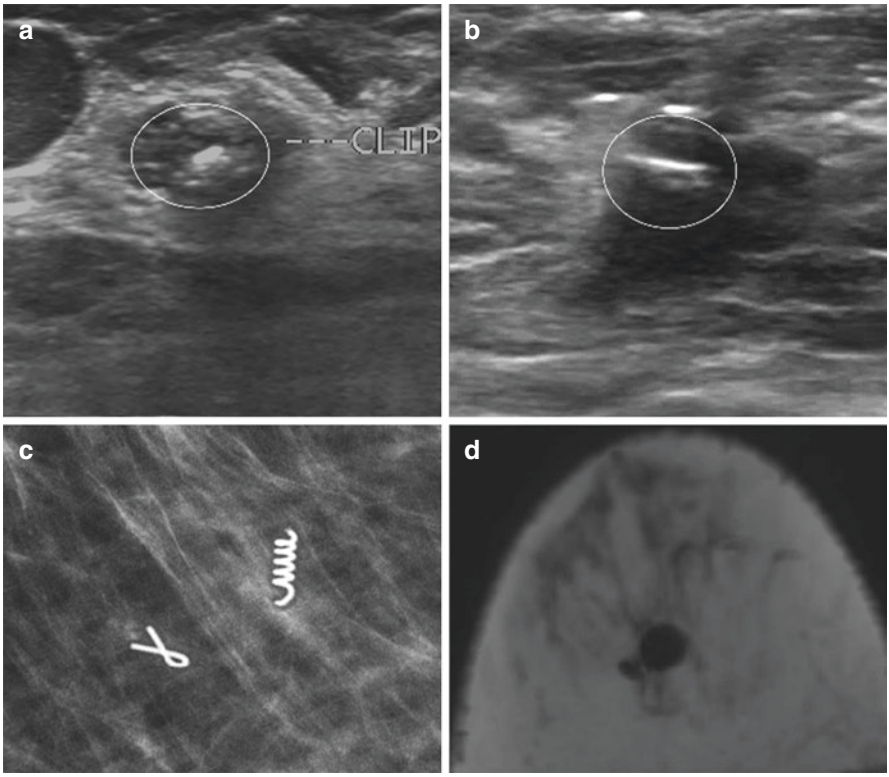

Fig. 10.1 Malignant mass marked for neoadjuvant chemotherapy, with two different clips. (**a**, **b**) sonography views of the markers before starting chemotherapy. One of the markers was deployed at the center of the mass (**a**) and the other at the posterior and lateral edge (**b**), to mark lesion extent. (**c**) Post-neoadjuvant chemotherapy mammography; the two markers are easily identified and no residual lesion is seen. (**d**) MRI T1W axial image; notice the different susceptibility artifacts produced by each different clip

10.6 Clip Placement Complications

The clip must be deployed at the biopsy site and must remain close to it to mark location accurately. Complications with clip placement are related to inaccurate deployment away from the lesion, mechanical failure to deploy the clip (rare), and clip migration, which may occur immediately after the procedure or later. Clip migration is the most frequent cause of clip displacement, and there are several reasons that can account for it:

1. The accordion effect: in procedures that require breast compression, such as mammography or MRI-guided biopsy, the clip might not adhere to the biopsy site and can be moved away from the biopsy site during compression release. The displacement of the clip in those cases occurs in the direction of the needle track (usually the Z axis, which will be further explained in the following sections).

2. Clip migration in fatty tissue: predominantly fatty tissue breasts are more likely to present clip migration within or outside the biopsy cavity, which is unrelated to breast compression.
3. Bleeding – post-procedure continuous bleeding may displace a clip that is not firmly attached to the biopsy cavity.
4. Hematoma – hematoma formation may prevent adequate clip attachment (floating clip inside the biopsy cavity) or even cause significant mass effect displacing the clip.
5. Changes in the biopsy site – Any factor that can modify the biopsy site may be responsible for clip migration, such as air reabsorption in the biopsy cavity or breast surgery.

Obtaining proper imaging documentation after clip deployment is essential. For ultrasound-guided procedures, it is critical to seek real-time visualization of the echogenic clip being deployed, while for MRI or mammography-guided procedures, post-procedure imaging provides immediate clip identification.

Regardless of the method being used to guide the procedure, it may be useful to obtain post procedure two orthogonal (craniocaudal (CC) and mediolateral (ML)) mammographic views to document clip location. Although uncommon, delayed migration may occur, and immediate post-clip documentation is critical to assess the extent of migration and accurate target location.

10.7 Ultrasound-Guided Biopsy

Ultrasound can guide fine-needle aspiration (FNA), CNB, and VAB. Currently, US-guided CNB is the most popular modality of breast tissue sampling and considered very safe, diagnostically accurate, and cost-effective compared to other modalities. In everyday practice, US-guided biopsy is the first option for sonographically visible lesions. In the following sections, we will discuss the three main types of US-guided procedures: FNA, CNB, and VAB.

All US-guided procedures can be performed either by a single operator or two operators. A single operator uses the free-hand technique, in which one hand holds the transducer in place while the “free hand” performs needle manipulation. Two operators may be helpful for challenging cases such as lesions too close to a blood vessel or in a very deep location, where one operator holds the transducer in place while the other is responsible for needle handling and sampling.

10.8 Fine-Needle Aspiration (FNA)

Fine-needle aspiration is performed with small disposable needles, usually 21–25 gauge, in a relatively rapid and simple way under ultrasound guidance. FNA is usually readily available and very well tolerated by patients, with no or minimal pain

during the procedure, even when no local anesthesia is used. Prior to the development of core biopsy in the 1990s, FNA was the standard test used for breast lesion assessment. However, FNA has several limitations compared to core biopsy and has been progressively replaced by the latter. FNA retrieves small amount of tissue, samples are frequently non-diagnostic or inadequate, and cytologic analysis is limited in differentiating invasive and in situ carcinoma, as well as tumoral subtype.

Currently, FNA is still employed in specific scenarios, especially for the evaluation of metastasis in axillary lymph nodes, workup of breast cysts, and evaluation of peri-implant effusions suspected of breast implant–associated anaplastic large cell lymphoma (BIA-ALCL). Rarely, FNA might be preferred for very superficial or deep lesions.

10.8.1 Axillary Assessment

Axillary management is an evolving and complex subject, and it is beyond the scope of this chapter to conduct a thorough discussion of axillary management and the role of image-guided biopsy of lymph nodes (see Chap. 4).

Staging of axillary lymph nodes is an important prognostic factor, and sentinel lymph node biopsy (SLNB) is the standard procedure to define axillary status. SLNB could be skipped in cases of positive image-guided biopsy of axillary nodes, leading straight to complete axillary dissection.

This paradigm has changed since the ACOSOG Z0011 study. The ACOSOG Z0011 trial showed that for clinical T1–T2 N0 invasive breast cancer patients, with up to two positive sentinel nodes in SNLB, there is no need for complete dissection of axillary nodes for patients undergoing conservative surgery and whole breast radiotherapy. In this setting, the role of preoperative axillary imaging has been questioned. Nevertheless, axillary image-guided biopsy with FNA or CNB still plays an important role in assessing axillary status in the clinically node-positive axilla and also in determining patients with extensive axillary disease burden, who may still benefit from additional axillary management. In addition, assessment of nodal status with ultrasound-guided biopsy should be considered for patients eligible for neoadjuvant chemotherapy, as SLNB can be plagued by a high false-negative rate afterward. Although with inferior diagnostic accuracy than CNB, FNA is still a reasonable option to assess lymph nodes, being less traumatic and more affordable.

10.8.2 Cysts

FNA is indicated for symptomatic large simple cysts, without a true solid component or other associated suspicious features (Fig. 10.2).

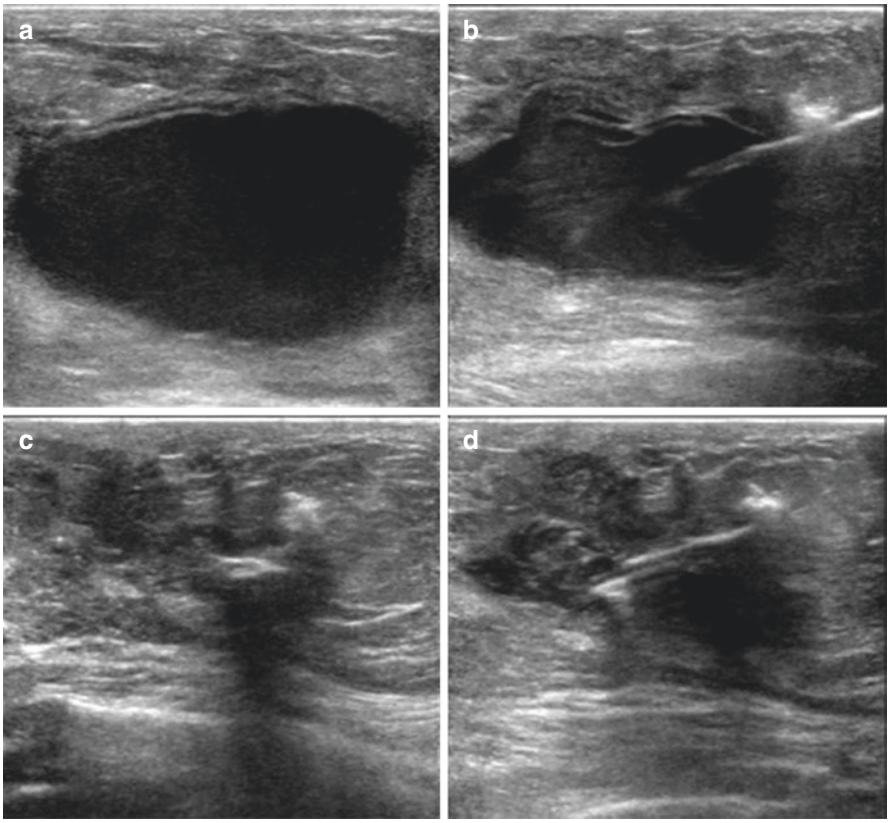

Fig. 10.2 (**a–d**) Consecutive images of a US-guided simple cyst FNA

Usually, simple cysts are easily aspirated, leaving no residual lesions in the imaging evaluation. For most of the cases, non-bloody and non-purulent aspirates are deemed benign and can be discarded. However, purulent aspirates should be sent for microbiologic analysis and culture, while bloody aspirates should be sent for cytologic evaluation. In the last case, it is also important to place a post-biopsy marker, especially if no residual lesion is visible.

Occasionally, cysts may be complicated and filled with echogenic material from pus, clot, or debris. If ultrasound and Doppler evaluation cannot discern whether the echogenic material is actually a solid component, FNA may be indicated to differentiate them. True complicated cysts will likely disappear, while true solid components will persist. It should be noted that if a true solid component is present, this should be submitted for histologic analysis preferably with VAB. Nevertheless, whenever US evaluation confirms a solid component within a cystic mass by flow detection on Doppler, FNA should not preclude histologic analysis by VAB or CNB [8].

10.8.3 Breast Implant–Associated Anaplastic Large Cell Lymphoma (BIA-ALCL)

BIA-ALCL is a recently recognized complication of texturized breast implants, usually presenting as late-onset effusion (85%), or less frequently as a mass (15%). Although patients with mass should undergo histologic analysis either by percutaneous biopsy or surgical excision, up to 85% of the cases are associated with late-onset effusion, defined as effusion occurring more than 1 year after breast augmentation. Whenever a suspected effusion is present, FNA is indicated, seeking to obtain at least 50 mL of effusion fluid for cytologic analysis and immunophenotyping, culture, cell counting, and protein [9].

10.8.4 Challenging Lesion Location

When compared to CNB, FNA maintains better tactile sensitivity, is considered easier to perform, and is less traumatic. Thus, FNA may be preferred for lesions just under the skin to avoid unwarranted skin trauma and also to sample lesions near the chest wall.

10.8.5 Diagnostic Accuracy and Availability

Although inferior to CNB, FNA is still a reasonable diagnostic option. A meta-analysis showed the sensitivity of FNA to be 74%, with a specificity of 96%. While CNB showed a sensitivity of 84% and a specificity of 98%. The area under the curve of CNB and FNA was high (98% vs 94%, respectively), confirming that both methods have excellent test performances [10]. The authors of this meta-analysis did not evaluate the impact of nondiagnostic insufficient samples, which is a major disadvantage of FNA. In another meta-analysis assessing the diagnostic value of FNA, although satisfactory samples of sensitivity and specificity of the test remained high (92% and 94%, respectively), the pooled proportion of unsatisfactory samples that were subsequently upgraded to cancers was 27.5% [11]. Since FNA is less expensive, it still plays an important diagnostic role in limited resource locations, such as developing countries [11].

10.9 Technique

The patient is positioned in a supine or supine oblique position, with the ipsilateral arm raised behind the head. Usually, the oblique position is preferred for lateral lesions, as well as axillary targets, especially in large breasts. In these situations, the

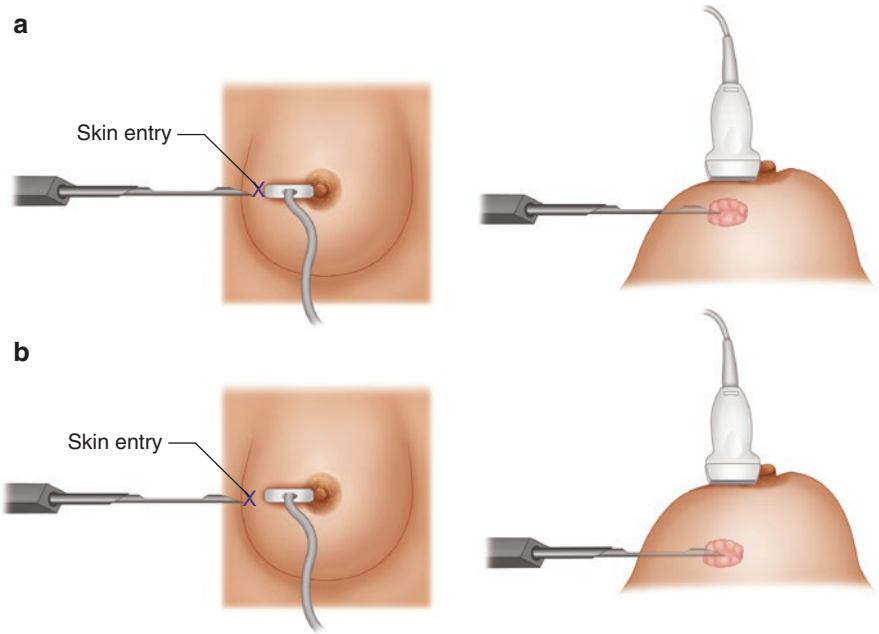

Fig. 10.3 Breast illustration for adequate needle entry point. (**a**) For superficial lesions, a closer entry point from the lesion is desired, while for deep lesions (**b**), a farther entry point is required to allow the needle to be parallel to the chest wall while sampling

oblique position may facilitate lesion visualization and improve needle path, allowing it to pass parallel to the chest wall.

The skin is cleansed, the transducer is properly covered with a sterile cover, and sterile gel is used to allow ultrasound imaging.

Planning the needle trajectory and skin entry site is one of the most crucial steps in the procedure. In general, the needle is better visualized while perpendicular to the transducer beam, and the needle tip should not be pointing to the chest wall to avoid unwarranted trauma (Fig. 10.3). Given the breast natural curvature, superficial lesions are better approached by a closer entry skin point in relation to the lesion, while deep lesions require a farther entry point. These considerations are valid for all US-guided procedures, including all types of biopsy needles, such as CNB and VAB, although different adjustments are required according to the needle length.

Once proper skin entry point has been selected, proceed applying local anesthesia, such as lidocaine, to decrease discomfort or pain during the procedure. The sampling needle attached to a 10–20-ml disposable syringe should be gently introduced and accurately placed within the lesion. The tip of the needle should be seen inside the target. For solid lesions, sampling is performed while applying suction to the syringe and using small and rapid back and forth stroke movements for cell harvesting. Coupling the syringe with a pistol-grip mechanic syringe holder (Fig. 10.4) is not required but highly recommended as it eases maintaining a negative pressure, allowing the operator to be more accurate during the back and forth movements.

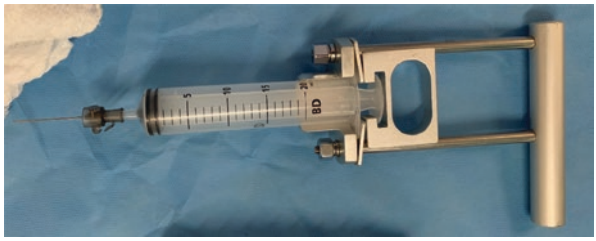

Fig. 10.4 Syringe attached to the pistol-grip mechanic syringe holder

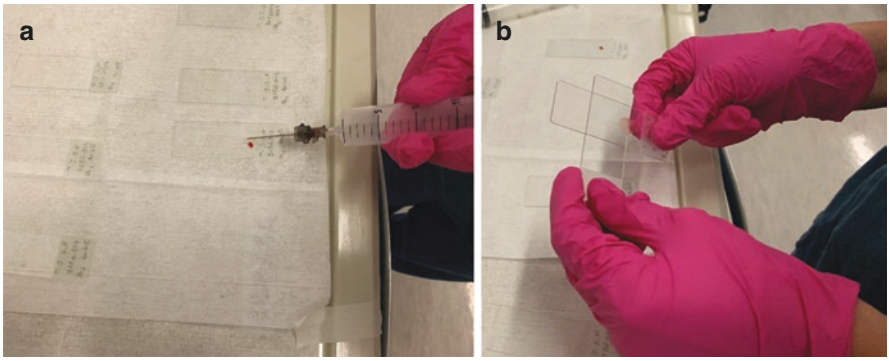

Fig. 10.5 After removing the needle and drawing air into the syringe, the operator replaces the needle onto the syringe and squirts one drop in the center of a slide (**a**). A second slide is used to gently spread the sample and make the smear (**b**)

Whenever suitable material is collected, the negative pressure is relieved and the needle withdrawn. Handling and preparation of the sampled cytologic material is as important as targeting.

If an on-site cytotechnologist or pathologist is not available, the operator must be familiar with pathology service standards and be able to prepare the direct smears on slides (Fig. 10.5) or any other desired preparation, such as cell blocks. If a slide is being submitted to fixation, it is imperative to be as expedite as possible, since delayed fixation may impair cellular preservation.

It is recommended to perform multiple needle passes, aiming to sample different portions of the target lesion to improve representativeness and diagnostic accuracy. A cytotechnologist or pathologist present on-site during the procedure can assist and ensure adequate sample collection.

10.10 Complications and Post-care

FNA is minimally invasive, usually very well tolerated by patients, and considered a safe breast procedure. Patients are released after the procedure and do not require further care. Rarely, the procedure may be complicated with pain, bleeding, or

infection. Even rarer is the occurrence of pneumothorax, which is usually treated conservatively without drainage.

10.10.1 Ultrasound-Guided Core Needle Biopsy and Vacuum-Assisted Biopsy

Core needle biopsies can be divided into two main groups: conventional core needle biopsy (CNB) and vacuum-assisted biopsy (VAB), which, although both use hollow needles to obtain the samples, are substantially different systems.

Conventional US-guided core needle biopsy (CNB) uses a hollow needle to retrieve tissue samples and overpowered FNA with its higher diagnostic accuracy, capability of differentiating in situ and invasive carcinomas, tumor grade, subtype, and receptor status. The procedure is currently the most popular modality of breast tissue sampling.

CNB uses a spring-loaded mechanism to obtain the samples with 18–12G needles. They are available as automatic or semiautomatic devices (Figs. 10.6 and 10.7).

The mechanism for cutting and collecting each sample is similar for both: the needle contains an outer cutting cannula and an inner stylet, with a notch for specimen collection. With the inner stylet retracted, the needle tip is first placed adjacent to the target border. The inner stylet is advanced inside the target. Once the inner trocar is in place, the outer cannula is rapidly advanced, cutting and storing each sample in the inner trocar notch. The whole needle is then withdrawn from the breast, and the sample is collected after being exposed in the trocar notch (Figs. 10.8, 10.9, 10.10, and 10.11).

The main difference between automatic and semiautomatic devices is to the advancement of the inner trocar. In semiautomatic devices, the inner trocar is manually advanced inside the lesion by the operator. Once the operator triggers (needle firing), the outer cutting cannula is spring deployed (one-stage mechanism). In automatic needles, the needle tip is positioned adjacent to the lesion border, and once the operator triggers, the inner trocar is spring deployed inside the lesion, followed by automatic spring deployment of the outer cutting cannula (two-stage mechanism). Since the inner trocar of the most commonly used 14-gauge needle has a throw of 2.2 cm, before firing the needle, the operator has to ensure the presence of adequate tissue beyond the lesion to avoid unwarranted trauma to the surroundings.

Because the procedure has to be repeated for each sample and requires multiple passes, a coaxial device may be used to facilitate repeated access to the biopsy site.

The semiautomatic method allows for a steady and operator-controlled advancement of the inner trocar, with real-time tracking of the needle tip. Thus, it is popular in challenging cases such as sampling of subtle atypical axillary lymph nodes, where it is possible to avoid the vascular hilum and better target the suspicious cortex, lesions near vascular structures or next to breast implants, avoiding unwarranted rupture of the implant shell. Nevertheless, the automatic procedure is slightly

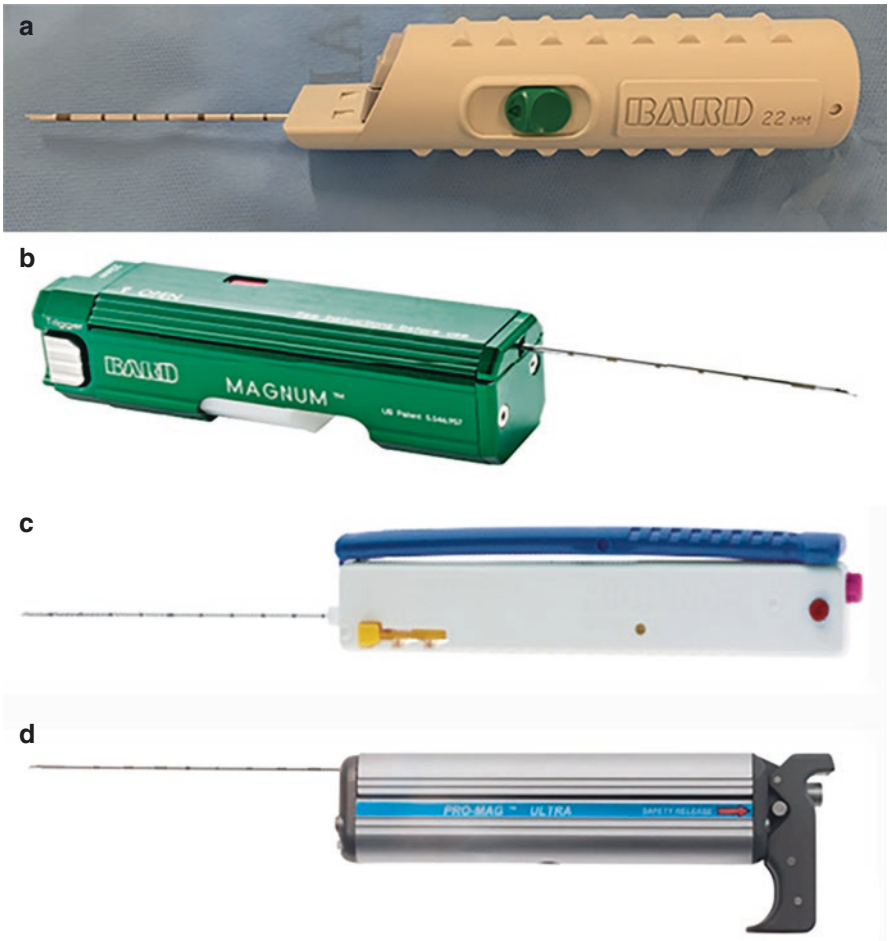

Fig. 10.6 Examples of automatic core biopsy devices: (**a**) Max-Core™ Disposable Core Biopsy (Bard Medical Division, Covington, GA, USA). (**b**) Magnum Reusable Core Biopsy Instrument (Bard Medical Division, Covington, GA, USA). (**c**) BioPince™ Full Core Biopsy (Argon Medical Devices, Inc., Athens, TX, USA). (**d**) Pro-Mag™ Ultra (Argon Medical Devices, Inc., Athens, TX, USA)

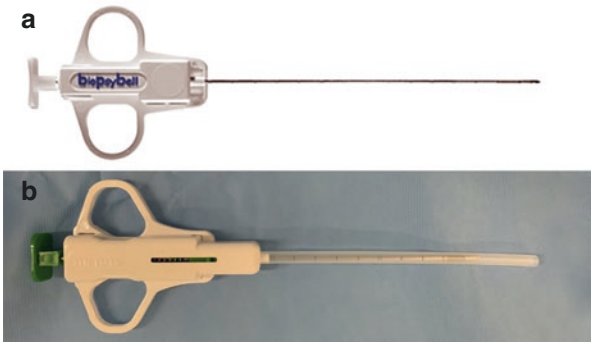

Fig. 10.7 Examples of semiautomatic biopsy devices. (**a**) SPEEDYBELL™ (BIOPSYBELL Srl., Mirandola, MO, Italy). (**b**) VELOX™ (Medax Srl Unipersonale, San Possidonio, MO, Italy)

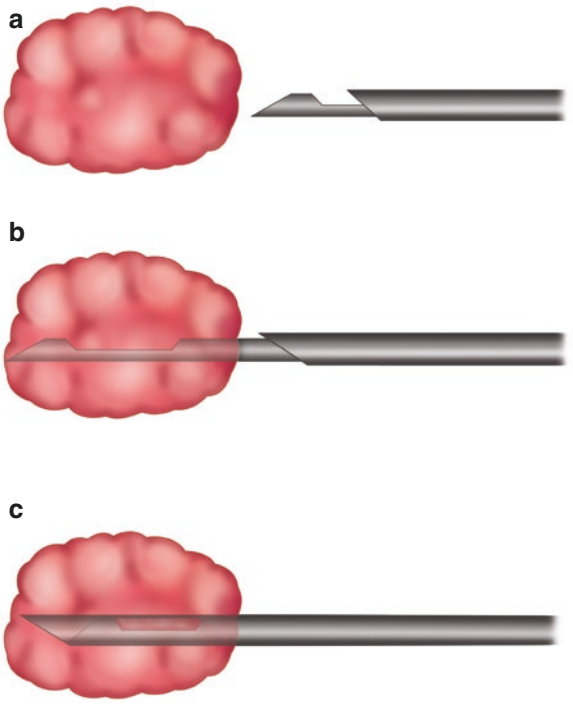

Fig. 10.8 Core needle sampling mechanism illustration. (**a**) Needle tip is positioned next to the target border. (**b**) The inner stylet is advanced inside the target, exposing the sampling notch. (**c**) The outer cannula is rapidly advanced, cutting and storing each sample in the inner trocar notch

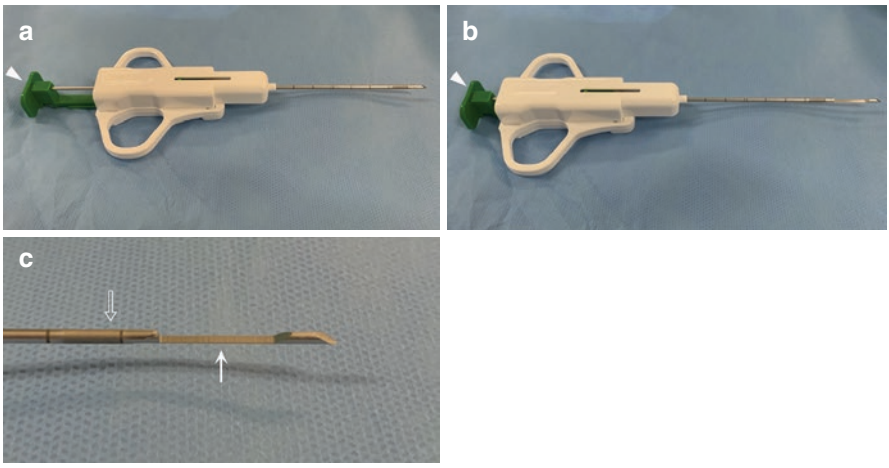

Fig. 10.9 (**a**) Semiautomatic needle device with the inner stylet retracted. (**b**) After pushing the plunger (arrowhead), the inner stylet is advanced, exposing the sampling notch. (**c**) In detail, the sampling notch (arrow) and outer cutting cannula (void arrow)

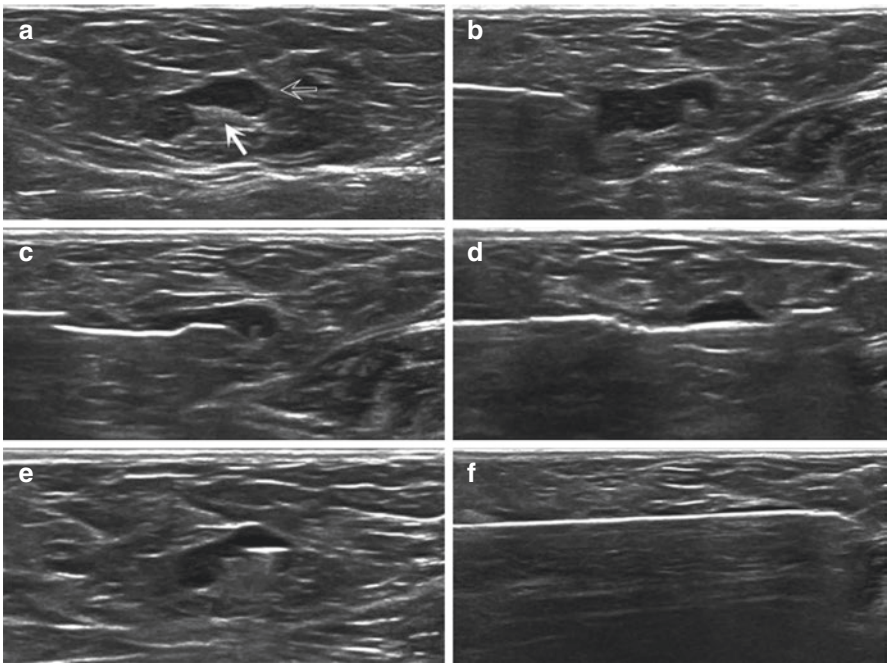

Fig. 10.10 Core biopsy of a lymph node with a semiautomatic device. (**a**) Ultrasound shows the abnormal cortical thickening (void arrow) and vascular hilum (arrow) of the target lymph node. (**b**) The needle is introduced fully retracted until reaching the border of the cortex. (**c**) Gradual and controlled advancement of the inner stylet, piercing the cortical and avoiding the vascular hilum. (**d**) The inner stylet fully extended while the sampling notch placed in the region of interest. (**e**) 90° rotation of the transducer confirming in both planes the accurate position of the sampling notch. (**f**) Post-fire with advancement of the outer cutting cannula over the sampling notch, colleting the sample

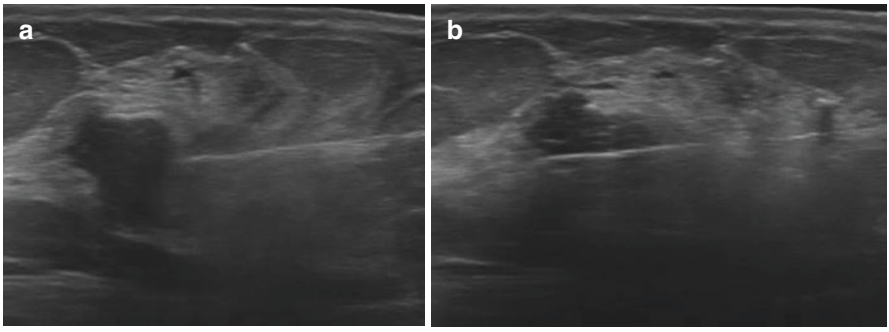

Fig. 10.11 Core biopsy of irregular mass with an automatic device (**a**) Pre-fire – the needle is introduced until the tip is positioned near the border of the mass. (**b**) Post-fire – both the inner stylet and outer cutting cannula have been spring deployed

more comfortable for the operator and less likely to displace the lesion as the inner trocar advances. Especially for hard lesions surrounded by breast soft tissue, the vigorous mechanical inner trocar throw in automatic devices is more likely to pierce the lesion instead of displacing it forward.

Vacuum-assisted breast biopsy (VAB) uses a vacuum-powered biopsy probe to obtain samples from larger core needles, available in a variety of sizes, needle gauges range from 14- to 7-gauge. The needle sampling chamber is positioned into or underneath the lesion, and after activation, the system continuously opens the needle sampling chamber while using suction to pull the tissue into it; a rotating cutting device advances through this tissue, closing the sampling chamber and aspirating the sampled material through the probe into a collection chamber. This process is repeated several times. The operator holds the probe in place and may rotate it to acquire samples from different locations, requiring only one needle pass for the whole procedure (Figs. 10.12 and 10.13).

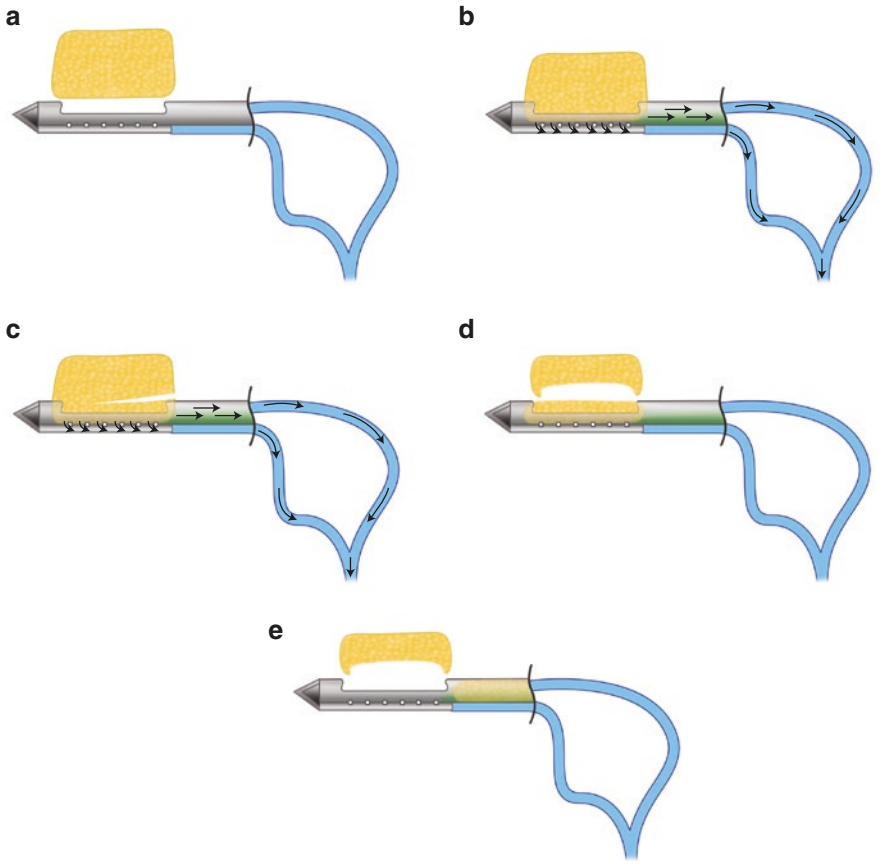

Fig. 10.12 (**a**) VAB needle with a sampling chamber positioned underneath the lesion. (**b**) Vacuum pulls the lesion inside the sampling chamber. (**c**) Cutting cannula advances and shaves part of the lesion. (**d**) The specimen is aspirated (**e**) followed by retraction of the cutting cannula, uncovering the sampling chamber for the next sample

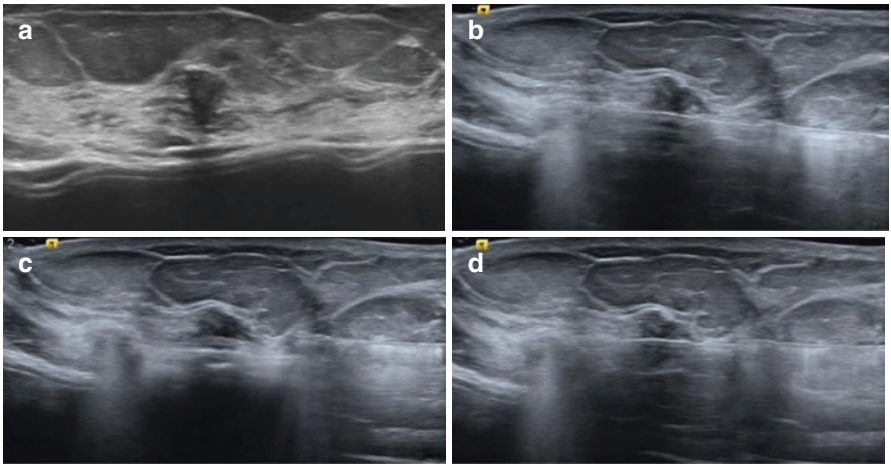

Fig. 10.13 VAB of an irregular mass. (**a**) A mass is situated near a breast implant. (**b**) The VAB needle is introduced until the sampling chamber is located underneath the target, being careful not to pierce the breast implant. Once in position, sampling is performed with (**c**) retraction of the cutting cannula, lesion aspiration, and (**d**) advancement of the cutting cannula

10.10.2 Sampling Considerations

Adequate sampling requires not only accurate targeting of the lesion but also representative and satisfactory sampling; in other words, adequate sampling requires samples of sufficient quality from the most suspicious parts of the lesion.

Adequate sampling is ultimately related to operator skills and needle selection. While the operator is responsible for adequately targeting the lesion, needle selection impacts the amount of tissue retrieved per biopsy and the quality of each sample.

10.11 Quantity and Quality of the Sample

The amount of tissue retrieved per biopsy and its quality are dependent on needle gauge as well as the method of choice: VAB vs CNB. Larger core needles yield larger sample sizes, and for the same needle gauge, vacuum-assisted biopsy obtains larger amounts of tissue when compared to CNB. For instance, the average specimen weight for the 14-gauge CNB sample is 17 mg, while per VAB, it is 37 mg. An 11-gauge VAB probe is capable of obtaining on average 94 mg per sampling, which is over five times the amount of tissue retrieved by the 14-gauge CNB [12]. In addition, another key factor is the quality of the sampled material. VAB devices can provide superior quality samples using suction, avoiding fragmented or floating specimens that are worse for pathologic assessment. For instance, bleeding in the biopsy cavity during the procedure may occur to varying degrees and can be severe

during a CNB, leading to the removal of a blood clot instead of an actual tissue. An interesting feature available in most VAB devices is manual aspiration of the biopsy cavity. Applying suction to the biopsy site can draw blood from the biopsy cavity, improving actual tissue sampling instead of blood clots.

10.12 Adequate Targeting

A skilled operator should sample different portions of the lesion and consider the minimum amount of required tissue for a definitive diagnosis, which is dependent on lesion type and size. For instance, when sampling a complex solid cystic mass, the main objective should be to target the solid portion, and when sampling a very heterogeneous lesion, the goal is to obtain fragments from different parts of the lesion. Due to the risk of carcinoma in situ, non-mass lesions require greater sampling for a definitive diagnosis. This is also true for irregular areas of distortion, comprising a differential diagnosis of sclerosing adenosis, radial scar, and invasive carcinoma [13].

There is no consensus on the number of fragments that must be retrieved during a standard CNB. The American College of Radiology suggests that at least three to six fragments should be obtained from each lesion. However, instead of looking for a fixed number of fragments, the operator should seek for adequate quality of the samples obtained according to the lesion type.

10.13 Choosing Between VAB and CNB

The two main advantages of VAB are the convenient single-pass procedure and capability of acquiring high-quality samples. A study by the American Society of Breast Surgeons Mastery of Breast Surgery Registry showed that larger core needles and tethered vacuum-assisted biopsy are associated with lower re-biopsy rates. One potential drawback from VAB devices is its higher cost per procedure when compared to standard CNB, although this might be balanced when comparing the cost per diagnosis, since VAB is more accurate [13].

Although the benefits of performing VAB in stereotactic biopsy for calcified lesions have been extensively shown in the literature, the evidence supporting VAB instead of CNB for US-guided biopsies, mainly for solid masses, is less clear. For biopsy of solid masses, both methods have shown excellent diagnostic performance, and CNB is a reasonable option in most scenarios. The operator should take into consideration its familiarity with each method, the type of the lesion, and cost of each method. In addition, while CNB is restricted to diagnostic purpose, VAB has been playing an increasing role as a therapeutic procedure, which will be further discussed below.

US-guided VAB should be considered for:

1. Re-biopsies after a non-concordant CNB or FNA findings.
2. Sampling of complex lesions (containing solid and cystic components).
3. Small lesions, usually under 5 mm, which may be challenging to perform with CNB.
4. Sampling of cluster of microcalcifications visible on US.
5. VAB may also be a better option for diffuse non-mass lesions, where a large sampling is indicated.
6. Therapeutic VAB.

10.13.1 Therapeutic VAB

VAB is also suitable for therapeutic removal of benign breast lesions, such as fibroadenomas. In such cases, the operator seeks the complete removal of a symptomatic benign entity, thus avoiding excisional surgery. Moreover, VAB has an increasing role in the management of benign lesions with heterogeneity in histological findings, such as papillary lesions.

Papillary lesions are a broad category ranging from definitely benign papilloma to lesions containing varying degrees of atypia, in situ and invasive carcinoma. One of the problems dealing with papillary lesions is that atypical cells can be found only in part of the lesion, as small foci, or even in adjacent areas outside the lesions themselves. Thus, although most papillary lesions are benign, CNB tends to mislead the pathologist and is associated with underestimation. For papillary lesions diagnosed through CNB, the risk of malignant upgrade on surgery has been reported as high as 15.7% [14].

Although surgical excision is still appropriated to atypical papilloma and malignant papillary lesions, most papillary lesions are in fact benign papilloma, which frequently present as a small intraductal solid mass and bloody nipple discharge. Surgical excision for papilloma without atypia diagnosed by VAB may not be necessary, since pathologic underestimation of heterogeneous lesions is reduced in biopsies with larger gauge needles, such as VAB. Moreover, VAB can be a therapeutic option when complete removal of the lesion is achieved, resolving the nipple discharge in symptomatic cases. An ongoing research has shown that if complete removal of papilloma has been achieved by VAB and no atypia is found, the upgrade rate to malignancy is close to 0% [15]. This approach to use VAB instead of surgery for papilloma without atypia may also be suitable for papilloma first diagnosed by standard CNB, where VAB could be used as a final diagnostic and therapeutic tool (Fig. 10.14).

This trend to de-escalate treatment with complete removal of the lesion by VAB has been expanding to other histological diagnosis with uncertain malignant potential and may be appropriate for selected cases of flat epithelial atypia, classic lobular neoplasia, radial scar, and benign phyllodes tumor [15, 16].

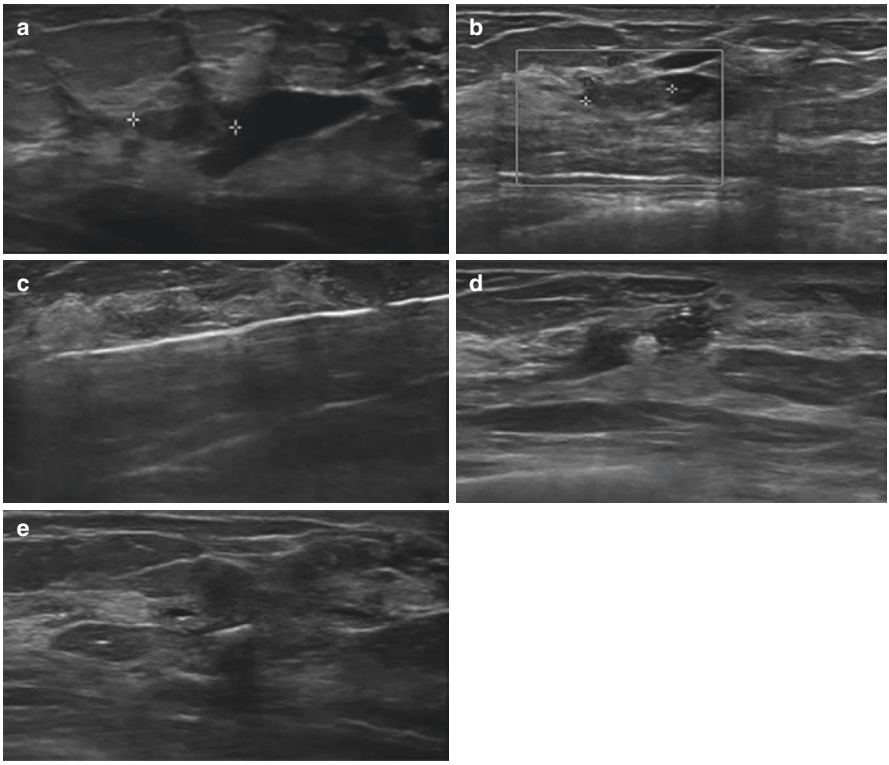

Fig. 10.14 Diagnostic and therapeutic VAB for an intraductal papilloma. (**a**) Intraductal solid mass in a patient presenting with bloody nipple discharge. (**b**) Color Doppler detected flow within the lesion, confirming the solid nature of the mass. (**c**) Complete removal of the intraductal mass with US-guided VAB. (**d**) Post-biopsy marker deployed immediately after the procedure. (**e**) Biopsy site 4 years after the procedure, with no residual lesion

10.13.2 VAB and CNB Technique

The initial planning of both VAB and CNB is very similar to FNA. The patient is positioned in a supine or supine oblique position, with the ipsilateral arm behind the head. The oblique position is preferred for lateral lesions, as well as axillary targets, especially in large breasts, improving lesion visualization and needle trajectory, allowing it to pass parallel to the chest wall.

Similar to FNA, the skin is cleansed and asepticized, the transducer is properly covered with a sterile cover, and sterile gel is used to allow ultrasound imaging of the targeted lesion. Once the initial preparations are complete, the operator has to plan the skin entry point of the needle and its trajectory, taking into account the lesion depth and location. The optimal needle visualization is obtained with a perpendicular angle between the needle and the transducer beam. Superficial lesions are best approached by a skin entry point closest to the transducer, while deep lesions require a farther entry point (Fig. 10.3).

Fig. 10.15 Skin entry point anesthesia

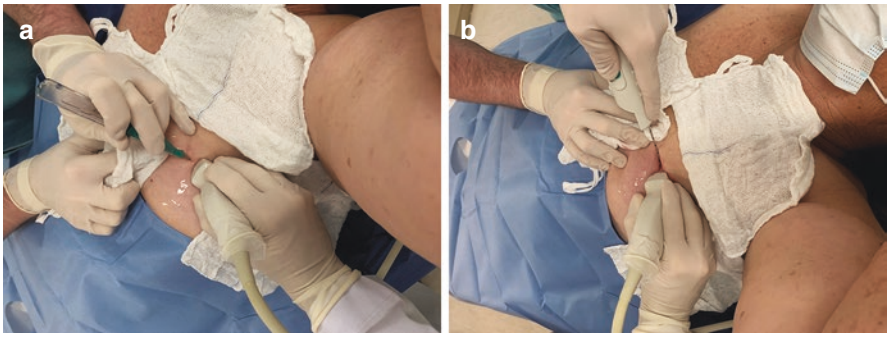

Fig. 10.16 (**a**) Scalpel incision in the skin and (**b**) core needle introduction

The entry skin point is anesthetized with lidocaine or other local anesthetic (Fig. 10.15). The needle trajectory should also be anesthetized with lidocaine alone or in combination with epinephrine, and the anesthetic liquid can be used to lift lesions close to the chest wall or breast implants. While delivering anesthesia, the operator uses this opportunity to confirm that the planned entry site in the skin and needle trajectory is optimal for performing the biopsy.

A small incision is made in the skin with a scalpel blade, and a needle is inserted under real-time guidance into the desired location for specimen collection (Fig. 10.16). VAB needles are ideally placed underneath the lesion, allowing the suction of the vacuum to assist in the lesion sampling, while CNB needles should pierce the lesion in each sampling (multiple passes). Once sampling is adequate, a marker should be deployed inside the lesion or in its original location in case of complete lesion removal with VAB.

Direct compression and ice should be applied to the breast for hemostasis for about 10 minutes. The most frequent biopsy complication is related to persistent bleeding and hematoma formation. Since VAB yields more tissue per biopsy, there

may be more tissue damage and bleeding, although the suction during the procedure is an effective measure to minimize hematomas in most cases. Usually 10 minutes of direct compression is sufficient for adequate hemostasis for both VAB and CNB; however, additional compression for 20 minutes or longer may be required in refractory cases. Continuous bleeding that requires surgical intervention is extremely rare. Albeit rare, other possible complications include infection, pneumothorax, and pseudoaneurysm formation. Implant rupture and milk fistula in lactating patients may occur, although they do not represent a threat but rather an inconvenient outcome.

Once hemostasis is achieved, a sterile dressing is applied to the skin wound, and the patient may be submitted to mammographic CC and ML views to document post-biopsy clip location. A compression bandage can be used for a few hours to further enhance hemostasis, and the patient is discharged after receiving general post-procedure orientations.

10.14 Mammography-Guided Biopsy

There are two methods of percutaneous mammography-guided breast biopsy: stereotactic and digital breast tomosynthesis (DBT)-guided biopsy. Stereotactic biopsy emerged first in the 1980s. The development of stereotactic biopsy was a huge breakthrough for diagnostic evaluation of suspicious breast lesions only seen at mammography.

Indications for stereotactic-guided and DBT-guided biopsies are identical, although the latter method is able to characterize and sample lesions not seen by standard 2D mammography, which will be further detailed in the following sections. Mammography-guided biopsies are mainly indicated to sample suspicious findings as calcifications, masses, architectural distortions, and focal and developing asymmetries not seen on ultrasound evaluation. In everyday practice, most stereotactic biopsies are related to clustered microcalcifications, since the individual calcifications are smaller than 0.5 mm and rarely seen on ultrasound.

For mammography-guided biopsies, although FNA and standard CNB can be performed, VAB is the current state of the art for the procedure. FNA does not have a reliable sensitivity in such procedures, and CNB is related to higher rates of rebiopsy due to insufficient sampling and image-pathology discordance, especially for calcifications [17, 18]. The vacuum system and larger gauge needles are associated with higher-quality samples, while the greater volume of tissue collected by VAB minimizes sampling error and compensates sampling error due to patient movement or due to deep injection of anesthetic. A recent meta-analysis has shown that VAB is related to lower Ductal carcinoma in situ (DCIS) underestimation rate compared to CNB (22.98% by CNB and 11.05% by VAB, $p < 0.001$) with higher rates of calcification retrieval (RR = 0.89, 95% CI 0.81 to 0.98, $p = 0.02$) [19]. The sensitivity and negative predictive value of VAB have been reported as high as >99% in a large retrospective study [17].

10.15 Stereotactic Biopsy

Stereotactic biopsy uses spatial triangulation and basic trigonometry to precisely target a breast lesion seen on mammography, providing coordinates in all axes (width, X; length, Y; and depth, Z) and allowing correct placement of the biopsy needle inside the breast for sampling.

Conventional 2D mammographic views alone cannot provide depth information. However, depth calculation is possible after adding a second view from a different position, based on the parallax principle. Stereotactic biopsy uses two different views of the target lesion, each one with different x-ray tube angulations, known as "stereopair," usually 15° off the midline. Bear in mind that the breast is fixed in place, while the x-ray tube is angled around a fixed center of rotation (Fig. 10.17). The different angulations between the images of the stereopair are responsible for the *apparent* change in the position of the lesion. The apparent change in position of an object in relation to a reference point from two different views is known as *parallax* shift. The target lesion does not actually move; however, it is projected at

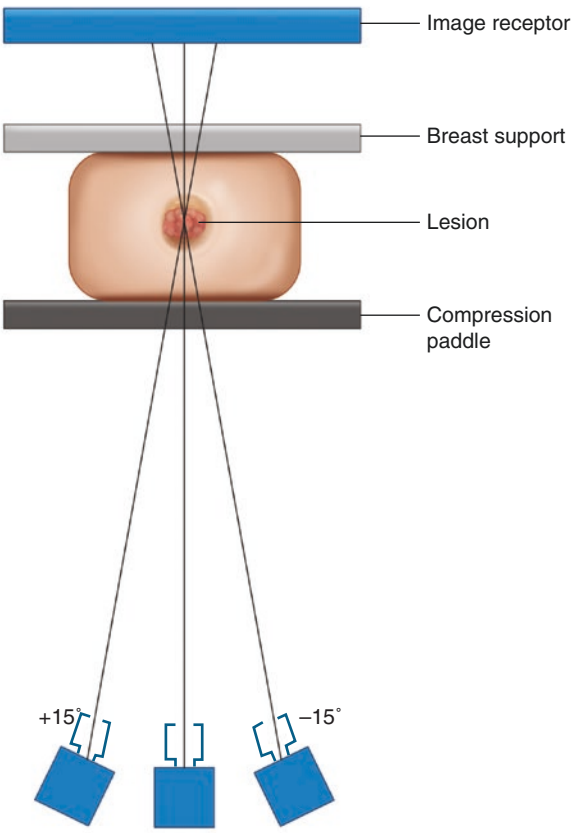

Fig. 10.17 The different angulations of the x-ray tube are responsible for the apparent change in position of the target at the image receptor, which is known as the parallax principle

different locations in each image. Using trigonometry and the apparent shift of the target lesion, the computer software is able to calculate the depth of the target lesion and provide coordinates in all axes.

10.16 Upright Add-On and Prone Table Biopsy Systems

Both stereotactic biopsy and DBT biopsy systems are offered by vendors as either dedicated prone tables or as add-on units to standard mammogram devices (Fig. 10.18).

In dedicated prone tables, the system is designed solely for breast biopsies. The patient is in prone position on the table, with the target breast inserted through a table opening. Under the table, the breast is compressed by a fenestrated compression paddle for needle introduction and tissue sampling.

On the other hand, upright add-on units are attached to a diagnostic mammography unit; the patient is positioned either in a lateral decubitus on a table or in an upright position seated on a chair, while the breast is compressed by a fenestrated compression paddle for sampling. The patient is able to see the whole procedure, including the needle manipulation and tissue sampling, which can increase vasovagal reactions.

The major advantage of the prone table system is that it is more comfortable for the patients; however, these systems are more expensive and cannot be used for routine mammographic imaging. The prone table system has a weight limit, which can preclude its use for overweight patients who exceed the limit. Also, targeting of far posterior lesions may be difficult as the breast cannot be pulled down enough

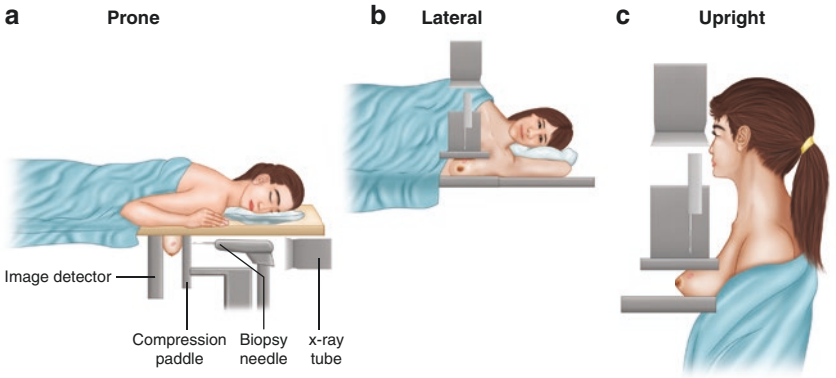

Fig. 10.18 (**a**) A dedicated prone table; the patient lies prone on the table, with the target breast inserted through a hole in the table. Under the table, the breast is compressed with a fenestrated paddle, through which the biopsy needle is inserted. (**b**, **c**) Conventional mammography unit with an add-on device for biopsy; the patient can be positioned either in a lateral decubitus or upright (seated)

through the table opening, often requiring the arm-through-the-hole technique. Upright add-on systems have the advantages of being less expensive, the mammographic unit can be used for routine mammographic examinations, and the system does not have a standard weight limit as the patients are placed on tables or chairs not attached to the system itself. In addition, far posterior lesions are more easily accessed. However, as previously explained, upright systems are known to be related to increased vasovagal reactions, which can impair the procedure.

10.17 The Procedure

The first step is to select the most appropriate approach for breast compression and needle introduction. The operator should review the CC and ML views and be attentive to two factors: conspicuity of the lesion in both views and in which view the lesion is more superficial to the skin. Ideally, the radiologist chooses the incidence in which the lesion is most superficial on the skin, as long as it is well visualized. In some situations, the operator has to choose one or the other (Fig. 10.19).

For instance, a lesion located at the junction of the inner quadrants has the mediolateral view as the shortest skin to lesion approach; however, if this lesion is best seen at the craniocaudal view, being very subtle at the lateromedial view, the operator may choose the CC approach to avoid sampling error.

After selecting the biopsy approach, the patient is positioned on the available biopsy system (prone or upright), and the technologist acquires a scout view visualizing the lesion through a fenestrated compression paddle. This preliminary image is acquired with the x-ray tube perpendicular to the breast (angle of 0°) to position the lesion at the center of the field of view (FOV). This step may be hard, long, and strenuous, especially for subtle findings in large breasts, given the small FOV of the

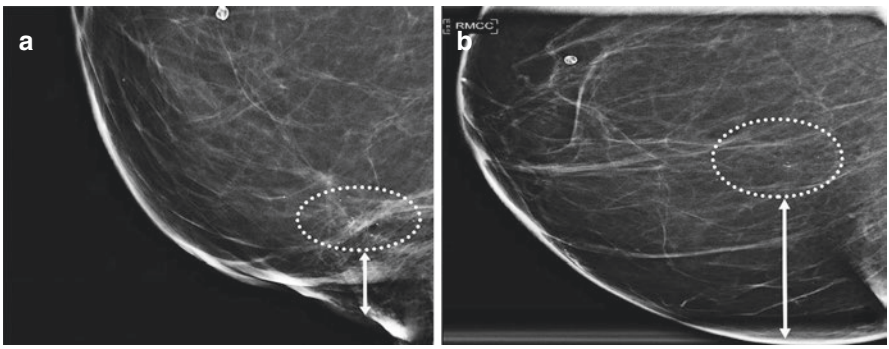

Fig. 10.19 Approach selection for a pleomorphic cluster of calcifications. (**a**) ML view and (**b**) CC view. The cluster of calcifications (circle) is closer to the inferior skin than the medial (arrows) and is well seen in both views; thus, the best approach is caudocranial

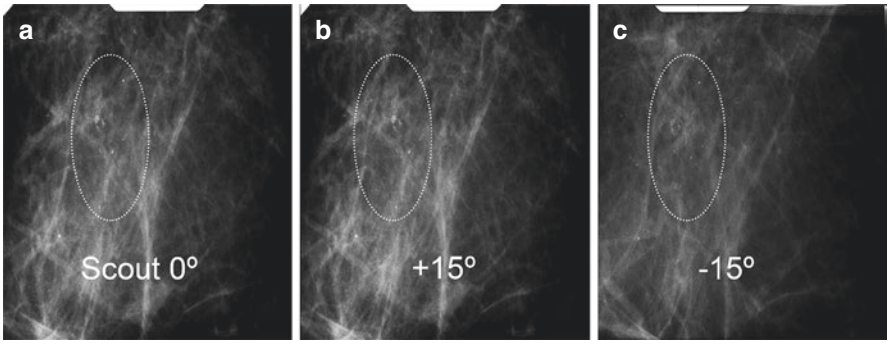

Fig. 10.20 (**a**) Scout image; (**b**, **c**) the "stereopair"

fenestrated paddle. If needed, the radiologist may help in positioning, using whatever helpful landmarks are available, such as blood vessels or coarse calcifications near the lesion to guide the correct positioning. The available screen in the procedure room does not have the same resolution as the dedicated breast workstations used for reporting, and therefore, the findings usually become less evident.

After finding the lesion, it is also important to check if there is any major blood vessel overlapping the lesion, a situation that will require repositioning, for instance, with maneuvers such as rolling.

Once the lesion is properly found and centered, the two views of the "stereopair" are obtained. Each stereopair view is 15° off the scout view, one angled to the left and the other angled to the right (+15° and −15°) (Fig. 10.20).

The radiologist should mark the target on each of the stereopair views so the software can calculate X-Y and Z coordinates. Using the Z coordinate (depth), the thickness of the breast, and the needle measurements, the radiologist has to check the "stroke margin" to ensure that the tip of the needle will not hit the posterior aspect of the breast (Fig. 10.21).

After targeting, the coordinates are transferred to the computer connected to the needle probe holder. The system automatically drives the needle to the desired location in the horizontal and vertical planes (X and Y coordinates), while advancing the needle in depth (Z-axis) is performed manually by the operator. The radiologist should disinfect the skin through the fenestrated paddle and administer local subcutaneous and deep anesthesia with lidocaine alone or in combination with epinephrine. For accurate local administration of anesthesia, it is helpful to manually advance the tip of the needle close to the skin to ensure the entry point is being numbed and seek for the needle trajectory for the deep anesthesia. A small scalpel incision (2–3 mm) is made in the skin, and the needle is manually advanced to the target. Once the needle is in place, the operator may request pre-fire images, two stereopair angulated views (+15 and −15 degrees) to ensure that the lesion has not moved due to anesthesia injection or inadvertent patient movement. The radiologist may obviate the pre-fire images if there is confidence that no movement has occurred. The needle is then fired deeper into the breast, and two post-fire stereopair

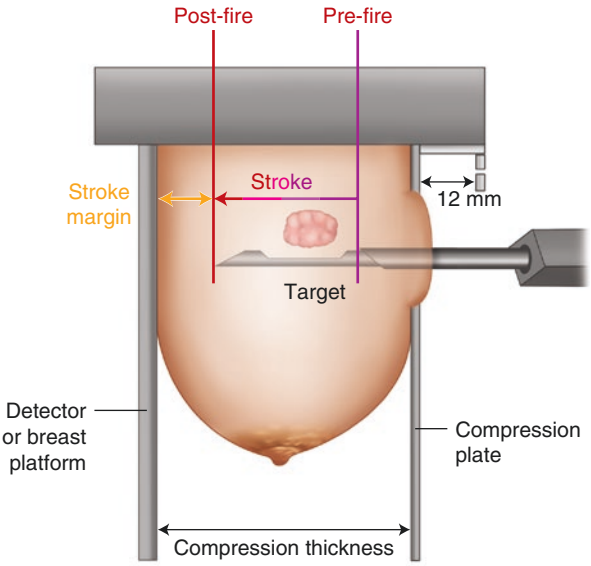

Fig. 10.21 Once in proper pre-fire position, the needle is fired into the tissue to avoid displacing the lesion. The distance of the post-fire needle tip to the image detector is the "stroke margin"

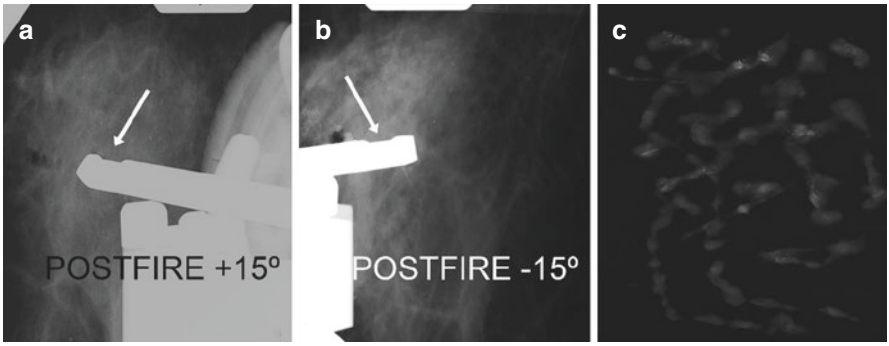

Fig. 10.22 (**a**, **b**) Post-fire stereopair images; part of the calcifications are obscured by the needle, with the sampling chamber correctly placed. (**c**) The specimen radiograph shows multiple fragments with pleomorphic calcifications

images are usually obtained to ensure the sampling chamber is within the target lesion (Fig. 10.22).

Generally, samples are obtained in a clockwise fashion if the needle is right in the center of the target; however, obtaining post-fire images can tailor sampling; for example, if more calcifications are seen under the sampling chamber, more samples should be obtained with the sampling chamber directed downward.

Usually, from 6 to 12 tissue fragments should be obtained. However, the number of fragments is variable and depends on the radiologist's discretion, needle gauge, and lesion size. For calcified lesions, radiographs of the sample should be obtained

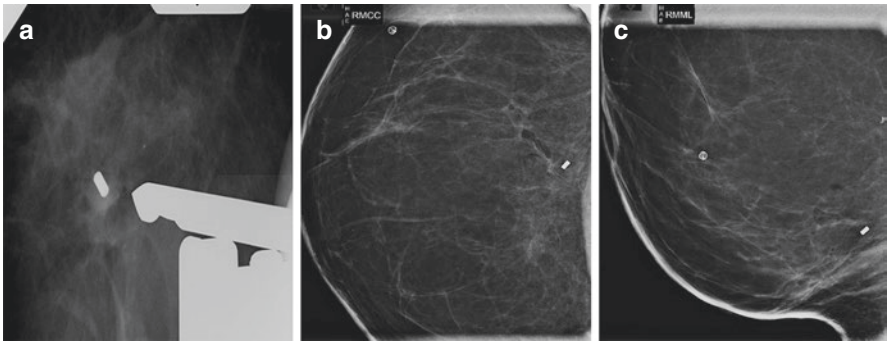

Fig. 10.23 (**a**) Biopsy probe slightly pulled back showing adequately deployed clip. (**b**, **c**) Post-biopsy clip documentation in CC and ML views

to confirm calcification retrieval and accurate targeting (Fig. 10.22c). There is no consensus about the optimal number of fragments in the literature; however, it has been suggested that for a larger needle gauge, such as 9G, nine fragments are optimal for diagnosis [20], while for a smaller needle gauge, such as 11G, at least 12 fragments should be retrieved [21]. The European Society of Breast Imaging suggests that at least 12 fragments should be retrieved [5].

Once sampling is finished, a marker should be deployed at the biopsy cavity through the biopsy probe. The probe should be slightly pulled back in order to confirm its placement with additional stereotactic views (Fig. 10.23).

If the marker is not seen, the probe is reinserted into the target's coordinates, and a second marker is deployed. Once adequate marker deployment has been ensured, the probe is withdrawn and the breast slowly released from compression to avoid clip migration ("accordion effect").

The main complications related to stereotactic biopsy are vasovagal reactions, bleeding, and hematoma formation, as seen in other breast procedures.

Direct compression and ice should be applied to the breast for hemostasis for at least 10 minutes. Once adequate hemostasis is achieved, a sterile strip dressing is applied to the skin incision to aid wound healing. Post-biopsy CC and ML views should be obtained to document the biopsy site, to confirm adequate sampling with partial or complete removal of the target lesion, and to document the location of the post-biopsy marker (Fig. 10.23b, c). Occasionally, the marker may be displaced from the biopsy site. This displacement usually occurs within the needle track; for instance, if the approach was either medial or lateral to the breast, the marker may be displaced lateral or medial to the biopsy cavity, while a craniocaudal approach may present superior or inferior displacement of the clip in relation to the biopsy cavity. In such cases, the radiologist should describe in the final report the amount of displacement of the marker in relation to the target site in centimeters as well as provide useful landmarks that can assist later localization of the biopsy site.

A compression bandage may be used for a few hours to further enhance hemostasis, and the patient is discharged with general post-procedure orientations.

Table 10.1 Positive predictive value for architectural distortions seen only on tomosynthesis

Author	AD only seen on DBT	Malignant outcome	PPV (%)
Alshafeiy TI et al.	59	6	10.2
Partyka L et al.	9	4	44
Patel BK et al.	34	9	26

AD architectural distortion, *PPV* positive predictive value

10.18 Digital Breast Tomosynthesis-Guided Biopsy

Digital breast tomosynthesis (DBT) has been increasingly used since the first device received its Food and Drug Administration (FDA) approval in 2011. The technology uses an x-ray tube that moves in an arc over the compressed breast and captures several images of each breast from different angles, which are reconstructed by software into a set of "three-dimensional" images. Also, acquired data can be collapsed into a single synthesized 2D image, which may obviate the need for conventional 2D images, reducing radiation dose in half. The three-dimensional set of images is converted into 1-mm sections of the breast, reducing tissue overlapping, improving analysis of the margins, facilitating the identification of subtle findings such as architectural distortions, and providing the location of lesions visible only in one mammographic view [22]. Studies have shown that DBT reduces false-positive and recall rates while improving cancer detection [8, 23, 24]. Its adoption by medical facilities has been increasing and replacing older mammographic 2D units (*conventional full field digital mammography and computed radiography units*). To illustrate, on December 1, 2017, 3866 certified facilities had DBT units in the United States of America (USA), and this number jumped to 6.111 on June 1, 2020. Currently, over 70% of all US certified facilities [25] have already adopted at least one DBT unit.

With increasing number of examinations being done with DBT technology, we have been facing a growth of findings visible only on DBT. There is still an ongoing debate of the positive predictive value of these findings; however, initial data suggests that biopsy is required. For architectural distortions (AD) seen only on DBT, 10–44% had a malignant biopsy outcome [26–28] (Table 10.1).

10.19 DBT Versus Stereotactic Guided Biopsy

DBT biopsy is critical for tissue sampling of findings only seen on DBT, such as AD, asymmetries, and some masses. Prior to DBT biopsy development, findings seen only on DBT had to be surgically excised after preoperative localization; thus, DBT biopsy reduces the costs and morbidity related to surgical excision. Moreover, even for noncalcified lesions seen at 2D mammography, DBT biopsy usually depicts these findings better than digital mammography (DM), which translates into better confidence in targeting.

Table 10.2 Comparison of technical success rate, mean procedure time, and radiation exposure between digital breast tomosynthesis and stereotactic biopsy

Author	Technical success rate		Mean procedure time (min)		Median number of images acquired	
	PSVAB	DBTVAB	PSVAB	DBTVAB		
Schrading et al.	154/165 (93%)	51/51 (100%)	27	13	8	5
Bahl et al.	410/431 (95.1%)	695/700 (99.3%)	27	12	12	3
Ariaratnam et al.	N/A	38/38 (100%)	N/A	15	N/A	N/A

PSVAB prone stereotactic vacuum-assisted biopsy,. *DBTVAB* digital breast tomosynthesis vacuum-assisted biopsy

In addition, DBT biopsy obviates the need for the stereopair images, with direct depth calculation (Z-axis), decreasing procedure time and radiation exposure. A large retrospective study conducted by Bahl et al. comparing 706 DBT-guided biopsies in upright positions with 439 stereotactic biopsies in prone tables suggested that DBT biopsy prevailed over stereotactic as a faster procedure (12 vs 27 min), with lower radiation dose (3 vs 12 exposures) and greater technical success (99.3% vs 95.1%) [29]. Those findings are similar to those of smaller earlier studies comparing DBT and stereotactic guided biopsies [30, 31] (Table 10.2).

10.20 The Procedure

Overall, aside from lesion identification and targeting, DBT-guided biopsy is very similar to the standard stereotactic biopsy. The choice of approach is identical, requiring the needle to go through the shortest distance to the skin or use the incidence that provides the best conspicuity of the lesion.

The patient is positioned according to the available system (upright or prone), and tomosynthesis images or a 2D scout image is obtained by the technologist centralizing the lesion within the FOV. Once the lesion is accurately identified, a tomosynthesis scout image is obtained. The radiologist scrolls through the slices until he/she finds the slice where the lesion is more conspicuous (Fig. 10.24).

In the computer screen, the target is marked and the software readily calculates the Cartesian coordinates X, Z, and Y. It is important to emphasize when going through the images, the radiologist should be aware if there are no vessels along the needle path, and if applicable, repositioning should be done. The breast can be rolled to remove the vessel from the path or change the approach view, such as orthogonal view.

After the proper coordinates are obtained, the radiologist has to ensure that there is sufficient tissue beyond the lesion for the needle to be fired within the breast without hitting the posterior aspect of the breast and also that the skin is not included in the sampling chamber of the needle. This has become very easy and intuitive with

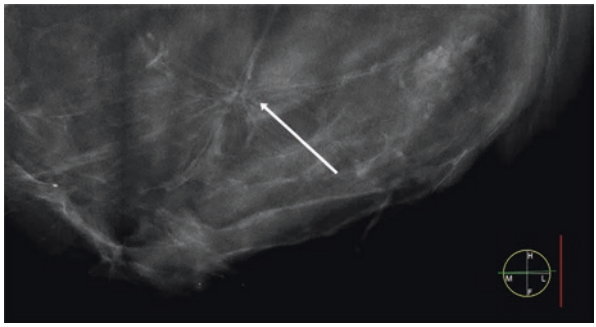

Fig. 10.24 DBT-guided biopsy of an architectural distortion. Once proper scout has been done, a tomosynthesis set of images are obtained. The radiologist scrolls the images until he/she reaches the slice where the lesion is most conspicuous (arrow)

newer software that displays a graphical representation of the needle inside the breast, as shown in Fig. 10.25.

Once targeting has been completed, the coordinates are sent to the computer attached to the needle probe. Asepsis of the skin, anesthesia, scalpel incision, and needle introduction are conducted similarly to stereotactic biopsy. Once in target, pre-fire images may be obtained, which can be either 2D stereopair angulated views (+15 and −15 degrees) or a pre-fire tomosynthesis image set. At this stage, it is crucial to check if there was patient movement after the lesion coordinates were obtained. After firing the needle, a post-fire tomosynthesis set or a 2D stereopair post-fire images may be obtained at the discretion of the radiologist; however, the stereopair adds more radiation than the tomosynthesis set of images (Fig. 10.26).

The handling of the probe for tissue sampling, the number of fragments required, the specimen radiographs, the procedure complications, and the post-procedure care are no different from what has been described for stereotactic biopsy. However, post-biopsy documentation to ensure the correct sampling with the marker in place is performed with a single set of tomosynthesis images (Fig. 10.27).

10.21 Technical Challenges and Possible Solutions (DBT and Stereotactic Biopsy)

10.21.1 Subtle Findings

Subtle findings may be hard to locate within the small field of view of the biopsy equipment. To overcome this problem, before positioning the patient on the stereotactic table, the lesion can be localized using a full-field 2D mammography and an alphanumeric grid. The alphanumeric grid is used to place a metallic marker (BB) overlying the skin, which can then be used during the procedure as a landmark to find the target lesion [32] (Fig. 10.28).

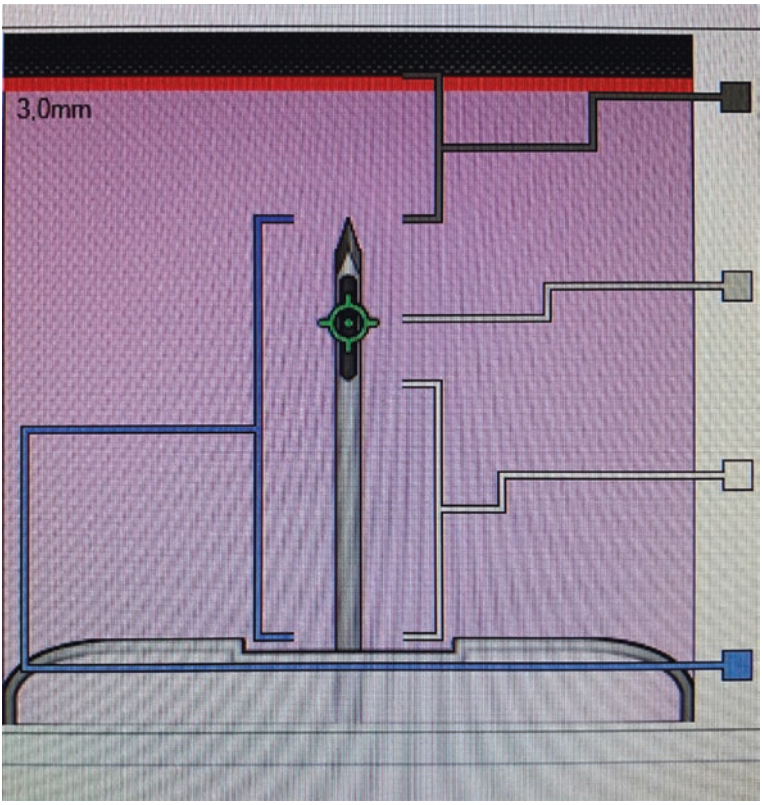

Fig. 10.25 The Hologic Affirm® Prone Biopsy System uses pre-programmed needle parameters to display a graphical representation of the selected needle, the target location, the compression paddle, and the image receptor. In an intuitive fashion, it is possible to see all relevant spatial relationships: the location of the marked target (green), the length of the needle inside the breast (blue), the distances between the point of entry of the skin and the beginning (white) and middle (light gray) of the sampling chamber, as well as the distance between the needle tip and the image receptor (dark gray)

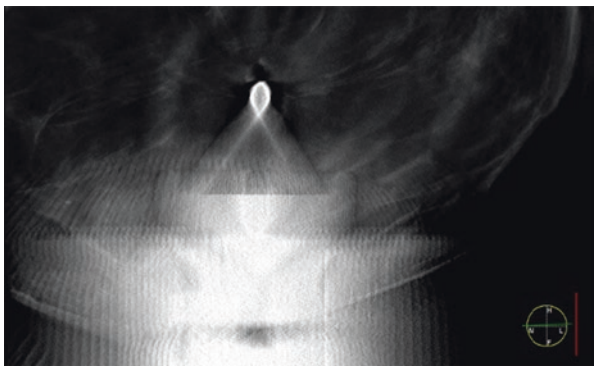

Fig. 10.26 Post-fire tomosynthesis showing the needle sampling chamber in an accurate position to sample an architectural distortion

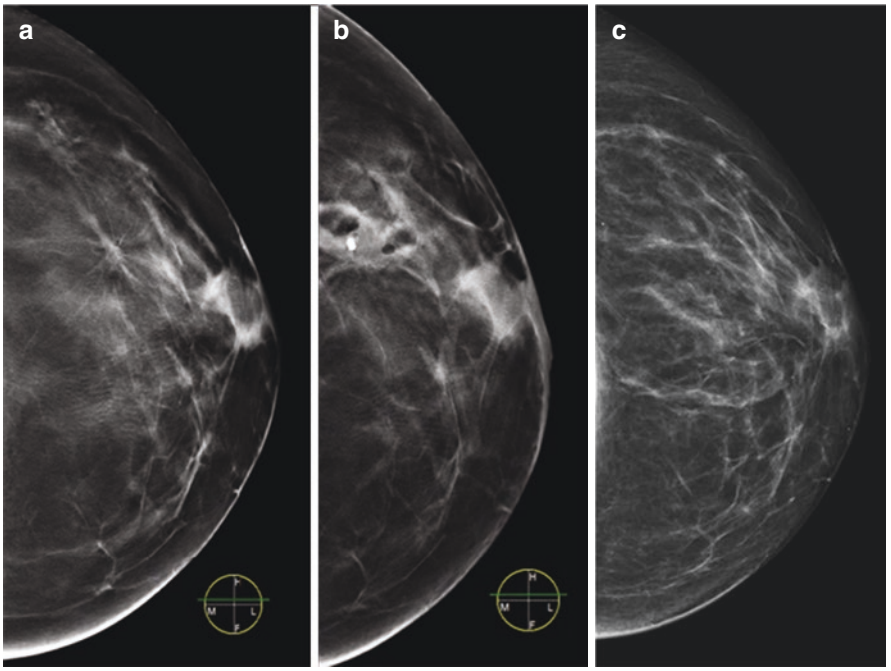

Fig. 10.27 Comparison of pre- and post-biopsy images to verify sampling accuracy. (**a**) Pre-biopsy tomosynthesis slice demonstrating the architectural distortion to be sampled; (**b**) post-biopsy tomosynthesis slice showing adequate sampling with the clip at the desired location; and (**c**) pre-biopsy 2D mammography for comparison. Note that the architectural distortion is barely seen without tomosynthesis

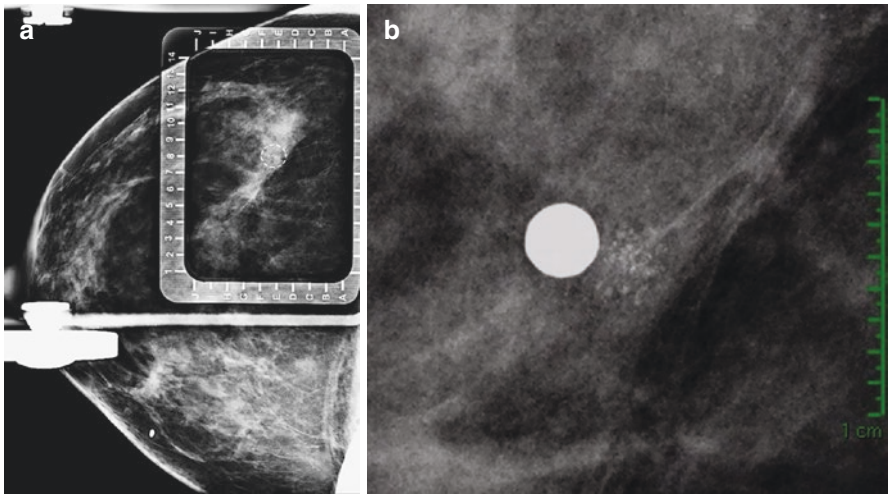

Fig. 10.28 (**a**) Full-field 2D mammography and alphanumeric grid used to locate subtle calcifications. (**b**) Magnified view after placing the marker overlying the skin. The BB can later be used as landmark to find the clustered calcifications

10.21.2 Far Posterior Lesions

Targeting deep lesions can be challenging, especially in prone tables. Occasionally, the breast cannot be sufficiently pulled down through the hole, and the lesion is not included in the field of view. If available, upright add-on systems are better suited for far posterior lesions.

There are several techniques that can be used to target far posterior lesions. Repositioning with lower breast compression and lateral or MLO approach can increase the inclusion of posterior and axillary tissue. For prone tables, the patient can be slightly rolled onto her side while placing her entire arm, shoulder, and breast through the table hole (arm-through-the-hole technique) [33].

10.21.3 Thin Breasts

During breast compression, a minimum thickness of the breast is required to fit the needle, including its tip and sampling chamber. A minimum thickness of 30 mm is required for standard VAB or 20 mm for a shortened sampling chamber needle, also called *petite* needle (Fig. 10.29).

If there is not enough room for the needle, the stroke margin becomes negative. In cases where even a *petite* needle is not enough, the operator can attempt to roll the

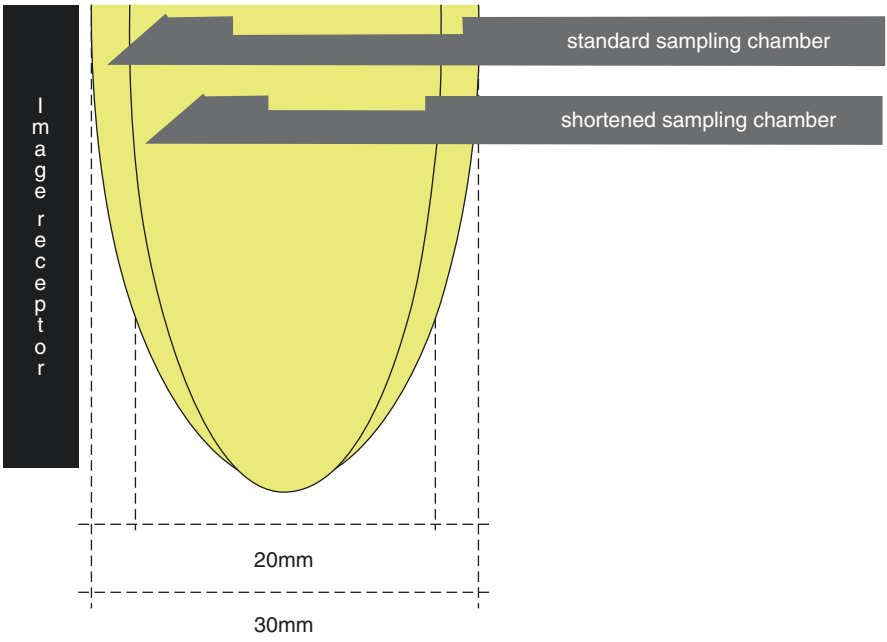

Fig. 10.29 Illustration showing the differences between standard and shortened sampling chamber needles

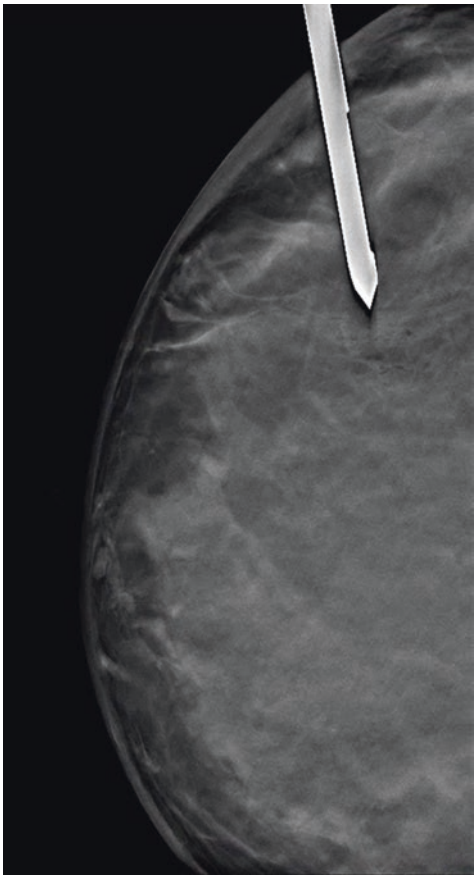

Fig. 10.30 Lateral arm approach for a very thin breast. The needle is manually inserted along the horizontal axis (X) into the breast

breast or tape up the breast against the chest wall in order to bulge the breast anteriorly through the opening of the paddle to increase thickness. Rarely, very thin breasts may require adding another biopsy paddle between the posterior aspect of the breast and the image receptor. In cases where the stroke margin is only slightly negative, injecting superficial anesthetic to increase the skin wheal can add a few millimeters.

If available, the operator can opt to use a lateral arm extension device to perform the insertion of the needle between the image receptor and the compression paddle, i.e., orthogonal to the compressed breast. In the lateral arm approach, the needle is inserted horizontally (X) into the breast; thus, the stroke margin is greatly improved (Fig. 10.30).

10.22 Superficial Lesions

To avoid unwarranted trauma of the skin, superficial lesions can be sampled with a shortened sampling chamber needle. In addition, although the software calculates the coordinates so that the target is right in the center of the sampling chamber,

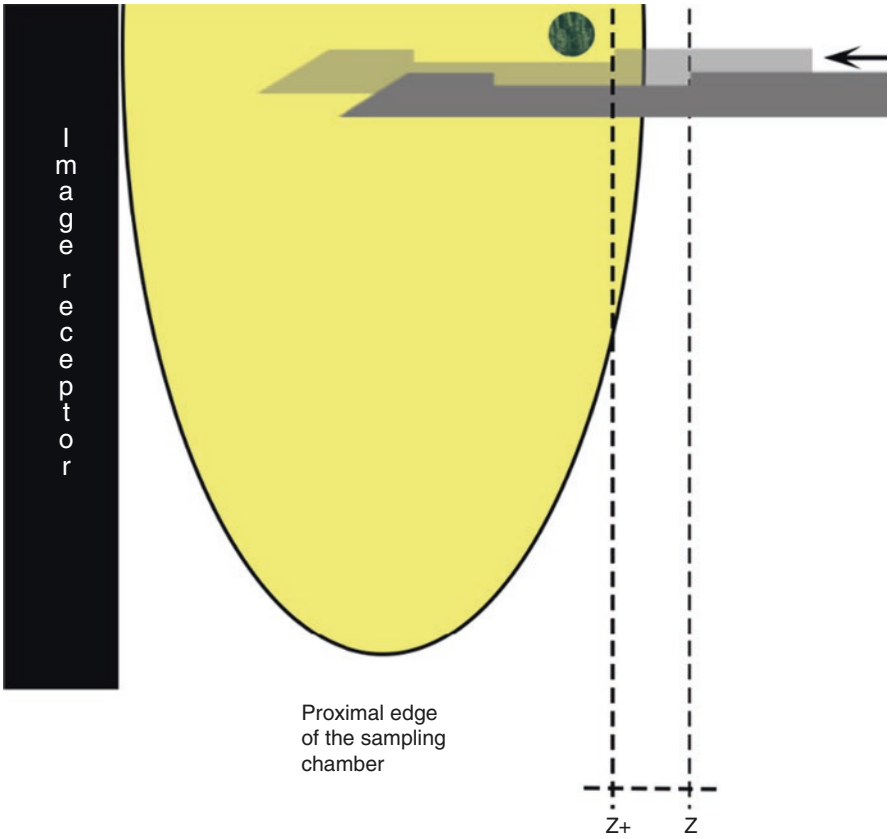

Fig. 10.31 Illustration showing the position of the sampling chamber and the skin at the calculated depth (Z) for the target. The operator can further introduce the needle (Z+) so the sampling chamber is able to sample the lesion at its proximal edge while avoiding the skin

sampling occurs throughout the whole sampling chamber. Taking into account the length of the sampling chamber and its relationship to the target allows the needle to advance a few millimeters to avoid skin trauma, while sampling is done at the beginning of the sampling chamber (Fig. 10.31).

10.23 MRI-Guided Biopsy

Of all imaging modalities, breast MRI has the highest sensitivity for detecting breast cancer. Two meta-analyses showed a sensitivity of 90–92% and a specificity of 70–72% [34, 35]. Thus, although MRI is very sensitive, up to 30% of suspicious findings are in fact benign, and histologic confirmation is required for a definitive evaluation of suspicious findings (BIRADS 4 and 5). The main indication for breast MRI-guided procedure is BIRADS 4 and 5 lesions that are not amenable to biopsies guided by ultrasound or mammography.

10.23.1 Second-Look Ultrasound and Second-Look Mammography

MRI-guided biopsy is an expensive and time-consuming procedure; it requires intravenous gadolinium injection and can be limited in deep or axillary lesions. The procedure may be time-consuming and uncomfortable for patients. Ultrasound sampling, whenever possible, should be the first option. Even in cases where breast ultrasound has already been performed, it may be useful to obtain a second-look ultrasound before undergoing breast MRI-guided biopsy.

A second-look ultrasound is a targeted examination with a purpose of finding a corresponding lesion on ultrasound. It should be performed using information from the MRI examination, such as lesion location and characteristics and available anatomic landmarks, taking into account imaging differences between the two modalities, including different breast position (supine vs prone) and related tissue deformation [36]. If a positive correlation is found, an ultrasound-guided biopsy is performed. It should be noted that the second-look ultrasound is often a challenging examination, requiring an experienced operator. The successful rate of positive correlation reported in the literature is markedly heterogeneous, ranging from 23% to 82%, and can be dependent on several factors, such as operator's experience, lesion type, size, depth, and size of the breast.

In 2009, Nakano et al. [37] described the use of a sonographic system that enables real-time sonography with MR navigation. Since then, several vendors have offered systems with different names that permit co-registration and allow synchronization of sonographic and MR images during real-time sonography [38]. These devices can track probe's position and couple real-time ultrasound images to a set of pre-acquired MR images uploaded in the system, displaying magnetic resonance multiplanar reconstruction (MPR) images along with real-time ultrasound images side by side or as overlying (fusion) images. A major limitation of these systems is that MR images are acquired in a prone position to reduce artifacts from breathing motion and heart beating, while ultrasound is usually performed in a supine position, and breast deformation in each position can lead to misalignment and morphological differences between the acquired images. Several solutions to reduce misalignment have been developed, such as performing both examinations in the same position (prone or supine) and improvements in algorithm to compensate deformation between the two modalities. These techniques have shown promising results, with reported rates of successful correlation ranging from 83% to 95.5% [38–41].

Although lesions that present a sonographic correlate are more likely to be malignant, malignancy is found in about 12% of cases where no sonographic correlate is found, and the lack of correlation does not obviate the need for histological analysis [42].

10.23.2 Second-Look Mammography

The rationale behind reviewing mammography images before performing an MRI-guided biopsy is similar to a second-look ultrasound. Performing a mammography-guided biopsy is more cost-effective and less time-consuming than performing an MRI-guided biopsy. The radiologist should look for any abnormalities on mammography that could correlate to the suspicious MRI finding. A careful review of calcifications is recommended for nonmass enhancements, as calcifications can be reliable targets and are frequently not seen on ultrasound evaluation.

Recent reports have also shown the value of second-look DBT. Clauser et al. published a study evaluating the performance of DBT and ultrasound in detecting 84 additional findings in 135 patients with breast cancer who underwent breast MRI. While ultrasound alone showed a positive correlation in 52% of the cases, when combined with DBT, the detection rate rose to 75% [43]. These results are in agreement with a study published by Mariscoti et al. analyzing 164 additional findings in 520 women with breast cancer who underwent breast MRI, showing that ultrasound alone was able to identify 69.5% of those additional lesions, while DBT increased the detection success rate by up to 89% [31]. This increase is probably related to the ability of tomosynthesis to evaluate masses, asymmetries, microcalcifications, or architectural distortions that may be subtle or not visible at all on US.

Similar to second-look ultrasound, the rest of the cases that do not have ultrasound or mammogram correlate require MRI-guided histological analysis.

10.23.3 The Procedure

MRI-guided biopsy requires a compatible and dedicated breast coil for the procedure, as well as an MRI-compatible vacuum-assisted biopsy device, usually containing an 8–12G needle and an introducer kit. As with stereotactic and DBT-guided biopsies, the use of VAB is the standard of care, ensuring the procedure is performed in a timely manner and that adequate samples are retrieved. Before starting the procedure, MRI safety should be checked, as well as contraindications to intravenous gadolinium injection. A thorough review of the original diagnostic MR examination is necessary to be familiar with the lesion's morphological features and location. The radiologist uses this information to aid in patient positioning and to select the best approach to sample the target lesion. Older systems are limited to lateromedial approach only; however, improvements in design made coils available from multiple vendors that also allow craniocaudal and mediolateral approaches, improving accessibility to the lesion.

The patient should be positioned in prone position, with the index breast placed on the breast coil. The breast is compressed between the compression plate and the biopsy grid, from which the radiologist manipulates the needle during the procedure.

Adequate compression is critical to ensure that the breast is fixed in place while the procedure is performed; however, care should be taken not to overcompress, which can interfere with enhancement of the target lesion.

The biopsy grid consists of evenly sized squared holes, one of which will be used for needle insertion. Some grids have a built-in marker in one of its holes that can be seen in non-enhanced T1-weighted sequences, while other grids require the placement of a fiducial marker in one of its holes. Since the marker can be seen on MR images and its actual location on the grid is known, it is used to identify a particular hole seen on the MR image and its actual location on the grid plate (Fig. 10.32).

Pre-contrast images are obtained to check for adequate fat saturation, and the radiologist attempts to see if the expected lesion location is within the limits of the grid, using landmarks and the location from the original diagnostic MRI (Fig. 10.33). Since the grid will be used to locate the needle in the horizontal and vertical planes, if the expected lesion is not seen within the limits of the grid, the patient can be repositioned before resuming the procedure.

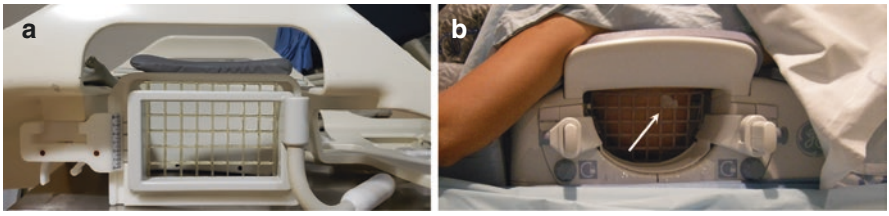

Fig. 10.32 (**a**) Breast coil and biopsy grid from Siemens (**a**) and from General Electric (**b**). The fiducial marker is placed in one of the grid holes (arrow) to serve as a landmark for hole identification on MR images

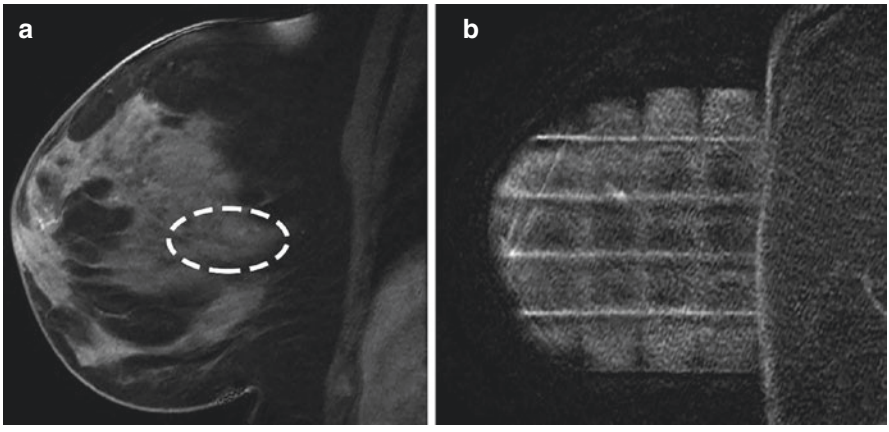

Fig. 10.33 (**a**, **b**) Non-enhanced sagittal T1 slices showing that the expected location of the lesion (circle), based on anatomical landmarks, is within the grid boundaries in (**b**)

Post-contrast dynamic sequences are obtained to accurately identify and target the lesion. If the enhancing lesion is not seen, the biopsy cannot be performed. Targeting the lesion can be either done visually or using designed software for this purpose. The visual method is very straightforward and consists of comparing the location of the lesion with the fiducial or built-in marker in the biopsy grid. For instance, when using sagittal sequences to perform the biopsy in a lateral approach, the radiologist must scroll through the slices until the lesion is clearly depicted. Once the lesion is found, the radiologist can pinpoint its center with a crosshair and then scroll back to the slices containing the fiducial marker. By comparing the pinpointed location with the fiducial marker, the radiologist chooses the most appropriate grid hole for needle introduction (X-Y coordinates) (Fig. 10.34).

Lesion depth is obtained by multiplying the number of slices between the skin and the lesion by the slice thickness (Z coordinate). With coordinates in hand, the patient is removed from the magnet and the biopsy area should be prepared with aseptic technique. The skin and needle path are anesthetized similarly to other procedures, and a small incision in the skin with a scalpel is made to facilitate the introduction of the coaxial device. The introducer kit contains a tunneled needle guide that is plugged into the grid hole to stabilize the needle and a three-part coaxial system, consisting of an outer plastic cannula, an inner metallic stylet, and an inner plastic obturator (Fig. 10.35).

After placing the needle guide into the chosen grid hole, the coaxial system is first introduced with the outer plastic cannula and the inner metallic stylet inside. The inner stylet is responsible for cutting and dissecting through the breast tissues, while the outer plastic cannula is marked with inches and centimeters that are used for depth control. Once the target depth is achieved, the inner stylet is removed and replaced by the inner plastic obturator. The patient reenters the magnet, and new images are obtained to ensure accurate positioning by comparing the signal from the obturator, target related landmarks, and slices. The lesion may be displaced by

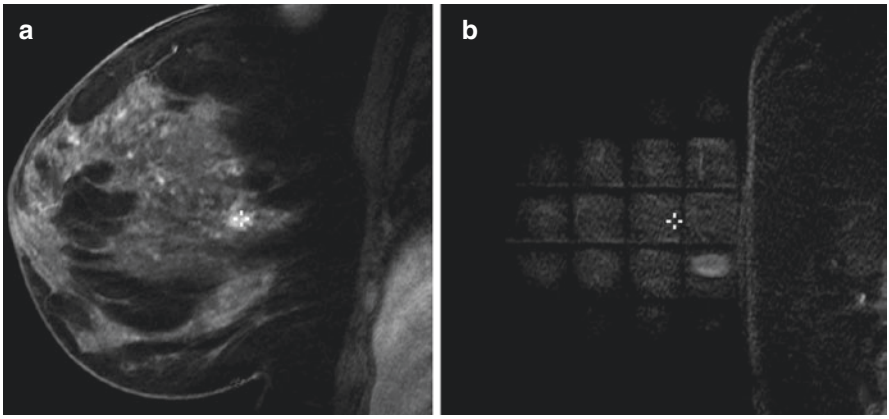

Fig. 10.34 (**a**) Crosshair placed in the center of target nonmass enhancement and (**b**) after scrolling back, the adequate grid hole for needle introduction is selected

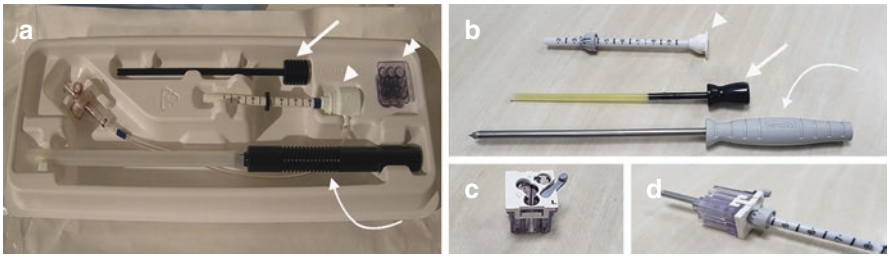

Fig. 10.35 Biopsy kit. (**a**) Suros biopsy kit and (**b**) Bard biopsy kit. Inner plastic obturator (arrow), outer plastic cannula (arrowhead) tunneled needle guide (double arrowhead) and inner stylet (curved arrow); (**c**) detail of Bard tunneled guide plastic and (**d**) obturator and inner stylet inserted into the needle guide

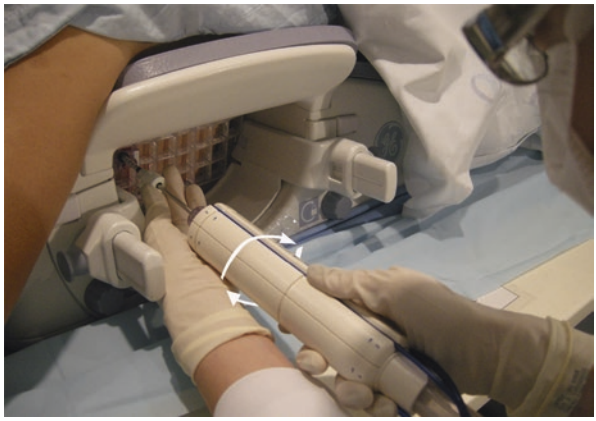

Fig. 10.36 Sampling is usually performed in a clockwise 360° fashion if the sampling chamber is centered in the lesion

anesthesia or bleeding, and occasionally, the coaxial system pushes and displaces the tissue instead of cutting, which is known as the "snowplow" effect. If needed, the inner stylet may be reinserted and necessary adjustments performed.

Once the coaxial system with the outer plastic cannula and the inner plastic obturator is confirmed in satisfactory position, the patient is again removed from the magnet, the obturator is removed and replaced by the actual VAB needle, and samples are obtained, usually in a clockwise fashion or according to suitable tailoring of the sampling chamber toward the lesion (Fig. 10.36).

Usually from 6 to 12 samples are obtained according to the radiologist's discretion. The VAB needle is then removed and replaced by the plastic obturator, and a new set of images are obtained to confirm if the expected lesion location has been sampled. Once adequate sampling has been confirmed, the obturator is removed and a clip marker is deployed at the biopsy site through the plastic cannula.

Technical issues with MRI-guided biopsy are usually associated with thin breasts or posterior lesions. MRI guidance allows a minimum thickness of 30 mm for standard needles and 18 mm for a *petite* needle. Most of the techniques previously

described to overcome technical problems with breast thickness in mammography-guided biopsy can be used in MRI-guided biopsy, such as rolling or taping the breast or increasing the anesthetic wheal. For posterior lesions, the patient may be rolled to include more posterior tissue, and the biopsy grid can be raised.

10.23.4 Complications and Post-biopsy Care

MRI-guided biopsy is at risk for complications similar to other VAB procedures, including bleeding, hematoma formation, skin damage, pneumothorax, and vasovagal reaction. In addition, although the risk for contrast reactions with gadolinium is low, the patient must be kept under surveillance for a certain amount of time. Other complications and post-procedure care and orientations are identical to other VAB procedures.

10.24 Imaging-Pathology Correlation

Imaging-pathology correlation consists of evaluation of the suspicious imaging finding and the final diagnosis provided by the pathology, assessing whether the histologic report is in agreement with the image and providing an appropriate management recommendation. This is a mandatory part of the final biopsy report, with the main purpose of preventing a malignant lesion with a benign pathology report after breast biopsy from receiving further investigation, delaying cancer treatment.

When establishing imaging-pathology correlation, two aspects have to be considered: (1) whether the target lesion was accurately sampled and (2) whether the histologic results can explain the imaging finding.

10.25 Discordant Biopsy

Whenever the lesions were missed during sampling, the results are considered discordant. A thorough review of all available images is required: the original diagnostic examination and the biopsy and post-biopsy images. Morphological features, size, and location of the target lesion are compared between the studies to ensure that the suspicious lesion was indeed targeted during the biopsy. Post-biopsy images may show reduction in size or complete removal of the lesion, especially when VAB has been performed. If a biopsy marker has been deployed, the radiologist can compare its location in relation to the target lesion, taking into account that migration may occur. For all procedures, it is very useful to check the proper positioning of the needle in relation to the target lesion during the procedure. For lesions with calcifications, the radiologist should obtain sample radiographs to ensure that the

calcifications have been retrieved, as well as to compare morphological features between the calcifications within the samples and the target area, to ensure that the correct group of calcifications has been sampled. Rarely, calcifications may not be seen in the sample radiographs but can be seen in histopathology. Another aspect to take into consideration is representativeness. If too few calcifications are present in the sample, it may be considered not representative of the original group. For heterogenous lesions, it is critical to ensure that the most suspicious part of the lesion has been sampled. Representativeness is also related to the needle gauge used to obtain the samples, with FNA at one end of the spectrum and VAB with larger gauge needles at the other end.

The next step is to establish whether the pathology report is consistent with the imaging finding. Imaging-pathology concordance is often a multidisciplinary task, involving the referring physician, the radiologist, and the pathologist. Parikh et al. described five scenarios of imaging-pathology correlation [44]:

10.25.1 Concordant Malignancy

The radiological features of the lesion are suspicious (BIRADS 4 and 5), and the pathology report is malignant, for instance, a spiculated mass diagnosed as infiltrating carcinoma, or a segmental enhancement or calcifications diagnosed as DCIS. The radiologist should communicate the results to the referring physician, and the patient contacted and referred for appropriate therapy.

10.25.1.1 Discordant Malignancy

The radiological features of the lesions suggest a benign etiology, but the pathology report is malignant. This can be either related to an incidental finding, inadequate prior assessment of image features, or the overlap between malignant and benign image features of some malignant lesions. Management of such cases is identical to concordant malignant.

10.25.2 Concordant Benign

The radiological features suggest a benign etiology, and the pathology report is a benign lesion. A classic example is an oval mass with circumscribed margins classified as a fibroadenoma. When establishing concordance of benign image features and a benign histological result, it is important to differentiate benign pathological entities that are a definitive diagnosis from benign entities that are nonspecific findings. Although the list of definitive and nonspecific diagnosis may be slightly variable within the literature, definitive diagnosis is lesions that have distinct image

features and are easily correlated with the image findings. Definitive diagnosis includes fibroadenoma, tubular adenoma, hematoma, abscess, hamartoma (fibroadenolipoma), fat necrosis, granulomatous disease, lymph node, myofibroma, and cyst contents.

On the other hand, nonspecific breast benign results on histopathology might be less reassuring and require a careful imaging-pathology correlation. Nonspecific benign entities include fibrocystic changes, apocrine metaplasia, duct hyperplasia, and stromal fibrosis. Although these lesions, alone or in combination, might be related to the image findings that led to biopsy, such as suspicious calcifications or an indistinct mass (e.g., fibrosis), these results are often incidental findings. Thus, establishing concordance for such entities frequently requires communication between the radiologist and the interpreting pathologist.

Short-term imaging follow-up protocol after a concordant benign finding is not consensual. The current NCCN guidelines (2020, version 1) support that either a 6- or 12-month follow-up is appropriate. Some authors suggest that for stereotactic or US-guided core biopsies, a short-term 6-month follow-up should be recommended to avoid delay in diagnosing a falsely negative biopsy [45, 46], while others suggest that a short-term follow-up may be appropriate for nonspecific diagnosis [44, 47, 48]. Recent reports have shown little benefit from short-term follow-up and that 12-month follow-up for benign concordant lesions is ideal [49–51].

Benign and concordant biopsies guided by MRI may benefit from short-term follow-up given its technical challenges: MRI-guided biopsy is not a real-time procedure; specimen radiograph to confirm lesion retrieval is not possible; contrast wash-out during the procedure and bleeding may limit sampling accuracy. A study by Hayward et al. showed a 2.4% rate of false-negative results after benign concordant assessment [52]. A short-term MRI follow-up may be useful for reassuring adequacy of tissue sampling and to avoid delays in false-negative results.

10.25.3 Discordant Benign

The radiological features suggest a malignant lesion, while the pathology report is benign and cannot explain the imaging features that lead to biopsy. For instance, a spiculated mass with microcalcifications cannot be explained by fibrocystic changes or a fibroadenoma result. A few benign entities can present findings highly suggestive of malignancy, such as granular cell tumor, fat necrosis, diabetic mastopathy, and granulomatous mastitis. These diagnoses may be concordant but require a careful correlation.

A discordant result is usually related to suboptimal or sampling error, and a thorough review is required to identify possible flaws during sampling. There are several reasons that can be related to a discordant result:

– Inaccurate targeting – wrong location was sampled, which can be related to subtle findings, patient movement, technical issues with the biopsy equipment, or

even complications during the procedure (such as hematoma and lesion displacement).
– The correct lesion may have been sampled, but due to heterogeneity in the lesion, only a benign portion was taken for histological analysis.
– Suboptimal quality of the samples.

The radiologist should contact the pathologist and referring physician to discuss the results and how to proceed with new biopsy. Both image-guided re-biopsy, usually with VAB, and surgical excision are viable alternatives.

10.25.4 High-Risk and Borderline Lesions

Some nonmalignant histologic results have a potential association with malignancy. Albeit benign, this diverse group of histologic results can coexist with malignant lesions, and the lesion itself confers a risk of increased malignancy over time. Borderline or high-risk lesions include atypical ductal hyperplasia (ADH), lobular neoplasia, papillary lesions, radial scars and complex sclerosing lesions, fibroepithelial lesions with atypia, atypical lobular hyperplasia (ALH), and lobular carcinoma in situ (LCIS).

Although atypical ductal hyperplasia has high well-known rates of underestimation from percutaneous biopsy, usually leading to an excision recommendation [53], the management of other high-risk or borderline lesions found after percutaneous biopsy is usually less well established and determined in a case-by-case basis due to the great variability of images, pathology, and clinical features that must be accounted for.

References

1. Parker SH, Lovin JD, Jobe WE, et al. Stereotactic breast biopsy with a biopsy gun. Radiology. 1990;176(3):741–7. https://doi.org/10.1148/radiology.176.3.2167501.
2. Parker SH, Lovin JD, Jobe WE, Burke BJ, Hopper KD, Yakes WF. Nonpalpable breast lesions: stereotactic automated large-core biopsies. Radiology. 1991;180(2):403–7. https://doi.org/10.1148/radiology.180.2.1648757.
3. Parker SH, Jobe WE, Dennis MA, et al. US-guided automated large-core breast biopsy. Radiology. 1993;187(2):507–11. https://doi.org/10.1148/radiology.187.2.8475299.
4. Liberman L. Percutaneous imaging-guided core breast biopsy. Am J Roentgenol. 2000;174(5):1191–9. https://doi.org/10.2214/ajr.174.5.1741191.
5. Wallis M, Tarvidon A, Helbich T, Schreer I. Guidelines from the European Society of Breast Imaging for diagnostic interventional breast procedures. Eur Radiol. 2007;17(2):581–8. https://doi.org/10.1007/s00330-006-0408-x.
6. Chetlen AL, Kasales C, Mack J, Schetter S, Zhu J. Hematoma formation during breast core needle biopsy in women taking antithrombotic therapy. Am J Roentgenol. 2013;201(1):215–22. https://doi.org/10.2214/AJR.12.9930.

7. Portnow LH, Thornton CM, Milch HS, Mango VL, Morris EA, Saphier NB. Biopsy marker standardization: what's in a name? Am J Roentgenol. 2019;212(6):1400–5. https://doi.org/10.2214/AJR.18.20577.
8. Durand MA, Haas BM, Yao X, et al. Early clinical experience with digital breast tomosynthesis for screening mammography. Radiology. 2015;274(1):85–92. https://doi.org/10.1148/radiol.14131319.
9. Sharma B, Jurgensen-Rauch A, Pace E, et al. Breast implant–associated anaplastic large cell lymphoma: review and multiparametric imaging paradigms. Radiographics. 2020;40(3):609–28. https://doi.org/10.1148/rg.2020190198.
10. Wang M, He X, Chang Y, Sun G, Thabane L. A sensitivity and specificity comparison of fine needle aspiration cytology and core needle biopsy in evaluation of suspicious breast lesions: a systematic review and meta-analysis. Breast Edinb Scotl. 2017;31:157–66. https://doi.org/10.1016/j.breast.2016.11.009.
11. Yu Y-H, Wei W, Liu J-L. Diagnostic value of fine-needle aspiration biopsy for breast mass: a systematic review and meta-analysis. BMC Cancer. 2012;12(1):41. https://doi.org/10.1186/1471-2407-12-41.
12. Berg WA, Krebs TL, Campassi C, Magder LS, Sun CC. Evaluation of 14- and 11-gauge directional, vacuum-assisted biopsy probes and 14-gauge biopsy guns in a breast parenchymal model. Radiology. 1997;205(1):203–8. https://doi.org/10.1148/radiology.205.1.9314986.
13. Nakano S, Imawari Y, Mibu A, Otsuka M, Oinuma T. Differentiating vacuum-assisted breast biopsy from core needle biopsy: is it necessary? Br J Radiol. 2018;91(1092) https://doi.org/10.1259/bjr.20180250.
14. Wen X, Cheng W. Nonmalignant breast papillary lesions at core-needle biopsy: a meta-analysis of underestimation and influencing factors. Ann Surg Oncol. 2013;20(1):94–101. https://doi.org/10.1245/s10434-012-2590-1.
15. Rageth CJ, O'Flynn EA, Comstock C, et al. First international consensus conference on lesions of uncertain malignant potential in the breast (B3 lesions). Breast Cancer Res Treat. 2016;159(2):203–13. https://doi.org/10.1007/s10549-016-3935-4.
16. Krishnamurthy S, Bevers T, Kuerer HM, Smith B, Yang WT. Paradigm shifts in breast care delivery: impact of imaging in a multidisciplinary environment. AJR Am J Roentgenol. 2017;208(2):248–55. https://doi.org/10.2214/AJR.16.17130.
17. Kettritz U, Rotter K, Schreer I, et al. Stereotactic vacuum-assisted breast biopsy in 2874 patients. Cancer. 2004;100(2):245–51. https://doi.org/10.1002/cncr.11887.
18. Philpotts LE, Shaheen NA, Carter D, Lange RC, Lee CH. Comparison of rebiopsy rates after stereotactic core needle biopsy of the breast with 11-gauge vacuum suction probe versus 14-gauge needle and automatic gun. Am J Roentgenol. 1999;172(3):683–7. https://doi.org/10.2214/ajr.172.3.10063860.
19. Huang XC, Hu XH, Wang XR, et al. A comparison of diagnostic performance of vacuum-assisted biopsy and core needle biopsy for breast microcalcification: a systematic review and meta-analysis. Ir J Med Sci 1971. 2018;187(4):999–1008. https://doi.org/10.1007/s11845-018-1781-6.
20. den Dekker BM, van Diest PJ, de Waard SN, Verkooijen HM, Pijnappel RM. Stereotactic 9-gauge vacuum-assisted breast biopsy, how many specimens are needed? Eur J Radiol. 2019;120:108665. https://doi.org/10.1016/j.ejrad.2019.108665.
21. Stereotactic 11-gauge Vacuum-Assisted Breast Biopsy: Influence of Number of Specimens on Diagnostic Accuracy - PubMed. Accessed June 21, 2020. https://pubmed.ncbi.nlm.nih.gov/15273332/
22. Durand MA, Wang S, Hooley RJ, Raghu M, Philpotts LE. Tomosynthesis-detected architectural distortion: management algorithm with radiologic-pathologic correlation. Radiographics. 2016;36(2):311–21. https://doi.org/10.1148/rg.2016150093.
23. Conant EF, Barlow WE, Herschorn SD, et al. Association of digital breast tomosynthesis vs digital mammography with cancer detection and recall rates by age and breast density. JAMA Oncol. 2019;5(5):635–42. https://doi.org/10.1001/jamaoncol.2018.7078.

24. Skaane P, Bandos AI, Gullien R, et al. Comparison of digital mammography alone and digital mammography plus tomosynthesis in a population-based screening program. Radiology. 2013;267(1):47–56. https://doi.org/10.1148/radiol.12121373.
25. Health C for D and R. MQSA National Statistics. FDA. Published online January 6, 2020. Accessed June 13, 2020. https://www.fda.gov/radiation-emitting-products/mqsa-insights/mqsa-national-statistics
26. Alshafeiy TI, Nguyen JV, Rochman CM, Nicholson BT, Patrie JT, Harvey JA. Outcome of architectural distortion detected only at breast tomosynthesis versus 2D mammography. Radiology. 2018;288(1):38–46. https://doi.org/10.1148/radiol.2018171159.
27. Partyka L, Lourenco AP, Mainiero MB. Detection of mammographically occult architectural distortion on digital breast tomosynthesis screening: initial clinical experience. Am J Roentgenol. 2014;203(1):216–22. https://doi.org/10.2214/AJR.13.11047.
28. Patel BK, Covington M, Pizzitola VJ, et al. Initial experience of tomosynthesis-guided vacuum-assisted biopsies of tomosynthesis-detected (2D mammography and ultrasound occult) architectural distortions. Am J Roentgenol. 2018;210(6):1395–400. https://doi.org/10.2214/AJR.17.18802.
29. Bahl M, Maunglay M, D'Alessandro HA, Lehman CD. Comparison of upright digital breast tomosynthesis–guided versus prone stereotactic vacuum-assisted breast biopsy. Radiology. 2018;290(2):298–304. https://doi.org/10.1148/radiol.2018181788.
30. Schrading S, Distelmaier M, Dirrichs T, et al. Digital breast tomosynthesis–guided vacuum-assisted breast biopsy: initial experiences and comparison with prone stereotactic vacuum-assisted biopsy. Radiology. 2015;274(3):654–62. https://doi.org/10.1148/radiol.14141397.
31. Ariaratnam NS, Little ST, Whitley MA, Ferguson K. Digital breast Tomosynthesis vacuum assisted biopsy for Tomosynthesis-detected Sonographically occult lesions. Clin Imaging. 2018;47:4–8. https://doi.org/10.1016/j.clinimag.2017.08.002.
32. Chesebro AL, Chikarmane SA, Ritner JA, Birdwell RL, Giess CS. Troubleshooting to overcome technical challenges in image-guided breast biopsy. Radiographics. 2017;37(3):705–18. https://doi.org/10.1148/rg.2017160117.
33. Soo MS, Walsh R, Patton J. Prone table stereotactic breast biopsy: facilitating biopsy of posterior lesions using the arm-through-the-hole technique. Am J Roentgenol. 1998;171(3):615–7. https://doi.org/10.2214/ajr.171.3.9725284.
34. Zhang Y, Ren H. Meta-analysis of diagnostic accuracy of magnetic resonance imaging and mammography for breast cancer. J Cancer Res Ther. 2017;13(5):862–8. https://doi.org/10.4103/jcrt.JCRT_678_17.
35. Peters NHGM, Borel Rinkes IHM, Zuithoff NPA, Mali WPTM, Moons KGM, Peeters PHM. Meta-analysis of MR imaging in the diagnosis of breast lesions. Radiology. 2008;246(1):116–24. https://doi.org/10.1148/radiol.2461061298.
36. Park VY, Kim MJ, Kim E-K, Moon HJ. Second-look US: how to find breast lesions with a suspicious MR imaging appearance. Radiographics. 2013;33(5):1361–75. https://doi.org/10.1148/rg.335125109.
37. Nakano S, Yoshida M, Fujii K, et al. Fusion of MRI and sonography image for breast cancer evaluation using real-time virtual sonography with magnetic navigation: first experience. Jpn J Clin Oncol. 2009;39(9):552–9. https://doi.org/10.1093/jjco/hyp087.
38. Mazzei MA, Di Giacomo L, Fausto A, Gentili F, Mazzei FG, Volterrani L. Efficacy of second-look ultrasound with MR coregistration for evaluating additional enhancing lesions of the breast: review of the literature. Biomed Res Int. 2018;2018 https://doi.org/10.1155/2018/3896946.
39. Nakano S, Kousaka J, Fujii K, et al. Impact of real-time virtual sonography, a coordinated sonography and MRI system that uses an image fusion technique, on the sonographic evaluation of MRI-detected lesions of the breast in second-look sonography. Breast Cancer Res Treat. 2012;134(3):1179–88. https://doi.org/10.1007/s10549-012-2163-9.
40. Nakano S, Yoshida M, Fujii K, et al. Real-time virtual sonography, a coordinated sonography and MRI system that uses magnetic navigation, improves the sonographic identification

of enhancing lesions on breast MRI. Ultrasound Med Biol. 2012;38(1):42–9. https://doi.org/10.1016/j.ultrasmedbio.2011.10.005.
41. Park AY, Seo BK, Han H, et al. Clinical value of real-time ultrasonography-MRI fusion imaging for second-look examination in preoperative breast cancer patients: additional lesion detection and treatment planning. Clin Breast Cancer. 2018;18(4):261–9. https://doi.org/10.1016/j.clbc.2017.07.007.
42. Spick C, Baltzer PAT. Diagnostic utility of second-look US for breast lesions identified at MR imaging: systematic review and meta-analysis. Radiology. 2014;273(2):401–9. https://doi.org/10.1148/radiol.14140474.
43. Clauser P, Carbonaro LA, Pancot M, et al. Additional findings at preoperative breast MRI: the value of second-look digital breast tomosynthesis. Eur Radiol. 2015;25(10):2830–9. https://doi.org/10.1007/s00330-015-3720-5.
44. Parikh J, Tickman R. Image-guided tissue sampling: where radiology meets pathology. Breast J. 2005;11(6):403–9. https://doi.org/10.1111/j.1075-122X.2005.00130.x.
45. Shin S, Schneider HB, Cole FJ, Laronga C. Follow-up recommendations for benign breast biopsies. Breast J. 2006;12(5):413–7. https://doi.org/10.1111/j.1075-122X.2006.00302.x.
46. Parker SH, Burbank F, Jackman RJ, et al. Percutaneous large-core breast biopsy: a multi-institutional study. Radiology. 1994;193(2):359–64. https://doi.org/10.1148/radiology.193.2.7972743.
47. Bassett LW, Mahoney MC, Apple SK. Interventional breast imaging: current procedures and assessing for concordance with pathology. Radiol Clin N Am. 2007;45(5):881–94. https://doi.org/10.1016/j.rcl.2007.06.010.
48. Wendie A. Berg JL. Diagnostic imaging: breast. 3rd ed; 2019. Accessed September 21, 2020. https://www.elsevier.com/books/diagnostic-imaging-breast/berg/978-0-323-54812-0
49. Johnson JM, Johnson AK, O'Meara ES, et al. Breast cancer detection with short-interval follow-up compared with return to annual screening in patients with benign stereotactic or US-guided breast biopsy results. Radiology. 2015;275(1):54–60. https://doi.org/10.1148/radiol.14140036.
50. Moon HJ, Jung I, Youk JH, Kim MJ, Kim E-K. Short-term follow-up in 6 months is unnecessary for asymptomatic breast lesions with benign concordant results obtained at ultrasonography-guided 14-gauge core needle biopsy. Am J Surg. 2016;211(1):152–8. https://doi.org/10.1016/j.amjsurg.2015.03.036.
51. Monticciolo DL, Hajdik RL, Hicks MG, et al. Six-month short-interval imaging follow-up for benign concordant core needle biopsy of the breast: outcomes in 1444 cases with long-term follow-up. Am J Roentgenol. 2016;207(4):912–7. https://doi.org/10.2214/AJR.15.15853.
52. Hayward JH, Ray KM, Wisner DJ, Joe BN. Follow-up outcomes after benign concordant MRI-guided breast biopsy. Clin Imaging. 2016;40(5):1034–9. https://doi.org/10.1016/j.clinimag.2016.06.005.
53. Kohr JR, Eby PR, Allison KH, et al. Risk of upgrade of atypical ductal hyperplasia after stereotactic breast biopsy: effects of number of foci and complete removal of calcifications. Radiology. 2010;255(3):723–30. https://doi.org/10.1148/radiol.09091406.

Chapter 11
Breast Imaging Preoperative Localization Procedure

Heni Debs Skaf, Juliana Hiraoka Catani, and Vivian Simone De Medeiros Ogata

Abbreviations

CC	Craniocaudal
FDA	Food and Drug Administration
LM	Lateromedial
MG	Mammography
ML	Mediolateral
MR	Magnetic resonance
MS	Magnetic seed
NRW	Nonrepositionable wires
NWL	Nonwire localization
OR	Operation room
PL	Preoperative localization
RFID	Radiofrequency identification tag
ROLL	Radio-guided occult lesion localization
RSL	Radioactive seed localization
RW	Repositionable wires
SNOLL	Sentinel node and occult lesion localization
US	Ultrasound
WL	Wire localization

H. D. Skaf · J. H. Catani · V. S. D. M. Ogata (✉)
Instituto de Radiologia INRAD, Hospital das Clinicas HCFMUSP, Faculdade de Medicina, Universidade de Sao Paulo, São Paulo, SP, Brazil
e-mail: h.skaf@hc.fm.usp.br; juliana.catani@hc.fm.usp.br; vivian.ogata@hc.fm.usp.br

S. J. Kim Hsieh, E. A. Morris (eds.), *Modern Breast Cancer Imaging*,
https://doi.org/10.1007/978-3-030-84546-9_11

11.1 Introduction

As breast imaging evolves, there is an increase in diagnosis of clinically occult small cancerous lesions, which represent approximately 25–35% of all breast cancers diagnosed in developed countries [1, 2]. In particular, mammographic screening-detected malignancies are often small and clinically occult, and many of these patients are candidates for conservative surgery, as it is a safe and effective method to treat early breast cancer. Additionally, breast conservation therapy may be indicated to treat larger lesions after neoadjuvant chemotherapy, resulting in significant tumor shrinkage.

In order to achieve excision of these lesions with adequate surgical margins in a conservation surgery, while providing a good cosmetic outcome, an imaging-guided localization procedure is advised and often performed before operation to guide the surgeon [3].

Our objective is to provide an overview of preoperative localization indications and of pre-procedure planning, the process itself guided by different imaging modalities, reviewing the most recent techniques available, as well as to expose problems that may arise during or after its execution and possible solutions.

11.2 Indications of Preoperative Localization

Preoperative localization (PL) is in general terms indicated for clinically occult lesions, hence non-palpable ones, that are detected by conventional breast imaging, requiring diagnostic or therapeutic surgical removal [4]. Furthermore, PL for diagnostic excision is required for some histologic entities resulting from percutaneous biopsy, which may require complete excision for adequate diagnosis due to the inherent risk of sample underestimation, for instance, atypical ductal hyperplasia [5, 6]. In addition, cases of radiologic-pathologic discordance or with insufficient sampling after percutaneous biopsy may also require PL for an excisional biopsy [7].

11.3 Pre-procedure Review of Preoperative Localization

Before the procedure, the radiologist reviews relevant imaging findings in order to become familiar with the target lesion and its topography and proceeds to choose the best imaging modality for guiding the localization procedure: typically, mammography (MG) or ultrasound (US) and, rarely, magnetic resonance (MR) [8, 9]. Previous discussion with the surgeon to review the PL planning is necessary to ensure that the chosen procedure will be the most helpful considering the lesion imaging presentation, its localization in the breast, the technical apparatus available in the operation room, the surgeon preferences, as well as the radiologist skill and familiarity with different localization modalities [10].

Informed consent is not routinely obtained by the radiologist performing the PL [11]. Frequently, consent is obtained by the surgeon and contemplates the localization and surgical procedures. Regardless of whether written or verbal consent is obtained by the radiologist, the procedure should be beforehand clearly explained to the patient as well as any possible complications exposed.

The patient should also be inquired about previous bleeding disorders in advance. It is not mandatory to submit a patient with no known coagulation disorders or a history of taking anticoagulant to blood coagulation tests [12]. However, these blood tests may be required when the patient is undergoing anticoagulant therapy.

Anticoagulant therapy may increase the risk of bleeding and hematoma formation during percutaneous procedures; however, there are potential life-threatening risks to stop such medications, mainly in a context of secondary prevention of thrombotic events. Current evidence supports that it is safe to perform percutaneous breast procedures under certain medications like acetylsalicylic acid. However, the necessity of temporary discontinuation of any anticoagulant therapy should be discussed in advance with the patient physician and be made on a case-by-case basis [13–17].

Another preprocedural care that should be discussed in advance with the patient physician includes the prescription of antibiotic prophylaxis for endocarditis in selected cases, not routinely. This is a topic of constant debate and evolution, and the currently adopted stance by most guidelines suggests antibiotic prophylaxis for patients at highest risk of endocarditis, such as bearers of a damaged heart valve, submitted for valve replacement; those diagnosed with structural congenital heart disease; and those with a history of previous infective endocarditis, among others [18].

Lastly, the patient should also be inquired about confirmed allergies [12]. Allergies to anesthetics that may eventually be used during PL, to latex, to metal or other components of the localization wire, and to the adhesive bandage tape are some examples.

11.4 Wire Localization

When performing wire localization (WL), a wire is introduced into the breast with the aid of a puncture needle (Fig. 11.1) [10]. The wire is then advanced out of the puncture needle when in the desired position, exposing its hook and anchoring in the lesion (Fig. 11.1) [19].

When dealing with small breast lesions, the hookwire should ideally penetrate the center of the lesion, and the maximum distance between the wire and the lesion should be 1 cm [20, 21]. Larger breast lesions, usually represented by clustered calcifications, may be best marked with multiple hookwires in order to achieve an excision with tumor-free resection margins [22]. The preferred imaging modality used for imaging-guided WL should be the one in which the target lesion is best visualized while being tolerated by the patient and at an acceptable cost [10].

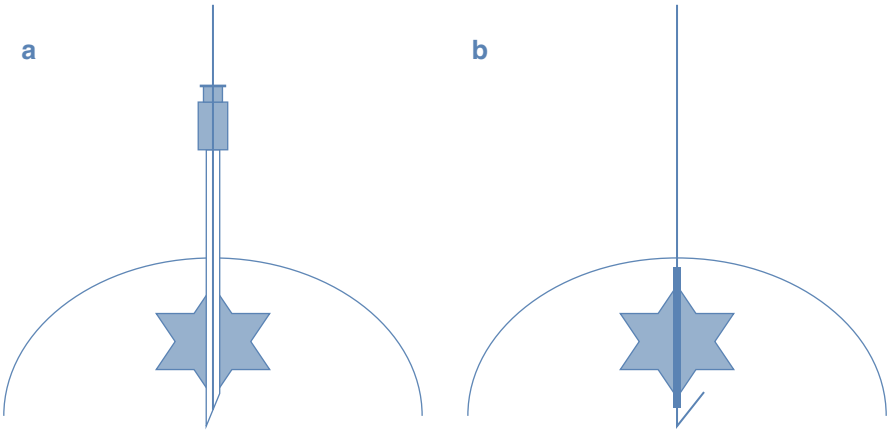

Fig. 11.1 WL. A wire is introduced into the breast with the aid of a puncture needle (**a**). The hookwire is then advanced out of the puncture needle, exposing the hook and anchoring itself in the lesion (**b**)

11.4.1 MG-Guided and Stereotactic-Guided Wire Localization

MG-guided or stereotactic-guided WL is usually performed when the lesions are conspicuous on MG but are not visualized on US [12]. Developing asymmetries, architectural distortions and small breast masses that are not visible on US, microcalcifications, and marker clips or coils that have been placed during a percutaneous biopsy or a pre-chemotherapy tissue marker are among examples of such lesions.

11.4.1.1 Technique Using a Perforated or Marked Compression Plate

The approach chosen for the puncture needle insertion when using a perforated or marked compression plate for WL should, ideally, result in the shortest distance from the skin surface to the target lesion with the intention of minimizing the distance that the needle must travel in the breast, decreasing the chance of needle deviation from the intended target [23]. In some situations, that approach may not be the most adequate. Inferior approaches, for example, may require uncomfortable positioning for the patient and for the radiologist performing the procedure, who must insert the needle from below, often from a kneeling position. Thus, breast lesions in the inferior quadrants may be more easily localized from either the medial or lateral side. Another situation when the shortest approach may not be used is when the lesion is visualized with greater clarity on another particular MG projection. Taking the surgical approach into consideration when planning the skin puncture site as well as the needle trajectory for PL is no longer mandatory as tumoral cell displacement or track seeding is no longer considered a relevant factor in the rate of local recurrence and overall survival in a context of conservative surgery plus adjuvant radiotherapy, as many studies have demonstrated [10].

WL is usually performed with the patient in a sitting position when a compression plate is employed. A reclinable chair can be useful for a prompt treatment of a vasovagal reaction, a common complication [24]. After deciding on the best approach to be used, based on the principles already emphasized, an initial MG image with the patient's breast in compression is acquired in the most adequate view using a perforated or a fenestrated compression plate with alphanumeric markings along its edge. Then, oriented by the compression plate markings, the skin insertion point is chosen according to the coordinates of the intended target. The skin over the lesion is cleansed, and the needle is inserted perpendicular to the compression plate and parallel to the chest wall; therefore, patients should never develop a pneumothorax in this context. The needle is inserted beyond a depth calculated on the second orthogonal view until it passes far enough through the lesion or, in order to minimize errors, until it touches the opposite skin in contact with the compressor. Next, a second MG image in the orthogonal plane is obtained. Based on this image, the depth of needle insertion is adjusted, if necessary, but only by retracting the needle, as it would deviate from the target if inserted in this plane. Once the needle is in the correct position, the wire is deployed. Correct needle insertion is then documented in two planes before the patient is sent to the operating room (Figs. 11.2, 11.3, and 11.4).

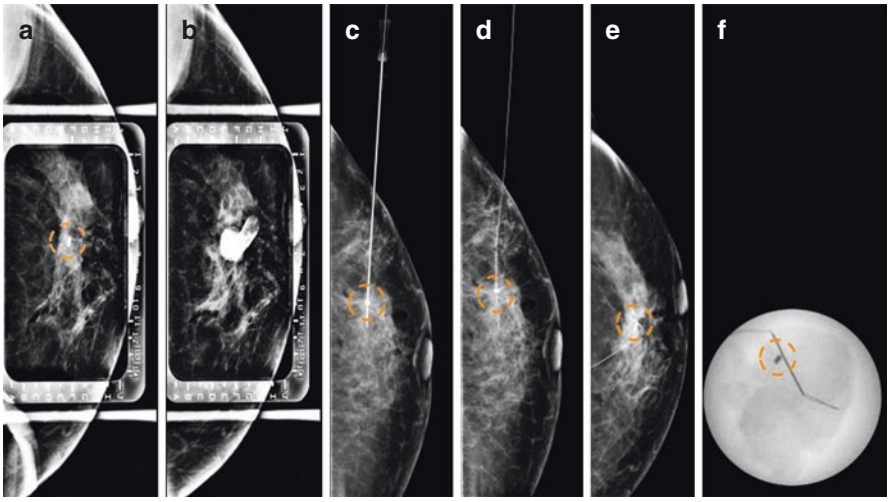

Fig. 11.2 MG-guided WL of a small non-palpable breast lesion using a marked compression plate. The first CC projection showed a clip marker (*dashed circle*) within the fenestrated paddle view (**a**). The puncture needle was inserted, oriented by the compression plate markings, perpendicularly to the skin, until it touched the opposite skin in contact with the compressor. The new CC projection showed the hub of the needle obscuring the clip marker (**b**). The orthogonal MLO projection obtained by using a nonfenestrated compression paddle showed the needle extending through and beyond the clip marker (**c**). Documentation in two planes after insertion of the wire and removal of the puncture needle showed the clip marker appropriately positioned at the thickened segment of the wire (**d**, **e**). The intraoperative specimen radiograph showed the distal portion of the hookwire and the clip marker (**f**)

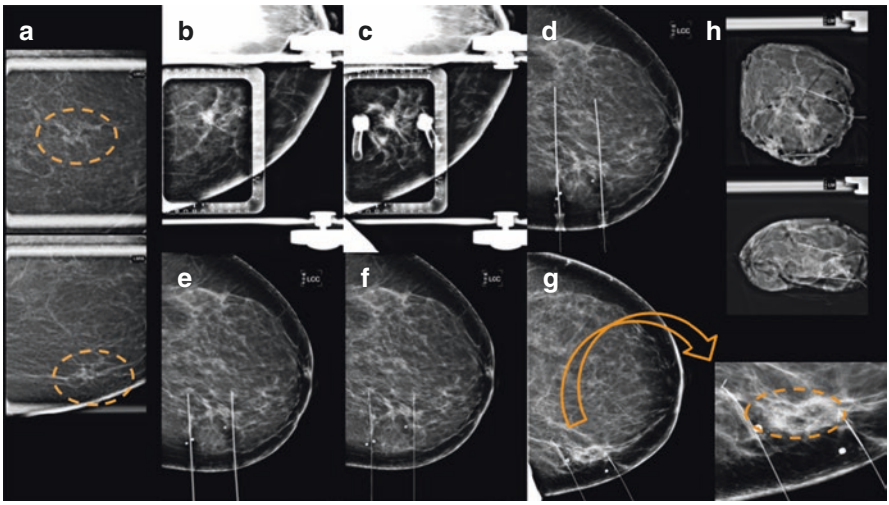

Fig. 11.3 MG-guided WL using a marked compression plate of a large non-palpable breast lesion. WL was performed on a cluster of pleomorphic calcifications (*dashed circle*) (**a**). The MLO projection showed the lesion within the fenestrated paddle view (**b**). In order to achieve complete excision of the lesion, the area of calcifications was bracketed by placing needles into both ends of the lesion (**c**). The needles were inserted perpendicularly to the skin until they touched the opposing skin in contact with the compressor. The first orthogonal CC projection obtained with a non-fenestrated compression paddle showed the needles extending through and beyond the lesion extremities, but further than necessary (**d**). The depth of the needle insertions was then adjusted by retracting them, and the new position was confirmed in another CC projection (**e**). Documentation in two planes after insertion of the wires and removal of the puncture needles showed the area of calcifications extending between the thickened segments of the two wires (**f**, **g**). The specimen radiograph obtained after surgery showed the distal portion of the hookwires and the calcifications (**h**)

11.4.1.2 Technique Using a Stereotactic Table

The accuracy of WL under stereotactic guidance is comparable to that using a perforated or marked compression plate [25]. It may be the method of choice to guide the localization when the target lesion is much more evident in one mammographic view than the other, because you do not necessarily need both orthogonal views to guide localization by this method, just a scout and a stereo pair image [23].

Before the procedure, MG imaging in two orthogonal views (CC and ML or LM) of the affected breast is required to identify the target position. Stereotactic localization is then initiated from the view in which the target is best identified. After positioning the patient on the stereotactic table, the compression plate's window is placed over the breast, and a scout image is acquired, preferably showing the lesion centered in the window. The x-, y-, and z-coordinates are determined by targeting the epicenter of the lesion on the unit's monitor using a stereo pair image (+15° and −15°) acquired based on the scout, in a similar way to stereotactic guided percutaneous biopsy. The puncture needle is placed in the holder, guided to the targeted

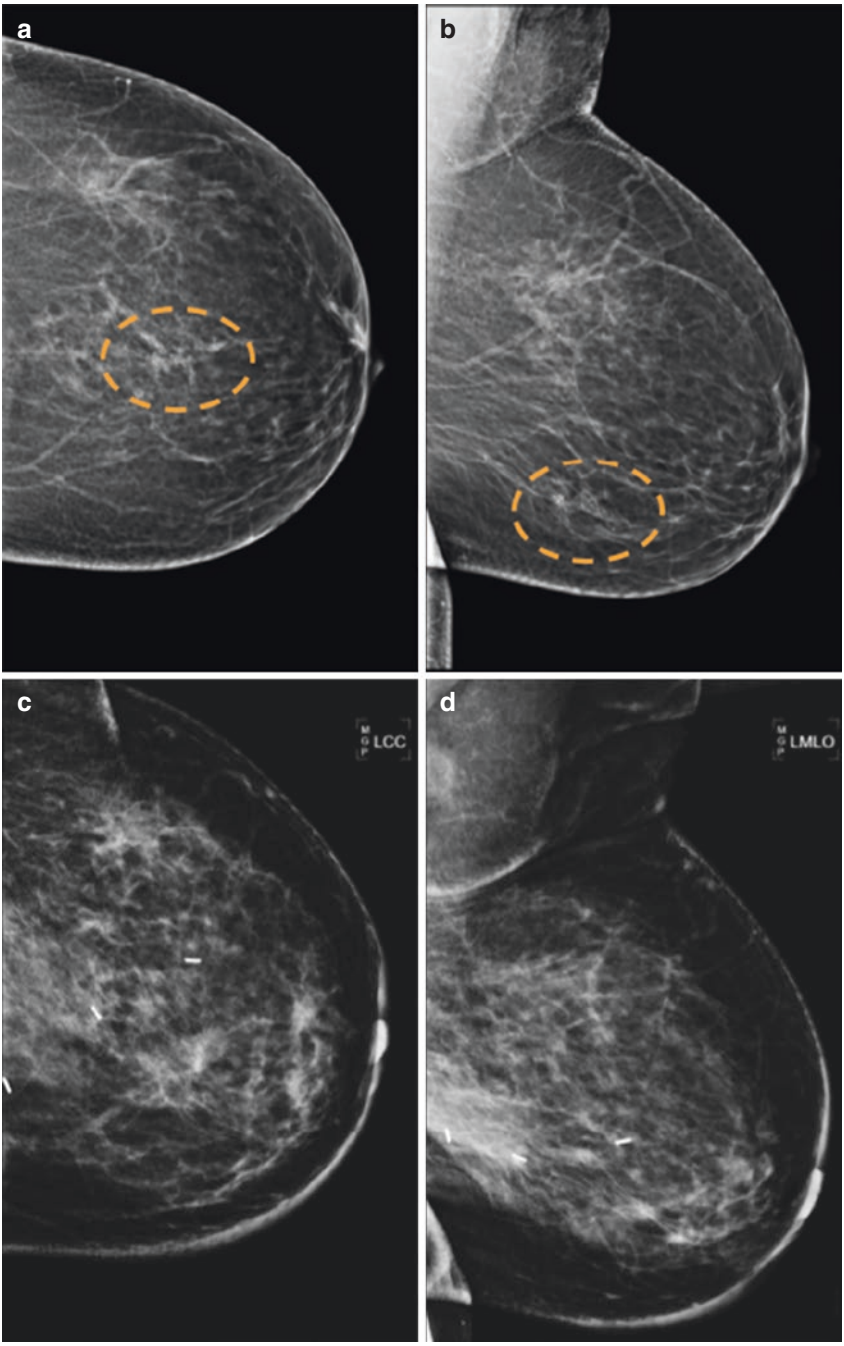

Fig. 11.4 CC and MLO projections of the case shown in Fig. 11.3 before (**a**, **b**) and after breast conservation surgery (**c**, **d**). By removing the smallest possible amount of healthy tissue with adequate surgical margins, conservation breast surgery provides optimal therapeutic results with good cosmetic outcomes

x- and y-coordinates, and advanced to the z-coordinate. The correct needle's tip position may be checked using a second stereo pair image, and it should be positioned within or directly behind the target lesion. The needle is then advanced nearly 1 cm beyond the z-coordinate and the wire is deployed. Lastly, another MG imaging in two orthogonal views is obtained to document the correct needle positioning.

When performing a stereotactic WL, especially with a hookwire, if the wire is deployed in the same plane as the initial compression one, for example, a craniocaudal compression and a caudal needle insertion, without changing to an orthogonal plane, it may hook onto tissues deeper ou superficially than the originally intented targeted point in the z-direction and, consequently, being incorrectly located after compression release (which is called "the accordion effect"). A positioning error of a few millimeters in the compressed breast can correspond to a large positioning error in the non-compressed breast. Some strategies to minimize this effect are to gently release the breast from compression after deploying the wire [23]. Another is to obtain a new stereo image in the orthogonal plane, then adjust the depth of needle insertion based on this image, and then insert the wire. In modern breast biopsy systems, another possibility is to perform the procedure using lateral needle approach, in which the needle is inserted orthogonally to the compression plane, thus eliminating the "accordion effect."

Additional challenges that may arise during stereotactic WL often are the same as those encountered during percutaneous biopsy guided by the same method and will be discussed in more detail in a specific chapter (Fig. 11.5).

11.4.2 US-Guided Wire Localization

US-guided WL is performed when the lesions are visualized on this image modality, and it should always be considered due to cost-effectiveness and improved patient comfort, especially when compared to other image modalities like stereotactic guidance.

The procedure starts by positioning the patient similar to that during a percutaneous biopsy. The puncture needle should advance through and 1 cm beyond the target lesion, and then the wire is deployed. Then, distances from lesion to skin and lesion to wire tip and total inserted wire length should be documented and reported to guide the surgeon.

Similarly, after MG or stereotactic guided WL and after US-guided procedure, MG views in two orthogonal planes should be obtained to document the correct needle insertion (Figs. 11.6, 11.7, and 11.8).

US-guided WL can be adapted for use in the axilla, but it has been infrequently utilized [26]. WL complications such as pain, hematoma, and adjacent tissue injury particularly occur in the axilla where sensitive structures (brachial plexus as well as axillary artery and vein) are nearby [3]. In addition, there is a higher wire migration and transection risk in the axilla compared to the breast due to arm movement and ratcheting effect or muscular contraction [27–29].

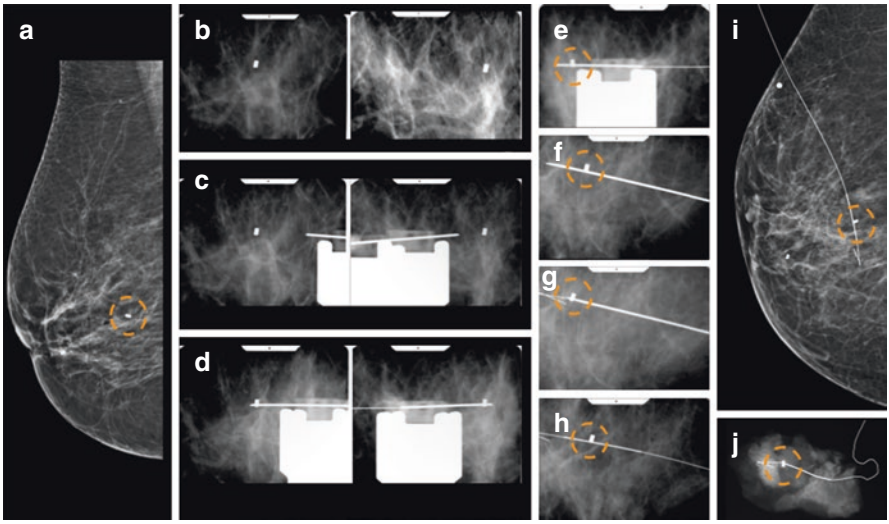

Fig. 11.5 WL using a stereotactic table. The MLO MG projection showed a clip marker (*dashed circle*) in the right breast (**a**). Stereo pair (±15°) images obtained based on the scout (0°) image were used to determine the x-, y-, and z-coordinates by targeting the clip (**b**). Pre-fire and postfire stereo pair (±15°) images showed the needle extending through and beyond the clip marker (**c**, **d**). An additional stereotactic image was obtained to confirm the depth of the needle (**e**). A new stereo image in the orthogonal plane of this last image was obtained, and the depth of the needle insertion was adjusted based on this orthogonal image in order to avoid "the accordion effect" (**f**). After depth adjustment, the wire was inserted and the puncture needle was carefully removed (**g**, **h**). MG documentation after stereotactic procedure showed the clip marker appropriately positioned at the thickened segment of the wire (**i**). The specimen radiograph obtained after surgery showed the distal portion of the hookwire and the clip marker (**j**)

11.4.3 MRI-Guided Wire Localization

MRI-guided WL is usually performed when the lesions are detected only on MRI, without US or MG imaging correlates. The target lesion may be identified using contrast-enhanced MRI guidance, in a similar way to MRI-guided percutaneous biopsy. To locate the lesion, an image is acquired in a sagittal plane associated to a plastic frame with reference markers (Fig. 11.9). A corresponding external location of the lesion on the patient's breast is determined relative to the frame and used to guide the point of needle insertion. The puncture needle is then placed in the holder and advanced nearly 1 cm beyond the depth estimated by using an axial reconstruction obtained from the sagittal acquisition or a new axial acquisition with a smaller field of view in order to decrease sequence duration and reduce the possibility of non-lesion characterization due to gadolinium washout (Fig. 11.10).

It is recommended to use wires made from MRI-compatible metals, which are typically alloys with high titanium and nickel content, to avoid imaging artifacts [10]. Because these special wires only have minor ferromagnetic properties, the

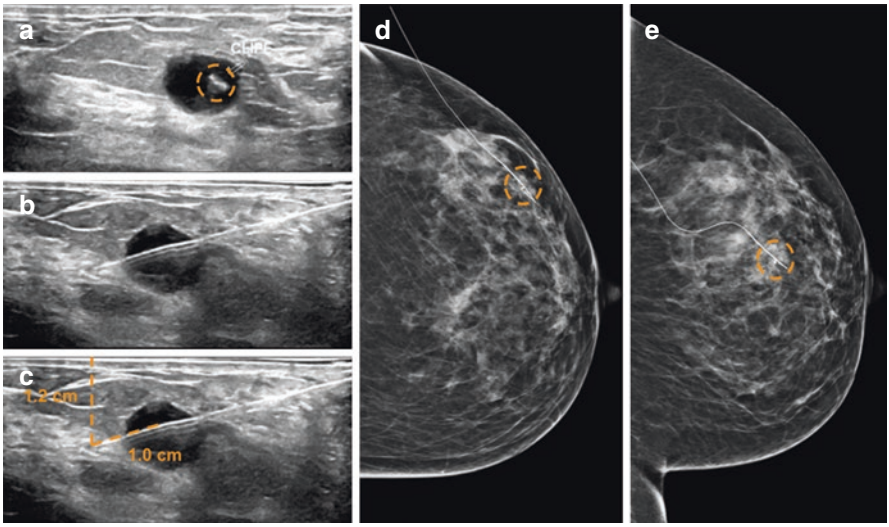

Fig. 11.6 US-guided WL with a hookwire. US image showing a hypoechoic mass with a clip marker (*dashed circle*) (**a**). The puncture needle was advanced through and 1 cm beyond the lesion, and then the wire was deployed (**b**). The distances from lesion to skin and lesion to wire tip are documented (**c**). MG documentation in two planes after the procedure showed the lesion appropriately positioned on the thickened segment of the wire (**d**, **e**)

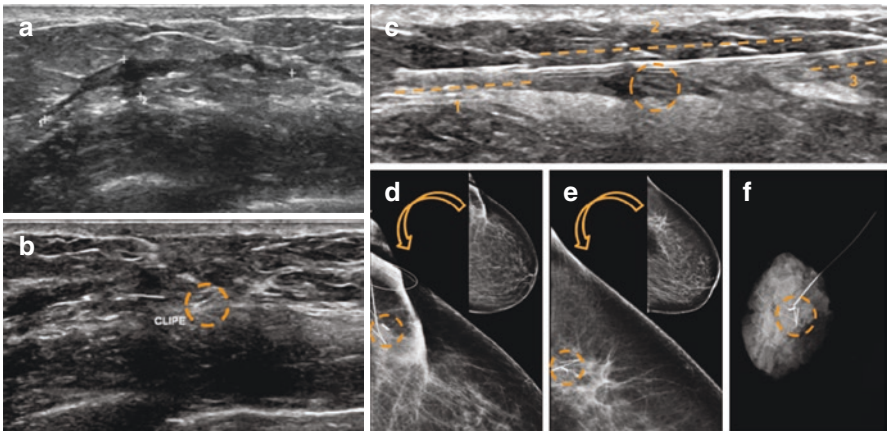

Fig. 11.7 US-guided WL with a hookwire. US performed after chemotherapy showed a non-mass breast lesion with a clip marker (*dashed circle*) (**a**, **b**). The puncture needle was carefully advanced through and beyond the lesion, and then the wire was deployed (*1: hookwire, 2: thickened segment, 3: wire*) (**c**). MG documentation in two planes obtained after the procedure showed the lesion appropriately positioned at the distal portion of the thickened segment of the wire (**d**, **e**). The specimen radiograph obtained after surgery showed the hookwire and the clip marker (**f**)

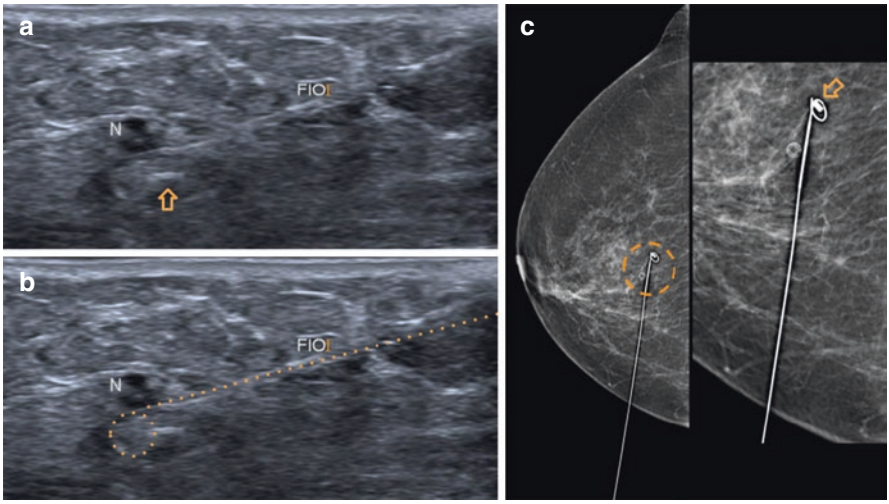

Fig. 11.8 US-guided WL with a retractable J-wire. The J-wire (*dotted line*) was placed adjacent to a clip marker (*arrow*) that could be clearly visualized on US (**a**, **b**). MG documentation after the procedure showed the clip marker appropriately positioned at the distal portion of the wire (*dashed circle*) (**c**)

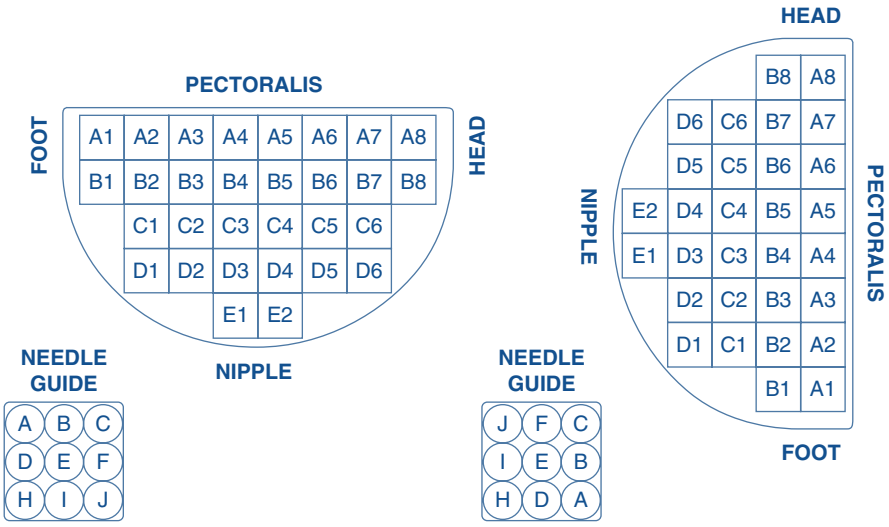

Fig. 11.9 To locate a lesion, the breast is imaged on MR while using a frame with reference markers which show up on the acquired image. The corresponding lesion location, relative to the frame, is then determined and used to determine the biopsy needle insertion site

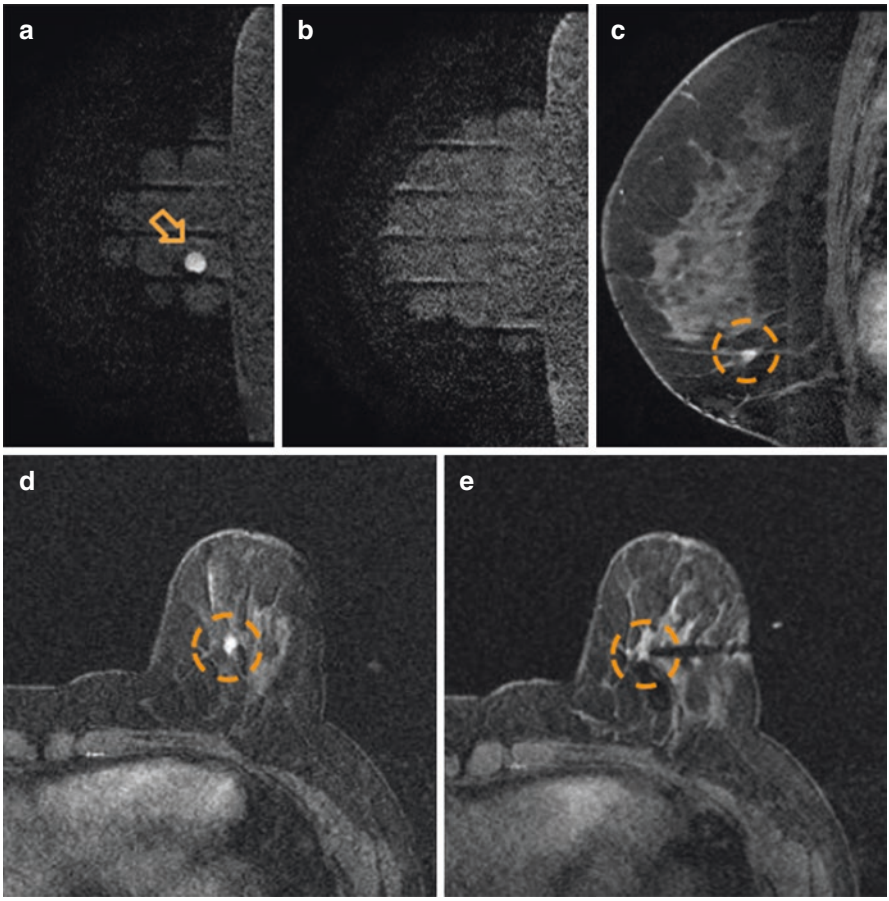

Fig. 11.10 WL under contrast-enhanced MRI guidance. To locate the lesion, the sagittal MRI was acquired associated with a plastic frame. A vitamin D capsule (*arrow*) was used as a skin marker to help determine the corresponding external location of the breast lesion relative to the frame (**a**, **b**). MR images acquired after contrast injection showed the target lesion, a focal non-mass enhancement (*dashed circle*) (**c**, **d**). MR image acquired after insertion of the coaxial needle showed its correct positioning within the focal non-mass enhancement (**e**)

susceptibility artifact caused by them produces a signal extinction that can be distinctly seen without masking relevant findings and fine structures.

Access to an MRI-guided WL is sometimes poor. It is worth mentioning that a clip marker placed in the cavity after an MRI-guided vacuum-assisted biopsy not only enables the radiologist to localize the biopsied area once again but also allows other imaging methods beyond MRI to be utilized in order to perform PL. Therefore, an originally MRI-visualized lesion can be preoperatively localized using cheaper imaging guidance, like mammography or ultrasound, for example, by using an MRI inserted marker.

11.4.4 Wire Variations

There are various designs of localization wires that influence the tenacity of it staying in place, which is also determined by the composition of the breast parenchyma [25]. In this regard, in patients with fatty breasts, the wire may dislocate more easily because of the limited stroma for anchorage.

In general, wire variations can be classified into nonrepositionable and repositionable types, and both have advantages and disadvantages (Figs. 11.11 and 11.12).

A nonrepositionable wire (NRW), such as a hookwire, is more stable than a repositionable one, preventing movement out of the breast. It also optimizes intraoperative identification of the localized lesion, since the NRW frequently presents a thickened distal segment that provides a tactile guide to the surgeon. However, this type allows only one-way forward movement, and once the hook is deployed, it cannot be drawn back into the puncture needle. Thus, if the hook is improperly placed or pushed into the breast, it can be permanently displaced away from the targeted area.

A repositionable wire (RW), such as a retractable J-wire, can be withdrawn from the puncture needle and repositioned if necessary, as many times as needed. Besides being less stable than a nonrepositionable one due to its design, the absence of the thickened distal segment on RW can also limit intraoperative identification of the localized lesion.

As both types have been shown to be effective in localizing breast lesions, the choice of the needle is largely a matter of service material availability and surgeon's and radiologist's preference [23].

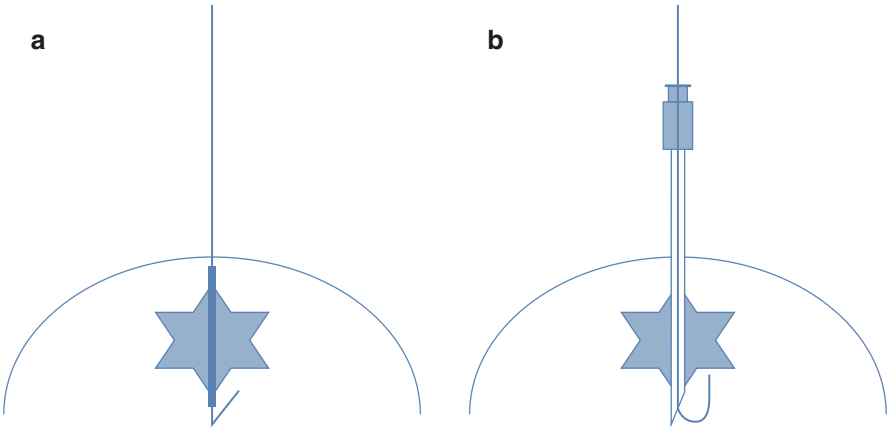

Fig. 11.11 WL. After accurate placement of the puncture needle in the breast, either a nonrepositionable hookwire (**a**) or a repositionable retractable curved-end wire (or J-wire) (**b**) can be inserted. Both types have been shown to be effective in localizing breast lesions

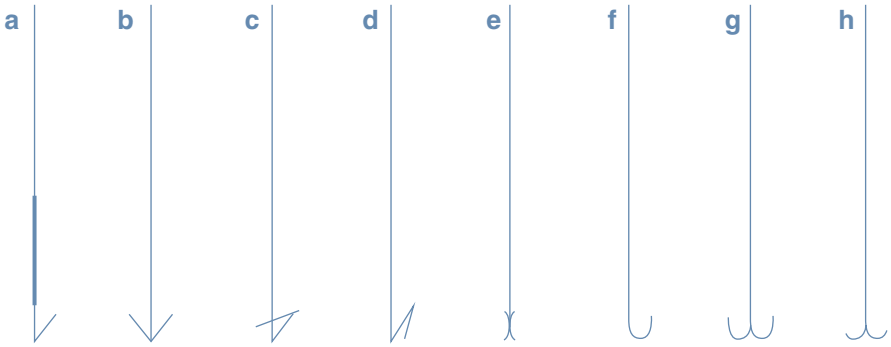

Fig. 11.12 Some of the various designs of localization wires. (**a**–**e**) represent nonrepositionable wires, and (**f**–**h**) represent repositionable wires

11.5 Nonwire Localization Methods

WL has been the standard for PL in breast imaging for decades due to its simplicity and low cost. However, the available options for performing it have expanded greatly and now include the use of substances (such as carbon and radiotracers) or nonwire localization (NWL) devices (such as radioactive and magnetic seeds, radar reflectors, and radiofrequency identification tags).

Compared with wires, these NWL alternatives, except for radiotracers, can be placed prior to the surgery date, at the patient's convenience, in contrast to the WL device procedures that are performed on the day of surgery. Radioactive seeds can be placed up to 5–7 days before, and carbon, radar reflectors, magnetic seeds, and RFID tags have been approved for long-term placement (more than 30 days), with no restriction on the length of time that they can remain in the breast tissue, which can be very useful in patients undergoing neoadjuvant systemic therapy. Consequently, this decoupling of the radiology and surgery schedules results in fewer delays, minimizes presurgical fasting as the resection can be the first surgery of the day, reduces the risk of vasovagal syncope, and overall improves patient satisfaction.

Another advantage of using NWL methods is the absence of a wire partially outside the breast, improving patient experience, and removing the possibility of wire migration.

Additionally, when the surgeon makes use of wire localization techniques, the wire and the healthy tissue along its course are usually retrieved. In contrast, with NWL, the surgeon keeps a continuous intraoperative target tracking in order to keep the lesion in the center of the specimen, retrieving a smaller quantity of nontargeted healthy tissue and improving cosmesis. Besides, wire placement affects the surgical planning because it must be fully retrieved, sometimes determining the incision site and increasing unnecessary healthy tissue removal.

11.5.1 Carbon Marking

There are commercially available carbon suspension products approved by the Food and Drug Administration (FDA) for tattooing the gastrointestinal tract that can be used in PL of breast lesions and axillary lymph nodes, although this use is not currently FDA approved and should be considered off label [30–37].

A sterile solution can be prepared using 4 g of activated charcoal in 100 ml of 0.9% saline solution. And 0.2–0.3 ml of nonionic radiographic contrast medium can be added when performing MG-guided localization for subsequent image documentation of correct dispersion, as charcoal is not often identified radiographically [23]. The charcoal is suspended quickly, so it is important to shake the bottle well before drawing it into the syringe. Approximately 1–1.5 ml of the solution is injected into the target lesion or directly proximal to it to achieve sufficient dispersion and visualization. Then a fine line of the solution extending all the way to the skin is injected as the needle is withdrawn. Being particulate and not soluble in water, the carbon solution remains on the path [23, 34–36]. During surgery, the targeted lesion is localized by visualization of the skin mark and dissection along the carbon track (Fig. 11.13).

A particular advantage of this PL method is the ease of locating the injection site during the specimen histopathological examination. However, the coal can render breast tissues more resistant to microtomy, occulting or distorting the lesion on microscopy.

There are few reported disadvantages of using carbon for PL. The carbon suspension does not diffuse significantly, but it can rarely spread into the surrounding tissues, particularly by accidental intraductal injection [23]. In this case, the demarcated area can be larger than initially expected, consequently increasing unnecessary healthy tissue removal. The surgeon can also remove a larger amount of breast

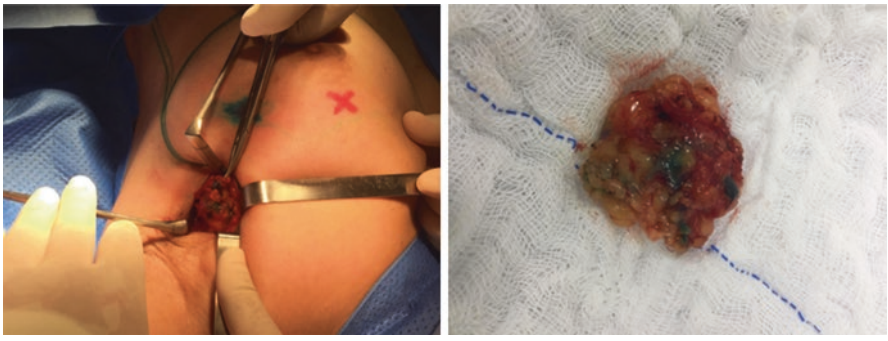

Fig. 11.13 Several of the methods currently used to localize lesions in the breast may be adapted for use in the axilla. Axillary lymph node carbon marking permits the surgeon to locate the target lymph node by visualization of the skin mark and dissection along the carbon trail to the lesion. (With permissions from Lucas Roskamp Budel, MD)

tissue when it faces difficulty to identify the demarcated area intraoperatively, especially in deeper tissues, where the carbon track is harder to palpate [30].

Carbon marking may be performed immediately after biopsy, obviating a separate PL, which is an advantage cost-wise [38]. However, when resection of the marked biopsy path is not accomplished in 6 months, local granulomatous reactions can occur and mimic suspicious lesions [39–41]. There are reported cases of mammographic lesions coinciding with previous coal marking sites, whose further investigation yielded charcoal granulomas.

11.5.2 Radio-Guided Occult Lesion Localization (ROLL)

Radio-guided occult lesion localization (ROLL) consists of a radiotracer injection into the target lesion on the same day as the surgery or on the day before, not exceeding 24 h between the injection and the procedure, guided by ultrasonography, stereotactic mammography, or even MRI [38]. This radiotracer is composed of a dose of human serum albumin macroaggregates, with particle diameter ranging between 80 nm and 150μm, labeled with 7–10 MBq of Tc-99 m (equivalent to 1–2% of the dose used for a whole-body bone scintigraphy) [42–44].

Scintigraphic images are usually acquired in front and lateral projections about 10 min after radiotracer injection. A cobalt-57 source is applied to outline the patient's contour during the acquisition in order to facilitate viewing of the inoculation site. The scanned images must highlight a focal spot of tracer accumulation with well-defined margins. In case of skin contamination, the acquisition must be repeated after properly cleaning with a decontaminant substance. If the tracer uptake spreads to the lesion surrounding tissues on the scanned images, PL must be repeated using another method, such as WL.

During surgery, the lesion is detected by using a gamma probe. All the tissue area with a higher radioactivity count compared to the background is removed. The edges are defined as points where radioactivity count drops sharply. After removing this area, if the radiotracer is still detected by the gamma probe at the surgical site, it is necessary to extend the resection until the counting rate disappears.

ROLL is comparable to WL in terms of costs; however, due to radiation concerns, it cannot be realized on an outpatient basis, resulting in scheduling restraints; additionally, it requires the need for a gamma radiation detector in the operating room (Figs. 11.14 and 11.15) [45].

11.5.2.1 Sentinel Node and Occult Lesion Localization (SNOLL)

Sentinel lymph node identification using radiotracers and ROLL can be performed in combination for the same surgical session in a procedure called sentinel node and occult lesion localization (SNOLL) [42, 46, 47]. It consists of peritumoral injection

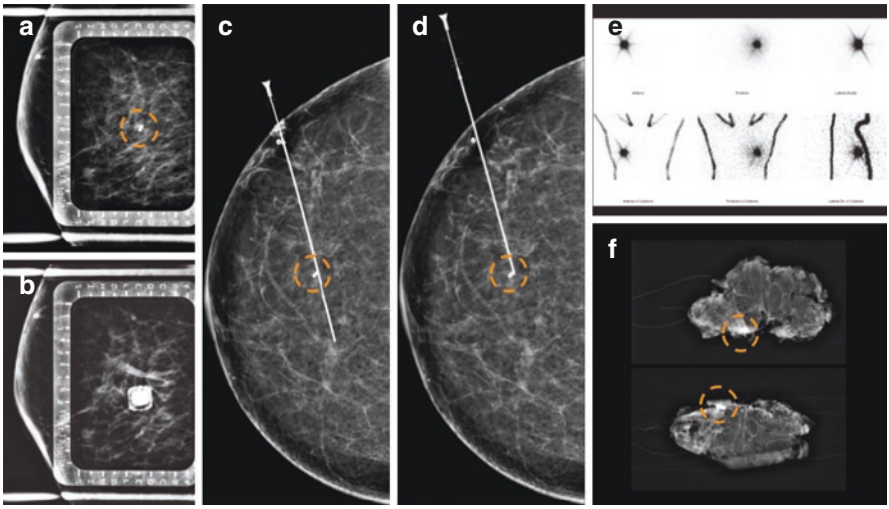

Fig. 11.14 MG-guided ROLL using a marked compression plate. The MLO projection showed a clip marker (*dashed circle*) while using a fenestrated paddle (**a**). The puncture needle was inserted, oriented by the compression plate markings similar to WL (**b**). The orthogonal CC projection obtained with a nonfenestrated compression paddle showed the needle extending through and beyond the clip marker, but further than necessary (**c**). The depth of the needle insertion was then adjusted, and the new position was confirmed in another CC projection. Once in the correct position, the radiotracer was injected through the puncture needle (**d**). The scintigraphic image obtained after the procedure showed the presence of a focal spot of tracer accumulation corresponding to the breast localized lesion (**e**). The specimen radiograph obtained after surgery showed the clip marker (**f**)

of a supplementary radiotracer carried by micromolecules, with particle sizes ranging between 16 and 100 nm, in addition to the macroaggregates used for ROLL [48]. Scanned images acquired after radiotracer injection must highlight the presence of at least two focal spots of the tracer accumulation with well-defined margins, the breast lesion and the sentinel lymph node (Figs. 11.16, 11.17, and 11.18). Furthermore, some studies also suggest that SNOLL may be associated with a higher identification rate of internal mammary chain drainage lymph nodes [49].

11.5.3 Current Lesion Localization Techniques

In order to overcome some of the WL inherent limitations, additional nonwire lesion localization techniques were more recently developed such as iodine-125 (^{125}I) radioactive seed (Advantage® I-125, IsoAid, Port Richey, FL), infrared radar reflectors (Savi SCOUT®, Cianna Medical, Aliso Viejo, CA), magnetic seed markers (Magseed®, Endomagnetics, Cambridge, England), and radiofrequency identification (RFID) tags (LOCalizer®, Hologic, Marlborough, MA) (Fig. 11.19).

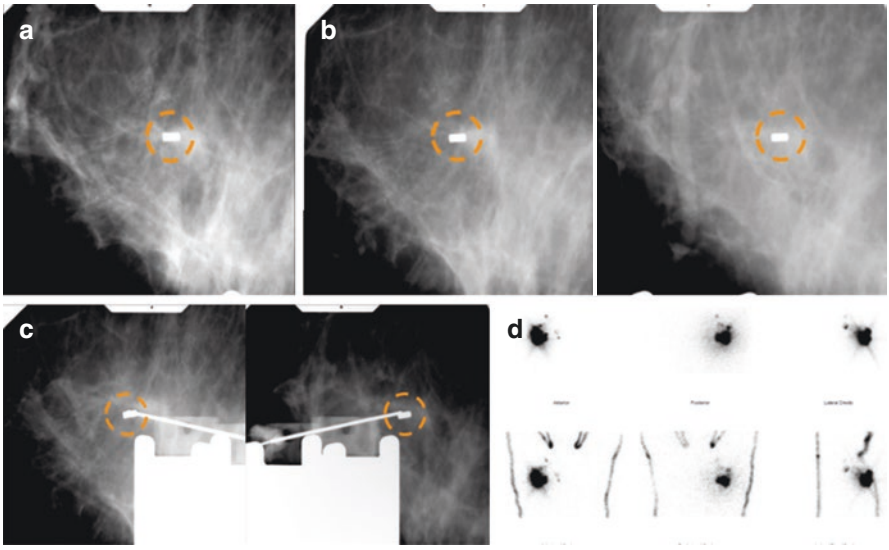

Fig. 11.15 Stereotactic guided ROLL. The scout (0°) image showed a clip marker (*dashed circle*) (**a**). The stereo pair (±15°) images obtained based on the scout were used to determine the x-, y-, and z-coordinates by targeting the clip (**b**). After needle insertion, a new stereo pair (±15°) image showed the tip of the needle in the correct position; then the radiotracer was injected (**c**). The scintigraphic image obtained after the procedure showed the presence of a focal spot of tracer accumulation corresponding to the clip (**d**)

These current nonwire devices may be deployed under mammography, ultrasound or stereotactic mammography guidance. Although they cannot be deployed under MRI guidance, due to the lack of an MRI-compatible introducer needle, patients with such devices may still undergo MRI under appropriate conditions, and the subsequently device-related susceptibility artifacts vary according to device and sequence parameters, as will be further discussed.

They are composed of three parts: a single-use sterilized device loaded in a needle introducer (12G to 18G), a reusable small console, and a handheld intraoperative probe, which may be available as a single-use sterilized device or a reusable one requiring an appropriate sterile cover. The intraoperative probe is capable of detecting the device, while the specific console emits numerous forms of feedback in order to guide the surgeon during the procedure.

Such devices cannot be repositioned once deployed, and multiple devices can be used to ensure the resection of the full lesion extent, particularly in patients with extensive microcalcifications, with large masses or with associated satellite nodules. However, superimposed multiple devices positioned in the anteroposterior plane may be detected as an isolated one in a supine patient, impairing the full extent disease excision and possibly the prognosis. Additionally, when multiple devices are deployed, they should approximately be at least 2 cm apart from one other in order to be detected separately [50, 51].

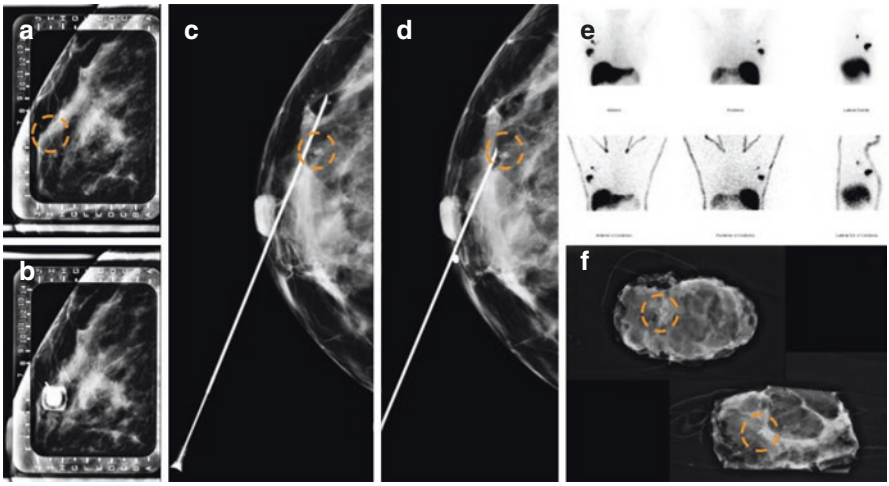

Fig. 11.16 MG-guided SNOLL. The MLO projection showed pleomorphic clustered calcifications (dashed circle) while using the fenestrated paddle (**a**). The puncture needle was inserted, oriented by the compression plate markings similar to WL (**b**). The orthogonal CC projection obtained with a nonfenestrated compression paddle showed the needle extending through and beyond the lesion (**c**). The depth of the needle insertion was then adjusted by retracting it, and the new position was confirmed in another CC projection. Once in the correct position, the radiotracer was injected (**d**). The scintigraphic image obtained after the procedure showed the presence of two spots of tracer accumulation corresponding to the lesion and the sentinel lymph node in the ipsilateral axilla (**e**). The specimen radiograph obtained after surgery successfully showed the presence of the targeted pleomorphic clustered calcifications in it (**f**)

Cost-wise, at first glance, these current nonwire localization devices may seem more expensive than wires. Implementing these systems requires investment in the reusable console and probe, which are the most expensive components, and the single-use device itself is costlier than a wire. But they may not be unfavorable on a cost-benefit analysis, as the elimination of operation room delays as well as increased schedule flexibility may result in cost savings, particularly in a bundled payment system [52].

11.5.3.1 Radioactive Nonwire Localization Device

Radioactive Seed Localization

Radioactive seed is a 5-mm titanium-encased implant containing iodine-125 (Fig. 11.20), first described as an alternative to wire localization in 2001. Since then, many studies have compared radioactive seed localization (RSL) with WL and have demonstrated no significant differences in the re-excision rate, ratio of tumor volume to specimen volume, cosmetic outcome, or the rate of close positive margins, with rates of clear surgical margins ranging from 75% to 97% [53–57].

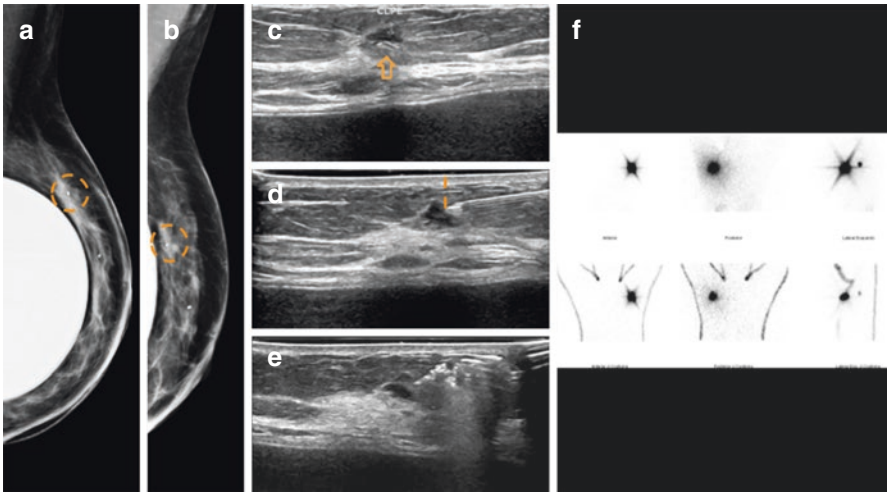

Fig. 11.17 US-guided SNOLL. MG images (**a**, **b**) obtained after chemotherapy showing a focal asymmetry with a clip marker (dashed circle), more evident with Eklund maneuver (**b**). US image showing a hypoechoic mass with a clip marker (arrow) corresponding to the lesion observed on the mammogram (**c**). The puncture needle was advanced to the lesion, and the distance from its tip to skin was documented (**d**). Once in the correct position, the radiotracer was injected adjacent to the lesion (**e**). The scintigraphic image obtained after the procedure showed the presence of two spots of tracer accumulation corresponding to the localized lesion and the sentinel lymph node in the ipsilateral axilla (**f**)

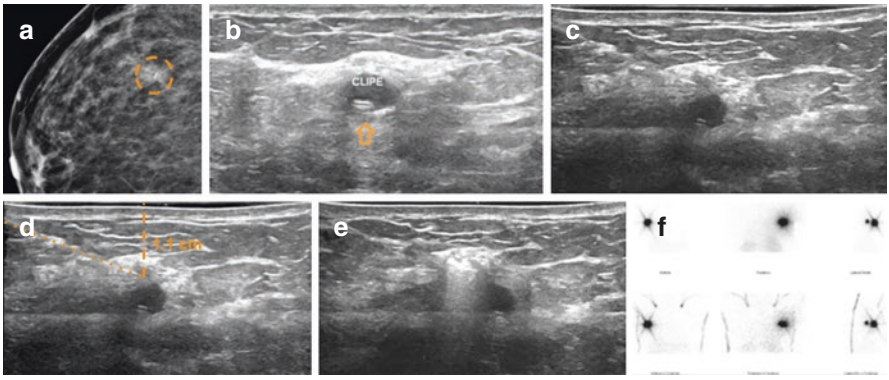

Fig. 11.18 Another example of US-guided SNOLL. MG image obtained after chemotherapy showing a small mass with a clip marker (dashed circle) (**a**). US image showing a hypoechoic mass associated with a clip marker (arrow) corresponding to the mammographic lesion (**b**). The puncture needle (dotted line) was advanced to the lesion, and the distance from its tip to skin was documented (**c**, **d**). Once in the correct position, the radiotracer was injected adjacent to the lesion (**e**). The scintigraphic image obtained after the procedure showed the presence of two spots of tracer accumulation corresponding to the localized lesion and the sentinel lymph node in the ipsilateral axilla (**f**)

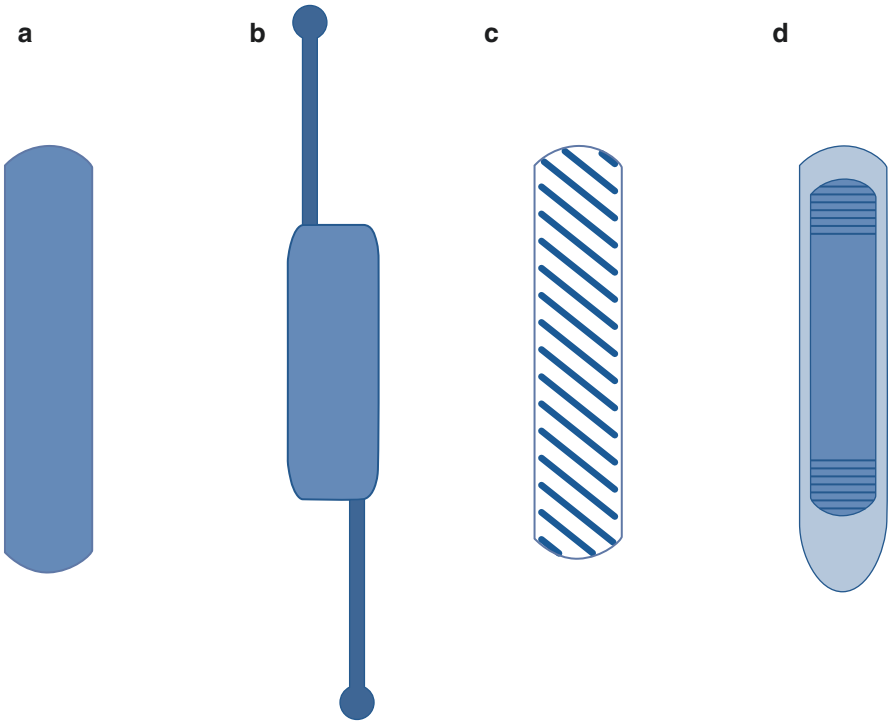

Fig. 11.19 Some schematic examples of current nonwire localization devices, such as iodine radioactive seed (**a**), radar reflector (**b**), magnetic seed (**c**), and radiofrequency identification tag (**d**)

Depending on the specific regulatory commission guideline, the seeds can be placed up to 5–7 days before surgery (they have a half-life of 60 days), and no special instructions need to be given to the patient or family after deployment because radioactivity is low (0.100–0.200 mCi [3.7 to 7.4 MBq]).

The seed is transported to the procedure room in a lead envelope. The presence of radioactivity in the seed must be confirmed before its placement in the breast with a Geiger counter. Either loose seed assemblies or preloaded seeds into needles can be used.

It is deployed into the breast by a technique similar to traditional wire localization (Figs. 11.21 and 11.22), within or adjacent to the lesion, and more than one may be used to bracket a defined area for excision. However, the maximum number of seeds allowed varies according to the institution due to safety concerns. After deployment and before anyone exits the room, the patient is assessed for radioactivity with a Geiger counter to confirm placement of the seed within the breast.

The surgeon then uses an intraoperative gamma probe to identify the target and excise the area. After surgery, the presence of ^{125}I activity in the resected tissue and lack of activity in the surgical bed confirm successful removal of the seed and the target lesion.

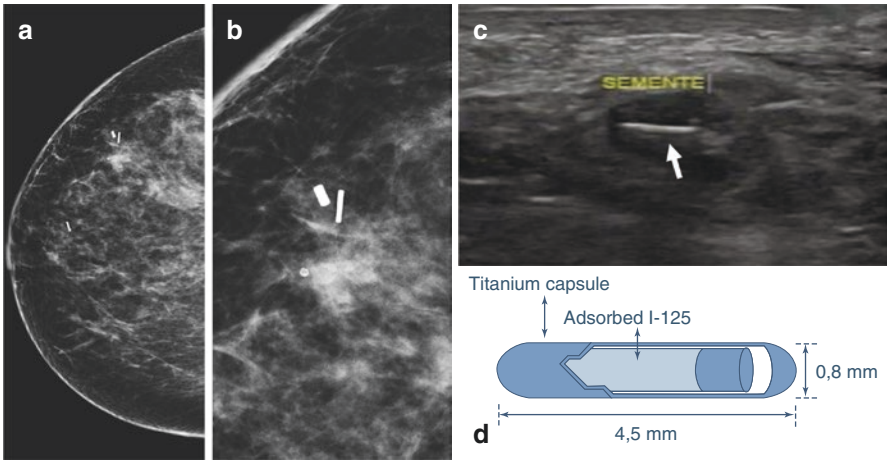

Fig. 11.20 A digital mammographic craniocaudal view of the right breast containing a post-biopsy marker alongside a radioactive seed (**a**). As depicted in the magnified view, despite having the same radiological density, the seed is thinner and longer than the marker (**b**). On ultrasound, the radioactive seed is clearly seen as a linear, echogenic structure, within the targeted breast mass (**c**). (With permissions from Fernanda Philadelpho Arantes Pereira, MD, PhD, from Dasa). Schematic drawing of a radioactive seed example (**d**)

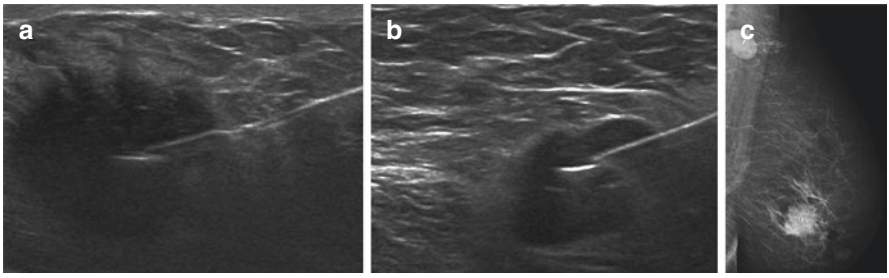

Fig. 11.21 Radioactive seed deployment under sonographic guidance of an irregular retroareolar mass on the left breast (**a**) as well as an ipsilateral suspicious axillary lymph node (**b**). Left breast mediolateral oblique mammographic view showing both lesions associated with correctly positioned markers (**c**). (With permissions from Aline Campos, MD, and Carla Tajima, MD, from BP – A Beneficência Portuguesa de São Paulo)

From the patient's point of view, those who undergo RSL had fewer vasovagal reactions at insertion in comparison to those who undergo wire localization, probably because patients were not fasting for surgery on the day the localization procedure was performed; additionaly, radioactive seeds are usually deployed quicker than wires are positioned, resulting in less algic stimulus thus decreasing the odds of a vasovagal reaction [58].

Another benefit of RSL is the possibility to use the same gamma probe, only adjusting the activity detection setting on the probe, to localize and excise sentinel

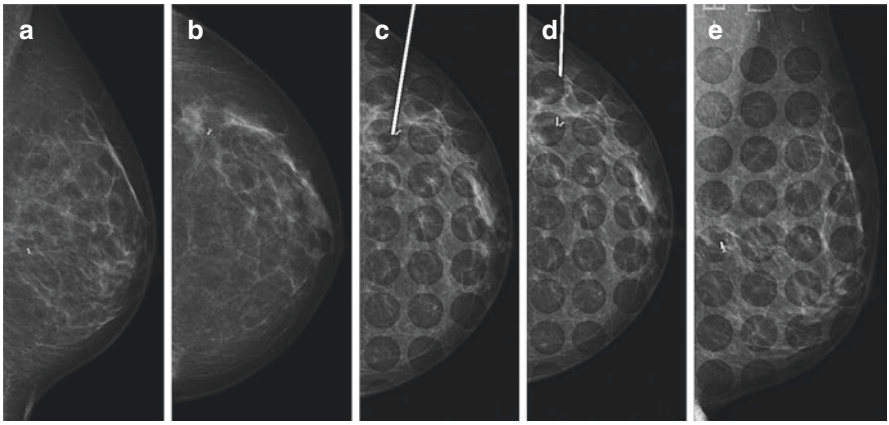

Fig. 11.22 Radioactive seed deployment under mammographic guidance using a marked compression plate. Digital mammography mediolateral (**a**) and craniocaudal (**b**) views depicting a post-biopsy marker on the junction of the outer quadrants of the left breast on the site with an established diagnosis. Digital mammography craniocaudal view using a marked compression plate showing the radioactive seed insertion needle in a lateral approach with its tip next to post-biopsy marker (**c**) and the seed adequate deployment (**d**, **e**). (With permissions from Aline Campos, MD, and Carla Tajima, MD, from BP – A Beneficência Portuguesa de São Paulo)

nodes submitted for technetium 99 m localization, as the ^{125}I seeds emit gamma rays with a photon energy of 27 keV, while technetium 99 m has a 140-keV activity signal.

Unlike other nonwire localization techniques, there is no reported depth limitation for detectability when RSL is utilized.

However, any RSL program must follow strict regulations due to the radioactivity involved and requires massive inter-departmental coordination for its execution. Therefore, establishing a radioactive seed program can take some time, in contrast to other nonwire localization programs which can be set up relatively quickly, and limits the widespread adoption of this localization technique.

Contrary to a migrated biopsy clip, a migrated radioactive seed must be excised and disposed accordingly due to the radioisotope presence. After the surgery, it is placed in a lead container and sent back to the nuclear medicine service for safe disposal. If the seed's removal takes longer than 5 days, a radiation safety officer must be notified, and the patient must be monitored until its removal.

Another RSL limitation is that these patients may not undergo MR imaging while the seed is in place due to the fact that the gamma probe to detect eventually extruded RSL seeds is not MR compatible (Zone IV), precluding recovering of a potentially lost seed and limiting long-term RSL use for patients who have MR follow-up imaging in the neoadjuvant setting.

During radioactive seed localization, it is crucial to not discard any material used in the procedure until the mammography confirms its placement, which will aid in the recovery if a seed is lost.

11.5.3.2 Non-radioactive Wireless Localization Devices

In the wake of limitations inherent to RSL, some non-radioactive wireless devices have recently emerged. Among their advantages, besides being devoid of radioactive emission, they are not constrained by specific regulations and protocols, do not require special license to be handled or operational adjustments to be made, and can be implemented quicker as well as inserted in one facility and removed in another.

Radar Reflector Localization

This localization technique uses radar technology and was first introduced in 2014, being composed of a device detected by a specific intraoperative probe that emits infrared light to excise the area of interest which can be placed under ultrasound or mammographic guidance in a similar way as a biopsy marker clip (Fig. 11.23).

One of the first radar reflector devices, the SAVI Scout System® (Merit Medical Systems, USA), measures 12 mm in length, with a 4-mm body and two 4-mm antennas on each side, including an infrared light detector. Being FDA approved for long-term placement, it is biocompatible and inert, responding only to signals emitted from the respective reader, and can be implanted at any time prior to surgery.

The reflector is deployed using a 16G needle by withdrawing a release button, rather than pushing the reflector, in order to prevent antenna bending. After

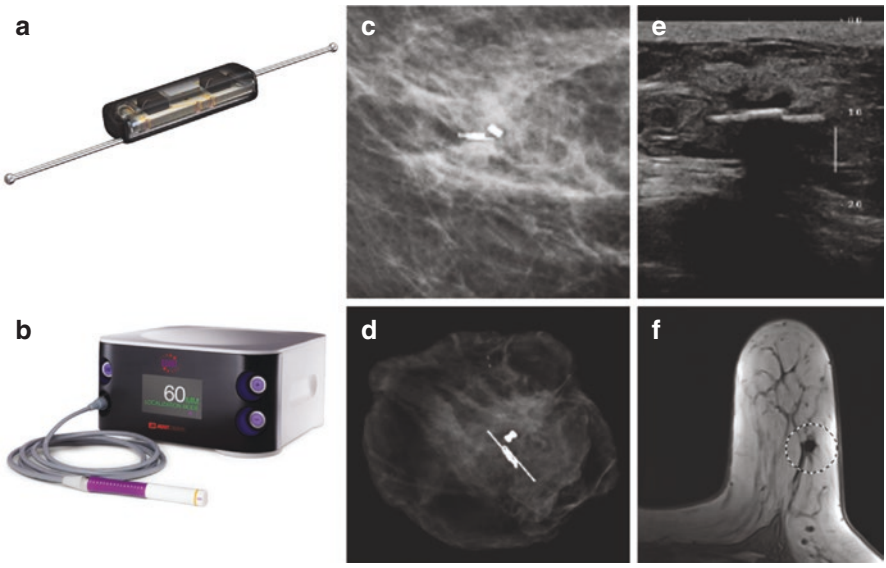

Fig. 11.23 A 12-mm radar reflector with a 4-mm body and two antennas on either side (**a**). Console with an attached handpiece probe (**b**). Mammographic (**c**), sonographic (**e**), surgical specimen (**d**), and MRI (**f**) appearance of the radar reflector, (© Merit Medical, reprinted with permission)

displacement, the radiologist uses a console to make sure that an audible signal can be obtained from the radar reflector. Researchers have successfully detected reflectors at a depth of up to 8 cm; however, in certain circumstances, a radar placed deeper than 6 cm may not produce a detectable signal through the skin, unlike radioactive seeds, and additional compression to tissue with the handpiece may be required [59, 60].

In the OR, the detector console emits power to the infrared light source through the hand probe, activating it, which results in the reflection of an electromagnetic wave signal back to the handpiece. The console then processes these signs and provides visual and audible feedback to the surgeon.

In contrast to the RFID tag and magnetic seed devices, which can cause MRI susceptibility signal void artifact, the radar reflector causes minimal artifact, and the patient with the device in place may safely undergo MRI at 3 T or less. However, the Scout system is costlier than WL or RSL.

Clear surgical margin rates achieved by using radar reflector-guided excision have ranged from 85% to 93%, and when compared to wire localization surgical outcomes, researchers found no substantial differences in margin positivity, close margin, and re-excision rates [19, 60, 61]. Another study comparing the SAVI Scout system to WGL and RSL found no difference in margin positivity, specimen volume, or 30-day complication rate but did find that the SAVI Scout device reduced the overall operating time [62].

Failures related to radar reflector technique are typically due to a lack of signal from the device: dense objects such as calcified masses, hematomas or wires, as well as certain plastics, positioned between the reflector and the handpiece, can interfere with signal detection [61, 63]. Halogen and some older model OR lights were shown to affect detection of the reflector as well; however, shielding the breast from these lights or redirecting them while using the handpiece solved these issues. Besides, LED lights, which are more prevalent than halogen lights in these settings, did not interfere with radar detection [60].

On top of it, this system cannot be placed in patients with a nickel allergy, as the radar reflector antennae are made of nitinol, an alloy of nickel and titanium.

In comparison to RSL, radar reflector localization lacks radioactivity and regulatory issues, can be implanted for longer periods and is associated with minimum susceptibility artifact on MRI. However, it should not be placed within or deep to a hematoma, there is the possibility of an allergic reaction in some patients due to the presence of nitinol and the Scout system costs more than WL or RSL.

Magnetic Seed Localization

The Magseed® (Endomagnetics, Cambridge, UK) device was FDA cleared in 2016, being a stainless-steel marker measuring 5 × 1 mm, the smallest among non-radioactive localization devices. It is deployed under mammogram or ultrasound guidance, in a similar way to a biopsy marker or RSL, through a preloaded 18G needle introducer.

These seeds have a textured surface to optimize their ultrasonographic visibility and may be placed up to 30 days before surgery. Recently, the FDA granted permanent implant status, so there is no time limit for retrieval and its signal strength does not decay.

Magseed is not permanently magnetic. It contains iron particles, which are not themselves magnetic but can be induced to transiently become a magnet under the influence of a Sentimag® probe (Endomagnetics, Cambridge, UK), creating a magnetic field. The probe then provides audible and numeric feedback for the strength of the magnetic field and consequently estimates the distance from the seed to the probe. Magseed® is intended to be placed up to a 3 to 4 cm depth, at the risk of not producing a detectable signal; however, seeds have been detected in locations deeper than this limit [50].

This same probe can also be used to perform sentinel node biopsy and lymphatic mapping by using Magtrace®, a liquid containing superparamagnetic iron oxide nanoparticles with a carboxydextran coating [64].

Magseed® is MRI conditional and has been tested in up to 3 T scanners; however, it produces a significant 4 cm signal void artifact due to its iron content, bigger than those associated with other nonwire localization methods, limiting diagnostic accuracy of breast MRI, and it should be taken into account in a preoperative setting.

Price et al. achieved 83% clear surgical margin by using magnetic seed-guided excision in a series of 64 patients [50]. Gera et al. reviewed 16 studies in a pooled analysis, obtaining a successful localization rate of 99.86% with a relatively low re-excision rate of 11.25% [65].

Some caveats are associated with its use in patients with pacemakers or implanted chest wall devices as the Sentimag® probe should not be placed within 15 mm from any part of an operating pacemaker. Non-metallic surgical tools are recommended while the probe is in use in order to not interfere with the signal, resulting in additional start-up costs.

Radiofrequency Identification Tag (RFID) Localization

Radiofrequency identification tags are a part of the LOCalizer® (Hologic Inc., Santa Clara, CA, USA) localization system introduced in 2017. The RFID tag is a passive device, measuring 9 × 2 mm, containing a ferrite rod wrapped in copper and a microprocessor, associated with an anti-migratory sheath. It is deployed through a preloaded 12G needle similar to a biopsy clip. The current license in the European Union permits deployment of the RFID tag within 30 days of surgery; however, this duration has been extended to “long term” in the United States, which permits deployment at the time of diagnostic core biopsy in patients requiring neoadjuvant chemotherapy. However, it has not yet been approved for placement in lymph nodes.

In the OR, a battery-powered RFID localizer reader sends a radiofrequency signal to the tag, which re-emits the signal modified to the portable handheld localizer device. The reader device operates in two different modes that can be used to reabsorb the signal, one with a 6 cm range and another with a 3 cm range. The probe

with the deeper range can be draped for use in a sterile surgical environment and is reusable, while the one with the smaller range is a pencil-sized, single-use device. On the reader screen, associated with an audible signal, the distance from the lesion to the probe can be viewed in millimeters as well as the tag's unique identification number.

There are no clear contraindications to RFID tags nor any adverse effects associated with their use. The tags have a long history of use similar to those embedded in livestock, pets, and breast implants as a form of identification.

Maggie et al. found that the clear surgical margin rate associated with RFID tag-guided excision was 97% in a subset of 33 patients [66].

It is MRI conditional; however, the ferrous and copper material creates a 2.5 cm susceptibility artifact when imaging is performed using a gradient-echo pulse sequence in a 3 T MRI unit.

We summarize and compare the main features of the aforementioned localization techniques in Table 11.1.

11.6 Post-procedure Complications

Complications of the preoperative imaging-guided localization procedures involve failure to excise the localized abnormality or procedure-associated complications [67].

The procedure-related complications include pain, vasovagal reactions, bleeding, hematoma formation, infection, pneumothorax, pseudoaneurysm formation, implant rupture, and milk fistula in lactating patients [51, 67, 68].

The majority of pain perceived by the patient is felt during insertion of the needle through the skin itself. Advancing the needle or wire through the breast tissue or injecting contrast solution (dye or carbon) is generally much less painful.

Bleeding is only a problem when an artery is inadvertently injured during localization. If this occurs, firm compression has to be applied for a sufficient period of time (approximately 10 minutes).

Vasovagal reactions are biphasic with an initial rise in heart rate, blood pressure, systemic resistance, and cardiac output. This rapidly reverses as bradycardia associated with splanchnic and muscle vasodilatation occurs associated with nausea, pallor, lightheadedness and diaphoresis. They are usually treated with simple supportive measures, including placing the patient in a supine position with legs raised at the onset of symptoms. The physician must always be prepared for vasovagal reactions since individual tolerance to the introduction of a needle into the breast varies greatly [24].

Ecchymoses or hematomas may follow after insertion of the needle into the breast. Although these most commonly occur in the region of the target lesion, an occasional more remote one may occur.

Although pneumothorax is probably the most serious potential complication, it is an extremely rare event, as is migration of wires into remote locations of the body.

Table 11.1 Comparison of different preoperative localization techniques

Features of localization Techniques							
	Wire	Carbon	ROLL	Radioactive Seed	Magnetic Seed	Radar Reflector	RFID Tag
Implantation Facilities	Hospital	Hospital/ outpatient	Hospital	Hospital	Hospital/outpatient	Hospital/ outpatient	Hospital/ outpatient
Repositionable	Certain types	No	No	No	No	No	No
Device size	3–15 cm	–	–	5 mm	5 mm	12 mm	9 mm
Device Isolated Cost	Low	Low	Low	Low	High	High	High
Additional equipment requirements	None	None	Console and Probe	Console and Probe	Console, probe, Non Ferromagnetic Surgical instruments	Console and Probe	Console and Probe
Depth limit for detectability	None	None	None	None	3–4 cm	6 cm	3–6 cm
Maximal duration of implantation	Same day as surgery	No restriction	Same day as surgery	5–7 days prior To surgery	No restriction	No restriction	No restriction
MRI Deployment	MRI-compatible Wires are available	Available	Available	Not available	Not available	Not available	Not available
MRI Device Safety	MRI-compatible Wires are available	Safe	Safe	MRI Conditional (3 T or less)	MRI Conditional (3 T or less)	MRI Conditional (3 T or less)	MRI Conditional (3 T or less)
FDA	Approved	Not approved for breast lesion localization	Approved	Approved	Approved	Approved	Approved

Strengths	Cost effective No depth limitation Can be placed with MRI guidance	Can be placed with MRI guidance	No depth limitation Can be placed with MRI guidance Axillary node localization	No depth limitation Console and probe are the Same used for sentinel lymph node biopsy	Small size Axillary node localization	Axillary node localization	Pencil size surgical probe available Each tag has a unique ID number visible on console
Weaknesses	Scheduling inflexibility Presurgical Patient will be in fasting state Potential discomfort while waiting for surgery	Potentially difficult visualization on imaging methods Foreign-body reaction that may mimic malignancy	Scheduling difficulties Radiation safety concerns Lengthy Process to begin Program	Radiation safety concerns Lengthy Process to begin Program	Requires nonferrous surgical tools Largest susceptibility artifact on MRI Contraindicated in patients with implanted cardiac devices	Contains nickel MRI artifact Multiple factors may limit signal detection on OR	MRI artifact Axillary use is still off label

WL specifically has a multitude of complications. Because part of the wire is external, it can dislocate, migrate, bend, fracture, or be transected before or during surgery [68]. An uncommon event is intramammary dislocation of the hook from its intended location. Distal migration of the wire within the breast can occur as repositioning and recompression result in more of the wire being enveloped by the breast. Respiratory and muscular activity during transportation, prolonged delays, and transfer from stretcher to operating table may result as well in distal wire displacements, particularly with posterior lesions. These complications are preventable by bending and securely taping the wire to the skin or, in the case of the curved-end J-wires, by using the skin clamp provided. In patients with fatty breasts, the wire may retract toward the skin surface because of limited stroma for hookwire anchorage.

Broken or transected wires are a problem that will have a variable incidence, depending on the surgical personnel involved. Failure to excise the localized mammographic abnormality has been reported in 2.5–6.7% of cases and is more likely with two lesions, small breast, microcalcifications, small lesions, and small specimen [21, 69]. Potential reasons for failure to excise include placement of the wire more than 1 cm from the lesion, placing the wire without reaching the lesion, advancing the wire significantly beyond the lesion, wire movement during patient transfer, and bleeding causing hematoma formation and wire displacement.

11.7 Post-procedure Assessment

The radiologist estimates the projection of the tumor on the skin surface, positions a marker in the corresponding spot, and reports the skin-to-lesion as well as skin-to–localization device depths, as well as the lesion distance from the nipple and pectoral muscle. After the procedure, the radiologist must summarize it for the surgeon and even consider a call to discuss the procedure, particularly if the localization device is not in an ideal position.

After the target tissue is excised, the specimen is labeled for orientation, and radiographs are obtained to confirm the removal of both the lesion and the localization device. Surgical specimens, excised under needle localization guidance, should be radiographed for several reasons. The radiography verifies that the entire lesion has been removed, serves as a lesion location guide in the specimen to the pathologist, and certifies that the wire has been removed from the breast. This is an absolute requirement when localization is performed for calcification, architectural distortion, or asymmetries. If the entire length of the wire is not visualized on the specimen radiograph, it is imperative to report this information to the surgeon. Intraoperative radiography or postoperative imaging is appropriate to identify the retained fragment [67].

References

1. Franceschi D, Crowe J, Zollinger R, Duchesneau R, Shenk R, Stefanek G, et al. Biopsy of the breast for mammographically detected lesions. Surg Gynecol Obstet. 1990;171(6):449–55.
2. Goedde TA, Frykberg ER, Crump JM, Lay SF, Turetsky DB, Linden SS. The impact of mammography on breast biopsy. Am Surg. 1992;58(11):661–6.
3. Hayes MK. Update on preoperative breast localization. Radiol Clin. 2017;55(3):591–603.
4. Gundry KR, Berg WA. Treatment issues and core needle breast biopsy: clinical context. AJR Am J Roentgenol. 1998;171(1):41–9.
5. Dershaw DD, Morris EA, Liberman L, Abramson AF. Nondiagnostic stereotaxic core breast biopsy: results of rebiopsy. Radiology. 1996;198(2):323–5.
6. Philpotts LE, Shaheen NA, Carter D, Lange RC, Lee CH. Comparison of rebiopsy rates after stereotactic core needle biopsy of the breast with 11-gauge vacuum suction probe versus 14-gauge needle and automatic gun. AJR Am J Roentgenol. 1999;172(3):683–7.
7. Liberman L. Clinical management issues in percutaneous core breast biopsy. Radiol Clin N Am. 2000;38(4):791–807.
8. Mayo RC III, Kalambo MJ, Parikh JR. Preoperative localization of breast lesions: current techniques. Clin Imaging. 2019;56:1–8.
9. Spillane RM, Whitman GJ, McCarthy KA, Hulka CA, Hall DA, Kopans DB. Computed tomography—guided needle localization of nonpalpable breast lesions: review of 24 cases. Acad Radiol. 1996;3(2):115–20.
10. Fischer U, Baum F, Luftner-Nagel S. Breast cancer: diagnostic imaging and therapeutic guidance. Thieme. 2018;9:166–73.
11. Reynolds HE, Jackson VP, Musick BS. A survey of interventional mammography practices. Radiology. 1993;187(1):71–3.
12. Fischer U, Baum F. Interventional breast imaging: ultrasound, mammography, and MR guidance techniques. Thieme; 2011.
13. Patel IJ, Davidson JC, Nikolic B, Salazar GM, Schwartzberg MS, Walker TG, et al. Consensus guidelines for periprocedural management of coagulation status and hemostasis risk in percutaneous image-guided interventions. J Vasc Interv Radiol. 2012;23(6):727–36.
14. Patel IJ, Davidson JC, Nikolic B, Salazar GM, Schwartzberg MS, Walker TG, et al. Addendum of newer anticoagulants to the SIR consensus guideline. J Vasc Interv Radiol. 2013;24(5):641–5.
15. Jaffe TA, Raiff D, Ho LM, Kim CY. Management of anticoagulant and antiplatelet medications in adults undergoing percutaneous interventions. Am J Roentgenol. 2015;205(2):421–8.
16. Veltri A, Bargellini I, Giorgi L, Almeida PAMS, Akhan O. CIRSE guidelines on percutaneous needle biopsy (PNB). Cardiovasc Intervent Radiol. 2017;40(10):1501–13.
17. Kaye AD, Kucera I, Sabar R. Perioperative anesthesia clinical considerations of alternative medicines. Anesthesiol Clin North Am. 2004;22(1):125–39.
18. Thornhill MH, Dayer M, Lockhart PB, Prendergast B. Antibiotic prophylaxis of infective endocarditis. Curr Infect Dis Rep. 2017;19(2):9.
19. Patel SN, Mango VL, Jadeja P, Friedlander L, Desperito E, Wynn R, et al. Reflector-guided breast tumor localization versus wire localization for lumpectomies: a comparison of surgical outcomes. Clin Imaging. 2018;47:14–7.
20. Chadwick D, Shorthouse A. Wire-directed localization biopsy of the breast: an audit of results and analysis of factors influencing therapeutic value in the treatment of breast cancer. Eur J Surg Oncol. 1997;23(2):128–33.
21. Jackman RJ, Marzoni FA Jr. Needle-localized breast biopsy: why do we fail? Radiology. 1997;204(3):677–84.
22. Butler R, Berg WA. Preoperative lesion localization, bracketing. Diagnostic imaging: breast. 3rd ed. Philadelphia, PA: Elsevier; 2019.

23. Dershaw DD. Imaging-guided interventional breast techniques. Springer Science & Business Media; 2002. p. 31–52.
24. Helvie MA, Ikeda DM, Adler DD. Localization and needle aspiration of breast lesions: complications in 370 cases. AJR Am J Roentgenol. 1991;157(4):711–4.
25. Sylvia H, Dershaw D, Schreer I. Diagnostic breast imaging; 2001. p. 152–60.
26. Woods RW, Camp MS, Durr NJ, Harvey SC. A review of options for localization of axillary lymph nodes in the treatment of invasive breast cancer. Acad Radiol. 2019;26(6):805–19.
27. Homer MJ. Transection of the localization hooked wire during breast biopsy. Am J Roentgenol. 1983;141(5):929–30.
28. Martinez SR, Gelfand M, Hourani HS, Sorrento JJ, Mohan EP. Cardiac injury during needle localized surgical breast biopsy. J Surg Oncol. 2003;82(4):261–5.
29. Bristol J, Jones P. Transgression of localizing wire into the pleural cavity prior to mammography. Br J Radiol. 1981;54(638):139–40.
30. Choy N, Lipson J, Porter C, Ozawa M, Kieryn A, Pal S, et al. Initial results with preoperative tattooing of biopsied axillary lymph nodes and correlation to sentinel lymph nodes in breast cancer patients. Ann Surg Oncol. 2015;22(2):377–82.
31. Patel R, MacKerricher W, Tsai J, Wood L, Allison K, Wapnir I. Pathological confirmation of pre-chemotherapy biopsied and tattooed axillary lymph nodes; 2018. p. 426–7.
32. Rose A, Collins J, Neerhut P, Bishop C, Mann G. Carbon localisation of impalpable breast lesions. Breast. 2003;12(4):264–9.
33. Ko K, Han B-K, Jang KM, Choe YH, Shin JH, Yang J-H, et al. The value of ultrasound-guided tattooing localization of nonpalpable breast lesions. Korean J Radiol. 2007;8(4):295–301.
34. Svane G. A stereotaxic technique for preoperative marking of non-palpable breast lesions. Acta Radiol Diagn. 1983;24(2):145–51.
35. Langlois SLP, Carter ML. Carbon localisation of impalpable mammographic abnormalities. Australas Radiol. 1991;35(3):237–41.
36. Canavese G, Catturich A, Vecchio C, Tomei D, Estienne M, Moresco L, et al. Pre-operative localization of non-palpable lesions in breast cancer by charcoal suspension. Eur J Surg Oncol. 1995;21(1):47–9.
37. Mullen DJ, Eisen RN, Newman RD, Perrone PM, Wilsey JC. The use of carbon marking after stereotactic large-core-needle breast biopsy. Radiology. 2001;218(1):255–60.
38. Franceschini G, Mason EJ, Grippo C, D'Archi S, D'Angelo A, Scardina L, et al. Image-guided localization techniques for surgical excision of non-palpable breast lesions: an overview of current literature and our experience with preoperative skin tattoo. J Personal Med. 2021;11(2):99.
39. Ruiz-Delgado M, López-Ruiz J, Sáiz-López A. Abnormal mammography and sonography associated with foreign-body giant-cell reaction after stereotactic vacuum-assisted breast biopsy with carbon marking. Acta Radiol. 2008;49(10):1112–8.
40. Cavalcanti TCS, Malafaia O, Nassif PAN, Skare TL, Ogata DC, Miguel MT, et al. Non-palpable breast lesions marked with coal suspension: evaluation of anatomopathological aspects, viability of interpretation and inflammatory response. Revista do Colegio Brasileiro de Cirurgioes. 2012;39(6):469–75.
41. de O Salvador GL, Barbieri PP, Maschke L, ALA N, Louveira MH, Budel VM. Charcoal granuloma mimicking breast cancer: an emerging diagnosis. Acta Radiol Open. 2018;7(12):2058460118815726.
42. Veronesi U. Conservative surgery 23. Breast cancer: innovations in research and management; 2017. p. 247–64.
43. Luini A, Zurrida S, Galimberti V, Paganelli G. Radioguided surgery of occult breast lesions. Eur J Cancer (Oxford, England: 1990). 1998;34(1):204–5.
44. Grüning T, Brogsitter C, Jones IW, Heales JC. Resolution recovery in planar bone scans: diagnostic value in metastatic disease. Nucl Med Commun. 2012;33(12):1307–10.
45. Postma EL, Koffijberg H, Verkooijen H, Witkamp A, Van Den Bosch M, Van Hillegersberg R. Cost-effectiveness of radioguided occult lesion localization (ROLL) versus wire-guided

localization (WGL) in breast conserving surgery for nonpalpable breast cancer: results from a randomized controlled multicenter trial. Ann Surg Oncol. 2013;20(7):2219–26.
46. Paganelli G, De Cicco C, Luini A, Cassano E, Pizzamiglio M, Fiorenza M, et al. Radioguided surgery in non-palpable breast lesions. Eur J Nucl Med Mol Imaging. 1997;24:893.
47. De Cicco C, Trifiro G, Intra M, Marotta G, Ciprian A, Frasson A, et al. Optimised nuclear medicine method for tumour marking and sentinel node detection in occult primary breast lesions. Eur J Nucl Med Mol Imaging. 2004;31(3):349–54.
48. Ahmed M, Douek M. Sentinel node and occult lesion localization (SNOLL): a systematic review. Breast. 2013;22(6):1034–40.
49. Krynyckyi BR, Shim J, Kim CK. Internal mammary chain drainage of breast cancer. Ann Surg. 2004;240(3):557.
50. Price ER, Khoury AL, Esserman LJ, Joe BN, Alvarado MD. Initial clinical experience with an inducible magnetic seed system for preoperative breast lesion localization. Am J Roentgenol. 2018;210(4):913–7.
51. US Nuclear Regulatory Commission. iodine-125 and palladium-103 low dose rate brachytherapy seeds used for localization of non-palpable lesions. Washington, DC: US Government Printing Office; 2015. p. 27. http://www.nrc.gov/materials/miau/med-use-toolkit/seed-localization.html
52. Loving VA, Edwards DB, Roche KT, Steele JR, Sapareto SA, Byrum SC, et al. Monte Carlo simulation to analyze the cost-benefit of radioactive seed localization versus wire localization for breast-conserving surgery in fee-for-service health care systems compared with accountable care organizations. Am J Roentgenol. 2014;202(6):1383–8.
53. Jakub JW, Gray RJ, Degnim AC, Boughey JC, Gardner M, Cox CE. Current status of radioactive seed for localization of nonpalpable breast lesions. Am J Surg. 2010;199(4):522–8.
54. McGhan LJ, McKeever SC, Pockaj BA, Wasif N, Giurescu ME, Walton HA, et al. Radioactive seed localization for nonpalpable breast lesions: review of 1,000 consecutive procedures at a single institution. Ann Surg Oncol. 2011;18(11):3096–101.
55. Hughes JH, Mason MC, Gray RJ, McLaughlin SA, Degnim AC, Fulmer JT, et al. A multi-site validation trial of radioactive seed localization as an alternative to wire localization. Breast J. 2008;14(2):153–7.
56. Sharek D, Zuley ML, Zhang JY, Soran A, Ahrendt GM, Ganott MA. Radioactive seed localization versus wire localization for lumpectomies: a comparison of outcomes. Am J Roentgenol. 2015;204(4):872–7.
57. Dryden MJ, Dogan BE, Fox P, Wang C, Black DM, Hunt K, et al. Imaging factors that influence surgical margins after preoperative 125I radioactive seed localization of breast lesions: comparison with wire localization. Am J Roentgenol. 2016;206(5):1112–8.
58. Zhang Y, Seely J, Cordeiro E, Hefler J, Thavorn K, Mahajan M, et al. Radioactive seed localization versus wire-guided localization for nonpalpable breast cancer: a cost and operating room efficiency analysis. Ann Surg Oncol. 2017;24(12):3567–73.
59. SAVI SCOUT reflector and delivery system instructions for use. Cianna Medical. 2016;2019. https://www.ciannamedical.com/wp-content/uploads/2016/11/Instructions-for-Use-Reflector-Delivery-System.pdf. Published 2016. Accessed 8 May 2019.
60. Cox CE, Russell S, Prowler V, Carter E, Beard A, Mehindru A, et al. A prospective, single arm, multi-site, clinical evaluation of a nonradioactive surgical guidance technology for the location of nonpalpable breast lesions during excision. Ann Surg Oncol. 2016;23(10):3168–74.
61. Mango VL, Wynn RT, Feldman S, Friedlander L, Desperito E, Patel SN, et al. Beyond wires and seeds: reflector-guided breast lesion localization and excision. Radiology. 2017;284(2):365–71.
62. Srour MK, Kim S, Amersi F, Giuliano AE, Chung A. Comparison of wire localization, radioactive seed, and Savi scout® radar for management of surgical breast disease. Breast J. 2020;26(3):406–13.
63. Falcon S, Weinfurtner RJ, Mooney B, Niell BL. SAVI SCOUT® localization of breast lesions as a practical alternative to wires: outcomes and suggestions for trouble-shooting. Clin Imaging. 2018;52:280–6.

64. Hersi A-F, Eriksson S, Ramos J, Abdsaleh S, Wärnberg F, Karakatsanis A. A combined, totally magnetic technique with a magnetic marker for non-palpable tumour localization and superparamagnetic iron oxide nanoparticles for sentinel lymph node detection in breast cancer surgery. Eur J Surg Oncol. 2019;45(4):544–9.
65. Gera R, Tayeh S, Al-Reefy S, Mokbel K. Evolving role of magseed in wireless localization of breast lesions: systematic review and pooled analysis of 1,559 procedures. Anticancer Res. 2020;40(4):1809–15.
66. DiNome ML, Kusske AM, Attai DJ, Fischer CP, Hoyt AC. Microchipping the breast: an effective new technology for localizing non-palpable breast lesions for surgery. Breast Cancer Res Treat. 2019;175(1):165–70.
67. Kapoor MM, Patel MM, Scoggins ME. The wire and beyond: recent advances in breast imaging preoperative needle localization. Radiographics. 2019;39(7):1886–906.
68. Cheang E, Ha R, Thornton CM, Mango VL. Innovations in image-guided preoperative breast lesion localization. Br J Radiol. 2018;91(1085):20170740.
69. Shetty MK. Presurgical localization of breast abnormalities: an overview and analysis of 202 cases. Indian J Surg Oncol. 2010;1(4):278–83.

Part III
Different Clinical Scenario: Clinical Management and Role of Imaging Modalities

Chapter 12
Screening

Mila Trementosa Garcia, Laura Aguiar Penteado, Flávia Abranches Corsetti Purcino, and Jose Roberto Filassi

12.1 Introduction

Screening tests are done to detect potential health disorders or diseases in people who do not have any symptoms of the disease. The goal is early detection to enable effective treatment or prevention through lifestyle changes. The disease must be serious and treatable. The exam must be safe, acceptable, and of low cost [1].

For breast cancer, mammography, as a screening test can offer conservative surgery and decrease mortality. Screening mammography detects 2–8 cancers per 1000 mammograms [2], and some guidelines show a 20% of mortality reduction [3].

Periodicity of mammography is controversial, as well as the ideal age to start and finish scheduled tests. Societies around the world offer different recommendations. The Brazilian College of Radiology and the Brazilian Society of Breast Cancer recommends from the age of 40 without a predetermined age for the interruption, testing women up to the life expectancy of 7 years. The US Preventive Services Task Force (USPSTF) recommendation (2009 and 2016) is biennial screening mammography for women aged 50–74 years. Annual screening mammography of women aged 40–84 is known to prevent more deaths from breast cancer than biennial screening of women 50–74 years old. No medical society recommends screening before 40 years.

On the other hand, mammography is not innocuous. Its main adverse effect is radiation exposure. Other problems may arise from false-positive results and overdiagnosis leading to overtreatment.

M. T. Garcia · L. A. Penteado · F. A. C. Purcino · J. R. Filassi (✉)
Departamento de Mastologia, Instituto do Cancer do Estado de Sao Paulo ICESP, São Paulo, SP, Brazil
e-mail: drfilassi@terra.com.br

S. J. Kim Hsieh, E. A. Morris (eds.), *Modern Breast Cancer Imaging*,
https://doi.org/10.1007/978-3-030-84546-9_12

Overdiagnosis refers to detection in the screening of invasive or noninvasive neoplasia that would not cause death or become symptomatic during the patient's life. It is a difficult task to state which cases have been overtreated, and literature vary widely from less than 5% to more than 50%. The greatest challenge for the future is to find ways to increase the accuracy of the detected cancer and if it threatens the patient's health or not [4, 5].

False-positive problems include recalls for further studies, follow-up, and biopsies with benign results, which increase the cost of screening and general anxiety. A good screening test must have high sensitivity so as not to lose cases of the disease present in the population tested, as well as high specificity, resulting in a few cases of false positives.

Considering radiation exposure, there are no direct demonstrations that periodic mammograms induce breast cancer. The glandular dose of two-view mammography ranges from 2 to 4 mGy. Anyway, it is prudent to avoid unnecessary exposure.

12.2 Screen-Film Mammography

This type of mammography was used in the initial studies that highlighted the advantage of screening for breast cancer (Table 12.1). The image needs to be developed and fixed chemically.

12.3 Digital Mammography

Digital mammography was compared with screen-film mammography, and there is no difference in accuracy for general screening. For women younger than 50 years old and dense breast tissue, digital mammography is more accurate.

Screen-film mammography has been replaced by digital mammography due to easier archiving and handling. Although digital mammography has advantages over

Table. 12.1 Reduced mortality in trials

Trial	% Mortality decrease	95% Confidence interval
HIP RCT	22	0 — 39
Malmo RCT	22	5 — 35
SWEDISH two-county RCT	27	11 — 41
Edinburgh RCT	21	−2 — 40
Stockholm RCT	10	−28 — 37
NBSS1 and 2 RCT	1	−12 — 12
Gothenburg RCT	23	0 — 40
Overall RCT	20	14 — 27

Source: Adapted from Niell et al. [6]

screen-film mammography, no medical society recommends the preferred use of digital mammography in screening the general population.

12.4 Tomosynthesis

In some cases, the fibroglandular tissue can hide lesions or hinder the interpretation of the exam. With tomosynthesis, a moving x-ray source acquires multiple projections in each incidence and creates thin sections that could help with the masking problem.

The combined use with mammography can reduce the rate of recall by 30%, but it increases exposure to radiation, which generates debate about its routine use in screening.

12.5 Magnetic Resonance Imaging (MRI)

Magnetic resonance imaging is used regularly to screen for breast cancer in women at high family risk (>20% lifetime), because MRI has the highest sensitivity for the detection of invasive as well as of intraductal cancer [7]. On the other hand, MRI screening has a lower specificity than mammography, and as a result, MRI will generate more findings judged as uncertain, requiring short-term follow-up or additional investigations [8].

Kriege et al., in a prospective study, compared the efficacy of mammographic and MRI screening for breast cancer in women with a positive family history or a genetic predisposition to breast cancer [9]. Among the women examined by both methods at the same screening visit, 45 breast cancers were detected (including 6 ductal carcinomas in situ): 32 by MRI (sensitivity, 71.1%) and 18 by mammography (40%). The sensitivity of MRI was higher than that of mammography, but both the specificity and positive predictive value of MRI were lower. MRI screening led to twice as many unnecessary additional examinations as mammography (420 vs. 207) and three times as many unnecessary biopsies (24 vs. 7) [9].

Despite MRI screening of the breast can detect occult malignancies better than mammography, several factors must be taken into consideration. MRI is very expensive and is an invasive procedure requiring an intravenous injection of a contrast agent. It is also contraindicated in women with claustrophobia, pacemakers, or aneurysm clips. Additionally, low specificity can cause an anxiety regarding the result of supplemental screening, such as emotional burden, concerns about false-positive results, or overdiagnosis and aversion to hospitals [10].

Berg et al. observed in the main ACRIN 6666 study that the increase in cancer detection seen in the MRI sub-study was greater than observed by the addition of annual ultrasound to mammography [11]. However, given the low rate of 8% of clinically detected interval cancer rate in the main ACRIN 6666 protocol and given

the fact that all interval cancers remained node-negative at diagnosis, it is unclear that the added cost and reduced tolerability of MRI screening are justified in women at intermediate risk for breast cancer in lieu of supplemental screening with ultrasound. Despite its higher sensitivity, the addition of MRI screening instead of ultrasound to mammography in broader populations of women at intermediate risk with dense breasts may not be appropriate, particularly when the current high false-positive rates, cost, and reduced tolerability of MRI are considered [11].

12.6 Ultrasound

Ultrasound (US) traditionally serves as an adjunctive diagnostic modality of mammographic in screening for abnormalities. Where mammography is available, US should be seen as a supplemental test for women with dense breasts who do not meet high-risk criteria for screening MRI and for high-risk women with dense breasts who are unable to tolerate MRI [12].

Dense breast tissue reduces the sensitivity of screening mammography to detect malignancy and is associated with an increased risk of breast cancer.

It is known that ultrasound is effective for the detection of small, invasive, node-negative cancers in dense breast tissue, where the sensitivity of mammography drops from 85% to 47.8–64.4% [13, 14]; therefore, women with mammographically dense breasts may benefit from supplemental screening with whole breast ultrasound.

Although most of the literature reviews ultrasound as a supplementary detection technique and its current evidence of effectiveness in the screening scenario is scarce, there is a growing body of literature describing the capability of ultrasound to detect breast cancer. Recent systematic review and meta-analysis of 26 studies with a total of 76,058 patients is the most comprehensive analysis of the sensitivity of ultrasound as a primary modality for breast cancer detection. The study showed that ultrasound had an overall pooled sensitivity and specificity (95% CI) of 80.1% (72.2–86.3%) and 88.4% (79.8–93.6%), respectively, for the detection of breast cancer. In addition, this high sensitivity and specificity did not differ based on subgroup analyses [15].

Considering that mammography is not widely available in all countries and breast cancer incidence is increasing, ultrasound, as a relatively inexpensive and available tool, can potentially play an important role in screening breast cancer in these sites. Furthermore, it is used as a primary diagnostic modality to assess focal breast symptoms in women under 40 years of age. Given that 23% of global breast cancer cases are seen in women aged 15 to 49 years old in developing countries [16], the use of ultrasound to screen asymptomatic women is also increasing rapidly.

The automated whole-breast ultrasound (AWBU) is a modality approved for medical use by the Food and Drug Administration (FDA) and allows the radiologist to read the images quickly, at a convenient time, while being free from doing the scan.

A blinded study of this system combined with screening mammography has shown that adding AWBU doubles the overall cancer detection and triples the invasive cancers of 1 cm or less found in women with dense breasts [17]. Training would be necessary for any facility planning to offer screening US [18].

12.7 Molecular Breast Imaging

Unlike mammography and ultrasound that are based on anatomy, molecular breast imaging (MBI) is a physiologic approach to breast cancer detection. MBI detects additional foci of occult breast cancer in 9.0% of women with newly diagnosed breast cancer, has a high sensitivity for detecting high-risk lesions, and detects 98% of invasive breast cancer and 91% of ductal carcinoma in situ [19]. Furthermore, in surveillance of high-risk women, breast-specific gamma imaging (BSGI)/MBI detects occult cancer in up to 16.5 per 1000 women. This modality is increasingly being used to assess response to treatment in women undergoing neoadjuvant chemotherapy and for adjunct screening in women with dense breasts. It has been shown to influence surgical management in nearly a quarter of women with newly diagnosed breast cancer. The Society of Nuclear Imaging has established clinical indications and the American College of Radiology has established appropriateness criteria as well as an accreditation program for MBI. A BIRADS-like lexicon for MBI has also been described.

12.8 Clinical Breast Examination

Clinical breast examination is described as the examination of the breasts performed by a doctor or a nurse. Commonly associated with screening mammography or executed alone on many low-income areas. Clinically detected cancers are larger, with a median size of 2.6 cm, compared with those found with screening mammography, with a median size of 1.5 cm [20].

Cancers found clinically are more likely to show axillary nodal metastases: 38–45% are node positive compared with 18–25% of cancers detected by mammographic screening [21, 22]. Even within the same stage of cancer, survival is higher in screen-detected cancers than in cancers detected clinically [23].

12.9 Breast Self-Examination

Described as an examination of the breasts performed by the patient herself. These methods do not require any technical equipment and can be performed by the women themselves if properly trained [24]. Data from two large trials do not

suggest a beneficial effect of screening by breast self-examination whereas there is evidence for harms. There were no randomized trials of clinical breast examination. At present, breast self-examination cannot be recommended [25].

The review of data from these trials did not find a beneficial effect of screening in terms of improvement in breast cancer mortality. This review searched for well-designed trials that assessed these methods and found two large population-based studies involving 388,535 women who compared breast self-examination with no intervention [25].

These meta-analyses also conclude that there is good evidence of harm from breast self-examination as a result of increased invasive diagnostic procedures [26, 27].

Other potential harms of screening include emotional distress even after a month after receiving a clear result after further investigation [28]. A multicenter follow-up study comparing different breast screening results groups 5 months after their last breast screening appointment showed that women who go on further investigation suffer greater adverse psychological consequences than women who do not [28, 29].

12.10 Thermography

A number of new and emerging technologies are being developed for breast cancer screening and diagnosis internationally. Emerging classes of technology promoted for breast cancer screening include digital infrared thermal imaging (DITI) – thermography. It is a noninvasive imaging method, which neither emits ionizing radiation nor compresses the breast and operates under differing physiological principles. DITI aims to detect localized increases in skin temperature, which are thought to occur as a result of increased vascularization, vasodilation, and recruitment of inflammatory cells to the site of a developing tumor [30]. Localized differences in skin temperature are captured by infrared cameras, which produce a heat map of the breast called a thermogram. Early attempts of thermal imaging technology for breast cancer detection had poor sensitivity (39%) [31]; however, the recent development of high-resolution infrared cameras has generated new interest in the use of DITI as a tool for breast cancer detection [32].

12.11 Elastography

Elastography incorporates multiple technological approaches. Two subclasses of elastography – ultrasound elastography (USE) and electronic palpation imaging (EPI) – will be described. EPI is a technology that generates pressure maps of breast tissue identifying tumors as more rigid structures than healthy tissue [33]. In contrast, USE can be interpreted as a measure of comparative strain between healthy and cancerous tissue [34], a five-point elasticity score index, or as an automatic classification of benign or malignant tumors using an artificial neural network [35].

12.12 Screening in Special Populations

12.12.1 Increased Breast Density

Screening is one of the main factors that contribute to the reduction of mortality from breast cancer worldwide. Mammographic screening is a well-known established method for all women who are between 50 and 70 years of age and can reduce mortality from breast cancer by about 25 percent [36]. About the value of breast cancer screening among women who are under 50 years old, there is no consensus [37]. One of the reasons for the lack of agreement is the difficulty in detecting tumors by mammographic screening in younger women, who have denser breasts than postmenopausal women [38].

Dense breasts are defined by mammographic appearance. The American College of Radiology's (ACR) Breast Imaging Reporting and Data System (BI-RADS) classifies breasts in four categories based on the fibroglandular breast density [39].

Extremely dense breast tissue is a risk factor for breast cancer and limits the detection of cancer with mammography. However, there is currently little evidence that the addition of breast ultrasound or MRI would change the mortality rate.

In J-START (Japan Strategic Anti-cancer Randomized Trial), investigators evaluated supplemental ultrasonographic breast screening among Japanese women aged 40–49 years old. 58% of the participants had dense breasts. Cancer-detection rates were 3.3 per 1000 screenings for mammography alone and 5.0 per 1000 screenings for mammography plus ultrasonography. The addition of ultrasonographic screening resulted in an interval-cancer rate of 0.5 per 1000 screenings, as compared with 1.0 per 1000 screenings with mammography alone, and an increase in the false-positive rate from 8.8% to 12.6% [40].

In a diagnostic setting, magnetic resonance imaging (MRI) is a sensitive method of breast imaging and is not influenced by breast density. The Dense Tissue and Early Breast Neoplasm Screening (DENSE) trial is a randomized, controlled trial to study the effect of supplemental MRI on the incidence of interval cancers in women with extremely dense breast tissue. The trial assigned 40,373 women between the ages of 50 and 75 years old with extremely dense breast tissue and randomized to a group that was invited to undergo supplemental MRI or to a group that received mammography screening only. The primary outcome was the difference between groups in the incidence of interval cancers during a 2-year screening period. It was observed a significantly lower interval-cancer rate in the MRI group (2.5 vs. 5.0 per 1000 screenings). Among the women who were invited to undergo MRI, 59% actually underwent the procedure. Of the 20 interval cancers diagnosed in the MRI-invitation group, 4 were diagnosed in the women who had undergone MRI and 16 in those who had not. A limitation of the trial is that it is not large enough to look at the effect of MRI screening on breast cancer-specific or overall mortality. This outcome would require a much larger sample size and longer follow-up [41].

12.12.2 High-Risk of Breast Cancer

A woman is considered at high risk of developing breast cancer if she has a lifetime risk of more than 20–25% of developing breast cancer based on available risk models, has a BRCA1 or BRCA2 mutations, or was exposed to therapeutic thoracic radiation (RT) before age 30. This population needs a special screening due to the high chances of developing breast cancer.

Kuhl et al. investigated in "the EVA Trial" the contribution of clinical breast examination (CBE), mammography, ultrasound, and quality-assured breast magnetic resonance imaging (MRI), used alone or in different combinations, for screening women at elevated risk for breast cancer. It was a prospective multicenter observational cohort study and analyzed 687 asymptomatic women at elevated familial risk (>20% lifetime). Twenty-seven women were diagnosed with breast cancer: 11 ductal carcinomas in situ (41%) and 16 invasive cancers (59%). All cancers were detected during annual screening; no interval cancer occurred; no cancer was identified during the half-yearly ultrasound. The cancer yield of ultrasound (6.0 of 1000) and mammography (5.4 of 1000) was equivalent; it increased nonsignificantly (7.7 of 1000) if both methods were combined. Cancer yield achieved by MRI alone (14.9 of 1000) was significantly higher; it was not significantly improved by adding mammography (MRI plus mammography: 16.0 of 1000) and did not change by adding ultrasound (MRI plus ultrasound: 14.9 of 1000). The positive predictive value was 39% for mammography, 36% for ultrasound, and 48% for MRI [42].

The National Comprehensive Cancer Network (NCCN) recommends that women who have a lifetime risk ≥20% should have an annual screening mammography (begin 10 years prior to when the youngest family member was diagnosed with breast cancer but not prior to age 30) and also recommends annual breast MRI (begin 10 years prior to when the youngest family member was diagnosed with breast cancer, but not prior to age 25) [43].

Special screening has been recommended for women who were exposed to therapeutic thoracic radiation, between the ages of 10 and 30 years. The NCCN recommends an annual screening mammography (begin 8 years after RT but not prior to age 30) and also recommends an annual breast MRI (begin 8 years after RT but not prior to age 25) [43].

12.12.3 Elderly Women

The upper age limit at which breast cancer screening should be applied is not established by guidelines. The woman's overall state of health should be considered in any decision to undertake or forgo screening.

References

1. The Johns Hopkins University, The Johns Hopkins Hospital, and The Johns Hopkins Health System Corporation, Johns Hopkins Medicine. Available at: https://www.hopkinsmedicine.org/. Accessed 10 Sept 2020.
2. Lee CS, Bhargavan-Chatfield M, Burnside ES, Nagy P, Sickles EA. The national mammography database: preliminary data. Am. J. Roentgenol [Internet]. American Roentgen Ray Society; 2016 ;206(4):883–90. Available at: https://doi.org/10.2214/AJR.15.14312.
3. Oeffinger KC, Fontham ETH, Etzioni R, Herzig A, Michaelson JS, Shih Y-CT, et al. Breast cancer screening for women at average risk: 2015 guideline update from the american cancer society. JAMA [Internet]. 2015;314(15):1599–614. Available at: https://doi.org/10.1001/jama.2015.12783.
4. Olsen AH, Agbaje OF, Myles JP, Lynge E, Duffy SW. Overdiagnosis, sojourn time, and sensitivity in the Copenhagen mammography screening program. Breast J [Internet]. 2006;12(4):338–42. Available at: http://doi.wiley.com/10.1111/j.1075-122X.2006.00272.x.
5. Jorgensen KJ, Gotzsche PC. Overdiagnosis in publicly organised mammography screening programmes: systematic review of incidence trends. BMJ [Internet]. 2009;339(jul09 1):b2587–b2587. Available at: https://www.bmj.com/lookup/doi/10.1136/bmj.b2587.
6. Niell BL, Freer PE, Weinfurtner RJ, Arleo EK, Drukteinis JS. Screening for breast cancer. Radiol Clin N Am. 2017;55(6):1145–62. https://doi.org/10.1016/j.rcl.2017.06.004. PMID: 28991557.
7. Kuhl CK, Schrading S, Leutner CC, Morakkabati-Spitz N, Wardelmann E, Fimmers R, et al. Mammography, breast ultrasound, and magnetic resonance imaging for surveillance of women at high familial risk for breast cancer. J Clin Oncol. 2005;23(33):8469–76.
8. Liberman L, Morris EA, Benton CL, Abramson AF, Dershaw DD. Probably benign lesions at breast magnetic resonance imaging: preliminary experience in high-risk women. Cancer. 2003;98(2):377–88.
9. Kriege M, Brekelmans CTM, Boetes C, Besnard PE, Zonderland HM, Obdeijn IM, et al. Efficacy of MRI and mammography for breast-cancer screening in women with a familial or genetic predisposition. N Engl J Med. 2004;351(5):427–37.
10. de Lange SV, Bakker MF, Monninkhof EM, PHM P, de Koekkoek-Doll PK, Mann RM, et al. Reasons for (non)participation in supplemental population-based MRI breast screening for women with extremely dense breasts. Clin Radiol. 2018;73(8):759.e1–9.
11. Berg WA, Zhang Z, Lehrer D, Jong RA, Pisano ED, Barr RG, et al. Detection of breast cancer with addition of annual screening ultrasound or a single screening MRI to mammography in women with elevated breast cancer risk. JAMA. 2012;307(13):1394–404.
12. Berg WA. Tailored supplemental screening for breast cancer: what now and what next? AJR Am J Roentgenol. 2009;192(2):390–9.
13. Thigpen D, Kappler A, Brem R. The role of ultrasound in screening dense breasts—a review of the literature and practical solutions for implementation. Diagnostics [Internet]. 2018;8(1):20. Available at: http://www.mdpi.com/2075-4418/8/1/20.
14. Rebolj M, Assi V, Brentnall A, Parmar D, Duffy SW. Addition of ultrasound to mammography in the case of dense breast tissue: systematic review and meta-analysis. Br J Cancer. 2018;118(12):1559–70.
15. Sood R, Rositch AF, Shakoor D, Ambinder E, Pool K-L, Pollack E, et al. Ultrasound for breast cancer detection globally: a systematic review and meta-analysis. J Glob Oncol. [Internet]. 2019;(5):1–17. Available at: https://ascopubs.org/doi/10.1200/JGO.19.00127.
16. Forouzanfar MH, Foreman KJ, Delossantos AM, Lozano R, Lopez AD, Murray CJL, et al. Breast and cervical cancer in 187 countries between 1980 and 2010: a systematic analysis. Lancet (London, England); 2011;378(9801):1461–84.
17. Kelly KM, Richwald GA. Automated whole-breast ultrasound: advancing the performance of breast cancer screening. Semin. Ultrasound, CT MRI [Internet]. 2011;32(4):273–80. Available at: https://linkinghub.elsevier.com/retrieve/pii/S088721711100031X.

18. Mendelson EB, Berg WA. Training and standards for performance, interpretation, and structured reporting for supplemental breast cancer screening. Am J Roentgenol. 2015;204(2):265–8.
19. Huppe AI, Mehta AK, Brem RF. Molecular breast imaging: a comprehensive review. Semin Ultrasound, CT MRI [Internet]. 2018;39(1):60–9. Available at: https://linkinghub.elsevier.com/retrieve/pii/S0887217117301105.
20. Mathis KL, Hoskin TL, Boughey JC, Crownhart BS, Brandt KR, Vachon CM, et al. Palpable presentation of breast cancer persists in the era of screening mammography. J Am Coll Surg [Internet]. 2010;210(3):314–8. Available at: https://linkinghub.elsevier.com/retrieve/pii/S1072751509016196.
21. Tabár L, Vitak B, Chen HH, Duffy SW, Yen MF, Chiang CF, et al. The Swedish Two-County Trial twenty years later. Updated mortality results and new insights from long-term follow-up. Radiol. Clin. North Am. 2000;38(4):625–51.
22. Vanier A, Leux C, Allioux C, Billon-Delacour S, Lombrail P, Molinié F. Are prognostic factors more favorable for breast cancer detected by organized screening than by opportunistic screening or clinical diagnosis? A study in Loire-Atlantique (France). Cancer Epidemiol. [Internet]. 2013;37(5):683–7. Available at: https://linkinghub.elsevier.com/retrieve/pii/S1877782113001070.
23. Moody-Ayers SY, Wells CK, Feinstein AR. Benign tumors and early detection in mammography-screened patients of a natural cohort with breast cancer. Arch Intern Med. American Medical Association;. 2000;160(8):1109–15.
24. Baines CJ, Wall C, Risch HA, Kuin JK, Fan IJ. Changes in breast self-examination behavior in a cohort of 8214 women in the Canadian National Breast Screening Study. Cancer. 1986;57(6):1209–16.
25. Kösters JP, Gøtzsche PC. Regular self-examination or clinical examination for early detection of breast cancer. Cochrane Database Syst Rev. 2003;2003(2):CD003373.
26. Baxter N, Care CTF on PH. Preventive health care, 2001 update: should women be routinely taught breast self-examination to screen for breast cancer? CMAJ [Internet]. 2001;164(13):1837–46. Available at: https://pubmed.ncbi.nlm.nih.gov/11450279.
27. Hackshaw AK, Paul EA. Breast self-examination and death from breast cancer: a meta-analysis. Br J Cancer. 2003;88(7):1047–53.
28. Brett J, Austoker J, Ong G. Do women who undergo further investigation for breast screening suffer adverse psychological consequences? A multi-centre follow-up study comparing different breast creening result groups five months after their last breast screening appointment. J. Public Health (Bangkok) [Internet]. 1998 1;20(4):396–403. Available at: https://academic.oup.com/jpubhealth/article-lookup/doi/10.1093/oxfordjournals.pubmed.a024793.
29. MacFarlane ME, Sony SD. Women, breast lump discovery, and associated stress. Health Care Women Int. 1992;13(1):23–32.
30. Anbar M. Clinical thermal imaging today. IEEE Eng Med Biol Mag. 1998;17(4):25–33.
31. Feig SA, Shaber GS, Schwartz GF, Patchefsky A, Libshitz HI, Edeiken J, et al. Thermography, mammography, and clinical examination in breast cancer screening. Review of 16,000 studies. Radiology. 1977;122(1):123–7.
32. Jones BF. A reappraisal of the use of infrared thermal image analysis in medicine. IEEE Trans Med Imaging [Internet]. 1998;17(6):1019–27. Available at: http://ieeexplore.ieee.org/document/746635/.
33. Egorov V, Kearney T, Pollak SB, Rohatgi C, Sarvazyan N, Airapetian S, et al. Differentiation of benign and malignant breast lesions by mechanical imaging. Breast Cancer Res Treat [Internet]. 2009;118(1):67–80. Available at: http://link.springer.com/10.1007/s10549-009-0369-2.
34. Garra BS. Imaging and estimation of tissue elasticity by ultrasound. Ultrasound Q LWW. 2007;23(4):255–68.
35. Moon WK, Chang R-F, Chen C-J, Chen D-R, Chen W-L. Solid breast masses: classification with computer-aided analysis of continuous US images obtained with probe compression. Radiology. 2005;236(2):458–64.

36. Nyström L, Andersson I, Bjurstam N, Frisell J, Nordenskjöld B, Rutqvist LE. Long-term effects of mammography screening: updated overview of the Swedish randomised trials. Lancet. 2002;359(9310):909–19.
37. Falun Meeting, Falun, Sweden OC and C. Breast-cancer screening with mammography in women aged 40–49 years. Int J Cancer [Internet]. 1996;68(6):693–9. Available at: https://onlinelibrary.wiley.com/doi/10.1002/(SICI)1097-0215(19961211)68:6%3C693::AID-IJC1%3E3.0.CO;2-Z.
38. Mandelson MT, Oestreicher N, Porter PL, White D, Finder CA, Taplin SH, et al. Breast density as a predictor of mammographic detection: comparison of interval- and screen-detected cancers. J Natl Cancer Inst. 2000;92(13):1081–7.
39. D'Orsi CJ. 2013 ACR BI-RADS atlas: breast imaging reporting and data system [Internet]. 5th ed. American College of Radiology; 2014. Available at: https://books.google.com.br/books?id=nhWSjwEACAAJ.
40. Ohuchi N, Suzuki A, Sobue T, Kawai M, Yamamoto S, Zheng YF, et al. Sensitivity and specificity of mammography and adjunctive ultrasonography to screen for breast cancer in the Japan Strategic Anti-cancer Randomized Trial (J-START): a randomised controlled trial. Lancet. 2016;387(10016):341–8.
41. Bakker MF, de Lange SV, Pijnappel RM, Mann RM, Peeters PHM, Monninkhof EM, et al. Supplemental MRI screening for women with extremely dense breast tissue. N Engl J Med. 2019;381(22):2091–102.
42. Kuhl C, Weigel S, Schrading S, Arand B, Bieling H, König R, et al. Prospective multicenter cohort study to refine management recommendations for women at elevated familial risk of breast cancer: the EVA trial. J Clin Oncol. 2010;28(9):1450–7.
43. NCCN – National Comprehensive Cancer Network. Breast Cancer Screening and Diagnosis. In: National Comprehensive Cancer Network (NCCN), editor. NCCN Clinical Practice Guidelines in Oncology. Version 1.2020 ed; 2020.

Chapter 13
Diagnostic

Karina Belickas Carreiro, Juliana Pierobon Gomes da Cunha, Jose Roberto Filassi, and Caio Dinelli

13.1 Diagnostic Management of Clinical Situations

13.1.1 Palpable Changes of the Breast

13.1.1.1 Breast Lump

The clinical complaint referred by the patient can be the first indication of the appearance of breast cancer and should always be valued. The most common clinical complaint is a palpable lump in the breast, but other complaints such as burning feeling, pain, and changes in color, texture, and appearance of the skin can also be mentioned. Despite this fact, it should be emphasized that most palpable complaints correspond to benign lesions in the breasts.

A breast lump is the most frequent presentation of breast cancer, regardless of the woman's age. It can be insidious or fast-growing, depending on the characteristics of the developing tumor. A breast lump is the second most frequent complaint in the breast surgeon's office, after breast pain, and is the most frequent complaint presented by patients with breast cancer.

A study by Barton et al. showed that 16% of the patients in primary healthcare offices had breast complaints during a 10-year period, with women under 50 years old having more complaints (twice as much) when compared to the group of women

K. B. Carreiro · J. P. G. da Cunha · J. R. Filassi (✉)
Departamento de Mastologia, Instituto do Cancer do Estado de Sao Paulo ICESP, São Paulo, SP, Brazil
e-mail: drfilassi@terra.com.br

C. Dinelli
Instituto de Radiologia INRAD, Hospital das Clinicas HCFMUSP, Faculdade de Medicina, Universidade de Sao Paulo, São Paulo, SP, Brazil

S. J. Kim Hsieh, E. A. Morris (eds.), *Modern Breast Cancer Imaging*,
https://doi.org/10.1007/978-3-030-84546-9_13

over 50 years old, and the diagnosis of cancer was made in 23 of the 372 women who presented symptoms (6.2%) [1].

Another palpable complaint that can be a symptom of cancer is breast thickening. This one differs from a mass as it does not have a three-dimensional configuration and presents itself differently from surrounding breast tissues on palpation and does not have a similar area in the contralateral breast, being asymmetrical. Thickening is associated with breast cancer about 5% of the time.

The masses and thickenings associated with breast cancer are ill-defined, are hardened, and may be attached to the skin or muscular plane and may be associated with changes in the skin and papillae, such as retraction.

Because many breast masses may not exhibit distinctive physical findings, imaging evaluation is necessary in almost all cases to characterize the palpable lesion. Any woman presenting with a palpable lesion should have a thorough clinical breast examination, usually by the referring clinician or by a clinical breast specialist, but the radiologist must also be able to establish a concordance between an imaging finding and a clinically detected mass [2].

When a suspicious finding is identified, an image-guided biopsy is indicated. It is preferable to do imaging examinations before biopsy, as changes related to the biopsy may confuse, alter, obscure, and/or limit image interpretation. The negative predictive value of mammography with ultrasound (US) in the context of a palpable mass ranges from 97.4% to 100% [2]. Nevertheless, a negative imaging evaluation should never overrule a strongly suspicious physical examination finding or vice versa. Any highly suspicious breast mass detected by imaging or palpation should undergo biopsy unless there are exceptional clinical circumstances such as the significant comorbid conditions presented by the patient.

Diagnostic mammography is indicated for women aged 40 years and over who present a palpable lump. In several series evaluating palpable breast abnormalities, the sensitivity of mammography alone was 86–91%, depending on the breast density (Fig. 13.1). If a clearly benign correlate for a palpable finding (oil cyst,

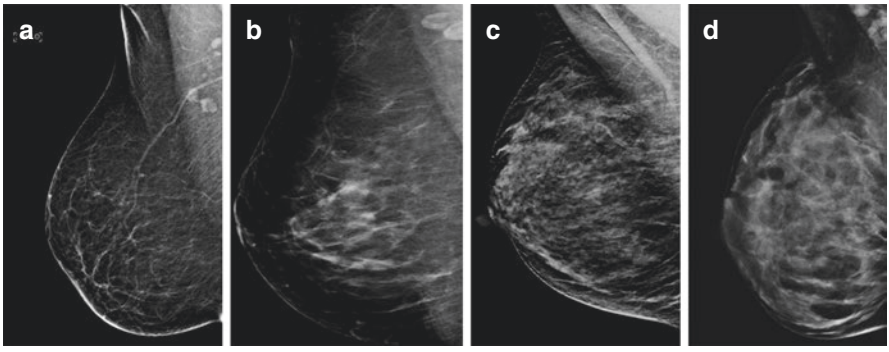

Fig. 13.1 Breast composition on mammography – comparison of breast density: (**a**) Almost entirely fatty. (**b**) Scattered areas of fibroglandular density. (**c**) Heterogeneously dense. (**d**) Extremely dense

hamartoma, degenerating fibroadenoma, lipoma, benign lymph node) can be identified on mammography, this modality alone may be sufficient and clinical follow-up rather than imaging follow-up or tissue sampling is appropriate [3, 4].

The diagnostic mammography technique is similar to screening mammography and may include complementation with additional views (true lateral view, magnification, and localized spot compression for instance), identification of the palpable complaint with a radiopaque marker (Fig. 13.2), and complementation with tomosynthesis if available [5].

If mammography is negative or an imaging correlate is identified that is not clearly benign, multimodality imaging is usually indicated, with targeted US directed toward the palpable finding [6] (Fig. 13.3). In most of these cases, supplemental ultrasound is helpful to further characterize the lesion.

In women younger than 40 years old, pregnant or lactating women, ultrasound should be used as the initial approach to a palpable complaint. Ultrasonography allows real-time image evaluation, can be correlated with mammography, and can

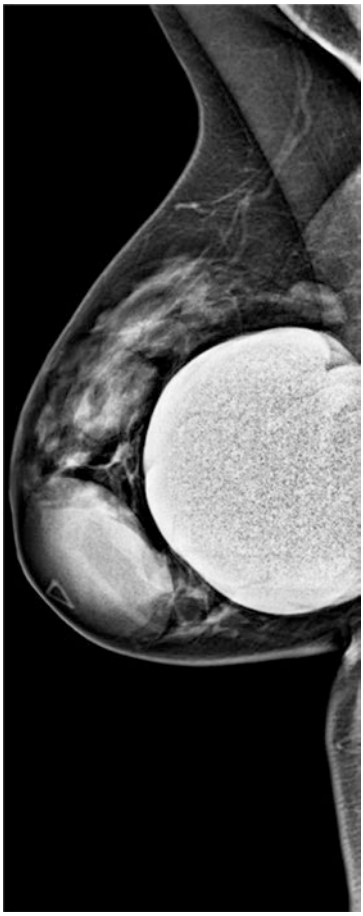

Fig. 13.2 A 30-year-old patient with a palpable lump in the right breast. Mammography shows the skin marker (radiopaque triangular marker) in the topography of a palpable, oval, and circumscribed mass. Histologically proven fibroadenoma

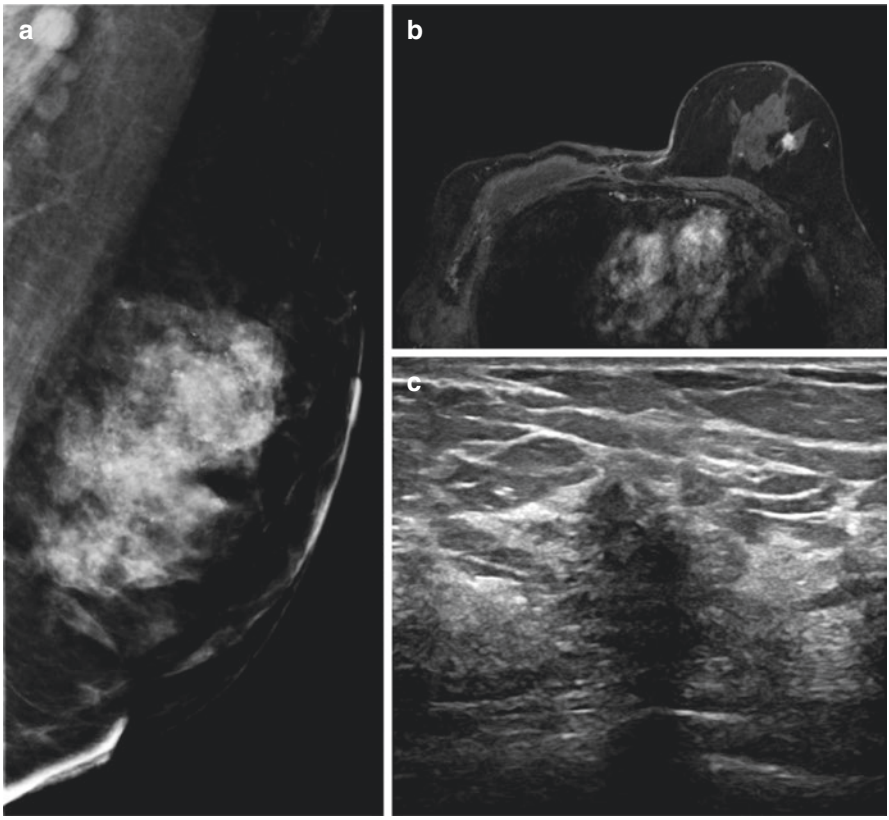

Fig. 13.3 Mammography and magnetic resonance imaging (MRI). (**a**) Mammography was negative for suspicious findings. (**b**) MRI (T1W post-contrast image) showed an irregular mass with homogeneous enhancement in the left breast. (**c**) Second-look ultrasound showed an irregular hypoechogenic mass with indistinct margins. Histologically proven grade 3 ductal carcinoma in situ (DCIS)

also assess superficial cutaneous and subcutaneous lesions with the use of high-frequency transducers and appropriate techniques.

In addition, younger women also tend to have relatively denser breast tissue, which is associated with decreased mammographic sensitivity [6]. However, in the event of a suspicious finding, mammography or digital breast tomosynthesis (DBT) is warranted even in younger women to better delineate disease and identify features of malignancy that may be seen on mammography or DBT alone.

If a palpable lump can be definitively characterized as benign on US (e.g., simple cyst, benign lymph node, duct ectasia, lipoma), clinical follow-up is the appropriate management, and imaging follow-up or tissue sampling is not indicated.

To improve the sensitivity and specificity, the combined use of diagnostic mammography and ultrasonography in palpable lesions has been recommended [2]. The combination of these two imaging modalities increases true positive rates and

allows the detection of masses hidden by dense tissue on mammography. When both tests are negative or show benign findings when assessing a palpable mass, the negative predictive value (NPV) is quite high (> 97%).

The presence of palpable masses with a benign feature on ultrasound has been evaluated in the literature, and it is known that the incidence of cancer in these situations ranges from 0% to 6% but most recent studies indicate an incidence of less than 2%, which would justify its semiannual sonographic follow-up, in a population ideally below 40 years old. In situations of palpable masses in women over 40 years old, with a high family or personal risk of breast cancer, and male patients, masses with documented significant growth or suspicious appearance in any of the imaging exams, a biopsy is always indicated [7].

Breast tomosynthesis added to the mammographic technique appears as an option for breast imaging that eliminates overlapping tissues [5]. In tomosynthesis, multiple projections are obtained while the x-rays emitted by the source follow a pre-defined semicircular angulation; the angle used varies according to the manufacturer; the projections obtained (slices) can still be reconstructed in a synthesized mammographic image, depending on the software model. The radiation dose of the method associated with digital mammography, both performed in a single time, does not exceed the average safe glandular dose [5].

A significant number of prospective studies and some retrospective studies compared the total field digital mammography alone with the total field digital mammography associated with tomosynthesis [8–10]; the results obtained show an increase of about 30% in the breast cancer detection rate, especially in the invasive form, and a decrease in the false-positive results of mammography, consequently reducing the recall rates when tomosynthesis is used. The addition of this technique to mammography shows evidence of increased specificity and sensitivity for invasive tumors. The most evident findings detected by tomosynthesis are architectural distortions and focal asymmetries. In the case of calcifications, these are better visualized by digital mammography, and tomosynthesis does not add significant benefit.

Digital breast tomosynthesis (DBT) can ease some of the limitations encountered with standard mammographic views. In addition to planar images, DBT allows the creation and viewing of thin-section reconstructed images that may decrease the lesion-masking effect of overlapping normal tissue and reveal the true nature of possible false-positive findings. DBT was evaluated predominantly in the screening setting, but it also proved to be useful in the diagnostic setting as well, improving lesion characterization in noncalcified lesions in comparison with the conventional mammographic workup [3, 11, 12].

In symptomatic patients setting, DBT demonstrated better diagnostic accuracy compared to 2D mammography, an improved reader confidence in distinguishing benign from malignant lesions, and higher accuracy in assessing tumor size and identifying multifocal diseases [13] (Fig. 13.4). New equipment are also available for image-guided biopsy using DBT guidance.

Several studies have specifically included women presenting clinical symptoms as palpable lumps, with promising results [4, 11, 12]. The diagnostic accuracy of one-view breast tomosynthesis in the diagnostic workup of women with clinical

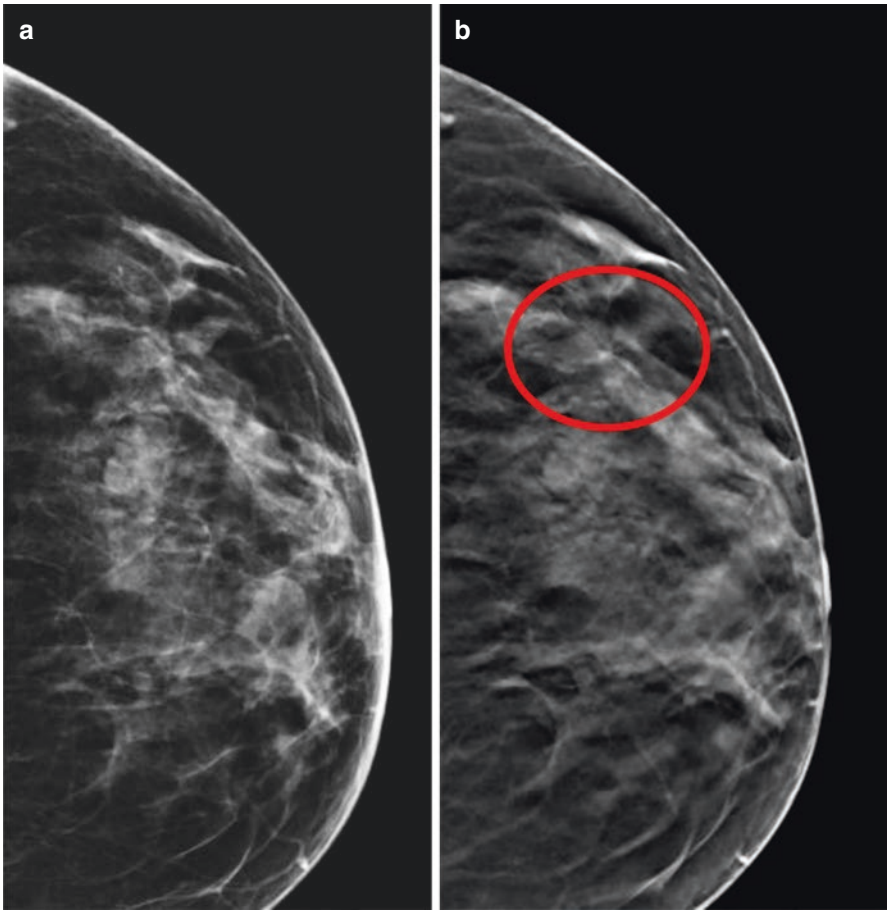

Fig. 13.4 A 42-year-old patient screening mammography with tomosynthesis. (**a**) Conventional 2D mammography was negative for suspicious findings. (**b**) Tomosynthesis showed an area of architectural distortion in the outer upper quadrant of the left breast (circle). Histologically proven grade 2 invasive lobular carcinoma

signs and symptoms and in women recalled from screening has also been shown to be equivalent to or better than supplemental diagnostic mammographic views in several studies [11, 14]. DBT can be used with or without spot compression views in the diagnostic context.

Interpretation time for DBT images is greater than for standard mammography [14, 15]. Additionally, the dose is increased if standard 2D images are obtained in addition to DBT images. However, synthesized reconstructed images (a virtual planar image created from the tomographic data set) may replace the need for a 2D correlate view, and current data suggest that these synthetic images perform as well as standard full-field digital images [14, 16].

In summary, mammography or DBT may be helpful in women between 30 and 39 years old as well as in women younger than 30 years old with palpable masses [5].

Although magnetic resonance imaging (MRI) can be used to assess patients with a palpable mass, it is not the method of choice to start the investigation, and its indication is more suitable for cases in which the palpable lesion is already defined as malignant, in order to assess the extent of disease [2].

In general, it is more cost-effective to use mammography or DBT and US as initial imaging examinations. There are few studies that evaluate the efficacy of MRI specifically in the setting of palpable lesions. A recent study from Moy et al. evaluating MRI workup for conventional imaging BI-RADS 0 cases included 29 palpable masses and found a sensitivity of 100% and specificity of 74% for this palpable lesion subset [2].

MRI may be of value in the very specific circumstance of distinguishing between scarring and recurrent disease in the context of a post lumpectomy patient with a palpable lump at the surgical site and inconclusive conventional imaging findings; however, the evidence for this indication is not well established. In addition, breast MRI without intravenous contrast has no role in the evaluation of a woman with a palpable breast mass.

In patients with a biopsy-proven breast cancer, MRI may be used to assess the extent of disease and detect additional lesions in the same quadrant (multifocal), in different quadrants (multicentric) or in the contralateral breast potentially impacting patient management. In this context, MRI is more useful than mammography and US in the staging of multifocal and multicentric disease or when DCIS is present. In addition, numerous studies have shown that MRI is superior to mammography and US for assessing tumor size, although there are still over- and underestimation in up to 15% of patients.

Magnetic resonance imaging may also detect cancers that were occult on mammography and/or sonography in the contralateral breast in approximately 3% of women with unilateral cancer detected by mammography or US. The detection of these initially unsuspected tumors may have a greater impact on patient outcomes than the detection of additional ipsilateral tumor foci since they would not be treated with concomitant radiation therapy [17].

13.1.1.2 Paget Disease

Since 1307 breast lesions have occurred similar to what we now recognize as Paget's breast disease, but which were only described as such in 1874 by Sir James Paget. Clinically, it corresponds to a lesion in the nipple-areola complex (NAC) represented by eczema, erythema, pruritus, and ulceration. Unlike papillary lesion due to invasion of the underlying tumor, Paget's breast disease is characterized by the cell described as large, pale-staining cells with round or oval nuclei and prominent nucleoli. It is considered a rare pathology, comprising 1–4% of cases of malignant breast disease [18].

In a paper published by Fu et al., 41 cases of Paget's disease treated at Providence Hospital & Medical Centers from 1980 to 1999 were analyzed. Of these patients, 17 had a palpable mass at diagnosis, which resulted in an invasive lesion in 100% of cases and positive axillary lymph node in 70%. Among the 24 patients who did not have a palpable mass, 30% had invasive lesions, 66% only ductal carcinoma in situ, and only 1 Paget's disease. The lymph node involvement in these patients reached 30% [19].

Song et al. analyzed 72 cases seen between 1991 and 2010 in their service in Wuhan, China, among which 60% had palpable masses; 25% suspected axillary lymph nodes, with the final histologic result of 45 cases associated with invasive carcinoma; 12 cases of ductal carcinoma in situ; and 9 cases with isolated Paget's disease. Of the total number of patients, there were 34 with affected axillary lymph node, 32 with invasive disease, and 2 with in situ disease. None of the patients with isolated Paget's disease had axillary involvement [20].

Although it is a noninvasive disease, about 8% of cases may present invasion of the basement membrane by Paget cells, being important to differentiate it from invasive diseases with skin involvement, due to the diverse prognosis between strains. Lee et al. in a retrospective study with 205 cases of breast Paget's disease identified 16 cases of invasive Paget's disease, of which 12 had invasive carcinoma and 3 associated ductal carcinomas in situ in another location of the breast. The comparison between cases with and without nipple invasion did not show worsening of prognosis during the follow-up of patients [20].

The evaluation using imaging methods is important for the identification of other breast lesions that may be associated, without alterations in the clinical examination, and for assessing the extent of involvement of the nipple-areola complex (NAC) (Fig. 13.5) [21]. Zakaria et al. published a retrospective study, with data collected between 1975 and 2000, including 86 patients diagnosed with Paget's disease of which 82 had data from the preoperative clinical evaluation and mammography. All patients with suspected mammographic and clinical findings including nipple complaints had invasive disease confirmed in the final specimen histology. Among patients without clinical changes, but with suspected mammographic findings, 93% had an additional malignant lesion in the breast, 45% of which was invasive, and 48% in situ. Even in the group in which neither clinical changes nor suspicious mammographic alterations were observed, there was an occurrence of 73% of previously undiagnosed lesions, being 68% in situ and 5% invasive [22].

Morrogh et al. published a series at the Memorial Sloan Kettering Cancer Center in which 69 patients with NAC-related breast complaints were selected from 2294 patients who sought the service for various breast complaints, without a previous diagnosis of cancer. Of the 69 patients submitted to NAC biopsy, 34 confirmed a diagnosis of Paget's disease. All patients underwent mammography to assess the extent of disease and to assess additional lesions, yielding 67% lesions characterized as BIRADS 3 and 33% lesions characterized as BIRADS 4 or 5. All BIRADS 3 patients underwent surgery (total of 15) or underwent complementary MRI (total

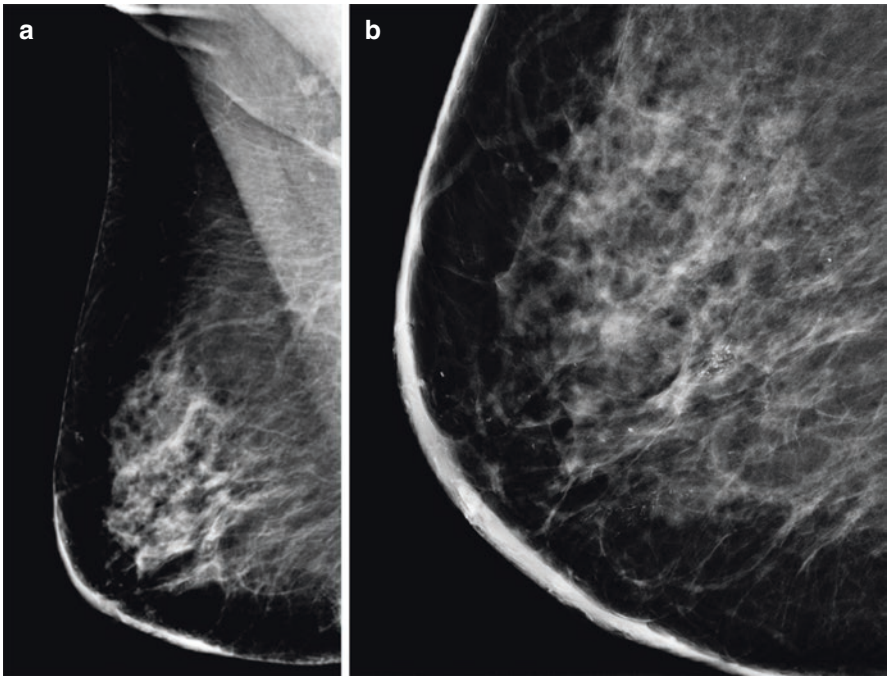

Fig. 13.5 A 63-year-old patient with Paget's disease of the right breast. (**a**) The mammography showing a diffuse thickening of the nipple-areola complex and fine pleomorphic calcifications in segmental distribution in the breast extending to the nipple. Histologically proven grade 3 DCIS. (**b**) Mammmographic magnification view showing pleomorphic calcifications in segmental distribution

of 8), and all patients with suspected lesions had a histological confirmation of an additional malignancy. Among the patients submitted to MRI, 50% had biopsy-proven suspicious lesions. The remaining four patients had confirmation of malignancy only in the final histological result from surgical specimen analysis. This work was able to demonstrate the possibility of an adequate surgical scheduling. The surgical procedures were divided into 21 mastectomies and 17 conservative surgeries, of which only 4 were converted to mastectomy after the final result. 59% of patients had disease only in the central breast sector [23].

Although Paget's disease affects only NAC and is almost exclusively in situ, it can present invasion of the basement membrane and lymph node involvement, influencing directly the proposed treatment. In addition, associated malignant lesions are often associated with Paget's disease, and proper assessment of the rest of the breast tissue is essential. Patients with suspected lesions on clinical examination are usually diagnosed with associated malignancy. Even those patients with no palpable changes should undergo mammography and eventually MRI, to define the extent of disease and look for additional lesions that need attention during treatment.

13.1.1.3 Occult Breast Cancer and Axillary Lymphadenopathy

Axillary lymph nodes receive drainage from the arm, chest wall, and breast, that is, any benign or malignant pathology that occurs in these regions may be associated with local lymphadenopathy. Some neoplastic diseases may also be associated with the involvement of axillary lymph nodes, even from distant sites, such as primary tumors of the pancreas, ovary, and bladder, in addition to lymphoma itself. We call it occult breast carcinoma when there is a metastatic axillary lesion with immunohistochemistry pointing to the breast as the primary tumor, with no changes in clinical or radiological examination (Fig. 13.6). The most commonly used radiological evaluation is mammography and ultrasound, but nowadays MRI shows better performance in detecting the primary tumor.

The incidence of occult breast carcinoma was around 0.3–1.0% between the 1950s and 1980s, as shown by the survey by Ge et al. in which the main radiological exam for breast investigation was mammography [24]. However, in a 2017 publication, Hessler et al. published their own statistics based on the National Cancer Database (NCDB). The NCDB is a clinical oncology database sponsored by the

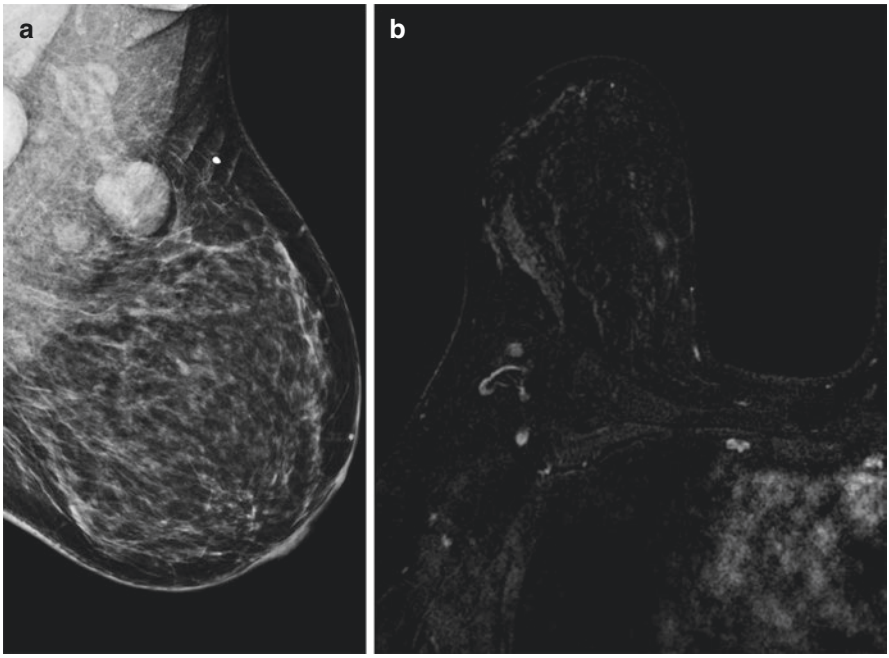

Fig. 13.6 Occult breast carcinoma in a 34-year-old patient with BRCA1 mutation presenting with palpable lumps in the left axilla. (**a**) Mammogram shows multiple enlarged axillary lymph nodes. No suspicious findings in the breast. (**b**) MRI (T1W post-contrast image with subtraction) of the same patient shows multiple round lymph nodes with obliteration of the fatty hilum and heterogeneous enhancement. No suspicious enhancements were found in the breast. *Histology of axillary lymph nodes:* metastatic triple-negative breast carcinoma

American College of Surgeons and the American Cancer Society. In this study, they found an incidence of 0.1%, with an analysis carried out between the years 2004 and 2013, with 1853 patients [25]. With the evolution of imaging exams and improved resolution of the images generated by the mammographic and ultrasound devices, in addition to the beginning of the MRI exams, it was possible to identify the primary breast lesions that were not possible before.

Vlastos et al. published a survey carried out at MD Anderson of patients treated at these sites with a metastatic axillary disease, with no specific primary site. Of the 479 identified patients, 45 were considered to be primarily of breast origin. The inclusion criteria were lymph node biopsy with histological diagnosis of adenocarcinoma or undifferentiated or unclassified carcinoma. All patients underwent surgical treatment, with 13 having mastectomies and 32 breast-conserving surgeries. The proposed conservative surgery was the resection of the superolateral quadrant of the breast, which is a denser region with the highest prevalence of breast tumors, comprising about 50%. It was possible to identify among the patients who underwent mastectomy 1 case of invasive tumor and 1 case of Paget's disease. Among the patients who underwent conservative surgery, 10 cases of malignant disease were identified, not stratified as invasive or in situ [26].

Within breast assessment, one factor that makes it difficult to diagnose breast lesions is the localization in the axillary tail or accessory mammary gland. However, MRI sensitivity can reach 95%, after negative mammography, ultrasound, and clinical examination, and 71% specificity, as demonstrated in a 2011 study [27]. Currently there are studies that question the existence of ectopic breast tissue in axillary lymph nodes, which would characterize occult carcinoma in this way, but with the possibility of definition only after surgery for histological confirmation [28].

Axillary metastasis can arise from the breast or any other extra-mammary site, requiring histological and immunohistochemical assessment to define the primary lesion. When compatible with breast origin without clinical evidence on physical examination, complementary radiological examinations are essential to search for the primary lesion. The initial workup consists of conventional imaging evaluation with mammography and ultrasound, and complementation with MRI when conventional imaging is negative. There are studies that include positron emission tomography (PET) scan, but this is not part of the initial recommendation for investigation yet [29].

13.1.2 Non-palpable Breast Changes

13.1.2.1 Image Screening Findings

The aim of mammographic screening is to reduce mortality rates from breast cancer through early detection compared to cancers diagnosed clinically at a later stage. Despite ongoing controversy, the effectiveness of mammographic screening

and the importance of diagnosing breast cancers at an early stage have been emphasized [30]. It is known that current screening with 2D digital mammography (2DDM) detects some cancers that might not cause symptoms during the woman's natural life. This has been termed "overdiagnosis," and the frequency of detecting such cases has been discussed in the independent review of breast screening. Screening with DBT will detect even more breast cancers at an earlier stage in some cases [5].

The accuracy of 2DDM screening is limited because of the effect of overlapping of normal breast structures and abnormal features on a two-dimensional image. The mammographic signs of breast cancer may be partially or completely obscured, particularly in women with a dense glandular parenchymal pattern on mammography, leading to delays in the diagnosis of breast cancer.

DBT demonstrates mammographic characteristics of soft-tissue lesions better than 2DDM, which leads to improved diagnostic accuracy, more accurate workup of soft-tissue lesions, and better local staging, with performance shown to be even more beneficial in women with dense breasts. There is improved interpretive performance of DBT in the detectability of invasive lobular cancers that present as distortions and spiculations as these lesions are more conspicuous on DBT.

Conversely, well-defined margins of benign lesions are more clearly demonstrated, potentially eliminating the need for biopsy and reducing recall rates. The better visibility of the margins of soft-tissue lesions improves the ability of the radiologist to distinguish between benign and malignant masses [5, 8, 31]. Circumscribed masses may also show a halo sign on DBT. For soft-tissue lesions, DBT improves the classification of the mammographic features seen on 2DDM and the accuracy of predicting malignancy.

In the largest retrospective study involving 7060 subjects, the TOMMY trial, the addition of DBT improved sensitivity in women with dense breasts (93% versus 86% for DBT versus 2DDM, in women with breast density of 50% or more; p1/40.03). Specificity was significantly improved in all subgroups (57% for 2DDM, 70% for 2DDM + DBT; $p < 0.001$ in both cases) [9].

13.1.2.2 Nipple Discharge

Nipple discharge corresponds to the majority of complaints from patients who seek breast surgeons, with an incidence of 2.5–5% [32–34]. Nipple discharge can be spontaneous or provoked, uniductal or multiductal, unilateral, or bilateral and can have several presentations: serous, bloody, milky, greenish, or transparent. The flow can be secondary to organic or structural causes. Among the organic causes, we can highlight the postpartum pregnancy cycle, metabolic changes, and the use of medications. Normally, in these situations, the flow is multiductal and bilateral and with a dairy aspect. In the case of structural changes, the flow most commonly presents itself as unilateral, with uni or multiductal secretion output, and can be spontaneous or provoked [35]. Among the most frequent causes of nipple discharge due to anatomical changes are papilloma (35–48%), carcinoma (5–21%), and ductal ectasia or

fibrocystic changes (3–50%), but it varies greatly between studies according to the type of complaint and clinical and radiological alteration included [32].

The initial assessment of patients with complaints of nipple discharge must contain clinical history and physical examination, in order to better characterize the flow and identify possible tangible changes. In the case of palpable complaints, it is possible to perform an examination directed to the site, through ultrasound or mammography. In cases of absence of palpable lesions, there is the benefit of evaluation by means of MRI [36]. Ductography is an evaluation of the affected duct through the injection of iodinated contrast and, afterwards, mammography with subareolar magnification to view possible defects of the ductal tree (Fig. 13.7). It is able to identify single or multiple lesions, in addition to peripheral lesions when the affected duct is well identified [33].

Adepoju et al. evaluated 168 cases of patients with spontaneous and uniductal papillary flow, of which 85% were bloody. Mandatory mammography, physical examination, and evaluation by complementary ductography and ultrasound, if the team considered it opportune, were performed before ductal resection to evaluate the etiology and its imaging correlation. Malignant lesions were diagnosed in 12% of cases and high-risk lesions in 11%. The mean age of patients with benign changes was 51 years old, with high-risk lesions 57 years old and malignant lesions 69 years. The sensitivity and specificity of ultrasound and mammography ranged from 10% to 35% and 68% to 94%, respectively, in high-risk and malignant lesions. Ductography, when performed, showed sensitivity and specificity of 75% and 49–53%, respectively, for high-risk and malignant lesions, but showed some limitations as scarcity of places and professionals able to perform the procedure, in

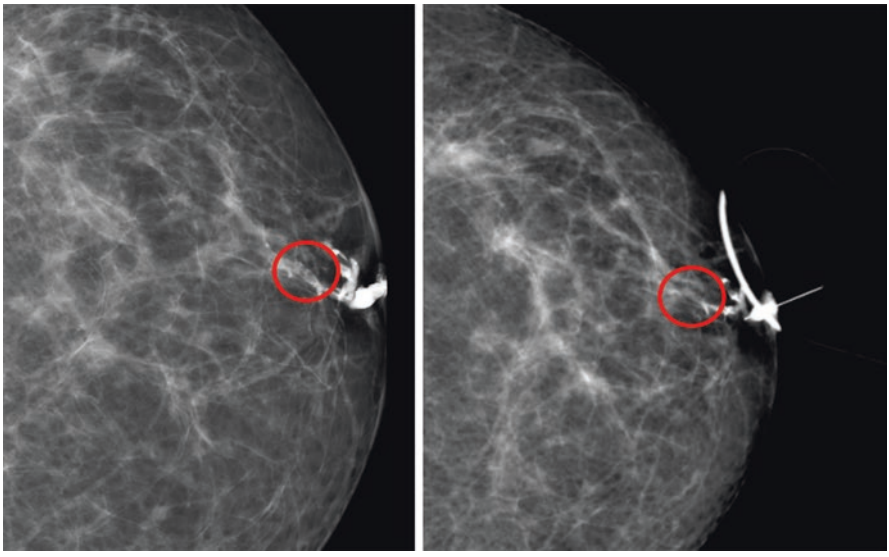

Fig. 13.7 Ductography in a 72-year-old patient with bloody nipple discharge in the left breast showing a filling defect (circle). Histologically proven intraductal papilloma

addition to anatomical variations that may make it impossible, such as ductal atrophy secondary to age [37].

Currently, the use of ductography has been questioned due to the discomfort potentially caused by duct catheterization and contrast injection, in addition to the need for a trained staff for the exam. Consequently, Baydoun et al. published an article evaluating 94 patients retrospectively, who underwent ductography between January 2005 and October 2010. The indications for the exam consisted of a woman with a negative image exam but with a persistent or bloody discharge in a 1-month clinical follow-up, and the biopsy result of an identified lesion was incongruous with the clinic or in a presurgical evaluation. In case the ductography was not performed properly or if it was negative, the patient was referred for contrast MRI exam (a total of 12 exams). Seven malignant lesions were identified (5 DCIS and 2 Invasive cancers) and 3 premalignant lesions (atypical hyperplasia). Comparing the exams, the sensitivity of mammography, ultrasound, and ductography were, respectively, 13%, 73%, and 76%. The low number of MRI performed in this study precluded the comparison with other modalities, but its sensibility appeared to be comparable to ductography (Fig. 13.8) [38].

Bahl et al. in a retrospective study evaluated a group of 118 women with papillary flow complaints with at least one of these characteristics: unilateral bloody, serous, or spontaneous. In these women, an evaluation with contrast MRI was performed after a negative mammography and ultrasound. Four cases of DCIS and two cases of invasive cancer not previously identified were diagnosed but with two false negatives cases (two cases of BIRADS 3 biopsied during the follow-up) [39].

Sanders et al. in a retrospective study evaluated 200 women with bloody nipple discharge with negative mammographic and ultrasound evaluation who would undergo duct resection. A total of 115 patients were submitted directly to surgery, and 85 underwent contrast MRI before. In both groups, the incidence of malignant breast cancer was 7%, and in the MRI group, only one case of false negative was identified (the final histological result of low-grade ductal carcinoma), but three malignant lesions were identified in the contralateral breast. The main causes for

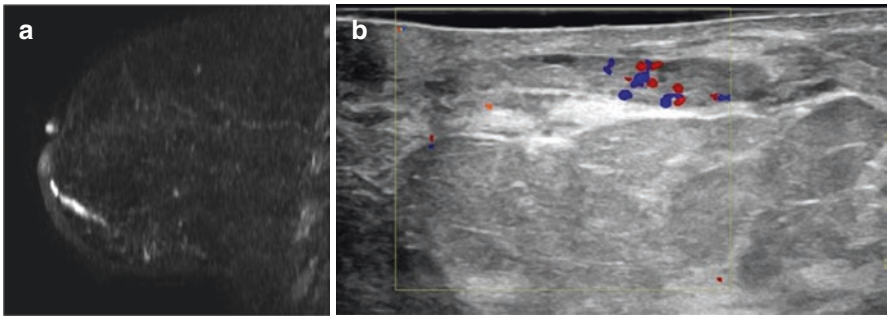

Fig. 13.8 A 46-year-old patient with bloody nipple discharge. (**a**) MRI (post-contrast subtracted image) shows a linear ductal enhancement in the left breast. (**b**) Second-look ultrasound depicted an intraductal mass with vascular flow on Doppler imaging. Biopsy proven Intraductal papilloma

papillary flow were papilloma, periductal inflammation, ectasia/ ductal hyperplasia, and fibrocystic disease [39].

Based on the literature, patients with suspected nipple discharge, which are, unilateral, uni- or multiductal, persistent, or spontaneous, associated with changes in physical examination, should undergo a targeted imaging examination to assess the flow etiology. If there is no palpable change, this radiological evaluation is indicated in order to determine possible non-palpable intraductal changes. Among the exams that can be performed, mammography and ultrasound can be included, and if these tests are negative, complementation with MRI is indicated. Ductoscopy can be performed to identify small lesions; however, a trained team is required to perform this procedure as it can cause discomfort to the patient associated with the exam. It is important to highlight that even the most complex changes in papillary flow are commonly associated with benign lesions, such as adenomas and papillomas.

Whenever there is a suspected lesion after radiological evaluation, histological evaluation of the alteration is necessary. It is possible to choose the evaluation through biopsies guided by the imaging method responsible for identifying the alteration or surgical biopsy, when a diagnosis was not possible.

13.1.3 Breast Biopsy in Clinical Scenario

If a suspicious mass has been identified on mammography, DBT, MRI, or US, tissue sampling is warranted except in rare circumstances (e.g., if the patient has comorbidities that would contraindicate biopsy). If a lesion is seen equally well on mammography and US, US guidance is preferred because of patient comfort, efficiency, economy, absence of ionizing radiation, and sampling accuracy due to real-time visualization of the needle within the lesion.

13.1.3.1 US and Mammography-Guided Biopsy (Fine-Needle Aspiration (FNA)/Core-Needle Biopsy (CNB)/Vacuum Aspiration Biopsy (VAB))

Although some practices demonstrate very good results using fine-needle aspiration (FNA) biopsy as the first means of diagnostic evaluation of a palpable breast mass, especially if a cytopathologist is available to interpret results in real time [16, 40], larger series demonstrate that core biopsy is superior to FNA in terms of sensitivity, specificity, and correct histological grading of palpable masses [41]. Core biopsy is therefore recommended in most cases. Either stereotactic or DBT (x-ray) or US guidance can be used for core biopsy, especially if the mass is vaguely palpable, small, deep, or mobile or if there are multiple lesions [40]. Even when a lesion is clinically palpable, image-guided biopsy has advantages over tissue sampling by palpation, allowing confirmation of biopsy accuracy and the possibility to place a post-biopsy marker clip.

The decision to perform surgical excisional versus percutaneous biopsy should involve the patient and her healthcare provider. However, image-guided core-needle biopsy has become the procedure of choice for most image-detected breast lesions requiring tissue diagnosis. Its advantages over surgical biopsy are well recognized, including less scarring, fewer complications, faster recovery, lower cost, and similar accuracy.

The cytological or histological diagnosis of suspected breast lesions by fine-needle aspiration cytology (FNAC)/core needle biopsy (CNB) has the advantage of allowing surgical planning or scheduling of neoadjuvant therapies for patients with malignancies and limiting the number of surgeries for patients who do not have a malignant disease. Concerning the preoperative assessment of breast cancer, both CNB and FNA are promising tools for the nonoperative pathological diagnosis of breast cancer. Nevertheless, FNA and CNB are methodologically different and have their advantages and disadvantages [16, 41, 42].

FNA is a diagnostic procedure in which a pathologist or radiologist or surgeon uses a very thin needle (usually 22 to 25 gauge) connected to a vacuumed syringe to aspirate a small amount of tissue from the suspicious area. FNA was first introduced by Martin and Ellis in 1930. Its use to detect breast lesion became increasingly important from the 1980s as a diagnostic adjunct in the population-based screening setting. FNA is a safe, economical, effective, and accurate technique, but its efficacy largely depends on the experience of those who perform the procedure and pathologists.

CNB is a technique that usually performed by a radiologist or surgeon using a large, hollow needle (a special 8–16 gauge) to withdraw small tissue fragments from the abnormal area in the breast. CNB was introduced as an assessment tool in the late 1990s. In addition to its high accuracy, CNB provides more material for grading tumors and for assessing predictive factors like hormone receptor status and HER2 (human epidermal growth factor receptor 2) status. On the other hand, it is more expensive and more invasive than FNA and has a rare but potential risk of track seeding in the biopsy path.

In most of the varied clinical studies, in general but not invariably, CNB has both higher sensitivity and specificity than FNA in diagnosing suspicious lesions, e.g., sensitivity and specificity values can range from 35% to 95% and 48% to 95% for FNA and 85% to 100% and 86% to 100% for CNB, respectively [42, 43].

Although thousands of people with suspected breast lesions have been enrolled in diagnostic studies for breast cancer by using FNA and/or CNB, no formal quantitative review of the available evidence has been published to comprehensively compare the accuracy performance of those two techniques. Nowadays, the use of FNA is in decline due to its limitations and its replacement by CNB, but it still remains as an important modality as FNA is fast, convenient, and economical [40].

Wang et al. studied 1802 patients and showed in a pooled analysis that the sensitivity of CNB is better than of FNA [87% (95% CI, 84%e88%, I2 1/4 88.5%) versus 74% (95% CI, 72%e77%, I2 1/4 88.3%)] and the specificity of CNB is similar to FNA [98% (95% CI, 96% e99%, I2 1/4 76.2%) versus 96% (95% CI, 94%e98%, I2 1/4 39.0%)]. For subgroup analysis, the sensitivities of both tests are better for

palpable lesions than for non-palpable lesions. The study suggests that both FNA and CNB have good clinical performance. In similar circumstances, the sensitivity of CNB is better than that of FNA, while their specificities are similar. FNA could be still considered the first choice to evaluate suspicious non-palpable breast lesions [42].

Under stereotactic guidance, vacuum-assisted biopsy (VAB) has proven to be more effective than CNB and less invasive than surgical excision of breast lesions. VAB is being increasingly utilized as an alternative to stereotactic-guided CNB. The advantages include biopsy of lesions only visible on DBT/2DDM, low-density lesions or lesions only identifiable on one view, fewer exposures required, better technical accuracy in localizing masses, distortions, and asymmetrical densities. Several studies have shown superior accuracy in lesion targeting and a lower complication rate [5, 44].

13.1.3.2 MRI- and DBT-Guided Biopsy

The result of the widespread use of MRI in breast diagnostics is an increase in incidental findings. Because of the high sensitivity and lower specificity of breast MRI, it is imperative that these findings be histologically assessed before any surgical intervention [41, 45].

The first step to investigate any MRI abnormalities should be a second-look targeted US. The efficacy of the second-look US is reported between 23% and 71%, with a malignancy detection rate of 15–56% [44, 45]. Larger enhancing masses and BIRADS 5 (highly suspicious for malignancy) lesions are more readily identified on a second-look targeted US, with a detection rate estimated between 25% and 62%; however, certain types of MRI lesions, such as non-mass enhancement or small foci less than10 mm, are less likely to have a US correlate, with a detection rate ranging from 11% to 42%. In a positive sonographic correlation, it is better to perform intervention under US guidance instead of MRI, because it is simpler, faster, and more cost-effective than MRI.

The possible MRI-guided interventions are wire localization of breast lesions followed by a surgical biopsy, CNB, and VAB [44].

Wire localization was one of the earliest procedures to be attempted under MR guidance. The technique has been performed freehand and with guidance systems in open and closed magnets with patients in supine, prone, and prone oblique positions. The relatively large surgical specimen reduces the chance of sampling error and compensates for some inaccuracy of needle placement. In a series of 101 patients, Eby et al. reported placement of the needle tip within 10 mm of the target in 53% of cases and between 11 and 20 mm in 46% of cases with successful excision in 100% [45].

CNB under MRI guidance also requires an extremely accurate targeting technique. Postfire sequences should demonstrate the needle within the target. Therefore, the patient must be scanned with the device in place. To achieve this goal, MRI-compatible CNB devices must be composed of nonferrous alloys including various

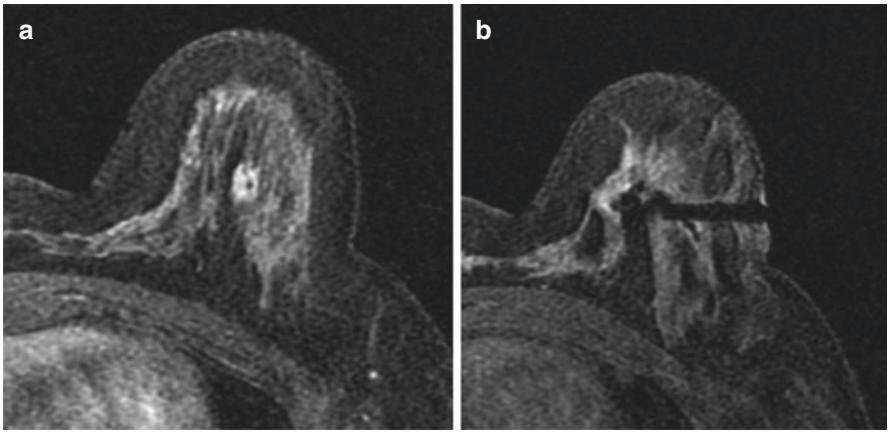

Fig. 13.9 MRI-guided biopsy in a 39-year-old patient with Li-Fraumeni syndrome. (**a**) Pre-biopsy image (T1W post-contrast image) shows an irregular mass with heterogeneous enhancement in the left breast. (**b**) Post-biopsy image (T1W post-contrast) shows a dark linear structure extending from the biopsy site to the lateral skin, corresponding to the artifact of the biopsy needle. Susceptibility artifacts from gas bubbles and tissue marker are also seen on the biopsy site. Histologic result: grade 1 tubulo lobular carcinoma

amounts of titanium and nickel. As a result of the advances and refinements, MRI-guided CNB is considered both safe and accurate with published reports of a high rate of technical success (95–100%) and cancer yields (20–38%) comparable to the accepted rates reported in mammographic- and sonographic-guided procedures.

The Mammotome (Ethicon Endo-Surgery) is an 11-gauge MRI-compatible VAB system. It was the first system to be developed and subsequently proved that VAB is possible under MRI guidance (Fig. 13.9). Clinical studies in Europe have demonstrated successful VAB in 98% of 341 lesions and have identified important barriers to the more widespread use of this technology, including needle artifact, tissue displacement during probe insertion, and washout of contrast enhancement during the procedure. These challenges limited the application of this early technology to lesions larger than 10 mm in diameter.

DBT-guided breast biopsy has been developed both for use with standard DBT mammographic equipment and dedicated prone table apparatus, often combined with stereotaxis. It is essential for lesions seen only with DBT and may be used as an alternative to stereotactic-guided VAB for both sonographically occult and soft-tissue lesions with micro-calcifications [44].

References

1. Barton MB, Elmore JG, Fletcher SW. Breast symptoms among women enrolled in a health maintenance organization: frequency, evaluation, and outcome. Ann Intern Med. 1999;130(8):651–7. https://doi.org/10.7326/0003-4819-130-8-199904200-00005.

2. Moy L, et al. ACR appropriateness criteria® palpable breast masses. J Am Coll Radiol. 2017;(5S):S203–S224. https://doi.org/10.1016/j.jacr.2017.02.033.
3. Ciatto S, Houssami N. Breast imaging and needle biopsy in women with clinically evident breast cancer: does combined imaging change overall diagnostic sensitivity? Breast. 2007;(4):382–6. https://doi.org/10.1016/j.breast.2007.01.007.
4. Murphy IG, et al. Analysis of patients with false negative mammography and symptomatic breast carcinoma. J Surg Oncol. 2007;16(4):382–6. https://doi.org/10.1002/jso.20801.
5. Michell MJ, Batohi B. Role of tomosynthesis in breast imaging going forward. Clin Radiol. 2018;73(4):358–71. https://doi.org/10.1016/j.crad.2018.01.001.
6. Durfee SM, et al. Sonographic evaluation of clinically palpable breast cancers invisible on mammography. Breast Journal. 2000;6(4):247–51. https://doi.org/10.1046/j.1524-4741.2000.99111.x.
7. Gilbert FJ, Pinker-Domenig K. Diagnosis and staging of breast Cancer: when and how to use mammography, tomosynthesis, ultrasound, contrast-enhanced mmmography, and magnetic resonance imaging; 2019 Feb 20. In: Hodler J, Kubik-Huch RA, von Schulthess GK, editors. Diseases of the Chest, Breast, Heart and Vessels 2019–2022: Diagnostic and Interventional Imaging [Internet]. Cham (CH): Springer; 2019. Chapter 13. https://doi.org/10.1007/978-3-030-11149-6_13.
8. Greenberg JS, et al. Clinical performance metrics of 3D digital breast tomosynthesis compared with 2D digital mammography for breast cancer screening in community practice. Am J Roentgenol. 2014;203(3):687–93. https://doi.org/10.2214/AJR.14.12642.
9. Gilbert FJ, et al. The TOMMY trial: a comparison of TOMosynthesis with digital mammography in the UK NHS breast screening programme – a multicentre retrospective reading study comparing the diagnostic performance of digital breast tomosynthesis and digital mammography with. Health Technol Assess. 2015;19(4):i–xxv, 1–136. https://doi.org/10.3310/hta19040.
10. Vedantham S, et al. Digital breast tomosynthesis: state of the art1. Radiology. 2015;277(3):663–84. https://doi.org/10.1148/radiol.2015141303.
11. Shetty MK, Shah YP, Sharman RS. Prospective evaluation of the value of combined mammographic and sonographic assessment in patients with palpable abnormalities of the breast. J Ultrasound Med. 2003;22(3):263–8; quiz 269–70. https://doi.org/10.7863/jum.2003.22.3.263.
12. Lehman CD, Lee AY, Lee CI. Imaging management of palpable breast abnormalities. Am J Roentgenol. 2014;203(5):1142–53. https://doi.org/10.2214/AJR.14.12725.
13. Dennis MA, et al. Breast biopsy avoidance: the value of normal mammograms and normal sonograms in the setting of a palpable lump. Radiology. 2001;219(1):186–91 https://doi.org/10.1148/radiology.219.1.r01ap35186.
14. Bernardi D, et al. Application of breast tomosynthesis in screening: incremental effect on mammography acquisition and reading time. Br J Radiol. 2012;85(1020):e1174–8. https://doi.org/10.1259/bjr/19385909.
15. Dang PA, et al. Addition of tomosynthesis to conventional digital mammography: effect on image interpretation time of screening examinations. Radiology. 2014;270:49–56. https://doi.org/10.1148/radiol.13130765.
16. Liew PL, et al. Rapid staining and immediate interpretation of fine-needle aspiration cytology for palpable breast lesions: diagnostic accuracy, mammographic, ultrasonographic and histopathologic correlations. Acta Cytol. 2011;55(1):30–7. https://doi.org/10.1159/000320869.
17. Spick C, et al. Breast MRI used as a problem-solving tool reliably excludes malignancy. Eur J Radiol. 2015;84(1):61–4. https://doi.org/10.1016/j.ejrad.2014.10.005.
18. Sven J, Kister MD, Cushman D, Haagensen M. Paget's disease of the breast. Am J Surg. 1970;119(5):606–9. https://doi.org/10.1016/S1776-9817(06)73026-7.
19. Fu W, Mittel VK, Young SC. Paget disease of the breast: analysis of 41 patients. Am J Clin Oncol. 2001;24(4):397–400. https://doi.org/10.1097/00000421-200108000-00019.
20. Lee HW, et al. Invasive Paget disease of the breast: 20 Years of experience at a single institution. Human Pathol. Elsevier Inc. 2014;45(12):2480–7. https://doi.org/10.1016/j.humpath.2014.08.015.

21. Lim HS, et al. Paget disease of the breast: mammographic, US, and MR imaging findings with pathologic corelation. Radiographics. 2011;31(7):1973–88. https://doi.org/10.1148/rg.317115070.
22. Zakaria S, et al. Paget's disease of the breast: accuracy of preoperative assessment. Breast Cancer Res Treat. 2007;102(2):137–42. https://doi.org/10.1007/s10549-006-9329-2.
23. Morrogh M, et al. MRI identifies otherwise occult disease in select patients with Paget disease of the nipple. J Am Coll Surg. 2008;206(2):316–21. https://doi.org/10.1016/j.jamcollsurg.2007.07.046.
24. Ge LP, et al. Clinicopathological characteristics and treatment outcomes of occult breast cancer: a SEER population-based study. Cancer Manag Res. 2018;10:4381–91. https://doi.org/10.2147/CMAR.S169019.
25. Hessler LK, et al. Factors influencing management and outcome in patients with occult breast cancer with axillary lymph node involvement: analysis of the national cancer database. Ann Surg Oncol. Springer International Publishing,. 2017;24(10):2907–14. https://doi.org/10.1245/s10434-017-5928-x.
26. Vlastos G, et al. Feasibility of breast preservation in the treatment of occult primary carcinoma presenting with axillary metastases. Ann Surg Oncol. 2001;8(5):425–31. https://doi.org/10.1007/s10434-001-0425-6.
27. Lu H, et al. Breast magnetic resonance imaging in patients with occult breast carcinoma: evaluation on feasibility and correlation with histopathological findings. Chin Med J. 2011;124(12):1790–5. https://doi.org/10.3760/cma.j.issn.0366-6999.
28. Terada M, et al. Occult breast cancer may originate from ectopic breast tissue present in axillary lymph nodes. Breast Cancer Res Treat. Springer US,. 2018;172(1):1–7. https://doi.org/10.1007/s10549-018-4898-4.
29. Wong YP, et al. Occult primary breast carcinoma presented as an axillary mass: a diagnostic challenge. Malays J Pathol. 2020;42(1):151–5.
30. Brandt KR, et al. Can digital breast tomosynthesis replace conventional diagnostic mammography views for screening recalls without calcifications? A comparison study in a simulated clinical setting. Am J Roentgenol. 2013;200(2):291–8. https://doi.org/10.2214/AJR.12.8881.
31. Gilbert FJ, Tucker L, Young KC. Digital breast tomosynthesis (DBT): a review of the evidence for use as a screening tool. Clin Radiol. 2016;71(2):141–50. https://doi.org/10.1016/j.crad.2015.11.008.
32. Murad TM, Contesso G, Mouriesse H. Nipple discharge from the breast. Ann Surg. 1982;195(3):259–64. https://doi.org/10.1097/00000658-198203000-00003.
33. Dawes LG, et al. Ductography for nipple discharge: no replacement for ductal excision. Surgery. 1998;124(4):685–91. https://doi.org/10.1067/msy.1998.91362.
34. King TA, et al. A simple approach to nipple discharge. Am Surg. 2000;66(10):960–5; discussion 965–6.
35. Montroni I, et al. Nipple discharge: is its significance as a risk factor for breast cancer fully understood? Observational study including 915 consecutive patients who underwent selective duct excision. Breast Cancer Res Treat. 2010;123(3):895–900. https://doi.org/10.1007/s10549-010-0815-1.
36. Morrogh M, et al. Lessons learned from 416 cases of nipple discharge of the breast. Am J Surg. Elsevier Inc. 2010;200(1):73–80. https://doi.org/10.1016/j.amjsurg.2009.06.021.
37. Adepoju LJ, et al. The value of clinical characteristics and breast-imaging studies in predicting a histopathologic diagnosis of cancer or high-risk lesion in patients with spontaneous nipple discharge. Am J Surg. 2005;190(4):644–6. https://doi.org/10.1016/j.amjsurg.2005.06.032.
38. Bahl M, Gadd MA, Lehman CD. Diagnostic utility of MRI after negative or inconclusive mammography for the evaluation of pathologic nipple discharge. Am J Roentgenol. 2017;209(6):1404–10. https://doi.org/10.2214/AJR.17.18139.
39. Sanders LM, Daigle M. The rightful role of MRI after negative conventional imaging in the management of bloody nipple discharge. Breast J. 2016;22(2):209–12. https://doi.org/10.1111/tbj.12551.

40. Rosa M, Mohammadi A, Masood S. The value of fine needle aspiration biopsy in the diagnosis and prognostic assessment of palpable breast lesions. Diagn Cytopathol. 2012;40(1):26–34. https://doi.org/10.1002/dc.21497.
41. Garg S, et al. A comparative analysis of core needle biopsy and fine-needle aspiration cytology in the evaluation of palpable and mammographically detected suspicious breast lesions. Diagn Cytopathol. 2007;35(11):681–9. https://doi.org/10.1002/dc.20721.
42. Wang M, et al. A sensitivity and specificity comparison of fine needle aspiration cytology and core needle biopsy in evaluation of suspicious breast lesions: a systematic review and meta-analysis. Breast. 2017;31:157–66. https://doi.org/10.1016/j.breast.2016.11.009.
43. Homesh NA, Issa MA, El-Sofiani HA. The diagnostic accuracy of fine needle aspiration cytology versus core needle biopsy for palpable breast lump(s). Saudi Med J. 2005;26(1):42–6.
44. Imschweiler T, et al. MRI-guided vacuum-assisted breast biopsy: comparison with stereotactically guided and ultrasoundguided techniques. Eur Radiol. 2014;24(1):128–35. https://doi.org/10.1007/s00330-013-2989-5.
45. Eby PR, Lehman C. MRI-guided breast interventions. In: Seminars in ultrasound, CT and MRI; 2006;27(4):339–50. https://doi.org/10.1053/j.sult.2006.05.008.

Chapter 14
Preoperative (Breast)

Jonathan Yugo Maesaka, Yedda Nunes Reis, and Jose Roberto Filassi

14.1 Preoperative Tests for the Breast

Newly diagnosed patients with breast cancer should be evaluated clinically and with imaging exams to guide locoregional surgical treatment (breast and axilla). In this context, understanding the locoregional extent of the disease assists the physician to make the best decision for the treatment and will enable the choice of the most appropriate surgical option, which can be a breast conservative surgery (quadrantectomy/lumpectomy), or a mastectomy; if there is a need for immediate breast reconstruction or even if there is an ipsilateral or contralateral synchronic disease that needs to be treated concomitantly or for contralateral breast symmetrization.

When assessing a patient who is a candidate for conservative surgery, the attending physician uses clinical and imaging parameters for safe decision-making. Important considerations are made about the tumor size, as well as the extent of the disease, the presence of multifocality/multicentricity, and involvement of adjacent structures.

Preoperative imaging exams will assist in understanding the true size of the tumor, so that adequate resection is programmed. Currently, "no ink on tumor" is the goal for patients with invasive breast disease undergoing conservative surgery, and in patients with pure ductal carcinoma *in situ* (DCIS), the recommended margin is 2 mm. Thus, the surgical approach must be personalized, and there is no longer contraindication for conservative surgery for multicentric tumors or with extensive

J. Y. Maesaka (✉) · Y. N. Reis · J. R. Filassi
Departamento de Mastologia, Instituto do Cancer do Estado de Sao Paulo ICESP, São Paulo, SP, Brazil
e-mail: jonathan.maesaka@hc.fm.usp.br; yedda.reis@hc.fm.usp.br; j.filassi@hc.fm.usp.br

S. J. Kim Hsieh, E. A. Morris (eds.), *Modern Breast Cancer Imaging*,
https://doi.org/10.1007/978-3-030-84546-9_14

DCIS components. Conservative surgery can be offered as long as the entire tumor is resected and the aesthetic result is adequate.

Special attention is required for patients with invasive lobular carcinoma (ILC) subtype. Invasive lobular carcinoma is the second most common histological type of breast cancer, representing 5–15% of cases, and due to its specific characteristics of involvement of the breast lobes, without significant inflammatory reaction, it can bring challenges in the clinical and imaging evaluation. Clinically, in most cases, it is not possible to identify well-defined palpable masses. This presentation is due to a slight change in the consistency of the breast. Invasion by malignant cells sometimes occurs insidiously, resulting in little or no desmoplasia. Masses and microcalcifications in lobular subtypes are incommon. In addition, lobular carcinoma has a tendency to multifocal proliferation, with greater challenge in safe delimitation of the disease. As we will mention further in this chapter, in view of this histological type, an individualized imaging evaluation must be performed.

14.1.1 Imaging Methods

14.1.1.1 Mammography

Mammography (MG) is the gold standard imaging method for preoperative breast assessment and should be performed by all patients diagnosed with breast cancer. As it is the main test used in screening, the diagnosis is often made based on the findings of this test.

In addition, mammography is widely used in patients scheduled for non-oncological aesthetic breast surgery. At this point, it is worth mentioning the Choosing Wisely statement of the American Society of Plastic Surgeons [1] that recommends avoiding the routine use of mammograms before breast surgery, reserving its use for patients with indications for screening. A study carried out by Sears et al. identified that mammography in patients under 40 years of age at preoperative mammoplasty (without other clinical indication) increased the rates of more exams (such as magnetic resonance imaging (MRI)) and more biopsies, without objective evidence of their benefit [2].

A characteristic to be mentioned in the use of preoperative mammography is the interobserver reproducibility. A study carried out by Kim et al. showed an almost perfect agreement of mammography between different observers, compared to others methods such as ultrasound (US) and MRI, when looking for prediction characteristics of an extensive intraductal component [3]. As it is a static method and easier to interpret, mammography is used by surgeons in the operating room to plan incisions and tumor location and assess the extent of the disease.

Berg et al. carried out in 2004 a study of the accuracy of MG, US, and MRI techniques in 111 patients [4]. MRI showed greater sensitivity when compared to MG. An interesting fact is that adding MRI led to a 12% increase in the diagnosis of new lesions, when compared to the use of MG + US. At the same time, in this same study, MRI showed a tendency to overestimate the final tumor size. In 2009,

Wasif et al. performed a comparative study between MG, US, and MRI [5]. Of the 61 patients evaluated, 52 were invasive ductal carcinomas. When the final size in pathology was used as a parameter, the correlation was better with MRI, followed by US and finally MG, identifying MRI as the exam with the best accuracy in relation to the pathological size of the lesion.

14.1.1.2 Ultrasound

Ultrasonography is the second most used exam, after mammography, for breast assessment. It is a widely available test, with a lower cost in relation to MRI, but it is also worth mentioning that this test depends on the operator and the device used. Preferably, it should be performed in conjunction with mammography, for a more complete and global assessment. During the exam, the patient is in the supine position, a position similar to that of the surgery, and the characterization of the lesions can assist in surgical planning, such as the skin distance, distance between lesions, and distance from the nipple.

Like mammography, ultrasonography also has a moderate correlation coefficient (0.68) with the pathological size of the tumor and is often due to the presence of uncalcified DCIS, lobular histologies or tumor isoechogenicity in relation to the breast parenchyma, especially in dense breasts.

14.1.1.3 Tomosynthesis

Tomosynthesis emerged as a new imaging technique that could overcome classic limitations of mammography, reducing the effect of overlapping breast tissue, decreasing recalls, and improving the method's detection capacity. However, studies showing real superior efficacy in assessing lesion size and multifocality have not been conclusive. In a patient with dense breasts, the benefit in terms of assessing tumor size seems to be greater with the use of tomosynthesis [6].

14.1.1.4 Breast Magnetic Resonance Imaging

Despite the increasingly frequent use in surgical programming, the use of MRI in preoperative locoregional staging is still controversial. Increased rates of mastectomy, high rates of false-positive findings, and absence of evidence that the use of MRI has an impact on patient survival are the main points of this controversy.

The objective of using MRI in the preoperative scenario should be the same as for screening: increased sensitivity. The sensitivity of MRI in detecting multicentric tumors and contralateral disease reaches 93% and 88%, respectively. Some studies suggest that this increase in sensitivity is particularly valid in patients with dense breasts and in lobular tumors. In theory, increased sensitivity should reduce positive margin rates, decrease reoperation rates, and potentially decrease local recurrence. However, the results of the studies are not consistent for these benefits and

sometimes bring an increase in mastectomy rates, without reducing reoperation rates or even impacting on survival, as a result of a published meta-analysis [7]. To date, there is no consensus on the use of preoperative MRI in patients with initial surgical treatment and it is suggested to use them in lobular tumors, as a consensus, and to consider it in patients with dense breasts.

Another limiting factor in the use of preoperative MRI is the low availability of services with the possibility of performing MRI-guided percutaneous biopsy. Therefore, an additional finding on MRI that cannot be verified by biopsy will end up being approached surgically, which would lead to more, not less, surgical procedures.

A situation in which the use of breast MRI is mandatory is in occult breast carcinoma. For patients who are candidates for neoadjuvant chemotherapy, it is suggested, even with the aforementioned scores and as long as there is no delay in treatment, to perform MRI before and after chemotherapy (before surgery), for better surgical planning [8].

14.1.1.5 Positron Emission Tomography-Computed Tomography (PET-CT)

The use of 18FDG PET-CT for breast is not routinely recommended. The method has low sensitivity and low specificity in the local assessment of breast cancer. For example, it has no capacity to detect lesions smaller than 1 cm, nor does it make the differential diagnosis with inflammatory diseases or even fibroadenoma [9].

14.2 Preoperative Tests for the Axilla

The presence of axillary disease in the context of breast cancer is an important prognostic factor for the disease. Proper assessment of this condition will guide the proposed therapy for each patient. The purpose of preoperative assessment is to define whether or not there is axillary involvement and when present, the magnitude of this involvement, also known as “axillary burden”. For this we can use, in addition to the physical examination, imaging methods. At the moment, no available imaging exam has an acceptable negative predictive value to contraindicate surgical assessment of the axilla when only normal lymph nodes are identified [10].

14.2.1 Indications

The axillary physical examination is always performed before surgery; however, it is not a good indicator of the presence or absence of lymph node metastases. In situations of clinically negative axilla, it will depend on the strategy adopted by the

surgeon to request tests directed to the axilla, as we will discuss below and also as explained in Chap. 4. In patients with clinically positive nodes, a scenario in which the sentinel lymph node is contraindicated, ultrasound-guided fine-needle aspiration (FNA) can confirm cytologically the presence of metastasis. In scenarios where the physical examination is inconclusive, additional tests should be ordered, and ultrasound can be of great use in conducting the case. The fact that ultrasound is an operator-dependent exam must also be taken into account when ordering and interpreting the results of the exam.

14.2.2 Methods

14.2.2.1 Ultrasound

Ultrasonography is the most established exam for axillary evaluation. The suspicion and diagnosis of axillary metastasis can modify the patient's therapeutic planning: negative axillae favors the performance of sentinel lymph node biopsy and, thus, reduces the morbidity associated with axillary dissection. Positive axillae favors the adoption of neoadjuvant treatment in order to reduce lymph node involvement by disease and enable axillary surgical de-escalation. Finally, in some cases, it may be contraindicated to perform the sentinel lymph node technique and guide the proposal for up-front axillary dissection. Such an approach is detailed in Chap. 4.

In the ultrasound evaluation, morphological criteria (concentric or focal cortical thickening greater than 3 mm, hilar obliteration, increased peri-hilar vascularization, round shape) can be used, as well as the size of the lymph node, to identify suspicious nodes. According to the criterion used, the specificity and sensitivity of the method may vary. In a systematic review, which included literature from 1980 to 2004, Alvarez and colleagues found that in patients with palpable lymph nodes, the sensitivity of the ultrasound was 68% on average when using the lymph node size criteria, with a specificity of 75.2%, whereas if morphological criteria were used, the sensitivity increased to 71% with a specificity of 96.1% on average. In the group of patients without palpable lymph nodes, mean sensitivity and specificity were 60.9% and 75.2%, respectively. However, when using the morphological criteria in these patients, the average sensitivity was 43.9%, with 92.4% specificity [11].

As we can see, there is a variety in the results found in the literature and in the accuracy of the ultrasound to identify the lymph nodes, and this can be explained by the variability of the method and criterion used, as well as whether the reference used was sentinel lymph node biopsy or axillary dissection.

A cost-effective analysis study was conducted by Boughey et al., for the performance of FNA guided by ultrasound in all lymph nodes with at least one altered morphological criterion and compared with the performance of sentinel lymph node biopsy intraoperatively, without performing axillary ultrasound (standard treatment). As a result, the strategy proved to be cost-effective with a minimal difference

(US $ 36 dollars) between the strategies, and in 63% of the patients, there were savings when the ultrasound was performed [12].

In 2017, a study published by Teixeira et al. created a nomogram for predicting the presence of metastases based on the tumor characteristics and ultrasound image of the axilla [13]. Using cortical thickening, tumor size, histological type, lesion location as variables in the breast (quadrant) and the patient's menopausal status, the nomogram achieved satisfactory discrimination, with an area under the curve (AUC) of 0.848.

14.2.2.2 Mammography

Although mammography is the main exam performed for breast assessment, its role in the preoperative assessment of the axilla is limited [14]. In general, the axilla is not fully included in the mammographic examination, and the accuracy of its findings is limited. Benign lymph nodes appear on the mammographic exam smaller than 2 cm in diameter and radiolucent hilar center. Suspicious findings are the increased size and density of the lymph node.

14.2.2.3 Magnetic Resonance Imaging

Most MRI breast protocols cover the entire axillary field and allow a good evaluation of this field. Suspicious findings in axillary lymph nodes on MRI include cortical thickening, loss of fatty hilum, and rounded shape. The presence of perifocal edema, defined as T2 hyperintensity in the adjacent fatty tissue ("marked T2 prolongation in the surrounding fat"), demonstrated the greatest accuracy among the descriptors, with a positive predictive value of 100% [15].

14.2.2.4 PET-CT

Another imaging method is the 18-FDG PET-CT, which has a role as a highly sensitive method for detecting distant metastases, even in early tumors. However, its role in axillary staging is limited: studies have shown a low to moderate sensitivity, and therefore, it is not recommended for routine axillary assessment [16]. A prospective trial involving 312 patients demonstrated that, compared to sentinel lymph node biopsy, the sensitivity of FDG-PET/CT was 24%, with a specificity of 99% [17]. Another classic study by Veronesi et al. demonstrated a sensitivity of 37% [18], and in a systematic review including 7 studies and 869 patients, PET-CT showed an average sensitivity of 56% (95% CI 44 to 67%), with an average specificity of 95% (95% CI 90 to 99%) [19].

14.3 Case Examples

14.3.1 Case 1

This is a case of invasive ductal carcinoma in the left breast. What is demonstrated here is the capacity of MRI in demonstrating larger extension of the tumor, including involvement of the nipple (Figs. 14.1 and 14.2).

14.3.2 Case 2

In this case, the mammography was unable to identify the index breast cancer lesion due to an extremely dense breast, but suspicious axillary lymph nodes were partially seen. The lesion was identified on breast ultrasound as a hypoechogenic mass. With MRI, we were able to confirm both the breast and the axillary lesions (Figs. 14.3, 14.4, and 14.5).

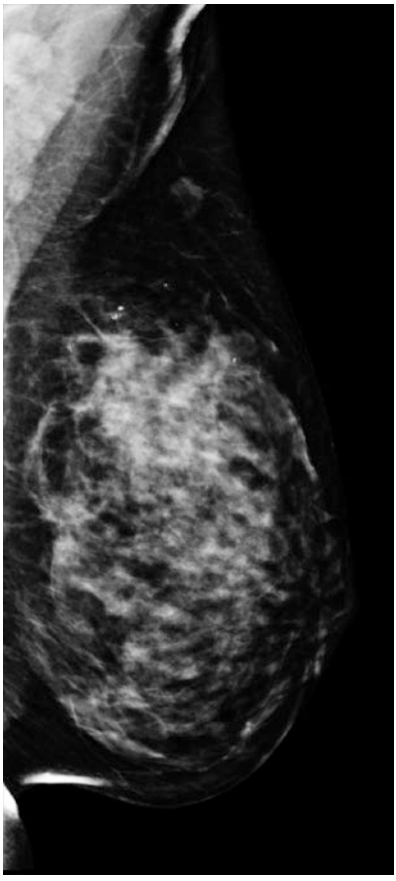

Fig. 14.1 Invasive ductal carcinoma in the left breast

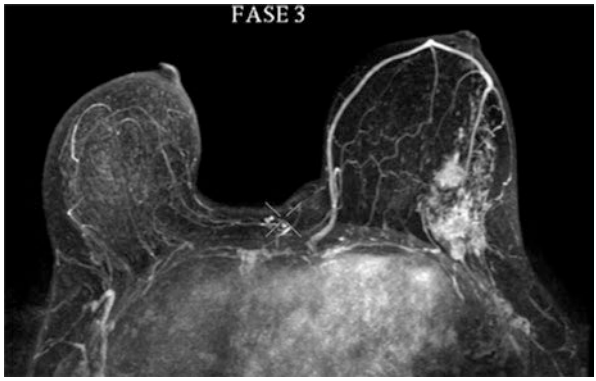

Fig. 14.2 Invasive ductal carcinoma with a greater extension on MRI than on mammography (Fig. 14.1). MRI demonstrates extension to the nipple

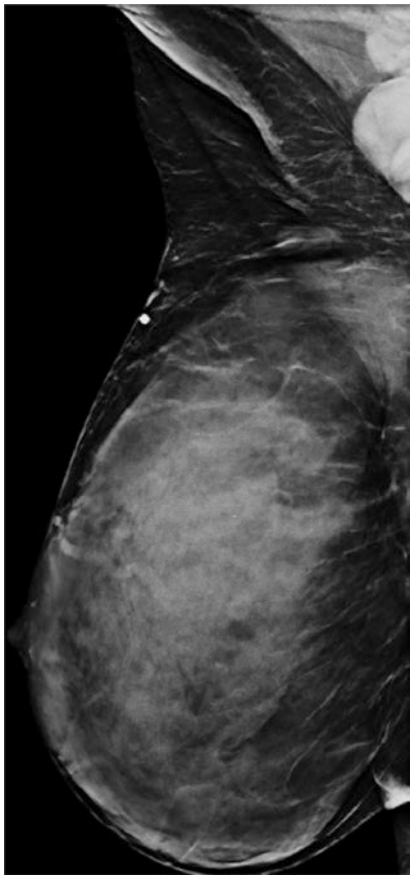

Fig. 14.3 Invasive carcinoma not identified on mammography, showing an extremely dense breast. Suspicious axillary lymph nodes are partially seen on mammography

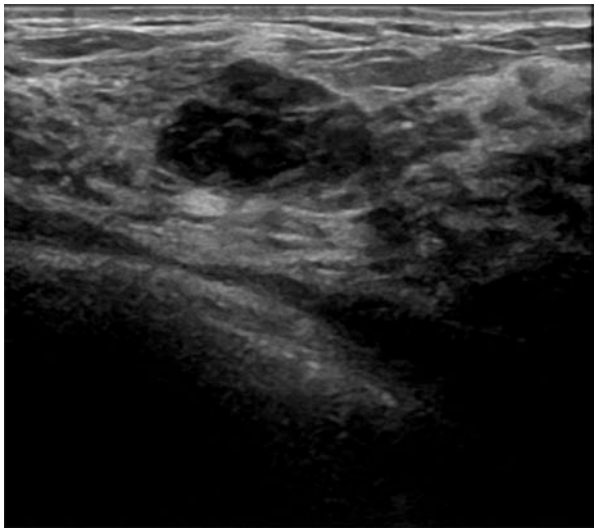

Fig. 14.4 Invasive carcinoma identified on ultrasound as a hypoechogenic mass (the same case from Fig. 14.3)

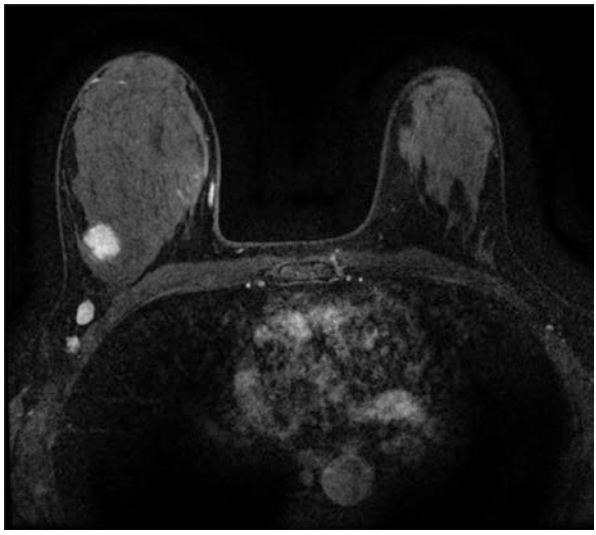

Fig. 14.5 Invasive carcinoma identified on MRI as an enhancing mass (the same case from Figs. 14.3 and 14.4). Suspicious axillary lymph nodes are better demonstrated on MRI

14.3.3 Case 3

In this case, all methods were able to accurately identify the breast lesion (Figs. 14.6, 14.7, and 14.8).

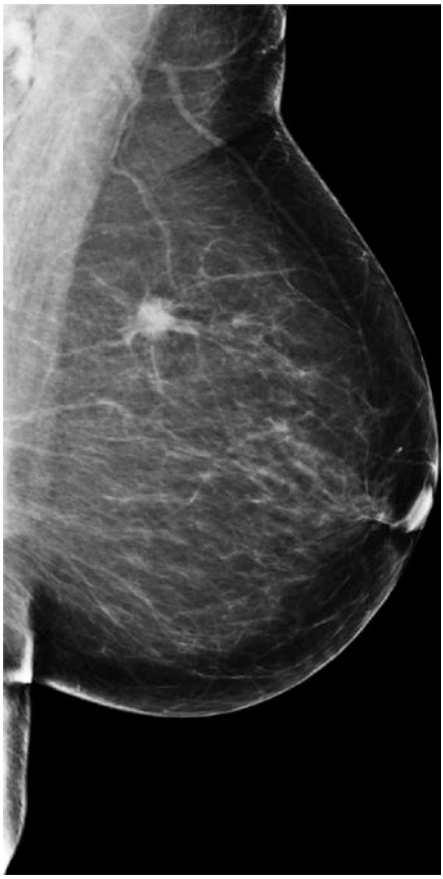

Fig. 14.6 Invasive carcinoma seen on mammography, with similar dimensions in other methods

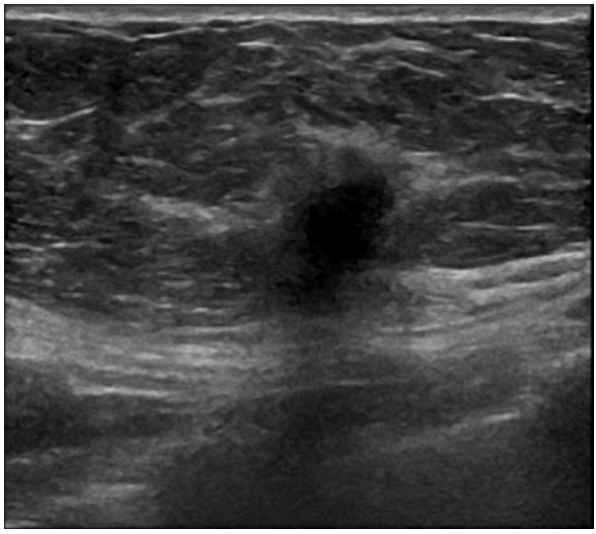

Fig. 14.7 Invasive carcinoma seen on ultrasound, with similar dimensions in other methods

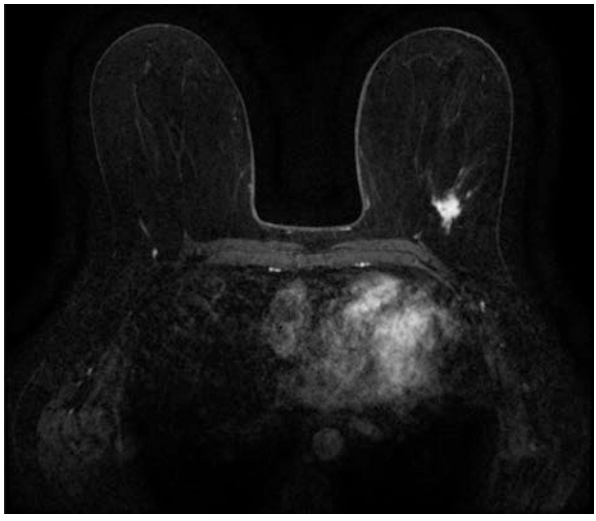

Fig. 14.8 Invasive carcinoma seen on MRI, with similar dimensions in other methods

14.3.4 Case 4

In this case, suspicions axillary lymph nodes were identified in mammography and confirmed on ultrasound (Figs. 14.9 and 14.10).

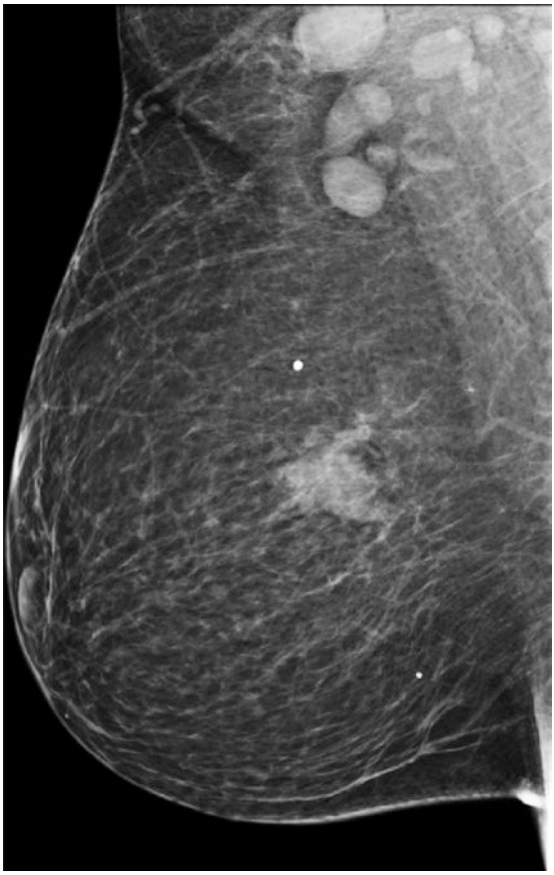

Fig. 14.9 Suspected axillary lymph nodes seen on mammography in a patient with invasive ductal carcinoma

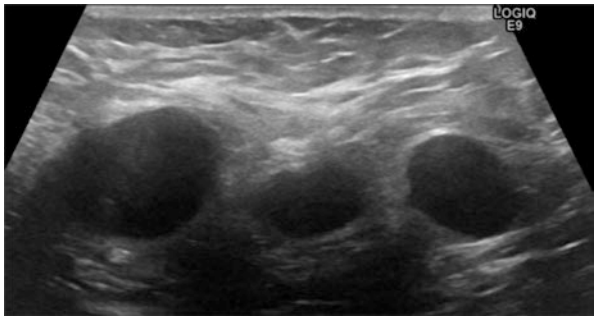

Fig. 14.10 Suspected axillary lymph nodes seen on ultrasound in a patient with invasive ductal carcinoma (the same case from Fig. 14.9)

14.3.5 Case 5

Example of normal lymph nodes identified on mammography and ultrasound (Figs. 14.11 and 14.12).

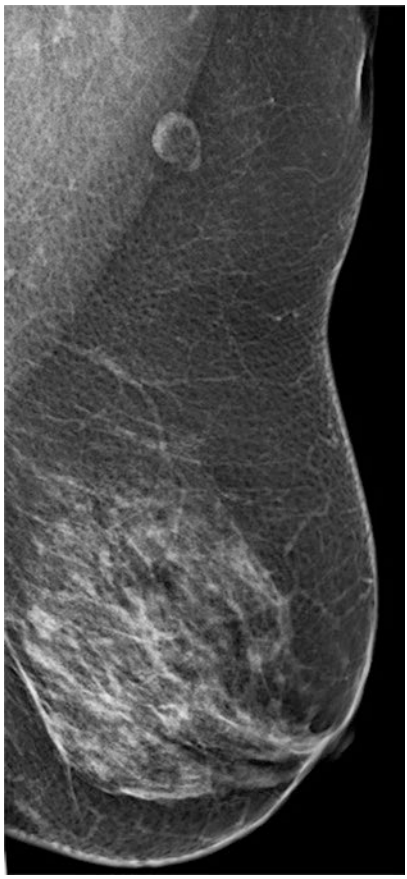

Fig. 14.11 Lymph nodes with usual features on mammography

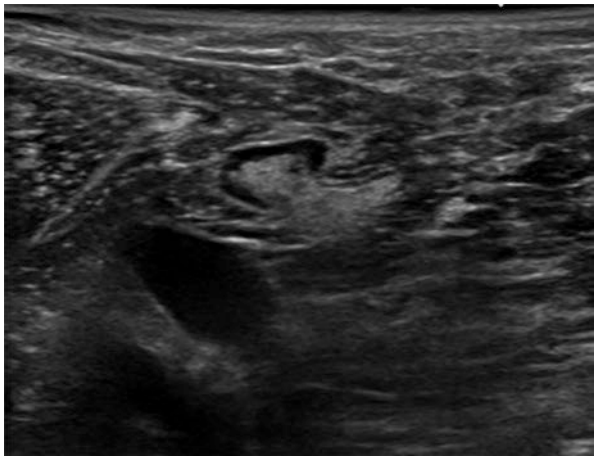

Fig. 14.12 Lymph nodes with usual features on ultrasound. Thin cortical and presence of a fatty hilum

References

1. Gutowski K, Gray D. The ASPS choosing wisely list for plastic surgery. Plast Reconstr Surg. 2014;134(4):853–5.
2. Sears ED, Lu YT, Swiatek PR, Chung TT, Kerr EA, Chung KC. Use of preoperative mammography during evaluation for nononcologic breast reduction surgery. JAMA Surg. 2019;154(4):356–8. https://doi.org/10.1001/jamasurg.2018.4875.
3. Kim HR, Jung HK, Ko KH, Kim SJ, Lee KS. Mammography, US, and MRI for preoperative prediction of extensive intraductal component of invasive breast cancer: interobserver variability and performances. Clin Breast Cancer. 2016;16(4):305–11. https://doi.org/10.1016/j.clbc.2016.02.005.
4. Berg WA, Gutierrez L, MS NA, Carter WB, Bhargavan M, Lewis RS, et al. Diagnostic accuracy of mammography, clinical examination, US, and MR imaging in preoperative assessment of breast cancer. Radiology. 2004;233(3):830–49. https://doi.org/10.1148/radiol.2333031484.
5. Wasif N, Garreau J, Terando A, Kirsch D, Mund DF, Giuliano AE. MRI versus ultrasonography and mammography for preoperative assessment of breast cancer. Am Surg. 2009;75(10):970–5.
6. Eghtedari M, Tsai C, Robles J, Blair SL, Ojeda-Fournier H. Tomosynthesis in breast cancer imaging: how does it fit into preoperative evaluation and surveillance? Surg Oncol Clin North Am. 2018;27:33–49. http://dx.doi.org/10.1016/j.soc.2017.07.004.
7. Houssami N, Turner R, Macaskill P, Turnbull LW, McCready DR, Tuttle TM, et al. An individual person data meta-analysis of preoperative magnetic resonance imaging and breast cancer recurrence. J Clin Oncol. 2014;32(5):392–401.
8. Sardanelli F, Boetes C, Borisch B, Decker T, Federico M, Gilbert FJ, et al. Magnetic resonance imaging of the breast: recommendations from the EUSOMA working group. Eur J Cancer. 2010;46(8):1296–316. https://doi.org/10.1016/j.ejca.2010.02.015.
9. Ulaner GA. PET/CT for patients with breast cancer: where is the clinical impact? Am J Roentgenol. 2019;213:254–65.
10. Rahbar H, Partridge SC, Javid SH, Lehman CD. Imaging axillary lymph nodes in patients with newly diagnosed breast cancer. Curr Probl in Diagn Radiol. 2012;41:149–58.
11. Alvarez S, Añorbe E, Alcorta P, López F, Alonso I, Cortés J. Role of sonography in the diagnosis of axillary lymph node metastases in breast cancer: a systematic review. Am J Roentgenol. 2006;186:1342–8.

12. Boughey JC, Moriarty JP, Degnim AC, Gregg MS, Egginton JS, Long KH. Cost modeling of preoperative axillary ultrasound and fine-needle aspiration to guide surgery for invasive breast cancer. Ann Surg Oncol. 2010;17(4):953–8.
13. Akissue de Camargo Teixeira P, Chala LF, Shimizu C, Filassi JR, Maesaka JY, de Barros N. Axillary lymph node sonographic features and breast tumor characteristics as predictors of malignancy: a nomogram to predict risk. Ultrasound Med Biol. 2017;43(9):1837–45. https://doi.org/10.1016/j.ultrasmedbio.2017.05.003.
14. Dialani V, James DF, Slanetz PJ. A practical approach to imaging the axilla. Insights Imaging. 2015;6:217–29.
15. Baltzer PAT, Dietzel M, Burmeister HP, Zoubi R, Gajda M, Camara O, et al. Application of MR mammography beyond local staging: is there a potential to accurately assess axillary lymph nodes? Evaluation of an extended protocol in an initial prospective study. Am J Roentgenol. 2011:196–5.
16. Liu Y. Role of FDG PET-CT in evaluation of locoregional nodal disease for initial staging of breast cancer. World J Clin Oncol. 2014;5:982–9.
17. Pritchard KI, Julian JA, Holloway CMB, McCready D, Gulenchyn KY, George R, et al. Prospective Study of 2-[18F]fluorodeoxyglucose positron emission tomography in the assessment of regional nodal spread of disease in patients with breast cancer: an Ontario Clinical Oncology Group study. J Clin Oncol. 2012;30(12):1274–9.
18. Veronesi U, De Cicco C, Galimberti VE, Fernandez JR, Rotmensz N, Viale G, et al. A comparative study on the value of FDG-PET and sentinel node biopsy to identify occult axillary metastases. Ann Oncol. 2007;18(3):473–8.
19. Cooper KL, Meng Y, Harnan S, Ward SE, Fitzgerald P, Papaioannou D, et al. Positron emission tomography (PET) and magnetic resonance imaging (MRI) for the assessment of axillary lymph node metastases in early breast cancer: Systematic review and economic evaluation. Health Technol Assess. 2011;15(4):iii–iv, 1–134. https://doi.org/10.3310/hta15040.

Chapter 15
Systemic Staging (Total Body – When, How)

Fabiano de Almeida Costa and Rudinei Diogo Marques Linck

15.1 Introduction

The staging of a neoplasm is an important step for the management of cancer patients and must be established as soon as cancer diagnosis occurs. Systematic staging allows the choice of the most appropriate treatments (local and systemic) and adequate comparison of results between institutions and clinical studies and provides initial prognostic information [1].

The initial evaluation of a patient with breast cancer should include anamnesis with special attention to menopausal status and familial history of breast or ovarian cancer, physical examination including bimanual breasts and regional lymph nodes palpation, as well as search for signs and symptoms that may indicate potential sites of metastasis. Initial laboratory evaluation with complete blood count, liver and kidney function tests, and assessment of serum alkaline phosphatase and calcium can alert about the possibility of systemic metastatic dissemination [2]. Despite the importance of anamnesis and physical examination and precise determination of tumor involvement extension with complementary exams, evaluating locoregional involvement and eventual systemic involvement is a fundamental step for initial therapeutic planning in breast cancer patients.

The decision to use imaging exams to assess possible systemic metastatic lesions must be made rationally since these exams led to increased financial costs and are associated with potential risks to patients' health. On the other hand, the failure to identify a metastatic lesion may lead to a futile indication of locoregional treatments or adjuvant therapies. Thus, this chapter will address the appropriate selection of

F. de Almeida Costa · R. D. M. Linck (✉)
Departamento de Oncologia, Instituto do Cancer do Estado de São Paulo ICESP, São Paulo, SP, Brazil
e-mail: rudinei.dmlinck@hsl.org.br

S. J. Kim Hsieh, E. A. Morris (eds.), *Modern Breast Cancer Imaging*,
https://doi.org/10.1007/978-3-030-84546-9_15

patients who are candidates for systemic staging by imaging, as well as the choice of the most appropriate complementary exams to be requested.

15.2 TNM Staging System

The TNM system was proposed by the American Joint Committee on Cancer (AJCC) and the Union for International Cancer Control (UICC) and is currently considered the standard staging system. For a most accurate prognostic information, the eighth edition of the TNM breast cancer classification in use since 2018 includes histological and molecular characteristics to the anatomical staging previously used [3].

Currently, it has been frequent the use of anatomical TNM classification criteria, especially important for the definition of cancer treatments and the use of the prognostic TNM classification (including histological and molecular information) for an improved definition of the survival impact of these treatments.

15.2.1 Anatomic Staging

The tumor size statement, either through physical examination and complementary evaluation using imaging methods (cT) or by the anatomopathological measure of the surgical specimen (pT), is a fundamental step of the TNM classification. The lymph node involvement of the ipsilateral regional chains of the compromised breast, either by clinical/imaging (cN) or anatomopathological (pN) evaluation, associated with the tumor size, make up the main prognostic factors in nonmetastatic breast cancer and are determinants in the therapeutic choice of this disease regardless of the tumor subtype [3].

Determining the metastasis existence or absence (M), on the other hand, clarifies about the virtual incurability of the disease when M1, although great advances have emerged in the last years as options for palliative therapies which brought significant improvements in survival and quality of life. Thus, the accurate recognition of the systemic metastatic disease is essential to define at the initial diagnosis the possibility of a treatment strategy with curative potential (definitive local treatment accompanied by neo/adjuvant systemic therapies) or the need for systemic palliative treatment to control the metastatic disease [4].

15.2.2 Biomarkers and Prognostic Staging

Biomarkers in breast cancer are important because they are able to establish the prognosis of the disease or, even, to predict the benefit of a specific treatment. Associated with tumor size and lymph node involvement, the histological grade

determination is the most important risk factor for disease recurrence after the initial treatment of a locoregional breast cancer [5]. The main factors that predict the benefit of antihormonal treatment are the positive expression of estrogen or progesterone receptors (HR-positive), as well as HER2 hyperexpression or amplification (HER2-positive) which are directly associated with the benefit with anti-HER2 therapies [6, 7]. Nowadays, tests for the tumor gene expression analysis have been able to refine the prognosis of the initial HR-positive, HER2-negative tumors, and even helping to select the patient who needs adjuvant chemotherapy [8].

The changes in AJCC staging proposed in its eighth edition included the information of histological grade, status of hormone receptors, HER2, and score of the oncotype DX gene expression test as components of its classification. These changes are taking into account the advances in the breast cancer treatment that occurred in the past years and the consequent improvement in the prognosis of certain tumor subtypes. With this new classification, the ability to predict the survival of breast cancer patients undergoing conventional treatments has been significantly improved [3]. However, the prognostic staging is less relevant for choosing which adjuvant treatment should or should not be indicated.

15.2.3 Therapeutic Decisions According to Staging

The TNM classification of locoregional breast cancer (stages I, II, and III) helps to determine the strategy of local and systemic treatment, since the more extensive the locoregional disease, the greater the risks of future recurrence and, therefore, the greater the absolute benefit of a more aggressive and extensive treatment. On the other hand, the definition of metastatic disease at the initial diagnosis (*de novo* metastatic cancer/stage IV) establishes a virtual incurability and indicates palliative strategies for its treatment. The failure to identify a metastatic lesion, with the consequent under-staging of the neoplasia, may result in unnecessary treatments, such as surgical or radiotherapy treatment of locoregional disease or even the indication of futile neo−/adjuvant treatments for this scenario. In addition, understaging can also represent inadequate choices for the treatment of metastatic disease [9].

15.3 Systemic Staging – When

Today, breast cancer represents the malignancy with the highest incidence in the world, with an estimated 2.3 million people having this diagnosis in 2020 [10]. Of these, approximately 90–95% are diagnosed as locoregional breast cancer, without systemic metastases [11]. The chances of systemic involvement are directly associated with the locoregional involvement extension. It is more likely to identify systemic metastases in more extensive locoregional disease or the more aggressive the characteristics of this tumor are [9]. Therefore, it is possible to define the need for

investigation of systemic metastases with complementary exams according to the chance of detecting disseminated neoplasia.

The initial assessment of any patient with breast cancer should include anamnesis and physical examination looking for signs and symptoms that may indicate potential sites of metastasis. In addition, the initial laboratory evaluation should include complete blood count, liver and kidney function tests, and serum alkaline phosphatase and calcium tests, since changes in these tests may suggest a possible systemic neoplastic dissemination [2]. Every patient who presents any signs or symptoms suggestive of systemic metastatic dissemination should be properly investigated with imaging exams. For instance, the presence of dyspnea, cough, or hemoptysis should trigger a further investigation in search of lung metastases; the presence of elevated alkaline phosphatase, abnormal liver marker tests, abdominal symptoms, or findings of abdominal changes on physical examination indicates the need for investigation for abdominal metastases; as well as bone pain or elevated alkaline phosphatase suggest the possibility of bone metastases.

In view of early diagnosis with small neoplasia and limited or absent lymph node involvement (staging up to T2N0 or T1N1) assessed as anatomical stage I or IIA, there is no need for routine imaging exams, unless with signs or symptoms suggestive of metastatic involvement [1, 2, 12]. However, retrospective studies suggest that early tumors, when they involve lymph node or aggressive tumor subtypes (especially HER2-positive or triple-negative), are more likely to have systemic metastasis [9].

15.4 Systemic Staging – How

Unlike initial tumors, those that present with extensive loco-regionally neoplasms may benefit from the systematic investigation of distant metastases. The incidence of metastatic lesions to other organs and systems, when asymptomatic, is low even in these cases. According to Ravaioli et al. [13], in a retrospective evaluation of 1218 cases of breast cancer in clinical stage (CS) III, the prevalence of abnormal abdominal ultrasound and chest radiography was 6% and 7%, respectively. Myers et al. [14] presented a meta-analysis of 11 studies, in which 8.3% of the CS III participants had bone scintigraphy suggestive of bone metastasis, 2.0% had an abdominal ultrasound with suspected liver metastasis. and 1.7% had chest x-ray with lesions suspected for metastasis.

In cases of locally advanced tumors, patients with T3 (≥5 cm) or N positive (CS ≥ IIB) must undergo a systemic assessment that includes chest computerized tomography (CT), CT or magnetic resonance imaging (MRI) of the abdomen, and bone scintigraphy [1, 2, 12]. Exams with less sensitivity for the detection of systemic metastases, such as abdominal ultrasound (US) and chest radiography, are generally not useful in clinical practice because they have high rates of false negative [9]. Assessment of central nervous system (CNS) metastasis should be performed exclusively when the patient has suggestive neurological symptoms and preferably with MRI [4].

The positron emission tomography with 18F-fluorodeoxyglucose (PET-CT FDG) is not routinely indicated [2, 12], but it can be useful when CT and bone scans are doubtful [1, 3]. Trials that demonstrate the superiority of PET-CT FDG over anatomical exams are already well established, but clinical benefits, which lead to recurrence-free survival and overall survival improvement, are less discussed and not defined. When PET-CT FDG is requested, it replaces chest and abdomen CT, abdominal MRI, and bone scintigraphy.

A prospective study conducted in Barcelona, Spain, evaluated 60 patients with tumors larger than 3 cm with chest CT, liver US, bone scintigraphy, and PET-CT FDG and compared the methods for at least one of year follow-up [15]. The sensitivity and specificity of PET-CT FDG to detect axillary lymph nodes were 70% and 100%, respectively. The overall sensitivity and specificity of PET-CT FDG to detect distant metastases were 100% and 98%, while the sensitivity and specificity of conventional exams were 60% and 83%, respectively. The most important finding in this study was that PET-CT FDG led to a change in initial staging in 42% of patients. Unfortunately, this study did not discuss clinical outcomes.

Another prospective study, conducted in Paris, France, evaluated 131 breast cancer patients with tumors larger than 2 cm [16]. In this study, PET-CT FDG was responsible for modifying the staging of 5.6% of patients previously diagnosed as stage IIA, 14.6% of previously diagnosed as stage IIB, and 27.6% of previously diagnosed as stage IIIA.

The PET-CT FDG is not routinely recommended in the first approach to systemic staging due to several issues: the high rate of false-negative for lesions smaller than 1 cm or low-grade tumors, the low sensitivity to detect axillary involvement, the low initial likelihood of these patients having measurable metastases, and the high rate of false positives [16]. We add the absence of evidence on most important clinical outcomes and the lack of cost-effectiveness studies suggesting that replacement of conventional investigation methods does not allow us to recommend routinely PET-CT FDG to initiate a systemic evaluation. However, there is limited evidence suggesting that PET-CT FDG may be a useful adjunct to standard imaging for systemic staging in high-risk patients (such as stage T4 or N2-3) due to its greater sensitivity to identify a more disseminated disease [1, 16, 17].

Complete blood count and liver function tests are recommended for all patients who are candidates for systemic neoadjuvant or adjuvant treatment. Other laboratory tests are indicated only if there are signs or symptoms [1, 3]. There is no recommendation for tumor markers such as CEA and Ca 15–3 in the initial evaluation [2, 12]. PET-CT with fluoroestradiol F-18 is a new methodology capable of identifying lesions with hormone receptors expression in patients with metastatic disease; however, there are no studies evaluating clinical utility [18, 19].

15.5 Biopsy or Rebiopsy

Patients who were suspected of having metastatic lesion on initial exams, whenever possible, must undergo a biopsy of the metastatic site, since the metastatic diagnosis is associated with a major impact on therapeutic planning. In addition to confirming

the diagnosis of systemic metastasis against alternative hypotheses such as an eventual benign condition or even a second primary tumor, access to the new immunohistochemical evaluation is highly recommended in breast cancer. Since breast cancer treatment is dictated by the result of hormone receptor expression and/or HER2 positivity, a different status of these markers at the metastasis site (becoming present when they were initially absent) could lead to a significant change in the treatment strategy [20].

At the neo/adjuvant and local treatment conclusion, the patient must start a planned medical follow-up for the possibility of tumor recurrence. Rebiopsy is of special value when a lesion suspected of recurrence is identified. Anatomopathological analysis can confirm the diagnosis of recurrent metastatic disease and also allows for new immunohistochemistry. It is possible to identify a discrepancy in the immunohistochemical profile between the primary tumor and metastasis, which can vary between 5% and 30% over the course of cancer treatment [1, 21, 22].

15.6 Follow-Up Patients

The follow-up of the patient with breast cancer begins after the conclusion of locoregional treatment and neo/adjuvant treatments and should be oriented towards the monitoring of any side effects associated with the treatment employed, as well as for the identification of any eventual neoplastic recurrence. Tumor relapse can be divided into two distinct conditions: when locoregional relapse occurs in the breast or in regional lymph nodes, which must be promptly identified as it is a potential curable situation, the reason why it is important to have routine follow-up by imaging exams, usually annual mammography, associated with physical exam [23], and when systemic relapse occurs, which are virtually incurable. Thus, early identification of systemic recurrence will not necessarily be able to change the natural history of the disease, and early palliative treatments will not be able to translate into increased chances of a cure or improved survival [24].

The main recommendation for the adequate breast cancer patients' follow-up is to carry out regular medical consultations for the active search for signs and symptoms suggestive of treatment toxicities and also the possibility of tumor recurrence [25]. There is no recommendation for routine exams to identify asymptomatic systemic metastases. However, any clinical suspicion should be promptly investigated.

15.7 Conclusion

Evaluation by imaging exams to investigate possible systemic metastatic disease should not be requested indiscriminately to all patients diagnosed with breast cancer. Most patients are diagnosed with locoregional tumors, and complementary exams are not free from risk, besides increasing financial costs for health systems.

On the other hand, failure to adequately identify metastatic disease can also lead to inappropriate choices in the therapeutic planning of these patients. Thus, complementary exams must be carefully considered.

Patients should always be assessed by anamnesis and physical examination, looking for signs and symptoms suggestive of metastatic spread, and any evidence or suspicion of abnormality should be promptly investigated with appropriate examinations. The main sites of metastasis in breast cancer are bones, lymph nodes, lungs, liver, and central nervous system (the latter especially important in neoplasms subtype HER2-positive or triple negative). Patients with loco-regionally advanced tumors, especially those with anatomical staging IIB or more, should undergo routine imaging assessment when the initial diagnosis is made. The exams indicated for this evaluation are chest CT, abdominal CT or MRI, and bone scintigraphy. PET-CT FDG evaluation may be an alternative, especially when the initial exams are not clear.

Biopsy for histological confirmation of systemic metastasis should be requested whenever possible, since there is a great impact on therapeutic definitions. The importance of biopsy of systemic metastases goes beyond the differential diagnosis between benign conditions or eventually a second primary tumor. In breast cancer, there is a great impact of immunohistochemical evaluation (related to the expression of hormone receptors and also of HER2) in the choice between different treatment alternatives. The immunohistochemical profile may, in some cases, differ between the primary and the metastatic tumor; also, there may be a change in the immunohistochemical profile after long periods of exposure to cancer treatments. Patients who are on follow-up after the end of treatment or in adjuvant endocrine therapy need to be evaluated by trained medical staff in search of signs and symptoms suggestive of systemic neoplastic recurrence. When there is a clinical suspicion of systemic metastasis, it necessarily needs to be promptly investigated with correct and accurate propaedeutics. However, asymptomatic patients with no suspicion of metastatic spread should not be subjected to indiscriminate routine imaging exams for systemic evaluation.

References

1. National Comprehensive Cancer Network. Breast Cancer (Version 8.2021). https://www.nccn.org/professionals/physician_gls/pdf/breast.pdf. Accessed September 14, 2021.
2. Barrios CH, Bedin SR, Reinert T, Tavares M, Sahade M, Cruz M, et al. Mama: Estadiamento. Diretrizes Trat Oncológicos da SBOC. 2020.
3. Amin MB, Edge SB, Greene FL. AJCC Cancer Staging Manual. 8th ed. Springer; 2017.
4. Cardoso F, Paluch-Shimon S, Senkus E, Curigliano G, Aapro MS, André F, et al. 5th ESO-ESMO international consensus guidelines for advanced breast cancer (ABC 5). Ann Oncol [Internet]. 2020;31(12):1623–49. Available from: https://linkinghub.elsevier.com/retrieve/pii/S0923753420424603
5. Pan H, Gray R, Braybrooke J, Davies C, Taylor C, McGale P, et al. 20-year risks of breast-cancer recurrence after stopping endocrine therapy at 5 years. N Engl J Med [Internet]. 2017;377(19):1836–46. Available at: http://www.nejm.org/doi/10.1056/NEJMoa1701830.

6. Breast E, Trialists C; Group C. Relevance of breast cancer hormone receptors and other factors to the efficacy of adjuvant tamoxifen: patient-level meta-analysis of randomised trials. Lancet [Internet]. 2011;378(9793):771–84. Available at: https://doi.org/10.1016/S0140-6736(11)60993-8.
7. Piccart-Gebhart MJ, Procter M, Leyland-Jones B, Goldhirsch A, Untch M, Smith I, et al. Trastuzumab after adjuvant chemotherapy in HER2-positive breast cancer. N Engl J Med [Internet]. 2005;353(16):1659–72. Available at: http://www.ncbi.nlm.nih.gov/pubmed/16236737.
8. Andre F, Ismaila N, Stearns V. Use of biomarkers to guide decisions on adjuvant systemic therapy for women with early-stage invasive breast cancer: ASCO clinical practice guideline update summary. J Oncol Pract [Internet]. 2019;15(9):495–7. Available at: http://ascopubs.org/doi/10.1200/JOP.19.00264.
9. Soares G, Pereira A, Vilas Boas M, Vaisberg V, Magalhães M, Linck R, et al. Value of systemic staging in asymptomatic early breast cancer. Rev Bras Ginecol e Obs/RBGO Gynecol Obstet [Internet]. 2018;40(07):403–9. Available at: http://www.thieme-connect.de/DOI/DOI?10.1055/s-0038-1666997.
10. Sung H, Ferlay J, Siegel RL, Laversanne M, Soerjomataram I, Jemal A, et al. Global cancer statistics 2020: GLOBOCAN estimates of incidence and mortality worldwide for 36 cancers in 185 countries. CA Cancer J Clin [Internet]. 2021:caac.21660. Available at: https://onlinelibrary.wiley.com/doi/10.3322/caac.21660.
11. Cardoso F, Spence D, Mertz S, Corneliussen-James D, Sabelko K, Gralow J, et al. Global analysis of advanced/metastatic breast cancer: decade report (2005–2015). Breast [Internet]. 2018;39:131–8. Available at: https://linkinghub.elsevier.com/retrieve/pii/S096097761830050X.
12. Cardoso F, Kyriakides S, Ohno S, Penault-Llorca F, Poortmans P, Rubio IT, et al. Early breast cancer: ESMO Clinical Practice Guidelines for diagnosis, treatment and follow-up. Ann Oncol. 2019;30(8):1194–220.
13. Ravaioli A, Pasini G, Polselli A, Papi M, Tassinari D, Arcangeli V, et al. Staging of breast cancer: new recommended standard procedure. Breast Cancer Res Treat. 2002;72(1):53–60.
14. Myers RE, Johnston M, Pritchard K, Levine M, Oliver T, Crump RM, et al. Baseline staging tests in primary breast cancer: a practice guideline. CMAJ. 2001;164(10):1439–44.
15. Fuster D, Duch J, Paredes P, Velasco M, Muñoz M, Santamaría G, et al. Preoperative staging of large primary breast cancer with [18F]fluorodeoxyglucose positron emission tomography/computed tomography compared with conventional imaging procedures. J Clin Oncol. 2008;26(29):4746–51.
16. Groheux D, Giacchetti S, Espié M, Vercellino L, Hamy AS, Delord M, et al. The yield of 18F-FDG PET/CT in patients with clinical stage IIA, IIB, or IIIA breast cancer: a prospective study. J Nucl Med. 2011;52(10):1526–34.
17. Carkaci S, Macapinlac HA, Cristofanilli M, Mawlawi O, Rohren E, Gonzalez Angulo AM, et al. Retrospective study of 18FFDG PET/CT in the diagnosis of inflammatory breast cancer: preliminary data. J Nucl Med. 2009;50(2):231–8. https://doi.org/10.2967/jnumed.108.056010.
18. Linden HM, Peterson LM, Fowler AM. Clinical potential of estrogen and progesterone receptor imaging. PET Clin [Internet]. 2018;13(3):415–22. Available at: http://www.ncbi.nlm.nih.gov/pubmed/30100079.
19. Jones EF, Ray KM, Li W, Chien AJ, Mukhtar RA, Esserman LJ, et al. Initial experience of dedicated breast PET imaging of ER+ breast cancers using [F-18]fluoroestradiol. NPJ Breast Cancer [Internet]. 2019;5:12. Available at: http://www.ncbi.nlm.nih.gov/pubmed/31016232.
20. Van Poznak C, Somerfield MR, Bast RC, Cristofanilli M, Goetz MP, Gonzalez-Angulo AM, et al. Use of biomarkers to guide decisions on systemic therapy for women with metastatic breast cancer: American Society of Clinical Oncology Clinical Practice Guideline. J Clin Oncol [Internet]. 2015;33(24):2695–704. Available at: http://www.ncbi.nlm.nih.gov/pubmed/26195705.

21. Aurilio G, Disalvatore D, Pruneri G, Bagnardi V, Viale G, Curigliano G, et al. A meta-analysis of oestrogen receptor, progesterone receptor and human epidermal growth factor receptor 2 discordance between primary breast cancer and metastases. Eur J Cancer [Internet]. 2014;50(2):277–89. Available at: http://www.ncbi.nlm.nih.gov/pubmed/24269135.
22. Pusztai L, Viale G, Kelly CM, Hudis CA. Estrogen and HER-2 receptor discordance between primary breast cancer and metastasis. Oncologist [Internet]. 2010;15(11):1164–8. Available at: http://www.ncbi.nlm.nih.gov/pubmed/21041379.
23. Schootman M, Jeffe DB, Lian M, Aft R, Gillanders WE. Surveillance mammography and the risk of death among elderly breast cancer patients. Breast Cancer Res Treat [Internet]. 2008;111(3):489–96. Available at: http://www.ncbi.nlm.nih.gov/pubmed/17957465.
24. Rojas MP, Telaro E, Russo A, Moschetti I, Coe L, Fossati R, et al. Follow-up strategies for women treated for early breast cancer. Cochrane database Syst Rev [Internet]. 2005;25(1):CD001768. Available at: http://www.ncbi.nlm.nih.gov/pubmed/15674884.
25. Khatcheressian JL, Hurley P, Bantug E, Esserman LJ, Grunfeld E, Halberg F, et al. Breast cancer follow-up and management after primary treatment: American Society of Clinical Oncology clinical practice guideline update. J Clin Oncol [Internet]. 2013;31(7):961–5. Available at: http://www.ncbi.nlm.nih.gov/pubmed/23129741.

Chapter 16
Neoadjuvant Systemic Therapy

Ana Carolina de Ataíde Góes, Heni Debs Skaf, and Laura Testa

Abbreviations

ADC	Apparent diffusion coefficient map
AI	Artificial intelligence
BCS	Breast-conserving surgery
CEM	Contrast-enhanced mammography
DCE-MRI	Dynamic contrast-enhanced MRI
DCIS	Ductal carcinoma in situ
DWI	Diffusion-weighted imaging
HER2	Human epidermal growth factor receptor 2
HR	Hormone receptor
IBC	Inflammatory breast cancer
LN	Lymph nodes
MRI	Magnetic resonance imaging
NCT	Neoadjuvant chemotherapy
NET	Neoadjuvant endocrine therapy
NST	Neoadjuvant systemic therapy
pCR	Pathological complete response to therapy
PPV	Positive predictive value
RECIST	Response Evaluation Criteria in Solid Tumors

A. C. de Ataíde Góes (✉) · H. D. Skaf
Instituto de Radiologia INRAD, Hospital das Clinicas HCFMUSP, Faculdade de Medicina, Universidade de Sao Paulo, São Paulo, SP, Brazil
e-mail: h.skaf@hc.fm.usp.br

L. Testa
Departamento de Oncologia, Instituto do Cancer do Estado de Sao Paulo ICESP, São Paulo, SP, Brazil

S. J. Kim Hsieh, E. A. Morris (eds.), *Modern Breast Cancer Imaging*,
https://doi.org/10.1007/978-3-030-84546-9_16

SLNB	Sentinel lymph node biopsy
TN	Triple negative
US	Ultrasound

16.1 Indications

Neoadjuvant systemic therapy (NST) was first introduced in breast cancer treatment to make surgery possible for inoperable tumors.

As systemic treatment evolved and survival benefits were shown for adjuvant treatment, the scenario changed, and once a patient has a clear indication of chemotherapy, for example, it could be used upfront, making breast conservation possible.

More recently, residual disease in pathological surgical specimens after neoadjuvant chemotherapy (NCT) is a marker for the need to escalate treatment, both for HER2 and triple-negative (TN) breast cancer.

The current understanding of the breast medical oncology community is that for TN disease we should offer NCT for patients with tumor size over 2 cm (some would say even 1 cm) irrespectively of nodal involvement. For HER2-positive disease, this is also the case, with some debate on the agents and regimens.

Patients that present with HR-positive breast cancer are usually referred to NCT when they have locally advanced disease or any node-positive patients who have other markers of better response to treatment such as Grade 3 or high Ki67 (Table 16.1).

Neoadjuvant endocrine therapy (NET) development followed a different path. Patients who had postmenopausal locally advanced disease but were not fit for chemotherapy were offered first tamoxifen with 50% of patients achieving clinical responses. When aromatase inhibitors became available, they showed improved rates of response and chances for BCS (breast-conserving surgery).

PCR is not as prognostic for HR (hormone receptor)-positive breast cancer as it is for TN- or HER2-positive disease, but patients who achieve low Ki67, tumor staging pT2 or less, and pN0 after 24 weeks of NET have excellent disease-free and overall survival. These tumor characteristics are evaluated with PEPI (preoperative endocrine prognostic index) score, and it has been useful. NET was better studied in postmenopausal patients, so it's not routinely recommended for premenopausal HR-positive breast cancer.

Table 16.1 Indications of neoadjuvant chemotherapy for breast cancer

Triple-negative disease	Tumor size over 2 cm (or 1 cm for some)
HER2-positive disease	Tumor size over 2 cm
HR-positive disease	Locally advanced breast cancer (clinical stage T3 N1–N3 M0) Or Any node positive + markers of response (e.g., grade 3 or high Ki67)
Inflammatory breast cancer	

16.2 Introduction to Multimodality Response Assessment

Presently there are no established guidelines to best evaluate tumoral response during or after NST. However, prior to initiation of chemotherapy, diagnostic imaging should be performed for both breasts, and, depending on the disease stage and the presence of symptoms, whole-body imaging should be conducted as well. Historically, this first evaluation consists of conventional breast imaging (mammography and ultrasound), besides physical examination.

Imaging monitoring during NST may help anticipate which patients aren't experiencing a response in cases of uncertain clinical progression, avoiding unnecessary chemotherapeutic toxicity. It also permits the oncologist to tailor specific therapy regimens to be used before or after surgery.

The same imaging modality and protocol should be executed after NST in order to assist to predict which patients will achieve pCR, as well as estimate residual tumoral size for the purpose of planning a BCS.

Breast tumor should be clipped with image-detectable marker prior to neoadjuvant therapy for future preoperative localization and identification of tumor bed. Similarly, it's important to clip metastatic axillary lymph node(s). Preferable to use clip that can be well seen on US for future localization (Fig. 16.1).

However, the surgical planning may dictate the decision whether or not to obtain posttreatment imaging studies: repeating breast imaging after neoadjuvant therapy may not be necessary for patients with multicentric disease, extensive lesions, or another clear contraindication to BCS.

Physical examination is subjective and relies on the physician's experience, and its accuracy to determine pCR is inferior to the usual breast imaging methods [1]. Besides, the presence of fibrosis and firm fibroglandular tissue may overestimate the amount of residual disease, and the absence of a palpable lesion does not exclude the presence of a remaining tumor, being notably inaccurate for small early-stage cancers, particularly smaller than 2 cm [2].

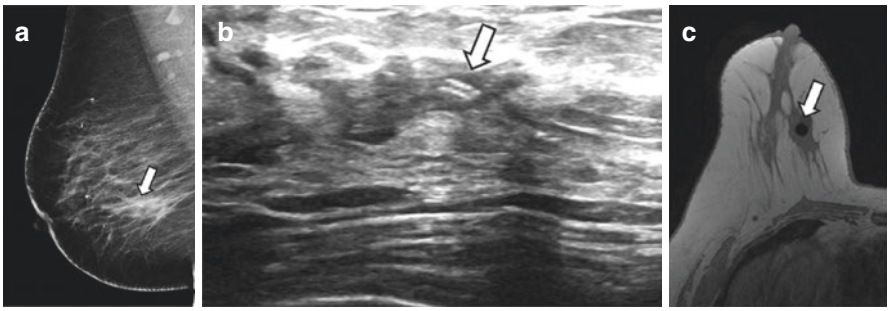

Fig. 16.1 Marker clip (arrows) within breast lesion on different imaging modalities. (**a**) Mammography shows a metallic clip. (**b**) The tissue marker is visible on ultrasound as hyperechogenic spots. (**c**) T1-weighted MR image shows local signal intensity void caused by marker clip

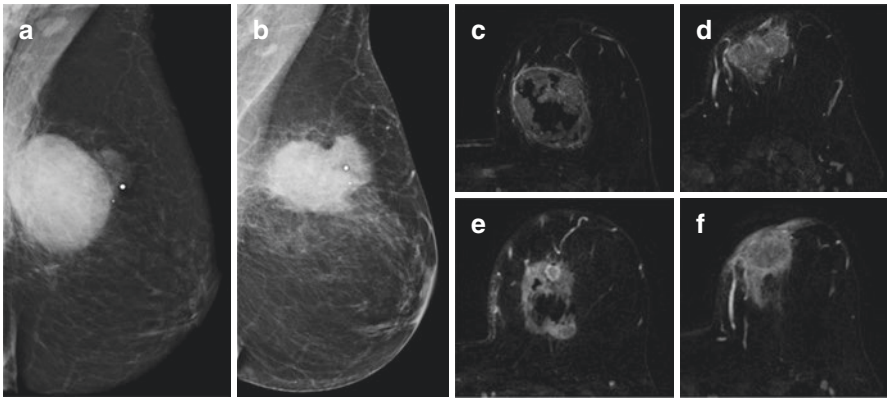

Fig. 16.2 CLM, 58-year-old female. MLO mammography before and after neoadjuvant systemic therapy shows two partially obscured masses (**a**), with signs of partial response to therapy characterized by reduced size associated to morphological changes of the lesions, now irregular and spiculated (**b**). However, despite the reduction in size after neoadjuvant systemic therapy (**c**, **e**), the cutaneous involvement became more pronounced on post-contrast MR subtracted images (**d**, **f**), emphasizing the intrinsic limitation of mammography in the skin evaluation

In the following sections, we will discuss each imaging modality, its advantages and limitations, as well as pitfalls and pearls in response evaluation. DCE-MRI offers the highest diagnostic accuracy in primary tumor therapy response assessment among the currently established imaging methods (mammography and ultrasound) [1], and its usage for response evaluation to NST is recommended by the American College of Radiology and European Society of Breast Imaging (Fig. 16.2) [3, 4].

Mammography and ultrasound (US) provide suboptimal evaluations in the accurate assessment of response to NST, and such limitations will be further discussed in this chapter. Predicting pCR is not highly accurate with US or mammography, correlating with these methods in only 13–25% of cases [5–7].

Despite DCE-MRI more accurately reflects true pathologic tumor size, it is more expensive, time-consuming, and less widely available and may still overestimate or underestimate residual disease but only within 1 cm of the final tumor size when compared to anatomopathological examination of the surgical specimen [8, 9]. The largest diameter of the lesion in the DCE-MRI showed the highest correlation with pathology in the evaluation of residual invasive disease after NST [10].

16.3 Mammography Interpretation

Mammography has a variable accuracy to assess residual tumor after neoadjuvant chemotherapy partly because of posttreatment image changes, such as the development of fibrosis or lesion fragmentation.

Furthermore, the pretreatment tumor mammographic presentation impacts the accuracy on assessment of the response to therapy, for example, lesions with circumscribed margins are better evaluated later, while indistinct or spiculated lesions negatively impact the method's accuracy [11]. This is partly due to the inherent method limitation in evaluating lesions with superimposed breast tissue, particularly in dense breasts, and may be alleviated by using digital breast tomosynthesis [12].

Some changes in mammographic images are more reliable response indicators than others, as the decrease in density and size is more common and trustworthy of response than changes in clustered calcifications, for instance.

Calcifications are often misleading, as they may remain stable, decrease, or increase after neoadjuvant chemotherapy (Fig. 16.3). A study analyzed 494 patients who underwent NST due to locally advanced breast cancer. There was no correlation between changes in clustered calcifications extent after pathologic complete response. In fact, they were associated at surgery with benign findings in 41% of patients. Regarding biological markers, positive estrogen receptor tumors were associated with a higher proportion of residual calcifications correlated with malignant findings at surgery when compared to negative estrogen receptor tumors, which

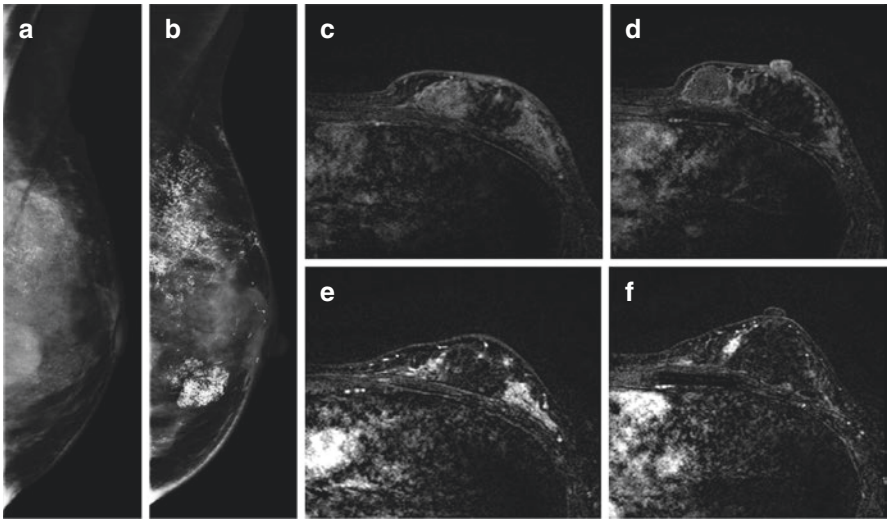

Fig. 16.3 GALO, 32-year-old female. MLO mammography before neoadjuvant systemic therapy shows an indistinct lesion occupying almost the entire left breast, diagnosed as invasive ductal carcinoma, associated with pleomorphic clustered calcifications (**a**). After the systemic therapy, there was partial regression of the lesion; nevertheless, we observed an increase in the extent and density of the calcifications (**b**). Post-contrast MRI before treatment characterizes an irregular mass with heterogeneous enhancement associated with non-mass diffuse enhancement of the left breast (**c**, **d**). After neoadjuvant systemic therapy, there were signs of a partial response characterized by a complete regression of the mass lesion with residual non-mass enhancement in multiple areas (**e**, **f**)

attained lower rates of pCR. Consequently, concerns about incomplete excision in this cancer subtype may be less of an issue [13].

Even though calcifications lacking enhancement more commonly represent benign findings, they can be malignant, as neoangiogenesis is not the same for all malignant breast lesions, not being always present in ductal carcinoma in situ or in lobular carcinomas. So regardless of enhancement dynamics, calcifications with malignant morphologic findings on mammography, without enhancement on MRI, which have not yet been histologically evaluated, should undergo biopsy [14].

According to some studies, mammography is more sensitive than physical examination for detecting residual tumor after neoadjuvant chemotherapy, especially in inflammatory carcinoma; however, it comes at the expense of decreased specificity and underestimation of the degree of response, with more false positives when compared to physical examination. False-positive mammographic assessments were mainly due to residual microcalcifications, benign at surgical specimen evaluation, and fibrosis [15, 16].

Contrast-enhanced mammography (CEM) is emerging as a feasible method capable of associating image features such as density and morphology with physiologic information due to tumoral neoangiogenesis.

CEM employs a dual-energy technique in order to highlight areas of contrast uptake in breast tissue by subtracting low-energy images from high-energy ones, canceling the enhancement of the background breast tissue. It uses standard mammography equipment upgraded to include copper filtration; the additional software needed for dual energy-imaging and a low-osmolar iodinated contrast material are also used.

Several studies have demonstrated CEM as an alternative to MRI to detect residual disease after NST. Patel et al. in 2018 retrospectively compared both methods in patients with invasive breast cancer after NST and both methods yielded comparable sensitivity and PPV in this matter [17]. Iotti and colleagues in 2017 made a prospectively evaluation of CEM and MRI in 54 patients and CEM demonstrated pCR better than MRI; nevertheless, both methods led to an underestimation of the extent of the residual tumor [18].

16.4 Ultrasound Interpretation

Breast and axillary US should be performed for malignant breast masses for clinical staging if neoadjuvant therapy is planned, being widely available and cost-effective.

There are some limitations though, as in physical examination and mammography, chemotherapy-induced fibrosis can be difficult to differentiate from residual disease by US and lesion fragmentation may underestimate its therapeutic response evaluation (Fig. 16.4).

Keune and colleagues retrospectively evaluated 196 patients diagnosed with invasive breast carcinoma and concluded that ultrasound was more accurate than

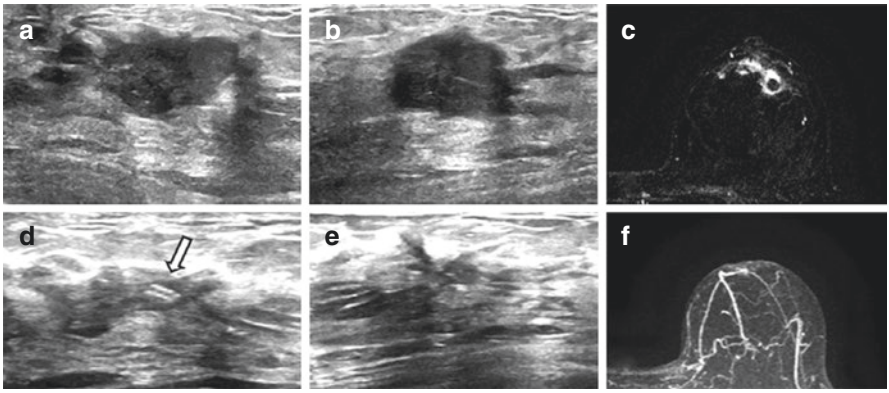

Fig. 16.4 BGK, 53-year-old female. Ultrasound of the left breast shows a hypoechoic irregular mass with angulated margins in the retroareolar region diagnosed as invasive ductal carcinoma (**a**, **b**), characterized on MRI as an irregular mass with heterogeneous enhancement (**c**). The lesion was marked with a clip (arrow) before systemic therapy and later characterized on ultrasound as a smaller hypoechoic irregular lesion (**d**, **e**) without corresponding enhancement on MRI (**f**). The final surgical specimen yielded a small ductal carcinoma in situ, without invasive component, with extensive regression signs

mammography in predicting residual tumor size after NST, demonstrating that 59.6% of residual tumors were accurately sized within 1 cm, when compared to surgical measurement, while mammography accurately sized 31.7% of the tumors [2]. Chagpar et al. corroborated these findings evaluating 189 patients, showing that US correlated with the size of the residual pathologic tumor (within an accuracy of 1 cm) in 75% of patients, mammography in 70%, and physical examination in 66% [19].

However, there was little difference in the ability of each method to predict pCR and the likelihood of a complete pathologic response was 80% when both imaging modalities did not demonstrate residual disease [2]. Peintinger et al. concluded that the combination of both methods, ultrasound and mammography, improves even more the accuracy of predicting a pCR to neoadjuvant chemotherapy to a greater degree than using either method isolated [20].

Ultrasound is listed on ACR Appropriateness Criteria® with a better rating than mammography to evaluate NST response, being a reliable modality to determine residual tumor size, particularly if it measures more than 7 mm and has been previously documented by the same method before NST [21, 22].

Regarding contrast-enhanced US, there is still not sufficient data to support its routine use in this setting, even though some studies suggest that change in time-intensity curves, representing quantitatively the tumoral perfusional changes after NST, may reliably predict response to therapy [23].

US also plays an important role in the management of the axilla due to its moderate sensibility and great specificity in the diagnosis of metastatic axillary involvement (Fig. 16.5) [24]. For those in whom axillary lymph nodes are palpated on physical exam, US is the first step in radiological investigation. If a suspicious

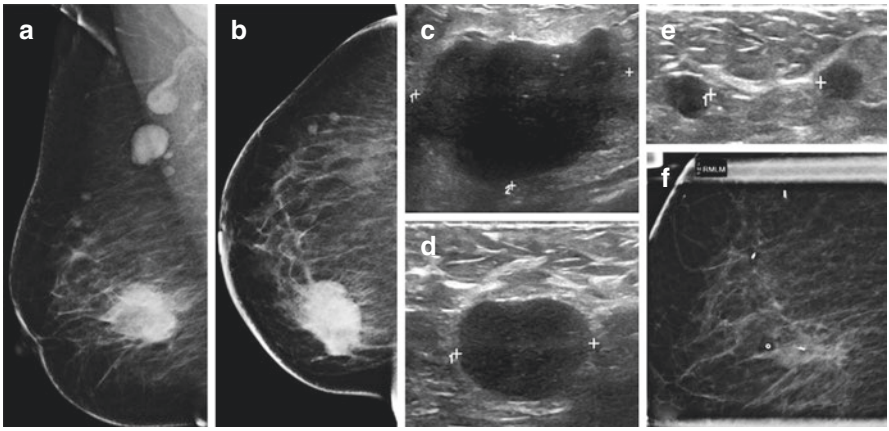

Fig. 16.5 MAS, 50-year-old female. MLO and CC mammography show an indistinct irregular mass at the junction of the inner quadrants on the right breast, diagnosed as invasive ductal carcinoma, as well as two smaller lesions at the upper outer quadrant and round enlarged axillary lymph nodes (**a**, **b**). These lymph nodes were better evaluated by ultrasound, both with thickened cortex and no visible hilum (**c**, **d**). Ultrasound better characterized both lesions in the upper outer quadrant which were diagnosed as compromised lymph nodes after core needle biopsy (**e**). All the breast lesions were marked with a clip before neoadjuvant systemic therapy for better surgical planning (**f**)

lymph node is found, ultrasound-guided needle biopsy should be performed to confirm pathologic involvement, and a marker can be placed in case a complete imaging response is obtained (see Lymph Node Evaluation).

This method is the most accurate predictor of NST response in axillary lymph nodes, when compared to physical examination and mammography [5], being the modality of choice according to the ACR Appropriateness Criteria®, as it permits the visualization of lymph nodes level I and II routinely, with a higher spatial resolution to evaluate these structures, better depicting cortical thickening or lobulations, absent hilum, and abnormal cortical vascularization by Doppler imaging, among other alterations.

16.5 MRI Interpretation

Magnetic resonance imaging (MRI) is the most accurate and reproducible method available to monitor breast cancer response to NST, being an excellent modality to define the extent of the disease and assist the surgeon in determining the optimal surgical approach. However, like any method, it has its advantages and limitations, and in this scenario, it can both overestimate and underestimate the tumor response.

According to the different aims for which NST is applied, MRI can be used for different purposes. From an oncologist's perspective, assessing the response to a

specific regimen and measuring changes in the size of the invasive tumor as early as possible helps to adapt the regimen in case of failure to respond [25, 26]. MRI has also been used to monitor the degree of response to induction chemotherapy as a surrogate marker for pCR, that is, to guide further systemic treatment [27]. For a surgeon, assessing the extent of possible residual disease, including DCIS, is important to guide subsequent surgery [28, 29]. Thus, separate strategies might be needed to determine response to a specific chemotherapy regimen and to determine residual tumor size after NST.

MRI Technique MRI is often acquired on a scanner of at least 1.5-T using a dedicated breast coil in the prone position. The imaging protocol usually consists of fat-suppressed axial T2-weighted images, diffusion-weighted imaging (DWI), and dynamic contrast-enhanced fat-suppressed T1-weighted images, besides standard subtraction images [30]. For further improvement of therapy response prediction and monitoring, other advanced imaging approaches are being evaluated. These include the quantitative dynamic contrast-enhanced imaging, advanced DWI techniques, and spectroscopic imaging, which are under investigation for the prediction of neoadjuvant therapy effects [31]. With the advent of artificial intelligence (AI) and machine learning, the large data sets provided by and potentially extractable from breast MRI make it suitable for AI applications. Recent developments in predicting the tumor response to the NST show promising results in objective interpretation of MR images using AI methods in personalized care for breast cancer patients [32]. However, there still no consensus on its broad application.

16.5.1 When to Assess Tumor Response

Imaging evaluation should be started prior to treatment, to identify the extent of disease. The ideal time for response analysis depends on the treatment, which can be performed in 6–9 weeks, and some authors suggest immediately after the first cycle of neoadjuvant therapy. Assessing the response at the beginning of treatment expands the clinical applications, detecting resistant tumor and avoiding the unnecessary toxicity of chemotherapeutic agents. Furthermore, previous studies suggest that MRI at the beginning of neoadjuvant treatment is more accurate and a stronger predictor of pCR than MRI after NST [33, 34]; however, it is currently mostly restricted to adaptive clinical trials. Early evaluation of tumor response could also allow to anticipate the timing of surgery if the tumor is found to be refractory to neoadjuvant therapy. Lastly, imaging after the completion of NST is important, as it evaluates residual disease to allow preoperative planning. However, with or without preceding NAC, preoperative MRI has not been proven to be associated with improved surgical outcomes or recurrence rates [35].

16.5.2 How to Assess Residual Tumor with MRI

The first step for suitable evaluation is cognizing the factors that affect the accuracy of MRI in demonstrating residual disease after NST, in order to adopt a tailored interpretation strategy. These factors include image acquisition parameters, methods of administration of contrast material, the histologic type of the tumor (ductal vs lobular), and the status of the tumor's HR and HER2 receptors. The size of lobular or HR-positive/ HER2-negative cancers tended to be underestimated on MRI compared to ductal or other subtypes, respectively (Fig. 16.6) [36]. In cases of HR-positive cancers, late phases of postcontrast MRI are better to evaluate response. In addition, factors such as therapy agents and baseline tumor morphology may modulate the MRI accuracy in identifying residual disease (see below).

To assess response to NST, changes in maximum tumor size, tumor volume, and enhancement kinetics have been used, as well as functional techniques, including various DWI, and molecular imaging techniques are being investigated [30]. The Response Evaluation Criteria in Solid Tumors (RECIST) 1.1 guidelines are standardized criteria widely used for response assessment [37]. Based upon measurement of a solid tumor in at least the longest diameter, four response categories are recognized: complete response, partial response, stable disease, and progressive disease (Table 16.2). Due to its emphasis on changes in lesion size and the unique

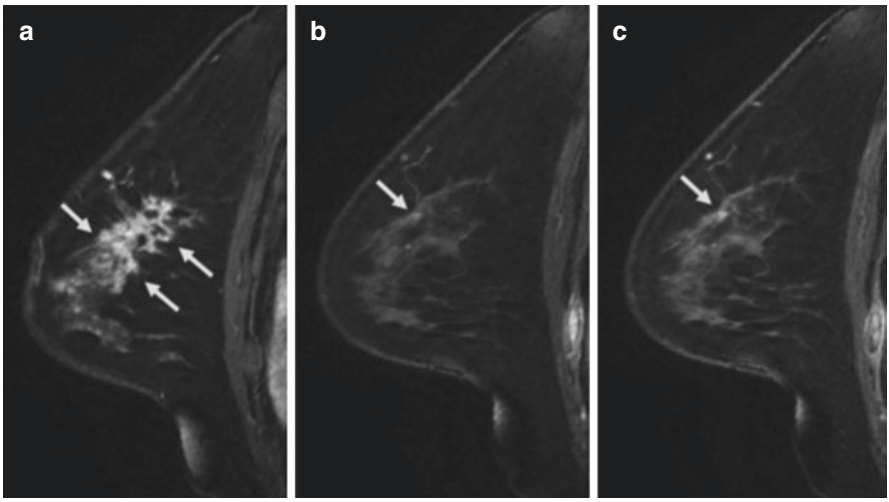

Fig. 16.6 A 50-year-old woman with invasive ductal carcinoma (estrogen receptor-positive and HER2-negative). (**a**) Prechemotherapy MRI shows a 6.0 cm irregular enhancing mass (arrows). (**b**) MRI obtained after completion of four cycles of doxorubicin/cyclophosphamide followed by four cycles of docetaxel in the early post-contrast phase (90 seconds) shows an 0.3 cm enhancing lesion (arrow). (**c**) An image obtained in the delayed phase (360 seconds) shows the lesion measuring 0.5 cm (arrow). Surgical histopathology revealed a 4.8 cm invasive ductal carcinoma and 5.0 cm total tumor size (including both invasive tumor and ductal carcinoma in situ). (Reprinted with permission from Reig et al. [47]. https://doi.org/10.1002/jmri.27145)

Table 16.2 Evaluation of target and nontarget lesions according to Response Evaluation Criteria in Solid Tumors (RECIST), version 1.1

Type of lesion and response	Criteria
Target lesion	
Complete response (CR)	Disappearance of all target lesions
Partial response (PR)	Decrease in the sum of the diameters of the target lesions ≥30%
Progressive disease (PD)	Increase in the sum of the diameters of the target lesions ≥20% Appearance of new lesions
Stable disease	Does not meet criteria for CR, PR, or PD
Non-target lesion	
Complete response (CR)	Disappearance of all non-target lesions
Non-CR/non-PD	Persistence of non-target lesions
Progressive disease (PD)	Appearance of new lesions Unequivocal progression of the non-target lesions

features of breast cancer, RECIST may not be reliable in this setting, being criticized for failing to capture meaningful changes in tumor biology [38].

The measurement of the functional tumor volume was a better predictor of response than the change in the longest diameter, as shown in the American College of Radiology Imaging Network (ACRIN) 6657 trial [34]. Furthermore, tumor volume change was found to be a predictor of recurrence-free survival even as early as after one cycle of chemotherapy (Fig. 16.7) [27].

Changes in time-signal intensity curve analysis or pharmacokinetic parameters may also be helpful in predicting response [39], with an early decrease in enhancement as an important predictor of response [40, 41].

Likewise, the apparent diffusion coefficient (ADC) has shown promise for detecting early response to therapy, with an increase in ADC after treatment as a predictor of response (Fig. 16.8). Although it sounds appealing, the use of DWI as an exclusive method to visualize residual disease is limited by its lower spatial resolution compared with DCE-MR imaging [42, 43].

The combination of changes in volumetric and functional assessment of the tumor may improve the specificity of the diagnosis; however, large-scale studies with standardized image acquisition are needed to implement these parameters as alternatives to conventional size measurements.

Still, to date there is no uniformly accepted method to obtain response assessment. In order to lead to a more standardized and less subjective evaluation of breast MRI acquisitions, a proposal for response types follows:

– **Complete response**: defined as total disappearance of the lesion (Fig. 16.9), being more unusual in separated or replaced lesions. The absence of enhancement in the tumor bed at visual assessment is the most commonly used imaging criterion for pCR, correlating well for HER2-positive and triple-negative subtypes, whereas this correlation is substantially weaker in HR-positive breast cancers [44, 45]. Note that complete radiologic response is different from the complete pathological response, which is most commonly defined as no residual

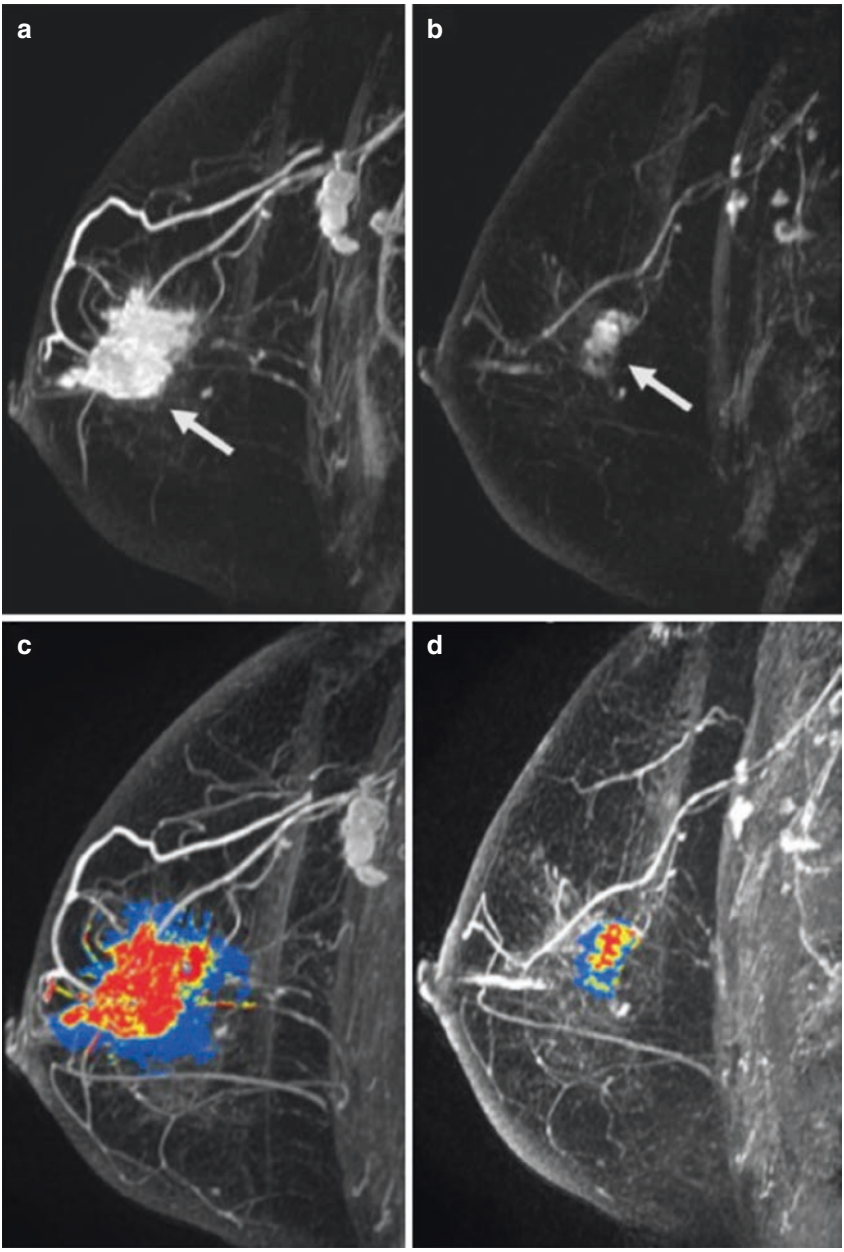

Fig.16.7 A 57-year-old woman with invasive ductal carcinoma. (**a**) Prechemotherapy maximal intensity projection (MIP) image of contrast-enhanced MRI shows a 4.5 cm irregular mass (arrow). (**b**) Post chemotherapy MIP image of contrast-enhanced MRI shows a 1.7 cm irregular mass (arrow) [(4.5–1.7)/4.5] × 100 = 62% reduction of the initial tumor diameter, suggestive of partial response. Computer-aided volumetry (red and yellow color) shows a 95% volume reduction from 27.4 cc (**c**) to 1.5 cc (**d**). (Reprinted with permission from Reig et al. [47]. https://doi.org/10.1002/jmri.27145)

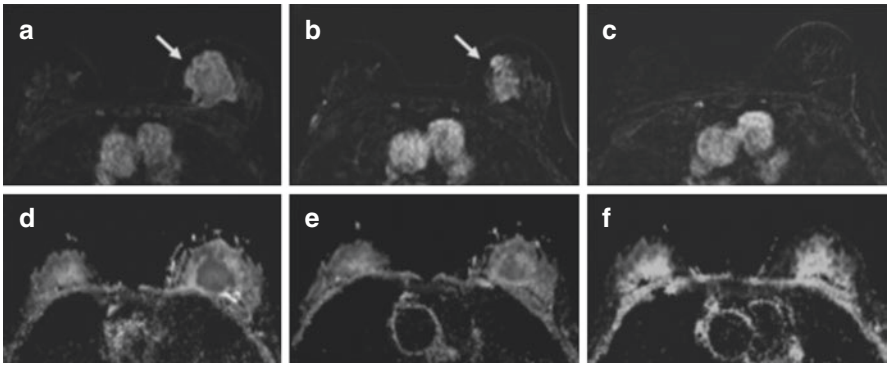

Fig. 16.8 A 44-year-old woman with invasive ductal carcinoma. (**a**) Prechemotherapy contrast-enhanced subtraction T1-weighted MRI shows an enhancing mass in the left breast (arrow). The maximal diameter of the mass was measured up to 7.4 cm. (**b**) After the first cycle of chemotherapy, the mass was measured up to 5.7 cm (arrow). (**c**) After the eight cycle of chemotherapy, the mass is not seen. ADC maps using b = 0 and 750 s/mm^2 at baseline (**d**), post-first cycle (**e**), and post-eight cycle chemotherapy timepoints (**f**) show the signal intensity increases after chemotherapy. The ADC value for the lowest signal intensity of the tumor was 1.103×10^{-3} mm^2/sec, 1.463×10^{-3} mm^2/sec, and 2.162×10^{-3} mm^2/sec, respectively. %ΔADC was 32.6% at post-first cycle chemotherapy. The patient underwent surgery, and surgical histopathology revealed no residual invasive ductal carcinoma. (Reprinted with permission from Reig et al. [47]. https://doi.org/10.1002/jmri.27145)

invasive disease or no residual invasive and in situ disease in the breast and axilla [46]. As MRI cannot reliably distinguish between invasive disease and ductal carcinoma in situ (DCIS), defining pCR as no residual invasive disease will increase MRI overestimation rates, as MRI identifies residual DCIS that is not counted in final pathology [47]. It is important to evaluate MRI enhancement in both early and delayed phases in any patient after NST to reduce underestimation of risk of residual disease, mainly in patients undergoing antiangiogenic therapies [48]. Although some groups have found that late enhancement may be seen in HER2+ cancers without residual disease [49], studies evaluating MRI parameters by breast cancer subtype are needed to further elucidate these findings. Lastly, remember that BI-RADS category 6 must be used even in cases of complete response.

– **Partial response**: tumor assessment on MRI might be challenging, as NST causes various histopathological changes in tumor cellularity, causing some tumors to show concentric shrinkage pattern (usually single mass) [50], while others may crumble ("fragmentation") into scattered islands of tumor cells (Fig. 16.10). In the latter case, a response is present, but the area of residual disease may remain similar to that prior to treatment. In addition, it is difficult to determine whether the multinodular enhancing lesions are residual invasive cancer, DCIS, or a reactive change after therapy [36]. A shrinkage pattern has also been found to be associated with tumor molecular subtype [51], with HER2+ tumors more likely to demonstrate concentric shrinkage, and HR-tumors are

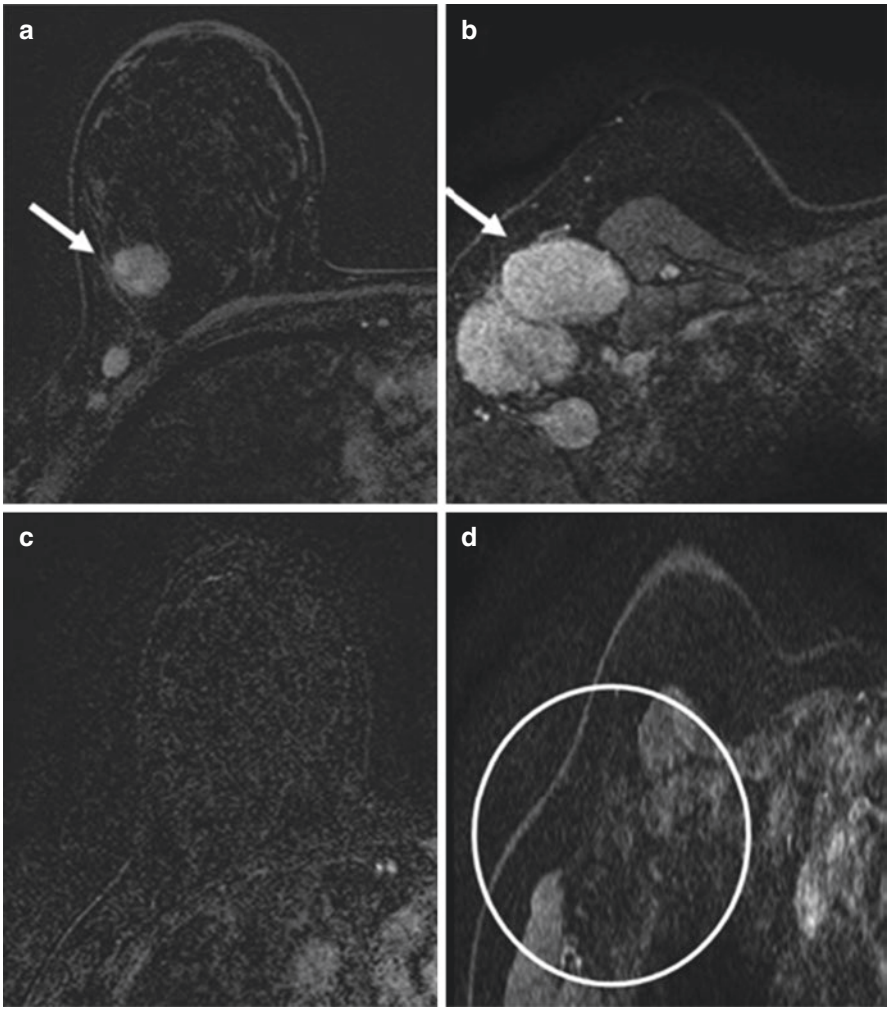

Fig. 16.9 A 38-year-old woman with triple-negative invasive ductal carcinoma of the right breast. Axial subtraction MRI: Image acquired before the NST demonstrates (**a**) a right breast mass (arrow) and (**b**) pathological lymph nodes (arrow). (**c**, **d**) Images after neoadjuvant chemotherapy show resolution of all lesions characterizing complete response. PCR confirmed after breast-conserving surgery

more likely to demonstrate a mixed pattern of concentric and crumbling shrinkage.

– **Stable disease:** unchanged compared with the baseline study, with unchanged defined as an enhancement rate of +/− 20% of baseline. It is usually related with tumor chemoresistance and strongly predictive of nonresponse by the end of therapy [47].

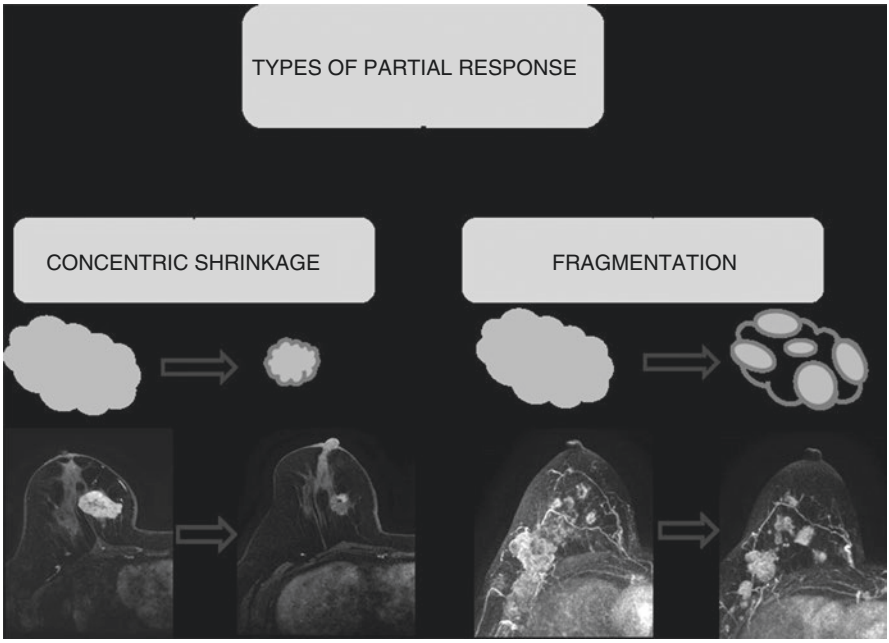

Fig. 16.10 Shrinkage patterns after neoadjuvant therapy includes concentric shrinkage and reduction into residual nodular lesions (fragmentation)

– **Progressive disease**: it represents the minority of cases and occurs with an increase in the size of lesion or appearance of new lesions. As breast cancer is a complex heterogeneous disease, primary tumor and micro metastases don't necessarily respond to the same therapy; thus, radiologists should be aware of progressive disease outside the primary tumor (Fig. 16.11) [38].

16.5.3 Pearls and Pitfalls in the Assessment of Response

Although MRI performs better than conventional modalities overall, it does have limits due to false-positive and false-negative results. Studies have found that MRI underestimated residual disease in 10% of cases and overestimated in 33% of cases by up to 1.0 cm [52, 53]. The potential clinical impact of overestimation of residual tumor is the resection of a larger amount of tissue during breast conservation surgery, which may negatively alter cosmetic outcome or influence a decision for mastectomy. The impact of underestimation of residual tumor is the potential for an incomplete resection with positive margins and the need for surgical re-excision.

Thus, it is important to be aware of the following factors [36, 47, 54–56]:

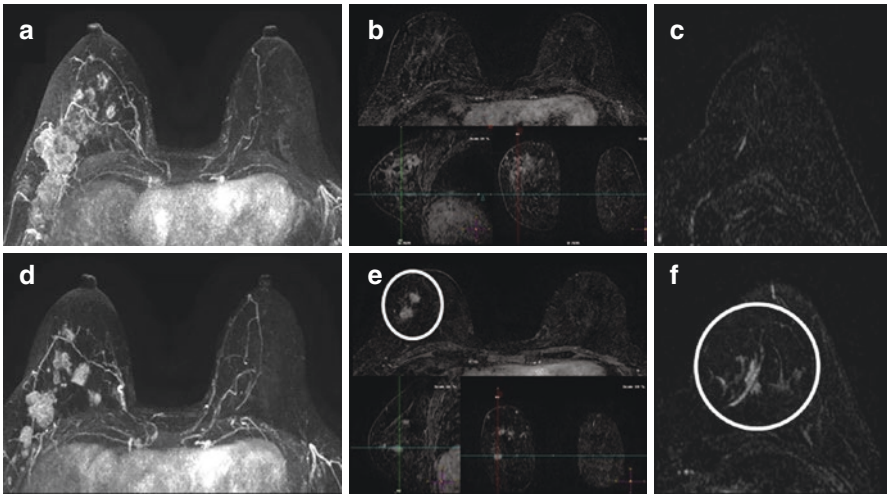

Fig. 16.11 A 31-year-old female with invasive breast carcinoma (not otherwise specified). Pre- (**a**) and post-therapy (**d**) MIP image shows an irregular and indistinct mass that decreased into a fragmented pattern after NST. Despite a partial response from the index lesion, new lesions have appeared on the lower outer quadrant of the right breast (**e** – circle) and left breast (**f** - circle), not shown on prechemotherapy images (**b**, **c**), characterizing progressive disease

16.5.3.1 Causes of Underestimation of Residual Disease

- **Invasive cancer cells without mass formation** may be underestimated due to their nonconcentric shrinkage pattern.
- Residual disease may only enhance in **late phases** of postcontrast MRI, particularly for HR-positive breast cancer.
- **Invasive lobular carcinoma** tends to be underestimated on MRI due to its growth pattern, subtle enhancement, distribution that mimics the normal breast parenchyma, and higher HR positivity.
- The anti-vascular effect of **taxane-containing neoadjuvant chemotherapy** may result in the decrease or resolution of enhancement despite residual disease.

16.5.3.2 Causes of Overestimation of Residual Disease

- **Fibrosis or posttreatment changes (inflammation and granulation tissue)** in the original tumor bed may contribute to the remaining contrast enhancement despite the treatment response, mimicking residual cancer.
- **Mucinous or necrotic tumor** may leave residual masses even without residual cancer. On mucinous carcinoma, persistent pools of mucin result in a continuous mass effect, so subsequent images may suggest a minimal response or even progressive disease despite an excellent pathological response (Fig. 16.12).

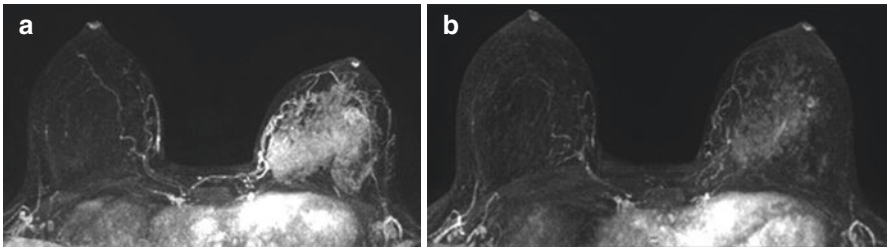

Fig. 16.12 A 40-year-old female with left invasive mucinous carcinoma (luminal B). (**a**) MIP image shows diffuse non-mass enhancement in the left breast that persists after NST (**b**). Despite the extent of enhancement in MRI, postoperative histopathologic findings showed an excellent pathological response (low cellularity)

– Fibroadenomas and other **benign lesions** may be stable after therapy, and biopsy may be required to differentiate them from residual disease.

16.5.4 Challenging Lesions for Assessment of Response

MRI has a significant role in some lesions that are difficult to assess by other modalities, especially in response to nonmeasurable lesions. In addition to non-mass enhancement, MRI is also useful in evaluating inflammatory breast cancer and complex cystic lesion.

The diagnosis of IBC is clinical, with a combination of skin changes and breast enlargement presenting rapidly (few weeks or few months), with or without an underlying palpable mass. MRI can detect a primary breast lesion in 98% of the cases, and the most common finding is an index mass or multiple small masses. Skin abnormalities, such as thickening, edema, and cutaneous masses or enhancing foci, are also better detected with MRI than other modalities. As the disease is best seen with MRI, response prediction and residual tumor size correlation with final pathology are also better with MRI than ultrasound or mammography [57]. Note that the assessment of the post-therapy response of the skin and nipple-areola complex thickening is limited and should be valued when these structures enhance, especially in a nodular and irregular pattern (Fig. 16.13).

Furthermore, the exact extent of the tumor in complex solid-cystic lesions may be difficult to delineate. MRI allows the identification of intratumoral necrosis when there is a very high signal intensity (similar to water) within the tumor in the fat-suppressed T2-weighted MRI scans [58]. In these cases, it is important to measure and follow the entire lesion and also the solid component, as necrotic tumors may leave residual acellular masses.

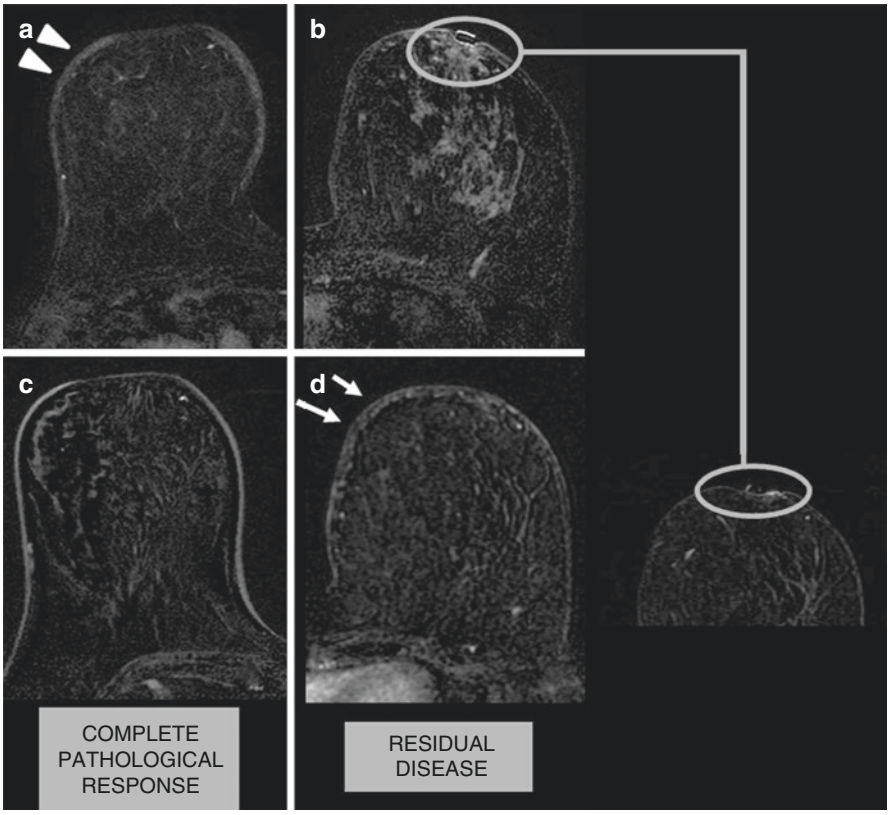

Fig. 16.13 Skin and nipple assessment of two different patients with inflammatory breast cancer (MRI T1W CE with subtraction). Images on the left from the same patient who presented global skin thickening of the right breast (**a** – arrowhead) that decreased after NST (**c**). Final pathologic findings after mastectomy surgery showed complete pathologic response. On the other hand, images on the right from another patient show diffuse non-mass enhancement with retraction and enhancement of nipple-areola complex (**b** – circle) in addition to skin enhancement that persists after NST (**d** – arrow), characterizing residual disease

16.6 Lymph Node Evaluation

NST can be used to reduce tumor burden and downstage the axilla, with pCR rates of 50–60% in the axillary lymph nodes (LN) [59]. In patients who are expected to achieve axillary pCR, omission of axillary LN dissection could prevent morbidity and complications such as lymphedema; therefore, sentinel LN biopsy (SLNB) could be an alternative surgical method [60]. Regarding axillary management after NST, two prospective observational trials – the Alliance Z1071 and SENTINA

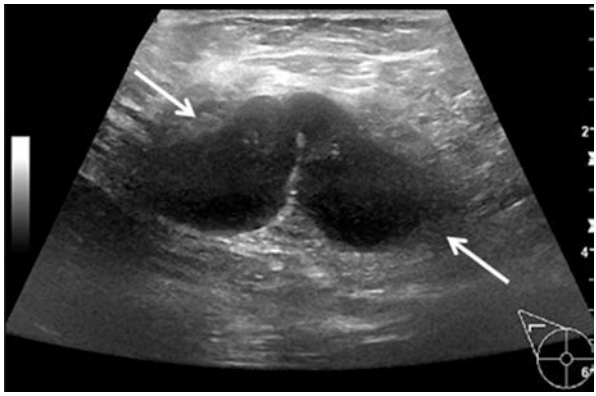

Fig. 16.14 Illustration of suspicious axillary lymph (ALN) node on ultrasound. Ultrasound image of metastatic ALN showing irregular shape, thickened hypoechoic cortex (> 3 mm), and deformity or absence of hyperechoic fatty hilum by compression (white arrows)

trials – suggested that if at least three sentinel LNs were obtained; then SLNB could be sufficient in patients who become clinically node-negative after NST [59, 61]. However, the overall false-negative rates of the two aforementioned studies were 13–14%, which is above the accepted cutoff value of 10%. Thus, axillary LN dissection has been the standard treatment in clinically node-positive breast cancer after NST due to the lack of consensus in the selection of proper candidates for SLNB [62] (see Chap. 4).

According to the American College of Radiology (ACR) Appropriateness Criteria, the most accurate imaging modality in the assessment of residual disease after NST is MRI for primary breast cancer and US for axillary LN [63].

Although some controversies remain with unsatisfactory false-negative rates, US is still known to be the most accurate modality in the evaluation of the axillary LN in NST setting [64, 65].

MRI may also play a role in evaluating LN; however, the sensitivity of post neoadjuvant MRI in the detection of persistent LN metastasis is only moderate, ranging from 61% to 72% [66, 67]. Likewise, axillary regions may be insufficiently included in MR images.

Suspicious features of axillary LNs include cortical thickening of more than 3 mm, round or irregular shape, or loss of fatty hilum [68] (Fig. 16.14). While a cut of a value of 3 mm of cortical thickness is used, a small residual metastatic focus can be missed, or fibrosis and reactive enlargement of 3 mm may be misinterpreted as residual disease [69].

Note that radiological and pathological response to NST in the breast and axilla are often correlated, but a proportion of patients (14.4%) have different responses in the two sites [69] (Fig. 16.15). Therefore, it is recommended that the axilla and the breast should be viewed and assessed as two separate entities for treatment planning.

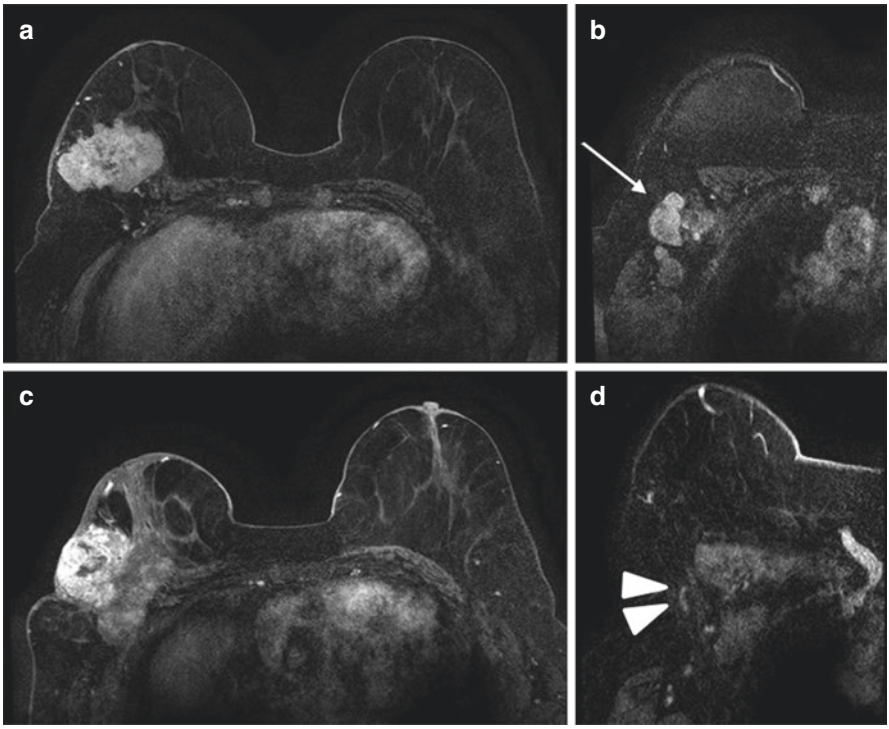

Fig. 16.15 T1W CE MRI in a 60-year-old female with triple-negative invasive ductal carcinoma in the right breast. Upper images demonstrate baseline MRI: (**a**) irregular mass in the right breast; (**b**) pathologic axillary lymph node (arrow). Bottom images: post-NST MRI shows an increase in the diameter of the breast mass and evidence of muscular and skin invasion (**c**), characterizing progressive breast disease. Even so, there was a reduced lymph node as shown in (**d**) (arrowheads), and no axillary metastasis was found at surgery, which impacted the management of the axilla. The response to NST in the breast and axilla is not always similar, so it is important to evaluate them separately

References

1. Croshaw R, Shapiro-Wright H, Svensson E, Erb K, Julian T. Accuracy of clinical examination, digital mammogram, ultrasound, and MRI in determining postneoadjuvant pathologic tumor response in operable breast cancer patients. Ann Surg Oncol. 2011;18(11):3160–3. https://doi.org/10.1245/s10434-011-1919-5.
2. Keune JD, Jeffe DB, Schootman M, Hoffman A, Gillanders WE, Aft RL. Accuracy of ultrasonography and mammography in predicting pathologic response after neoadjuvant chemotherapy for breast cancer. Am J Surg. 2010;199(4):477–84. https://doi.org/10.1016/j.amjsurg.2009.03.012.
3. Lehman C. ACR practice parameter for the performance of contrast-enhanced magnetic resonance imaging (MRI) of the breast. Am Coll Radiol. 2013. Available at: https://www.acr.org/-/media/ACR/Files/Practice-Parameters/mr-contrast-breast.pdf
4. Mann RM, Kuhl CK, Kinkel K, Boetes C. Breast MRI: guidelines from the European Society of Breast Imaging. Eur Radiol. 2008;18(7):1307–18. https://doi.org/10.1007/s00330-008-0863-7.

5. Herrada J, Iyer RB, Atkinson EN, Sneige N, Buzdar AU, Hortobagyi GN. Relative value of physical examination, mammography, and breast sonography in evaluating the size of the primary tumor and regional lymph node metastases in women receiving neoadjuvant chemotherapy for locally advanced breast carcinoma. Clin Cancer Res. 1997;3(9):1565–9.
6. Vinnicombe SJ, MacVicar AD, Guy RL, Sloane JP, Powles TJ, Knee G, Husband JE. Primary breast cancer: mammographic changes after neoadjuvant chemotherapy, with pathologic correlation. Radiology. 1996;198(2):333–40. https://doi.org/10.1148/radiology.198.2.8596827.
7. von Minckwitz G, Dan Costa S, Eiermann W, Blohmer JU, Tulusan AH, Jackisch C, Kaufmann M. Maximized reduction of primary breast tumor size using preoperative chemotherapy with doxorubicin and docetaxel. J Clin Oncol. 1999;17(7):1999–2005. https://doi.org/10.1200/jco.1999.17.7.1999.
8. Yeh E, Slanetz P, Kopans DB, Rafferty E, Georgian-Smith D, Moy L, Halpern E, Moore R, Kuter I, Taghian A. Prospective comparison of mammography, sonography, and MRI in patients undergoing neoadjuvant chemotherapy for palpable breast cancer. Am J Roentgenol. 2005;184(3):868–77. https://doi.org/10.2214/ajr.184.3.01840868.
9. Rosen EL, Blackwell KL, Baker JA, Soo MS, Bentley RC, Yu D, Samulski TV, Dewhirst MW. Accuracy of MRI in the detection of residual breast cancer after neoadjuvant chemotherapy. Am J Roentgenol. 2003;181(5):1275–82. https://doi.org/10.2214/ajr.181.5.1811275.
10. Scheel JR, Kim E, Partridge SC, et al. MRI, clinical examination, and mammography for preoperative assessment of residual disease and pathologic complete response after neoadjuvant chemotherapy for breast cancer: ACRIN 6657 trial. Am J Roentgenol. 2018;210(6):1376–85. https://doi.org/10.2214/AJR.17.18323.
11. Huber S, Wagner M, Zuna I, Medl M, Czembirek H, Delorme S. Locally advanced breast carcinoma: evaluation of mammography in the prediction of residual disease after induction chemotherapy. Anticancer Res. 2000;20(1B):553–8.
12. Förnvik D, Zackrisson S, Ljungberg O, Svahn T, Timberg P, Tingberg A, Andersson I. Breast tomosynthesis: accuracy of tumor measurement compared with digital mammography and ultrasonography. Acta Radiol. 2010;51(3):240–7. https://doi.org/10.3109/02841850903524447.
13. Adrada BE, Huo L, Lane DL, Arribas EM, Resetkova E, Yang W. Histopathologic correlation of residual mammographic microcalcifications after neoadjuvant chemotherapy for locally advanced breast cancer. Ann Surg Oncol. 2015;22(4):1111–7. https://doi.org/10.1245/s10434-014-4113-8.
14. Kuhl CK. MRI of breast tumors. Eur Radiol. 2000;10(1):46–58. https://doi.org/10.1007/s003300050006.
15. Helvie MA, Joynt LK, Cody RL, Pierce LJ, Adler DD, Merajver SD. Locally advanced breast carcinoma: accuracy of mammography versus clinical examination in the prediction of residual disease after chemotherapy. Radiology. 1996;198(2):327–32. https://doi.org/10.1148/radiology.198.2.8596826.
16. Moskovic EC, Mansi JL, King DM, Murch CR, Smith IE. Mammography in the assessment of response to medical treatment of large primary breast cancer. Clin Radiol. 1993;47(5):339–44. https://doi.org/10.1016/S0009-9260(05)81451-5.
17. Patel BK, Hilal T, Covington M, Zhang N, Kosiorek HE, Lobbes M, Northfelt DW, Pockaj BA. Contrast-enhanced spectral mammography is comparable to MRI in the assessment of residual breast cancer following neoadjuvant systemic therapy. Ann Surg Oncol. 2018;25(5):1350–56. https://doi.org/10.1245/s10434-018-6413-x.
18. Iotti V, Ravaioli S, Vacondio R, Coriani C, Caffarri S, Sghedoni R, et al. Contrast-enhanced spectral mammography in neoadjuvant chemotherapy monitoring: a comparison with breast magnetic resonance imaging. Breast Cancer Res. 2017;19(1):106. https://doi.org/10.1186/s13058-017-0899-1.
19. Chagpar AB, Middleton LP, Sahin AA, et al. Accuracy of physical examination, ultrasonography, and mammography in predicting residual pathologic tumor size in patients treated with neoadjuvant chemotherapy. Ann Surg. 2006;243(2):257–64. https://doi.org/10.1097/01.sla.0000197714.14318.6f.

20. Peintinger F, Kuerer HM, Anderson K, et al. Accuracy of the combination of mammography and sonography in predicting tumor response in breast cancer patients after neoadjuvant chemotherapy. Ann Surg Oncol. 2006;13(11):1443–9. https://doi.org/10.1245/s10434-006-9086-9.
21. Ollivier L, Balu-Maestro C, Leclére J. Imaging in evaluation of response to neoadjuvant breast cancer treatment. Cancer Imaging. 2005;5(1):27–31. https://doi.org/10.1102/1470-7330.2005.0009.
22. Roubidoux MA, LeCarpentier GL, Fowlkes JB, Bartz B, Pai D, Gordon SP, Schott AF, Johnson TD, Carson PL. Sonographic evaluation of early-stage breast cancers that undergo neoadjuvant chemotherapy. J Ultrasound Med. 2005;24(7):885–95. https://doi.org/10.7863/jum.2005.24.7.885.
23. Cao X, Xue J, Zhao B. Potential application value of contrast-enhanced ultrasound in neoadjuvant chemotherapy of breast cancer. Ultrasound Med Biol. 2012;38(12):2065–71. https://doi.org/10.1016/j.ultrasmedbio.2012.07.027.
24. Alvarez S, Añorbe E, Alcorta P, López F, Alonso I, Cortés J. Role of sonography in the diagnosis of axillary lymph node metastases in breast cancer: a systematic review. Am J Roentgenol. 2006;186(5):1342–8. https://doi.org/10.2214/AJR.05.0936.
25. Mano MS, Awada A. Primary chemotherapy for breast cancer: the evidence and the future. Ann Oncol. 2004;15:1161–71.
26. Maur M, Guarneri V, Frassoldati A, Conte PF. Primary systemic therapy in operable breast cancer: clinical data and biological fall-out. Ann Oncol. 2006;17 Suppl 5:158–64.
27. Hylton NM, Blume JD, Bernreuter WK, et al. Locally advanced breast cancer: MR imaging for prediction of response to neoadjuvant chemotherapy—results from ACRIN 6657/I-SPY TRIAL. Radiology. 2012;263(3):663–72.
28. Pediconi F, Miglio E, Telesca M, et al. Effect of preoperative breast magnetic resonance imaging on surgical decision making and cancer recurrence rates. Investig Radiol. 2012;47(2):128–35.
29. Pettit K, Swatske ME, Gao F, et al. The impact of breast MRI on surgical decision-making: are patients at risk for mastectomy? J Surg Oncol. 2009;100(7):553–8.
30. Le-Petross HT, Lim B. Role of MR imaging in neoadjuvant therapy monitoring. Magn Reson Imaging Clin N Am. 2018;26:207–20.
31. Mann RM, Cho N, Moy L. Breast MRI: state of the art. Radiology. 2019;292:520–36.
32. Codari M, Schiaffino S, Sardanelli F, Trimboli RM. Artificial intelligence for breast MRI in 2008–2018: a systematic mapping review. AJR. 2019;212:280–92.
33. Goorts B, Dreuning KMA, Houwers JB, Kooreman LFS, Boerma EG, Mann RM, et al. MRI-based response patterns during neoadjuvant chemotherapy can predict pathological (complete) response in patients with breast cancer. Breast Cancer Res. 2018:20–34.
34. Hylton NM, Gatsonis CA, Rosen MA, Lehman CD, Newitt DC, Partridge SC, et al. Neoadjuvant chemotherapy for breast cancer: functional tumor volume by MR imaging predicts recurrence-free survival—results from the ACRIN 6657/CALGB 150007 I-SPY 1 TRIAL. Radiology. 2016;279(1):44–55.
35. Hylton NM. Residual disease after neoadjuvant therapy for breast cancer: can MRI help? Radiology. 2018;289(2):335–6.
36. Kim TH, Kang DK, Yim H, Jung YS, Kim KS, Kang SY. Magnetic resonance imaging patterns of tumor regression after neoadjuvant chemotherapy in breast cancer patients: correlation with pathological response grading system based on tumor cellularity. J Comput Assist Tomogr. 2012;36:200–6.
37. Watanabe H, Okada M, Kaji Y, Satouchi M, Sato Y, Yamabe Y, et al. New response evaluation criteria in solid tumours – revised RECIST guideline (version 1.1). JPN J Cancer Chemother. 2009;36(13):2495–501.
38. Kuhl CK, Alparslan Y, Schmoee J, Sequeira B, Keulers A, Brümmendorf TH, Keil S. Validity of RECIST version 1.1 for response assessment in metastatic cancer: a prospective, multireader study. Radiology. 2019;290(3):349–56.
39. Martincich L, Montemurro F, De Rosa G, et al. Monitoring response to primary chemotherapy in breast cancer using dynamic contrast-enhanced magnetic resonance imaging. Breast Cancer Res Treat. 2004;83(1):67–76.

40. Ah-See ML, Makris A, Taylor NJ, et al. Early changes in functional dynamics magnetic resonance imaging predict for pathologic response to neoadjuvant chemotherapy in primary breast cancer. Clin Cancer Res. 2008;14(20):6580–9.
41. Dogan BE, Yuan Q, Bassett R, et al. Comparing the performances of magnetic resonance imaging size vs pharmacokinetic parameters to predict response to neoadjuvant chemotherapy and survival in patients with breast cancer. Curr Probl Diagn Radiol. 2019;48(3):235–40.
42. Partridge SC, Zhang Z, Newitt DC, et al. Diffusion-weighted MRI findings predict pathologic response in neoadjuvant treatment of breast cancer: the ACRIN 6698 multicenter trial. Radiology. 2018;289(3):618–27.
43. Chu W, Jin W, Liu D, et al. Diffusion-weighted imaging in identifying breast cancer pathological response to neoadjuvant chemotherapy: a meta-analysis. Oncotarget. 2017;9(6):7088–100.
44. Chen CA, Hayward JH, Woodard GA, Ray KM, Starr CJ, Hylton NM, et al. Complete breast MRI response to neoadjuvant chemotherapy and prediction of pathologic complete response. J Breast Imaging. 2019;1(3):217–22.
45. Santamaría G, Bargalló X, Fernández PL, Farrús B, Caparrós X, Velasco M. Neoadjuvant systemic therapy in breast cancer: association of contrast-enhanced MR imaging findings, diffusion-weighted imaging findings, and tumor subtype with tumor response. Radiology. 2017;283(3):663–72.
46. US Department of Health and Human Services Food and Drug Administration Center for Drug Evaluation and Research. Guidance for industry: Pathological complete response in neoadjuvant treatment of highrisk early-stage breast cancer (version 2020). Accessed October 1, 2020. Available at: http://www.fda.gov/Drugs/GuidanceComplianceRegulatoryInformation/Guidances/default.htm
47. Reig B, Heacock L, Lewin A, Cho N, Moy L. Role of MRI to assess response to neoadjuvant therapy for breast cancer. J Magn Reson Imaging. 2020;52(6). https://doi.org/10.1002/jmri.27145.
48. Kim SY, Cho N, Park IA, et al. Dynamic contrast-enhanced breast MRI for evaluating residual tumor size after neoadjuvant chemotherapy. Radiology. 2018;289(2):327–34.
49. Kim Y, Sim SH, Park B, et al. Magnetic resonance imaging (MRI) assessment of residual breast cancer after neoadjuvant chemotherapy: relevance to tumor subtypes and MRI interpretation threshold. Clin Breast Cancer. 2018;18(6):459–67. e451
50. Negrão EMS, Souza JA, Marques EF, Bitencourt AGV. Breast cancer phenotype influences MRI response evaluation after neoadjuvant chemotherapy. Eur J Radiol. 2019;120:108701.
51. Ballesio L, Gigli S, Di Pastena F, et al. Magnetic resonance imaging tumor regression shrinkage patterns after neoadjuvant chemotherapy in patients with locally advanced breast cancer: correlation with tumor biological subtypes and pathological response after therapy. Tumour Biol. 2017;39(3):1010428317694540. https://doi.org/10.1177/1010428317694540.
52. Rosen EL, Blackwell KL, Baker JA, et al. Accuracy of MRI in the detection of residual breast cancer after neoadjuvant chemotherapy. AJR Am J Roentgenol. 2003;181(5):1275–82.
53. Lorenzon M, Zuiani C, Londero V, et al. Assessment of breast cancer response to neoadjuvant chemotherapy: is volumetric MRI a reliable tool? Eur J Radiol. 2009;71(1):82–8.
54. Schrading S, Kuhl CK. Breast cancer: influence of Taxanes on response assessment with dynamic contrast-enhanced MR imaging. Radiology. 2015;277(3):687–96.
55. Chen JH, Bahri S, Mehta RS, et al. Impact of factors affecting the residual tumor size diagnosed by MRI following neoadjuvant chemotherapy in comparison to pathology. J Surg Oncol. 2014;109(2):158–67.
56. Kopans DB. Breast imaging. 3rd ed. Philadelphia, PA: Lippincott Williams & Wilkins; 2007.
57. Shin HJ, Kim HH, Ahn JH, et al. Comparison of mammography, sonography, MRI and clinical examination in patients with locally advanced or inflammatory breast cancer who underwent neoadjuvant chemotherapy. Br J Radiol. 2011;84(1003):612–20.
58. Kawashima H, Inokuchi M, Furukawa H, Kitamura S. Triple-negative breast cancer: are the imaging findings different between responders and nonresponders to neoadjuvant chemotherapy? Acad Radiol. 2011;18(8):963–9.
59. Boughey JC, Suman VJ, Mittendorf EA, et al. Sentinel lymph node surgery after neoadjuvant chemotherapy in patients with node-positive breast cancer: the ACOSOG Z1071 (Alliance) clinical trial. JAMA. 2013;310(14):1455–61.

60. Pilewskie M, Morrow M. Axillary nodal management following neoadjuvant chemotherapy: a review. JAMA Oncol. 2017;3(4):549–55.
61. Kuehn T, Bauerfeind I, Fehm T, et al. Sentinel-lymph-node biopsy in patients with breast cancer before and after neoadjuvant chemotherapy (SENTINA): a prospective, multicentre cohort study. Lancet Oncol. 2013;14:609–18.
62. Hennessy BT, Hortobagyi GN, Rouzier R, et al. Outcome after pathologic complete eradication of cytologically proven breast cancer axillary node metastases following primary chemotherapy. J Clin Oncol. 2005;23(36):9304–11.
63. Expert Panel on Breast Imaging; Slanetz PJ, Moy L, et al. ACR appropriateness criteria® monitoring response to neoadjuvant systemic therapy for breast cancer. J Am Coll Radiol. 2017;14(11S):S462–75.
64. Boughey JC, Ballman KV, Hunt KK, et al. Axillary ultrasound after neoadjuvant chemotherapy and its impact on sentinel lymph node surgery: results from the american college of surgeons oncology group Z1071 trial (Alliance). J Clin Oncol. 2015;33(30):3386–93.
65. Le-Petross HT, McCall LM, Hunt KK, et al. Axillary ultrasound identifies residual nodal disease after chemotherapy: results from the american college of surgeons oncology group Z1071 trial (Alliance). AJR Am J Roentgenol. 2018;210(3):669–76.
66. Hieken TJ, Boughey JC, Jones KN, Shah SS, Glazebrook KN. Imaging response and residual metastatic axillary lymph node disease after neoadjuvant chemotherapy for primary breast cancer. Ann Surg Oncol. 2013;20(10):3199–204.
67. You S, Kang DK, Jung YS, An YS, Jeon GS, Kim TH. Evaluation of lymph node status after neoadjuvant chemotherapy in breast cancer patients: comparison of diagnostic performance of ultrasound, MRI and ^{18}F-FDG PET/CT. Br J Radiol. 2015;88(1052):20150143. https://doi.org/10.1259/bjr.20150143.
68. Saffar B, Bennett M, Metcalf C, Burrows S. Retrospective preoperative assessment of the axillary lymph nodes in patients with breast cancer and literature review. Clin Radiol. 2015;70:954–9.
69. Morgan C, Stringfellow TD, Rolph R, Kovacs T, Kothari A, Pinder SE, Hamed H, Sever AR. Neoadjuvant chemotherapy in patients with breast cancer: does response in the breast predict axillary node response? Eur J Surg Oncol. 2020;46(4 Pt A):522–6.

Chapter 17
Postoperative Breast

Larissa Muramoto Yano and Monica Akahoshi Rudner

17.1 Normal Postoperative Changes (for Benign Disease)

For the proper examination to be performed, the radiologist and technologist must be aware of pertinent aspects of the patient's history, such as signs and symptoms, locations of masses, pain, and prior surgeries that the patient must indicate in a diagram. Extensive surgical procedures, such as mammoplasty, must be shown diagrammatically only, without the use of skin markers. Smaller scars are marked with pieces of thin wire that are taped to the skin to correlate with possible mammographic findings (Fig. 17.1), but it may not always correlate with the surgical excision site located deeper in the breast. The entire surgical area must be included on at least one mammographic view and, if necessary, additional views, such as spot compression, magnification, and tangential and various angulations, may be useful and should be performed in the projection where the area is better and more completely seen. Diagnostic accuracy increases with awareness of how procedures were performed, knowledge of time since surgery, and breast density (detection and interpretation are more difficult in dense breasts).

Normal postoperative imaging findings include architectural distortion, increased density and parenchymal scarring, and decrease in severity over time, more rapidly

L. M. Yano
Hospital Albert Einstein, São Paulo, SP, Brazil

Instituto de Radiologia INRAD, Hospital das Clinicas HCFMUSP, Faculdade de Medicina, Universidade de Sao Paulo, São Paulo, SP, Brazil
e-mail: larissa.yano@einstein.br

M. A. Rudner (✉)
Hospital Albert Einstein, São Paulo, SP, Brazil

Instituto de Radiologia INRAD, Hospital das Clinicas HCFMUSP, Faculdade de Medicina, Universidade de Sao Paulo, São Paulo, SP, Brazil

Hospital Moriah and Prevent Senior, São Paulo, SP, Brazil
e-mail: monicaak@einstein.br

S. J. Kim Hsieh, E. A. Morris (eds.), *Modern Breast Cancer Imaging*,
https://doi.org/10.1007/978-3-030-84546-9_17

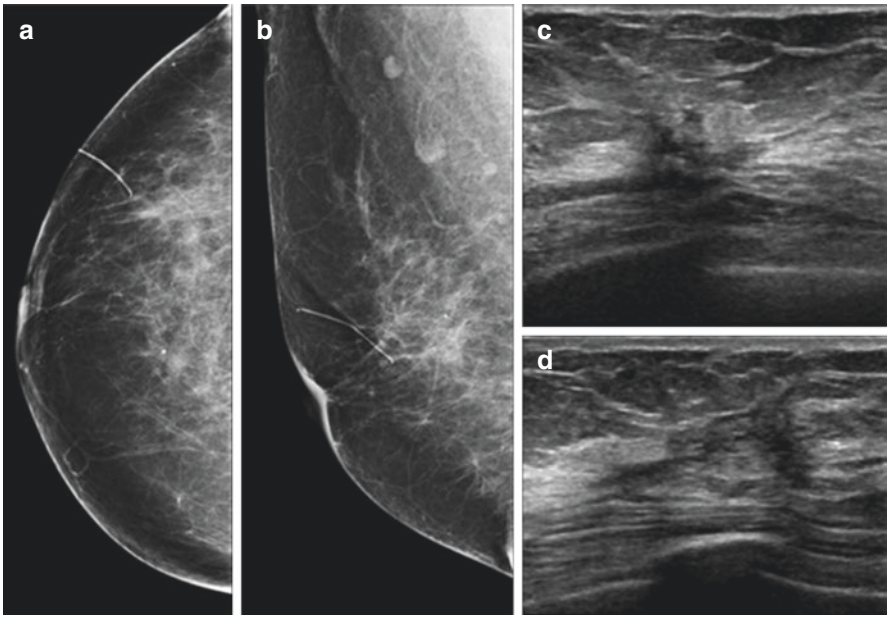

Fig. 17.1 Postoperative scarring. Mammography shows thin wire taped to the skin marking the cutaneous scar to correlate with possible mammographic findings (**a**, **b**). Ultrasound depicted a hypoechoic irregular area with architectural distortion, with different morphologic aspects in different planes, representing a scar (**c**, **d**)

and completely in benign biopsies (Fig. 17.2) or aesthetic procedures (Fig. 17.3). Immediately after the procedure, mammography will show a round/oval mass or asymmetric soft-tissue density in the postoperative site representing seroma or hematoma, with or without air in the biopsy cavity. The incidence of postsurgical fluid collections reflects the surgical technique. Breast edema usually occurs close to the incision area and may last for the first 1 or 2 months. Outlined by subcutaneous fat, linear parenchymal trabeculations extend toward the skin, representing engorged lymphatics and interstitial fluid. Depending on the extension of the surgery, the breast enlarges, and mammographic compression is more difficult. As the edema recedes, the breast size also normalizes. Skin thickening and breast edema are usually seen together and have similar time courses and resolution. Contralateral asymmetries may be explained by the absence of equivalent tissue on the operative side and can be mistaken as an abnormality. If there is doubt, sonography can identify the fluid-filled nature of the mass (Fig. 17.4). Initially, some hematomas show internal echoes but most soon become anechoic with posterior acoustic enhancement and may present septa (which do not mean complications). The incision can occasionally be traced from the biopsy cavity to the skin, which is thickened (Fig. 17.2). Management of a complex mass requires knowledge of the clinical context. If an abscess is not suspected, observation may be preferred [1].

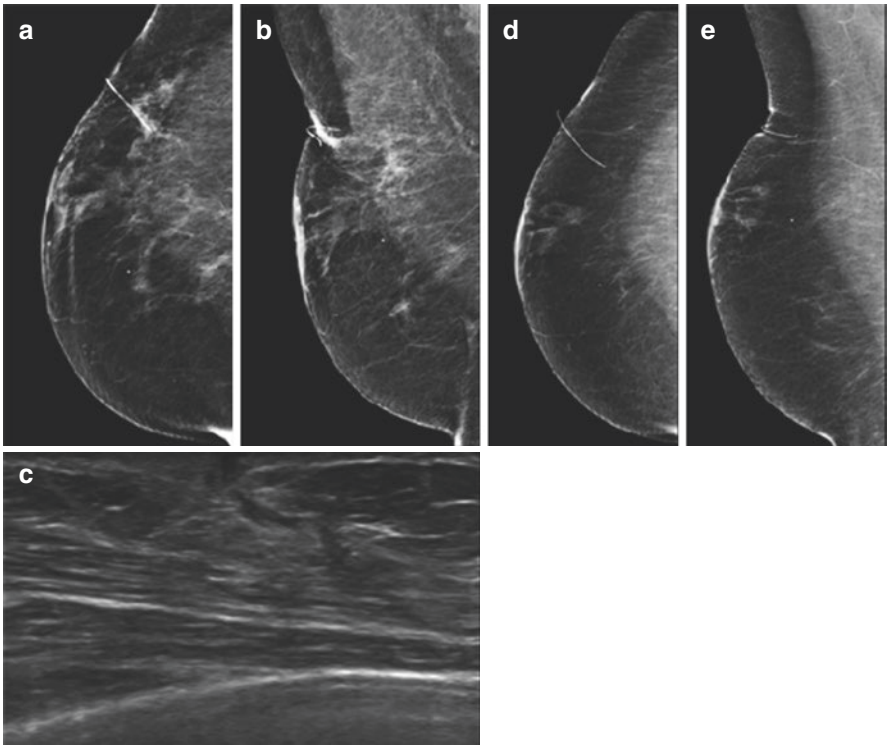

Fig. 17.2 Normal postoperative aspect. Mammogram 1 month after benign biopsy depicts skin thickening, architectural distortion, increased density, and parenchymal scarring (**a**, **b**). Ultrasound of the same date shows architectural distortion and scarring of the incision from the biopsy cavity to the skin, which is thickened (**c**). Late control shows that these findings had diminished over time (**d**, **e**)

In very rare cases, seroma cavities persist 1 year after a benign biopsy [1]. Generally, after a few weeks to 18 months, the fluid collection is gradually reabsorbed; the lesion decreases in size and becomes poorly defined. Areas of radiolucency representing fat entrapped by the developing scar are seen interspersed with soft-tissue density [1]. Scars change appearance in different projections: a spiculated mass like soft tissue in one view may elongate in other projections. After 1 or 2 years, an evolving scar contracts and shrinks as it matures, and architectural distortion or a spiculated density may be seen. On sequential mammograms, decrease in size may be barely perceptible or seen in only one projection. It is important to note that the linear metallic scar marker on the skin will not always be immediately adjacent to the surgical bed because the skin is pressed away from the underlying parenchyma. Preoperative mammograms should always be reviewed, fundamentally if a spiculated mass is found far from the marker, and biopsy may be necessary to eliminate the possibility of cancer. Ultrasound reveals a hypoechoic spiculated

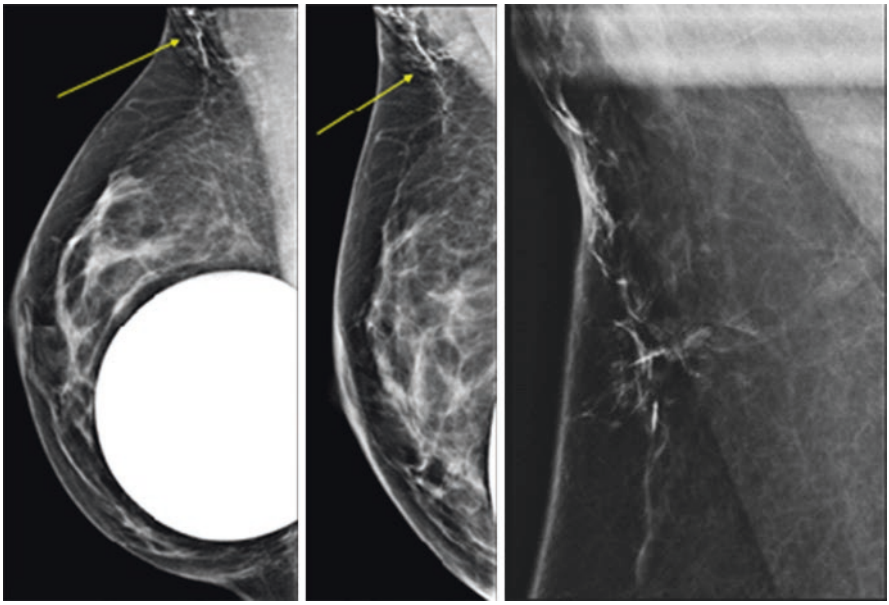

Fig. 17.3 Increased density and parenchymal scarring after liposuction on the axilla (normal findings)

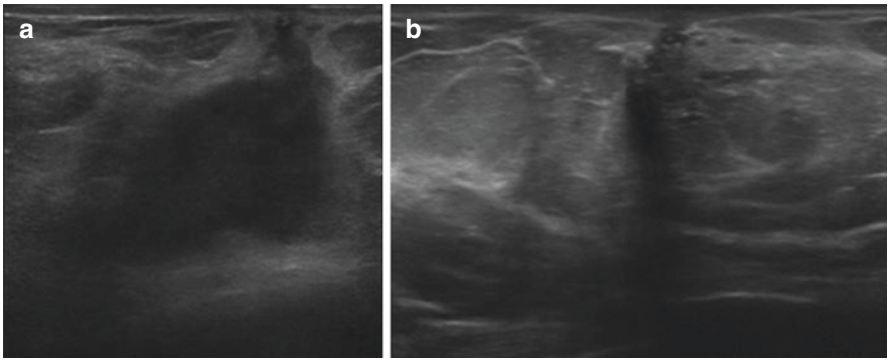

Fig. 17.4 Postsurgical seroma/hematoma. Ultrasound depicts the fluid-filled nature of the mass with the surgical path through the breast tissue up to the skin and hyper-echogenicity of the surrounding parenchyma (**a**). A 1-year control (**b**) depicts complete resolution of the fluid collection with architectural distortion and parenchymal scarring, as well as skin thickening and retraction

mass, and, occasionally, retraction of the scar skin is noted (Figs. 17.1 and 17.5). History and physical findings in the skin can help distinguish this normal postoperative finding from cancer. Scarring not complicated by fat necrosis is perceived as induration rather than a mass. The period of change is variable and does not depend on the type of breast parenchyma, but some aspects can induce the rate of scar formation, such as resection size, postsurgical fluid collection volume, and whether or

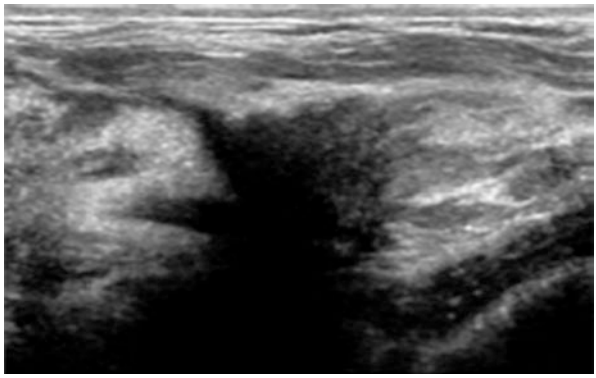

Fig. 17.5 Postoperative scarring. Ultrasound shows a hypoechoic spiculated mass in the surgical bed with posterior shadowing

not it was drained. After 3 to 5 years, between 50 and 55% of cases show complete resolution of the biopsy cavity, leaving no scar or distortion in the underlying breast parenchyma [2]. The findings should be stable on subsequent mammograms.

To evaluate calcifications at the surgical site, the same morphological and distributional features used in the preoperative period should be applied to classify the probability of malignancy. In early stages, they may be quite fine, faint, and difficult to characterize, usually becoming coarser later on. Dystrophic calcifications may have similar pathogenesis of secretory disease or ductal ectasia, associated with areas of necrotic tissue, sloughed cells, and cellular detritus, evolving into scars and in the subcutaneous tissue under surgical incisions. Tangential mammographic views to the skin can demonstrate their superficial locations. Calcified remnants of suture material can also be seen, with several millimeters long and quite wide, presenting as knots, branching linear and double tracking calcifications. If the benign nature of these calcifications cannot be determined, biopsy is indicated [1].

The thickened skin in the incision may be superimposed on the surgical area causing a mass-like increased density, particularly when a keloid has formed. A complementary tangential view to the scar permits separation of the skin and parenchymal elements, so the surgical bed can be better accessed. Sonographically, a band of thickened skin will be seen in the incision [1].

Fat necrosis originates from aseptic fat saponification and is associated with all types of surgical procedures in the breast. It usually appears as a radiolucent lipid-filled mass. When symptomatic, fat necrosis may present as a lump. In earlier phases, a hematoma may be present. In all types of imaging methods, it is a common finding and sometimes a challenging pitfall, manifesting different presentations that may be indistinguishable from cancer, depending on the stage of the process (Fig. 17.6). Mammography is pathognomonic if it shows oily cysts or typical eggshell rim calcifications around a mass with radiolucent center. There is a wide range of sonographic presentations that include solid mass, complex mass with mural masses, complex mass with echogenic bands, anechoic mass with posterior acoustic enhancement, anechoic mass with shadowing, or an isoechoic mass. The margins of the mass vary from well circumscribed to indistinct or spiculated.

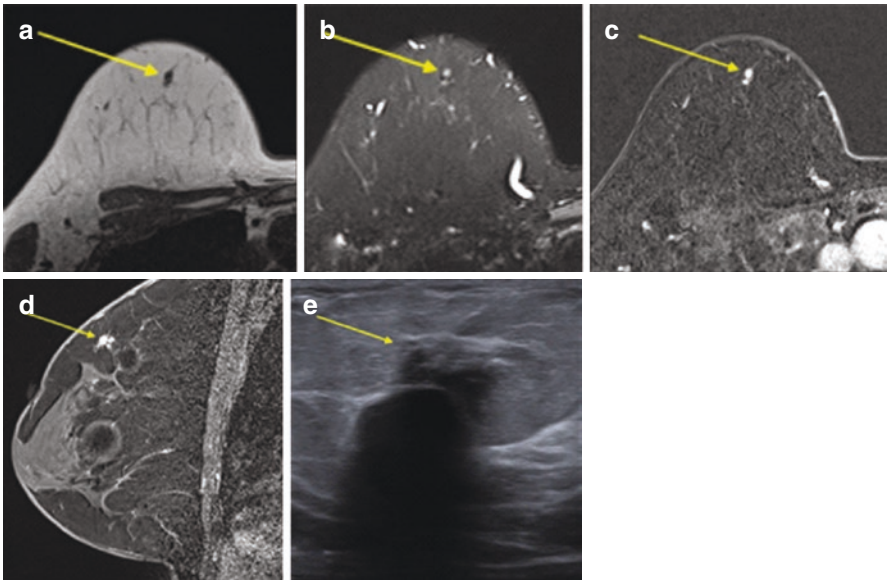

Fig. 17.6 Fat necrosis. MRI shows an irregular mass, hypointense on axial T1-weighted image without fat saturation (**a**) and hyperintense on axial fat-saturated T2-weighted image (**b**). Axial contrast-enhanced fat-suppressed T1-weighted MR subtraction image (**c**) and sagittal contrast-enhanced fat-suppressed T1-weighted image (**d**) show homogeneous enhancement. Ultrasound depicts an irregular, ill-defined, heterogeneous mass (**e**). Core needle biopsy was consistent with fat necrosis

On magnetic resonance imaging (MRI), fat necrosis usually presents as a round or oval mass showing high signal intensity on T1-weighted images without fat saturation, high signal intensity on T2-weighted images without fat saturation, and low signal intensity on fat-saturated images. T1-weighted fat-suppressed sequences are helpful in differentiating fat from blood (Figs. 17.7 and 17.8). A fat-fluid level may be present. Fibrosis may appear as high, intermediate, or low signal on T1-weighted images. Degree of enhancement depends on the stage of the inflammatory process: recent lesions may have variable enhancement surrounding them, whereas chronic lesions show marked irregularity and retraction (scar), generally without enhancement. Needle biopsy may be indicated if the diagnosis of fat necrosis is not certain.

MRI can be very useful in evaluation of the postoperative breast, since it shows high sensitivity and specificity in differentiation between benign postoperative changes and malignant tumors, eventually minimizing unnecessary intervention. The most important factor is the correlation of lesion morphology and enhancement kinetics following administration of gadolinium contrast material. Skin thickening, architectural distortion (Fig. 17.9), resolving edema, fat necrosis, signal voids or signal flare from prior bleeding (hemosiderin), a small focal area of non-mass like

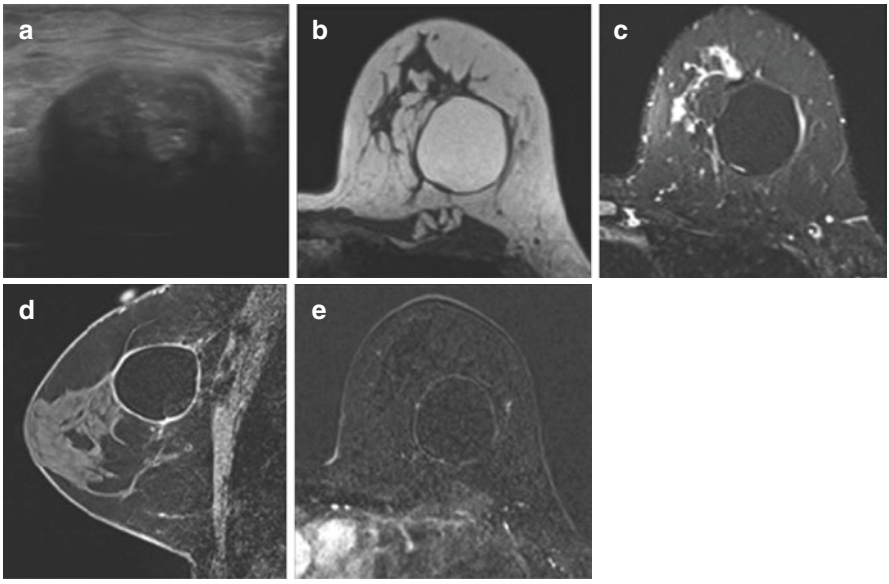

Fig. 17.7 Fat necrosis. Ultrasound shows an oval, circumscribed, and heterogeneous mass (**a**). Axial non-fat-saturated T1-weighted (**b**), axial fat-saturated T2-weighted (**c**), sagittal contrast-enhanced fat-suppressed T1-weighted (**d**), and axial contrast-enhanced fat-suppressed T1-weighted MR subtraction images (**e**) show a T1-hyperintense mass with signal loss on the fat-saturated images and thin discrete peripheral enhancement

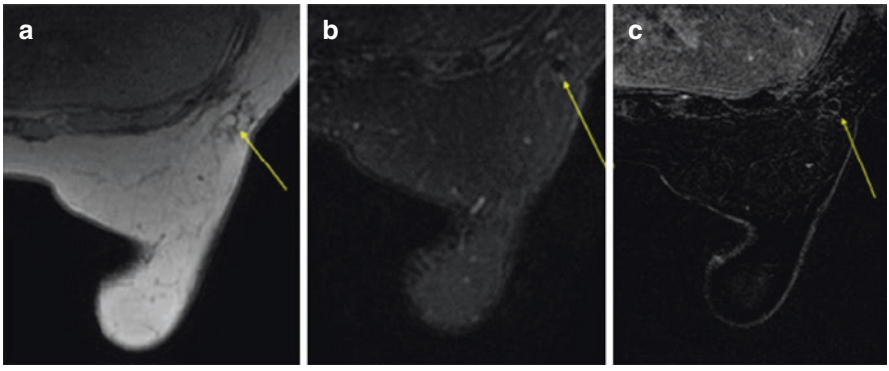

Fig. 17.8 Fat necrosis. Axial T1-weighted image without fat saturation (**a**), axial fat-saturated T2- weighted (**b**), and axial contrast-enhanced fat-suppressed T1-weighted MR subtraction images (**c**) show a T1-hyperintense mass with signal loss on the fat-saturated images and thin discrete peripheral enhancement

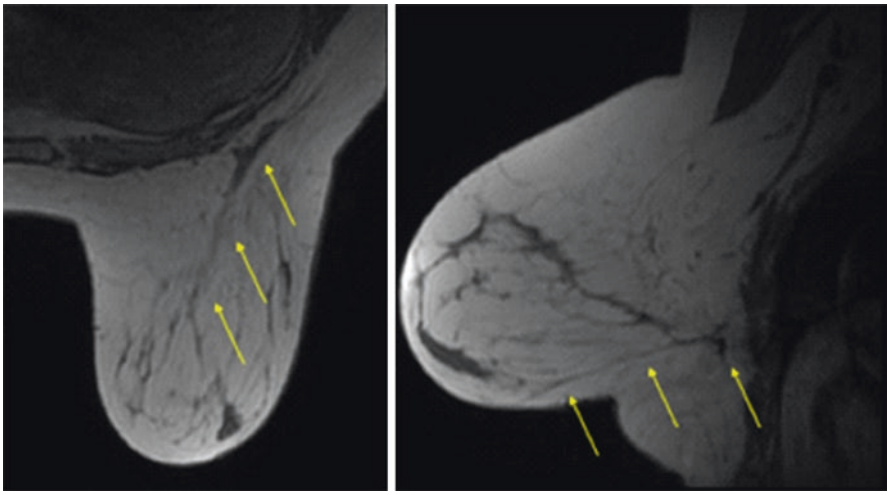

Fig. 17.9 T1-weighted MR images without fat suppression show architectural distortion and scarring on mammoplasty bed (arrows)

enhancement, and thin linear non-mass-like enhancement at the surgical area can all be expected findings. Non-enhancing areas have a high negative predictive value for malignancy (88–96%). Postoperative seromas have high signal intensity (fluid-filled structure signal) on T2-weighted images and smooth, thin rim enhancement. Benign postoperative changes generally demonstrate more gradual uptake of contrast material. Breast hematomas show a varying signal according to the hemoglobin degradation status (high signal on T1-weighted at subacute stage, low signal on T1/T2-weighted at chronic stage). As they dissipate, fibrous tissue in the site of the fluid collection can appear as an architectural distortion. Scarring enhancement (a minimal or small focal area of enhancement or thin linear enhancement) can be seen for up to 18 months or even longer. At follow-up imaging, the enhancement should demonstrate stability or progressive decrease [2].

17.2 Aesthetic Breast Surgery

17.2.1 Reduction Mammoplasty and Mastopexy

Mammoplasty and mastopexy are different procedures; the central focus of mammoplasty is breast volume reduction (most often performed for macromastia) and for mastopexy is breast shape. Nevertheless, there are many similarities regarding the techniques used and also postoperative imaging aspects. The multiplicity of surgical techniques, with different accesses (inframammary and peri-areolar fold access; peri-areolar, vertical, and horizontal (inverted T); peri-areolar and vertical;

peri-areolar, vertical and lateral horizontal; isolated peri-areolar), evidence the challenge to achieve a harmonious and symmetrical aesthetic result, with minimal scarring. The resulting surgery leaves a smaller breast with normal skin visible in the region of the cleavage. Both surgical procedures may be performed concurrently with breast conservation therapy. Awareness of normal postoperative imaging features of these oncoplastic procedures is important to avoid false-positive results.

The most common surgical procedure involves a circumareolar incision, an inframammary incision, and a vertical incision between the two (traditional inverted-T scar, or Wise pattern), with removal of the skin, breast parenchyma, and fat, predominantly from the lower portion, followed by superior relocation of the nipple (Fig. 17.9). This will result in elevation of the nipple-areolar complex (NAC) and reduction of the cutaneous envelope of the breast. With the advent of smaller skin-incision techniques, new vertical scar techniques feature only one vertical incision leaving a lollipop-shaped scar, compared with the anchor-shaped appearance of the inverted-T scar. These smaller skin-incision techniques decrease scarring and distortion of the inframammary fold, allowing parenchymal rearrangement and pedicle creation, which maintains blood supply to the NAC [3].

Usually, the nipple is kept attached to the breast ducts, but in very ptotic or very large breasts, the surgeon may choose to remove the nipple and then graft it back into the breast, which may increase the risk of nipple necrosis and difficulty breast-feeding. The new nipple site may have little parenchyma behind it and may result in a relative shift, resulting in transposition of parenchyma to the dependent portion of the breast, with nonanatomic distribution, linear strands, parenchymal bands, and calcifications. Depending on the amount of tissue removed from different areas of the breast, redistribution of glandular tissue occurs, and breast parenchymal pattern can be patchy [4]. This fact, associated with scarring, makes comparison with previous images difficult.

Postoperative mammograms show characteristic skin thickening in the region of the scars, generally over the lower breast, which is most evident on the mediolateral oblique or mediolateral view. The lower breast shows architectural distortion, and its general pattern is distorted from the scar (Fig. 17.10). Fibrous bands can be seen extending to the repositioned NAC in 20% of the patients, representing scarring associated with the vascular pedicle (Fig. 17.11) [3]. Fat necrosis or oil cysts are common findings and may have a characteristic appearance or may be atypical, forming a palpable mass when symptomatic. Epidermal inclusion cysts can also form in scars and produce a smooth dense round or oval mass close to the skin surface but not connected to it. They represent epidermal cells displaced into breast tissue during surgery. Skin calcifications along incisions can be distinguished from intraparenchymal calcifications or cancer because of their typical skin location. Periareolar dermal calcifications and thickening related to the repositioned NAC can be seen; therefore, imaging of the nipple in profile is critical (Fig. 17.12) [3]. Recalls may be higher in this group of patients due to surgical architectural distortions and possible areas of fat necrosis with atypical presentations, but tomosynthesis can resolve some doubts and reduce recall rates.

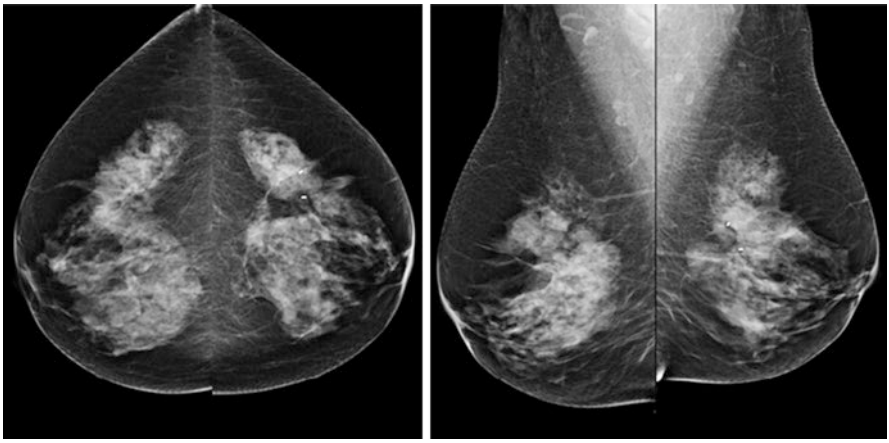

Fig. 17.10 Mammoplasty. Mammography shows architectural distortion in the lower quadrants, and breast overall pattern is distorted from the scar

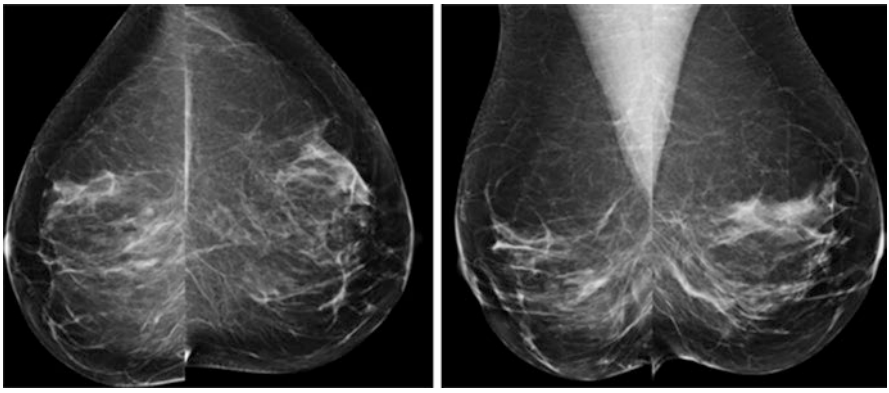

Fig. 17.11 Mastopexy. Fibrous bands extending to the repositioned NAC, representing scarring associated with the vascular pedicle

17.2.2 Breast Implants

Aesthetic surgery rates are raising worldwide, and the use of silicone breast implants is the main procedure used in breast augmentation. They were introduced in 1962 by Cronin and Gerow, presenting several modifications in the design, texturing, and gel cohesiveness over subsequent generations [5]. Approximately 80% is placed for cosmetic reasons and the other 20% for breast reconstruction after mastectomy [6].

The silicone implants can be positioned via periareolar, axillary, transpapillae, or inframammary incisions. All implants are placed behind the breast tissue, and surgeons will choose the ideal place regarding the pectoralis muscle, which may be subglandular, subfascial, submuscular, or double plane (Figs. 17.13 and 17.14).

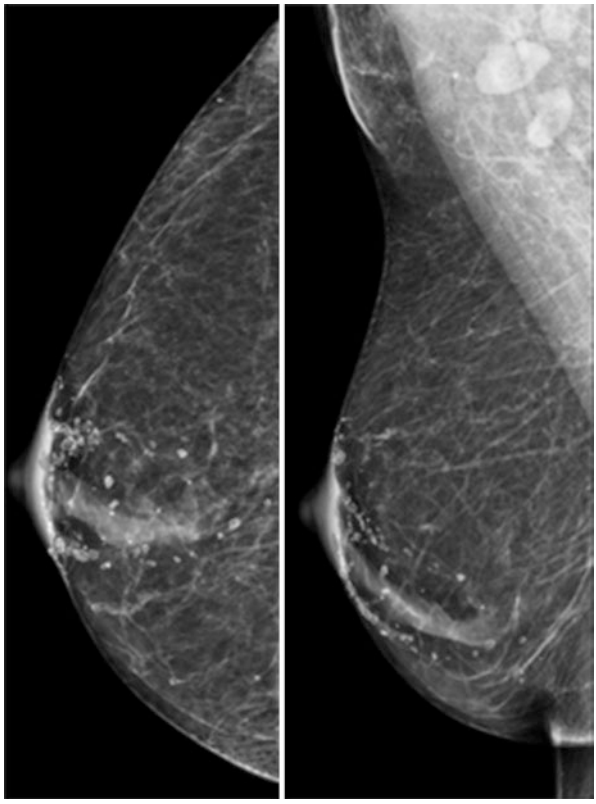

Fig. 17.12 Periareolar dermal calcifications and thickening related to the repositioned NAC can be seen on mammogram. Dermal calcifications over the vertical incision are also present

Breast implants are not lifetime devices [7, 8]. The older the implants, the more likely they will require removal or substitution [9, 10]. There is no current evidence that breast augmentation with silicone implants may present increased risk for developing connective disorders, breast cancer, no proven delay in breast cancer detection, and no difference in survival or recurrence rates compared with women with no augmentation [11–18].

17.2.2.1 Implant Types

Breast implants are classified according to its material, shape, surface texturing, and number of chambers.

Saline implants are composed of an outer silicone shell and an inner envelope filled with saline solution. Some are pre-filled, and others can be filled during the surgical procedure. Single-lumen silicone implants are the most common type and consist in a silicone elastomer shell filled with silicone made from a synthetic polymer of cross-linked chains of dimethyl siloxane. The inner silicone can have a liquid, gel, or solid consistency depending on the length of the individual chains and the degree to which these chains are cross-linked.

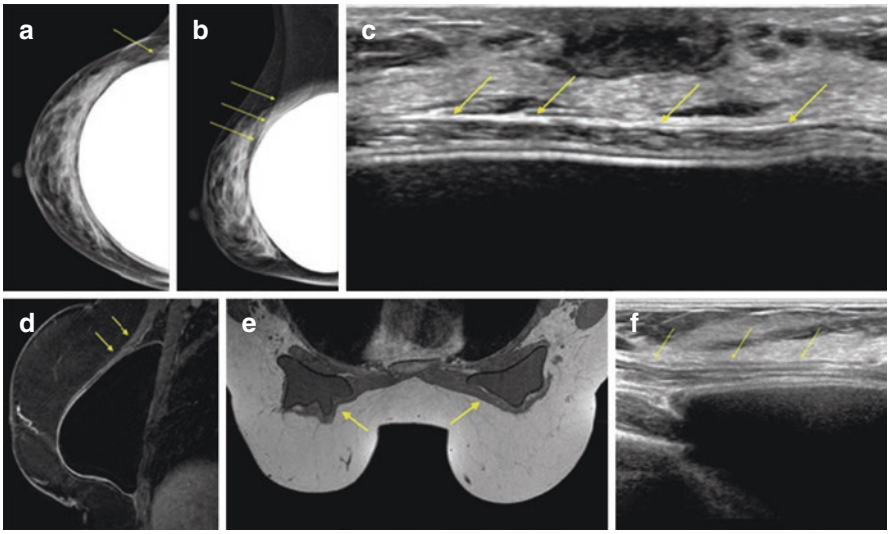

Fig. 17.13 Submuscular implant. Mammogram (**a**, **b**), ultrasound (**c**, **d**), and MRI (**e**, **f**) show the pectoralis muscle (arrows) over the implant

Saline and silicone implants are either round or anatomic (teardrop) in shape, and the outer envelope can be textured or smooth (uncoated). Textured coating stabilizes the implant within the breast pocket, reducing the risk of rotation and resulting in lower rates of capsular contraction, decreasing the risk of a secondary procedure. Early texturized implants were coated with polyurethane foam, but they were withdrawn from the market due to concerns about in vivo degradation to carcinogenic compounds [5]. Therefore, implant shells started to be texturized mechanically, creating pores of different sizes [19].

Double-lumen implants/expanders have two envelopes inside one another, and each can contain saline or silicone gel. It is common to find saline filling the inner lumen and silicone in the outer lumen, but the opposite can also occur (Fig. 17.15). Tissue expanders present different sizes and shapes and may have a smooth or textured outer surface. They are inserted under the breast skin, autologous tissue, or pectoralis muscle, immediately following mastectomy reconstruction or in subsequent surgery months or years later. As soon as possible, the tissue expander is slowly inflated through a series of saline solution injections or through a patient-controlled device, which releases carbon dioxide gas into the expander. The objective is to stretch the patient's tissue for insertion of an implant or the patient's own tissue as part of the reconstruction process (after mastectomy, to reconstruct injured or congenitally deformed breasts, or as part of gender reassignment surgery).

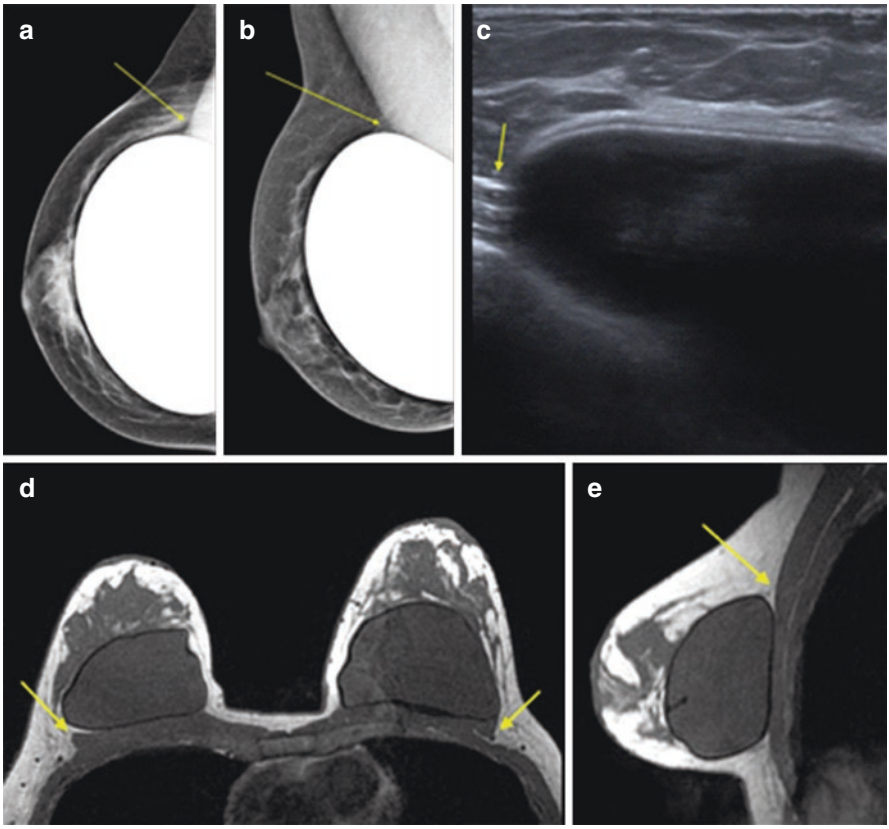

Fig. 17.14 Subglandular implant. Mammogram (**a**, **b**), ultrasound (**c**), and MRI (**d**, **e**) show the pectoralis muscle (arrows) behind the implant

Stretching may result in breast tissue damage, skin thinning, pain (especially during saline filling), rupture, and infection.

Motiva implants present a 3D imprinted surface texturing. Radiofrequency identification transponders are attached to it and can transmit data about the implant wirelessly. They have a linear radiopaque appearance on mammography and CT (Figs. 17.16 and 17.17) and produce an important magnetic susceptibility artefact on MRI (Fig. 17.17).

Stacked implants are two single-lumen, smooth-surface silicone gel-filled implants placed one on top of the other, firmly joined in the middle. Both have different volumes, the smaller representing 20% of the entire volume and positioned anteriorly. Each one has its own separate shell so the filling of each portion is not shared.

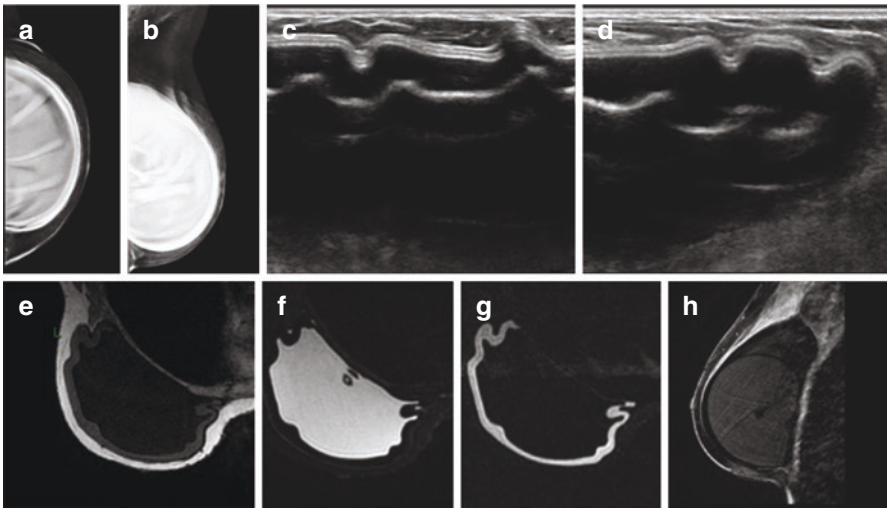

Fig. 17.15 Double-lumen implants/expander. The inner lumen is filled with saline surrounded by a smaller outer lumen that contains silicone. Mammogram shows a double contour with a low-density inner lumen and a high-density outer lumen (**a**, **b**). Ultrasound depicts the inner envelope with undulations that may be mistaken for the stepladder sign (**c**, **d**). Axial T1-weighted without fat suppression (**e**), axial fat- suppressed T2-weighted (**f**), axial short T1 inversion-recovery silicone-excited image (**g**), and sagittal contrast-enhanced fat-suppressed T1-weighted MR images (**h**) demonstrate the inner and outer lumens with different signal intensities, depending on the pulse sequence

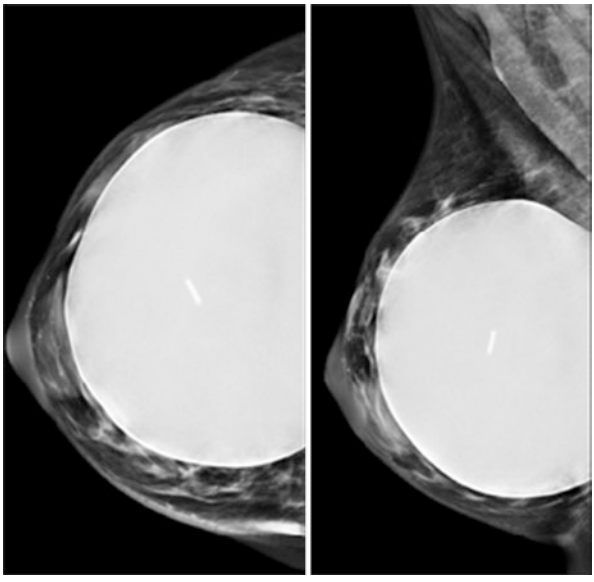

Fig. 17.16 Motiva implant. Radiofrequency identification transponder presents a linear radiopaque appearance on mammography

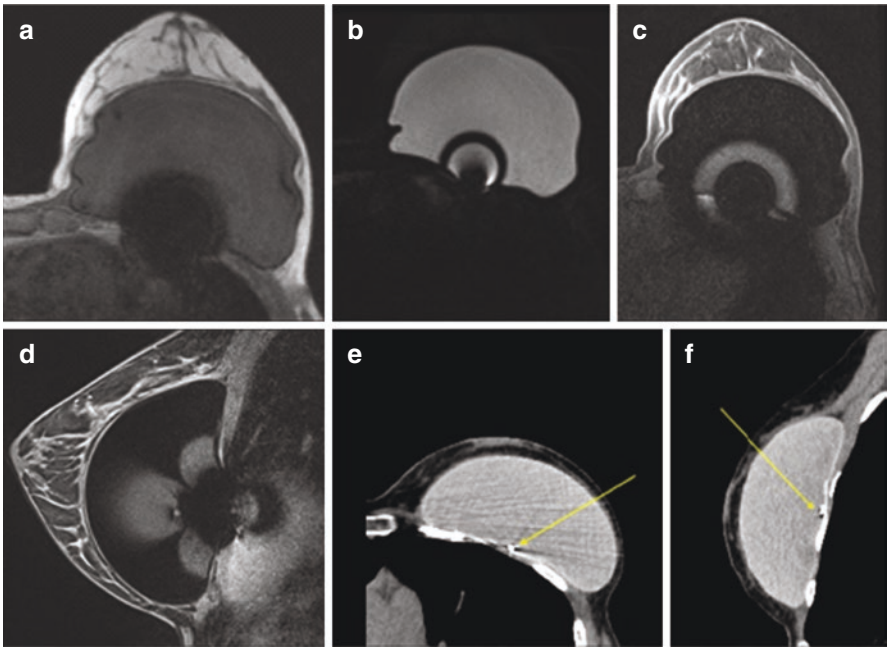

Fig. 17.17 Motiva implant. Important magnetic susceptibility artefact on T1-weighted image without fat suppression (**a**), short T1 inversion-recovery silicone-excited image (**b**), fat-suppressed T2-weighted (**c**), and contrast-enhanced fat-suppressed T1-weighted MR images (**d**) related to Motiva's transponder. Radiofrequency identification transponder presents a linear radiopaque appearance on CT (**e**, **f**)

17.2.2.2 Mammographic Technique, Normal Aspects, and Screening Considerations

Although breast implants withstand some degree of compression, some situations can subject them to so much pressure that the implants may rupture (e.g., during mammography or closed capsulotomy) [20]. Nevertheless, mammographic views without the necessary compression decreases the sensitivity of the exam in detecting cancer.

Thus, to potentialize mammography detection rate and minimalize the risk of implant rupture, the recommendation for each implanted breast is two views that include the implant and surrounding tissue with limited compression, in addition to two implant displaced views in which the implant is pushed posteriorly against the chest wall while the breast tissue is pulled over in front of the implant and strongly compressed (Eklund Maneuver) (Fig. 17.18). The compression paddle avoids the implant from reentering the field, reducing implant overlap on breast tissue, improving image resolution and diagnosis of breast pathologies. This technique may increase 2–5 cm of additional breast compression, and no ruptures were reported. However, some breast tissue will always be hidden by the implant even with the

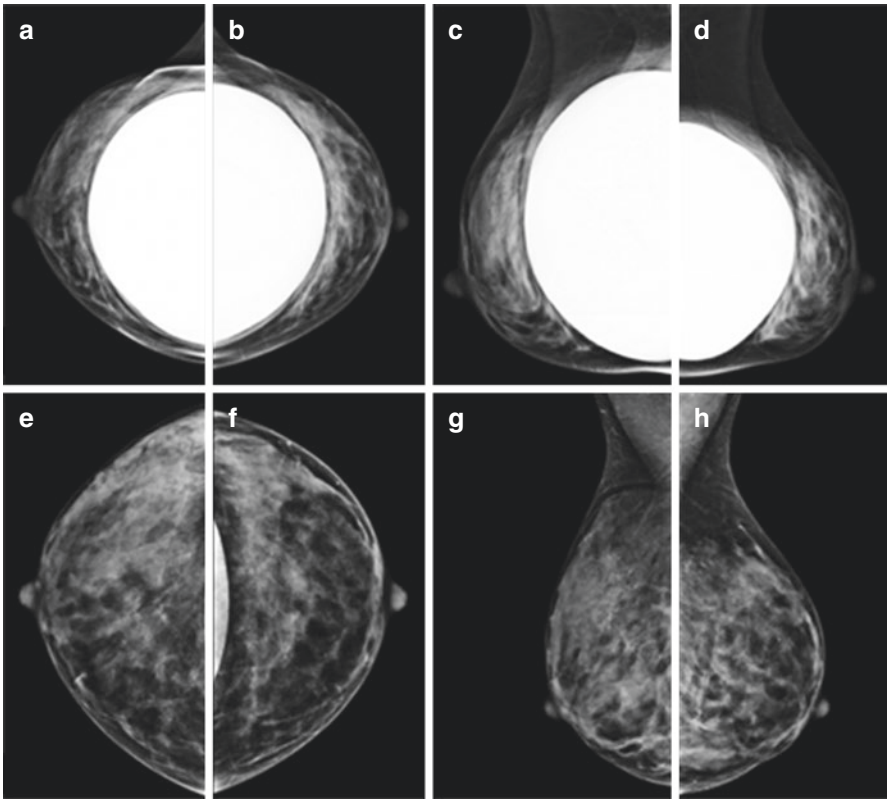

Fig. 17.18 Modified views for implants (Eklund maneuver). Projections of each breast obtained with routine positioning show the implants contours and only a small amount of breast tissue (**a**–**d**). Projections of each breast after the implant has been displaced posteriorly and the anterior breast tissue pulled into the compression plates demonstrate more parenchyma (**e**–**h**)

implant-displaced views, and only about 80% of the breast tissue is seen, raising the concern of a possible reduction in detectability of breast (Fig. 17.19) [21–25].

The recommendation for breast cancer screening is the same as that for patients with no implants. Presurgical and postsurgical mammograms are useful in distinguishing benign postoperative changes from other breast pathologies [25]. Limited-compression views may display a lesion near the implant not evidenced on implant-displaced views, because masses on the fibrous capsule can be pushed away from the field of view after Eklund maneuver [22]. Additional views or tomosynthesis may be useful for evaluating abnormalities in patients with implants. All types of percutaneous biopsies and presurgical localization can be performed in the presence of implants as well, but an informed consent should be obtained, including implant rupture as a possible complication [24].

To evaluate intracapsular rupture of implants and to detect other complications such as hematomas and seromas, ultrasound is an important tool. With the exception

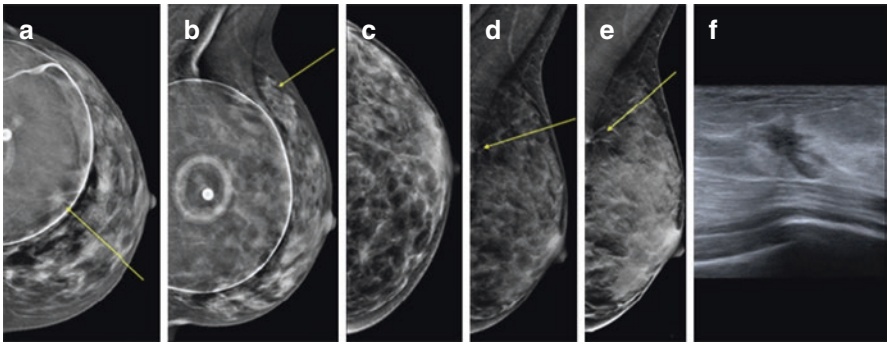

Fig. 17.19 Reduction in detectability of breast carcinoma in augmentation. Spiculated mass hidden by the implant (**a**, **b**), the saline filler diminished the risk of overlooking this lesion, but it is important to note that on the implant-displaced views (**c**, **d**), it was very difficult to diagnose the mass. Tomosynthesis (**e**) shows the irregular spiculated mass in a very posterior area that could easily have been lost with a bad positioning. Ultrasound (**f**) confirmed the irregular mass

of cases with dense breast tissue, in which ultrasound may increase detection of masses obscured by implants, there is no specific screening protocol that includes this imaging test. Ultrasound is also helpful as an adjunct to mammography in evaluating detected breast masses or palpable findings, as it can evaluate the entire depth of the breast tissue down to the implant, and it may distinguish breast masses from silicone granulomas caused by ruptured implants. Ultrasound-guided procedures also reduce the chance of implant perforation.

The US Food and Drug Administration (FDA) recommends evaluating implant integrity with magnetic resonance imaging (MRI) 3 years after surgery and every 2 years thereafter to depict silent ruptures (asymptomatic) [3, 26]. MRI is considered the gold standard in evaluating implant integrity and should be performed whenever mammography and ultrasound detect any abnormality. Regarding screening, MRI has the same recommendations according to age and risk factors. A dedicated breast coil obtains high-resolution images, and it is possible to suppress or emphasize the signal from water, fat, or silicone [27]. Saline implants follow fluid signal on all sequences. Silicone appears hypointense on T1-weighted image and hyperintense on T2-weighted image (Fig. 17.20). The envelope and fibrous capsule have low signal on all sequences. Like other imaging methods, radial folds and periprosthetic fluid are normal findings and should not be mistaken for rupture (Fig. 17.21).

On mammography, silicone implant appears near the chest wall and behind the breast tissue as a dense, smooth, oval, and completely opaque image that partially obscures the surrounding breast tissue. On the other hand, saline implants are radiolucent in the center, surrounded by a dense silicone outer envelope, which makes wrinkles easily detected, unlike on opaque silicone implants. Wrinkles are normal findings, accentuated by compression because the envelope is easily folded but are sometimes related to capsular contraction (Fig. 17.22). Double-lumen implants are a common type of implant, usually filled with saline in the inner lumen and silicone in the outer lumen. The subglandular position consists in the implant behind the

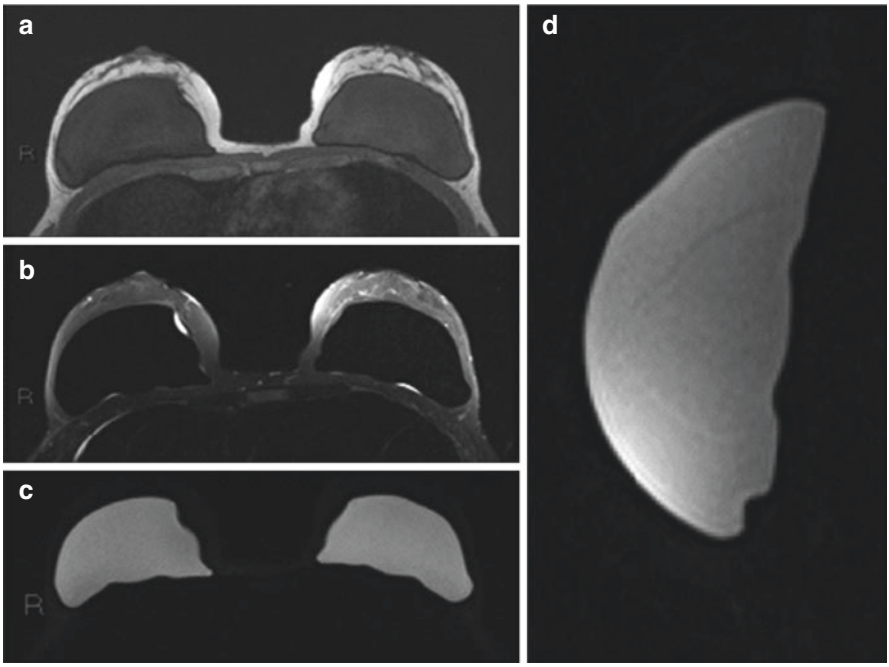

Fig. 17.20 Normal aspects of silicone implants on MRI. Silicone appears hypointense on T1-weighted image without fat suppression (**a**) and on short T1 inversion-recovery silicone-excited images (**b**) and hyperintense sign on fat-suppressed T2-weighted MR images (**c**, **d**)

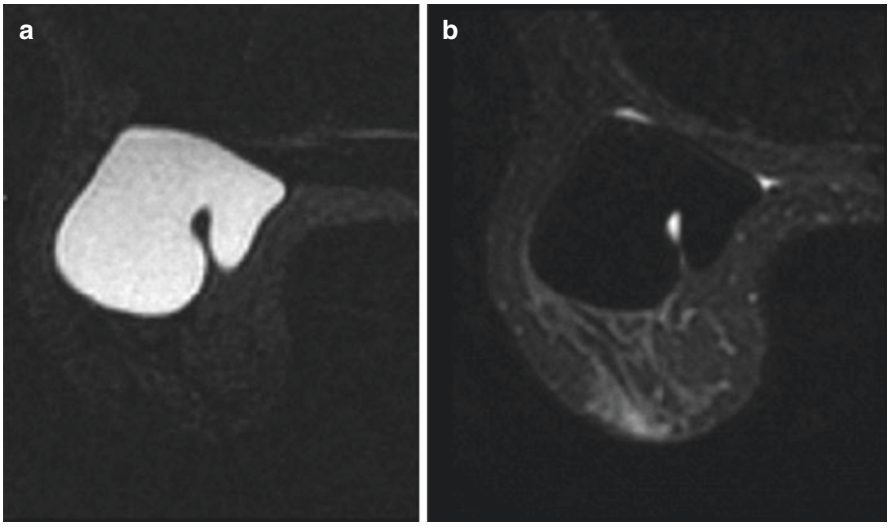

Fig. 17.21 Fluid inside a radial fold (normal aspect). Axial short T1 inversion-recovery silicone-excited image (**a**) and axial fat-suppressed T2-weighted MR image (**b**)

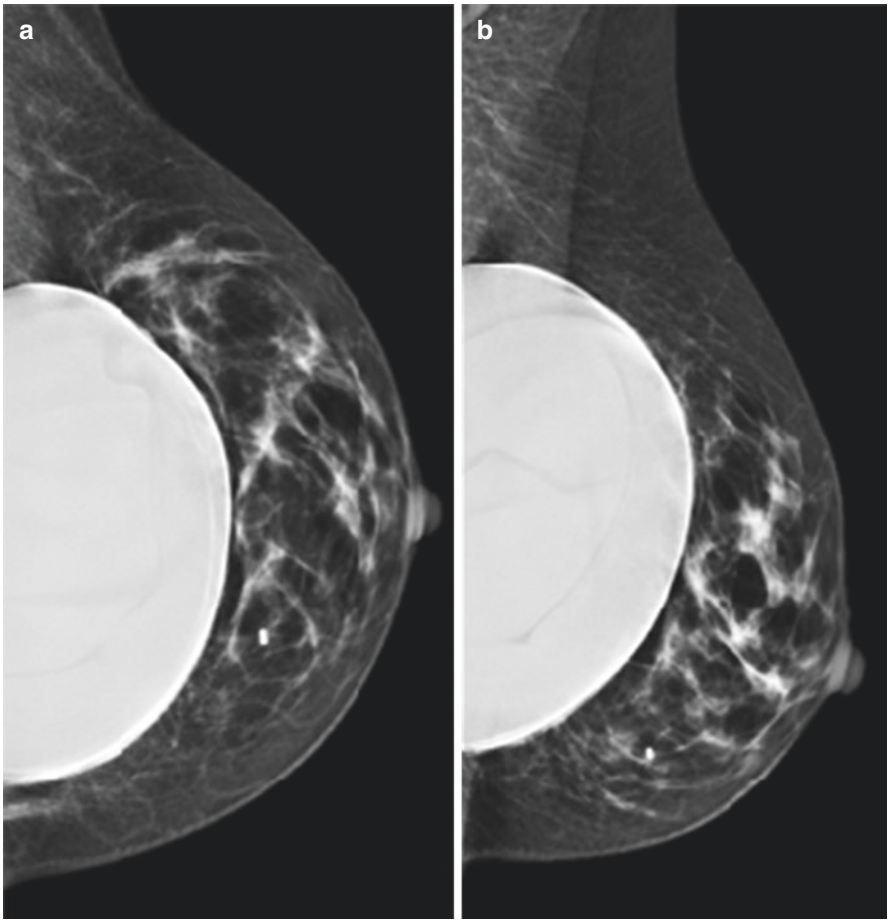

Fig. 17.22 Wrinkles on the surface of the implant on mammogram (normal finding)

glandular tissue, overlapping the pectoralis muscle, whose anterior contour will be underneath the implant on mammography, mostly on the mediolateral oblique view. On the other hand, in the subpectoral position, the implant is behind the breast tissue and the pectoralis muscle, which covers the implant [23].

A fibrous capsule is always formed around the implant, usually soft and undetectable by physical examination or mammography, unless it hardens or calcifies [28]. Dystrophic sheetlike calcifications appear dense, thin, and irregular next to the implant (Figs. 17.23 and 17.24) [29]. Polyurethane-covered implants are covered with a spongelike material and, when calcified, produce a typical fine mesh-like calcification. Implant-displaced views displace the capsular calcifications away from the implant (Fig. 17.25) [22]. Spot magnification can help differentiate if the calcifications are in the parenchyma (which may represent postoperative fibrosis or a more worrisome diagnosis) or in the implant capsule. Sometimes this

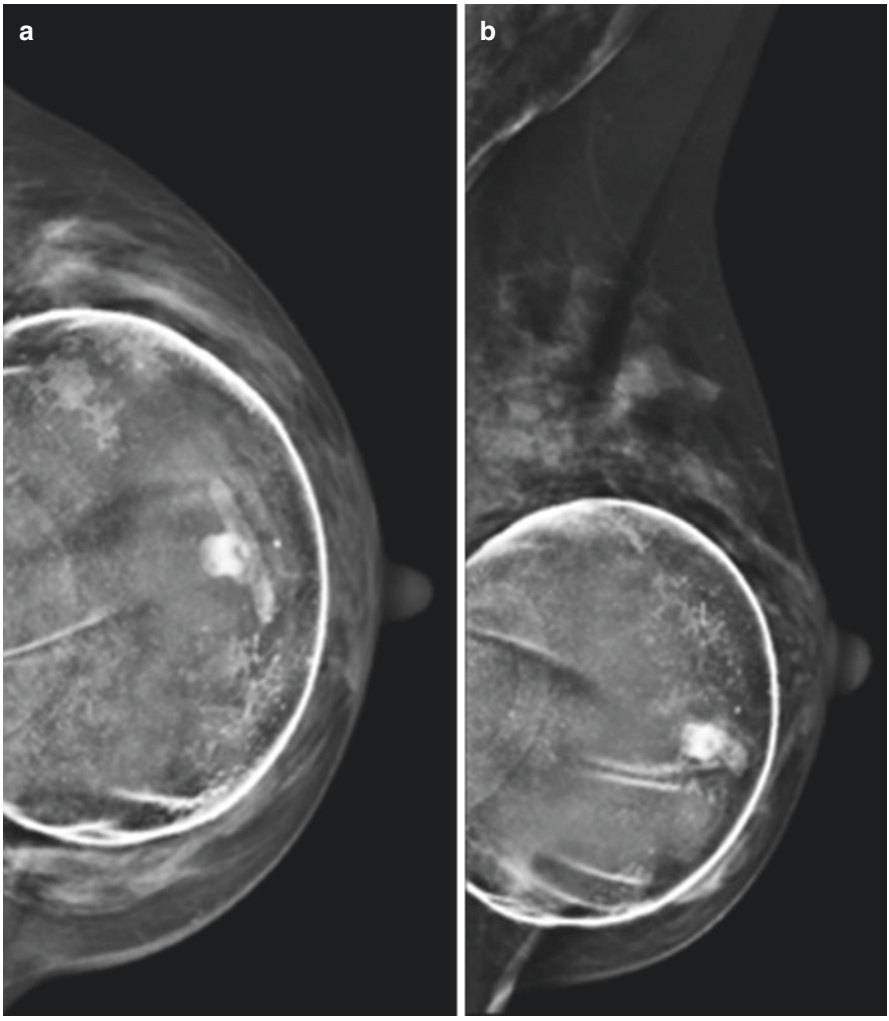

Fig. 17.23 Calcified fibrous capsule of a saline implant after 22 years of placement

differentiation is not possible, and capsular calcifications can be mistaken for malignancy, leading to a false-positive examination [29].

Ultrasound cannot differentiate between silicone or saline implant types, but in double-lumen implants, it is possible to characterize the inner and outer envelopes as two distinct chambers. The normal implant (Fig. 17.26) is an anechoic mass with an echogenic shell, a three-layered appearance, two thin echogenic lines, and an anechoic line between them ("Oreo cookie sign") [30]. Reverberation artifacts can be identified as multiple bands of noise caused by repeat reflections of the beam between the skin surface and the anterior wall of the implant, characteristically seen in the near field, parallel to the anterior implant wall, showing the same width as the

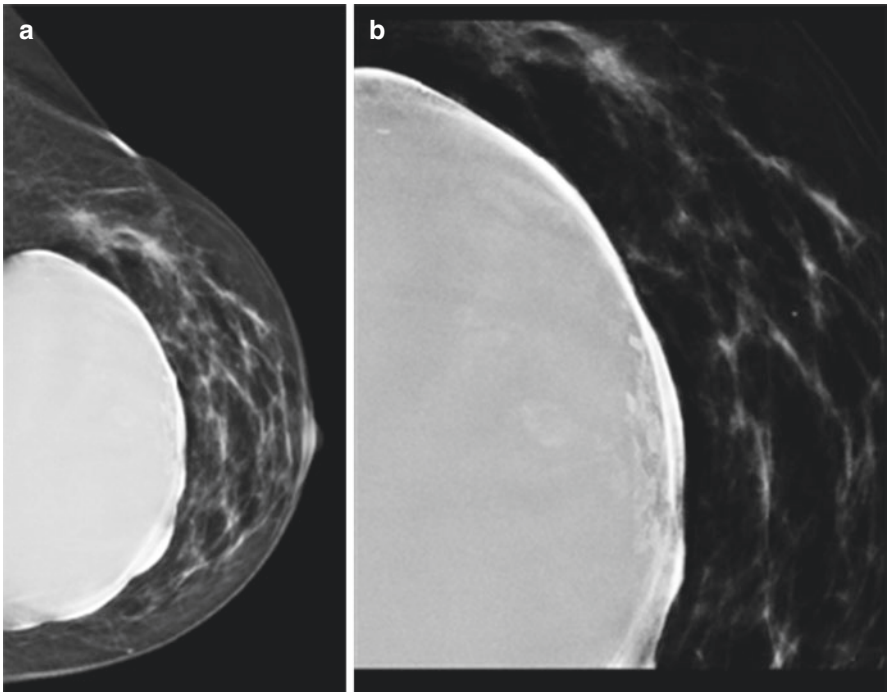

Fig. 17.24 Calcified fibrous capsule of a silicone implant. Dystrophic sheetlike calcifications appears dense, thin, and irregular next to the implant

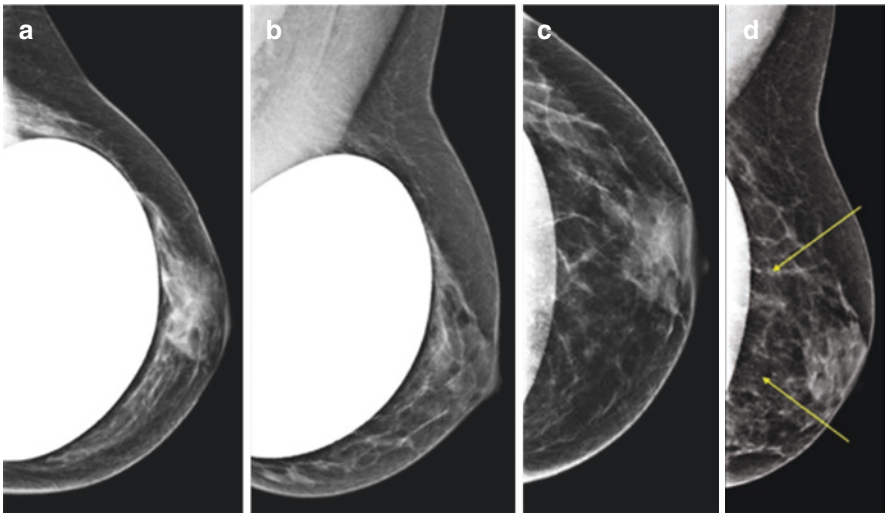

Fig. 17.25 Capsular calcifications (**c**, **d**) displaced away from the implant after Eklund maneuver

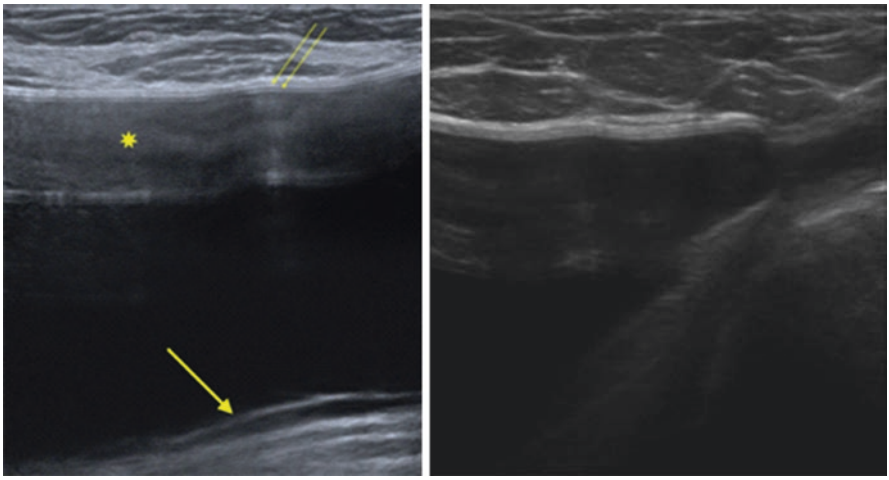

Fig. 17.26 Normal implant on ultrasound. Anechoic mass with an echogenic shell with a three-layered appearance with two thin echogenic lines (thin arrows) and an anechoic line between them ("Oreo cookie sign"). Reverberation artifacts (star) and the posterior localization of the seal (thicker arrow) are also characterized

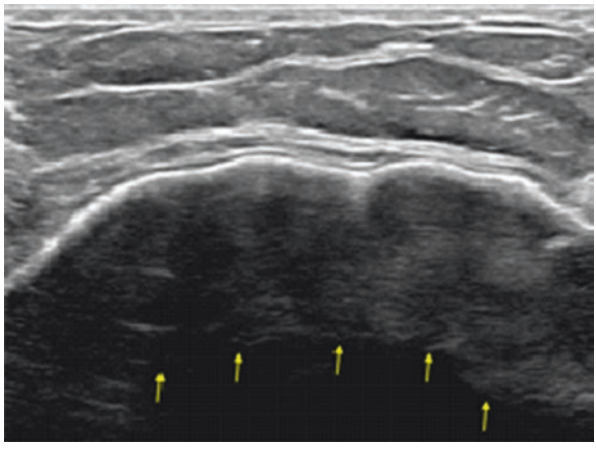

Fig. 17.27 Reverberation artifacts (normal findings). Multiple bands of noise caused by repeat reflections of the beam between the skin surface and the anterior wall of the implant, characteristically seen in the near field, parallel to the anterior implant wall, showing the same width as the breast tissue anterior to the implant

breast tissue anterior to the implant (Fig. 17.27) [23, 28]. Radial folds are common findings and represent infoldings of the intact envelope that look like echogenic lines extending to the periphery of the envelope [30]. The fibrous capsule may be seen as another echogenic line superficial to the implant shell separated by a small anechoic line. Implants that have a sponge structure of the outer shell present the fibrous capsule growth into this coverage; therefore, it cannot be seen. The clue that helps to evidence the fibrous capsule is the search for a small radial fold, in which the fibrous capsule is usually lifted from the implant and easy to measure (Fig. 17.28).

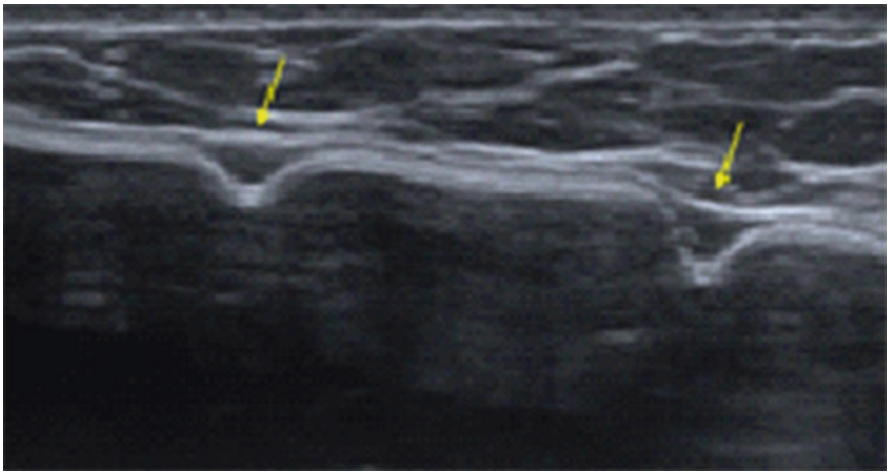

Fig. 17.28 Fibrous capsule. Ultrasound shows small radial folds filled with fluid. In these spots, fibrous capsule is usually lifted from the implant and easy to measure

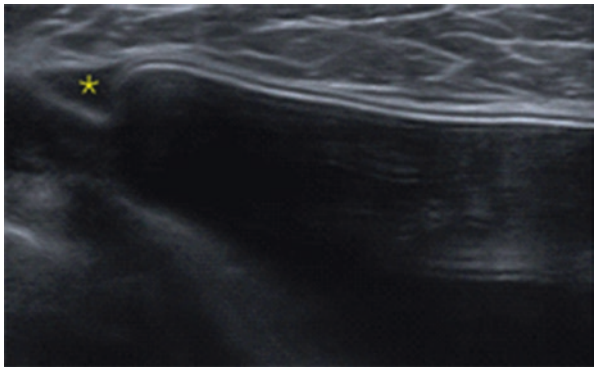

Fig. 17.29 Small amount of periprosthetic fluid (normal finding) on ultrasound

Small radial folds and a small amount of periprosthetic fluid are also considered normal findings (Fig. 17.29) [31].

17.2.2.3 Imaging Findings After Implant Removal (Explantation)

The main reasons patients decide to remove their implants are suspected silicone-related health problems; suspected rupture; breast firmness; breast and musculoskeletal pain; or other complications. Mammography, ultrasound, and magnetic resonance imaging after explantation are broad and may simulate malignant tumors. In this context, the comparison with previous exams and a detailed surgical history are crucial. The imaging findings range from a nearly normal appearance to

architectural distortion (Fig. 17.30), focal asymmetry, residual fibrous capsules or spiculated silicone granulomas, residual free silicon, or collections [4, 32, 33].

After the removal of the implants, the fibrous capsule often remains totally or partially in the breasts, which may be seen on subsequent imaging studies (Fig. 17.31) [32]. The implant cavity may resolve completely but, in some cases may scar, causing architectural distortion (Fig. 17.32) or may fill with fluid in the non-collapsed fibrous capsule (seroma), which may simulate an abscess (Fig. 17.33). Mammogram may show dystrophic calcifications if the fibrous capsule calcifies,

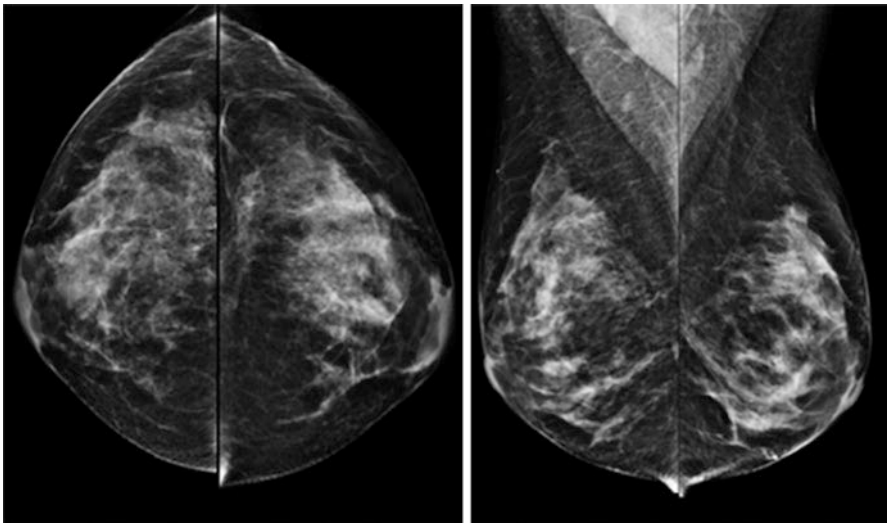

Fig. 17.30 Explantation. There are no signs of the implant removal, except for the discrete architectural distortion

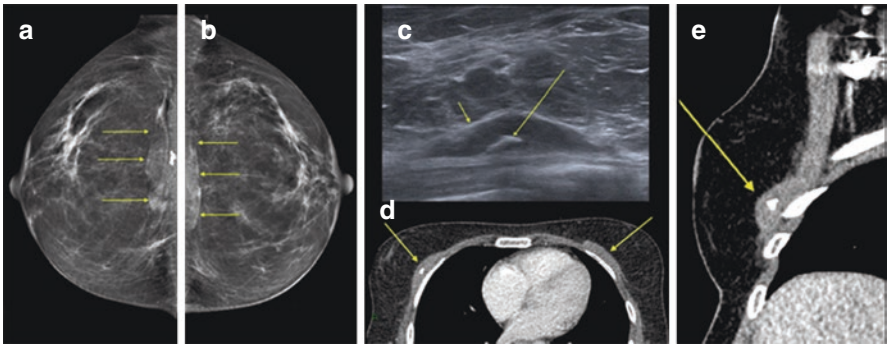

Fig. 17.31 Explantation. Mammogram (**a**, **b**) and CT (**d**, **e**) show coarse calcifications in the residual fibrous capsule after implants removal. On ultrasound (**c**), the fibrous capsule presents as a hypoechoic mass next to the thoracic wall with a hyperechoic image in the center that represents the calcification

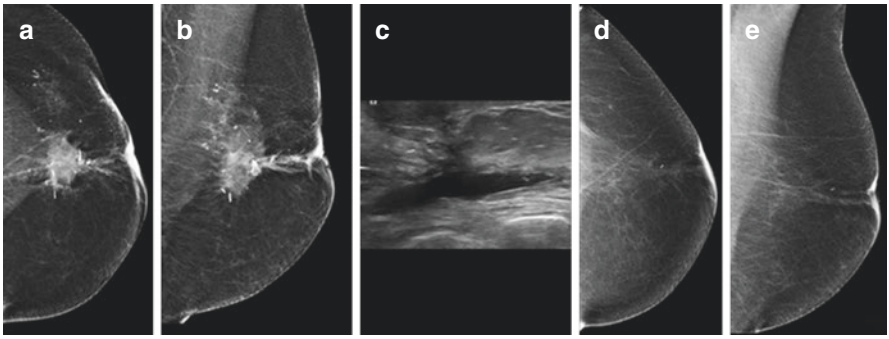

Fig. 17.32 Explantation. Mammogram performed 1 month after explantation depicts architectural distortion associated with a spiculated mass and calcifications (**a**, **b**). Ultrasound of the same date shows the distortion as a hypoechoic path from the fluid filled implant cavity up to the NAC (**c**). Late control mammogram shows an almost completely resolved cavity with a discrete architectural distortion (**d**, **e**)

typically presenting as a sheetlike curvilinear pattern at the chest wall (Fig. 17.34) but occasionally can show an undetermined pattern, which can be hard to distinguish from other breast pathologies (Fig. 17.35) [4, 29, 33].

It is usually difficult to remove all the extracapsular free silicone from a ruptured implant, without removing too much of the breast [28]. In this case, some free silicone images, infiltrated lymph nodes (Fig. 17.34), or silicone in the residual fibrous capsule (Fig. 17.36) can be seen [4]. Ultrasound shows the typical snowstorm sign, and the free silicone signal on MRI should not be misinterpreted as an acute rupture of new implants [32].

17.2.2.4 Implant Complications

Complications associated with silicone implants are categorized as early or late changes. They include contracture of the fibrous capsule, calcification of the fibrous capsule, implant rippling, seroma, implant displacement, malposition, extrusion, breastfeeding difficulties, hematoma, infection (Figs. 17.37 and 17.38), breast pain, scarring, implant rupture, rotation, herniation, and silicone gel "bleed" [34].

Breast implant-associated anaplastic large cell lymphoma (BIA-ALCL) is a rare clinicopathologic entity associated with implants. Multimodality imaging examinations are useful in investigating a possible complication, fundamentally ultrasonography (US) and MR imaging. Mammography with special views and sonography can frequently delineate a locule within the implant that mimics a parenchymal breast mass.

Breast implant illness (BII) is a clinical condition in which some patients report a variety of systemic symptoms, such as chronic fatigue, brain fog, and joint and muscle pain. There are no typical imaging finding, and radiologic examinations are useful to exclude other pathologies that could be related to these symptoms. The

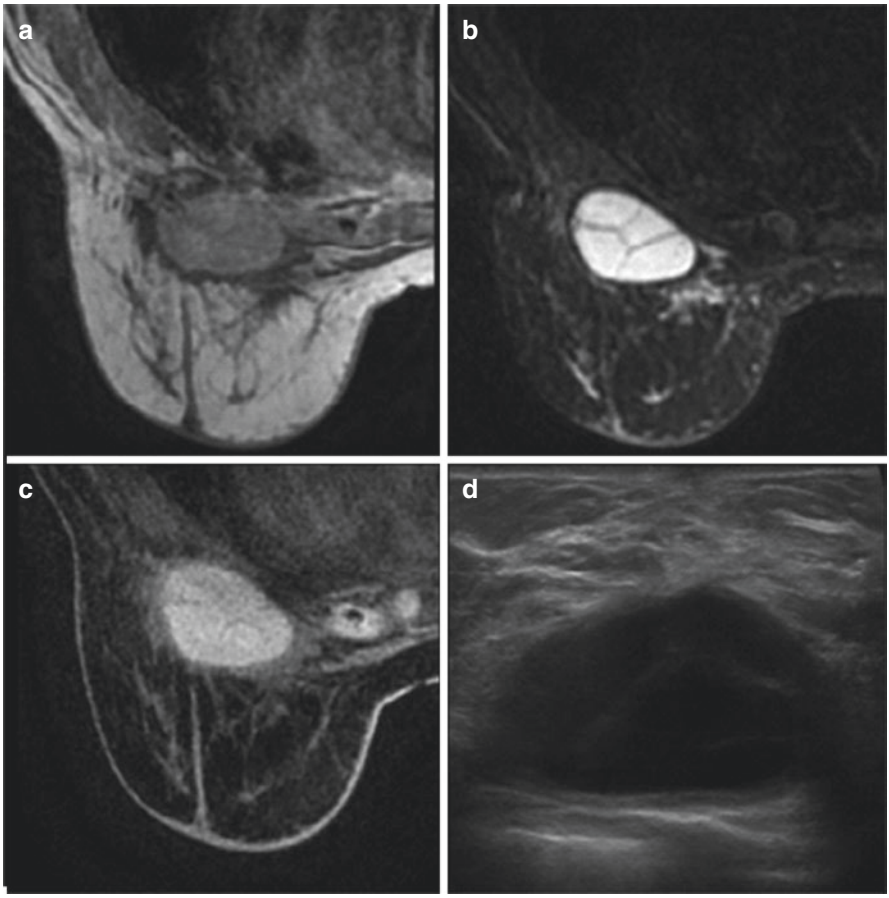

Fig. 17.33 Explantation. Axial T1-weighted without fat suppression (**a**), axial fat- suppressed T2-weighted (**b**), and axial contrast-enhanced fat-suppressed T1-weighted MR images (**c**) depict the implant cavity after 2 months of implant removal filled with fluid in a non-collapsed fibrous capsule, mimicking an abscess. Ultrasound shows a seroma with thin septa (**d**)

removal of breast implants without replacement sometimes appears to reverse their symptoms.

Systemic autoimmune adverse reactions related to silicone have rarely been reported. Autoimmune/inflammatory syndrome induced by adjuvants (ASIA) syndrome was first described in 2011 by Shoenfeld and Agmon-Levin and incorporates several conditions linked to previous exposure to an adjuvant substance, including silicone. Clinical manifestations are highly heterogeneous, with development of both nonspecific and specific manifestations of autoimmune diseases, which cannot be classified as classic connective tissue disorders. It is currently still being investigated whether silicone implants increase the risk of autoimmunity [35].

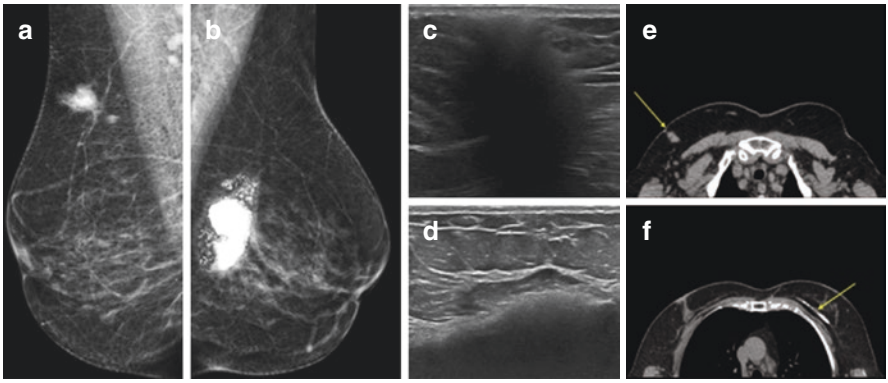

Fig. 17.34 Explantation. Late postoperative mages of an explantation of 45-year-old implants. Mammogram shows silicone within intramammary lymph node in the upper quadrants of the right breast (**a**) and residual fibrous capsule with calcifications and silicone on the left breast (**b**). Corresponding ultrasound images depict a spiculated mass with snowstorm sign (**c**) and a linear posterior image with residual silicone (**d**). CT shows an oval, circumscribed mass corresponding to the lymph node with silicone (**e**) and a posterior calcified linear image representing the fibrous capsule (**f**)

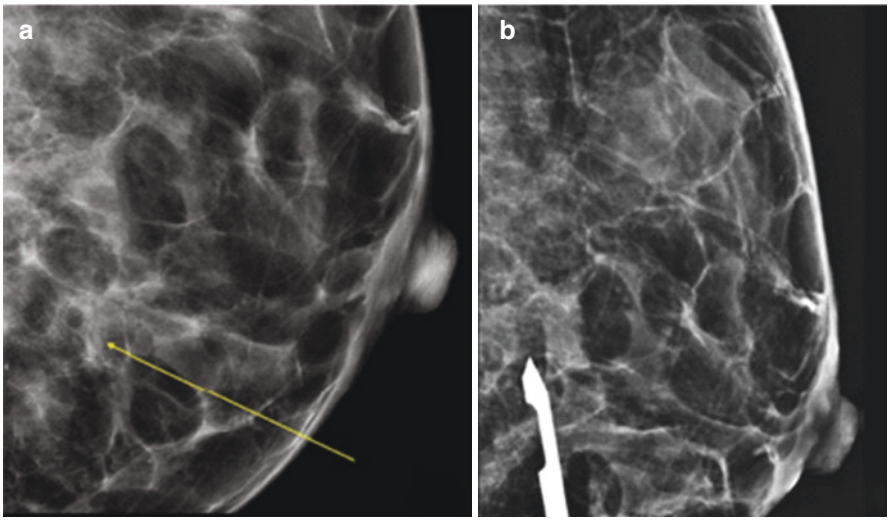

Fig. 17.35 Explantation. Amorphous calcifications (arrow) after explantation of an 18-year-old implants (**a**). Vacuum-assisted needle biopsy (**b**) was indicated, and the histological result was calcifications in the fibrous capsule

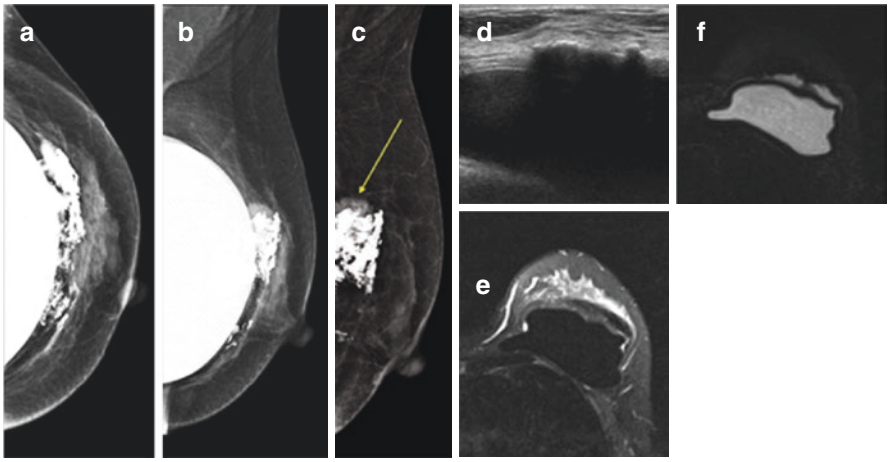

Fig. 17.36 Explantation. Mammogram (**a**–**c**) shows a dense residual fibrous capsule with an associated small spiculated density (arrow). An irregular linear image with posterior shadowing is seen anteriorly to the implant on ultrasound (**d**). On axial fat- suppressed T2-weighted (**e**) and axial short T1 inversion-recovery silicone-excited MR images (**f**), this image shows signal compatible with silicone from previous ruptured implant

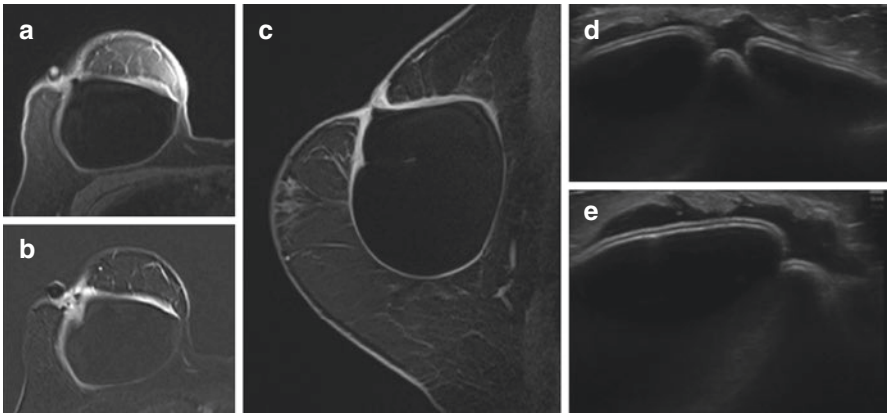

Fig. 17.37 Infection. Axial fat-suppressed T2-weighted (**a**) and axial contrast-enhanced fat-suppressed T1-weighted subtraction image (**b**) and sagittal contrast-enhanced fat-suppressed T1-weighted MR images (**c**) show fibrous capsule thickening with enhancement. Patient had inflammatory signs with fistulization of purulent content in the upper quadrants which resulted in skin retraction. Ultrasound depicts a small collection with anfractuous contours next to the implant and hyper echogenicity of the nearby tissue (**d**, **e**)

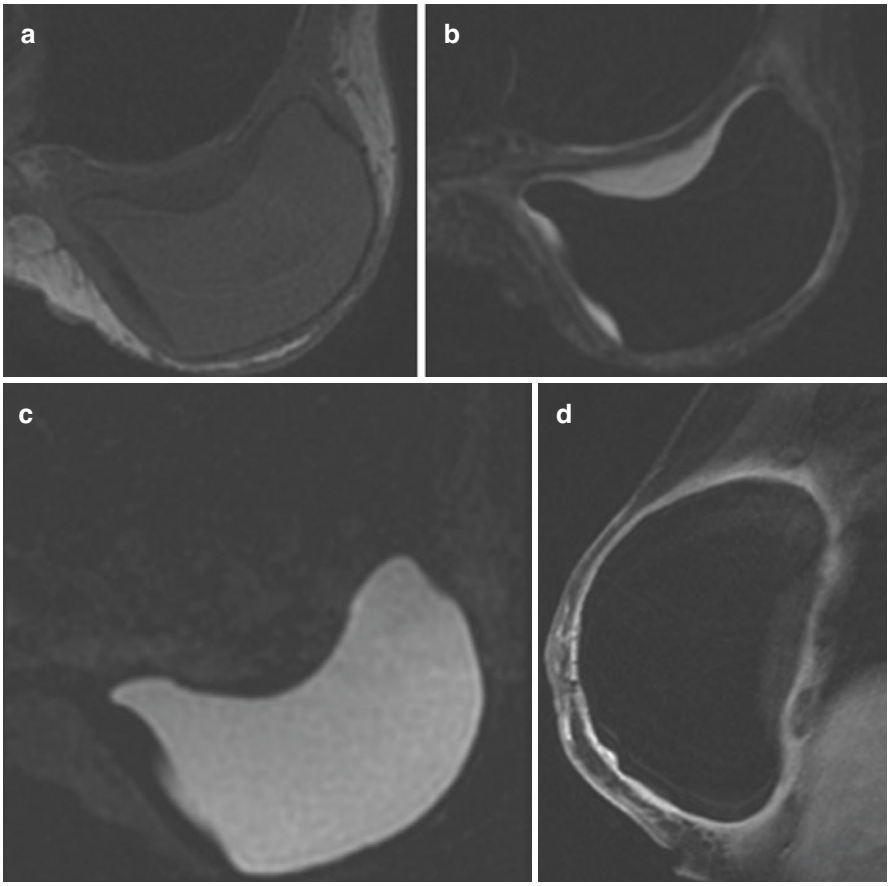

Fig. 17.38 Infection. Axial T1-weighted without fat suppression (**a**), axial fat-suppressed T2-weighted (**b**), axial short T1 inversion-recovery silicone-excited (**c**), and sagittal contrast-enhanced fat-suppressed T1-weighted MR images (**d**) show periprosthetic effusion and fibrous capsule thickening with enhancement

Rotation

Implant rotation may be clinically suspected from a new asymmetry or deviation from normal breast contours. Rotation rates vary in the literature and can be related to lack of development of a connective tissue adhesion layer between the implant and the capsule, a surgical pocket that is too large for the implant of the patient, capsular fluid, anatomical shape (asymmetry of anatomical implants can act as the geometric base for their rotation), double capsules, periprosthetic mesh, and prosthetic massage. Texturized surfaces are supposed to have an adhesive effect with the surrounding tissue after surgical implantation to reduce incorrect positioning. In most cases, rotation is asymptomatic and does not imply any clinical issue.

Imaging diagnosis can be made by searching for the raised silicone ridge/projections (Fig. 17.39) used for intraoperative orientation of the implant that usually are placed between 5 and 7 o'clock, easily visualized on ultrasound. In implants that do not have an orientation marker, we must look for the posterior seal (Fig. 17.40). If it is visible on the anterior part of the envelope, it is compatible with rotation (Fig. 17.41). MRI is a useful tool since it can demonstrate any localization of the seal, not only anterior or posterior (Fig. 17.42).

Capsular Contraction

Capsular contraction is the most common implant complication [36], with a reported incidence of more than 70% in older series and about 20% in more recent literature (lower rates of capsular contracture have been observed with later-generation,

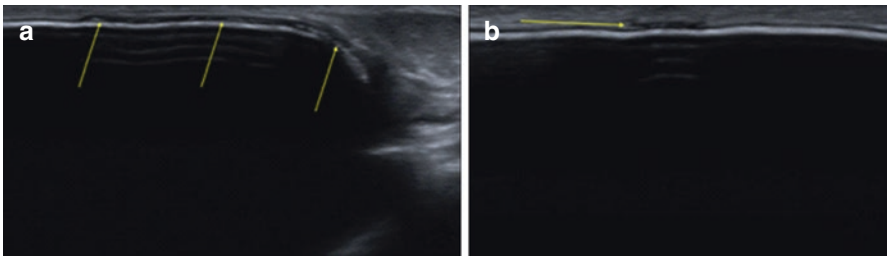

Fig. 17.39 Raised silicone ridge. Ultrasound shows the orientation marker on longitudinal (**a**) and transversal position (**b**) as a hypoechoic periprosthetic layer (arrows)

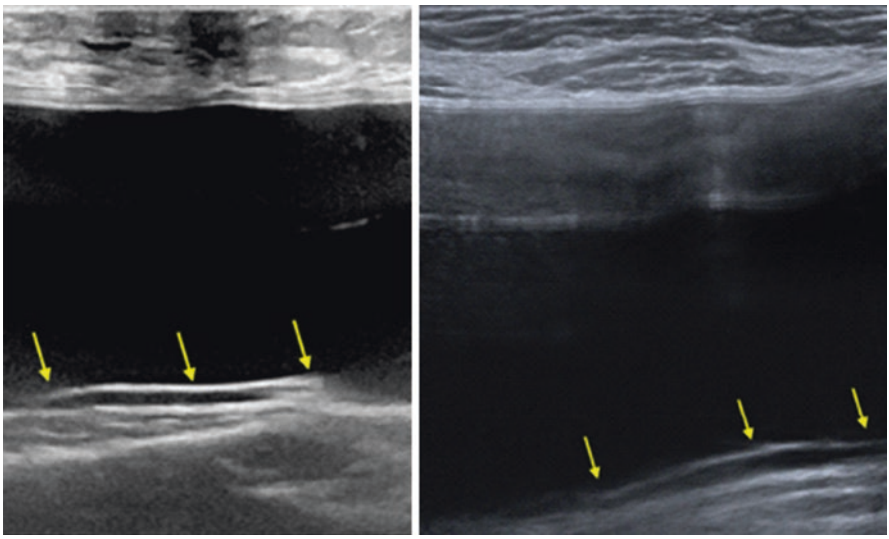

Fig. 17.40 Posterior seal. Normal positioning of the implant can be confirmed by the posterior location of the seal that is characterized by its echogenic linear appearance (arrows) separated from the envelope by a thicker anechoic line

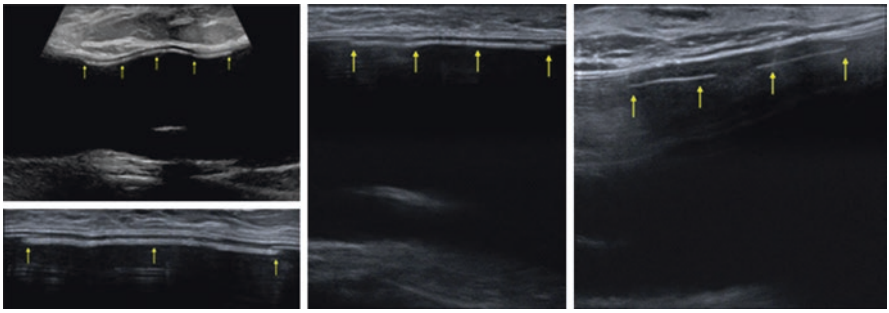

Fig. 17.41 Rotation. Ultrasound of different implants show the posterior seal with an anterior location

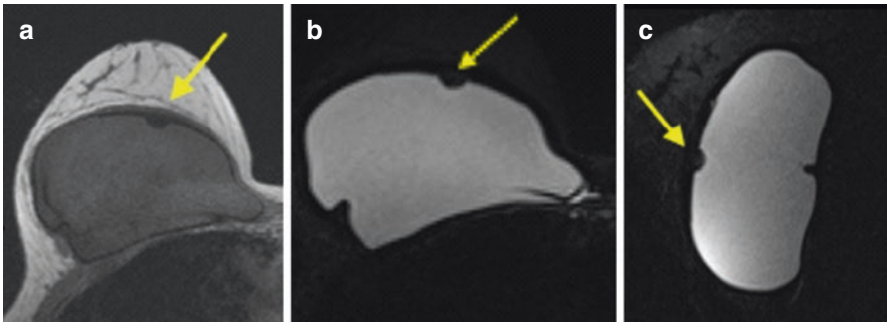

Fig. 17.42 Rotation. Non-fat-suppressed T1-weighted (**a**) and short T1 inversion-recovery silicone-excited MR images (**b**, **c**) show the seal as a linear thickening with a little oval projection into the lumen in an anterior position (arrows). Other types of implants may have different seal presentations

cohesive-gel, form-stable implants than with those of earlier generations), usually starting within the first year of implantation and an increasing risk over time [5, 23]. The physiopathology is not well established and is presumed to be multifactorial, with proposed mechanisms that include bacterial contamination, surface texturing, selection of implant pocket, the incision type, drain placement, antibiotic use, and smoking [19]. It may be in part related to a subclinical implant infection caused by *Staphylococcus epidermidis* from the breast ducts. The incidence of capsular contracture is higher with transaxillary and periareolar incisions and lower with inframammary incisions.

Implants become hard and resistant, presenting a round morphology, with or without prominent wrinkles. The diagnosis is based on clinical examination, but imaging can suggest capsular contraction in some cases and discard other complications [23, 36]. Baker classification describes increasing levels of capsular contracture and hardening of breast implants on physical inspection and examination (Table 17.1).

Table 17.1 Baker classification for capsular contraction

Grade	Breast firmness	Implant visibility
I	Soft	Nonpalpable; nonvisible
II	Minimal	Palpable; nonvisible
III	Moderate	Easily palpable; distortion visible
IV	Severe	Hard, tender, cold; distortion may be marked

Fig. 17.43 Bilateral capsular contraction. Increased anteroposterior diameter due to the spherical shape. It is very difficult to suggest a bilateral diagnosis only with mammogram. Clinical history is critical in these cases

Typical imaging findings are increased anteroposterior diameter due to the spherical shape (deformation of the implant) (Fig. 17.43), capsular wrinkles and folds that often mimic breaks especially on ultrasound, and thickening and enhancement of the fibrous capsule on MRI (called capsulitis that may represent an active stage of capsular contracture) [23]. The diagnosis may be easier if these findings are unilateral (Fig. 17.44). There are reports showing high correlation between the clinical Baker score and elastography measurements. Contrast-enhanced ultrasound could be an alternative due to its higher accessibility when compared to MRI to study the possible changes in enhancement of the capsule (Fig. 17.45) [36].

Treatments for capsular contracture include open surgical capsulotomy (make incisions in the scar capsule encasing the implant to release and relax it), capsulectomy (excision of portions or the entire capsule), and replacing the implant to another location. Another option is the closed capsulotomy, which consists of squeezing the implant manually trying to break the hardened fibrous capsule to allow the implant to soften again, but this technique can result in implant rupture and moderate breast pain [28]. Contractures that fail to respond to these treatments may ultimately benefit from implant removal and autologous reconstruction (auto augmentation) rather than implant replacement [23].

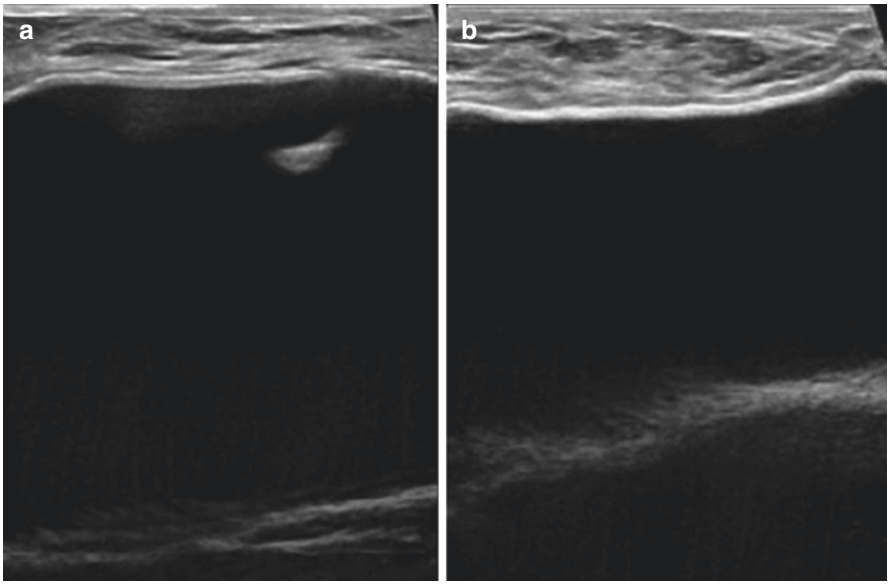

Fig. 17.44 Unilateral capsular contraction on ultrasound. Increased anteroposterior diameter due to the spherical shape (**a**) is better seen when compared to the other side (**b**)

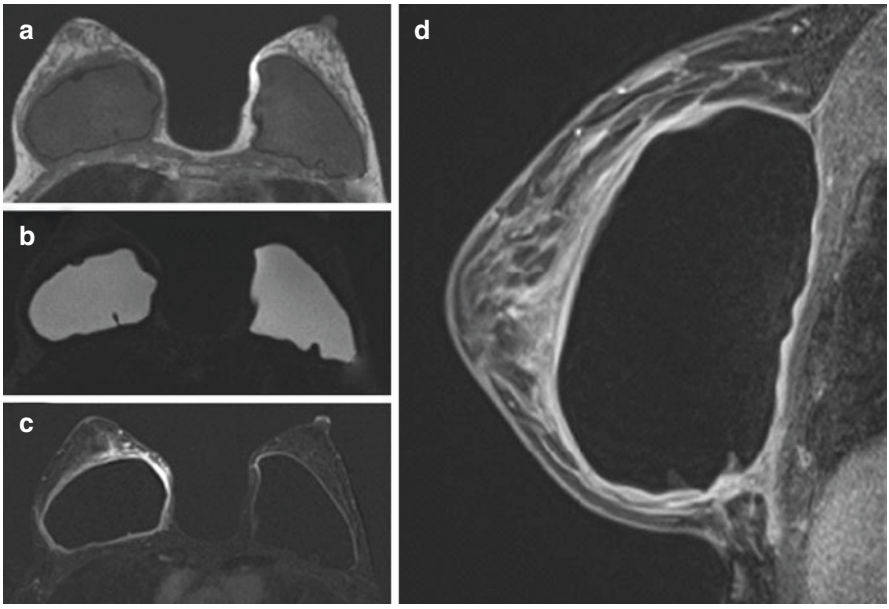

Fig. 17.45 Unilateral capsular contraction on MRI. Patient with induration of the right breast. Axial T1-weighted without fat suppression (**a**), axial short T1 inversion-recovery silicone-excited image (**b**), axial contrast-enhanced fat-suppressed T1-weighted subtraction (**c**), and sagittal contrast-enhanced fat-suppressed T1-weighted MR images (**d**) show bilateral rotation with increased anteroposterior diameter due to the spherical shape and enhancement of the fibrous capsule of the right implant

Subglandular implants have the highest incidence of capsular contracture, unlike textured submuscular implants that present the lowest incidence. In theory, the overlying muscular tissue compresses and massages the implant between the muscle fibers and the chest wall, inhibiting the development of capsular contracture and minimizing the unnatural firmness of the implant. Trilucent implants were removed from the market with a subsequent recommendation that the implants be removed from patients due to their association with rippling, breast pain, contracture, and deflation. There are some reports of implants that contain carboxymethylcellulose (hydrogel), which presented low rates of capsular contracture.

Implant Rupture

Breast implant ruptures consists in partial or total collapse of the envelope, mostly associated with trauma, closed capsulotomy, and older generation implants [20, 37, 38]. Newer generations of silicone implants are more stable and have rupture rates estimated in 2.0–3.8% in 6-year follow-up (fifth-generation implants) [3, 5, 8, 38–41]. Implant type (ruptures in double-lumen and polyurethane-covered implants are less frequent than in smooth implants) and manufacturers also have influence in risk factors [5, 36]. Poly Implant Prothèse (PIP) silicone implants have been responsible for a crisis in this growing aesthetic field, by containing nonmedical industrial silicone and a higher reported rupture rate.

When a saline implant ruptures, the envelope retracts, and deflation is usually noticeable as the breast becomes smaller [23, 37]. The breast tissue absorbs the saline solution with no major complications.

The silicone implant usually keeps the original shape and volume if the fibrous capsule is intact and continues to contain the free silicone (intracapsular rupture). Intracapsular ruptures account for 77–89% of ruptures, and the patient is usually asymptomatic. These are also called silent ruptures and occurs in 5% of screening patients [21].

The collapse of the silicone implant envelope may be associated with a rupture of the fibrous capsule, with the extrusion of the silicone gel into the breast tissue, which are not absorbed by the body (extracapsular rupture).

Gel bleed is a situation in which silicone gel leakage is observed through an apparent intact implant envelope (the existence of undetectable ruptures remains controversial).

Diagnosis of silicone implant rupture is often difficult based only on clinical manifestations because they are frequently nonspecific [5, 42]. Reported symptoms include palpable masses in the axilla, breast, or chest wall (older generations); pain; or changes in the size, shape, or texture of the breast [3, 28, 43, 44]. Imaging assessment plays a main role in the detection of implant ruptures because physical examination misses approximately 50% of them [6, 42].

Mammography

Intracapsular ruptures in implants filled with silicone gel are almost undetectable in mammograms because the silicone gel is still contained within an intact fibrous capsule [28, 45]. A flared contour may be related to intracapsular rupture (Fig. 17.46) but also to capsular contracture or herniation of an intact implant envelope through a rupture in the surrounding fibrous capsule [44].

Silicone beyond the fibrous capsule is a typical and specific finding of an extracapsular rupture (Fig. 17.47) [45, 46]. However, mammograms may show only contour abnormality of the ruptured implant when the extruded silicone is not far enough from the implant to be seen as a separate finding (Fig. 17.48). Eventually extracapsular rupture may have no apparent abnormality on mammograms, and the diagnosis must be confirmed by either ultrasound or MRI [44, 47].

Dense axillary lymph nodes are rare and represent silicone infiltration in the lymphatics, highly suggestive of an extracapsular rupture [23, 28, 48].

It is impossible to remove all of the free silicone without removing too much of the breast tissue after removal of an implant with extracapsular rupture. The residual gel stays within the breast tissue without absorption, making it difficult to correctly assess a new implant. Radiolucent centered coarse eggshell calcifications of silicone granulomas may be seen after implant rupture.

In ruptured saline implants, mammography usually shows only a slightly dense collapsed envelope near the chest wall because the saline fluid is absorbed by breast tissue.

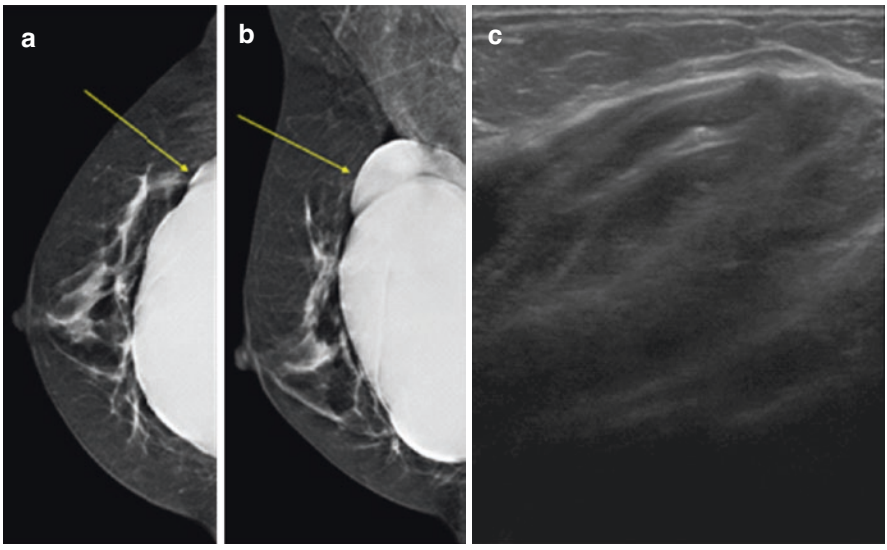

Fig. 17.46 Intracapsular silicone implant rupture. The silicone gel is still contained within an intact fibrous capsule. A flared lobulated contour may be seen on mammogram (**a**, **b**). Ultrasound depicts the stepladder sign (**c**)

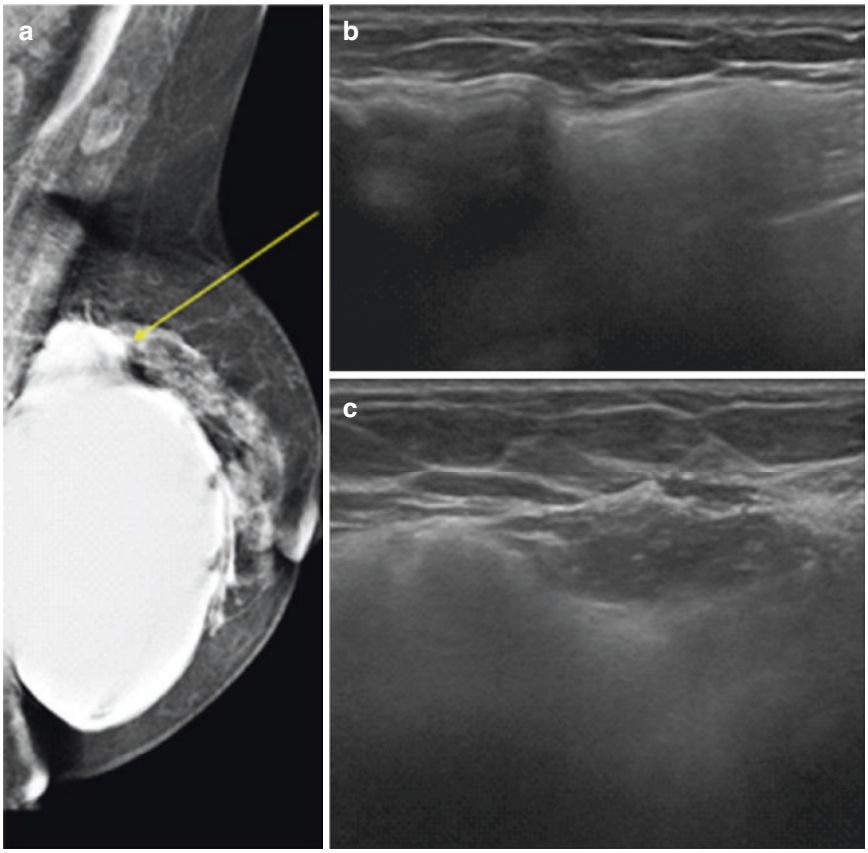

Fig. 17.47 Extracapsular rupture. Mammogram (**a**) shows silicone beyond the fibrous capsule (arrow). Ultrasound depicts the snowstorm sign (echogenic noise), a typical intense echogenic artifact caused by the slow velocity of sound in the silicone as compared to the surrounding parenchyma, obscuring all findings below it (**b**, **c**)

Ultrasound

Ultrasound is a useful tool in screening for ruptured breast implants, less expensive and more cost-effective than MRI, with sensitivity of 25–65%, specificity of 57–98%, and a negative predictive value of 85% [45].

The classic finding in extracapsular rupture of a silicone implant is the snowstorm sign (echogenic noise), which is a typical intense echogenic artifact caused by the slow velocity of sound in silicone when compared to the surrounding parenchyma that obscures all findings below it (Figs. 17.47 and 17.48) [43, 45, 49, 50]. The snowstorm sign is present when scanned from all angles, whereas edge artifact may change or disappear. Echogenic noise may also be seen in lymph nodes with silicone infiltration (Fig. 17.49), gel bleed, and direct silicone or paraffin injections, which can be so intense that ultrasound is nondiagnostic (Figs. 17.64 and 17.65) [28].

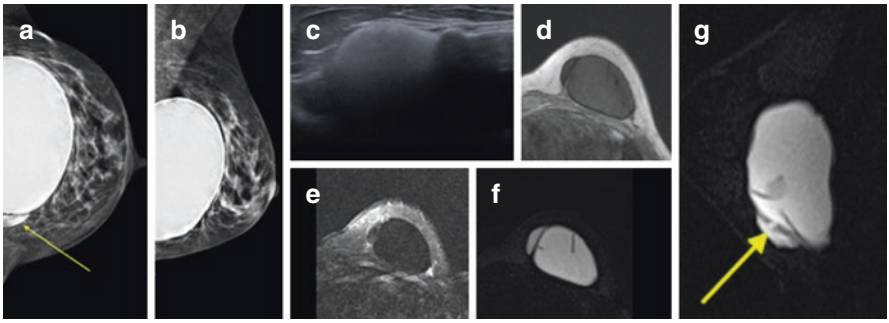

Fig. 17.48 Extracapsular rupture. Mammogram (**a**, **b**) shows contour abnormality due to extruded silicone that is not far enough from the implant to be seen as a separate finding. It may be difficult to differentiate from a double contour of periprosthetic effusion. Ultrasound depicts the snowstorm sign on this topography (**c**). Axial T1-weighted without fat suppression (**d**), axial fat-suppressed T2-weighted (**e**), and axial short T1 inversion-recovery silicone-excited images (**f**) demonstrate the outer silicone next to the implant, and the reconstructed sagittal short T1 inversion-recovery silicone-excited image (**g**) shows the discontinuous envelope (arrow)

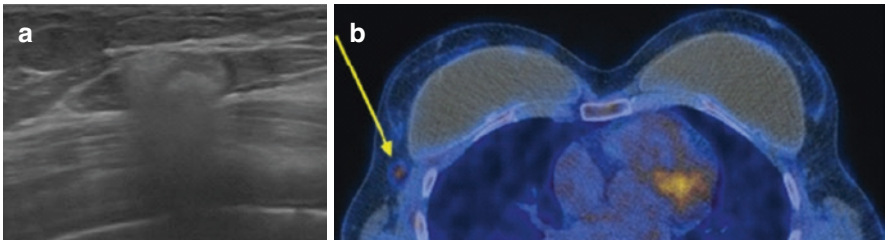

Fig. 17.49 Snowstorm sign in an intramammary lymph node with silicone infiltration (**a**), corresponding to the finding with high uptake on PET-CT (**b**)

The intact fibrous capsule in intracapsular rupture ensures that the silicone is isolated from the breast parenchyma, so there will be no snowstorm sign, unless when associated with extracapsular rupture. Instead, stepladder sign may be present, which is characterized by multiple thin echogenic lines within the silicone gel that looks like the steps of a stepladder (Figs. 17.46 and 17.50) [14, 30, 46, 49, 50]. This sign represents the collapsed envelope from ruptured implant contained by the intact fibrous capsule. False-positive stepladder signs can be caused by radial folds (which always extend to the implant periphery) (Fig. 17.60) and intact multilumen implants producing multiple linear echoes [45, 52]. Less specific signs of intracapsular rupture are discontinuous envelope lines (Figs. 17.51 and 17.54), diffuse linear echoes, debris, or diffuse low-level echoes within the implant [50, 53]. When these signs a re dubious, MRI can confirm the diagnosis [47].

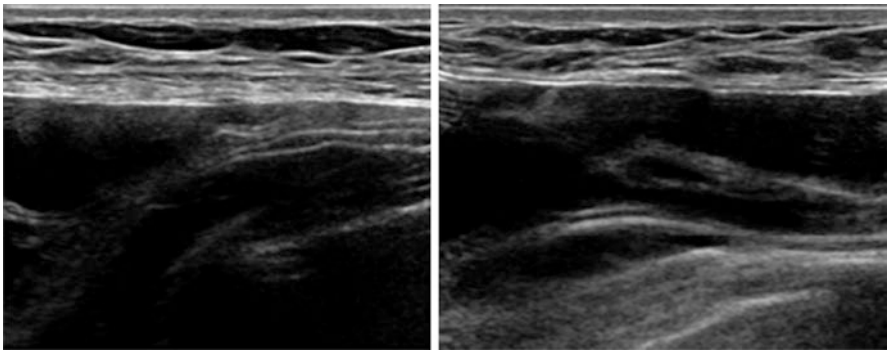

Fig. 17.50 Stepladder sign. The collapsed envelope from ruptured implant contained by the intact fibrous capsule, characterized by multiple thin echogenic lines within the silicone gel

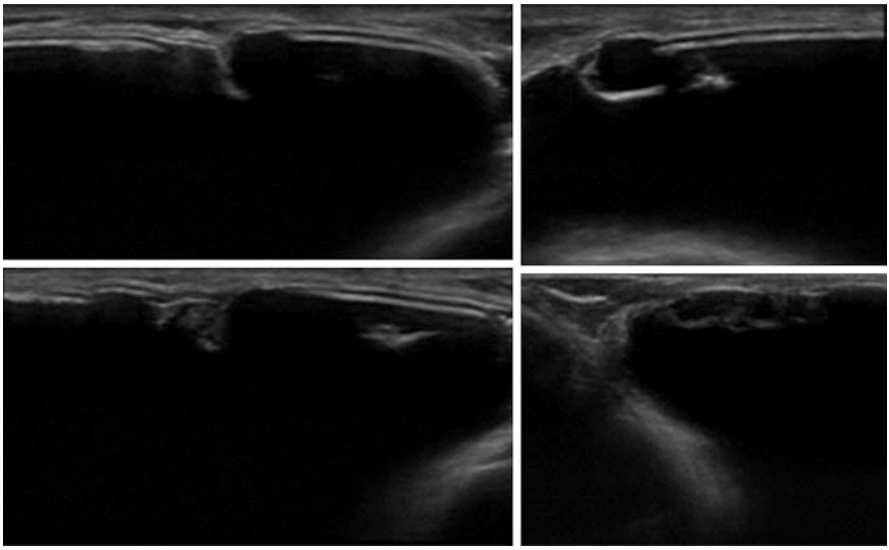

Fig. 17.51 Intracapsular rupture. Ultrasound shows discontinuous envelope lines

Magnetic Resonance Imaging

MRI remains the most sensitive and specific modality to detect silicone implant rupture. The Food and Drug Administration's recommendation for MRI screening for "silent" rupture is 3 years after implantation and every 2 years thereafter, raising diagnostic rates of ruptures still in the intracapsular phase, making surgery less traumatic and shorter [3, 54, 55]. There is no proven systemic health impact with rupture and extravasation of silicone to adjacent tissues.

It is possible to differentiate silicone gel from fat, water, glandular tissue, and any other tissues based on their unique relaxation properties using specific pulse

sequences. Silicone and water have high signals on T2-weighted images and combined silicone and water images, but signal suppression of either one makes it possible to distinguish these components [3, 43, 56, 57]. Intravenous contrast is not necessary for the detection of implant ruptures but may be useful for evaluating BIA-ALCL, implant-associated infections, and breast cancer in a patient with implants (known or suspected).

Normal saline implant shows the intact envelope filled with water, which has high signal on water-specific images but dark on silicone-specific images. MRI is usually not used to assess integrity of a saline implant because its rupture is clinically diagnosed by an acute reduction in breast size (Fig. 17.52). Normal single-lumen silicone implant shows high signal from the silicone gel with a smooth oval border on silicone-specific images. Radial folds in the envelope are dark lines in all sequences that extend to the periphery of the implant (Fig. 17.53). Multiplanar acquisitions enable to look at all implant contours and to differentiate them from ruptured envelopes [57]. Reactive fluid around the implant and water droplets in a radial fold topographically outside the envelope are common and nonspecific findings [46].

Intracapsular rupture can be characterized by the keyhole or teardrop sign, the subcapsular line, or the linguine sign [3, 26, 43, 49, 56, 58–60]. The keyhole or inverted teardrop sign represents silicone outside the implant envelope within a short radial fold, characterized with hyperintensity on silicone-specific images (Fig. 17.54). A subcapsular line is a dark line parallel to the implant shell that does not reach the implant periphery, representing incomplete shell collapse (Fig. 17.55). The linguine sign is the collapsed shell represented as curvy noodle-shaped dark lines inside the implant that do not extend to the periphery and is reported as the

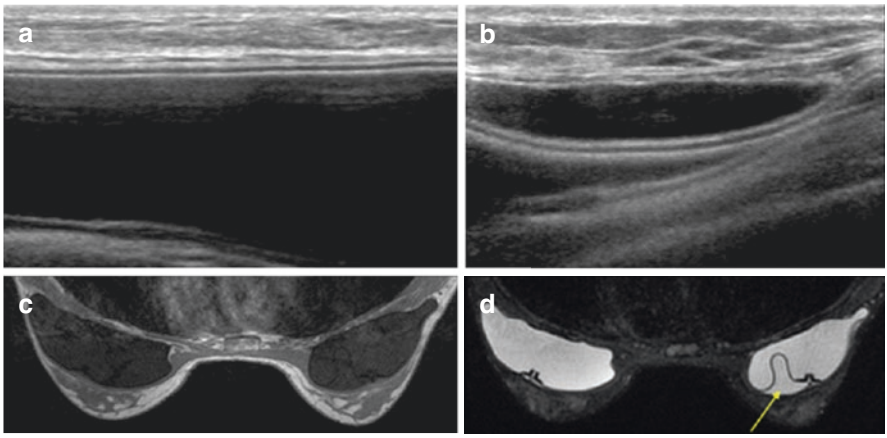

Fig. 17.52 Ruptured saline implant. Ultrasound shows a smaller implant when compared to the other side, with a normal appearance of the reduced implant (**a**) and only with a small amount of periprosthetic fluid (**b**). Axial T1-weighted MR image without fat suppression (**c**) shows symmetric hypointense signal inside the fibrous capsule. Axial fat-suppressed T2-weighted MR image (**d**) presents a reduced implant with a small amount of periprosthetic fluid (arrow)

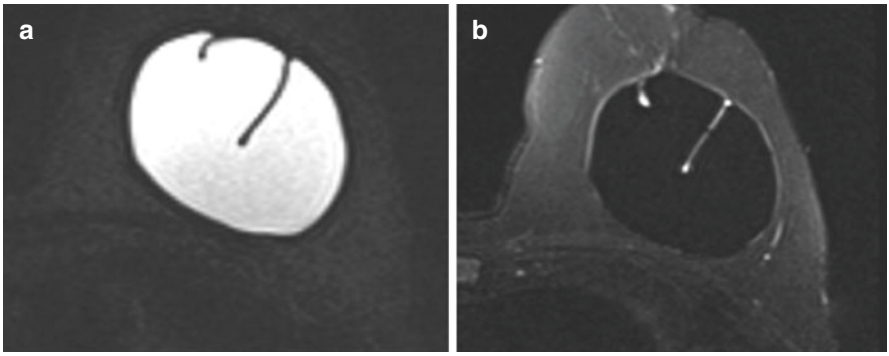

Fig. 17.53 Normal radial folds in the envelope on short T1 inversion-recovery silicone-excited image (**a**) and fat-suppressed T2-weighted MR images (**b**), with a small amount of fluid inside the last one

most sensitive (93%) and specific (65%) finding for rupture (Figs. 17.56 and 17.57) [26, 28, 47, 58]. Extracapsular rupture is characterized by silicone outside the fibrous capsule (Fig. 17.48), within the breast parenchyma or axilla, almost always associated with signs of intracapsular rupture [28, 56]. Severe gel bleed can present as a thin layer of silicone around the periphery of the implant but with an apparently intact envelope and fibrous capsule.

Multilumen or multiple implants (Fig. 17.58), stacked implants or implants made of rare materials, poor positioning of the breast, and a "redo" from a prior rupture (implant replacement after removal of ruptured implants) are causes of false-positives when screening for silicone implants rupture [49, 52]. Wrong positioning may produce artificial bulges by squeezing a part of implant between the coil and the chest wall. Silicon material extruded from previous rupture may not be completely removed during an implant replacement surgery and the residual silicone droplets near the new intact implant may result in misinterpretation as a new extracapsular rupture.

Breast Implant-Associated Anaplastic Large Cell Lymphoma (BIA-LCL)

The World Health Organization (WHO) recognized in 2016, BIA-ALCL, an extremely rare lymphoma reported in patients with implants, as a rare type of non-Hodgkin's lymphoma that accounts for only 3% of this pathology [60–62]. A major increase in incidence was noted over the last few years, but it may be due to increased awareness and earlier diagnosis of BIA-ALCL [61, 63]. The absolute risk estimated in the literature should be considered approximate and potentially biased estimates, since it has not been based on large population-based studies and there is a lack of reliable information on the prevalence of women with breast implants over time [60].

The physiopathology is unclear but is probably based on a chronic local inflammation due to the presence of implants and the degradation products derived from

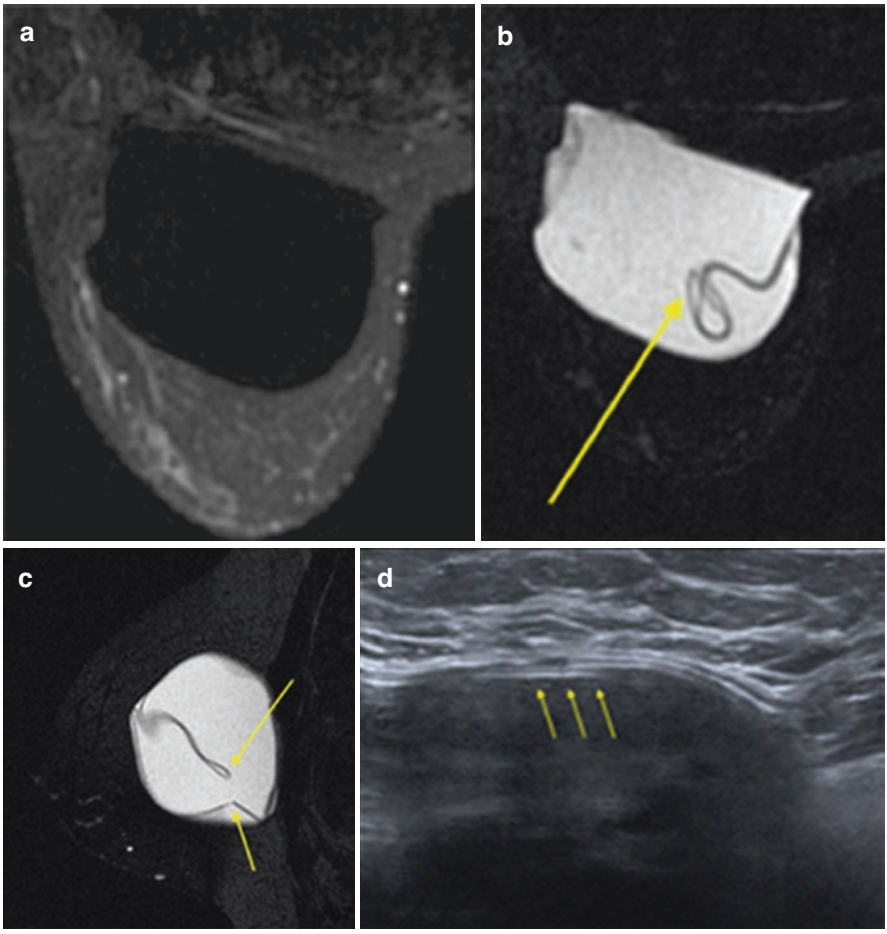

Fig. 17.54 Intracapsular rupture. Axial fat-suppressed T2-weighted MR image (**a**) shows the absence of periprosthetic fluid. Silicone-specific images (**b**, **c**) show silicone outside the implant envelope within a short radial fold (keyhole sign) and discontinuity of the envelope (arrows). Ultrasound was only capable to demonstrate the latter finding (**d**)

them, which can be retained by trauma, genetic predisposition, immunological alterations, or bacterial infections (specific bacterial species adherent to the prosthesis surface (biofilm) may play a role, possibly via an auto-immune response) [61–65]. It does not seem to correlate significantly with the type of implant material (silicone, hydrogel, saline), surgery (oncological or aesthetic), or position of the prosthesis (subglandular or submuscular). An important association that has been noticed worldwide is with macro textured implants [62–64].

ALCL is a T-cell lymphoma emerging within the fibrous capsule that surrounds the implant and not from the breast tissue. The median reported time interval between surgery and lymphoma diagnosis is 8 years [62]. The most common

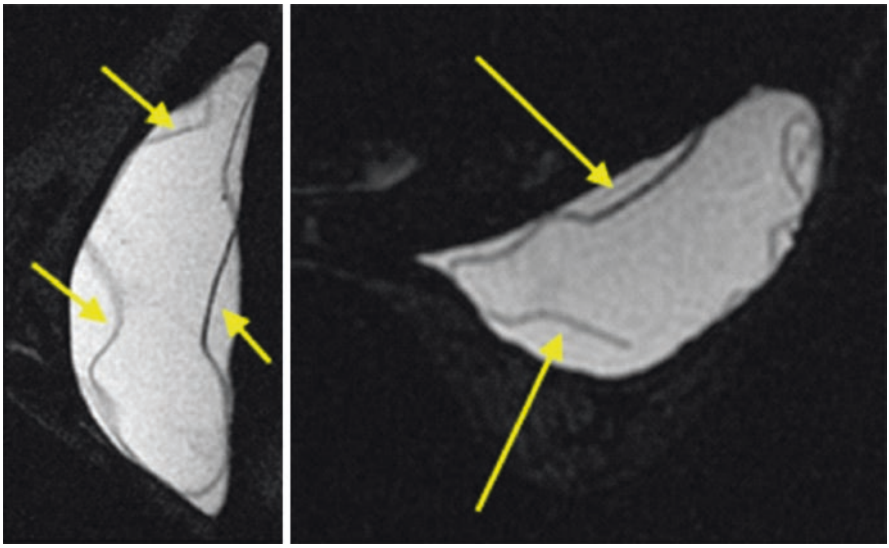

Fig. 17.55 Subcapsular line. Silicone-specific images demonstrate dark lines parallel to the implant shell that do not reach the periphery of the implant, representing incomplete shell collapse

clinical presentation is an abundant and persistent late seroma around the implant (more than 70%), which presents more than 1 year after implantation [61]. Other clinical presentations include a solid mass (20%), distant metastases, asymmetry and breast pain (21%), aggressive capsular contracture (7%), axillary lymphadenopathy, skin lesions (7%), fever (7%), and B-type symptoms (5%) [65]. Two-thirds of the cases are restricted to the fibrous capsule, and in the remaining cases, it presents as an infiltrative form associated with nodal and systemic extension. These forms could represent different stages of the same disease with a very different prognosis: a favorable outcome in cases of disease limited to the fibrous capsule (>90% remission following capsulectomy) and a more aggressive outcome in advanced stages [64]. Limited observations suggest that BIA-ALCL is a clinically indolent disease, but fatal outcomes have revealed the importance of early diagnosis and treatment, which can be delayed by lack of knowledge and the absence of unequivocal signs of disease, which often do not allow the identification of early pathognomonic radiological signs [65].

Radiological signs are often dubious, highlighting either the periprosthetic effusion or breast masses with varying sensitivity and specificity (Table 17.2) [60]. Periprosthetic effusion presents as a “double contour” in a mammogram, indistinguishable between seroma, or a mass (Fig. 17.59). Other mammographic findings are capsular thickening (Fig. 17.60), irregular contours of implants, and masses emerging from the fibrous capsule to the breast parenchyma (Fig. 17.61). In some cases, even when the patient has an abnormality in other tests, mammogram can be normal. Ultrasound can detect effusion and masses that can be complex solid cystic or even circumscribed and hypoechoic, not necessarily hyper vascularized.

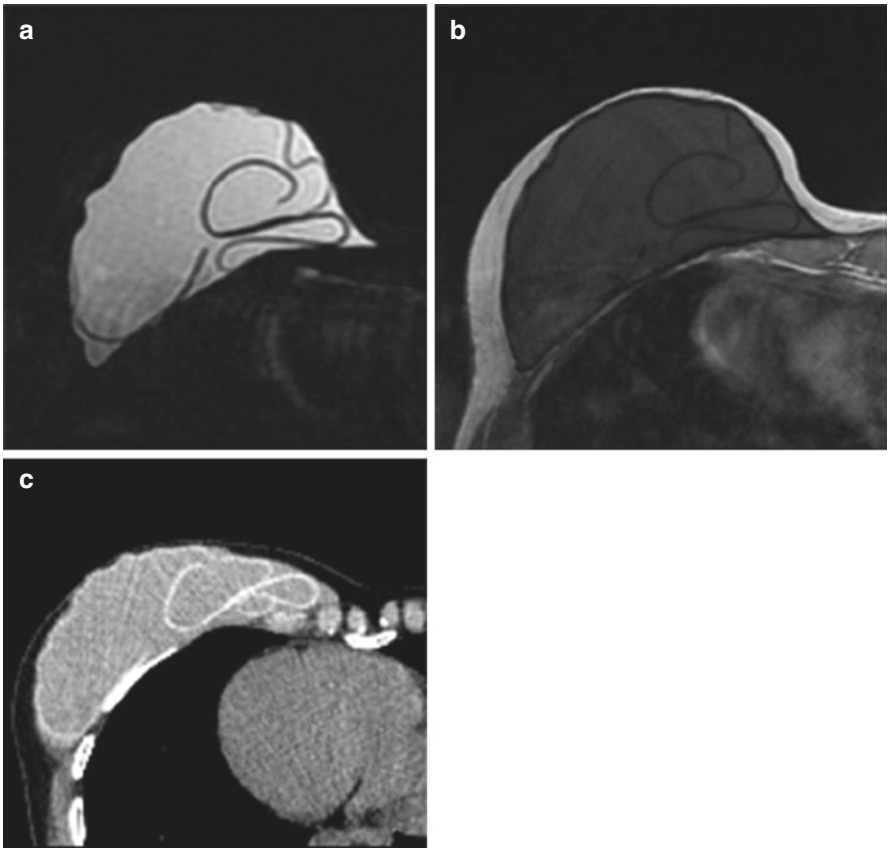

Fig. 17.56 Linguine sign. The collapsed shell is represented as curvy noodle-shaped dark lines inside the implant that do not extend to the periphery, better seen on axial T1-weighted MR image without fat suppression (**a**) and axial short T1 inversion-recovery silicone-excited image (**b**). Computed tomography (CT) also displays the collapsed envelope (**c**)

Computed tomography (CT) can show masses, lymphadenopathy, capsular thickening, and irregularity of implant contours, mainly in the contrast phases. MRI show the same abnormalities in addition to capsule enhancement and can be used in cases of ambiguous US exams, accurately evaluating other implant complications, such as ruptures as a cause of periprosthetic collection. Peri-implant seroma typically appears as a hyperintense fluid collection around the implant on T2-weighted sequences that can assess and quantify the amount of effusion more accurately than US, probably due to the different positioning of the breast. PET-CT shows diffuse or focal uptake surrounding the implants as well as in the lymph nodes (axillary, supra-, or infraclavicular and internal mammary chains). Hybrid PET/MRI is new promising imaging technique, especially for oncological workup, and BIA-ALCL cases could benefit for the high contrast resolution of MRI and for quantitative data derived from PET.

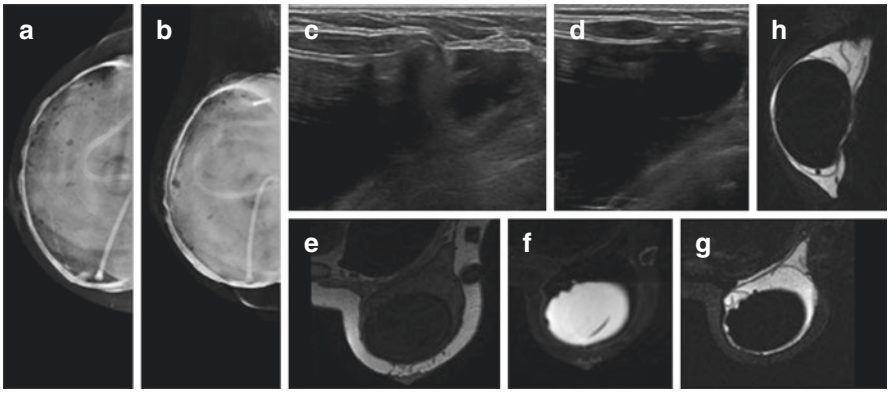

Fig. 17.57 Intracapsular rupture of a double lumen implant. Mammogram shows hypodense images inside the implant (**a**, **b**). Ultrasound depicts a heterogeneous outer lumen and the snow-storm sign which make impossible to evaluate the inner envelope completely (**c**, **d**). Axial T1-weighted image without fat suppression (**e**), axial fat- suppressed T2-weighted (**f**), and axial and sagittal short T1 inversion-recovery silicone-excited MR images (**g**, **h**) show the intact inner saline lumen and a collapsed outer silicone lumen but with no signs of extracapsular rupture

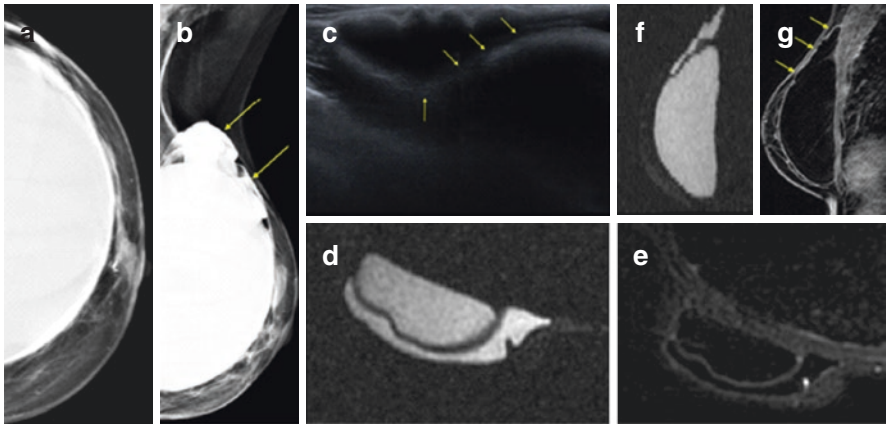

Fig. 17.58 False-positive rupture. Mammogram show the implant with irregular contour in its upper aspect (**a**, **b**), being very difficult to exclude a diagnosis of rupture. Ultrasound (**c**) depicts undulated contours of the implant with a regular thin echogenic line inside the implant that reaches the periphery of the envelope, but with an angulation and a convexity posterior in its trajectory (arrows). Axial short T1 inversion-recovery silicone-excited image (**d**) and axial fat-suppressed T2-weighted MR image (**e**) show silicone covering the implant that presents regular contours, with no signs of rupture. Sagittal short T1 inversion-recovery silicone-excited reconstructed image (**f**) and sagittal contrast-enhanced fat-suppressed T1-weighted MR image (**g**) delimits better the normal aspect of the implant and depicts another image similar to it, inside the fibrous capsule (arrow). This patient corrected an aesthetic defect with another silicone implant, placed over the first one. Knowledge about patient's medical history is the key to avoid misdiagnosis

Table 17.2 Sensitivity and specificity for effusion and a detection rate for masses for each imaging test

Imaging test	Sensitivity for effusion	Specificity for effusion	detection rate for masses
Mammography	73%	50%	***
Ultrasound	84%	75%	46%
MRI	82%	33%	50%
Computed tomography	55%	83%	50%
Positron emission tomography (PET-CT)	38%	83%	64%

***Mammogram is unable to distinguish between effusion and masses

It is important to remember that nonspecific seromas around implants are usual postoperative findings and that late effusions beyond 1 year after surgery are much less common, so cytology should be considered. BIA-ALCL peri-implant effusion does not correspond actually to a seroma, since it is composed of dense liquid from necrotic tumoral cells. US-guided FNA is performed to sample the peri-prosthetic collection, and the maximum amount of fluid possible should be collected (minimum 50 ml) to provide sufficient material for cytological examination. The correct position of the patient allows locating the fluid collection in its most dependent position, and applying light pressure to expand the target window for aspiration can help in cases with small effusions. BIA-ALCL is characterized by "hallmark cells," large lymphoid cells with abundant cytoplasm, and horseshoe-shaped nuclei. Immunophenotypically, all tumors' cells are positive for CD30 and negative for ALK, with variable expression of one or more T-cell markers, such as CD3 and CD4 [61, 62]. Still, available data are limited for screening implant-associated ALCL. Awareness of the spectrum of imaging findings may improve early detection and proper management of ALCL in the future.

Gossypibomas

Gossypibomas are retained surgical material that remains inside the body after surgery, extremely rare in superficial sites (there are few locations of difficult access that can impair the visibility of a gauze or sponge). Radiologic presentation is broad and reflects the type of response presented. Acute responses may be exudative, leading to infection, abscess, and even fistula formation. Chronic responses may present as aseptic fibrinous, with adhesion/encapsulation, clinically silent or appear within years after surgery [66].

Mammography pathognomonic finding is the characterization of a radio-opaque marker (Fig. 17.62). Sponges without radio-opaque markers or markers that are fragmented or disintegrated may present as a mass with mottled radiolucency, due to air trapping. Ultrasound may show sponges as a highly echogenic anterior band

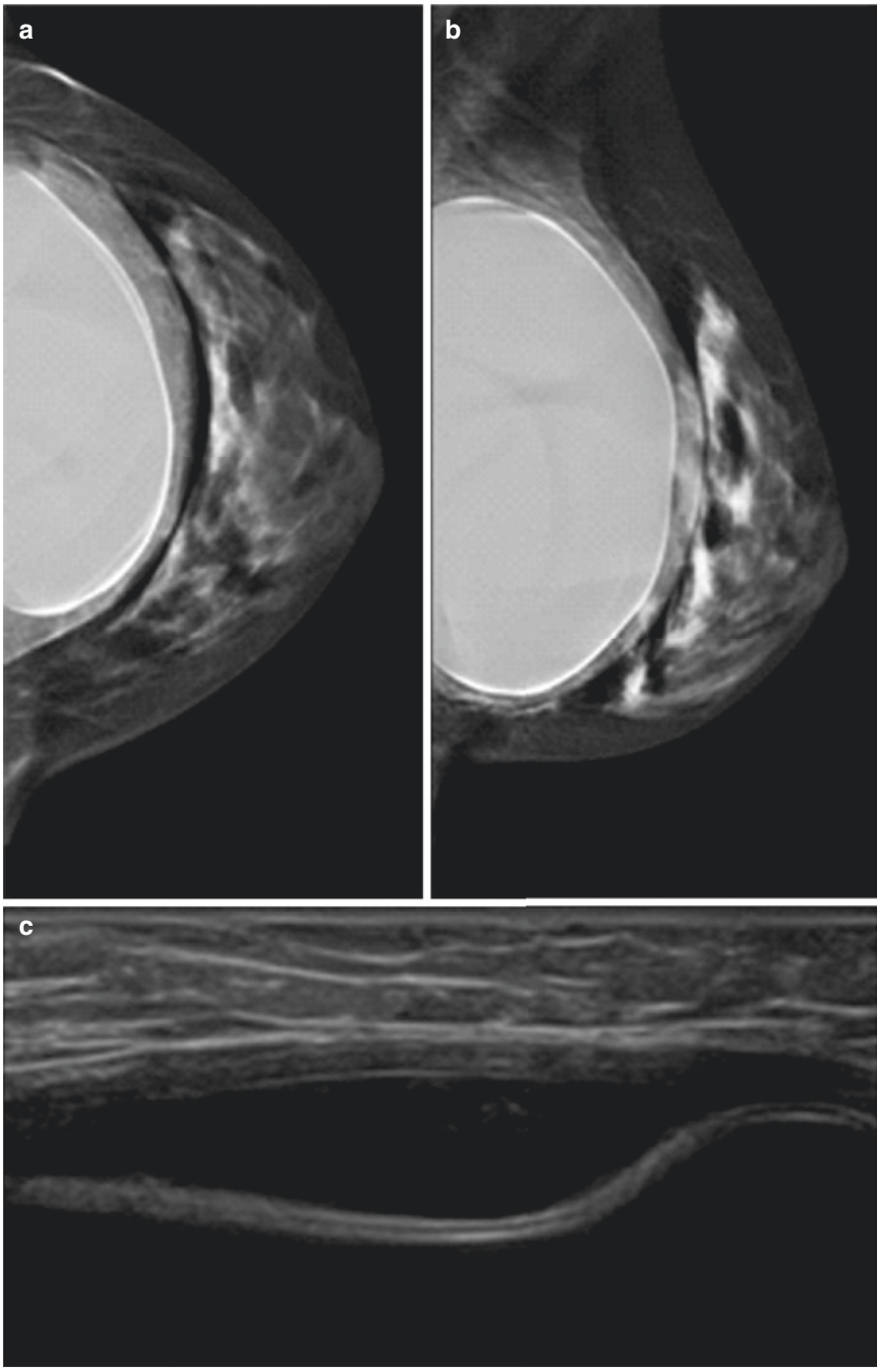

Fig. 17.59 Seroma. Mammography (**a**, **b**) shows a "double contour" around the implant consistent with periprosthetic effusion on ultrasound (**c**)

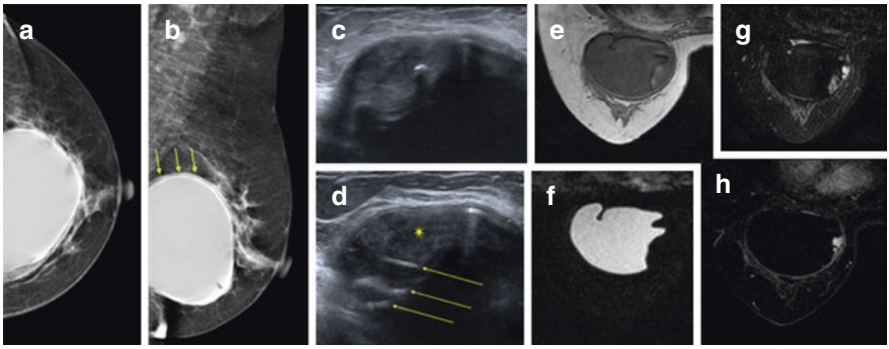

Fig. 17.60 False-positive exam. Mammogram (**a**, **b**) shows a discrete double-contour and capsular thickening (arrow). Ultrasound (**c**, **d**) depicts a false-positive stepladder sign caused by radial folds and a heterogeneous intracapsular mass (star) above them making really hard to characterize the envelope margin. Axial T1-weighted MR image without fat suppression (**e**) and axial short T1 inversion-recovery silicone-excited image (**f**) show the intact envelope being deformed by a intracapsular mass. Axial fat- suppressed T2-weighted MR image (**g**) demonstrates a heterogeneous mass with enhancement on contrast-enhanced fat-suppressed T1-weighted MR subtraction image (**h**). Explantation was performed and the diagnosis was an organized bruise

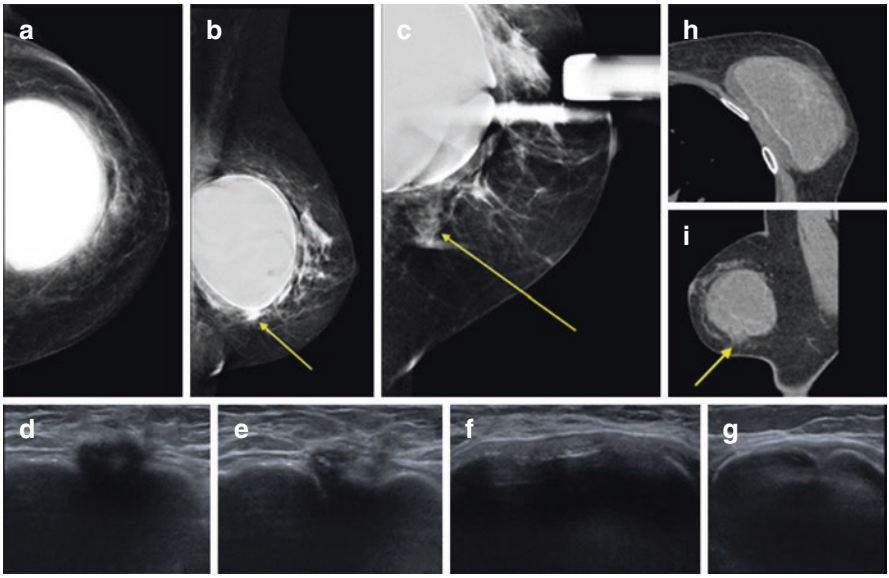

Fig. 17.61 Breast implant-associated anaplastic large cell lymphoma. Mammogram shows a double contour implant and an irregular density on the lower part of the implant, next to the fibrous capsule (**a**–**c**). Ultrasound depicts an echogenic periprosthetic effusion (**f**, **g**) and an irregular ill-defined mass next to the fibrous capsule (**d**, **e**). CT demonstrates irregular margins of the implant and the periprosthetic effusion (**h**). CT sagittal reconstruction (**i**) shows a discrete irregular density on the lower part of the implant, next to the fibrous capsule. This patient was submitted to a surgical explantation and the histological result was BIA-ALCL

with posterior acoustic shadowing that may be associated with fluid collections. On MRI, a mass with low-signal intensity stripes seen on T2-weighted images is highly suggestive. In addition, breast augmentation with implants presents diagnostic difficulties in the evaluation of structures posterior to the implant, both on ultrasound and on mammography, and MRI is more sensitive in these cases. Strong enhancement on contrast-enhanced sequences is rare and may mimic neoplasm, prompting biopsy (Fig. 17.63) [66, 67].

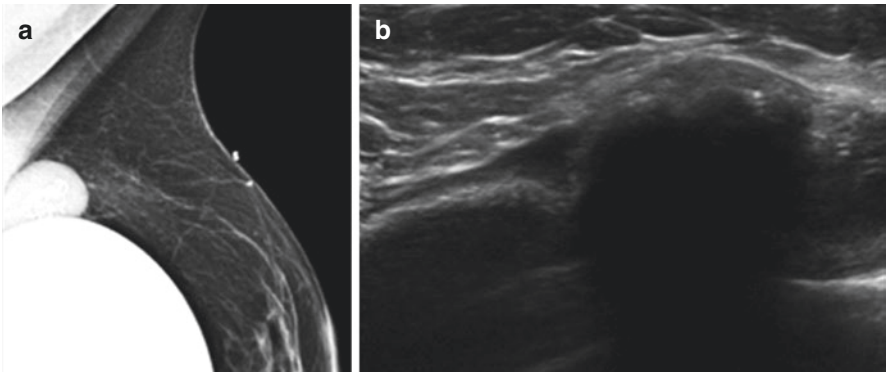

Fig. 17.62 Gossypiboma. Mammography (**a**) shows a circumscribed mass, with typical radiopaque marker inside, adjacent to the upper contour of the implant. Ultrasound (**b**) depicted an intracapsular complex mass with posterior acoustic shadowing. These findings were consistent with surgical gauze

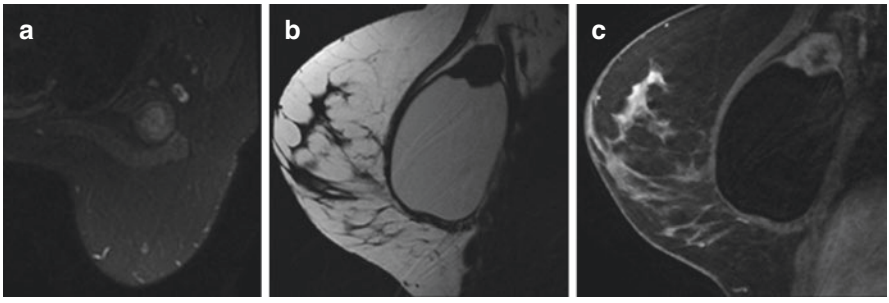

Fig. 17.63 Gossypiboma. MRI shows a circumscribed intracapsular mass, with heterogeneous signal intensity on axial fat-suppressed T2-weighted image (**a**) and homogeneous signal intensity on T1 (**b**). Sagittal contrast-enhanced fat-suppressed T1-weighted MR image (**c**) revealed internal heterogeneous and persistent enhancement, with a small non-enhancing central zone. Surgical removal of the retained gauze was performed

17.3 Other Aesthetic Procedures

17.3.1 Direct Synthetic Substance Injection (Fillers)

Noninvasive cosmetic surgery is a growing market with a crescent demand, sometimes performed by untrained and unlicensed personnel. Many countries do not have laws that regulate the performance of cosmetic procedures by properly trained physicians, and most of the materials used are not approved for medical use.

Injections of non-resorbable synthetic biomaterials for large volume breast augmentation are limited as they usually present a high cost and risk to patient safety, causing irreversible damage, requiring debridement procedures and breast reconstructions. Patients who underwent breast injections with permanent biomaterials, whether symptomatic or not, should avoid breastfeeding as there is a risk of material displacement in the breast tissue and rupture of the capsule that surrounds it, causing material leakage and inflammation.

17.3.1.1 Paraffin Injection

Paraffin is a group of hydrocarbons relatively inert. To facilitate injection, the paraffin is heated to form a semiliquid material prior to injection. The early cosmetic results were often quite acceptable, and the complications related to the injection frequently did not show up until 5 or 10 years later.

Complications are broad and range from aesthetic failure to death. They include pulmonary embolism, migration, ulceration, fistulae, infection, and necrosis, most of which often lead to mastectomy.

Radiologically, it does not form an isolated mass, usually consisting of many droplets, widely dispersed in the tissues. On mammography, early paraffin injections appear as multiple, circumscribed, noncalcified masses in the retroglandular and subpectoral regions. Late-stage paraffin injections demonstrate paraffinomas that are chronic inflammatory granulomatous reactions, involving skin and underlying soft tissues, not restricted to the injection area. Clinical presentation is characterized by the development of indurated masses, pain, ulceration, fistulae, and necrosis. Mammograms show numerous multiple dense masses with arc and ring calcifications.

17.3.1.2 Silicone Injection

Injectable silicones are extensively cross-linked polymers of dimethyl siloxane, some of them include impurities and additives in the preparation, purposely added to cause a sclerotic reaction in the breasts, intended to contain the liquid silicone and prevent migration to other sites.

Many of the complications of paraffin injections were repeated a half-century later, including migration of silicone to other parts of the body, inflammation, discoloration, formation of granulomas masses (siliconomas), ulceration, fistulae, fibrosis, chronic sinus tracts, lymphadenopathy, infection, and necrosis. Systemic complications include hypersensitivity pneumonitis, silicone embolism syndrome, pulmonary edema, and sepsis.

Clinical manifestations of liquid silicone injected into the breasts vary considerably, reflecting different susceptibility to the deleterious effects of silicone. Some patients do not develop significant symptoms. There are two main types of clinical presentations. The first type of patient usually presents with multiple and/or painful lumps in their breasts. These may occur within 2–3 years until 15 years after injection. In attempt to decrease the inflammatory reaction, some patients also received multiple injections of cortisone, which can complicate the clinical picture. The second type of patient presents impending breakdown with skin inflammation. The breasts may show increased capillary filling time and various stages of skin circulatory difficulties, from fine telangiectasia to necrosis, as silicone invades the dermis and epidermis of the overlying skin. Migration of the silicone is common.

Mammography shows silicone globules as multiple radiopaque masses with or without rim calcifications (former eggshell-type) that obscure the underlying breast tissue, reducing the accuracy of screening mammograms (Figs. 17.64 and 17.65) [23]. It also demonstrates two patterns: multiple high-density round and circumscribed masses ranging from 0.2 up to 2.0 cm in diameter, often with peripheral calcifications, or large areas of opacity if larger volumes have been injected into areas of the breast. Spiculated or ill-defined margins may be present on siliconomas and lead to biopsy even with the history of silicone injection. Extremely dense axillary lymph nodes may be present. Ultrasound of silicone granulomas shows the snowstorm sign (echogenic noise), which obscures all findings below it, also associated with hypoechoic or anechoic masses representing large silicone globules. At CT, scattered nodular soft-tissue foci is seen, calcified or noncalcified, and discrete or confluent (Fig. 17.66). At MRI, these nodular foci tend to demonstrate

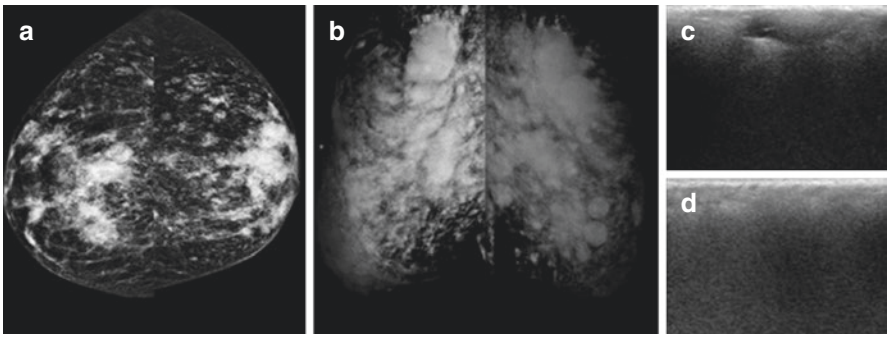

Fig. 17.64 Liquid silicone injection. Mammogram views (**a**, **b**) show diffuse multiple radiopaque masses in different patterns. Ultrasound (**c**, **d**) shows the snowstorm sign diffusively, which obscures all findings below it

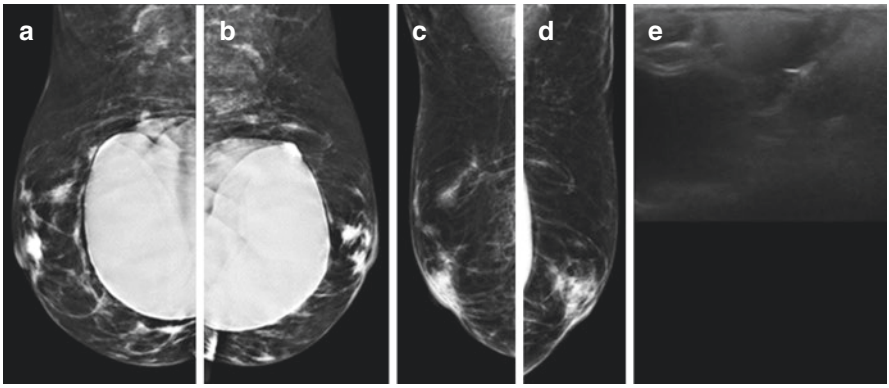

Fig. 17.65 Liquid silicone injection. Patient underwent a second surgery to remove the previously injected liquid silicone and repair breasts aesthetically with implants placement. Mammogram (**a**–**d**) shows radiopaque irregular densities with tiny punctate images that resemble calcifications, representing the residual injected silicone. Ultrasound (**e**) shows the snowstorm sign, adjacent to the implant contour, which can make it difficult to diagnose a possible rupture

intermediate signal intensity on T1-weighted images and variable intensity on T2-weighted images, because high-viscosity silicone is usually more hypointense on T2-weighted images. Chemical shift artifact and fat suppression may also be present. Silicone granulomas may enhance suspiciously, mimicking cancer.

Because granulomas may become clinically quite hard and reduce the characterization of the underlying breast tissue, the assessment for breast cancer with physical examination, mammography, and ultrasound can be quite challenging. MRI may be needed for further assessment.

17.3.1.3 Acrylate Injection

Some nonabsorbable materials contain a family of polymers made from acrylate monomers, including acrylamide (in the form of polyacrylamide hydrogel PAAG) or methacrylate (in the form of polymethyl-methacrylate PMMA, ethyl-methacrylate EMA or hydroxyethyl-methacrylate HEMA). Their use has been banned due to its myriad complications.

The semisolid consistence of acrylates is a challenge to the complete removal of the injected material because of its extensive displacement (involving the back, lower abdomen, upper arm, and sternum), extensive infiltration, dispersive induration, and confusing injection level. Residual material can be left behind after cannula aspiration; therefore, an open procedure with surgical debridement is recommended, but several complications create unsuitable conditions for immediate implant reconstruction [68].

PMMA is a polymer with irregular surface particles that cannot be phagocytized, leading to formation of granulomas. Its low cost resulted in indiscriminate use with

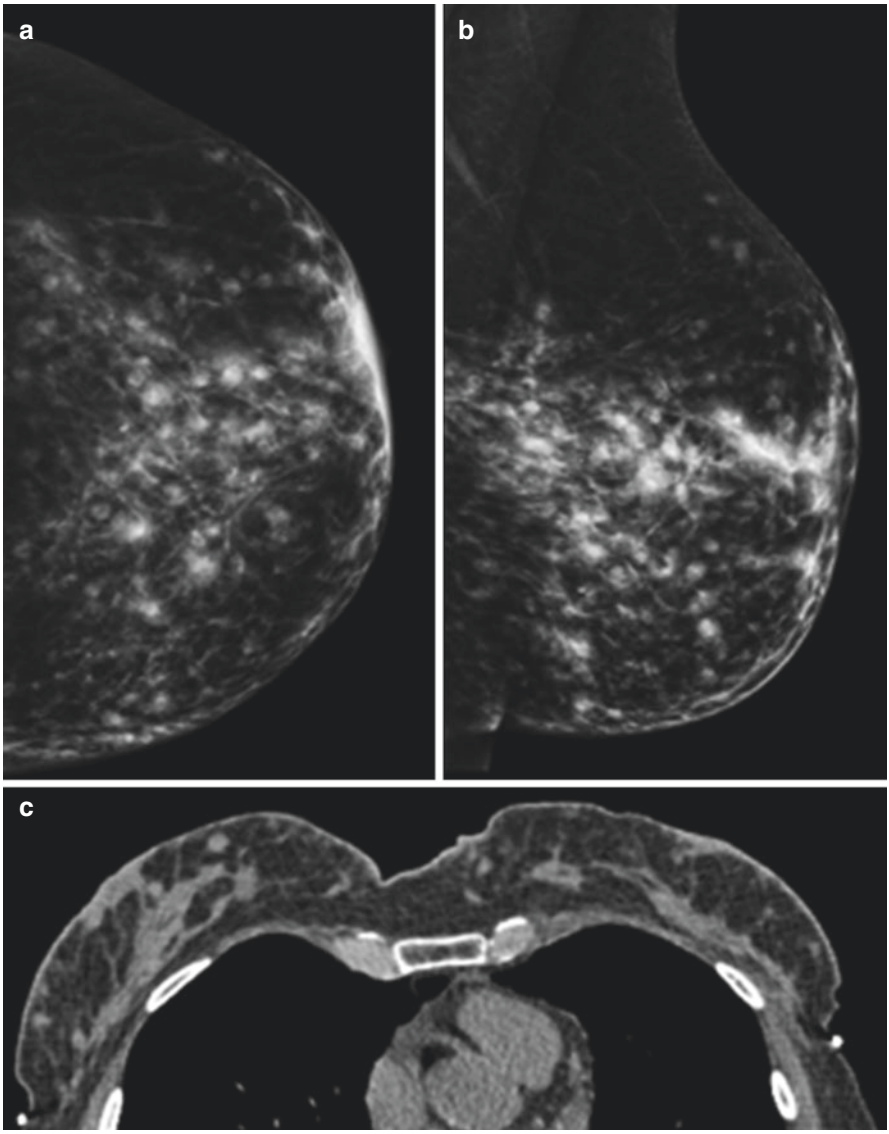

Fig. 17.66 Liquid silicone injection. Mammogram (**a**, **b**) shows diffuse multiple radiopaque masses in different patterns. On CT (**c**), scattered noncalcified nodular soft-tissue foci is seen

unpredictable cosmetic results due to serious immunologic and inflammatory reactions that may lead to deformities. CT findings include fluid attenuation masses, with surrounding subcutaneous infiltration. On MRI, PMMA is T1 hypointense and T2 hyperintense and shows mild peripheral enhancement up to 2 months after procedure (Fig. 17.67) [69].

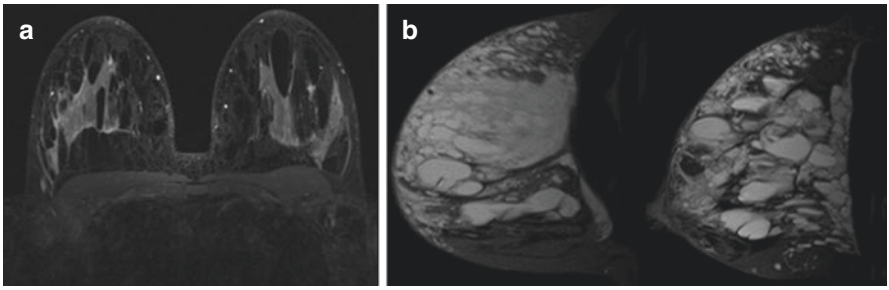

Fig. 17.67 PMMA injection. MRI shows multiple confluents, oval, circumscribed masses, hypointense on axial fat-suppressed T1-weighted MR image (**a**) and hyperintense on axial fat- suppressed T2-weighted MR image (**b**)

PAAG is a polymer synthesized from 2.5% acrylamide and 97.5% water highly exchangeable with the water molecules of tissue fluids. Thereby a 10% reduction in volume occurs during the first days, as a consequence of osmotic exchange. Once considered a nonbiodegradable hydrogel that was nontoxic, non-sensitizing, and non-teratogenic, with long-term clinical application, many complications began to be reported, such as pain, induration, displacement, deformation, milk deposition/galactocele formation, and psychological fear. Some studies suggested that PAAG may decompose acrylamide monomers under multiple factors, with carcinogenic and toxic effects on the nervous and reproductive systems. Injection of approximately 150–200 mL of polyacrylamide gel is made into the retroglandular space of each breast at the inframammary fold or at the upper region of the breast. At MRI, PAAG presents hypointense to isointense signal on T1-weighted images; hyperintense with hypointense peripheral rim on T2-weighted images; and T2-weighted fat-saturated images are useful because of high water content (Fig. 17.68) [68, 70].

Mammography may show multiple randomly distributed bizarre densities of varying shapes and sizes, indistinguishable from the adjacent breast tissues or with a well-defined oval density (generally on single injection). On sonography, PAAG injection may be seen as a single collection of globular fluid in a retroglandular pre pectoral location with variable internal echogenicity similar to the asymptomatic patients. Other manifestation of acrylate injection is the same of mammogram, multiple bizarre, and randomly distributed masses. The infected breast may show marked increase in the size of collection as well as a diffuse increase in its internal echogenicity to midlevel echoes. The position of the acrylate collections is well depicted on MRI. Superimposed inflammatory changes increase the intermediate heterogeneous T1 signal and decrease heterogeneous T2 signal, along with irregular and thickened rim enhancement. A thin regular rim of delayed enhancement can also be seen around PAAG collection in asymptomatic patient, similar to the rim enhancement of breast cysts [68, 70].

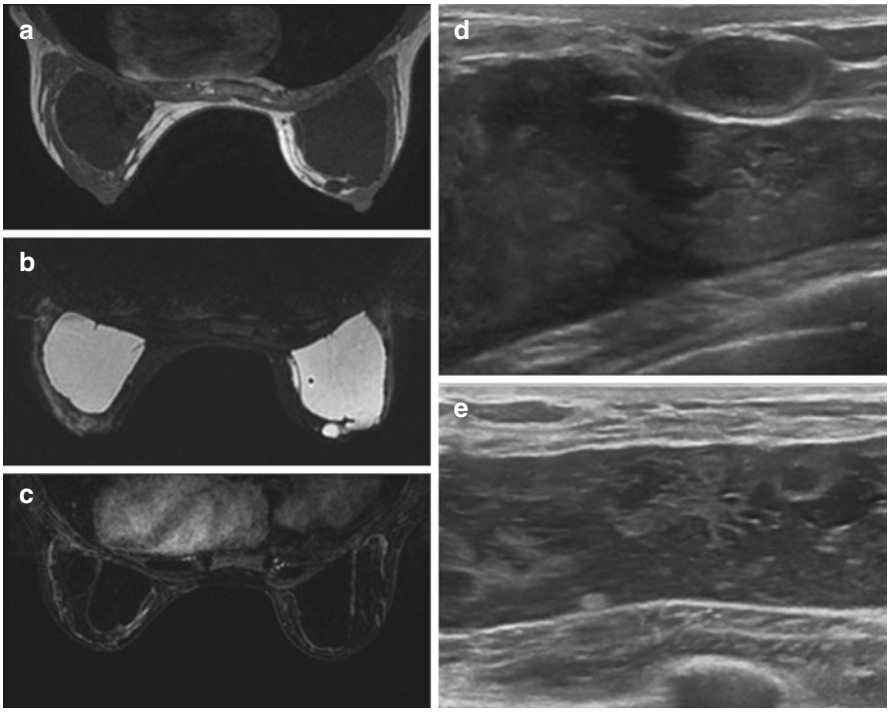

Fig. 17.68 PAAG injection. MRI presents large lobulated masses, with hypointense signal on axial T1-weighted image without fat suppression (**a**), hyperintense with hypointense peripheral rim on fat-suppressed T2-weighted image (**b**) and a thin peripheral enhancement on contrast-enhanced fat-suppressed T1-weighted subtraction image (**c**). Ultrasound (**d**, **e**) shows circumscribed and heterogeneous masses

17.3.1.4 Hyaluronic Acid

Hyaluronic acid (HA) is an absorbable filler, and its aesthetic effects are considered transitory for its natural and progressive degradability. Despite this significant reabsorption, there are some reports of absence of radiological signs of reabsorption even 24 months after the procedure. Some adverse effects related to the product are development of masses and breast pain. Infection and abscesses formation are also described. In spite the potential for additional applications in the future, it increases the total cost and the risk for development of granulomas.

HA injection determines an increase in breast parenchyma radiodensity on mammography, either diffuse or as multiple radiodense lesions. This finding corresponds to multiple predominantly anechoic collections with internal echoes of variable sizes and echogenicity on ultrasound (Figs. 17.69 and 17.70). On MRI, HA collections appear as well delimited areas with hyperintensity on T2-weighted and hypointensity on T1-weighted images. They may be involved by fibrotic capsules, assuming suspect appearance.

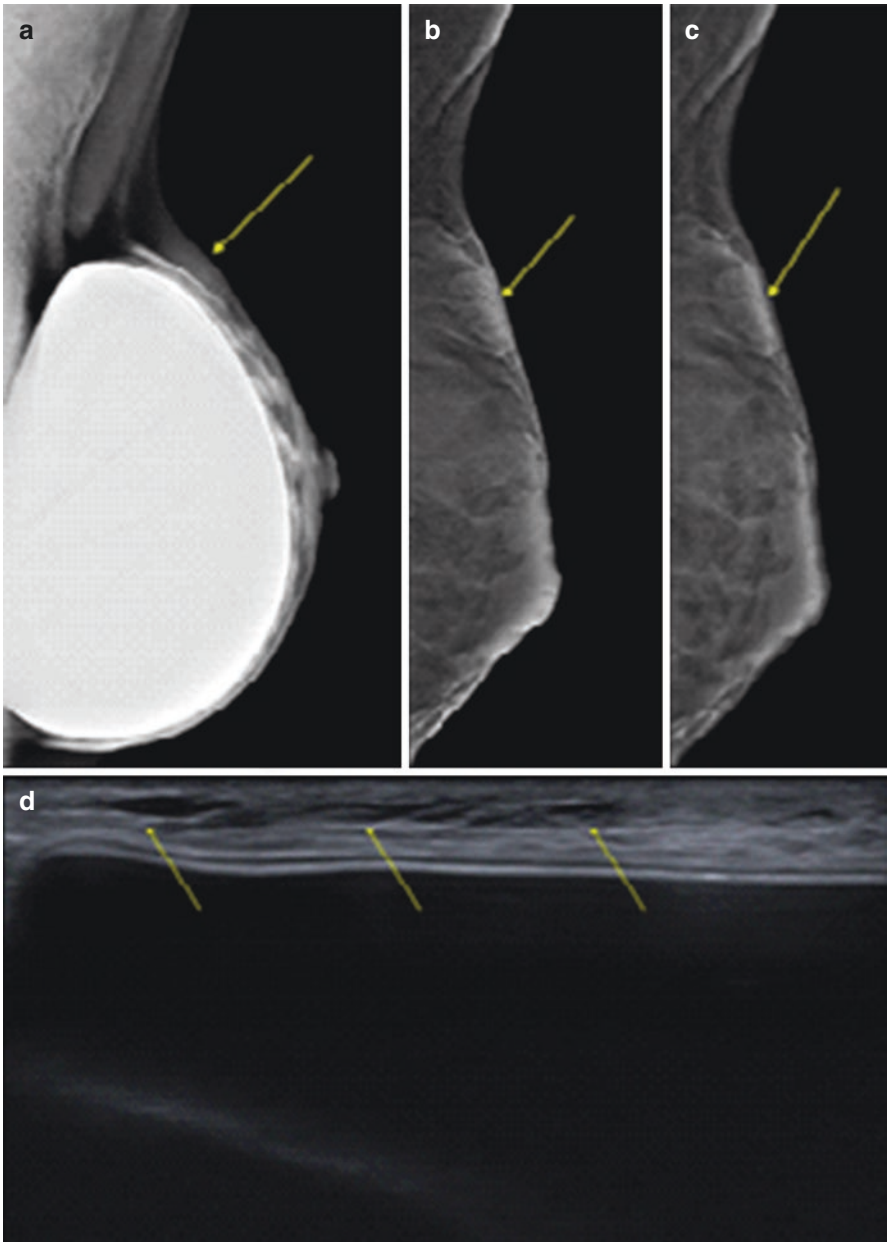

Fig. 17.69 Hyaluronic acid injection. Mammogram (**a**, **b**) and tomosynthesis (**c**) show a slightly dense asymmetry on superficial planes of the upper quadrants. Ultrasound depicts elongated cystic images on the subcutaneous fat (**d**)

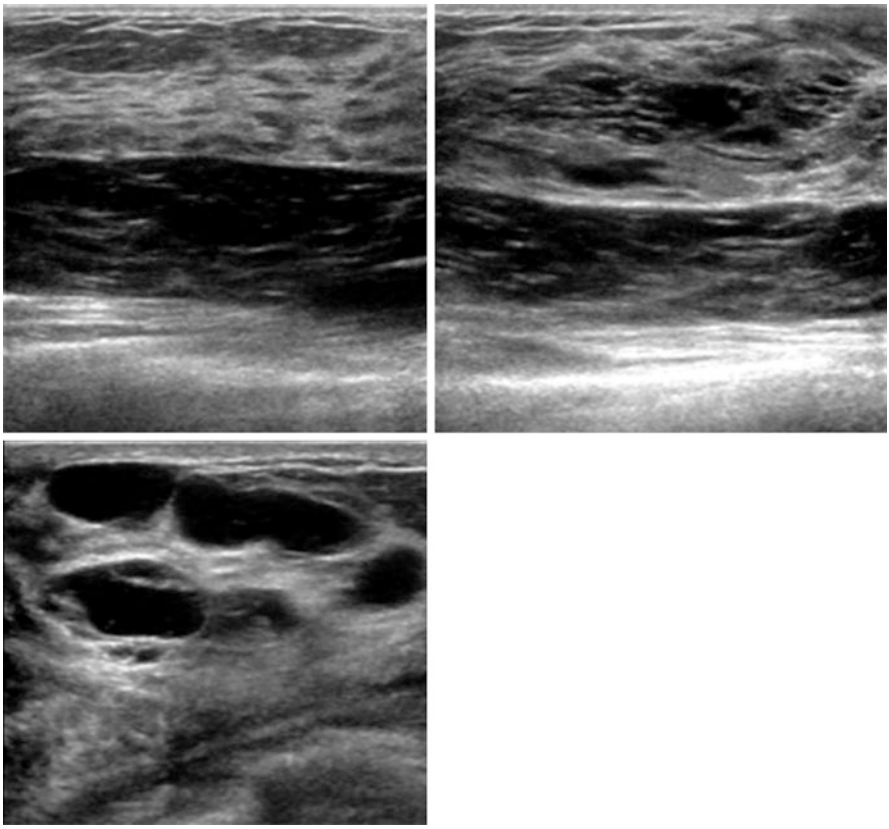

Fig. 17.70 Hyaluronic acid injection. Ultrasound shows multiple cystic images of different sizes, some of them with thin septa and internal echoes

17.3.2 Lipofilling (Fat Grafting)

Autologous fat grafting (FG) is a reconstructive and aesthetic technique increasingly used in breast surgery, consisting in harvesting fat from one site, preferably where removal is aesthetically desired and possible, and transferring the fat to other areas for augmentation in the same patient, also called autologous fat transfer, lipografting, lipotransfer, liposculpting, and lipofilling. There are various harvesting methods from the donor site, including vacuum aspiration, syringe suction, and cutting. The reason why so many techniques exist is to yield viable and functional adipocytes. Liposuction should be gentle, involving the use of syringes or a low-pressure apparatus, and avoid exposure to ambient air (closed technique) to handle the fatty material as little as possible. It should then be purified using low-speed centrifugation. FG is performed using small cannulas in small quantities to ensure that the grafted tissue is in full contact with the vascularized tissue of the receptor region to ensure appropriate nutrition in the first days after surgery. Graft survival

percentage depends on the methods used to aspirate, prepare, and transplant the fat and the destination of the graft (in well-vascularized muscles, the survival rate is higher than in a relatively oxygen-poor environment such as scar tissue from previous breast surgery) [71]. Most studies estimate that 30–40% of the volume is lost after the first procedure, which might require subsequent procedures or graft overcorrection [72]. There is no significant difference in the volume or viability of the fat grafted from different donor sources. FG is considered a safe procedure with a low number of major complications [73].

Fat grafting is a more targeted augmentation technique than implants, but the two methods combined are increasingly common. It does not cause hypersensitivity or foreign-body reactions. The complications related to FG are seroma, under correction, infection, asymmetry, fat necrosis, and fat embolism [72]. The main diagnostic difficulties are related to fat necrosis [3, 73]. Patients may be symptomatic, and the mammographic and US images may be misleading. In such cases, MRI may be helpful to differentiate between cancer recurrence and liponecrosis, due to fat-suppressed and post-contrast sequences that demonstrate an unenhanced fat-containing mass on T1-weighted images [3, 74]. Fat necrosis rate is directly proportional to the amount of fat injected into the same breast, particularly if performed in a single procedure. It can be prevented by injecting small quantities of fat in different directions and layers [73].

A wide spectrum of mammographic changes after fat grafting have been reported in the literature, ranging from benign looking lipid cysts (Fig. 17.71) and architectural distortion of normal breast tissue, to findings suspicious for malignancy such as clustered microcalcifications, spiculated areas of increased opacity, and focal masses [3, 75]. Pectoral muscle may appear heterogeneous in density and also present low-density strips. On CT or MR images, linear subcutaneous fat stranding can be seen in the harvesting area. At the site of fat transfer, nonspecific subcutaneous fat stranding may be seen on CT images, because the injected fat can be difficult to discern from the native subcutaneous fat layer. If intramuscular injections are performed, lobular foci of fat can be identified. Literature reports no statistically

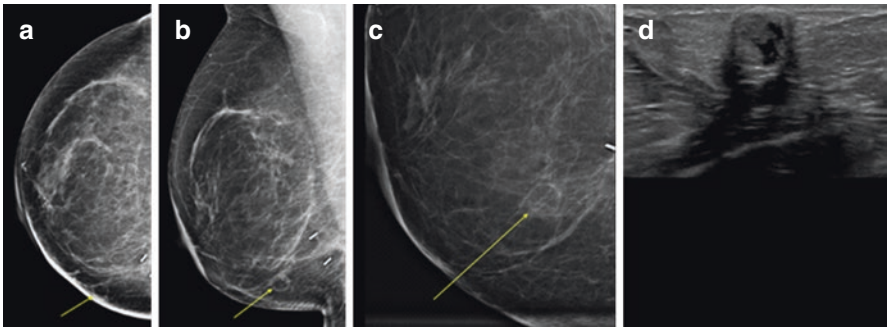

Fig. 17.71 Lipofilling. Mammogram shows a lipid cyst in the palpable area after a fat grafting procedure to reshape the skin depression from previous oncologic surgery (**a**–**c**). On ultrasound, this area was a subcutaneous complex mass with little shadowing (**d**)

significant difference between breast density findings before and after fat injection and no interference in cancer detection after breast fat grafting [3, 72, 73, 75, 76].

17.3.3 Biological and Synthetic Mesh

Matrices have been inserted successfully and safely in breast reconstruction and in cosmetic procedures, with biological or synthetic matrices. Mesh support is used to restore the lost strength, improving the longevity of ptosis correction in mastopexies. The main objective is to achieve the right balance between persistence, inflammation, biocompatibility, and incorporation without interfering with mammography or presenting a long-term infection risk. Another advantage is the direct-to-implant breast reconstruction technique that does not require tissue expansion before implant insertion, avoids donor site morbidity and lengthy recovery time associated with autologous flap reconstruction, and substantially reduces operating time, compared to autologous flap and expander-based breast reconstruction. The high cost of meshes is a factor to be added when choosing a reconstructive technique, but considering its good cosmetic outcomes and lower rate of surgical revisions, it can be a low-cost alternative. The proper selection of patients, considering possible comorbidities and risk factors, helps to choose the best reconstructive options for each one. A low rate of inflammation may not generate the fibrous tissue reaction necessary to prevent recurrent breast ptosis, while higher rates may lead to matrix non-incorporation and loss.

A biological mesh (acellular dermal matrix – ADM) is a scaffold of dermis produced from cadaveric human, porcine (Figs. 17.72 and 17.73), bovine, or bovine pericardium tissue that is stripped of its antigenic cells. It allows rapid host revascularization and cell repopulation, which may favor a better outcome, with statistically reduced bottoming-out, rippling, capsular contracture of the implant, and

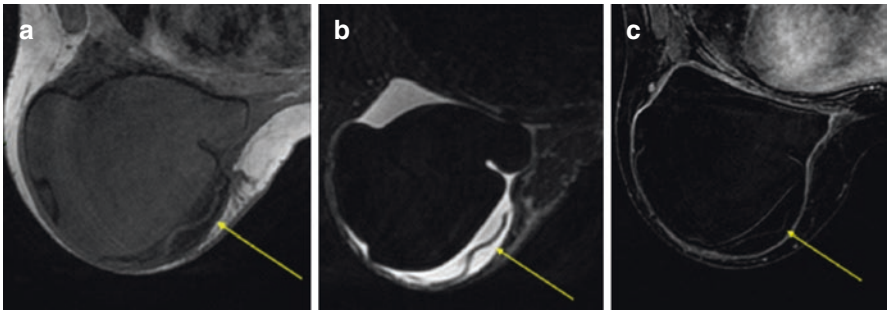

Fig. 17.72 Porcine biological mesh. Axial T1-weighted without fat suppression (**a**), fat- suppressed T2-weighted (**b**) and contrast-enhanced fat-suppressed T1-weighted MR subtraction images (**c**) demonstrate a thin intracapsular linear image with hypointense signal in all sequences, without significant enhancement, which does not cover the entire implant surface, easier to see because the patient developed a seroma

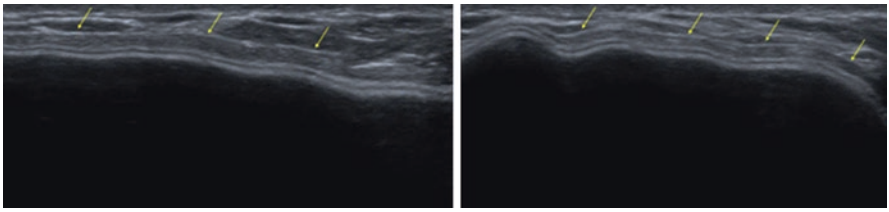

Fig. 17.73 Porcine biological mesh. Ultrasound shows a hypoechoic periprosthetic layer representing the biological membrane (arrows). Usually few months after surgery, it is not still identifiable. This is probably due to the high biocompatibility of the biological membrane, causing a mild fibroblastic reaction with focal tissue integration of the matrix and, thus, appearing less visible during follow-up

mechanical shift when compared to the absence of matrix reconstruction. ADM might be attached to the inferior-lateral pole of the pectoralis major muscle, expanding the space available for the insertion of an implant, filling the void left between the muscle and fascia, thereby creating a natural inframammary fold, providing additional cover and support inferiorly, with faster tissue expansion, larger implant volumes, and improvement of lower pole projection. Complications include infection, seroma, hematoma, skin flap necrosis, capsular contracture, implant extrusion/exposure with explantation/implant loss, besides that ADM may present adverse effects associated with radiotherapy [77]. Other disadvantages include increased incidence of seroma; lack of sterility (they are aseptic rather than sterile); and exposure to antibiotics, which may result in allergic reaction, increased incidence of infection, and high cost [78].

Synthetic matrices are made of absorbable (Vicryl), long-term absorbable, or nonabsorbable (titanium-coated polypropylene mesh) plastic-like material. Mesh induces only a thin layer of collagenous tissue, which enhances the overall strength, acting as a composite material, so strong that rupture or failure is extremely unlikely, with high flexibility and not palpable under the skin. Synthetic meshes can be inserted between subcutaneous fat and the glandular tissue and be fixed on thoracic wall, sometimes with metallic clips. It remains unclear whether the complication rates between synthetic and biological matrices differ. The surgical outcomes from both types are similar, and synthetic meshes are cheaper than ADM [78]. Combination of absorbable and nonabsorbable synthetic meshes have been found to work, despite inflammation and non-incorporation. Infection of a nonabsorbable mesh remains a persistent risk factor. Single-stage direct-to-implant breast reconstruction demonstrated a low complication rate, excellent cosmetic outcome, and significant cost savings in comparison to the use of ADM. On mammography, it may be possible to see the fixation clips (Fig. 17.74) and the mesh, but radiological aspects will vary depending on the material. On subsequent exams, it can be reabsorbed or calcify partially or totally (Figs. 17.75 and 17.76). Ultrasound can depict a superficial irregular linear echogenic image, with varying posterior acoustic shadowing, representing the mesh (Fig. 17.77). Both methods have limitations in detecting breast lesions with mesh implantation. MRI can be helpful in cases of doubt.

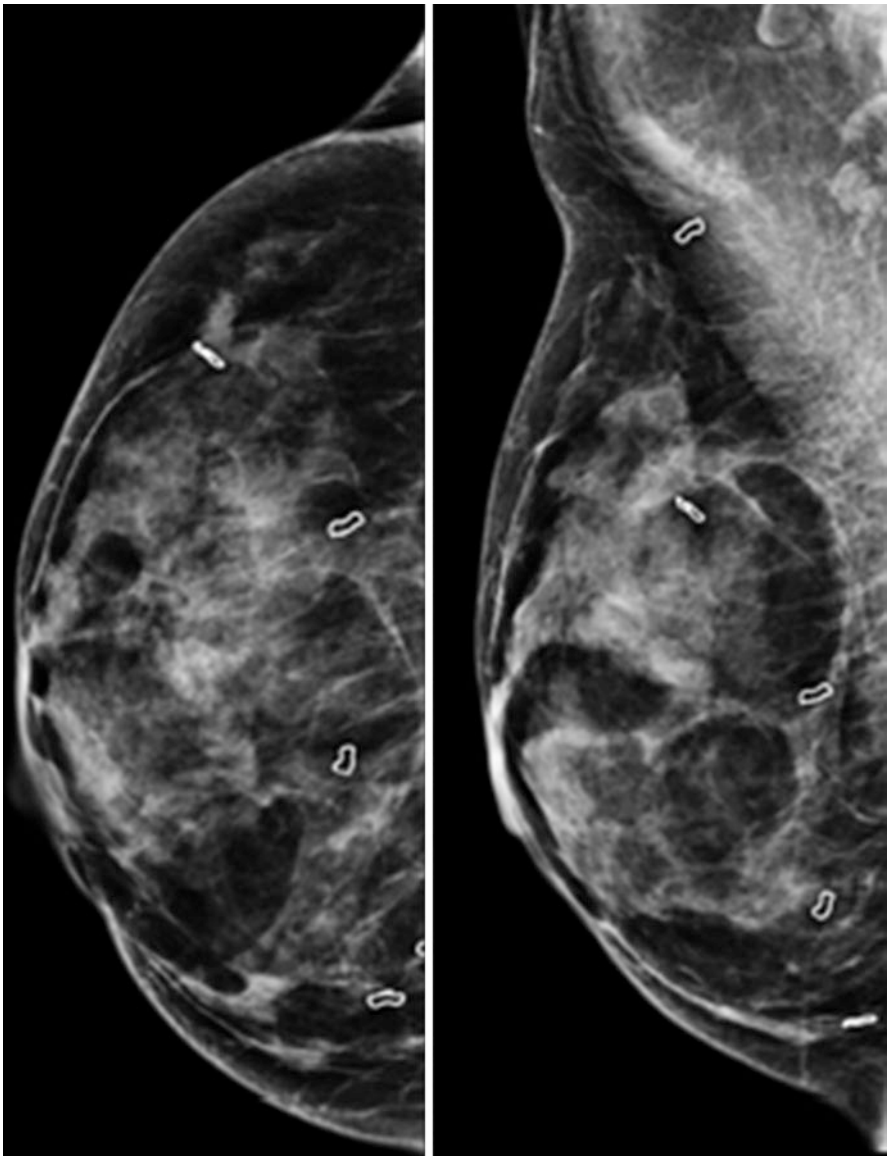

Fig. 17.74 Fixation clips of a synthetic mesh

17.4 Breast Cancer Treatment

Breast cancer treatment depends on the tumor size and stage (TNM) to establish the surgical management (lumpectomy or mastectomy) and the need for adjuvant therapy (radiotherapy and/ or systemic therapy). The goals are removing all the cancer from the breast (tumor-free margins), locoregional control, and eradicate occult

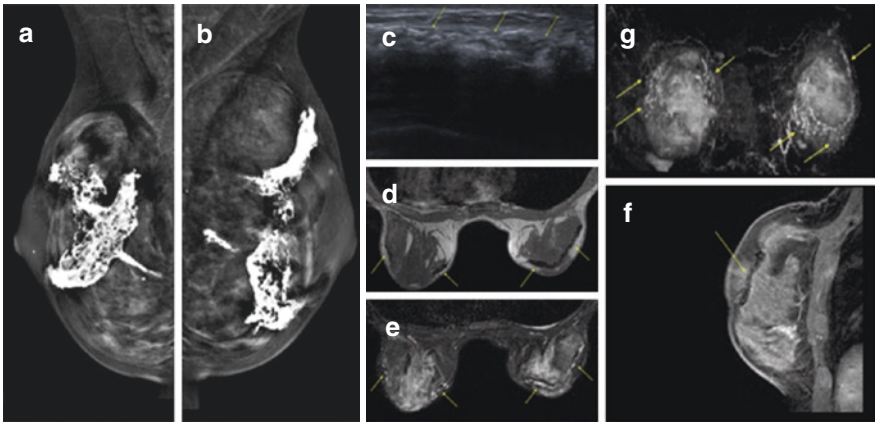

Fig. 17.75 Synthetic mesh. Mammogram shows meshes almost totally calcified with coarse and linear patterns (**a**, **b**). Ultrasound (**c**) shows an irregular linear echogenic image, with posterior acoustic shadow (arrows). Axial T1-weighted without fat suppression (**d**) axial fat-suppressed T2-weighted (**e**), sagittal contrast-enhanced fat-suppressed T1-weighted MR images (**f**), and 3D reconstruction (**g**) depict the mesh as a linear coarse image usually in the interface between the subcutaneous fat and the fibroglandular tissue, with hypointense signal on T1 sequences and hyperintense signal on T2 sequences

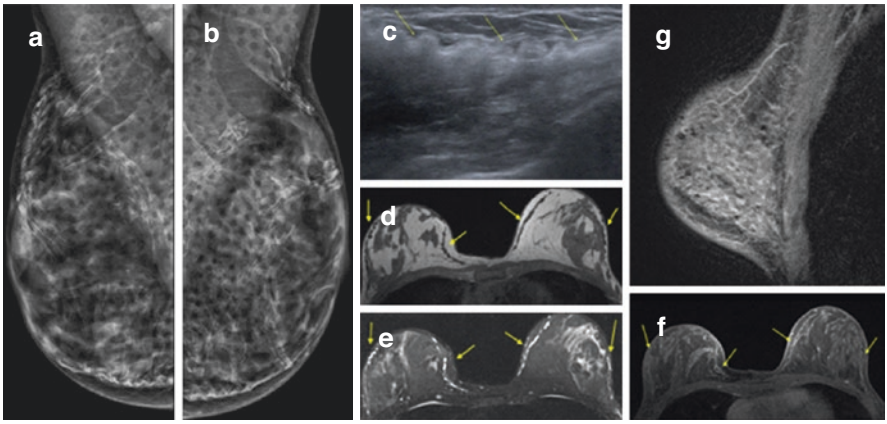

Fig. 17.76 Synthetic mesh. Mammogram (**a**, **b**), ultrasound (**c**) and MRI axial T1-weighted without fat suppression (**d**), axial fat-suppressed T2-weighted (**e**), and axial contrast-enhanced fat-suppressed T1-weighted subtraction images (**f**) show similar aspects of Fig. 17.75. Sagittal contrast-enhanced fat-suppressed T1-weighted MR images (**g**) demonstrate the same aspect shown on mammogram

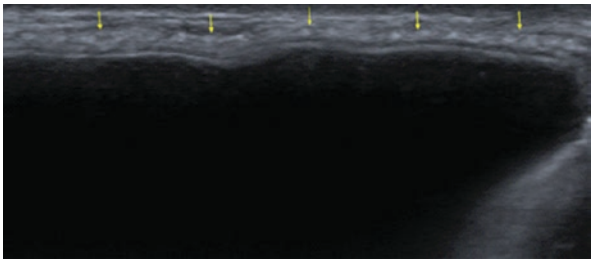

Fig. 17.77 Synthetic mesh. Ultrasound shows a superficial irregular linear echogenic image, next to the anterior contour of the implant (arrows)

metastatic disease. The treatment plan is based on the tumor TNM classification, imaging, physical findings, and the patient's wishes, involving breast radiologists, breast surgeons, medical oncologists, radiation oncologists, pathologists, and plastic surgeons [79].

Breast-conserving surgery (also known as lumpectomy, setorectomy, partial mastectomy, or quadrantectomy) is used when the entire tumor can be removed with a good cosmetic result. These patients usually undergo postsurgical whole-breast irradiation to control residual microscopic disease.

Mastectomy is chosen when the entire tumor cannot be excised with a good cosmetic result, for women with contraindications to radiation therapy (i.e., pregnancy, previous breast radiation therapy, multicentric or diffuse disease, collagen vascular disease) or if it is the patient's preference [80].

Both approaches offer equivalent local control disease and identical survival rates in women with tumors 4 cm or less in diameter and positive or negative axillary lymph nodes, as shown by Protocol B-06 conducted by National Surgical Adjuvant Breast and Bowel Project (NSABP). Currently, available data suggest that local recurrence is more related to tumor biology than to surgical technique.

The definition of tumor-free margin has varied among institutions. A recent consensus guideline from the Society of Surgical Oncology (SSO) and the American Society of Radiation Oncology (ASTRO) has recommended that a negative margin be defined as "no tumor on ink" based on a review of multiple studies [81].

17.5 Breast-Conserving Surgery (BCS)

Breast-conserving surgery (also known as lumpectomy, setorectomy, partial mastectomy, or quadrantectomy) consists of surgical removal of the primary tumor, with negative margins. It is the ideal treatment for most cases of breast cancer, and the conditions for performing it are the following: the patient's desire, possibility of oncological control, and preservation of breast aesthetics [82].

The addition of whole breast external beam radiotherapy (WB-XRT) to conservative surgery reduces the rate of local recurrence by 50%, with an impact on 15-year mortality, according to a meta-analysis by the Early Breast Cancer Trialists Collaborative Group (EBCTCG); therefore, omission of radiotherapy in BCS is not recommended.

To perform a local excision for diagnostic or therapeutic purposes, the surgeon makes an incision in the skin, usually periareolar or in the inframammary fold (more cosmetic), and removes the tumor with macroscopic margins and appropriate guidance for histological analysis. The adjacent breast tissue, the subcutaneous tissue, and the skin are then closed. The surgical cavity can be filled with fluid and granulation tissue.

Mammography is rarely obtained immediately after surgery. But if performed, the image would show a round or oval mass in the postoperative site representing a seroma or hematoma, with or without air, which should resolve over time. Thickening of the skin at the incision is usually present, and adjacent breast tissue shows thickening of trabeculae in subcutaneous fat and increased density caused by local edema or hemorrhage. On MRI the postoperative site is filled with blood or seroma, with high signal intensity on T2-weighted images without contrast or fat suppression. On ultrasound, the early postoperative findings are seroma or hematoma, breast edema, and focal skin thickening. Postoperative seroma or hematoma is normal and is gradually absorbed. However, if the fluid collection persists or there is a clinical sign of infection (fever, erythema, swelling and pain), drainage with subsequent culture of fluid can be performed under US guidance to exclude the possibility of abscess formation.

After subsequent weeks, the postoperative site resorbs the air and fluid collection, which is replaced by fibrosis and scarring, with residual focal skin thickening and breast edema.

On MRI, enhancement of the surrounding normal healing tissue is possible for up to 18 months after the surgery (regular rim enhancement). There is also architectural distortion and sometimes a scar that can simulate cancer with rapid uptake and washout kinetics and is a common cause for false-positive reading, resulting in biopsy unless the radiologist investigates the patient's history. Recurrent invasive cancers usually appear as a mass at or near the biopsy site in the first few years. It is important to know that chemotherapy changes the enhancement pattern of the breast by diminishing the enhancement of normal breast parenchyma and tumor, due to loss of abnormal tumor vascularity. Thus, enhancement at the site of prior cancer should be considered residual tumor even if the kinetic curves are benign. In the ipsilateral axilla, reactive lymph nodes that cannot be distinguished from metastatic disease may develop.

On mammography the findings include architectural distortion, increased density, and parenchymal scarring. These findings diminish in severity over time and should be stable after 3–5 years. Almost 50% of patients continue to have variable mammographic findings ranging from spiculated mass like scars to slight architectural distortion. As these findings can simulate cancer, it is important to document the date and location of the surgical procedure, use skin markers (usually linear metallic marker placed on the scar before the mammogram), and compare with previous exams. The other half has no scar or distortion in the underlying breast parenchyma, and only comparison with preoperative images can indicate that breast tissue has been removed. Fat necrosis is another common finding and usually

appears as a radiolucent lipid-filled mass or a typically calcified eggshell-type rim around a radiolucent center, pathognomonic in mammography [83].

On ultrasound, the incision can usually be traced from the biopsy cavity to the skin and appears as a linear scar that disturbs the normal breast architecture. The seroma or hematoma is gradually absorbed, and only fibrotic scar remains, as a hypoechoic spiculated mass with acoustic shadowing that simulates breast cancer. So, the comparison with previous images and the correlation with physical finding of a scar on the skin can distinguish normal postoperative scarring from cancer.

The whole breast, external beam radiotherapy (WB-XRT) usually is performed after lumpectomy to eliminate microscopic residual disease and to suppress tumor recurrence both in the remaining breast parenchyma and in the tissue around the lumpectomy cavity. During WB-XRT the breast skin becomes erythematous, and the breast may become edematous, particularly in those patients with larger breasts. After completion of radiotherapy, the breast edema slowly subsides, and the skin becomes less edematous and more normal in appearance as the breast heals. Some options as accelerated partial breast irradiation (APBI) that delivers radiotherapy only to the lumpectomy cavity plus margins have also emerged as a potential option for selected patients. Various APBI techniques include intraoperative radiotherapy (IORT), interstitial brachytherapy, intracavitary brachytherapy, or three-dimensional (3D) conformal external beam radiation. All types of APBI use a higher dose per fraction to achieve an effective total dose. Given the higher fractionated dose, post-treatment changes in the breast after APBI may be different from that seen after WB-XRT. The shortened time course of radiotherapy increases accessibility of breast conservation treatment and may increase the proportion of women who receive appropriate adjuvant radiotherapy after breast-conserving surgery. In addition, limiting the field of treatment to the local tumor bed should, in theory, reduce treatment-related morbidities such as radiation pneumonitis, breast lymphedema, and radiation-induced sarcoma [84].

Normal changes after radiation therapy include the usual post-biopsy changes at the surgical site plus diffuse skin thickening and whole breast edema from WB-XRT. Skin thickening in the immediate postradiation therapy period is caused by breast edema due to small-vessel damage, and in the later period, it is caused by fibrotic changes. These findings are most obvious compared with the contralateral side or older mammograms. On mammography, the edema is seen as stromal thickening, diffuse increased breast density and trabecular thickening in subcutaneous fat. These changes usually decrease after 2.5–3 years or may remain stable. Progression of breast edema is abnormal and should be investigated to exclude inflammatory breast cancer, mastitis, trauma, and obstructed breast lymphatic or venous drainage. Obtaining a mammogram relatively early (6–12 months) after completion of radiation therapy establishes a baseline for future reference. After completion of whole-breast irradiation, many facilities use a lumpectomy cavity boost to sterilize the operative site that is marked with radiopaque clips. In about a quarter of women, calcifications develop in the treated breast at the biopsy site. Although most of these calcifications will be caused by benign dystrophic calcification, fat necrosis, or calcified suture material, magnification views of the

calcifications at the biopsy site are required to distinguish them from cancer recurrence pleomorphic calcifications. When there are no distinguishing features to diagnose dystrophic or fat necrosis calcifications, a biopsy should be performed. Nonspecific microcalcifications that form at or near the biopsy site are a problem. Unchanged nonspecific calcifications should be monitored because they may represent either benign findings or incompletely resected tumor. Increasing microcalcifications are suggestive of breast cancer recurrence and should prompt biopsy unless they are specific for dystrophic calcifications or fat necrosis [51, 85] (Fig. 17.78). On MRI, the APBI results in characteristic posttreatment changes, which extend from the skin to the chest wall. Typically, there is only localized skin thickening in the APBI area and the absence of the diffuse skin thickening seen with WB-XRT. In addition, signal voids are common in the postoperative breast after APBI and may persist up to 25 months after treatment [3].

17.6 Ipsilateral Breast Tumor Recurrence (IBTR)

The incidence of treatment failure is approximately 1% per year. Women who are at greatest risk for failure include those under age 35 (especially younger than 30) and treated for invasive cancer with an extensive intraductal component or infiltrating ductal carcinoma with a large intraductal component; with intraductal carcinoma of comedo type, intraductal cancer measuring 2.5 cm or greater in diameter, and multicentric lesions; treated for more than one synchronous cancer in the same breast; and with angiolymphatic invasion. Microscopic residual disease may not imply a greater risk of IBTR, but gross residual tumor also has a poor prognosis. Despite the slightly greater tendency for recurrence in these groups, no risk factor is an absolute contraindication for breast conservation.

For women who choose lumpectomy, IBTR rates are approximately 5% at 5 years and between 10 and 15% at 10 years after therapy. Invasive IBTR is most common between 18 months and 7 years after treatment. During this period IBTR is more common in or around the lumpectomy cavity. After 7 years, IBTR is most often a random event in any quadrant of the affected breast, not necessarily at the original site, and is usually unrelated to the original lesion in the breast [86]. Recurrences at the original tumor site are usually caused by original failure to eradicate the cancer and represent true treatment failures and occur earlier than the development of a tumor elsewhere in the breast (Fig. 17.79).

On mammography, treatment failures manifest as new pleomorphic calcifications, scar edges becoming rounder or larger, or masses developing in or around the lumpectomy cavity [13]. On ultrasound, an IBTR shows a mass with or without continuity with the surgical scar if it occurs near the original lumpectomy site. Radiologists must investigate any new mass, because even benign-appearing new solid masses may represent a new cancer. On MRI, clumped enhancement or an eccentric residual mass can be seen around the lumpectomy cavity (Fig. 17.80).

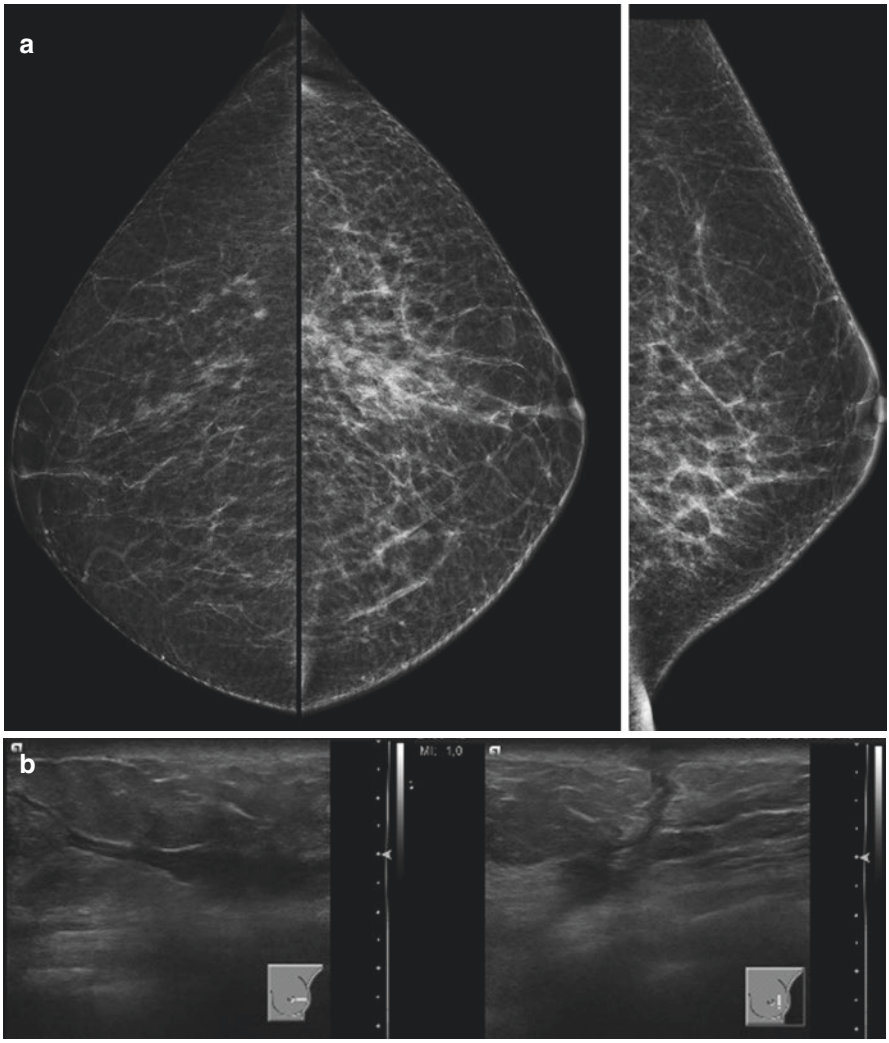

Fig. 17.78 Breast-conserving treatment. Imaging findings of a 54-year-old woman with personal history of Invasive ductal carcinoma (IDC) in the left breast, treated with breast conserving surgery 7 months ago and radiotherapy. (**a**) Mammogram shows architectural distortion and cutaneous and trabecular thickening due to radiation therapy on the left breast. (**b**) US images show the incision from the surgical cavity to the skin and cutaneous thickening

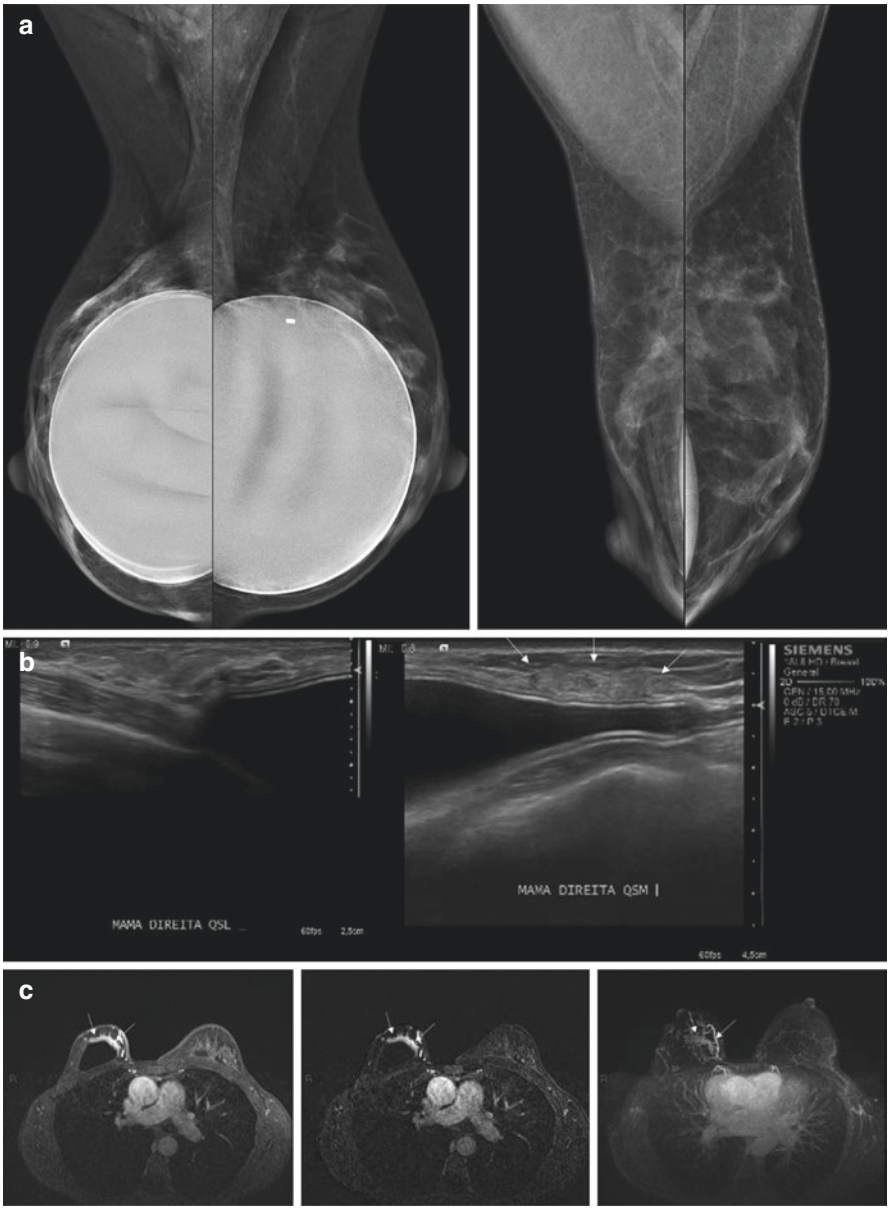

Fig. 17.79 Recurrence after breast-conserving treatment. Imaging findings of a 48-year-old woman with personal history of IDC in the right breast 4 years ago, treated with breast conserving surgery, and familial history of breast cancer. (**a**) Mammography (with and without Eklund's maneuver) showing heterogeneously dense tissue, architectural distortion on the right breast, a marker clip on the left breast (benign calcifications), and subglandular implants. (**b**) Ultrasound images showing a hyperechoic non-mass lesion on the upper inner quadrant of the right breast. (**c**) Axial post-contrast fat-suppressed T1-weighted MR images show heterogeneous non-mass enhancement with segmental distribution on the right breast. DCIS confirmed in US-guided core biopsy

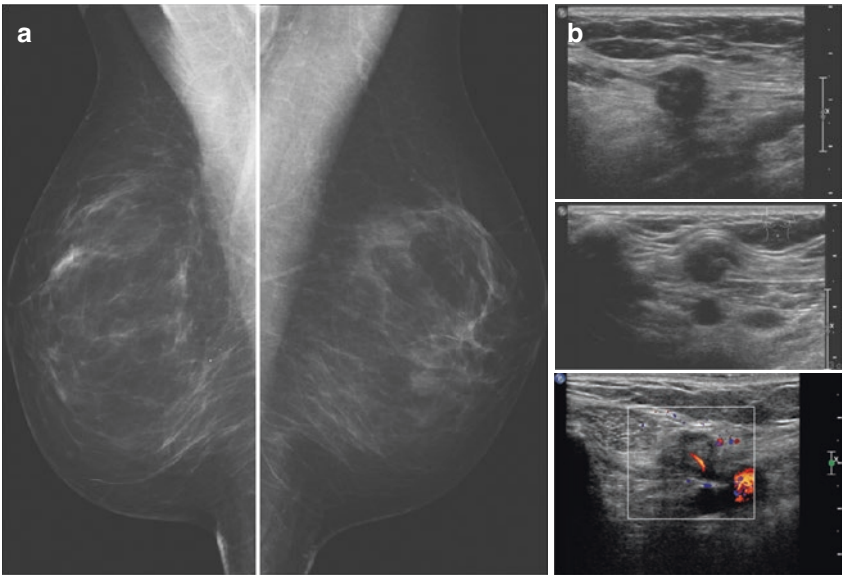

Fig. 17.80 Infraclavicular recurrence after breast-conserving treatment. Imaging findings of a 58-year-old woman with personal history of IDC in the right breast 13 years ago, treated with breast-conserving surgery. (**a**) Mammography showing scattered areas of fibroglandular density, bilateral surgical architectural distortion, and a benign mass on the left breast. (**b**) Ultrasound images show an irregular spiculated mass in the subclavicular chain. There was correspondence on PET-CT images (not shown), and metastatic breast carcinoma was confirmed on core biopsy

Treatment failures after lumpectomy and WB-XRT are usually treated by salvage mastectomy with or without reconstruction. The choice of repeating lumpectomy without additional radiotherapy or repeating lumpectomy with additional APBI has little long-term data to conclude on safety and effectiveness [87, 88].

17.7 Mastectomy

Mastectomy is the surgical removal of the mammary gland and is chosen when the entire tumor cannot be excised with a good cosmetic result, for the women with contraindications to radiation therapy (i.e., pregnancy, previous breast radiation therapy, multicentric or diffuse disease, collagen vascular disease), for disease involving the skin or if preferred by the patient. Even large lesions (more than 5 cm) or multifocal disease can be treated with breast-conserving surgery if a neoadjuvant chemotherapy is offered before surgery, and there is a decrease in tumor size [89–91].

There are various types of mastectomies, and they can be associated or not with axillary lymph node dissection. In simple mastectomy, the nipple-areolar complex

(NAC) is removed with an ellipse of skin with underlying breast tissue. In the conservative mastectomies (skin-sparing mastectomy and nipple-sparing mastectomy), the aim is to save as much tissue as possible to provide better aesthetic results in breast reconstruction. Insufficient removal of the breast tissue may increase the risk of cancer, and the excessive removal impairs the outcome of the reconstruction. Residual breast parenchymal tissue should be reported by the radiologist as long-term surveillance imaging may be indicated. A skin-sparing mastectomy (SSM) suggests that some of the skin on the breast that would normally have been removed may remain. It involves complete removal of all breast tissue and the NAC while preserving the skin envelope and is followed by immediate breast reconstruction. The postoperative appearance of a skin-sparing mastectomy is variable in terms of the amount of skin remaining, and imaging will demonstrate a skin flap from the native skin and subcutaneous fat and either autologous or implant augmentation in place of the glandular tissue [92]. In case of nipple-sparing mastectomy (NSM, adeno-mastectomy or subcutaneous mastectomy), the breast tissue is removed as it is done in a simple mastectomy but with preservation of the nipple-areolar complex. Some ductal tissue may remain within the nipple itself, as well as in the underlying tissue, which ensures adequate nipple vascularization. This is usually requested by patients who are having mastectomy for prophylactic reasons. When this technique is performed in a cancer treatment setting, tumors should be smaller than <3 cm in size and more than 2 cm away from the NAC, with negative lymph nodes. There are no randomized studies comparing the effectiveness of these techniques; however, retrospective studies have shown an acceptable rate of local recurrence. Typically, radiotherapy is not routinely performed after a nipple-sparing mastectomy unless there are pathological indications such as involvement of multiple nodes or a large tumor. The surgical complication rate of conservative mastectomies is higher when compared to conventional mastectomies. The main complications are the skin flap and nipple-areolar complex necrosis, which occur in 3–9% of cases (Fig. 17.81).

Unless there is a medical contraindication to breast reconstruction, patients who choose mastectomy are always offered breast reconstruction with a tissue expander, implant, or autologous tissue flap. The breast reconstruction options include an implant, a latissimus dorsi flap with an implant when significant breast skin has been lost, or a transverse rectus abdominis myocutaneous (TRAM) flap or one of its derivative procedures, such as a deep inferior epigastric perforator flap (DIEP). Imaging of the reconstructed breast is not normally performed after placement of an expander, implant, or after autologous tissue reconstruction [3].

Reduction mammoplasty may be required in the unaffected contralateral breast to achieve symmetry with the treated breast. The appearance of breasts reconstructed with autologous tissue and contralateral normal breasts submitted to reduction mammoplasty are characteristic and should not be mistaken for cancer.

Recurrence of breast cancer in the mastectomy site without reconstruction is usually detected by physical examination. Due to the low yield of breast cancer detection from the small amount of remaining breast tissue, surveillance mammography of the mastectomy site is not usually performed. Ultrasound can evaluate

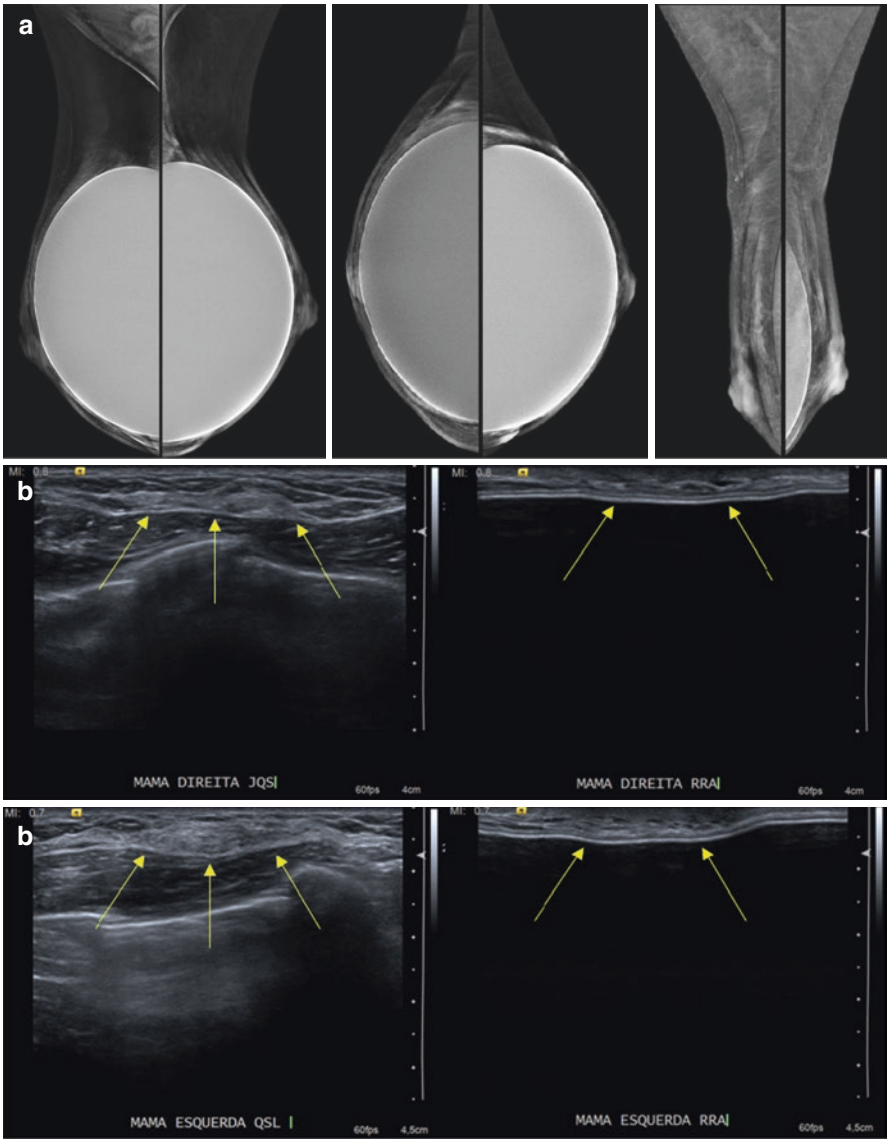

Fig. 17.81 Prophylactic nipple-sparing mastectomy. Imaging findings of a 47-year-old woman after prophylactic nipple-sparing mastectomy. (**a**) Mammography showing retropectoral implants, minimal subareolar fibroglandular parenchyma, and preserved NAC. (**b**) Ultrasound showing residual parenchyma also in the junction of upper quadrants of the right breast and in the upper outer quadrant of the left breast

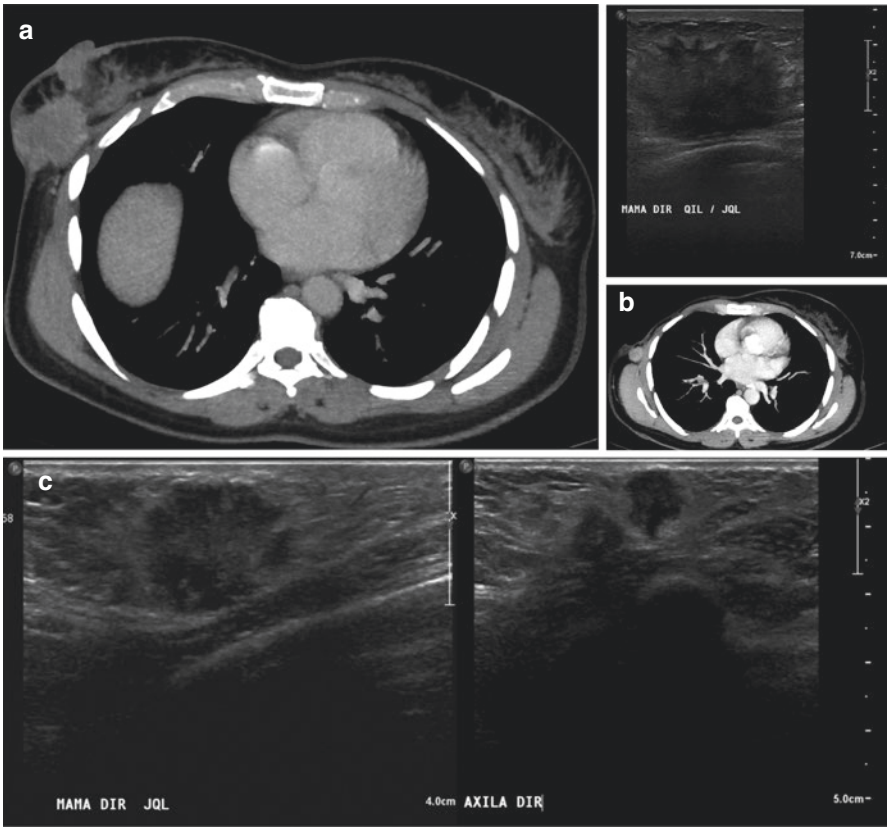

Fig. 17.82 Recurrence after mastectomy without reconstruction. Imaging findings of a 41-year-old woman before and after mastectomy. (**a**) Preoperative CT and US show a solid spiculated mass involving the skin, confirmed IDC. (**b**) Postoperative routine CT shows the right mastectomy site without reconstruction after 10 months and a mass in the axillary tail. (**c**) US shows a solid spiculated mass and some atypical axillary lymph nodes, core biopsy confirmed new IDC, and metastatic lymph nodes

seroma, lymphadenopathy, and cancer recurrence in the chest wall, subcutaneous fat, and skin (Fig. 17.82).

17.8 Breast Reconstruction

After mastectomy, the breast may be reconstructed with autologous tissue, implant, or a combination of both. The aim of breast reconstruction is to create a new breast and restore chest symmetry, reducing the psychosocial consequences related to the mastectomy. There is no ideal technique. It is expected to be effective, fast-performed, with few complications. The choice of breast reconstruction depends on

the patient's goals, medical history, physical examination, and potential need for adjuvant therapy [93].

Regardless of the chosen technique, cancer may recur in the reconstructed breast. To detect breast cancer recurrences at a smaller size, radiologists must be familiar with the range of normal and abnormal imaging appearances of reconstructed breasts that occur in different surgical techniques.

Implant reconstruction is the most used technique (80% of cases) and requires placement of a tissue expander in a retropectoral position at the time of mastectomy (skin-sparing mastectomy) for expansion of the skin. Usually, a saline expander is used that is gradually filled until the skin is sufficiently stretched and the space is adequate to hold an appropriately sized implant. Subsequent surgery is done to replace the tissue expander with a permanent implant behind the pectoral muscle (Fig. 17.83). Patients with small breasts and little ptosis present more favorable results since the skin flap completely accommodates the volume of the implant. For the other hand, women with large and ptotic breasts present less satisfactory results, often requiring skin reduction, which increases the risk of skin and the nipple-areola complex necrosis. The need for radiotherapy after mastectomy is not an absolute contraindication for this type of reconstruction, but it can be associated with poor outcome, capsular contracture, and even loss of the implant.

The most common form of autologous tissue reconstruction is made with the transverse rectus abdominis myocutaneous (TRAM) flap (Fig. 17.84). It can be performed as a pedicle (pedicled TRAM) or free flap (muscle-sparing TRAM flap, DIEP flap, SIEA flap). Another option used when an additional skin is needed to close the wound or additional soft tissue is required in an implant-based reconstruction is a latissimus dorsi myocutaneous flap (Fig. 17.85). In all these cases, skin, fat, and muscle are transferred to the mastectomy site with attachments to vascular structures and are shaped to form a breast. The choice of flap relies on the tissue abundance at the donor site and the viability of the vascular pedicle. The method of choice for vascular mapping (before TRAM and DIEP flaps) is computed tomographic (CT) angiography. It has an excellent sensitivity (99.6%) and a high positive predictive value (99.6%) for identifying clinically relevant perforating branches, allowing a better assessment of perforating vessel size, hemodynamics (maximal enhancement quantification), and location within the muscle [94]. In recent years, MR angiography has gained in popularity with similar results to those obtained with CT angiography [95, 96]. Complications may be related to the donor area or the flap itself. The most feared flap-related complication is necrosis, in addition to dehiscence and hematoma, which are more frequent.

Another form of breast reconstruction involves autologous fat graft injection (also known as lipofilling) to augment the volume of the reconstructed breast, usually in combination to other reconstruction form. This procedure transfers mature adipocytes and adipocyte-derived stem cells (ADSCs) to the defective breast region. These ADSCs have the ability to stimulate local neoangiogenesis and stimulate fibroblasts locally, allowing these mature adipocytes to survive and integrate into the graft-receiving mammary environment. The main disadvantage of this technique is the impossibility of predicting how much fat will be reabsorbed, often requiring

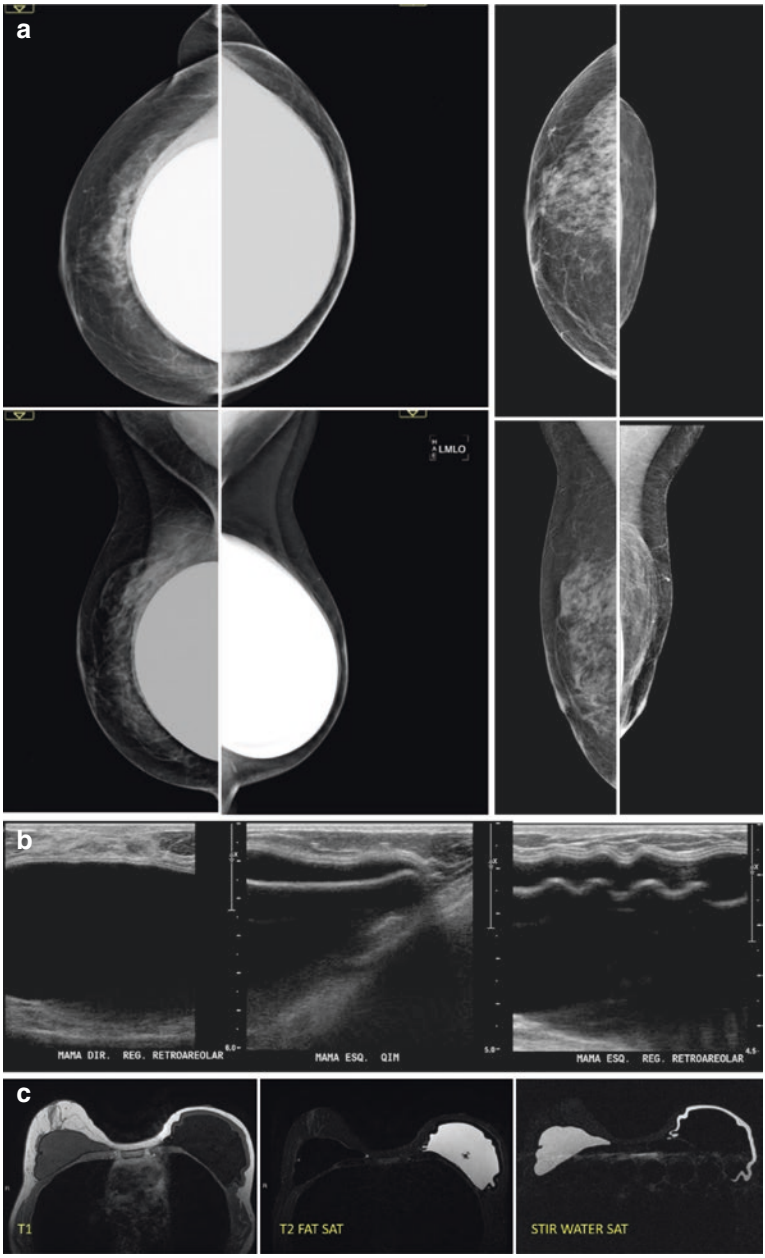

Fig. 17.83 Breast reconstruction with double-lumen implant. Imaging findings of a 51-year-old woman with personal history of IDC in the left breast 4 years ago, treated with nipple-sparing mastectomy. (**a**) Mammography showing retropectoral implants, minimal subareolar fibroglandular parenchyma, and preserved NAC in the left breast. (**b**) Ultrasound shows the differences between the single-lumen implant in the right breast (first image) and the expander or double-lumen implant in the left breast. (**c**) Axial MR images showing single-lumen silicone implant in the right breast and double-lumen implant (inner saline compartment; outer silicone gel compartment) in the left breast

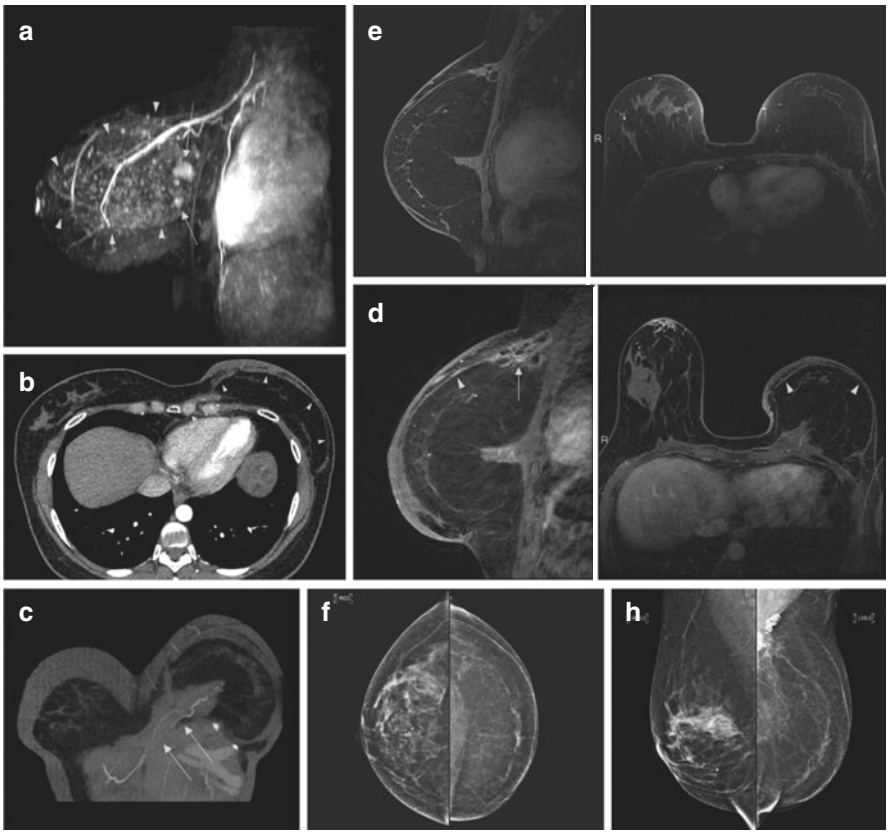

Fig. 17.84 Tram-flap reconstruction. Imaging findings of a 41-year-old woman who presented amorphous clustered calcifications in the screening mammogram, confirmed histologically as DCIS. (**a**) Preoperative contrast-enhanced MIP reconstruction image shows two irregular masses (arrow) and large clumped non-mass enhancement (arrowhead). Mastectomy with a pedicled TRAM flap reconstruction was performed. Biopsy confirmed IDC, ILC, and DCIS*. (**b**, **c**) Postoperative CT and coronal T1-weighted MR image show the contralateral rectus abdominis muscle tunneled through the inframammary fold to the mastectomy pocket (arrow). Imaging findings 1 year after mastectomy, chemotherapy, and radiation therapy. (**d**) Sagittal and axial T1-weighted MR images show cutaneous thickening and steatonecrosis (arrow) due to radiation therapy and a thin line separating the fat from the skin of the TRAM flap (arrowhead). Imaging findings 4 year after treatment. (**e**) Sagittal and axial T1-weighted MR images show decrease of the postoperative findings. (**f**) Mammogram shows autologous flap appearing as fat centrally and calcifications from fat necrosis in the left breast and findings of reduction mammoplasty in the right breast (made for symmetry). (**g**) Ultrasound shows the differences between the fat distribution of the TRAM flap in the left breast and the usual breast parenchyma of the right breast. *IDC invasive ductal carcinoma, ILC invasive lobular carcinoma, DCIS ductal carcinoma in situ

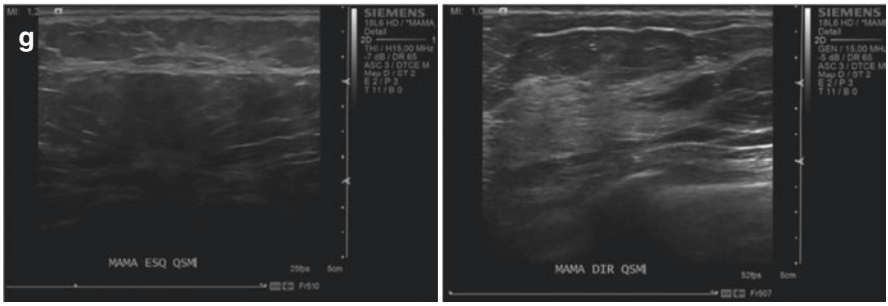

Fig. 17.84 (continued)

more than one procedure to obtain the expected result. The main complication is fat necrosis and cellulitis. The imaging studies show oil cysts and fat necrosis that are easily identified on mammography, ultrasound, and MRI. The interaction between mature adipocytes, ADSC, and the normal mammary cell, as well as the carcinogen cell, is still unclear [95].

Also, the nipple can be reconstructed out of the skin and tattooed to provide color similar to the contralateral side.

Mammography is indicated if any breast tissue has been left at the mastectomy site (with or without implants). Breast cancer recurrences can appear as masses or suspicious calcifications. The mammographic evaluation is useful in the autologous tissue reconstruction, especially when there are suspicious physical findings. Autologous flaps appear radiographically as fat centrally, with or without muscle fibers around the edges of the flaps. Common findings are calcifications from fat necrosis, benign dermal calcifications, and calcified hematoma. In patients undergoing radiotherapy after reconstruction, diffuse thickening of the skin and trabeculae may be seen, usually within the first 6 months after completion of radiotherapy. Suspicious findings are masses and clusters of microcalcifications. Recurrence is more likely to occur if the margins were closer to less than 1 cm or if there was prior lymphovascular invasion. But some studies have shown that mammographic screening of asymptomatic women does not increase life expectancy and there is no reason to do so [96].

MR images may be helpful in showing postoperative findings in autologous reconstructions and to find cancer in the opposite breast. They show that the flap has fat signal intensity and the pedicle is isointense to pectoralis muscle, with easily visible fat necrosis, skin thickening, edema, fluid collection, hematoma, or lipofilling changes. The postoperative findings decrease on subsequent MRI studies [3].

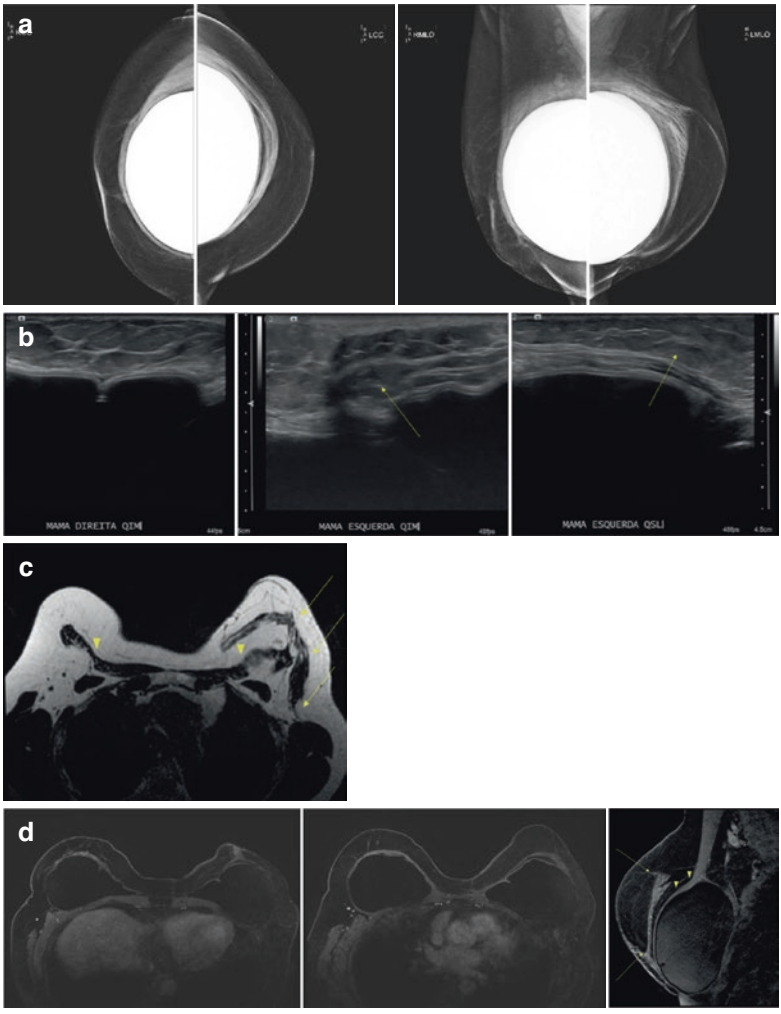

Fig. 17.85 Dorsal-flap reconstruction. Imaging findings of a 53-year-old woman with personal history of IDC in the left breast 6 years ago with recurrence after 4 years, treated with mastectomy and latissimus dorsi flap with implant reconstruction and prophylactic nipple-sparing mastectomy in the contralateral breast. (**a**) Mammography showing retromuscular implants, autologous flap appearing as fat centrally in the left breast and minimal subareolar fibroglandular parenchyma, and preserved NAC in the right breast. (**b**) Ultrasound shows the differences between the fat distribution of the TRAM flap in the left breast (arrows) and the usual breast parenchyma of the right breast (first image). (**c**) Axial T2-weighted MR image shows major pectoral muscle (arrowhead) and latissimus dorsi muscle tunneled in the left breast (arrows). (**d**) Sagittal and axial post-contrast fat-suppressed T1-weighted MR image show the major pectoral muscle (arrowhead) and a thin line separating the fat autologous flap (arrow)

17.9 Breast Cancer Recurrence

Although the risk for breast cancer is reduced by more than 90% after mastectomy, it is not eliminated, because the breast tissue is incompletely excised (usually remaining in the anterolateral aspect of the chest wall and in the axilla). The reported breast cancer recurrence rate after TRAM flap reconstruction ranges between 4.2% and 11.7%, (depending on the primary tumor stage, histology and patient's genetic risk). Early detection of recurrent tumors in reconstructed breasts may have benefits, but any benefit would come at the cost of many false-positive findings, and a benefit in terms of patient survival has yet to be proven [97].

The most common finding of recurrent cancer in the reconstructed breast is a palpable mass and occurs in the skin envelope superficially to the autologous flap reconstruction. Other signs and symptoms include local pain and tenderness, irregularity of the flap surface, erythematous rash, as well as nodal metastasis. Local recurrences arise mostly at the medial aspect of the flap because of lymphatic drainage to the internal mammary nodes, which are not dissected during mastectomy and reconstruction. A recurrence can also arise from the chest wall (this one with the worst prognosis).

The mammographic and sonographic findings may resemble those of the primary tumor and may include a solid irregular and spiculated mass, distortion, microcalcifications, and skin thickening. Ultrasound is more sensitive than mammography for detecting occult recurrences [98], especially smaller ones and those in peripherical location (not included in the mammographic field of view).

MR images show an irregular mass with avid early enhancement and delayed washout. Nodal recurrence manifests as an increase in the number and size of axillary or internal mammary lymph nodes [99, 100] (Fig. 17.86).

There is not a consensus on the methods for patient follow-up after mastectomy and breast reconstruction. Many authors recommend performing a physical examination to detect subcutaneous recurrences and mammography to detect recurrent tumors in the chest wall. Follow-up with breast MRI may benefit women at high risk for breast cancer recurrence (histologically aggressive type or genetic susceptibility). Early detection of recurrence has not been shown to decrease mortality, as most patients with recurrent breast cancer have metastases when recurrence is diagnosed [101, 102].

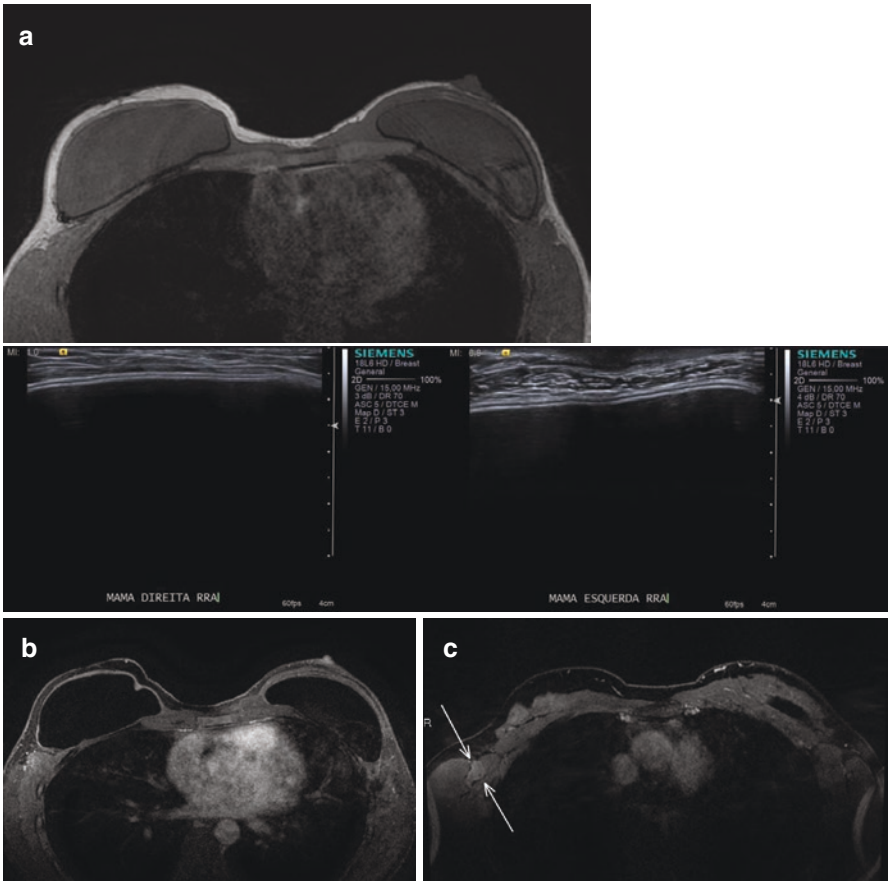

Fig. 17.86 Recurrence after skin sparing mastectomy (SSM). Imaging findings of a 33-year-old woman with personal history of DCIS in the right breast 7 years ago, treated with skin sparing mastectomy. After 5 years she underwent a prophylactic SSM on the left breast. (**a**) Axial T1-weighted MR image (anatomical features) and US images show retropectoral implants, absence of the NAC on the right breast (SSM), and minimal subareolar fibroglandular parenchyma and preserved NAC on the left breast (NSM). (**b**) Axial post-contrast fat-suppressed T1-weighted MR image shows no intramammary suspicious enhancement. (**c**, **d**) Axial and sagittal post-contrast fat-suppressed T1-weighted MR images show an oval, circumscribed axillary mass. (**e**, **f**) Corresponding PET-CT and US images, 7 years after the first treatment. (**g**) Core biopsy proven IDC luminal B

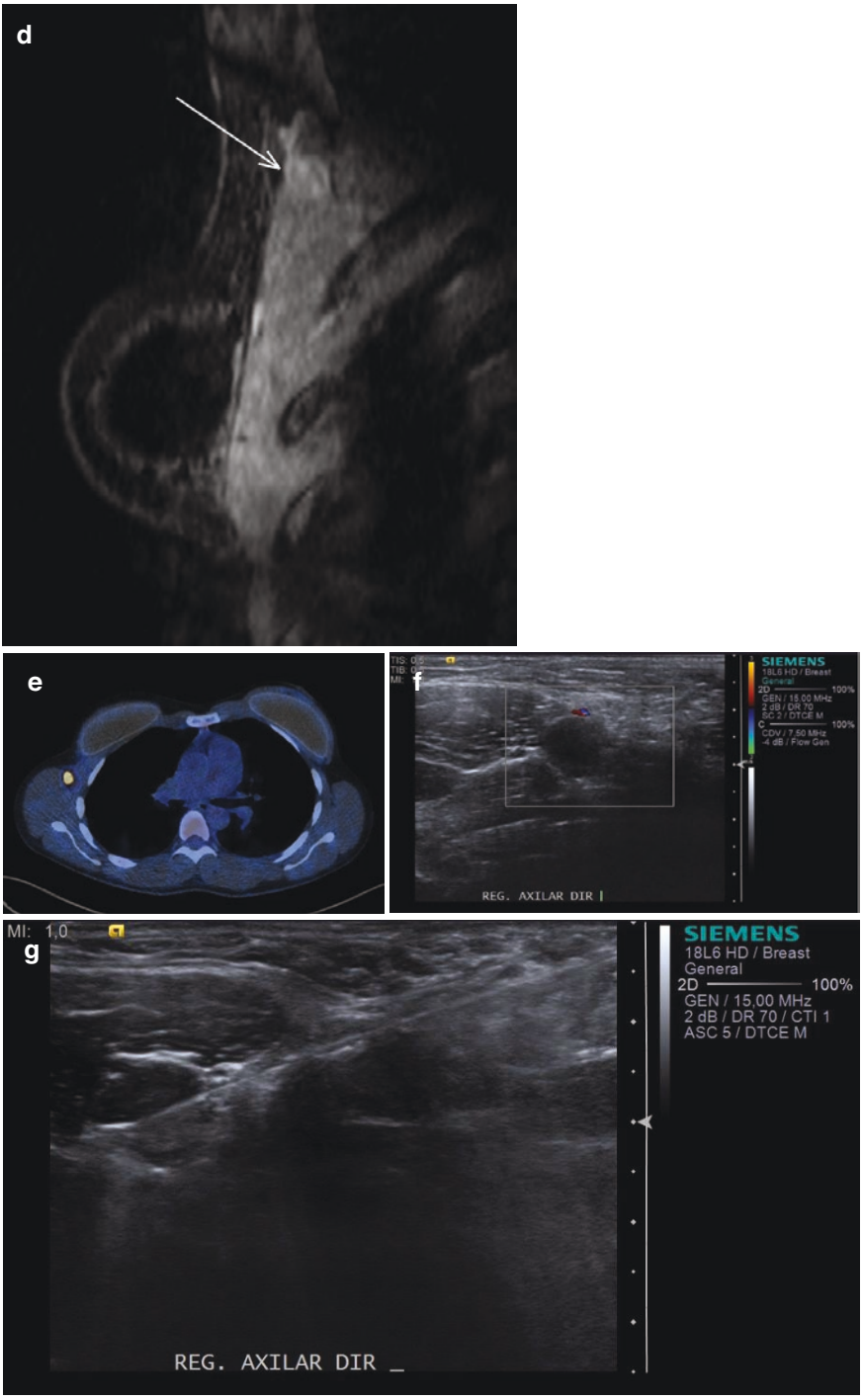

Fig. 17.86 (continued)

17.10 Conclusion

Patients have a wide range of surgical options and adjuvant therapies. Radiologists should be familiar with them, including normal and abnormal imaging appearances from surgical procedures, reconstructed breasts, and radiation therapy changes, as posttreatment changes can sometimes mimic malignancy or obscure locally recurrent breast cancer.

References

1. Mendelson EB. Evaluation of the postoperative breast. Breast Imaging: Curr Status Future Dir. 1992;30:107–38.
2. Drukteinis JS, Gombos EC, Raza S, et al. MR imaging assessment of the breast after breast conservation therapy: distinguishing benign from malignant lesions. Radiographics. 2012;32:219–34.
3. Margolis NE, Morley C, Lotfi P, et al. Update on imaging of the postsurgical breast. Radiographics. 2014;34:642–60.
4. Hayes MK, Gold RH, Bassett LW. Mammographic findings after the removal of breast implants. AJR Am J Roentgenol. 1993;160:487–90.
5. Collis N, Sharpe DT. Silicone gel-filled breast implant integrity: a retrospective review of 478 consecutively explanted implants. Plast Reconstr Surg. 2000;105:1979–85.
6. Ikeda DM, Borofsky HB, Herfkens RJ, et al. Silicone breast implant rupture: pitfalls of magnetic resonance imaging and relative efficacies of magnetic resonance, mammography, and ultrasound. Plast Reconstr Surg. 1999;104:2054–62.
7. Cicchetti S, Leone MS, Franchelli S, Santi PL. Evaluation of the tolerability of hydrogel breast implants: a pilot study. Minerva Chir. 2002;57:53–7.
8. Collis N, Litherland J, Enion D, Sharpe DT. Magnetic resonance imaging and explantation investigation of long-term silicone gel implant integrity. Plast Reconstr Surg. 2007;120:1401–6.
9. Kreymerman P, Patrick RJ, Rim A, et al. Guidelines for using breast magnetic resonance imaging to evaluate implant integrity. Ann Plast Surg. 2009;62:355–7.
10. Marotta JS, Widenhouse CW, Habal MB, Goldberg EP. Silicone gel breast implant failure and frequency of additional surgeries: analysis of 35 studies reporting examination of more than 8,000 explants. J Biomed Mater Res. 1999;48:354–64.
11. Janowsky EC, Kupper LL, Hulka BS. Meta-analyses of the relation between silicone breast implants and the risk of connective-tissue diseases. N Engl J Med. 2000;342:781–90.
12. Kessler DA. The basis of the FDA's decision on breast implants. N Engl J Med. 1992;326:1713–5.
13. Lipworth L, Holmich LR, McLaughlin JK. Silicone breast implants and connective tissue disease: no association. Semin Immunopathol. 2011;33:287–94.
14. McLaughlin JK, Lipworth L, Murphy DK, Walker PS. The safety of silicone gel-filled breast implants: a review of the epidemiologic evidence. Ann Plast Surg. 2007;59:569–80.
15. Muzaffar AR, Rohrich RJ. The silicone gel-filled breast implant controversy: an update. Plast Reconstr Surg. 2002;109:742–8.
16. Noels EC, Lapid O, Lideman JH, Bastiaanner E. Breast implants and the risk of breast cancer: a meta-analysis of cohort studies. Aesthet Surg J. 2015;35:55–62.
17. Spear SL, Mardini S. Alternative filler materials and new implant designs: what's available and what's on the horizon? Clin Plast Surg. 2001;28:435–43.

18. Tugwell P, Wells G, Peterson J, et al. Do silicone breast implants cause rheumatologic disorders? A systematic review for a court-appointed national science panel. Arthritis Rheum. 2001;44:2477–84.
19. Derby BM, Codner MA. Textured silicone breast implant use in primary augmentation: core data update and review. Plast Reconstr Surg. 2015;135:113–24.
20. Handel N, Garcia ME, Wixtrom R. Breast implant rupture: causes, incidence, clinical impact, and management. Plast Reconstr Surg. 2013;132:1128–37.
21. Destouet JM, Monsees BS, Oser RF, et al. Screening mammography in 350 women with breast implants: prevalence and findings of implant complications. AJR Am J Roentgenol. 1992;159:973–81.
22. Eklund GW, Busby RC, Miller SH, Job JS. Improved imaging of the augmented breast. AJR Am J Roentgenol. 1988;151:469–73.
23. Ganott MA, Harris KM, Ilkhanipour ZS, Costa-Greco MA. Augmentation mammoplasty: normal and abnormal findings with mammography and US. Radiographics. 1992;12:281–95.
24. Silverstein MJ, Handel N, Gamagami P. The effect of silicone-gel-filled implants on mammography. Cancer. 1991;68(Suppl):1159–63.
25. Silverstein MJ, Handel N, Gamagami P, et al. Mammographic measurements before and after augmentation mammaplasty. Plast Reconstr Surg. 1990;86:1126–30.
26. Shah M, Tanna N, Margolies L. Magnetic resonance imaging of breast implants. Top Magn Reson Imaging. 2014;23:345–53.
27. Monticciolo DL, Nelson RC, Dixon WT, et al. MR detection of leakage from silicone breast implants: value of a silicone-selective pulse sequence. AJR Am J Roentgenol. 1994;163:51–6.
28. Berg WA, Caskey CI, Hamper UM, et al. Diagnosing breast implant rupture with MR imaging, US, and mammography. Radiographics. 1993;13:1323–36.
29. Young VL, Bartell T, Destouet JM, et al. Calcification of breast implant capsule. South Med J. 1989;82:1171–3.
30. DeBruhl ND, Gorczyca DP, Ahn CY, Shaw WW, Bassett LW. Silicone breast implants: US evaluation. Radiology. 1993;189:95–8.
31. Gossner J. Sonography in capsular contracture after breast augmentation: value of established criteria, new techniques and directions for research. J Ultrasound. 2017;20:87–9.
32. Ahn CY, Shaw WW, Narayanan K, et al. Residual silicone detection using MRI following previous breast implant removal: case reports. Aesthet Plast Surg. 1995;19:361–7.
33. Stewart NR, Monsees BS, Destouet JM, Rudloff MA. Mammographic appearance following implant removal. Radiology. 1992;185:83–5.
34. Henriksen TF, Holmich LR, Fryzek JP, et al. Incidence and severity of short-term complications after breast augmentation: results from a nationwide breast implant registry. Ann Plast Surg. 2003;51:531–9.
35. Cortes MIC, Valadez ER, Martinez RDZ, et al. Breast prosthesis syndrome: pathophysiology and management algorithm. Aesth Plast Surg. 2020;44:1423–37.
36. Feng LJ, Amini SB. Analysis of risk factors associated with rupture of silicone gel breast implants. Plast Reconstr Surg. 1999;104:955–63.
37. Holmich LR, Friis S, Fryzek JP, Vejborg IM, et al. Incidence of silicone breast implant rupture. Arch Surg. 2003;138:801–6.
38. Bengtson BP, Eaves FF 3rd. High-resolution ultrasound in the detection of silicone gel breast implant shell failure: background, in vitro studies, and early clinical results. Aesthet Surg J. 2012;32:157–74.
39. Heden P, Bone B, Murphy DK, et al. Style 410 cohesive silicone breast implants: safety and effectiveness at 5 to 9 years after implantation. Plast Reconstr Surg. 2006;118:1281–7.
40. Heden P, Bronz G, Elberg JJ, et al. Long-term safety and effectiveness of style 410 highly cohesive silicone breast implants. Aesthet Plast Surg. 2009;33:430–6.
41. Heden P, Nava MB, van Tetering JP, et al. Prevalence of rupture in Inamed silicone breast implants. Plast Reconstr Surg. 2006;118:303–12.

42. Holmich LR, Fryzek JP, Kjoller K, et al. The diagnosis of silicone breast-implant rupture: clinical findings compared with findings at magnetic resonance imaging. Ann Plast Surg. 2005;54:583–9.
43. Beekman WH, Hage JJ, Taets van Amerongen AH, Mulder JW. Accuracy of ultrasonography and magnetic resonance imaging in detecting failure of breast implants filled with silicone gel. Scand J Plast Reconstr Surg Hand Surg. 1999;33:415–8.
44. Rosculet KA, Ikeda DM, Forrest ME, et al. Ruptured gel-filled silicone breast implants: sonographic findings in 19 cases. AJR Am J Roentgenol. 1992;159:711–6.
45. Chung KC, Wilkins EG, Beil RJ Jr, et al. Diagnosis of silicone gel breast implant rupture by ultrasonography. Plast Reconstr Surg. 1996;97:104–9.
46. Di Benedetto G, Cecchini S, Grassetti L, et al. Comparative study of breast implant rupture using mammography, sonography, and magnetic resonance imaging: correlation with surgical findings. Breast J. 2008;14:532–7.
47. Ahn CY, DeBruhl ND, Gorczyca DP, et al. Comparative silicone breast implant evaluation using mammography, sonography, and magnetic resonance imaging: experience with 59 implants. Plast Reconstr Surg. 1994;94:620–7.
48. Rivero MA, Schwartz DS, Mies C. Silicone lymphadenopathy involving intramammary lymph nodes: a new complication of silicone mammaplasty. AJR Am J Roentgenol. 1994;162:1089–90.
49. Berg WA, Caskey CI, Hamper UM, et al. Single- and double-lumen silicone breast implant integrity: prospective evaluation of MR and US criteria. Radiology. 1995;197:45–52.
50. Harris KM, Ganott MA, Shestak KC, et al. Silicone implant rupture: detection with US. Radiology. 1993;187:761–8.
51. Kuzmiak CM, et al. Mammographic findings of partial breast irradiation. Acad Radiol. 2009;16(7):819–25.
52. Kwek JW, Choi H, Ma J, Miller MJ. Gel-gel double-lumen silicone breast implant: mimic of intracapsular implant rupture. AJR Am J Roentgenol. 2006;187:W436–7.
53. Palmon LU, Foshager MC, Parantainen H, et al. Ruptured or intact: what can linear echoes within silicone breast implants tell us? AJR Am J Roentgenol. 1997;168:1595–8.
54. Cher DJ, Conwell JA, Mandel JS. MRI for detecting silicone breast implant rupture: meta-analysis and implications. Ann Plast Surg. 2001;47:367–80.
55. Holmich LR, Vejborg I, Conrad C, et al. The diagnosis of breast implant rupture: MRI findings compared with findings at explantation. Eur J Radiol. 2005;53:213–25.
56. Gorczyca DP. MR imaging of breast implants. Magn Reson Imaging Clin N Am. 1994;2:659–72.
57. Kim SH, Lipson JA, Moran CJ, et al. Image quality and diagnostic performance of silicone-specific breast MRI. Magn Reson Imaging. 2013;31:1472–8.
58. Herborn CU, Marincek B, Erfmann D, et al. Breast augmentation and reconstructive surgery: MR imaging of implant rupture and malignancy. Eur Radiol. 2002;12:2198–206.
59. Soo MS, Kornguth PJ, Walsh R, et al. Intracapsular implant rupture: MR findings of incomplete shell collapse. J Magn Reson Imaging. 1997;7:724–30.
60. Adrada BE, Miranda RN, Rauch GM, et al. Breast implant-associated anaplastic large cell lymphoma: sensitivity, specificity, and findings of imaging studies in 44 patients. Breast Cancer Res Treat. 2014;147:1–14.
61. Chacko A, Lloyd T. Breast implant-associated anaplastic large cell lymphoma: a pictorial review. Insights Imaging. 2018;9:683–6.
62. Xu J, Wei S. Breast implant-associated anaplastic large cell lymphoma: review of a distinct clinicopathologic entity. Arch Pathol Lab Med. 2014;138:842–6.
63. Boer M, Leeuwen FE, Hauptmann M, et al. Breast implants and the risk of anaplastic large-cell lymphoma in the breast. JAMA Oncol. 2018;4(3):335–41.
64. Forgia DL, Catino A, Fausto A, et al. Diagnostic challenges and potential early indicators of breast periprosthetic anaplastic large cell lymphoma A case report. Medicine. 2020;99:30.

65. Miranda RN, Aladily TN, Prince HM, et al. Breast implant-associated anaplastic largecell lymphoma: long-term follow-up of 60 patients. J Clin Oncol. 2014;32:114–20.
66. Zanetta VC, Rudner MA, et al. Gossypibomas after breast augmentation: an almost-forgotten diagnosis. Breast J. 2020;26:2125–8.
67. Morris EA, Comstock CE, Lee CH, et al. ACR BI-RADS® magnetic resonance imaging. ACR BI-RADS® atlas, breast imaging reporting and data system. Reston: American College of Radiology; 2013.
68. Qian B, Xiong L, Guo K, et al. Comprehensive management of breast augmentation with polyacrylamide hydrogel injection based on 15 years of experience: a report on 325 cases. Ann Transl Med. 2020;8(7):475.
69. Grella R, Almadori A, D'Ari A, et al. Management of complication after breast augmentation with methacrylate. Int J Surg Case Rep. 2015;15:17–20.
70. Teo SY, Wang SC. Radiologic features of polyacrylamide gel mammoplasty. AJR. 2008;191:W89–95.
71. Khouri RK, Eisenmann-Klein M, Cardoso E, et al. Brava and autologous fat transfer is a safe and effective breast augmentation alternative: results of a 6-year, 81-patient, prospective multicenter study. Plast Reconstr Surg. 2012;129:1173–87.
72. Blumenschein AR, Freitas-Junior R, Tuffanin AT, et al. Breast fat grafting: experimental or established procedure? Rev Bras Cir Plást. 2012;27(4):616–22.
73. Atia AA, Ghareeb FM, Ellabban MG, et al. Clinical and radiological assessment of autologous fat transfer to the breast. Eur J Plast Surg. 2020;43:139–46.
74. Gigli S, Amabile MI, Pastena FD, et al. Magnetic resonance imaging after breast oncoplastic surgery: an update. Breast Care. 2017;12:260–5.
75. Veber M, Tourasse C, Toussoun G, et al. Radiographic findings after breast augmentation by autologous fat transfer. Plast Reconstr Surg. 2011;127(3):1289–99.
76. Rubin JP, Coon D, Zuley M, et al. Mammographic changes after fat transfer to the breast compared with changes after breast reduction: a blinded study. Plast Reconstr Surg. 2012;129:1029–38.
77. Loo YL, Haider S. The use of porcine acellular dermal matrix in single-stage, implant-based immediate breast reconstruction: a 2-center retrospective outcome study. Plast Reconstr Surg Glob Open. 2018;6(8):e1895.
78. Faulkner HR, Shikowitz-Behr L, McLeod M, et al. The use of absorbable mesh in implant-based breast reconstruction: a 7-year review. Plast Reconstr Surg. 2020;146(6):731e–6e.
79. Bedrosian I, et al. Changes in the surgical management of patients with breast carcinoma based on preoperative magnetic resonance imaging. Cancer. 2003;98:468–73.
80. Bleicher RJ, et al. Association of routine pretreatment magnetic resonance imaging with time to surgery, mastectomy rate, and margin status. J Am Coll Surg. 2009;209:180–7.
81. Bleicher RJ, Morrow M. MRI and breast cancer: role in detection, diagnosis, and staging. Oncology. 2007;21:1521–33.
82. Morrow M. Should routine breast cancer staging include MRI? Nat Clin Pract Oncol. 2009;6:72–3.
83. Sickles EA, Herzog KA. Mammography of the postsurgical breast. AJR Am J Roentgenol. 1981;136:585–8.
84. Godinez J, et al. Breast MRI in the evaluation of eligibility for accelerated partial breast irradiation. AJR Am J Roentgenol. 2008;191:272–7.
85. Liberman L, et al. Mammographic features of local recurrence in women who have undergone breast-conserving therapy for ductal carcinoma in situ. AJR Am J Roentgenol. 1997;168:489–93.
86. Tuli R, et al. Prognostic indicators following ipsilateral tumor recurrence in patients treated with breast-conserving therapy. Am J Surg. 2009;198:557–61.
87. Gorechlad JW, et al. Screening for recurrences in patients treated with breast-conserving surgery: is there a role for MRI? Ann Surg Oncol. 2008;15:1703–9.

88. Houssami N, Hayes DF. Review of preoperative magnetic resonance imaging (MRI) in breast cancer: should MRI be performed on all women with newly diagnosed, early stage breast cancer? CA Cancer J Clin. 2009;59:290–302.
89. Brennan ME, et al. Magnetic resonance imaging screening of the contralateral breast in women with newly diagnosed breast cancer: systematic review and meta-analysis of incremental cancer detection and impact on surgical management. J Clin Oncol. 2009;27:5640–9.
90. Chen JH, et al. MRI evaluation of pathologically complete response and residual tumors in breast cancer after neoadjuvant chemotherapy. Cancer. 2008;112:17–26.
91. Dang CM, et al. Increased use of MRI for breast cancer surveillance and staging is not associated with increased rate of mastectomy. Am Surg. 2009;75:937–40.
92. Pinel-Giroux FM, et al. Breast reconstruction: review of surgical methods and spectrum of imaging findings. Radiographics. 2013;33:435–53.
93. Clavero JA, et al. MDCT in the preoperative planning of abdominal perforator surgery for postmastectomy breast reconstruction. AJR Am J Roentgenol. 2008;191(3):670–6.
94. Phillips TJ, et al. Abdominal wall CT angiography: a detailed account of a newly established preoperative imaging technique. Radiology. 2008;249(1):32–44.
95. Özalp B, Aydinol M. Breast augmentation combining fat injection and breast implants in patients with atrophied breasts. Ann Plast Surg. 2017;78:623–8.
96. Helvie MA, et al. Mammographic screening of TRAM flap breast reconstructions for detection of nonpalpable recurrent cancer. Radiology. 2002;224(1):211–6.
97. Medina-Franco H, et al. Factors associated with local recurrence after skin-sparing mastectomy and immediate breast reconstruction for invasive breast cancer. Ann Surg. 2002;235(6):814–9.
98. Edeiken BS, et al. Recurrence in autogenous myocutaneous flap reconstruction after mastectomy for primary breast cancer: US diagnosis. Radiology. 2003;227(2):542–8.
99. Shaikh N, et al. Detection of recurrent breast cancer after TRAM flap reconstruction. Ann Plast Surg. 2001;47(6):602–7.
100. Vaughan A, et al. Patterns of local breast cancer recurrence after skin-sparing mastectomy and immediate breast reconstruction. Am J Surg. 2007;194(4):438–43.
101. Lu WL, et al. Impact on survival of early detection of isolated breast recurrences after the primary treatment for breast cancer: a meta-analysis. Breast Cancer Res Treat. 2009;114:403–12.
102. Seely JM, et al. Breast MRI in the evaluation of locally recurrent or new breast cancer in the postoperative patient: correlation of morphology and enhancement features with the BI-RADS category. Acta Radiol. 2007;8:838–45.

Chapter 18
Radiation Therapy

Paula de Camargo Moraes

18.1 Introduction

It has been long established that postsurgical radiotherapy reduces the risk of locoregional failure. A survival advantage, however, has recently also been demonstrated [1, 2]. Therefore, some women with breast cancer will need radiation therapy, in addition to other treatments, as summarized below:

- After breast-conserving surgery (BCS) to reduce locoregional failure in the same breast or nearby lymph nodes. Breast radiotherapy is recommended in patients with invasive breast cancer treated with breast-conserving surgery where complete microscopic excision has been achieved, unless life expectancy is less than 3 years due to comorbidities.
- This approach has enormously improved the quality of life and cosmetic outcome for appropriately selected and treated patients while achieving excellent long-term survival rates.
- After a mastectomy, especially if the cancer was large (T3/T4), if cancer is found in many lymph nodes, or if certain surgical margins have cancer such as the skin or muscle.
- The need for radiotherapy in patients with ductal carcinoma in situ (CDIS) can be guided by use of the Van Nuys Prognostic Index (VNPI) score that accounts for tumor size, grade, margin, presence of necrosis, and patient age.
- If cancer has spread to other parts of the body, such as the bones or brain.

P. de Camargo Moraes (✉)
Instituto de Radiologia INRAD, Hospital das Clinicas HCFMUSP, Faculdade de Medicina, Universidade de Sao Paulo, São Paulo, SP, Brazil

CDB (Centro Diagnóstico Brasil) – Grupo Alliar, São Paulo, SP, Brazil

Alta Medicina Diagnóstica – Grupo DASA, São Paulo, SP, Brazil
e-mail: paula.moraes.ext@dasa.com.br

S. J. Kim Hsieh, E. A. Morris (eds.), *Modern Breast Cancer Imaging*,
https://doi.org/10.1007/978-3-030-84546-9_18

18.2 Imaging Findings

Before addressing the findings expected after radiotherapy, it is important to reinforce that since radiotherapy generally follows surgical treatment, the findings of these two procedures often overlap. Besides that, imaging the treated breast presents challenges due to its limited compressibility and the overlapping features of benign posttreatment alterations and tumor recurrence, as described below.

18.2.1 Mastectomy

After any type of mastectomy procedure, most of the breast cells are removed. However, there is a chance of a small amount of breast tissue remaining, and therefore the chance of recurrence exists. The rate of recurrence at the chest wall following mastectomy is between 5% and 27%.

Recurrence involving the chest wall or skin can frequently be detected on clinical or breast self-exam, as they are often obvious changes such as palpable masses, skin thickening, retraction, edema, and redness. The addition of US to clinical exams may prove to be more accurate than mammography when evaluating a palpable or visible abnormality, as recurrence tends to be small and close to the skin surface. Magnetic resonance imaging (MRI) is another imaging tool that can be used to evaluate the mastectomy site and plays an important role in detecting recurrent lesions.

For the asymptomatic patients, there is a continuing debate concerning imaging following mastectomy, because it is said that imaging modalities may not be helpful after this kind of surgery. So the findings commonly associated with this type of surgical procedure, followed or not by radiation therapy, will not be addressed in this chapter.

18.2.2 Breast Conservation Surgery

Breast conservation treatment achieves local tumor control by the surgical removal of the cancer with margins and is usually followed by radiation therapy. The combination of conservative surgery and radiation therapy offers the advantage of preserving the breast, usually with a satisfactory cosmetic result. Given equivalent survival rates for breast conservation therapy and mastectomy, breast conservation therapy has become the treatment of choice for early-stage breast cancer.

However, radiologists are faced with increased imaging and diagnostic challenges when dealing with the conservative treated breast. The treated breasts may be difficult to position adequately and to compress sufficiently due to surgical

deformities, pain, or radiation changes. Also, the interpretation of imaging findings can be difficult because imaging features after treatment may mimic or hide tumor recurrence [3, 4].

The findings after lumpectomy and radiation therapy often overlap, and it is important to recognize that radiation therapy often intensifies and delays resolution of postsurgical changes [3, 4].

Although certain posttreatment alterations may persist, most changes after breast conservation therapy diminish and regress over time and then remain stable. Stability, defined as the lack of interval change on two successive studies, usually occurs at 2–3 years after the completion of radiation therapy, which is around the same time tumor recurrences typically begin to appear [5]. After stability has been achieved, any increase in the changes, development of new asymmetries, or calcifications should raise suspicion for tumor recurrence [4].

It is important to acknowledge that both surgery and radiotherapy alter the appearance of the breasts and sometimes distinguishing between recurrence and benign postsurgical changes can be challenging due to overlapping features. Despite this, differentiation between these two entities is usually possible by recognizing characteristic features of posttreatment sequelae and the evolution of the appearance of the conservatively treated breast by comparing interval findings on serial studies. There is an expected chronological appearance for these findings on the conservatively treated breast, as described below (Fig. 18.1).

The most common posttreatment findings that include breast edema, skin thickening, fluid collections, fat necrosis, architectural distortion, and calcifications [3, 6] will be revised and illustrated.

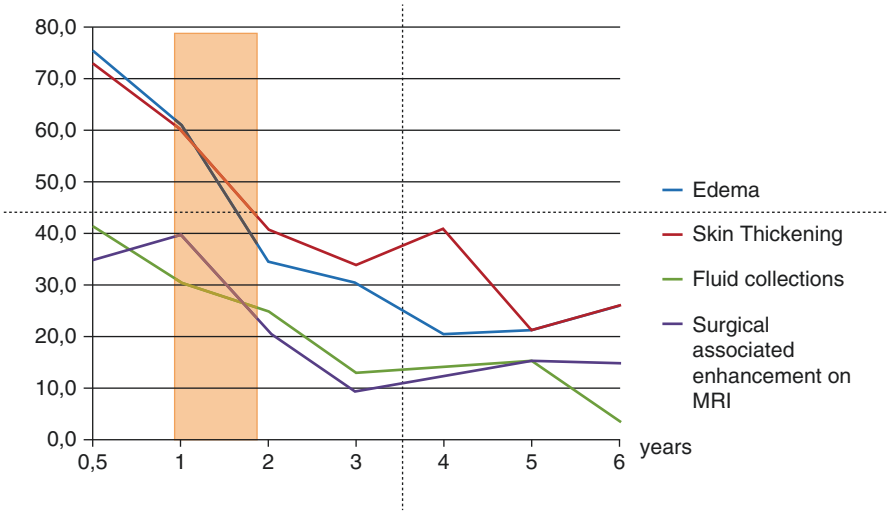

Fig. 18.1 Expected chronological appearance of the surgical findings on the conservatively treated breast

18.2.2.1 Fluid Collections

A common finding on posttreatment mammography is fluid collections at the lumpectomy site. Dead space is often intentionally left at surgery of a malignant breast neoplasm to allow fluid to fill in the space and, in this way, achieve better cosmesis [3].

Fluid with or without blood which collects in the postoperative cavity appears on mammography as an oval or round circumscribed or obscured mass that is most commonly seen within the surgical bed and should not be confused with recurrent tumor (Figs. 18.2 and 18.3).

Sonography of these collections often reveals a complex cystic mass with septations, loculations, thick walls, or a combination of these findings (Figs. 18.2 and 18.3).

Approximately half of breast cancer patients have fluid collections at the surgical site at 4 weeks after surgery and about 25% at 6 months. Over subsequent months, postoperative seromas, and hematomas are gradually resorbed and are replaced by scarring and fibrosis.

Fluid collections generally diminish in size over time and resolve completely by 12–18 months after surgery, although they may persist in a minority of patients. Any increase in the size of a fluid collection over time should alert the radiologist to a possible recurrence.

18.2.2.2 Breast Edema and Skin Thickening

Breast edema and skin thickening are posttreatment findings with similar time courses for appearance and regression. Typically, post-lumpectomy edema is localized to the area of the incision, and breast edema from radiation therapy usually encompasses the entire breast.

Breast edema may present as more of an accentuated trabecular pattern or as overall increased breast density depending on the degree of the edema (Figs. 18.4 and 18.5). The perceived increased density in the irradiated breast may also be explained by suboptimal exposure because the treated breast often is swollen and less compressible.

Skin thickening during the period after radiation is secondary to breast edema from the damage of small vessels. Skin thickening is the most common finding after breast-conserving therapy, reported in up to 90% of patients. Normal skin thickness of the breast as seen on mammograms is 2 mm. The skin thickness after radiation therapy may reach 1 cm or more (Figs. 18.4 and 18.5).

Breast edema and skin thickening are best appreciated when compared with the contralateral breast or with pretreatment mammograms (Figs. 18.4 and 18.5).

At mammography, maximal breast edema and skin thickening are usually seen during the first 6 months after completion of radiation therapy. These alterations then diminish and attain stability within 2–3 years.

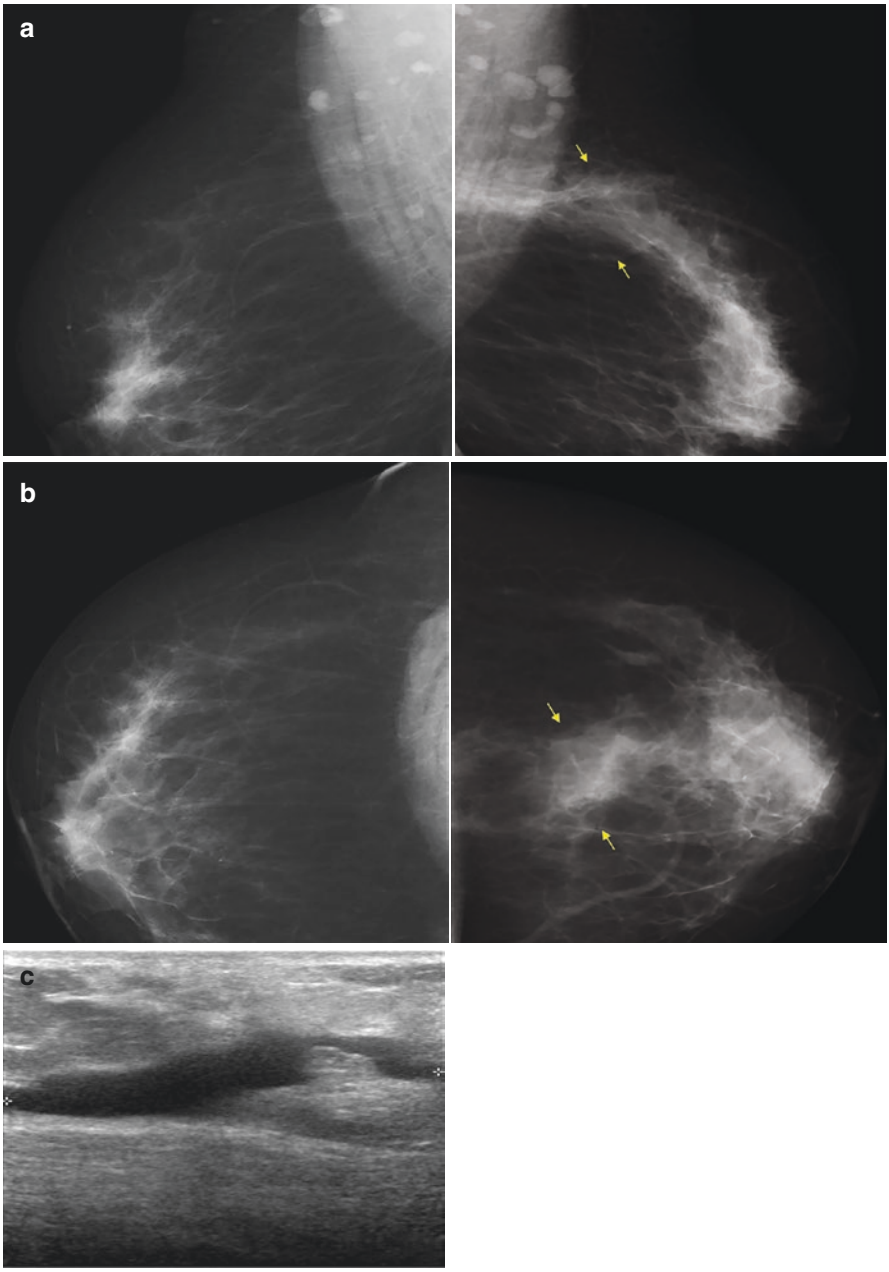

Fig. 18.2 Postoperative seroma in a 62-year-old woman with history of invasive left breast carcinoma. Mediolateral oblique (**a**) and craniocaudal (**b**) mammograms obtained 6 months after radiation therapy show an ill-defined mass in upper outer left breast consistent with postoperative seroma (arrows). The ultrasound image (**c**) shows a complex solid-cystic mass. These findings are consistent with postoperative seroma given history of breast conservation therapy in this area

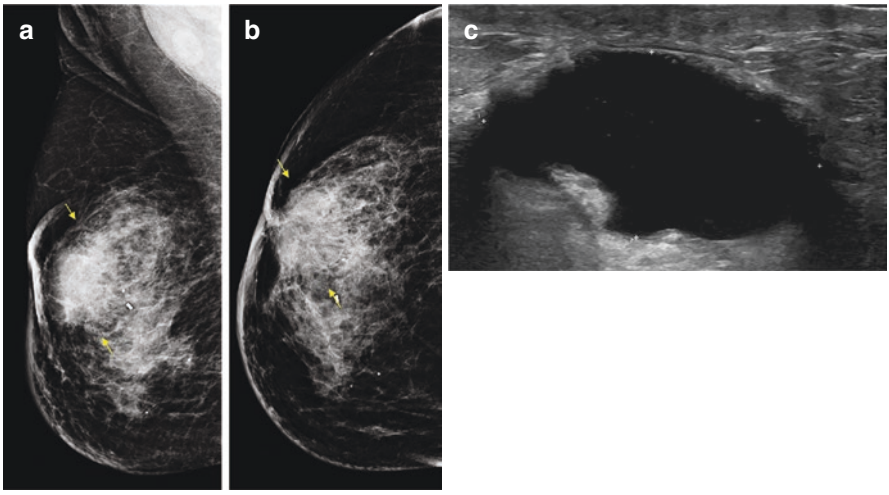

Fig. 18.3 Postoperative seroma in a 44-year-old woman with history of in situ right breast carcinoma. Mediolateral (**a**) and craniocaudal (**b**) mammograms obtained 6 months after radiation therapy show an obscured oval mass in upper outer right breast consistent with postoperative seroma (arrows). Increased breast density and skin thickening can also be seen. The ultrasound image (**c**) shows a complex solid-cystic mass with thick walls. These findings are consistent with postoperative seroma given history of breast conservation therapy in this area

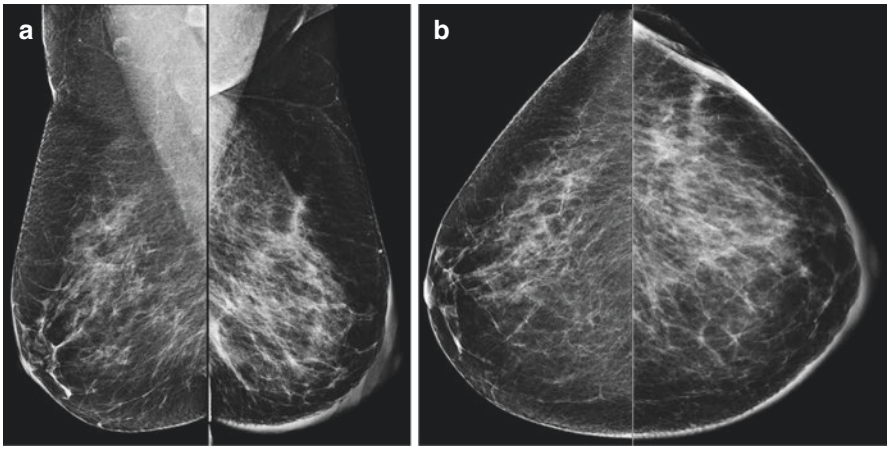

Fig. 18.4 Breast edema and skin thickening due to radiation therapy in a 74-year-old woman with history of invasive left breast carcinoma. Mediolateral oblique (**a**) and craniocaudal (**b**) mammograms of the right and left breasts obtained 1 year after radiation therapy show increased breast density and skin thickening of the left breast

Edema or skin thickening that increases after stability has been achieved should alert radiologists to the need for further investigation. The differential diagnoses of recurrent or worsening breast edema include lymphatic spread of cancer, obstructed venous drainage, congestive heart failure, and infection.

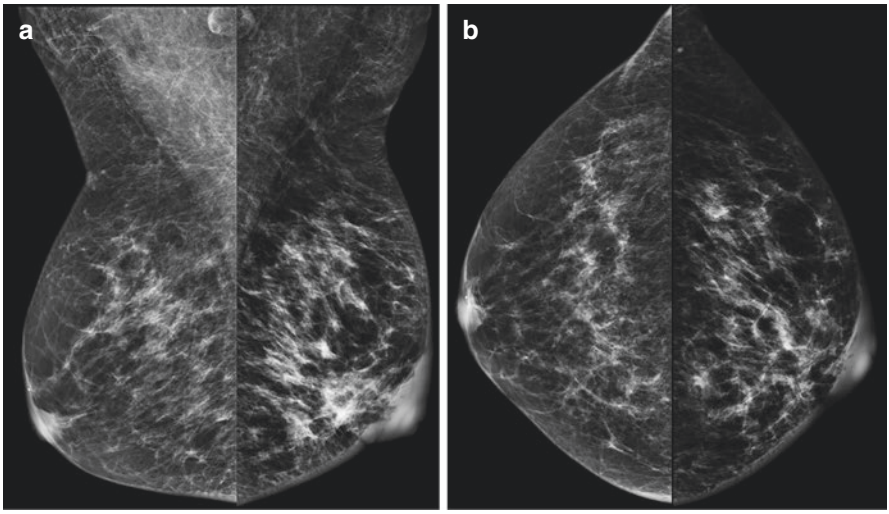

Fig. 18.5 Breast edema and skin thickening due to radiation therapy in an 80-year-old woman with history of invasive left breast carcinoma. Mediolateral oblique (**a**) and craniocaudal (**b**) mammograms of right and left breasts obtained 3 years after radiation therapy show increased breast density and skin thickening of the left breast, which is most prominent in the periareolar area

18.2.2.3 Fat Necrosis

Fat necrosis of the breast is a benign entity which may be seen after trauma, surgery, and radiotherapy, among other conditions [6–8]. Clinically, the patients may be asymptomatic or may present with a palpable lump, skin tethering, and induration.

In imaging studies, the appearance of fat necrosis ranges from typically benign to worrisome for malignancy, depending on the time at which diagnostic imaging is performed. This is directly related to whether inflammation or fibrosis is predominating within the lesion, and correlation with clinical history is very important for the correct evaluation of these lesions [6].

The classically benign appearing mammographic findings for fat necrosis are the oil cysts, which are masses with central lucency. These oil cysts may be accompanied by peripheral rim or "eggshell" calcifications (Fig. 18.6).

The presence of calcifications on mammography suggests that most of the calcifications will evolve to a dystrophic morphology as the lesions become older. At the beginning of the calcification process, sometimes we can intercept pleomorphic or amorphous appearing calcifications on mammography.

Fat necrosis appearing as suspicious noncalcified masses may demonstrate increased density due to progressive parenchymal fibrosis resulting in an ill-defined, spiculated mass on mammography, and biopsy may be warranted for the adequate diagnosis.

Fat necrosis ranges from simple cyst to complex cystic or solid masses on sonography (Fig. 18.7). As the appearance of fat necrosis can be undetermined

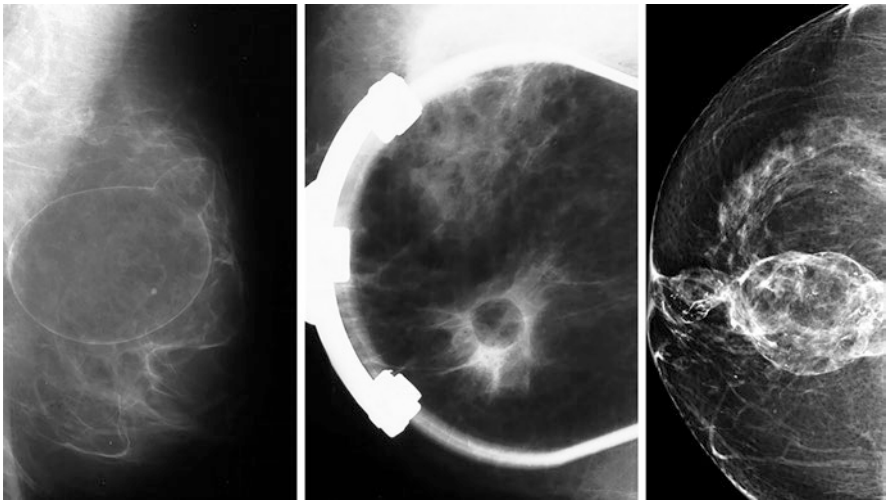

Fig. 18.6 Different examples of fat necrosis on mammography

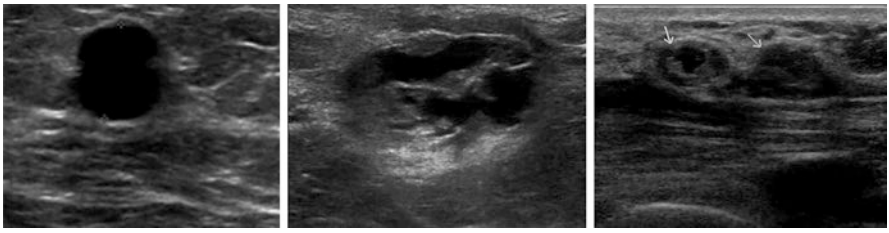

Fig. 18.7 Different examples of fat necrosis on ultrasound

on ultrasound, whenever we are faced with complex or inconclusive masses in a posttreated breast, mammographic correlation is essential for their proper evaluation.

The amount of inflammatory reaction, presence of liquefied fat, and the degree of fibrosis determine the varying findings of fat necrosis on MRI (Fig. 18.8). Administration of contrast may result in enhancement, particularly during the early stages of the inflammatory process. The presence of fat signal on MRI findings usually suggests its benignity.

Nonfatty signal intensity irregular masses with variable enhancement patterns are likely a reflection of the later stages of fat necrosis, when the fibrotic chances are more prominent.

In summary, mammography is more specific than sonography, and emphasis should be placed on mammography in making the diagnosis of fat necrosis. In selected cases, MRI may be helpful in showing findings consistent with fat necrosis, especially when fat signal can be detected inside the imaging findings.

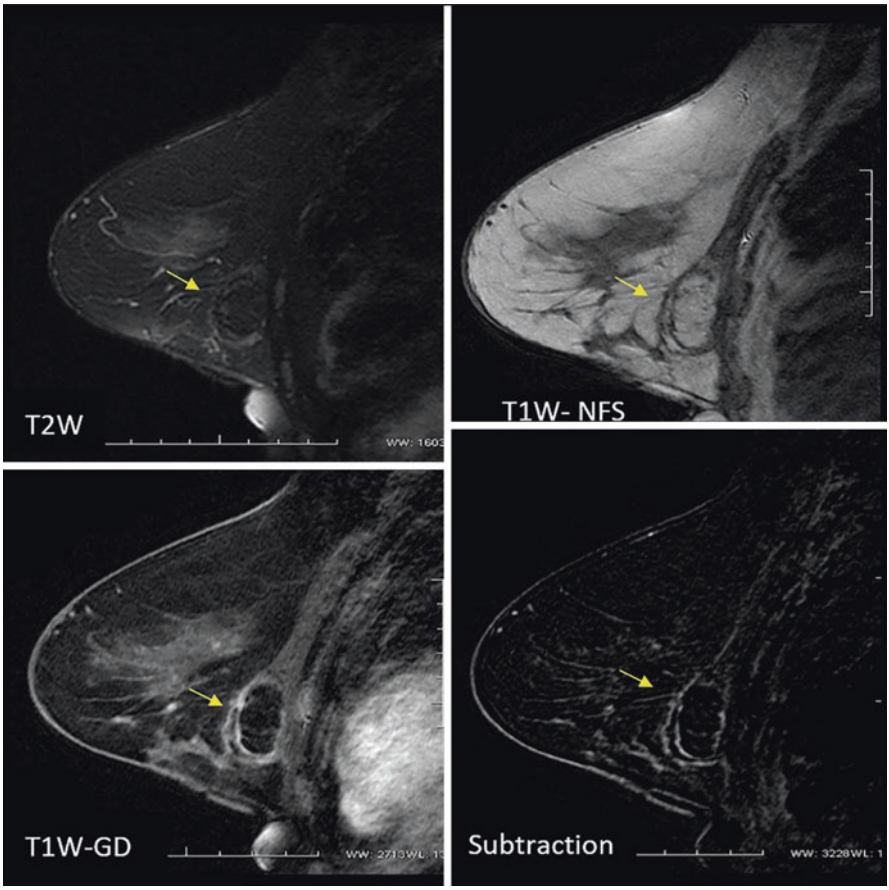

Fig. 18.8 Fat necrosis on MRI. T1-weighted nonfat-saturated image (NFS) shows a hyperintense circumscribed mass with a hypointense rim (arrow). The mass signal is similar to the adjacent fat, characteristic of fat necrosis. Sagittal T1-enhanced and fat-suppressed and subtraction images show the fat-containing mass with a non-enhancing thin fibrous rim (arrow)

18.2.2.4 Architectural Distortion

Architectural distortion in the treated breast develops secondary to scar formation and fat necrosis. Architectural distortion is commonly seen in the lumpectomy bed and within the lower axilla if sentinel node biopsy or axillary node dissection was performed (Fig. 18.9).

Parenchymal scarring and fat necrosis can cause an irregular spiculated or indistinct mass, associated with skin retraction that mimics recurrent malignancy.

However, the presence of the following mammographic features is more likely to suggest benign architectural distortion rather than tumor recurrence: the presence of

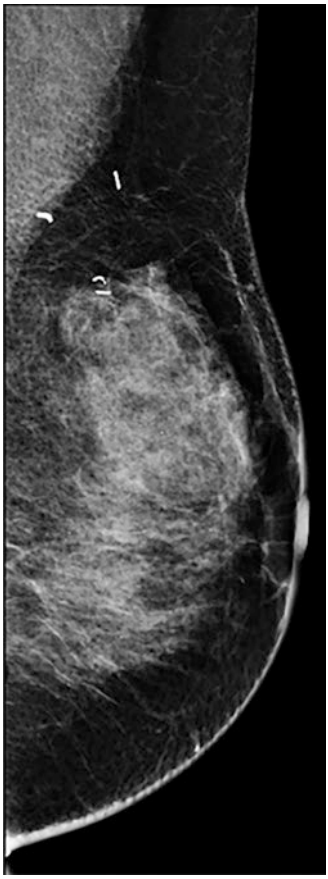

Fig. 18.9 Mediolateral oblique mammogram of the left breast shows post lumpectomy site as an area of architectural distortion in the upper quadrant. Surgical clips delineate site of tumor removal

central lucencies; a changing appearance on different projections; and thick, curvilinear spiculations [3] (Fig. 18.10).

Central lucencies suggest scarring because they represent fat trapped by fibrous stranding in the scar. These differentiating features can often be helpful, although they are not always reliable. For instance, some breast carcinomas, notably, infiltrating lobular, may contain central lucencies and may not have a central mass.

Architectural distortion usually diminishes in conspicuity and stabilizes over a 2-year period. In evaluating suspicious lesions, spot compression, magnification, and tomosynthesis views are helpful in showing the features of scarring and in excluding recurrent tumors.

Annual follow-up mammograms are necessary to show the sequential decrease in the size and prominence of the density to ensure its benignity. If the scar grows in size or if it becomes denser or more mass like, recurrent tumor should be suspected and should prompt biopsy [4, 9].

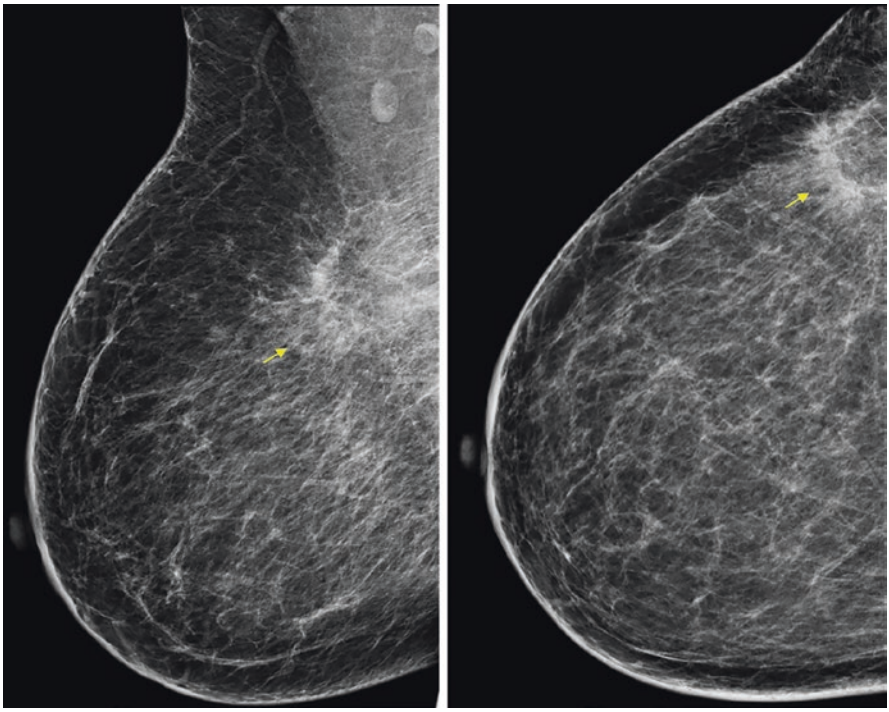

Fig. 18.10 Mediolateral oblique and craniocaudal mammogram of the right breast shows post-lumpectomy site as an area of architectural distortion in the upper outer quadrant (arrows). Note the presence of central lucency and thick, curvilinear spiculations suggestive of surgical scar

18.2.2.5 Benign Calcifications

Benign calcifications may develop at the postoperative site, with a reported incidence of 28% within the first 6–12 months after radiation therapy.

Dystrophic calcifications generally develop in areas of fat necrosis and are usually round and coarse and typically large and often have lucent centers (Fig. 18.11). Suture material left in the breast may also calcify, forming distinctive shapes such as knot like, rod-shaped, and curvilinear (Fig. 18.12).

On magnification views, these benign forms of calcifications can often be recognized and differentiated from pleomorphic or other suspicious calcifications associated with malignancy (Fig. 18.13).

At times, however, dystrophic calcifications may simulate malignancy. As previously described, early calcification of evolving fat necrosis may produce an appearance that is mammographically inconclusive. In such cases, careful inspection of the previous mammograms may help by showing regression of the calcifications over time or formation of the calcifications around a radiolucent center of fat, suggesting the benign nature (Fig. 18.14). If calcifications cannot be distinguished from a possible malignant process radiographically, biopsy should be considered.

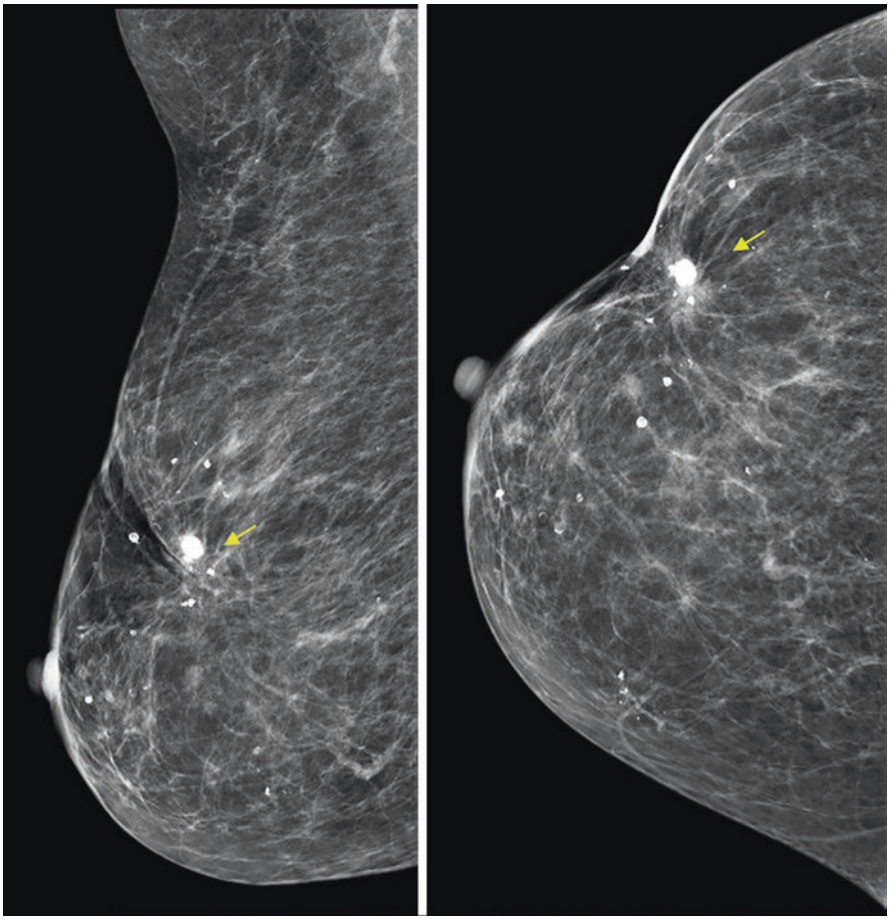

Fig. 18.11 Dystrophic calcifications in 72-year-old woman with history of right breast carcinoma. Mediolateral oblique and craniocaudal mammograms of right breast obtained 12 years after lumpectomy and radiation therapy. Large coarse calcifications (arrows), representing dystrophic calcifications, are seen within tumor excision site

18.3 Imaging Methods

18.3.1 Mammography

There is currently no universal guideline for posttreatment imaging surveillance. There are multiple proposed guidelines, and they recommend mammography as part of routine follow-up after BCT [10].

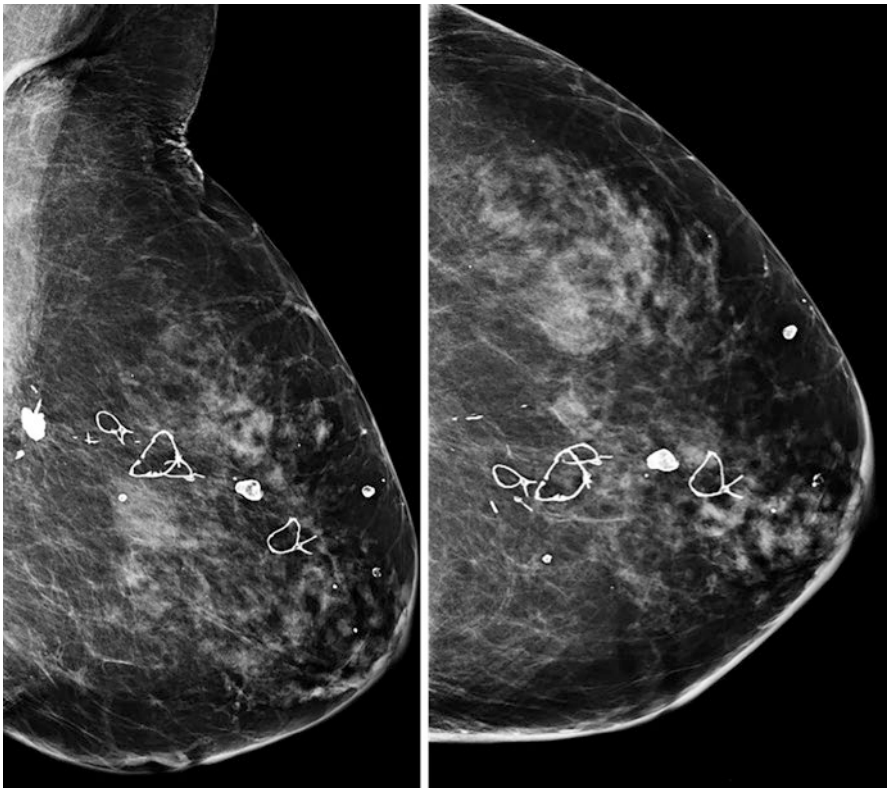

Fig. 18.12 Sutural calcifications in a 91-year-old woman with a history of left breast cancer that was treated with lumpectomy and radiation therapy. Mediolateral oblique and craniocaudal mammograms of post-lumpectomy and radiation of the left breast show curvilinear and knot-shaped calcifications. These findings are characteristic of sutural calcifications, which are most commonly seen in the irradiated breast and are rarely observed after benign breast surgery

Postsurgical mammograms can be obtained before the initiation of radiation therapy on selected cases to determine the completeness of tumor excision by identifying residual calcifications within the breast.

In most cases, however, mammograms of both breasts are obtained 6 months after the completion of radiation therapy. Images obtained at that time include craniocaudal and mediolateral oblique views. Magnification views of the lumpectomy bed are also routinely obtained even though there is no evidence to support improved outcome. Subsequently, annual mammography is normally performed [3, 5].

Mammographic imaging in patients after breast conservation surgery is challenging because surgery alters the normal breast architecture. The distinction of normal postoperative changes from true findings of recurrence becomes demanding making it essential to know what are the expected posttreatment findings.

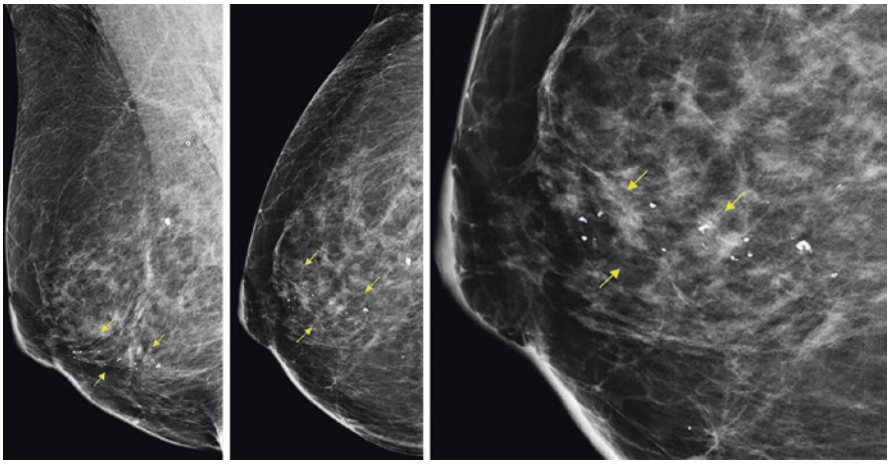

Fig. 18.13 Dystrophic calcifications in a 65-year-old woman with history of right breast carcinoma. Mediolateral oblique and craniocaudal mammograms of right breast obtained 5 years after lumpectomy and radiation therapy. Coarse calcifications (arrows), representing dystrophic calcifications, are seen within tumor excision site

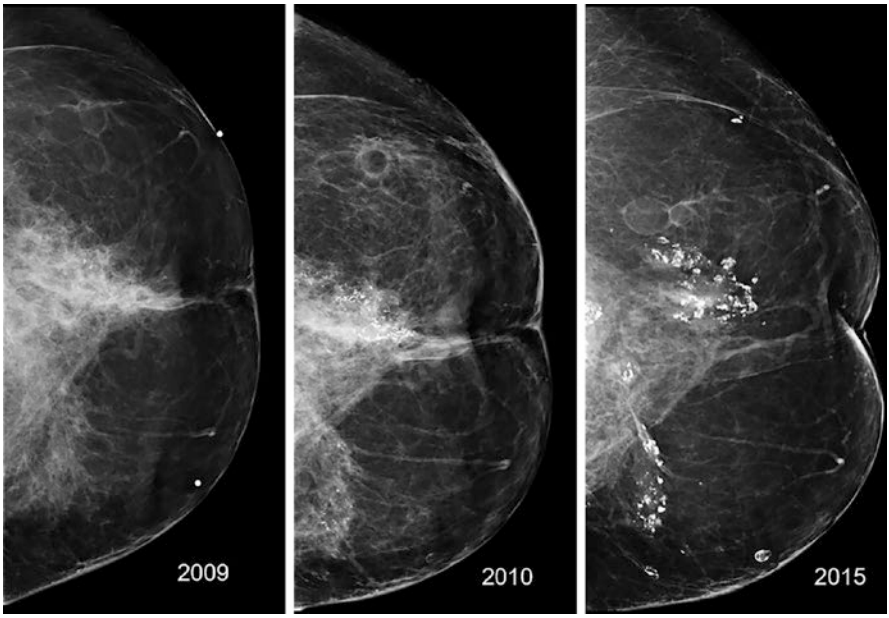

Fig. 18.14 Follow-up mammograms help showing the formation of the calcifications around the area of fat necrosis, suggesting the benign nature

18.3.2 Tomosynthesis

Digital breast tomosynthesis (DBT) is a mammographic technique that entails imaging of the breast tissue in multiple sections at varied angles. The overlap of parenchymal tissues is largely resolved, reducing the false positives as well as adequately identifying true lesions, increasing the sensitivity of a mammogram [7, 11].

DBT not only helps in triangulation of a lesion but also reduces the requirement for additional views and lowers the patient call-back rate.

Similar to screening mammography, DBT also helps resolve post conservation changes such as a scar or other asymmetries due to parenchymal edema from a true recurrence. The fat density within the scar and that associated with benign calcification may also be better appreciated on DBT whereas a true recurrence would demonstrate a mass.

A study by Sia et al. [11] also reported that DBT decreases the rate of indeterminate findings in surveillance imaging of conservatively treated breasts.

18.3.3 Ultrasound

Breast ultrasound is a widely used method adjuvant to mammography for the further characterization of lesions identified on mammography. It provides additional information on lesions' margin, shape, internal echotexture, vascularity, and elasticity [7, 12].

Ultrasonography is also useful in demonstrating the origin of a palpable mass either within the breast parenchyma or the implant, in cases of breast reconstruction.

If a lesion has suspicious morphology on any breast imaging method and is visible on ultrasound, ultrasound-guided biopsy is the procedure of choice. When performed correctly, this procedure is safe and minimally invasive and has a high diagnostic accuracy, comparable to surgical biopsy.

18.3.4 Magnetic Resonance

An important component in evaluating the role of MRI following BCS is to compare to the current standard of mammography. Whereas data support the concept that MRI is more sensitive than mammography as part of high-risk screening, less data are available in the post-BCT setting. Robertson et al. [10] performed a systematic review of nine studies and found that for ipsilateral breast tumor recurrences,

the sensitivity/specificity of MRI was 86–100%/93% as compared with 64–67%/85–97% for mammography with MRI also having higher sensitivity for nonroutine ipsilateral breast recurrences.

Another potential role for MRI in patients following BCS is to evaluate findings identified on surveillance mammography. Differentiating benign and malignant lesions on MRI were summarized by Drukteinis et al. [13] who concluded that MRI is useful in evaluating posttreatment changes. Breast MR imaging is especially useful in differentiating scar tissue from tumor recurrence, as non-enhancing areas have a high negative predictive value for malignancy (88–96%).

Another challenging finding is fat necrosis, which can mimic tumor recurrence on mammography and ultrasonography and lead to increased numbers of biopsies/interventions. As described above, MRI can help identify fat signals within lesions and characterize these areas as benign.

Skin thickening, architectural distortion, resolving edema, and signal voids from surgical or biopsy clips or from prior bleeding (hemosiderin) are frequent findings in the post-BCT breast [4, 12–14].

The majority of these findings progressively decrease over time. Stability or less prominent findings are expected and typically occur within 3 years. Edema in the post-BCS breast may never resolve entirely, but increasing edema may be a sign of recurrent cancer.

The normal appearance of a post-lumpectomy breast often includes a fluid cavity filled with blood or serum (seroma) at the surgical site. Smooth, thin (≤5 mm) rim enhancement around a seroma should be considered benign (Fig. 18.15). Most seromas slowly diminish in size and evolve into scars (architectural distortion) by 1 year after surgery.

A minimal or small focal area of enhancement or thin linear non-mass-like enhancement (NME) without an associated mass can be seen for up to 18 months at the lumpectomy site. This enhancement likely represents the healing process after surgery and radiation therapy and can be considered appropriate for 6-month follow-up (BI-RADS 3 category) if no previous study is available for comparison, and no clinical or worrisome mammographic findings are present.

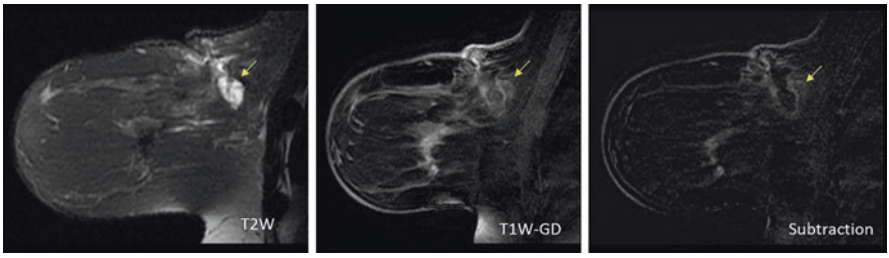

Fig. 18.15 MRI of post-lumpectomy and radiation therapy of the right breast shows fluid cavity at the surgical site with smooth, thin rim enhancement (arrows)

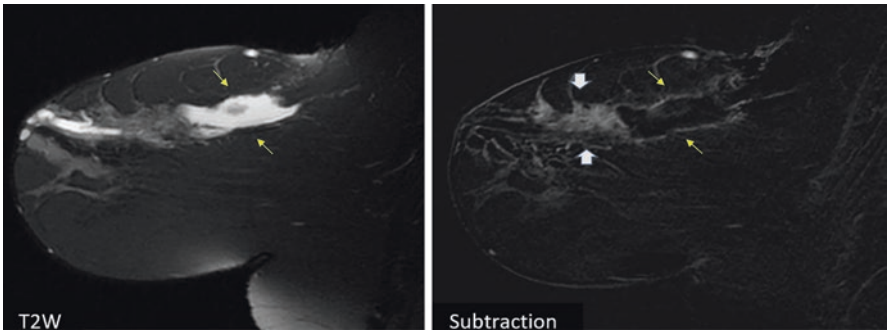

Fig. 18.16 Post-lumpectomy with positive margins MRI was performed before the radiation therapy of the right breast. Fluid cavity at the surgical site with smooth, thin rim enhancement (thin arrows). Anterior to the seroma, it is possible to identify a suspicious non-mass-like segmental enhancement (large arrows)

In contrast, mass-like enhancement or NME of ductal or segmental distribution can indicate recurrence (Fig. 18.16). Therefore, at MR imaging of the post-BCS breast, it is important to identify lesions that are benign or appropriate for short-interval imaging surveillance to minimize unnecessary intervention, as well as to discern suspicious lesions and optimize the diagnosis of recurrence.

Although there is no randomized evidence supporting the routine use of MRI in surveillance post-BCS, a review of the literature by Fisher et al. [2] demonstrates that MRI has increased sensitivity compared to mammography to detect recurrences and can help evaluate inconclusive mammographic abnormalities before biopsy (Fig. 18.17).

In patients with higher risk of local recurrence, surveillance with MRI may represent an effective surveillance strategy although no subgroups have been identified that could benefit from its use and neither has the impact on cost and quality of life been evaluated.

18.4 Conclusion

After breast-conserving surgery and radiation therapy, several alterations of the breast occur and evolve over time.

As surgery and radiotherapy alter the appearance of the breasts, distinguishing between recurrence and benign postsurgical changes can be challenging due to overlapping features. Despite this, differentiation between these two entities is usually possible by recognizing characteristic features of posttreatment sequelae and the evolution of the appearance of the conservatively treated breast by comparing interval findings on serial studies. However, certain features of these benign changes may simulate patterns of tumor recurrence and biopsy may be warranted.

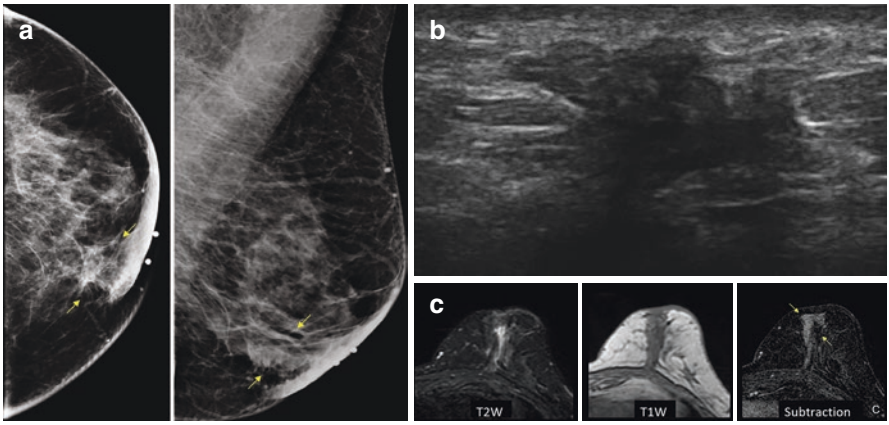

Fig. 18.17 Mediolateral oblique and craniocaudal mammogram (**a**) of the left breast after lumpectomy and radiation therapy shows area of architectural distortion at the lumpectomy site in the retroareolar region, with associated increased density (arrows). Target ultrasound (**b**) shows irregular mass with angulated margins. MRI (**c**) was performed to better access this finding and demonstrated segmentar enhancement of the area and biopsy was recommended. Histologic result was steatonecrosis associated with chronic granulomatous inflammatory process with multinucleated giant foreign body cells

18.5 Summary

The posttreatment alterations include fluid collections, breast edema, skin thickening, fat necrosis, architectural distortion, and calcifications. There is an expected chronological appearance for these findings on the conservatively treated breast, and this is important to know for the correct diagnosis and conduct.

Mammograms and other imaging modalities should be evaluated and compared with earlier studies to maximize detection of recurrent breast carcinoma while minimizing unnecessary recalls and biopsies.

References

1. Joshi SC, Khan FA, Pant I, Shukla A. Role of radiotherapy in early breast cancer: an overview. Int J Health Sci (Qassim). 2007;1(2):259.
2. Fisher B, Anderson S, Bryant J, Margolese RG, Deutsch M, Fisher ER, et al. Twenty-year follow-up of a randomized trial comparing total mastectomy, lumpectomy, and lumpectomy plus irradiation for the treatment of invasive breast cancer. N Engl J Med. 2002;347(16):1233–41.
3. Chansakul T, Lai KC, Slanetz PJ. The postconservation breast: part 1, expected imaging findings. Am J Roentgenol. 2012;198:321–30.
4. Chansakul T, Lai KC, Slanetz PJ. The postconservation breast: part 2, imaging findings of tumor recurrence and other long-term sequelae. Am J Roentgenol. 2012;198(2):331–43.
5. Krishnamurthy R, Whitman GJ, Stelling CB, Kushwaha AC. Mammographic findings after breast conservation therapy. Radiographics. 1999;19(suppl_1):S53–62.

6. Fernandes Chala L, de Barros N, de Camargo Moraes P, Endo É, Kim SJ, Maciel Pincerato K, et al. Fat necrosis of the breast: mammographic, sonographic, computed tomography, and magnetic resonance imaging findings. Curr Probl Diagn Radiol. 2004;33(3):106–26.
7. Tayyab SJ, Adrada BE, Rauch GM, Yang WT. A pictorial review: multimodality imaging of benign and suspicious features of fat necrosis in the breast. Br J Radiol. 2018;91(1092):2018021.
8. Kerridge WD, Kryvenko ON, Thompson A, Shah BA. Fat necrosis of the breast: a pictorial review of the mammographic, ultrasound, CT, and MRI findings with histopathologic correlation. Radiol Res Pract. 2015;2015:613139.
9. Günhan-Bilgen I, Oktay A. Mammographic features of local recurrence after conservative surgery and radiation therapy: comparison with that of the primary tumor. Acta radiol. 2007;48(4):390–7.
10. Robertson C, Ragupathy SKA, Boachie C, Fraser C, Heys SD, MacLennan G, et al. Surveillance mammography for detecting ipsilateral breast tumour recurrence and metachronous contralateral breast cancer: a systematic review. Eur Radiol. 2011;21(12):2484–91.
11. Sia J, Moodie K, Bressel M, Lau E, Gyorki D, Skandarajah A, et al. A prospective study comparing digital breast tomosynthesis with digital mammography in surveillance after breast cancer treatment. Eur J Cancer. 2016;61:122–7.
12. Ramli Hamid MT, Rahmat K, Hamid SA, Kirat Singh SK, Hooi TG. Spectrum of multimodality findings in post-surgical breast cancer imaging. Curr Med Imaging Former Curr Med Imaging Rev. 2018;15(9):866–72.
13. Drukteinis JS, Gombos EC, Raza S, Chikarmane SA, Swami A, Birdwell RL. MR imaging assessment of the breast after breast conservation therapy: distinguishing benign from malignant lesions. Radiographics. 2012;32(1):219–34.
14. Margolis NE, Morley C, Lotfi P, Shaylor SD, Palestrant S, Moy L, et al. Update on imaging of the postsurgical breast. Radiographics. 2014;34(3):642–60.

Chapter 19
Adjuvant Therapy

Laura Testa and Renata Colombo Bonadio

19.1 Indications

Adjuvant systemic treatment improved the outcomes of patients with localized breast cancer significantly, impacting the reduction of breast cancer mortality. Nevertheless, appropriate selection of candidates is crucial, since it may be associated with severe side effects, including late toxicities from chemotherapy such as secondary myelodysplasia and leukemia. Moreover, some patients have a high chance of cure without requiring systemic therapy.

For localized disease treated with curative intent, the addition of systemic therapy aims to control microscopic cancer cells, decreasing the risk of recurrence. The systemic therapy can be used before or after surgery (neoadjuvant or adjuvant, respectively). Here, we discuss indications of systemic therapy for patients already submitted to surgery. Indications of neoadjuvant therapy are discussed in a separate chapter.

The indication of adjuvant chemotherapy will depend on tumor characteristics such as size, grade, lymph node status, and expression of hormone receptor (estrogen receptor (ER) and progesterone receptor (PR)) and HER2. Patient characteristics, including age, performance status, and comorbidities, are also important for the decision-making process.

For hormone receptor (ER or PR)-positive breast cancer, adjuvant endocrine therapy should be considered for all patients [1]. Otherwise, the use of adjuvant chemotherapy in this group is more complex, with diverse factors influencing the decision. Adjuvant chemotherapy is usually recommended for those with more than

L. Testa (✉) · R. C. Bonadio
Departamento de Oncologia, Instituto do Cancer do Estado de Sao Paulo ICESP, São Paulo, SP, Brazil
e-mail: laura.testa@hc.fm.usp.br

S. J. Kim Hsieh, E. A. Morris (eds.), *Modern Breast Cancer Imaging*,
https://doi.org/10.1007/978-3-030-84546-9_19

four positive lymph nodes. For patients with negative or less than four positive lymph nodes, clinical characteristics and tumor pathology need to be evaluated to assess patients' risk of recurrence and the benefit of chemotherapy. Features associated with a higher risk of recurrence include younger age, premenopausal status, grade 3, positive lymph nodes, presence of angiolymphatic invasion, and low expression of ER/ PR.

More recently, a helpful tool that can be considered is the use of assays that evaluate recurrence risk based on gene expression profiles from tumor samples. The oncotype DX recurrence score (RS) is the most well-validated assay to predict adjuvant chemotherapy benefit. Oncotype DX RS provided a score based on gene expression that allows a classification of the risk of recurrence in low (RS < 11), intermediate (RS 11–25), or high (RS > 25). The TAILORx trial, a phase III trial, evaluated the use of oncotype DX to predict the benefit of chemotherapy for hormone receptor-positive node-negative breast cancer. Patients with low-risk received endocrine therapy alone, those with high risk received endocrine therapy plus chemotherapy, and those with intermediate risk were randomized to endocrine therapy alone or endocrine therapy plus chemotherapy. Results showed that patients in the intermediate group can be treated with endocrine therapy alone with satisfactory outcomes [2]. However, subgroup analysis suggested that women younger than 50 years with a RS of 16–25 might benefit from the addition of chemotherapy [3]. Based on these results, patients with node-negative disease may be spared from adjuvant chemotherapy if they present a RS less than 16 for women with any age or less than 26 for those older than 50 years.

HER2 amplification is an important driver of HER2-positive breast cancer. Adjuvant anti-HER2 therapy is indicated in addition to chemotherapy for HER2-positive tumors greater than 1 cm or node-positive [1, 4]. Pivotal trials of anti-HER2 therapy did not have a representative population of node-negative tumors smaller than 1 cm. Nevertheless, anti-HER2 therapy may also be considered for this group based on a significant risk of relapse described in some studies, especially when high-risk features are present [5, 6].

Finally, neoadjuvant or adjuvant chemotherapy has a major role for triple-negative (TN) breast cancer, usually characterized by aggressive behavior and high recurrence risk. For these patients, chemotherapy should be considered for any tumor greater than 0.5 cm or with positive lymph node (regardless of primary tumor size) [1].

19.2 Treatment Options

Treatment regimens based on anthracyclines and taxanes are standard regimens for breast cancer patients with an indication of adjuvant chemotherapy. These drugs may be combined in different ways, depending on local expertise and preference. A largely used regimen is AC-T, based on doxorubicin and cyclophosphamide,

sequential with paclitaxel [7]. AC is done for four cycles (every 3 weeks or every 2 weeks in the dense dose regimen), followed by weekly paclitaxel for 12 weeks.

However, anthracyclines may lead to some concerning adverse events such as cardiotoxicity and secondary leukemia. Regimens without anthracyclines constitute an alternative, especially for patients with contraindications to anthracyclines. In this way, TC (docetaxel and cyclophosphamide, every 3 weeks, for four to six cycles) and CMF (cyclophosphamide, methotrexate, 5-fluorouracil, every 4 weeks, for six cycles) regimens are also common options of adjuvant chemotherapy [7, 8].

In recent years, relevant studies suggested that patients who received neoadjuvant systemic therapy may have their adjuvant treatment modulated by the response to neoadjuvant therapy. For patients with triple-negative breast cancer, those who present residual disease in the surgical specimen after neoadjuvant therapy benefit from additional adjuvant therapy with capecitabine for 6 months [9].

As anti-HER2 adjuvant therapy, the monoclonal antibody trastuzumab remains the cornerstone [10]. Adjuvant trastuzumab is used for a year and is started concurrently with a taxane. For locally advanced tumors, AC-TH (doxorubicin and cyclophosphamide, followed by paclitaxel and trastuzumab) and TCH (docetaxel, carboplatin, and trastuzumab) are preferred regimens [11, 12]. Recent studies have favored non-anthracycline regimens due to a similar efficacy and lower rate of late toxicities than anthracycline-based regimens in HER2-positive breast cancer [13]. Finally, for early HER2-positive breast cancer, TH (taxane and trastuzumab) regimen is an option, which is preferred, especially for node-negative tumors smaller than 2 cm [14]. An intensification of adjuvant anti-HER2 therapy, with the addition of pertuzumab to trastuzumab, has a small benefit in disease-free survival and may be considered for selected high-risk patients [15].

For HER-2 positive breast cancer patients who received neoadjuvant treatment, the anti-HER2 therapy is continued after surgery for a total duration of 1 year. When a complete pathological response is observed, the same anti-HER2 therapy is continued as adjuvant therapy. Otherwise, patients with residual disease have a relevant disease-free survival gain with the modification of the adjuvant therapy to T-DM1, an antibody-drug conjugate of trastuzumab and emtansine [16].

As adjuvant endocrine therapy, tamoxifen or an aromatase inhibitor is usually indicated. Treatment with an aromatase inhibitor is preferred for postmenopausal women, as the single endocrine therapy or with a switch to tamoxifen [17]. Tamoxifen is the treatment of choice for premenopausal women who will not receive ovarian suppression. As an alternative, premenopausal women, especially high-risk patients, may be treated with the addition of ovarian suppression to endocrine therapy (tamoxifen or an aromatase inhibitor) [18].

After treatment of localized disease, patients are followed with periodic consult and physical examination (every 3–6 months). Mammography should be done annually to detect local recurrence and second primary breast cancer that are amenable to potentially curative treatment. Other routine image tests are not indicated during follow-up and should be performed in case of suspicion of metastatic disease based on patients' signs and symptoms.

References

1. Cardoso F, Kyriakides S, Ohno S, Penault-Llorca F, Poortmans P, Rubio IT, et al. Early breast cancer: ESMO clinical practice guidelines for diagnosis, treatment and follow-up. Ann Oncol. 2019;30(10):1674.
2. Sparano JA, Gray RJ, Makower DF, Pritchard KI, Albain KS, Hayes DF, et al. Adjuvant chemotherapy guided by a 21-gene expression assay in breast cancer. N Engl J Med. 2018;379(2):111–21.
3. Sparano JA, Gray RJ, Ravdin PM, Makower DF, Pritchard KI, Albain KS, et al. Clinical and genomic risk to guide the use of adjuvant therapy for breast cancer. N Engl J Med. 2019;380(25):2395–405.
4. Denduluri N, Somerfield MR, Giordano SH. Selection of optimal adjuvant chemotherapy and targeted therapy for early breast Cancer: ASCO clinical practice guideline focused update summary. J Oncol Pract. 2018;14(8):508–10.
5. Gonzalez-Angulo AM, Litton JK, Broglio KR, Meric-Bernstam F, Rakkhit R, Cardoso F, et al. High risk of recurrence for patients with breast cancer who have human epidermal growth factor receptor 2-positive, node-negative tumors 1 cm or smaller. J Clin Oncol. 2009;27(34):5700–6.
6. Livi L, Meattini I, Saieva C, Franzese C, Di Cataldo V, Greto D, et al. Prognostic value of positive human epidermal growth factor receptor 2 status and negative hormone status in patients with T1a/T1b, lymph node-negative breast cancer. Cancer. 2012;118(13):3236–43.
7. Peto R, Davies C, Godwin J, Gray R, Pan HC, Clarke M, et al. Comparisons between different polychemotherapy regimens for early breast cancer: meta-analyses of long-term outcome among 100,000 women in 123 randomised trials. Lancet. 2012;379(9814):432–44.
8. Blum JL, Flynn PJ, Yothers G, Asmar L, Geyer CE, Jacobs SA, et al. Anthracyclines in Early Breast Cancer: The ABC Trials-USOR 06-090, NSABP B-46-I/USOR 07132, and NSABP B-49 (NRG Oncology). J Clin Oncol. 2017;35(23):2647–55.
9. Masuda N, Lee SJ, Ohtani S, Im YH, Lee ES, Yokota I, et al. Adjuvant capecitabine for breast cancer after preoperative chemotherapy. N Engl J Med. 2017;376(22):2147–59.
10. Moja L, Tagliabue L, Balduzzi S, Parmelli E, Pistotti V, Guarneri V, et al. Trastuzumab containing regimens for early breast cancer. Cochrane Database Syst Rev. 2012;4:CD006243.
11. Romond EH, Perez EA, Bryant J, Suman VJ, Geyer CE, Davidson NE, et al. Trastuzumab plus adjuvant chemotherapy for operable HER2-positive breast cancer. N Engl J Med. 2005;353(16):1673–84.
12. Slamon D, Eiermann W, Robert N, Pienkowski T, Martin M, Press M, et al. Adjuvant trastuzumab in HER2-positive breast cancer. N Engl J Med. 2011;365(14):1273–83.
13. van der Voort A, van Ramshorst M, van Werkhoven E, et al. Three-year follow-up of neoadjuvant chemotherapy with or without anthracyclines in the presence of dual HER2-blockade for HER2-positive breast cancer (TRAIN-2): a randomized phase III trial. J Clin Oncol. 2020;15_suppl:501.
14. Tolaney SM, Barry WT, Dang CT, Yardley DA, Moy B, Marcom PK, et al. Adjuvant paclitaxel and trastuzumab for node-negative, HER2-positive breast cancer. N Engl J Med. 2015;372(2):134–41.
15. von Minckwitz G, Procter M, de Azambuja E, et al. Adjuvant pertuzumab and trastuzumab in early HER2-positive breast cancer. N Engl J Med. 2017;377(7):122.
16. von Minckwitz G, Huang CS, Mano MS, Loibl S, Mamounas EP, Untch M, et al. Trastuzumab emtansine for residual invasive HER2-positive breast cancer. N Engl J Med. 2019;380(7):617–28.
17. (EBCTCG) EBCTCG. Aromatase inhibitors versus tamoxifen in early breast cancer: patient-level meta-analysis of the randomised trials. Lancet. 2015;386(10001):1341–52.
18. Francis PA, Pagani O, Fleming GF, Walley BA, Colleoni M, Láng I, et al. Tailoring adjuvant endocrine therapy for premenopausal breast cancer. N Engl J Med. 2018;379(2):122–37.

Chapter 20
Follow-Up After Treatment

Bruno Salvador Sobreira Lima, Fernanda Barbosa, Maria Carolina Formigoni, Sergio Masili-Oku, and Jose Roberto Filassi

20.1 Introduction

According to statistics from the International Agency for Research on Cancer (IARC), 44 million people live with the disease worldwide. With the establishment of effective screening policies and improvement of diagnostic and therapeutic methods, the number of patients who survive the disease is considerable. Specifically, for breast cancer, the 5-year survival rate in countries like the United States is around 90% [1].

For those patients who survived the primary neoplasia, the follow-up will have to consider specific issues of the natural aging process, in addition to the particularities related to the cancer therapy received. Some aspects, such as the risk of late recurrence, the occurrence of a new primary tumor of the mammary site or not, and sequelae of short- and long-term treatment are added to psychological, genetic, reproductive, and social issues. All of these aspects must be involved in the follow-up after cancer treatment.

We can didactically divide the follow-up into some items:

1. Follow-up appointments (anamnesis and physical examination).
2. Imaging exams.
3. Laboratory tests.
4. Genetic counseling.
5. Quality of life and lifestyle change.
6. Sexual and reproductive aspects.

B. S. S. Lima · F. Barbosa · M. C. Formigoni · S. Masili-Oku (✉) · J. R. Filassi
Departamento de Mastologia, Instituto do Cancer do Estado de Sao Paulo ICESP, São Paulo, SP, Brazil
e-mail: m.formigoni@hc.fm.usp.br; drfilassi@terra.com.br

S. J. Kim Hsieh, E. A. Morris (eds.), *Modern Breast Cancer Imaging*,
https://doi.org/10.1007/978-3-030-84546-9_20

20.1.1 Follow-Up Appointments (Anamnesis and Physical Examination)

The most important ways to detect recurrences are still considered [2–4]. Consultations should be held every 3–6 months in the first 3 years, semiannually for another 2 years, and annually after the fifth year [5].

In anamnesis, one should ask about symptoms of local recurrence or metastasis, ask about symptoms side by side with the therapy, in addition to reinforcing adherence to it:

Some important topics to be covered include [6, 7]:

- Constitutional symptoms - anorexia, weight loss, fatigue, insomnia.
- Bone health – bone pain, location and characteristic, associated symptoms, improvement, and worsening factors.
- Pulmonary symptoms – persistent cough, dyspnea.
- Neurological symptoms – headache, nausea, vomiting, visual changes.
- Gastrointestinal symptoms – abdominal pain, change in bowel habits, and characteristics of the stool.
- Genito-urinary symptoms – vaginal bleeding, difficulty urinating.
- Psychological symptoms – depression and anxiety.
- Endocrine/reproductive symptoms – hot flashes, dyspareunia, vaginal dryness, preservation of fertility.

The physical examination should include a general exam with an assessment of vital data, cardiac and pulmonary auscultation, and skeletal muscle, abdominal, and neurological examination. The importance of gynecological follow-up must be reinforced, especially for tamoxifen users [6]. Physical analysis of the breasts and armpit must be carried out rigorously, looking for local and lymph node recurrence signs.

In mastectomy cases with reconstruction, special attention should be given to implants and possible complications related to contractures and or ruptures. In cases of reconstruction using flaps such as transverse rectus abdominis (TRAM) or great dorsal attention to steatonecrosis, which, due to its characteristics, can simulate a recurrence, mammography has typical features that exclude a possible recurrence, without the need for biopsy.

20.1.2 Imaging Exams

Mammography should be performed on the contralateral breast or after conservative surgery. It should be performed annually, with the first control exam conducted 6 months after radiotherapy in conservative surgery [8, 9].

Magnetic resonance imaging is not routinely indicated, and such data was demonstrated by a systematic review carried out in 2012 [10]. It can be crucial in cases

where mammography is not conclusive and formally indicated in patients with BRCA mutations and patients with a family history of breast cancer [11].

Ultrasound is also not routinely indicated. It should be performed to complement possible mammographic changes or clinical examination findings without correspondence to the mammogram.

For older patients or those with comorbidities that limit life expectancy to less than 5–10 years, one can consider not having a mammographic follow-up [12].

In addition to the breast image assessment, we must emphasize the importance of bone health assessment. It is known that breast cancer treatment increases the risk of osteoporosis, especially in users of aromatase inhibitors [13]. Therefore, American Society of Clinical Oncology (ASCO) recommends bone densitometry in the following cases:

- Women over 65 years old.
- Women aged 60–64 years in the presence of one of the following factors: family history of osteoporosis, weight <70 kg, history of fracture unrelated to trauma or other risk factors (smoking, physical inactivity, alcoholism).
- Premenopausal women with indication and/ or use of an aromatase inhibitor.
- Premenopausal women who developed early menopause secondary to cancer treatment.

20.1.3 Laboratory Tests

Intensive surveillance with laboratory and imaging (systemic) examinations is not recommended for asymptomatic patients, as this strategy has not shown an increase in disease-free survival or overall survival [14].

The early diagnosis of metastases provided by these tests increases the number of interventions with a consequent increase in toxicity, increased cost, with no evident benefit in survival or quality of life [15].

The guideline for follow-up after breast cancer treatment by ASCO (2012) reinforces not performing these exams in asymptomatic patients, among them it is worth mentioning:

- Tumor markers.
- Liver function tests.
- Bone scintigraphy.
- Alkaline phosphatase.
- Chest imaging exams (x-ray and tomography).
- Abdominal imaging and PET-CT.

Exception made only in those cases in which recurrence is suspected [5].

20.1.4 Genetic Counseling

In the follow-up, evaluate those patients who indicate the need for genetic research and who may not have been tested during the initial investigation and evaluation phase.

The patients with family cancer history (breast, ovary, colon) and at high risk of hereditary tumors, such as breast cancer patients before age 50, patients with triple-negative tumors before age 60, families descended from Jewish Ashkenazis, and male patients [16].

The BRCA mutation is the most frequent, although other rarer mutations should be investigated depending on the personal and family history of several types of cancer, such as Li-Fraumeni and Cowden syndromes.

The performance of these tests and genetic counseling (with a geneticist or another trained professional) is essential for evaluating other family members. In this case, with the identification of high-risk individuals, it is possible to establish risk-reducing measures.

Although it is possible to perform genetic tests on patients not affected by cancer, these results can often be inconclusive. The ideal is to conduct genetic testing on the affected individual, and if a particular mutation is identified, it should be investigated on their descendants.

20.1.5 Quality of Life and Lifestyle Change

Several observational studies suggest that physical exercise, avoiding obesity, adequate diet, and low alcohol intake decrease breast cancer recurrence risk [17, 18].

High doses of vitamin D at diagnosis, especially in premenopausal patients, have been associated with a better prognosis; however, no randomized clinical data associate vitamin D supplementation with a lower risk of recurrence.

Complementary therapies, such as acupuncture, mindfulness, music therapy, and yoga, have been studied in breast cancer survivors. Although there is no evidence of the relationship between these therapies and a lowest recurrence rate, there is a significant improvement in the patients' quality of life [19]. Some studies suggest that these practices can improve joint pain in patients using aromatase inhibitors and physical and psychological pain from breast cancer diagnosis and treatment [20].

20.1.6 Sexual and Reproductive Aspects

Symptoms of menopause, such as hot flushes and vaginal dryness, can be due to age, chemotherapy treatment (in premenopausal patients), and hormone therapy.

Hormone therapy at menopause should be avoided in patients with a previous history of breast cancer. Symptom management should be done with nonhormonal drugs, such as gabapentin or serotonin reuptake inhibitors. Particular attention should be given to serotonin reuptake inhibitors in patients using tamoxifen, with venlafaxine and desvenlafaxine being preferred [21].

Acupuncture is a non-pharmacological therapy that has shown promising results in clinical studies. Cognitive-behavioral therapy also improved hot flushes, night sweats, and sleep quality [22, 23].

Sexual activity may become less pleasurable in patients with breast cancer. Psychological sequelae can affect body image and affect relationships, with impaired sexual function. Sexual dysfunction is associated with depression in breast cancer survivors [24]. The treatment of vaginal atrophy includes nonhormonal options such as lubricants.

Although some experts recommend waiting 2 years to conceive, some studies suggest that pregnancy is safe, even in the first 2 years, the time of the most significant risk of early recurrence [25].

The World Health Organization (WHO) suggests using nonhormonal contraception in patients with a history of breast cancer, as a copper or silver intrauterine device (nonhormonal IUD), condom, and diaphragm.

20.2 Summary and Recommendations

- Recommend adherence to treatment and healthy lifestyle habits.
- Follow-up should include medical history, complete clinical examination, and mammography.
- Follow-up should not focus only on cancer recurrence but also on treatment complications and psychological aspects.
- Evaluate the need for genetic counseling.
- Do not perform laboratory or imaging exams in asymptomatic patients.
- Recommend adoption of a healthy lifestyle: adequate diet, regular physical activity, low alcohol intake, and smoking cessation.
- Assess possible sexual dysfunctions.
- Assess and treat menopausal symptoms.
- Pregnancy does not worsen breast cancer prognosis.
- Give preference to nonhormonal contraception.

References

1. Siegel RL, Miller KD, Jemal A. Cancer statistics, 2018. CA Cancer J Clin. 2018;68:7.
2. de Bock GH, Bonnema J, van der Hage J, et al. Effectiveness of routine visits and routine tests in detecting isolated locoregional recurrences after treatment for early-stage invasive breast cancer: a meta-analysis and systematic review. J Clin Oncol. 2004;22:4010.
3. Montgomery DA, Krupa K, Cooke TG. Follow-up in breast cancer: does routine clinical examination improve outcome? A systematic review of the literature. Br J Cancer. 2007;97:1632.
4. Lu W, de Bock GH, Schaapveld M, et al. The value of routine physical examination in the follow up of women with a history of early breast cancer. Eur J Cancer. 2011;47:676.
5. Runowicz CD, Leach CR, Henry NL, et al. American Cancer Society/American Society of Clinical Oncology Breast Cancer Survivorship Care Guideline. J Clin Oncol. 2016;34:611.
6. Loomer L, Brockschmidt JK, Muss HB, Saylor G. Postoperative follow-up of patients with early breast cancer. Patterns of care among clinical oncologists and a review of the literature. Cancer. 1991;67:55.
7. Pace BW, Tinker MA. Follow-up of patients with breast cancer. Clin Obstet Gynecol. 1994;37:998.
8. Grunfeld E, Noorani H, McGahan L, et al. Surveillance mammography after treatment of primary breast cancer: a systematic review. Breast. 2002;11:228.
9. Lash TL, Fox MP, Buist DS, et al. Mammography surveillance and mortality in older breast cancer survivors. J Clin Oncol. 2007;25:3001.
10. Quinn EM, Coveney AP, Redmond HP. Use of magnetic resonance imaging in detection of breast cancer recurrence: a systematic review. Ann Surg Oncol. 2012;19:3035.
11. National Comprehensive Cancer Network. NCCN Clinical Practice Guidelines in Oncology. Genetic/familial high-risk assessment: breast and ovarian. https://www.nccn.org/professionals/physician_gls/pdf/genetics_bop.pdf. Accessed on 04 Feb 2020.
12. Freedman RA, Keating NL, Partridge AH, et al. Surveillance mammography in older patients with breast cancer-can we ever stop?: a review. JAMA Oncol. 2017;3:402.
13. Pant S, Shapiro CL. Aromatase inhibitor-associated bone loss: clinical considerations. Drugs. 2008;68:2591.
14. Rojas MP, Telaro E, Russo A, et al. Follow-up strategies for women treated for early breast cancer. Cochrane Database Syst Rev. 2005:CD001768.
15. Henry NL, Hayes DF, Ramsey SD, et al. Promoting quality and evidence-based care in early-stage breast cancer follow-up. J Natl Cancer Inst. 2014;106:dju034.
16. National Comprehensive Cancer Network. www.nccn.org
17. Friedenreich CM, Gregory J, Kopciuk KA, et al. Prospective cohort study of lifetime physical activity and breast cancer survival. Int J Cancer. 2009;124:1954.
18. Kwan ML, Kushi LH, Weltzien E, et al. Alcohol consumption and breast cancer recurrence and survival among women with early-stage breast cancer: the life after cancer epidemiology study. J Clin Oncol. 2010;28:4410.
19. Lyman GH, Greenlee H, Bohlke K, et al. Integrative Therapies During and After Breast Cancer Treatment: ASCO Endorsement of the SIO Clinical Practice Guideline. J Clin Oncol. 2018;36:2647.
20. Park S, Sato Y, Takita Y, et al. Mindfulness-based cognitive therapy for psychological distress, fear of cancer recurrence, fatigue, spiritual well-being, and quality of life in patients with breast cancer-a randomized controlled trial. J Pain Symptom Manag. 2020;60:381.
21. Barnabei VM, Cochrane BB, Aragaki AK, et al. Menopausal symptoms and treatment-related effects of estrogen and progestin in the Women's Health Initiative. Obstet Gynecol. 2005;105:1063.
22. Lesi G, Razzini G, Musti MA, et al. Acupuncture as an integrative approach for the treatment of hot flashes in women with breast cancer: a prospective multicenter randomized controlled trial (AcCliMaT). J Clin Oncol. 2016;34:1795.

23. Atema V, van Leeuwen M, Kieffer JM, et al. Efficacy of internet-based cognitive behavioral therapy for treatment-induced menopausal symptoms in breast cancer survivors: results of a randomized controlled trial. J Clin Oncol. 2019;37:809.
24. Avis NE, Crawford S, Manuel J. Psychosocial problems among younger women with breast cancer. Psychooncology. 2004;13:295.
25. Azim H Jr, Kroman N, Ameye L, et al. Pregnancy following estrogen receptor-positive breast cancer is safe – results from a large multi-center case-control study. Eur J Cancer. 2012;48S: European Breast Cancer Conference #21.

Chapter 21
Breast Cancer During Pregnancy and Lactation

Yoon Seung Chang and Monica Akahoshi Rudner

21.1 Introduction

Breast diseases associated with pregnancy are those diagnosed during pregnancy and 1 year after delivery.

During pregnancy and lactation, complete development of the mammary glands occurs due to increase in hormone levels (estrogen and progesterone) and is promoted by the placenta. Glandular proliferation, ductal distension, and stromal involution occur. Such structural changes are manifested clinically by progressive increase in the volume, firmness, and nodularity of the breasts, making physical examination difficult. Therefore, imaging evaluation is necessary.

During these periods, the breasts can be affected by diseases directly related to physiological changes, inflammatory and infectious diseases, juvenile papillomatosis, and benign and malignant tumors.

Palpable changes are responsible for initiating investigation in these patients. All masses found during pregnancy and lactation must be carefully evaluated, as the diagnosis of injuries or physiological changes secondary to hormonal stimulation can only be established after a thorough radiological evaluation.

Y. S. Chang
Breast Imaging Section, Centro de Diagnósticos Brasil (CDB – Alliar), São Paulo, SP, Brazil

Instituto de Radiologia INRAD, Hospital das Clinicas HCFMUSP, Faculdade de Medicina, Universidade de Sao Paulo, São Paulo, SP, Brazil
e-mail: yoon.chang@cdb.com.br

M. A. Rudner (✉)
Hospital Albert Einstein, São Paulo, SP, Brazil

Instituto de Radiologia INRAD, Hospital das Clinicas HCFMUSP, Faculdade de Medicina, Universidade de Sao Paulo, São Paulo, SP, Brazil

Hospital Moriah and Prevent Senior, São Paulo, SP, Brazil
e-mail: monicaak@einstein.br

S. J. Kim Hsieh, E. A. Morris (eds.), *Modern Breast Cancer Imaging*,
https://doi.org/10.1007/978-3-030-84546-9_21

The ideal protocol for radiological evaluation of the breasts of symptomatic pregnant or lactating women is controversial. Physiological changes that occur during pregnancy and lactation lead to a diffuse and pronounced increase in the density of the breast parenchyma. On mammography, the gland appears very dense, heterogeneous, nodular, and with a sharp decrease in adipose tissue and a prominent ductal pattern. These characteristics, associated with the high density that is generally observed in young women, reduce the sensitivity of mammography, which usually ranges from 70% to 90% [1]. In lactating women, mammography should be performed immediately after breastfeeding, when breast density decreases.

Although some researchers suggest that mammography should be reserved for pregnant and lactating women with proven malignancy [2], others argue that mammography is a useful diagnostic tool during these periods [3, 4].

In contrast to the controversy regarding the use of mammography, there is a consensus on the application of ultrasound (US) when evaluating a pregnant or lactating woman with breast diseases [1, 5]. During pregnancy, the breast parenchyma is characterized by the proliferation of the fibroglandular component with slight diffuse heterogeneous hypoechogenicity. In contrast, during lactation the parenchyma is diffusely hyperechogenic, with a prominent ductal system and increased vascularity (Fig. 21.1).

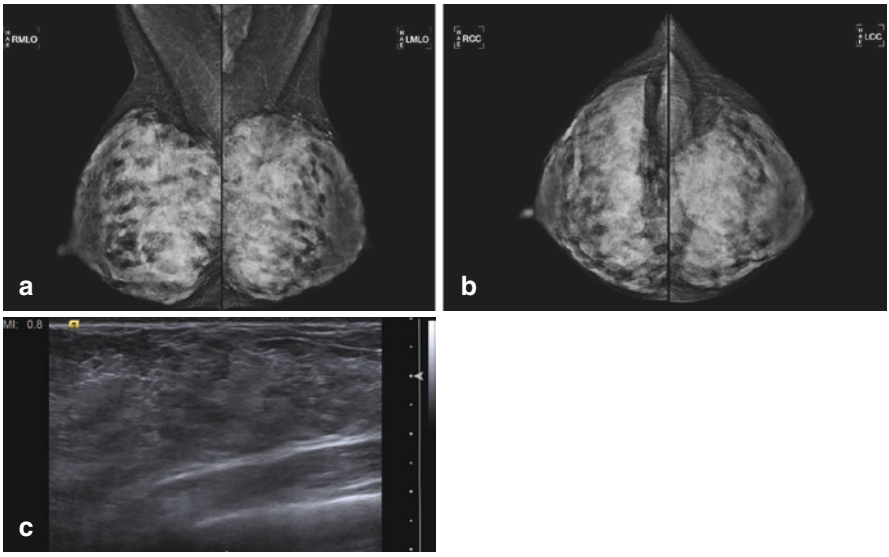

Fig. 21.1 Lactational breast parenchyma. Imaging findings of a 35-year-old lactating woman with family history of breast cancer. Medio lateral (**a**) and craniocaudal (**b**) views of screening mammogram show pronounced increase in density of breast parenchyma, which is very dense, heterogeneous, nodular, and confluent. US image (**c**) shows diffusely hyperechoic breast parenchyma with prominent ducts

Ultrasonography is more sensitive (almost 100%) compared to mammography in the evaluation of patients with carcinoma during these periods. In addition, ultrasound helps to differentiate whether the palpable change represents a mass or normal parenchyma [3].

A recent retrospective review evaluated the accuracy of mammography and ultrasonography in 155 pregnant, lactating, or postpartum women. Among pregnant and lactating women, mammography and ultrasound had a negative predictive value of 100% and identified few cases of cancer [6].

The mammographic and ultrasound characteristics of breast lesions in pregnant and lactating patients do not differ from nonpregnant patients. However, some benign lesions may have suspicious characteristics for malignancy during these periods.

The routine use of magnetic resonance imaging (MRI) in the breast evaluation of pregnant women is a topic that raises debate. MRI evaluation of malignant neoplasms during lactation is controversial and difficult, because during this period the parenchyma has avid contrast impregnation, which can hide or mimic malignant lesions [7]. However, some studies have shown that MRI can differentiate malignant masses from background parenchyma enhancement by evaluating the morphology and kinetics of the enhancement [8]. Three months after the end of lactation, the background enhancement tends to return to the usual pattern. However, if the patient plans to breastfeed for a long period or is at high risk for breast cancer, MRI during lactation should be considered.

In summary, ultrasound should be considered as the initial image exam for the assessment of symptomatic pregnant and lactating women. Although the use of mammography is controversial, this modality should be performed if malignancy is suspected, as it is particularly effective in detecting calcifications and subtle architectural distortions, which are not commonly identified on ultrasound [5].

21.2 Ethical and Legal Aspects

21.2.1 Mammography

The impact of prenatal exposure to ionizing radiation is influenced by three factors: radiation dose, anatomical distribution of radiation, and fetal developmental stage at the time of exposure. During the first 2 months of pregnancy (organogenesis), the fetus is more susceptible to malformations induced by radiation exposure, which include congenital lesions, growth retardation, perinatal death, and risk of developing neoplasms after birth.

Such malformations are more frequent with exposure greater than 0.05 Gy of radiation [9]. Standard mammography exposes the fetus to 0.004 Gy of radiation. Thus, mammography with the use of abdominal protection can be performed during

pregnancy to stage breast cancer with minimal risk to the fetus [6]. However, it is recommended to avoid having a mammogram during the first trimester of pregnancy, proceeding with the evaluation of breast diseases through ultrasound [5].

21.2.2 Cytological Analysis

Several cellular changes occur in the epithelium of the breasts of pregnant or lactating women. Most of these changes are so pronounced that they can lead to a false positive diagnosis of carcinoma. Therefore, the cytological diagnosis of breast lesions during pregnancy and lactation should be done with caution. An experienced cytopathologist, with knowledge of pregnancy-specific changes, is needed to avoid false-positive diagnoses.

21.2.3 Percutaneous Biopsy

Percutaneous biopsy (core biopsy or vacuum-assisted biopsy) is the standard procedure for assessing breast masses during pregnancy and lactation. It is a safe, effective, and easy method for accurate diagnosis, avoiding surgical biopsy.

However, caution is recommended, as the risk of bleeding is relatively high due to increased vascularization during these periods. Other complications include formation of milk fistulae and increased risk of infection due to ductal dilation and trauma-related to breastfeeding [10].

Although these complications are more likely to occur with core biopsy than with fine needle aspiration (FNA) biopsy, they occur with low frequency [5].

21.2.4 Magnetic Resonance Imaging (MRI)

The American College of Radiology (ACR) recommends the use of MRI only in situations where the risk-benefit ratio is well established and specifically states that contrast agents should not be used routinely in pregnant patients, as they cross the placental barrier and enter fetal circulation [11, 12]. Although there are no reports of adverse effects on the fetus due to gadolinium, there are few data available that corroborate the use or not of contrast.

The use of gadolinium does not contraindicate breastfeeding, so interruption is not recommended. In the first 24 hours, only 0.04% of the injected contrast is present in breast milk. Of this amount that is in milk, only 1% is absorbed in the baby's gastrointestinal tract [13].

21.3 Benign Diseases Closely Related to Physiological Changes

21.3.1 Gestational and Secretory Hyperplasia

Calcifications secondary to gestational or secretory hyperplasia can be identified on mammography. Calcifications are most commonly punctate and round, with diffuse or focal distribution. Less commonly, they have an irregular appearance, linear distribution, and a branching pattern similar to those with malignant characteristics. The two manifestations can coexist, as punctate calcifications represent hyperplasia in the lobular acini, while linear calcifications correspond to ductal hyperplasia [14]. Nodular presentation is rare (Fig. 21.2).

21.3.2 Spontaneous Papillary Discharge

Bloody spontaneous papillary discharge is a condition that can occur in up to 20% of pregnant women. It most often occurs in the third trimester of pregnancy when the vascularization of the breast is significantly increased. It is usually self-limited. In cases of persistence, infection, papilloma and, more rarely, breast cancer should be suspected.

In the event of suspected secretion, US and/or mammography should be performed to exclude intraductal proliferations, such as intraductal papilloma or carcinoma. MRI eventually can be considered.

21.3.3 Galactocele

Galactoceles are the most common benign breast lesions in breastfeeding women. They occur more frequently after the interruption of breastfeeding when the milk is contained in the breast [15]. They are cysts formed by cuboidal or flattened

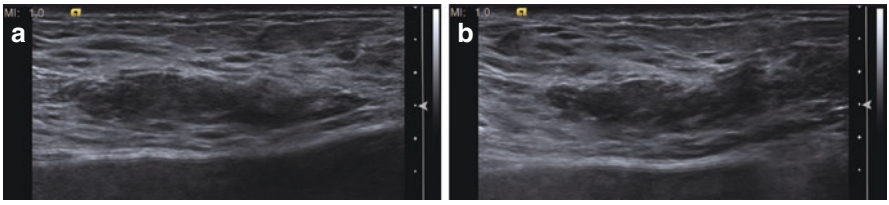

Fig. 21.2 Gestational and secretory hyperplasia. Imaging findings of a 33-year-old pregnant woman (16 weeks) with a palpable mass in the left breast. US images (**a**, **b**) show an oval, hypoechoic with indistinct margin mass). Core biopsy confirmed secretory hyperplasia

epithelium containing fluid similar to milk. The cysts result from ductal dilation and are often enclosed by a fibrous wall of different thicknesses that can be associated with an inflammatory component. Clinically, it presents as a softened mass that is painless on palpation, which can often present as a result of complications such as infection.

In ultrasonography it presents itself in several ways, including simple cysts, cysts with posterior acoustic shadow, and debris inside (fat particles in suspension, masses with liquid-fat level (pathognomonic), among other presentations. Due to the variable amount of fat, protein, and water, echogenicity can be heterogeneous and have suspicious characteristics, such as irregular shape and non-circumscribed margin. The most important differential diagnosis includes intracystic carcinomas [16, 17] (Fig. 21.3).

The mammographic aspect of the galactocele depends on its composition, density, and viscosity of the fluid [16].

Aspiration puncture is a diagnostic and therapeutic procedure, extracting fluid milk when performed during lactation and thickened milk when obtained from older lesions after the end of lactation [15].

21.4 Inflammatory and Infectious Diseases

21.4.1 Puerperal Mastitis

Infectious diseases of the breast are uncommon during pregnancy, but they occur relatively frequently during breastfeeding, with an estimated incidence of 6.6–31% [18]. The most common agent that causes infection is *S. aureus*, followed by *Streptococcus*. The source is the infant's nose or oropharynx. The infection occurs due to fissures in the epithelium of the papilla and areola with retrograde dissemination of the organisms. Milk stasis is an important risk factor, as it represents an excellent culture medium [15].

Mammography is generally not necessary to investigate mastitis in lactating women, unless malignancy is suspected. On the other hand, US plays an important role in the diagnosis and treatment of mastitis, especially in the face of suspected abscess formation.

Abscesses develop in 5–11% of lactating women with mastitis and usually manifest as complex hypoechogenic masses or irregular anechoic masses, sometimes with fluid levels, debris, posterior acoustic reinforcement, and increased vascularization. The inflammatory tissue manifests itself as a poorly defined, hypoechogenic region around the lesion [19] (Fig. 21.4).

Abscesses are usually treated with antibiotic therapy and surgical incision and drainage, but they can also be treated with needle aspiration or catheter drainage, especially when smaller than 2.5 cm. US-guided drainage has the advantage of identifying the necrotic cavity, distinguishing it from inflammatory tissue. The high rate of recurrence is the most common complication related to abscesses.

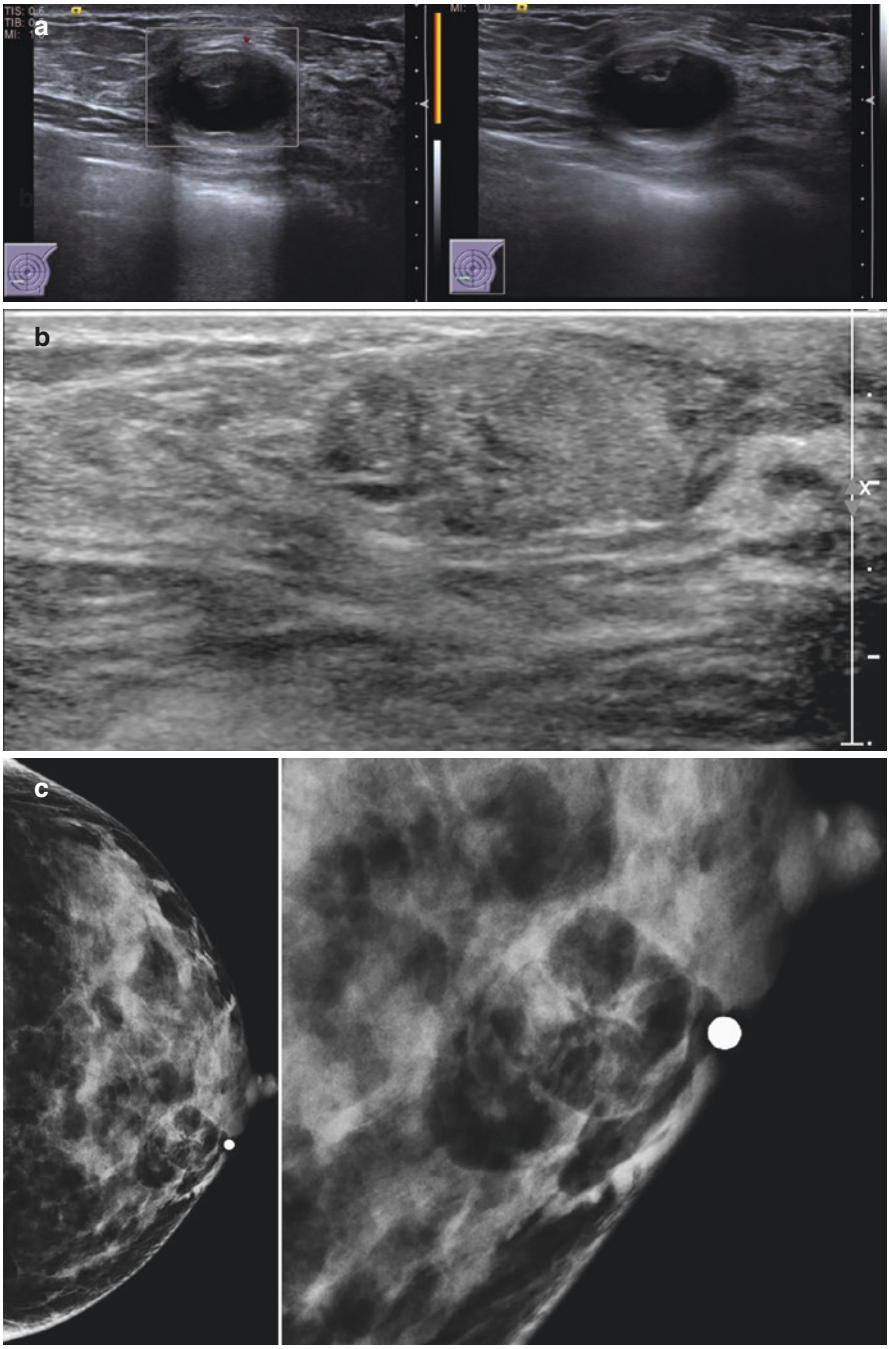

Fig. 21.3 Galactocele**.** Imaging findings of a 37-year-old, 4 months after delivery with a palpable mass in the left breast. (**a**) US images show an oval, circumscribed complex solid and cystic mass, not seen in mammogram (not shown). FNA suggested galactocele. (**b**) US image of another patient with a palpable oval, circumscribed, isoechoic heterogeneous mass. (**c**) Mammogram shows a fat containing mass (galactocele, marked with a BB)

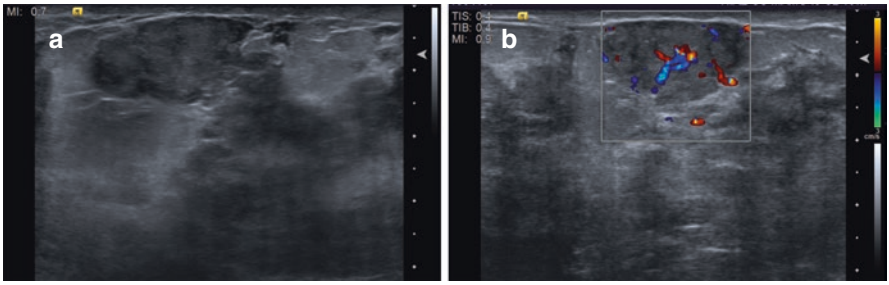

Fig. 21.4 Acute mastitis (puerperal mastitis). Imaging findings of a 33-year-old woman, 6 months after stop breastfeeding, with erythematous and swollen right breast. US images (**a**) show an oval hypoechoic mass, with indistinct margin and internal vascularity at color Doppler (**b**) in the right breast (2.7 cm). Core biopsy confirmed acute mastitis (puerperal mastitis)

21.4.2 Increased Intramammary and Axillary Lymph Nodes

During lactation, enlarged lymph nodes may appear, both intramammary and axillary, being related to bacterial propagation from the nipple during breastfeeding.

On ultrasound, these lymph nodes have thickened cortical and globular morphology in a symmetrical distribution.

21.4.3 Granulomatous Mastitis

Granulomatous mastitis is a rare chronic inflammatory disease of unknown cause, which has been closely linked to pregnancy and lactation. It affects young women usually up to 5 years after a pregnancy.

It often manifests with clinical and radiological changes suggestive of inflammatory carcinoma and breast abscess. For this reason and also due to the tendency of recurrence, the anatomopathological study is indispensable.

Mammographic characteristics vary from the normal presentation in patients with dense breast tissue to focal asymmetries, architectural distortion, and masses with benign or malignant aspects.

Ultrasonography shows hypoechogenic, tubular, and contiguous lesions, sometimes associated with a large hypoechogenic mass (Fig. 21.5).

21.4.4 Juvenile Papillomatosis of the Breast

It is a rare disease during pregnancy and lactation, whose manifestation involves a tumor consisting of multiple cysts separated by fibrous septa and relatively well demarcated regarding the surrounding normal parenchyma.

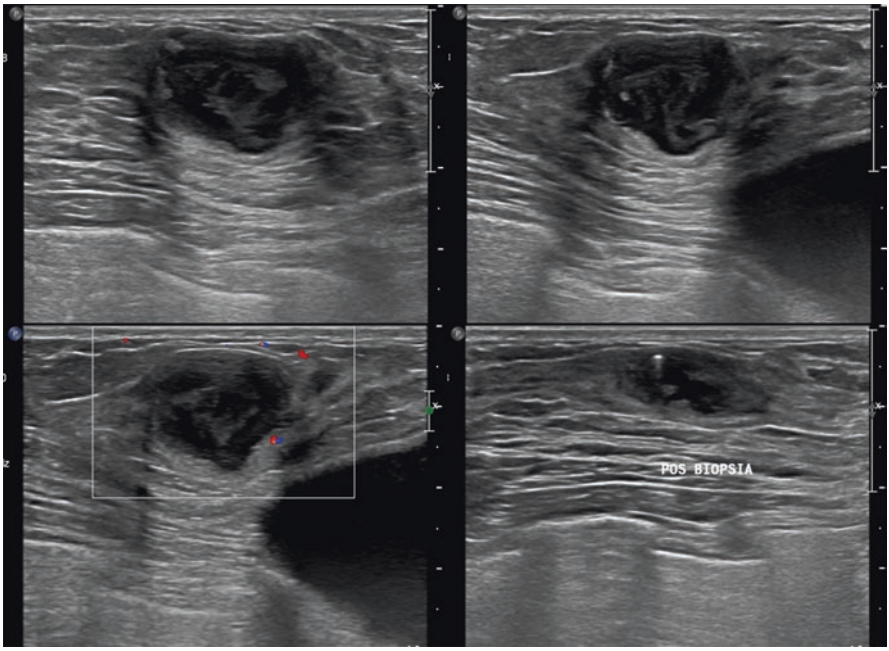

Fig. 21.5 Granulomatous mastitis. Imaging findings of a 31-year-old woman, 4 months after delivery and 2 months after stop breastfeeding, with a palpable mass in the left breast. US images show a complex solid and cystic mass with indistinct margin (2.6 cm). Core biopsy confirmed granulomatous mastitis

On ultrasound, juvenile papillomatosis manifests itself as poorly defined hypoechogenic masses that are demarcated from the normal parenchyma and composed of multiple cysts of varying sizes.

Mammography is usually negative or may show focal asymmetry and calcifications.

The diagnosis of juvenile papillomatosis is made only with histopathological evaluation [5].

21.5 Benign Tumors

21.5.1 Lactational Adenoma

Lactational adenoma is a benign lesion of the breast in response to the physiological changes that characterize pregnancy and lactation (increased estrogen levels) but with controversial etiology. It is sometimes interpreted as a variant of fibroadenoma, tubular adenoma, and lobular hyperplasia, which are also caused by physiological changes.

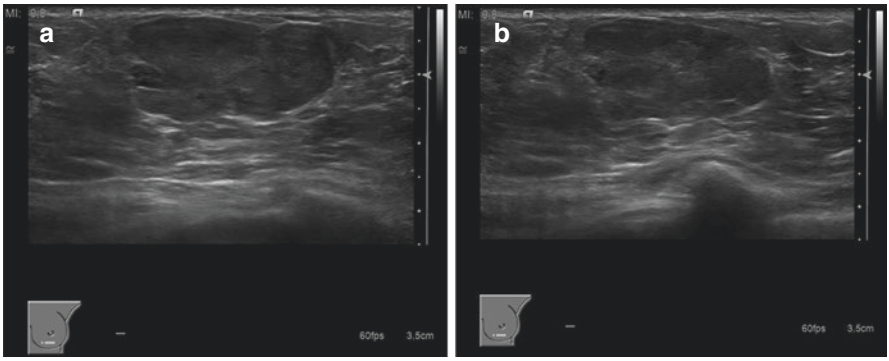

Fig. 21.6 Lactational adenoma 1 – pregnant. Imaging findings of a 32-year-old pregnant woman (38 weeks) with a palpable mass in the left breast. (**a**, **b**) US shows a solid, oval, circumscribed mass, parallel, hypoechoic with 3.2 cm. Core biopsy confirmed lactational adenoma

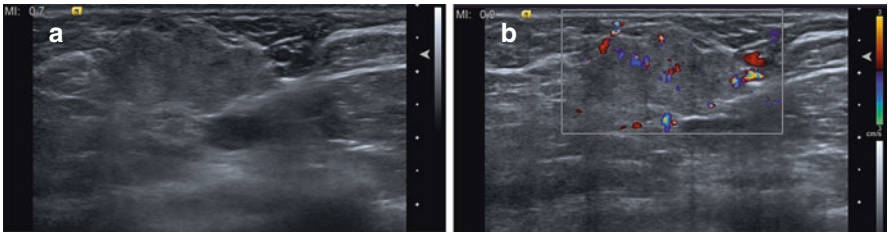

Fig. 21.7 Lactational adenoma 2 – lactating. Imaging findings of a 38-year-old lactating woman with a palpable mass in the right breast. US image (**a**) show a solid, irregular, hyperechoic mass with indistinct margin, parallel, with 3.7 cm, hypervascularized on color doppler (**b**). Core biopsy confirmed lactational adenoma

Lactational adenomas manifest radiologically as benign masses that are indistinguishable from fibroadenomas. However, some of them, especially when suffering infarction, have characteristics that can be confused with malignant lesions, such as irregular shape, microlobulated contours, and posterior and intense acoustic shadow [20] (Figs. 21.6, 21.7, and 21.8).

The natural course of these lesions is regression after breastfeeding cessation.

21.6 Morphological and Physiological Changes in Fibroadenomas Secondary to Pregnancy and Lactation

Fibroadenoma is the most common tumor found during pregnancy and lactation, due to the increase in hormone levels that can induce their growth. For this reason, preexisting or undiagnosed fibroadenomas can be identified during pregnancy. The radiological aspects do not differ from the nonpregnant state.

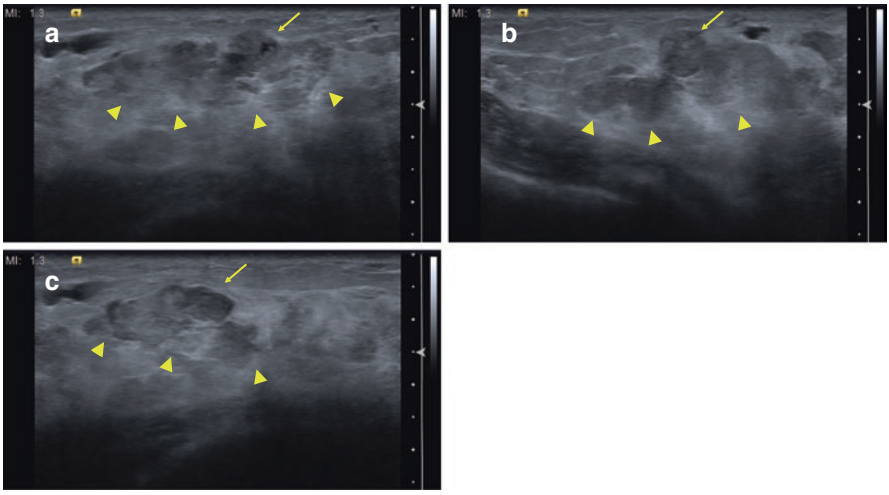

Fig. 21.8 Lactational adenoma 3 – lactating. Imaging findings of a 35-year-old lactating woman with a palpable mass in the left breast and family history of breast cancer (mother). US images (**a**–**c**) show a solid, oval, circumscribed hypoechoic mass, parallel, with 1.0cm (arrows) associated with a non-mass heterogeneous lesion (arrowheads). Core biopsy confirmed lactational adenoma. Control exam 10-months after biopsy didn't show any lesion

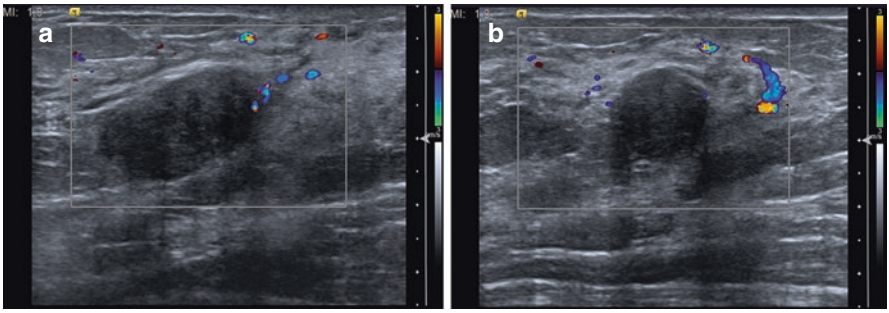

Fig. 21.9 Fibroadenoma (pregnant). Imaging findings of a 35-year-old pregnant woman (16 weeks) with a palpable mass in the right breast. US images (**a**, **b**) show a solid, oval, circumscribed, hypoechoic mass (increased compared to the last exam). Core biopsy confirmed fibroadenoma

A relevant aspect is that fibroadenomas, and lactational adenomas can develop foci of infarction during the third trimester of pregnancy or after childbirth, manifesting clinically as sudden pain in a previously painless fibroadenoma.

On ultrasound, it has an oval shape, homogeneous texture, circumscribed margin, and normal adjacent tissue. However, during pregnancy, it may have an atypical presentation, with cystic component increased vascularity, and heterogeneous texture [19] (Fig. 21.9).

21.7 Malignant Tumors

21.7.1 Pregnancy-Associated Breast Carcinoma (PABC)

PABC is defined as breast cancer that occurs during pregnancy or within 1 year after delivery. PABC affects 1 in every 3000–10,000 pregnancies and represents up to 3% of all malignant breast tumors. In general, it is biologically aggressive, with negative hormone receptors (estrogen and progesterone) and positive for type 2 receptors for human epidermal growth factor (Her2-neu).

Currently, women have chosen to become pregnant later, after 30 years of age, which may contribute to an increase in the incidence of PABC [10].

Patients with a palpable lesion complaint are investigated, so it is important that the clinical examination of the breasts be performed at the beginning of pregnancy before breast engorgement occurs, which makes its assessment difficult.

PABC patients tend to have larger tumors and are diagnosed at more advanced stages, which reflects worse prognosis compared to nonpregnant women of the same age with breast carcinoma.

The sensitivity of mammography to PABC is lower in pregnant or lactating women due to increased glandular density. As mentioned earlier, US is the most appropriate radiological method for assessing PABC. More than 90% of women with PABC present with masses that are easily assessed using US. In addition, it is useful in assessing lymph node involvement and monitoring the response to neoadjuvant chemotherapy. However, mammography plays a complementary role and should always be performed if cancer is suspected, since it is essential for the assessment of calcifications. The imaging aspects are the same as for nonpregnant patients [21, 22].

The diagnosis is made preferably by percutaneous biopsy (core), as it is the safest and most accurate method.

Treatment for patients diagnosed with PABC in the first trimester of pregnancy consists of modified radical mastectomy with adjuvant chemotherapy after the second trimester. For patients with a diagnosis established after the second trimester, neoadjuvant chemotherapy and conservative surgery with radiotherapy after delivery can be considered (Figs. 21.10 and 21.11).

After making the diagnosis of PABC, one should assess the risk-benefit of the mother and fetus before the start of treatment. Therapeutic abortion does not increase patient survival and should not be indicated.

Survival and recurrence of patients with a previous diagnosis of breast cancer do not appear to be affected by posttreatment pregnancy.

21.8 Conclusions

The diseases that affect the breasts during pregnancy and lactation have similar aspects to those observed in nonpregnant women. However, the peculiarities in the presentation of the lesions together with the physiological changes typical of these

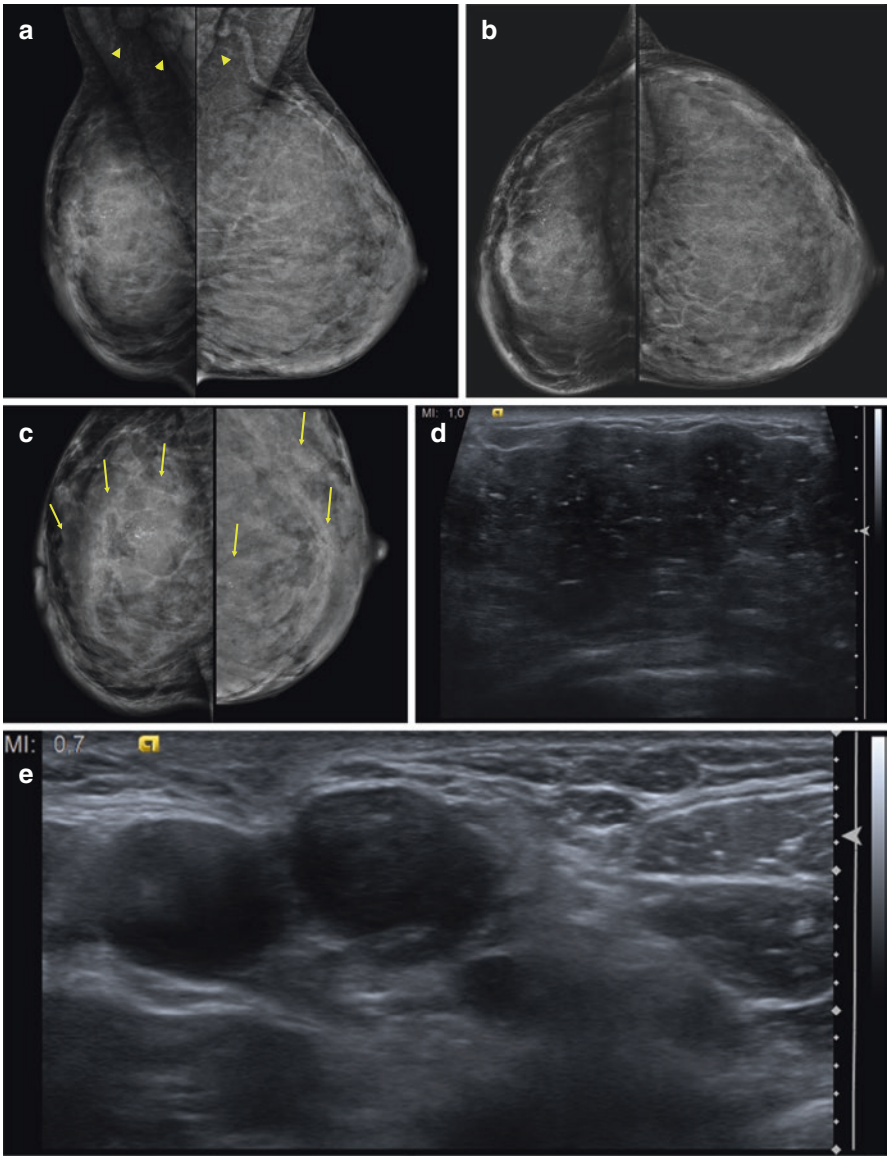

Fig. 21.10 PABC lactating. Imaging findings of a 34-year-old lactating woman (left breast preferential breastfeeding) with a palpable mass in the left breast. Mediolateral (**a**), craniocaudal (**b**), and magnifications views (**c**) mammography shows fine pleomorphic segmental calcifications in the left breast, fine pleomorphic segmental calcifications, and skin thickening in the right breast (arrows in **c**), atypical right axillary lymph nodes (arrowheads in **a**). US images (**d**, **e**) show diffuse hyperechoic parenchyma with prominent ductal system, skin thickening, and an extensive non-mass hypoechoic lesion that occupies the entire right breast and atypical right axillary lymph nodes (I, II and III levels in **c**). Core biopsy (right breast) confirmed invasive carcinoma and ductal carcinoma in situ. Patient has axillary and hepatic metastasis. Vacuum-assisted biopsy of the left breast confirmed secretory hyperplasia

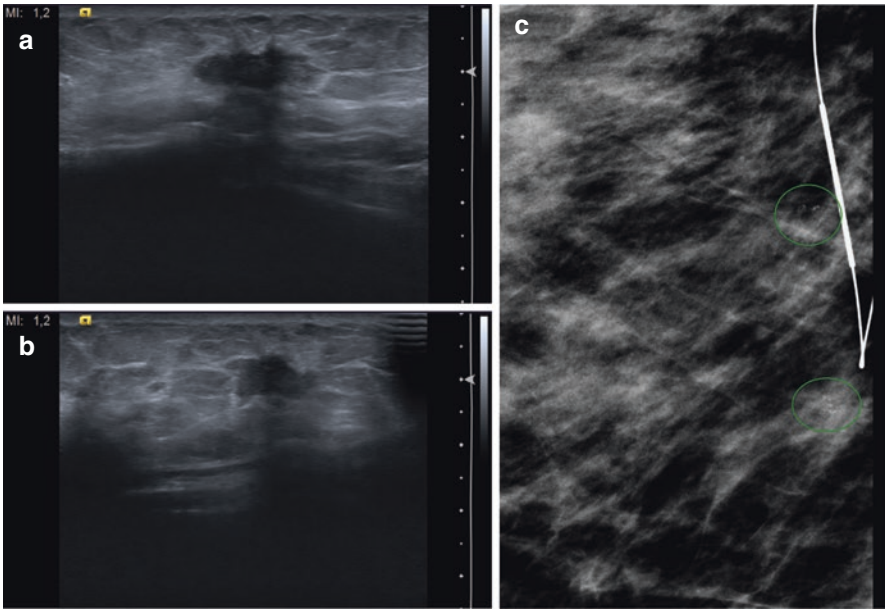

Fig. 21.11 PABC pregnant. Imaging findings of a 41-year-old pregnant woman (12 weeks twin pregnancy) with personal history of surgical excision of Phyllodes tumor in the left breast. US routine images (**a**, **b**) show new solid, irregular mass, with angular margin in the right breast. Core biopsy confirmed invasive carcinoma and ductal carcinoma in situ. Preoperative needle localization mammogram (**c**) shows coarse heterogeneous grouped calcifications (circles in **c**). Patient underwent conservative surgery 1 week after the diagnosis with radiation therapy and chemotherapy after childbirth. No suspicious lesions were seen after 4 years of follow-up

periods must be considered for the correct diagnosis. Delayed diagnosis is the main cause of worse prognosis commonly found in pregnant or lactating patients with breast carcinoma.

References

1. Obenauer S, Dammert S. Palpable masses in breast during lactation. Clin Imaging. 2007;31:1–5.
2. Hogge JP, De Paredes ES, Magnant CM, Lage J. Imaging and management of breast masses during pregnancy and lactation. Breast J. 1999;5:272–83.
3. Ahn BY, Kim HH, Moon WK. Pregnancy and lactation-associated breast cancer: mammographic and sonographic findings. J Ultrasound Med. 2003;22:491–7.
4. Yang WT, Dryden MJ, Gwyn K, Whitman GJ, Theriault R. Imaging of breast cancer diagnosed and treated with chemotherapy during pregnancy. Radiology. 2006;239:52–60.
5. Sabate JM, Clotet M, Torrubia S, Gomez A, Guerrero R, de las Heras P, Lerma E. Radiologic evaluation of breast disorders related to pregnancy and lactation. Radiographics. 2007;27 Suppl 1:S101–24.
6. Robbins J, et al. Accuracy of diagnostic mammography and breast ultrasound during pregnancy and lactation. AJR. 2011;196:716–22.

7. Talele AC, Slanetz PJ, Edmister WB, Yeh ED, Kopans DB. The lactating breast: MRI findings and literature review. Breast J. 2003;9(3):237–40.
8. diFlorio-Alexander, et al. Breast imaging of pregnant and lactating women. J Am Coll Radiol. 2018;15:11S.
9. Greskovich JF Jr, Macklis RM. Radiation therapy in pregnancy: risk calculation and risk minimization. Semin Oncol. 2000;27:633–45.
10. Ayyappan AP, Kulkarni S, Crystal P. Pregnancy-associated breast cancer: spectrum of imaging appearances. Br J Radiol. 2010;83(990):529–34.
11. Amant F, Deckers S, Van Calsteren K, Loibl S, Halaska M, Brepoels L, Beijnen J, Cardoso F, Gentilini O, Lagae L, Mir O, Neven P, Ottevanger N, Pans S, Peccatori F, Rouzier R, Senn HJ, Struikmans H, Christiaens MR, Cameron D, Du Bois A. Breast cancer in pregnancy: recommendations of an international consensus meeting. Eur J Cancer. 2010;46(18):3158–68.
12. Kanal E, Borgstede JP, Barkovich AJ, et al. American College of radiology white paper on MR safety. AJR Am J Roentgenol. 2002;178:1335–47.
13. Committee opinion – diagnostic imaging during pregnancy and lactation. Obstet Gynecol. 2017;130:4.
14. Mercado CL, Koenigsberg TC, Hamele-Bena D, Smith SJ. Calcifications associated with lactational changes of the breast: mammographic findings with histologic correlation. AJR Am J Roentgenol. 2002;179:685–9.
15. Scott-Conner CEH. Diagnosing and managing breast disease during pregnancy and lactation. Medscape Womens Health eJournal. 1997;2(3). Available at: http://www.medscape.com/viewarticle/408859.
16. Son EJ, Oh KK, Kim EK. Pregnancy-associated breast disease: radiologic features and diagnostic dilemmas. Yonsei Med J. 2006;47(1):34–46.
17. Stevens K, Burrell HC, Evans AJ, Sibbering DM. The ultrasound appearances of galactoceles. Br J Radiol. 1997;70:239–41.
18. Holanda AAR, Gonçalves AKS, Medeiros RD, Oliveira AMG, Maranhão TMO. Ultrasound findings of the physiological changes and most common breast diseases during pregnancy and lactation. Radiol Bras. 2016;49(6):389–96.
19. Yu Q, Chang C, Zhang H. Ultrasound imaging characteristics of breast lesions diagnosed during pregnancy and lactation. Breastfeed Med. 2019;14(10):712–7.
20. Sumkin JH, Perrone AM, Harris KM, Nath ME, Amortegui AJ, Weinstein BJ. Lactating adenoma: US features and literature review. Radiology. 1998;206:271–4.
21. Espinosa LA, Daniel BL, Vidarsson L, Zakhour M, Ikeda DM, Herfkens RJ. The lactating breast: contrast-enhanced MR imaging of normal tissue and cancer. Radiology. 2005;237:429–36.
22. Taylor D, Lazberger J, Ives A, Wylie E, Saunders C. Reducing delay in the diagnosis of pregnancy-associated breast cancer: how imaging can help us. J Med Imaging Radiat Oncol. 2011;55(1):33–42.

Index

A
Abnormal lymph node, 128
Accelerated partial breast irradiation (APBI), 394
Acrylate injection, 381–383
Acupuncture, 442, 443
Acute mastitis, 454
Adipocyte-derived stem cells (ADSCs), 402
Adjuvant anti-HER2 therapy, 436
Adjuvant chemotherapy, 435–437
Aesthetic breast surgery
  acrylate injection, 381, 383
  breast implants (*see* Silicone breast implants)
  direct synthetic substances injection (fillers), 379
  hyaluronic acid injection, 384–386
  lipofilling (fat grafting), 386
  mammoplasty, 338–340
  mastopexy, 338, 340
  paraffin injection, 379
  periareolar dermal calcifications, 341
  porcine biological mesh, 388, 389
  silicone injection, 379–381
  synthetic mesh, 390–392
Alliance A11202 study, 44
American college of radiology (ACR), 450
American College of Surgeons Oncology Group (ACOSOG) Z1071 trial, 43
American society of clinical oncology (ASCO), 10, 441
American society of radiation oncology (ASTRO), 392
Anamnesis, 440
Anthracyclines, 436, 437
Anti-HER2 adjuvant therapy, 437
Apparent diffusion coefficient (ADC), 317
Architectural distortion, 331
Aspiration puncture, 452
Associated findings, 126
Atypical hyperplasia, 22
Atypical lobular hyperplasia (ALH), 206
Autoimmune/inflammatory syndrome induced by adjuvants (ASIA) syndrome, 356
Autologous fat grafting (FG), 386
Autologous fat graft injection, 402
Automated breast ultrasound (ABUS), 107, 109
Axillary disease, 284
  indications, 284–285
  mammography, 286
  MRI, 286
  PET-CT, 286
  ultrasonography, 285
Axillary lymph node dissection (ALND), 39
Axillary management
  in clinically node-negative patients, 40–42
  in clinically node-positive patients, 42–44
  in micro metastases (N1m1), 40
Axillary surgery, 39

B
Baker classification, 361, 362
Benign calcifications, 425
Bilateral capsular contraction, 362
Biological mesh, 388
BI-RADS® Categories, 127–129

S. J. Kim Hsieh, E. A. Morris (eds.), *Modern Breast Cancer Imaging*,
https://doi.org/10.1007/978-3-030-84546-9

BI-RADS® Lexicon, 114, 115, 117, 118, 120
Bone health, 440
BRCA mutation, 26, 442
Breast biopsy, 273
  core needle biopsy (CNB), 274
  DBT-guided breast biopsy, 276
  fine needle aspiration (FNA) biopsy, 273
  MRI-guided biopsy, 275, 276
  vacuum-assisted biopsy (VAB), 275
  wire localization, 275
Breast cancer
  basal carcinomas and triple negative carcinomas, 4
  BRCA1 mutation, 3
  genes and associated syndromes, 24–26
  genome analysis technologies, 3
  HER2-enriched carcinomas, 9–12
  hereditary syndromes, 23, 24
  heterogeneity of, 3
  incidence of, 17
  luminal carcinomas, 6, 8, 9
  neoadjuvant chemotherapy, 151
  non-FDG tracers for, 155, 156
  recurrence, 150
  risk factors
    alcohol consumption and smoking, 21
    contraception and hormone replacement therapy, 19, 20
    gender and age, 17
    gestation and lactation, 18, 19
    obesity, 20, 21
    precursor injuries, 22
    reproductive factors, 18
    thoracic radiation therapy, 21, 22
Breast Cancer Index (BCI) assay, 34
Breast cancer treatment, 390, 392
Breast conservation therapy, 339
Breast-conserving surgery (BCS), 392–394, 396, 415
Breast edema, 332, 393, 394
Breast imaging, 71
Breast implant-associated anaplastic large cell lymphoma (BIA-ALCL), 170, 355, 370, 372, 373, 375, 377
Breast implant illness (BII), 355
Breast implant rupture, 128
Breast implants, 136
Breast reconstruction
  autologous fat graft injection, 402
  DIEP flap, 402
  dorsal-flap reconstruction, 406
  double-lumen implant, 402, 403
  TRAM flap, 402, 404
Breast self-examination, 251

C
Calcifications, 120, 123
Calcified fibrous capsule, 351
Canadian Sentinel Node Biopsy Following Neoadjuvant Chemotherapy (SN FNAC) trials, 43
Cancer recurrence, 407, 408
Capsular calcifications, 351
Capsular contraction, 360
Capsulitis, 362
Carboxymethylcellulose (hydrogel), 364
Chromogenic in situ hybridization (CISH), 10
Chromosome enumeration probe (CEP17), 10
Clinical breast examination, 251
Clip placement, 165, 166
Closed capsulotomy, 362
Clustered microcysts, 125, 126
Complementary therapies, 442
Complicated cyst, 127
Constitutional symptoms, 440
Cytological analysis, 450

D
Deep inferior epigastric perforator flap (DIEP), 399
Diffusion-weighted images (DWI), 135
Digital breast tomosynthesis (DBT), 190, 263, 429
Digital breast tomosynthesis vacuum-assisted biopsy (DBTVAB), 191
Digital mammography, 248
Direct synthetic substances injection (Fillers), 379
Discordant biopsy, 203–206
  concordant benign, 204–205
  concordant malignancy, 204
  discordant benign, 205–206
  discordant malignancy, 204
  high-risk and borderline lesions, 206
DNA microarrays, 6
Doppler evaluation, 102–104
Dorsal-flap reconstruction, 406
Double-lumen implants/expanders, 342, 344, 347
Ductal carcinoma in situ (DCIS), 23, 415
Ductography, 271
Dystrophic calcifications, 335, 425, 426, 428

E
Early breast cancer trialists collaborative group (EBCTCG), 392
18F-FDG-PET

diffuse intense activity, 143
histologic subtypes and receptor status, 144, 145
indications in breast cancer, 144
metastatic staging, 147, 149
nodal metastases, 147
physiological uptake, 143
primary breast tumor detection and staging, 146
prognostic value, 153
Eklund maneuver, 345, 346
Elastography, 252
automated breast ultrasound, 107, 109
shear wave elastography, 106, 108
strain elastography, 105
Endocrine/reproductive symptoms, 440
Endocrine therapy, 435–437
EndoPredict assay, 33
Epidermal inclusion cysts, 339
Ethyl-methacrylate (EMA), 381
European SENTinel NeoAdjuvant (SENTINA) trial, 43
Exam documentation, 111–114
Expression of epidermal growth factor (EGFR), 4
Extracapsular rupture, 366, 370

F
False-positive rupture, 374
Fat grafting, 386, 387
Fat necrosis, 125, 334–337, 339, 387, 393, 395, 404, 405
Fibroadenoma, 456, 457
Fibrous capsule, 353
Fine needle aspiration (FNA), 42, 285
Fixation clips, synthetic mesh, 390
Flat epithelial atypia (FEA), 22
Fluorescence in situ hybridization (FISH), 10
Follow-up after treatment
appointments, 440
genetic counseling, 442
imaging examination, 440, 441
laboratory tests, 441
lifestyle changes, 442
quality of life, 442

G
Galactocele, 451, 453
Gamma rays, 142
Gastrointestinal symptoms, 440
Gel bleed, 364
Gene expression assays
concordance of expression assays, 34
genomic tests for, 35
MammaPrint assay, 33
Oncotype DX assay, 32
Genetic counseling, 442
Genito-urinary symptoms, 440
Genomic tests, 31
Gestational and secretory hyperplasia, 451
Gossypibomas, 375, 378
Granulomatous mastitis, 454, 455

H
Hematoma, 332, 334, 335, 338, 346, 389, 393, 394, 402, 405
HER2 amplification, 436
HER2 gene-protein assay (GPA) technique, 12
Hereditary syndromes, 23, 24
Hormone therapy, 443
Hyaluronic acid injection, 385, 386
Hydroxyethyl-methacrylate (HEMA), 381
Hypoechoic spiculated mass, 333–335, 394

I
Image acquisition, 141
Imaging-guided percutaneous biopsy
complications, 164
historical perspective, 161
percutaneous breast biopsy, 164
post-biopsy marker, 165
pre-biopsy assessment, 163, 164
purpose of the procedure, 164
surgical biopsy, 164
Imaging methods, 109, 111
Imaging pathology correlation, *see* Discordant biopsy
Immunohistochemical reaction, 11, 61
Infraclavicular recurrence, 398
Injections of non-resorbable synthetic biomaterials, 379
In situ hybridization (ISH), 10
International agency for research on cancer (IARC), 439
International Breast Cancer Study Group (IBCSG) 23-01 trial, 41
Interstitial brachytherapy, 394
Intracapsular rupture, 368
Intracapsular silicone implant rupture, 365
Intracavitary brachytherapy, 394
Intraoperative radiotherapy (IORT), 394

Invasive carcinoma, 55, 56
mammography, 288, 290
MRI, 289, 291
ultrasound, 289, 291
Invasive ductal carcinoma
mammography, 288
MRI, 287
Ipsilateral breast tumor recurrence (IBTR), 395, 397, 398

J
Juvenile papillomatosis, 454

L
Lactational adenoma, 455–457
Lactational breast parenchyma, 448
Lesion morphology, 131
Linguine sign, 373
Lipofilling (fat grafting), 386–388, 402
Liquid silicone injection, 380–382
Lobular carcinoma in situ (LCIS), 23, 206
Loco regional recurrence (LRR) rates, 44
Luminal androgenic subtype (LAR), 5
Luminal carcinomas, 6, 8, 9
Lymph nodes, 293
mammography, 293
ultrasound, 294

M
Magnetic resonance imaging, 249, 250
breast implants, 136
diffusion-weighted images (DWI), 135
imaging acquisition, 131
PET/MR mammography, 154
signal intensity, 133
standard MRI examination, 132
3D MIP images, 135
T1-weighted images, 134
T2-weighted images, 133
Malignant tumors, 458, 459
MammaPrint assay, 33
Mammography
ACR-BIRADS® final assessment, 91
advantages, 71
architectural distortion, 85
associated findings, 90
asymmetries, 85
beast composition, 80
calcifications, 82
cleavage view on, 77
indications, 77, 80
intramammary lymph node, 86
irregular mass with microlobulated margins, 74
large rod-like calcifications, 74
lesions location, 90
magnification view, 74
masses, 81
PET/MR mammography, 153
pregnancy and lactation, 449
recommendation, 93
regular and exaggerated CC view, 76
regular and rolled CC view, 75
single dilated duct, 90
skin breast lesions, 89
spot compression view on, 74
true lateral view on, 73
Mammography-guided biopsy, 183
biopsy probe, 189
CC and ML views, 186
DBT biopsy, 190
DBT *vs.* stereotactic biopsy, 190
far posterior lesions, 195
field of view (FOV), 191
hologic affirm® prone biopsy system, 193
post-fire tomosynthesis, 192
pre- and post-biopsy images, 194
subtle findings, 192
superficial lesions, 196
thin breasts, 195–196
field of view (FOV), 186
prone table biopsy systems, 185, 186
six to 12 tissue fragments, 188
stereopair view, 187
stereotactic biopsy, 184, 189
Mammoplasty, postoperative breast, 340
Mammotome (ethicon endo-surgery), 276
Mastectomy, 392, 398, 399
Mastopexy, postoperative breast, 340
Menopause, 443
Metastatic disease, 152
Metastatic staging, 147, 149
Mindfulness, 442
Molecular breast imaging, 251
Motiva implants, 343, 345
MRI-guided biopsy, 197
adequate compression, 200
biopsy kit, 202
coaxial system, 202
complications, 203
lesion depth, 201
non-enhanced sagittal T1 slices, 200
post procedure care, 203
pre-contrast images, 200
second-look mammography, 199
second-look ultrasound, 198
visual method, 201
Music therapy, 442

N
National comprehensive cancer network (NCCN) guidelines, 27, 42, 144
National surgical adjuvant breast and bowel project (NSABP), 392
National Surgical Adjuvant Breast and Bowel Project (NSABP) B-32 trial, 40
Neoadjuvant chemotherapy (NAC), 151
Neoadjuvant systemic therapy (NST), 308
  lymph node evaluation, 324–326
  mammography interpretation, 310, 312
  MRI interpretation, 314
    assess response, 316
    challenging lesions, 323, 324
    complete response, 317
    DCE-MR imaging, 317
    DCIS, 315
    DWI techniques, 315
    functional tumor volume, 317
    overestimation of residual disease, 322–323
    partial response, 319
    progressive disease, 321
    residual tumor, 316
    stable disease, 320
    time-signal intensity curve analysis, 317
    underestimation of residual disease, 322
    using AI methods, 315
  multimodality response assessment, 309–310
  NCT indications, 308
  neoadjuvant endocrine therapy (NET), 308
  PCR, 308
  ultrasound interpretation, 312, 314
Neurological symptoms, 440
Next generation sequencing, 62
Nipple-areolar complex (NAC), 265, 266, 339, 398–399
Nipple-sparing mastectomy (NSM), 399
Noninvasive cosmetic surgery, 379
Non-mass-like enhancement (NME), 430
Non-palpable breast changes, 269–273
  image screening, 269–270
  nipple discharge, 270
    BIRADS 3 biopsied, 272
    ductography, 271
    ductoscopy, 273
    initial assessment, 271
    MRI, 272
Non-radioactive wireless devices
  magseed localization, 236
  radar reflector localization, 234
  RFID localizer, 236

O
Obesity, 20, 21
Oil cysts, 339
Oncotype DX assay, 32
Oncotype DX recurrence score (RS), 436
Open surgical capsulotomy, 362
Oreo cookie sign, 350

P
Palpable changes
  axillary lymph nodes, 268
  axillary metastasis, 269
  breast lump, 259
    biopsy-proven breast cancer, 265
    breast tomosynthesis, 263
    DBT, 263
    diagnostic mammography technique, 260
    ductal carcinoma in situ, 262
    fibroadenoma, 261
    magnetic resonance imaging, 262, 265
    negative predictive value, 263
  occult breast carcinoma, 268
  Paget's disease
    BIRADS 3 patients, 266
    imaging methods, 266
    nipple areola complex, 265, 266
    noninvasive disease, 266
    right breast, 267
Papillary neoplasms, 49, 50
Parenchymal scarring, 331
Pathologic complete response (pCR), 5
Pathology, breast cancer of
  atypical ductal hyperplasia and low-grade carcinoma in situ, 51
  benign high-risk lesions and precursors, 50
  biomarkers in ductal carcinoma in situ, 53
  fibroepithelial lesions, 48, 49
  immunohistochemistry, 61
  in situ hybridization, 61
  intermediate and high-grade ductal carcinoma in situ, 51, 52
  invasive carcinoma, 55, 56
  macroscopic evaluation, 57, 58
  next generation sequencing, 62
  papillary neoplasms, 49, 50
  pleomorphic lobular carcinoma in situ (PLCIS), 52, 53
  pre-analytical procedures, 47
  radiological-pathological correlation, 47, 48
  special subtype, 59
Percutaneous biopsy, 450
Periareolar dermal calcifications, 339

Periprosthetic fluid, 347, 353, 369, 371
Phyllodes tumor, 49
Polyacrylamide hydrogel (PAAG), 383, 384
Polymethyl-methacrylate (PMMA), 381
Porcine biological mesh, 388, 389
Positron emission tomography-computed tomography (PET-CT), 284
Postoperative breast
  aesthetic breast surgery (*see* Aesthetic breast surgery)
  architectural distortion and scarring, 336, 338
  breast-conserving surgery, 392, 394, 396
  calcifications at surgical site, 335
  fat necrosis, 336, 337
  increased density and parenchymal scarring, 334
  ipsilateral breast tumor recurrence, 395, 398
  mammogram one month after benign biopsy, 333
  mastectomy, 398, 401
  periareolar dermal calcifications, 339
  scarring, 331, 332, 335
  seroma/hematoma, 334
Post-processed images, 135
Postsurgical fluid collection, 125, 129
Pregnancy and lactation
  benign diseases
    galactocele, 451, 453
    gestational/secretory hyperplasia, 451
    spontaneous papillary discharge, 451
  benign tumors, lactational adenoma, 455–457
  cytological analysis, 450
  fibroadenoma, 456, 457
  inflammatory and infectious diseases
    granulomatous mastitis, 454, 455
    increased intramammary and axillary lymph nodes, 454
    juvenile papillomatosis, 454
    puerperal mastitis, 452
  lactational breast parenchyma, 448
  magnetic resonance imaging, 449, 450
  mammography, 449, 450
  percutaneous biopsy, 450
  physiological changes, 448
  pregnancy-associated breast carcinoma, 458–460
  ultrasonography, 449
Pregnancy-associated breast carcinoma (PABC), 458, 459
Preoperative imaging, 281
  breast magnetic resonance imaging, 283–284
  mammography, 282
  PET-CT, 284
  tomosynthesis, 283
  ultrasonography, 283
Preoperative localization (PL)
  complications, 237
    bleeding, 237
    broken/transected wires, 240
    ecchymoses, 237
    pneumothorax, 237
    vasovagal reactions, 237
  indications, 212
  post-procedure assessment, 240
  pre-procedure review, 212
  wire localization (WL) (*see* Wire localization (WL))
Prone stereotactic vacuum-assisted biopsy (PSVAB), 191
Prophylactic nipple-sparing mastectomy, 400
Prosigna assay, 34
Protocol B-06, 392
Psychological symptoms, 440
Puerperal mastitis, 452, 454
Pulmonary symptoms, 440

R
Radial and anti-radial scanning, 99
Radiation therapy
  breast-conserving surgery, 415
    architectural distortion, 423, 424
    benign calcifications, 425
    breast edema and skin thickening, 418, 420, 421
    expected chronological appearance, 416, 417
    fat necrosis, 421, 422
    fluid collections, 418
  CDIS, 415
  digital breast tomosynthesis, 429
  magnetic resonance, 429–431
  mammography, 426
  mastectomy, 415, 416
  ultrasound, 429
Radioactive seed localization (RSL), 229, 232, 233
Radiofrequency identification tag (RFID) localization, 236
Radio-guided occult lesion localization (ROLL), 226
  gamma probe, 226
  MG-guided ROLL, 227
  scintigraphic images, 226
  stereotactic guided ROLL, 228
Raised silicone ridge, 360
Recurrence, 397, 399, 401, 407, 408

Reduction mammoplasty, 399, 404
Response evaluation criteria in solid tumors (RECIST), 316, 317
Retraction, of scar, 334, 336
Reverberation artifacts, 350, 352
Ruptured saline implant, 369

S
Saline implants, 341, 347
Scanning technique
  anatomy, 100
  compound imaging, 102
  doppler evaluation, 102–104
  harmonic image, 101
  longitudinal and transverse scan, 99
Screen-film mammography, 248
Screening
  breast self-examination, 251
  clinical breast examination, 251
  digital mammography, 248
  elastography, 252
  magnetic resonance imaging, 249, 250
  molecular breast imaging, 251
  screen-film mammography, 248
  in special populations, 253, 254
  thermography, 252
  tomosynthesis, 249
  ultrasound (US), 250
Sentinel lymph node biopsy (SLNB), 39
Sentinel node and occult lesion localization (SNOLL), 226
  MG-guided SNOLL, 229
  US-guided SNOLL, 230
Seroma, 332–334, 338, 346, 354–356, 372, 373, 375, 376, 389, 393, 394, 401
Sexual activity, 443
Shear wave elastography, 106, 108
Silicone breast implants
  capsular calcifications, 349, 351
  complications
    ASIA syndrome, 356
    BIA-LCL, 370, 371, 373, 375
    breast implant illness, 355
    capsular contraction, 360, 362–364
    gossypibomas, 375, 378
    infection, 358, 359
    posterior seal, 360
    raised silicone ridge, 360
    rotation, 359, 361
    rupture (*see* Silicone implant rupture)
  double-lumen implants/expanders, 342, 344
  Eklund Maneuver, 346
  fibrous capsule, 349–351, 353
  implant removal
    abscess, 356
    amorphous calcifications, 357
    architectural distortion, 355
    dystrophic calcifications, 354, 357
    fibrous capsule, 354
    residual fibrous capsule, 355, 358
  magnetic resonance imaging, 347, 348
  motiva implants, 343–345
  periprosthetic fluid, 347, 348, 353
  radial folds, 347, 348, 352
  reduction in detectability of breast carcinoma, 346, 347
  reverberation artifacts, 350, 352
  saline implants, 341, 342
  stacked implants, 343
  subglandular implant, 343
  submuscular implant, 342
  ultrasound, 347, 350, 352
  wrinkles, 347
Silicone implant rupture
  gel bleed, 364
  magnetic resonance imaging
    false-positive rupture, 374
    intracapsular rupture, 369, 371, 374
    linguine sign, 373
    normal radial folds, 370
    ruptured saline implant, 369
    subcapsular line, 372
  mammography
    extracapsular rupture, 366, 367
    intracapsular silicone implant rupture, 365
  rates, 364
  ultrasound
    intracapsular rupture, 368
    snowstorm sign, 367
    stepladder sign, 368
Silver-enhanced in situ hybridization (SISH), 10
Skin lesion, 127
Skin sparing mastectomy (SSM), 399, 408
Skin thickening, 332–334, 336, 339, 393–395, 405, 407
Snowstorm sign, 366, 367
Society of surgical oncology (SSO), 392
Sonographic based imaging, 97, 98
Spontaneous papillary discharge, 451
Stacked implants, 343
Standard mammography, 72
Stepladder sign, 368
Strain elastography, 105
Subcapsular line, 372
Subglandular implant, 343, 364
Submuscular implant, 342, 364

Suspicions axillary lymph nodes, 292
Sutural calcifications, 427
Synthetic matrices, 388, 389
Synthetic mesh, 389–392
Systematic staging, 297
  biopsy/rebiopsy, 301
  early diagnosis, 300
  follow-up patients, 302
  initial assessment, 300
  metastatic lesion, 297
  PET-CT FDG, 301
  systemic assessment, 300
  TNM system, 298
    anatomic staging, 298
    biomarkers, 298
    prognostic staging, 298–299
    therapeutic decisions, 299
Systemic autoimmune adverse reactions, 356

T
T1-weighted images, 134
T2-weighted images, 133
TAILORx trial, 436
Taxanes, 436
Thermography, 252
Thoracic radiation therapy, 21, 22
Three-dimensional (3D) conformal external beam radiation, 394
Tomosynthesis, 249
Tram-flap reconstruction, 404
Transverse rectus abdominis myocutaneous (TRAM) flap, 399, 402, 440
Trilucent implants, 364
Triple-negative (TN) breast cancer, 436
Tsukuba scoring system, 106
Tumor-free margin, 392
Tumor mutational burden (TMB), 6
2D digital mammography (2DDM), 270

U
Ultrasound-guided biopsy, 167
  accuracy and availability, 170
  adequate sampling, 178
  adequate targeting, 179
  axillary management, 168
  BIA-ALCL, 170
  CNB, 173
    automatic core biopsy, 174
    irregular mass, 176
    lymph node, 176
    semiautomatic devices, 174, 175
    spring-loaded mechanism, 173
  complications, 172
  cysts, 168
  fine-needle aspiration (FNA), 167
  lesion location, 170
  on-site cytotechnologist or pathologist, 172
  optimal needle visualization, 181
  pistol-grip mechanic syringe holder, 171
  quantity and quality, 178–179
  scalpel incision, 182
  skin entry point anesthesia, 182
  supine oblique position, 170
  unwarranted trauma, 171
  VAB, 173, 177, 178
    advantages, 179
    de-escalate treatment, 180
    diagnostic and therapeutic, 181
    papillary lesions, 180
    stereotactic biopsy, 179
    surgical excision, 180
    US-guided, 180
Unilateral capsular contraction, 363

V
Vacuum-assisted biopsy (VAB), 459
Vacuum-assisted breast biopsy, 177
Vacuum-assisted needle biopsy, 357
Vascular abnormalities, 125
Vitamin D, 442

W
Whole breast external beam radiotherapy (WB-XRT), 392, 394
Wire localization (WL)
  hookwire, 213
  MRI-guided, 214, 219
    marked compression plate, 214, 217
    sagittal-MRI, 222
    stereotactic guidance, 216, 219
    vacuum-assisted biopsy, 222
  nonwire localization methods, 224
    advantages, 224
    carbon marking, 225
    current lesion localization techniques, 227, 231

non-radioactive wireless devices (*see* Non-radioactive wireless devices)
radioactive seed localization, 229, 232, 233
ROLL, 226
SNOLL, 227, 230
puncture needle, 214
US-guided, 218
hypoechoic mass, 220
mass breast lesion, 220
retractable J-wire, 221
wire variations, 223
Wrinkles, 349

Y
Yoga, 442